REALISTIC MODELLING OF LEAKAGE IN WATER DISTRIBUTION PIPE NETWORKS

Asaph Mercy Kabaasha

Thesis presented for the Degree of

DOCTOR OF PHILOSOPHY

in the Department of Civil Engineering

Faculty of Engineering and the Built Environment

UNIVERSITY OF CAPE TOWN

June 2018

Declaration

I, Asaph Mercy Kabaasha, hereby declare that the work in this document is my own except where acknowledgements indicate otherwise. Neither the whole work nor any part of it has been, is being, or is to be submitted for another degree in this or any other university.

Signature: Signed by candidate Date: 18/06/2018

Acknowledgements

I am sincerely grateful to my supervisor, Prof J. E van Zyl, for providing me with the original idea and his continued believe in me throughout this research. The timely responses to my queries and our regular meetings have been undoubtedly crucial for the completion of this research in time.

I also thank Prof G (Kumar) Mahinthakumar, for his ideas that were incorporated into this research. I specifically thank him for giving me access to the leak detection models that were developed by his research group at the North Carolina State University. These models were used to develop Chapter 6 of this thesis.

The Carnegie Corporation of New York was a generous funder of this research for the first three years. This was through its programme "Developing the Next Generation of Academics in Africa". I am sincerely thankful to them. Once again, I thank Prof J. E van Zyl for ensuring that I had access to funding during the 4th year of this research.

My fellow students in the water distribution systems research group have been a source of inspiration and support. Although your names are too many for a one-page acknowledgment, I say thank you.

Heartfelt thanks go to my Mom and Dad. You sacrificed a lot throughout my studies. I would never had achieved the education I have, if it were not because of you. Thank you for understanding the value of education even in a society where it was not valued by many.

Lastly, many thanks to my dear wife Dorothy Murekatete and my sons Noble and Ian. This PhD journey would have been difficult without your support. Thank you for unselfishly allowing me this opportunity, even when it meant that I must be away from you this long.

Abstract

Several experimental and modelling studies have established that leak areas are mostly not fixed but vary linearly with pressure. Introducing this linear relationship into the orifice equation, results in a two-part modified orifice equation for leakage modelling with pressure head exponents of 0.5 and 1.5 respectively.

Current hydraulic network solvers apply the conventional power leakage equation to model pressure dependent demands such as leakage. The empirically derived power leakage equation does not explicitly consider the leak area variation with pressure and it has been found to be flawed under certain conditions.

The aim of this study therefore, was to incorporate the modified orifice equation into the algorithm of a hydraulic network solver and evaluate the impact this has on leakage modelling. Epanet is the hydraulic modelling software whose algorithm of the network solver was modified. In addition, a stochastic model for network leak generation and distribution was developed.

The conventional and the modified software were applied to different levels of stochastically generated and distributed leakage in three differently sized pipe networks. It was found that the conventional power leakage equation results in significant leakage volume and flow rate errors under certain conditions.

A methodology was also developed to correct the conventional power leakage equation so that it can be used to model leakage realistically without a change of the software to one that uses the modified orifice equation. The methodology was thereafter applied to an existing model that detects leaks in standard water distribution pipe networks, and the results showed significant improvements in the performance of the model.

Table of contents

List of tables

List of figures

Acronyms and abbreviations

ALC	Active Leakage Control
AZNP	Average Zone Night Pressure
AZP	Average Zone Pressure
BABE	Burst and Background Estimates
BG	Background leaks
CARL	Current Annual Real Losses
Conn	Consumer connection
DMA	District Metered Area
GGA	Global Gradient Algorithm
GUI	Graphical User Interface
IDE	Integrated Development Environment
ILI	Infrastructure Leakage Index
IWA	International Water Association
LP	Linear Programming
MILP	Mixed Integer Linear Programming
MNF	Minimum Night Flow
MR	Mains Reported

MU	Mains Unreported
NDF	Night Day Factor
PD	Potentially Detectable leaks
PM	Pressure Management
SR	Service Reported
SU	Service Unreported
UARL	Unavoidable Annual Real Losses
UBL	Unavoidable Background Leakage
USA	United States of America
WADISO	Water Distribution and System Optimization

Symbols

A_0	Initial leak area
A_{0s}	System initial leak area
C_d	Coefficient of discharge
C_{ds}	System coefficient of discharge
C_c	Coefficient of contraction
C_v	Coefficient of velocity
cv	Coefficient of variation
g	Acceleration due to gravity
h	Pressure head
L_N	Leakage number
m	Head-area slope
m_s	System head-area slope
$N1$	Leakage exponent
P_{av}	System average pressure
Q	Discharge flow rate
σ	Standard deviation
μ	Mean

1. Introduction

1.1. Background and context

Leakage in water distribution pipe networks is a problem internationally. It affects service delivery and causes financial losses to water utilities. For more than two decades, there have therefore been research efforts towards better understanding of leakage. One of the efforts is the development of equations for more accurate modelling of leakage flow rates.

From a hydraulic point of view leaks are orifices that should adhere to the orifice equation:

$$Q = C_d A\sqrt{2gh} \quad (1)$$

In the above equation, Q is the orifice flow rate, C_d the discharge coefficient, A the orifice area, g the acceleration due to gravity, and h is the pressure head differential over the leak.

Researchers and practitioners in the field of leakage modelling have, however, realized that leakage does often not adhere to the theoretical orifice equation (1). Instead, it mostly requires higher pressure head exponents (Ogura 1979; Hiki 1981) .

Mechanisms that were thought to be responsible for the pressure head exponent diverging from the theoretical value of 0.5 in equation (1) have been explored. The dominant cause was found to be that leak areas are not fixed but vary with pressure head (May 1994; van Zyl and Clayton 2007; Cassa et al. 2010).

Practitioners therefore proposed a power leakage equation (also known as the $N1$ equation) to model leakage flow rate:

$$Q = Ch^{N1} \quad (2)$$

In the above equation, Q is the leakage flow rate, C the leakage coefficient and $N1$ the leakage exponent. The exponent $N1$, which is empirically calibrated from data sets of leakage flow rates and pressure heads, is sometimes replaced by researchers with the symbol α.

Despite being used widely by both practitioners and researchers, the power leakage equation has been found to be flawed under certain circumstances. In fact, van Zyl et al. (2017) concluded that if the parameters of the power leakage equation are extrapolated beyond its calibration pressure range and at high exponent values, this may result in serious errors in the modelled leakage flow rates.

On the other hand, experimental and modelling studies have revealed that leak areas vary in a linear fashion with pressure heads under both elastic and viscoelastic deformation conditions. This is the case irrespective of the leak type, pipe material and loading states (Cassa and van Zyl 2013; van Zyl and Cassa 2014; Malde 2015; Ssozi et al. 2016). The relationship between leak area and pressure head may thus be described as:

$$\mathrm{A} = \mathrm{A}_0 + \mathrm{mh} \tag{3}$$

Where A_0 is the initial leak area (i.e. the area of the leak opening when the pressure head differential is zero) and m the head-area slope, which defines the potential of the leak to expand under pressure.

Inserting equation (3) into (1) results in the modified orifice equation, known in leakage practice as the FAVAD (Fixed and Variable Area Discharges) equation:

$$\mathrm{Q} = \mathrm{C_d}\sqrt{2\mathrm{g}}(\mathrm{A_0h}^{0.5} + \mathrm{mh}^{1.5}) \tag{4}$$

The FAVAD equation was initially suggested by May (1994) and defines leakage flow rate as comprising of two components, namely leakage through the initial leak area and leakage through the expanding part of the leak area.

The relationship between leak area and the pressure head is thus assumed to be linear. An important aspect of this assumption is that the total leak area of a system with many leaks will also display a linear relationship between leak area and pressure head. In other words, the initial leak area of the whole system will be the sum of all the individual initial leak areas, and the total system head-area slope will be the sum of all the head-area slopes of the individual leaks (Schwaller et al. 2015). This means that equation (4) may be applied equally to a system (or pipe) with either single or multiple leaks.

Although the behaviour of leaks is now well described theoretically, hydraulic simulation software packages currently apply the power equation to model leakage in water pipe networks. From this, it has emerged that there is a lack of knowledge on the implications in modelling leakage in water distribution pipe networks if the linear relationship between pressure head and leak area is explicitly considered.

This study therefore sought to explicitly integrate the linear relationship between pressure head and leak area into the hydraulic modelling of water distribution pipe networks. To do this, the modified orifice equation was integrated into a hydraulic network solver in the widely used Epanet software package (Rossman 2000).

The implications of integrating the linear relationship between the pressure head and the leak area were thereafter investigated for different leakage levels in systems. Differently sized water pipe networks were considered. A stochastic model was used to generate and distribute leaks realistically in the water pipe networks.

Leakage modelling has applications in water distribution pipe networks. Some of these applications include leak detection (i.e. the identification of leak size and location), pipe network optimization (e.g. finding an optimum solution for the installation of pipe network components like valves and meters), to mention a few. This study hypothesised that the explicit integration of the linear relationship between pressure head and leak area into the hydraulic simulation software would improve the results of these applications.

1.2. Goal and objectives

1.2.1. Goal

The goal of this study was to incorporate current best understanding of leakage behaviour into leakage modelling in water distribution networks. For this end, the modified orifice equation which explicitly considers the linear relationship between pressure head and leak area was integrated into the standard hydraulic solver for pipe networks. The possible implications were then investigated.

1.2.2. Objectives

To achieve the above goal, the following objectives were pursued:

1. to gain the latest insights into pressure and leakage modelling and the related concepts as applied to water distribution networks
2. to incorporate the modified orifice equation into the algorithm of the hydraulic network solver of the Epanet software package
3. to develop a stochastic model that generates and distributes leaks realistically in water distribution networks
4. to investigate the impact of the modified orifice equation on leakage modelling behaviour, both for a normal diurnal demand pattern and for cases where the system pressure is significantly reduced to model pressure management conditions
5. to compare the proposed modified orifice leakage model with the conventional power leakage model in terms of leakage flow rates, pressure heads, simulation accuracy and convergence for different network sizes and leakage levels

6. to investigate the impact of the integration of the modified orifice equation into the hydraulic network solver for pipe networks on the applications that use leakage modelling, e.g. pipe network leak detection
7. to develop a methodology that may be used to correct the conventional power leakage equation, so that software packages that apply the power leakage equation may be used to model leakage realistically, without changes to them by incorporating the modified orifice equation. Most researchers and practitioners still use the conventional power leakage equation.

1.3. Contributions to knowledge

This study makes the following contributions to knowledge:

- A modified orifice equation that explicitly considers a linear relationship between the pressure head and the leak area has been incorporated into a standard hydraulic network solver for realistic leakage modelling. Currently, known hydraulic network solvers incorporate the power leakage equation which was found to be flawed under certain circumstances.
- Ranges of leakage flow rate and pressure head errors that may occur when leaks are modelled using the conventional power leakage equation have been shown for both system and individual nodes. For the leakage flow rate errors, cases of normal diurnal demand patterns were considered, but also instances when system pressure is reduced significantly to implement pressure management.
- Simulation and convergence issues associated with the power leakage equation have been identified, especially when the leakage exponent $N1$ is equal or greater than 2.
- A stochastic model that uses the infrastructure leakage index (ILI) to appraise the level of leakage has been developed. It considers the network's physical properties and is aimed to generate and distribute leaks realistically in any water distribution network.
- It has been demonstrated that use of the modified orifice equation improves the performance of applications which use leakage modelling, for example the leak detection methods.
- A methodology has been developed to correct the parameters of the conventional power leakage equation and enable realistic modelling of leakage without a change of the software to the one that uses the modified orifice equation.

1.4. Thesis layout

This thesis consists of 7 chapters, a list of references, a list of published works and 14 appendices. Also included is a CD with source code files of the Epanet software package with the modified orifice equation and the stochastic model for leak generation and distribution.

Chapter 1 presents the background and context of the study. The goals and objectives and the contribution of this study to the knowledge in this field are also presented.

Chapter 2 provides a review of relevant literature. Equations that are used to model leakage and how they relate to the leakage – pressure relationship are reviewed. This is followed by a review of the techniques that are used to manage leakage in water distribution networks. Some benchmarking concepts and internationally used terminology relevant to this study are then presented. The chapter ends with a review of the methods that are used to estimate average pressures in water networks.

Chapter 3 presents the approach and methodology that was used to incorporate the modified orifice equation into the algorithm of the standard hydraulic network solver of Epanet software package.

Chapter 4 explains the procedure that was applied to develop a stochastic model to generate and distribute leaks in a water distribution network.

Chapter 5 discusses the impact of the results obtained when modelling leakage using either the modified orifice or the conventional power leakage equations. Different size networks and leakage levels are considered.

Chapter 6 presents a methodology that was developed to correct the conventional power leakage equation to model leakage realistically without a change of the software to one that

uses the modified orifice equation. The methodology was thereafter tested on an application that identifies the size and location of leaks in a water distribution network.

Chapter 7 discusses the overall findings of the study. General concluding remarks and recommendations for further studies are presented.

2. Literature review

2.1. Introduction

This chapter provides a review of literature relevant to this study. Section 2.2 discusses literature on the modelling of leakage in water distribution networks. Equations that are used to model the pressure and leakage relationship are reviewed.

Section 2.3 reviews literature on the techniques that are used to classify, assess, control and manage leakage in water distribution networks. Internationally used leakage benchmarking concepts are also discussed.

In section 2.4 some guidelines for the estimation of system average pressures are reviewed.

2.2. Leakage modelling in water distribution networks

In hydraulics, a leak is an orifice that should adhere to the orifice equation. The orifice equation is developed from the fundamental hydraulic principle of conservation of energy - the Bernoulli principle.

This section provides a description of the Bernoulli principle, followed by an account of how the orifice equation was developed. The conventional power leakage equation is then described and an explanation given of how it is implemented in one of the standard hydraulic modelling software packages, Epanet.

Following this, the development and application of the modified orifice equation in leakage modelling is described. The section ends with a discussion of the concept that was developed to link the modified orifice and the conventional power leakage equations.

2.2.1. The Bernoulli principle

The Bernoulli principle is the fundamental hydraulic principle of energy conservation that forms the orifice equation which is used to model leaks.

If an incompressible fluid particle is considered, the components of energy per unit weight it possesses are expressed as:

- the potential energy due to its position (z),
- the potential energy due to the pressure ($p/\rho g$), and
- the kinetic energy due to the velocity of flow ($v^2/2g$).

The total energy per unit weight of the particle is obtained through addition of the energy components:

$$H = z + \frac{p}{\rho g} + \frac{v^2}{2g} \tag{5}$$

The above equation is known as the Bernoulli equation in which H is the total energy per unit weight of the fluid particle, z the elevation from the datum, p the pressure, ρ the density, v the velocity with which the fluid particle is moving, and g the acceleration due to gravity.

If the fluid particle moves from one location to another with no or negligible energy losses, the total energy per unit weight does not change (conservation of energy). However, the energy components may vary as in equation (6), where subscripts *1* and *2* refer to the two locations.

$$H = z_1 + \frac{p_1}{\rho g} + \frac{{v_1}^2}{2g} = z_2 + \frac{p_2}{\rho g} + \frac{{v_2}^2}{2g} \tag{6}$$

The orifice equation is derived from a special case of the Bernoulli principle as described in the next subsection.

2.2.2. The orifice equation

Brater et al. (1996) define an orifice as "an opening with closed perimeter and of regular form through which water flows". A stream of water through an orifice is called a jet. When issuing from an orifice, a jet contracts until it reaches the *vena contracta*, which is a point at which the jet has a minimum diameter. This is shown in figure 1.

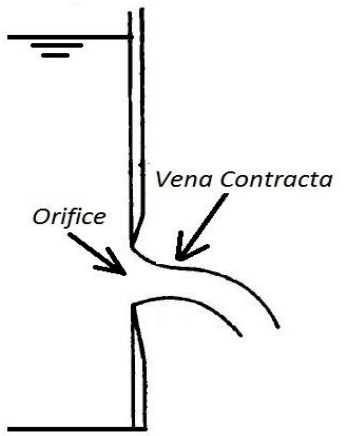

Figure 1: Location of a vena contracta on a jet from an orifice (King 1918).

The cross-section area of the *vena contracta* a_2 is related to the cross-section area of the orifice A as in equation (7), where C_c is the coefficient of contraction.

$$a_2 = C_c A \tag{7}$$

The coefficient of contraction varies mainly with the geometry of the orifice and the pressure head. Smith and Walker (1923), as cited in Brater et al. (1996) carried out experiments and found that coefficients of contraction decreased when the orifice cross-section area increased.

To obtain the discharge flow rate through an orifice, the speed of the fluid must be known in addition to the cross-section area. The speed of a fluid through the cross-section area of the orifice at the *vena contracta* is described using the Torricelli theorem, discovered by an Italian scientist Evangelista Torricelli in 1643 (Wikipedia 2017). The Torricelli theorem states that

"the speed of efflux of a fluid through a hole at the bottom of a tank filled to a depth h is the same as the speed of a body falling freely under gravity from the height h" (Wikipedia 2017). Theoretically, velocity V_t of water passing through an orifice is thus the velocity acquired by a body falling freely in a vacuum through a distance equal to the difference in elevation between the surface of the water and the elevation of the centre of the orifice (equation 8).

$$\mathrm{V_t} = \sqrt{2\mathrm{gh}} \tag{8}$$

The above equation is a specific case of Bernoulli's principle (i.e. equation 6) under the following assumptions:

- the pressure acting on both the surface of water in the container and the jet at the *vena contracta* is atmospheric pressure, and
- the velocity at the surface of the water in the container is negligible.

In equation (8), a coefficient of velocity C_v is introduced to cater for energy losses. The corrected velocity of the jet at the *vena contracta*, after applying the coefficient of velocity, is:

$$\mathrm{V_2} = \mathrm{C_v V_t} = \mathrm{C_v}\sqrt{2\mathrm{gh}} \tag{9}$$

The above equation is the Torricelli equation for velocity of the jet. The discharge of a jet Q is thus a product of its velocity at the *vena contracta* and its corresponding cross-sectional area:

$$\mathrm{Q} = \mathrm{a_2 V_2} = \mathrm{C_c A}\left(\mathrm{C_v}\sqrt{2\mathrm{gh}}\right) \tag{10}$$

The coefficient of contraction C_c multiplied by the coefficient of velocity C_v becomes the coefficient of discharge C_d. The flow rate through an orifice is therefore given by:

$$\mathrm{Q} = \mathrm{C_d A}\sqrt{2\mathrm{gh}} \tag{11}$$

Equation (11) is known as the orifice equation and is used to model leaks.

In practice, the coefficients of contraction and velocity are not necessarily known. It is the coefficient of discharge that is required and can be determined experimentally. Many experiments have found that the coefficient of discharge is not independent but is affected by factors like pressure. Figure 2 shows results of different experiments on an orifice of size 2.5cm (Brater et al. 1996). Although the diameter of the orifice remains the same, the coefficients of discharge found were different. Brater et al. (1996) argue that the differences in values are not wholly due to experimental errors. Other factors like the ratio of the diameter of the orifice to the tank wall dimensions, the sharpness of the orifice edge, the inner surface roughness, the orifice plate and the water temperature may have contributed. The important point evident in figure 2 is that coefficients of discharge decrease initially but then stabilize and become constant for higher pressure values.

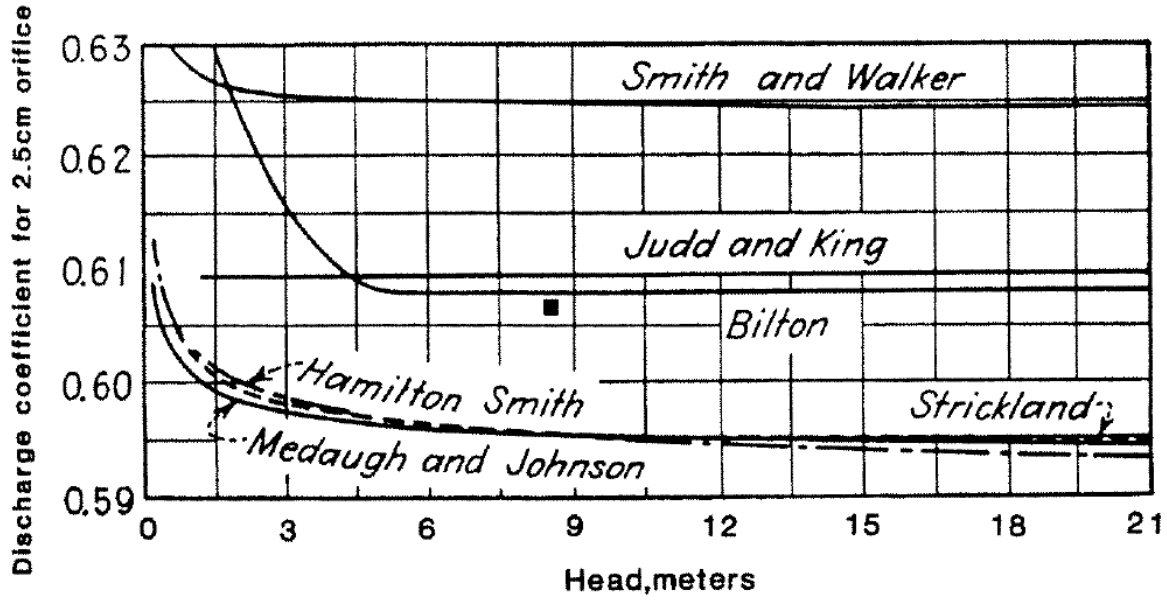

Figure 2: Discharge coefficient variation with pressure (Brater et al. 1996).

Lea (1942), as cited in Brater et al. (1996), plotted experimental values of the coefficients of discharge against Reynolds number (figure 3). The flow regime is laminar for Reynolds numbers less than 12 and fully turbulent when Reynolds number is greater than 10,000. In-between values correspond to the transitional region. The coefficients of discharge varied from

0 to approximately 0.4 in the laminar flow regime. When the flow regime was transitional, the coefficients of discharge ranged from approximately 0.4 to 0.8. For fully turbulent flow regimes, the coefficients of discharge were in the constant range of 0.60 to 0.62. Generally, the coefficients of discharge increased as the Reynolds numbers increased but stabilized at very high Reynolds numbers.

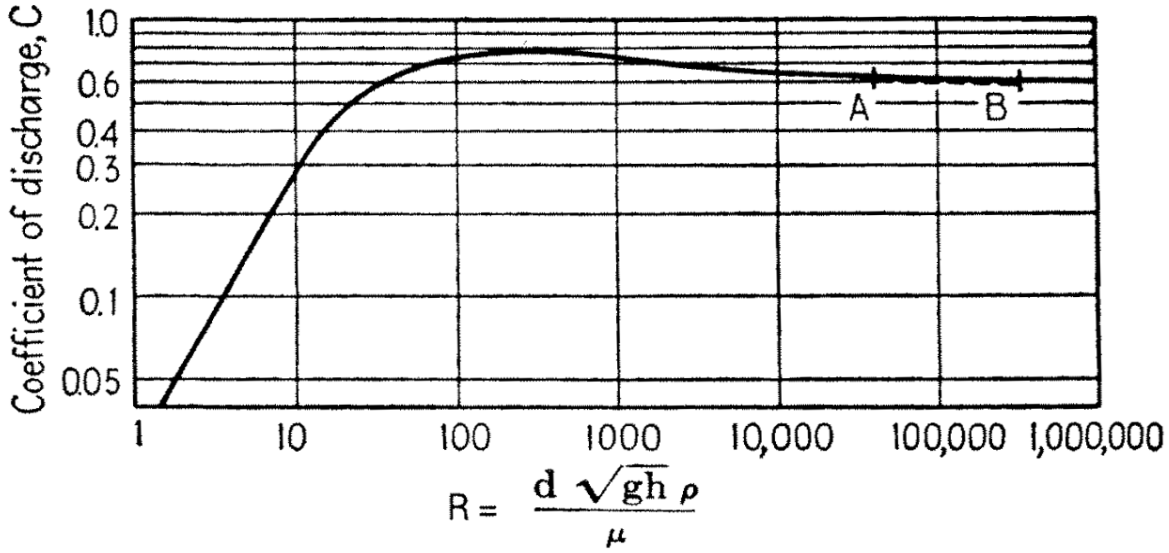

Figure 3: Coefficients of discharge against Reynolds number (Brater et al. 1996).

2.2.3. The conventional power leakage equation

Whereas the orifice equation models leakage flow rate as proportional to the pressure head with an exponent of 0.5, field tests in the UK, Japan and Brazil resulted in the pressure head exponents ranging from 0.36 to 2.95 (Lambert 2014). Laboratory tests that were conducted in different countries for different types of leak areas and materials resulted in a similar range of exponents (May 1994; Greyvenstein and van Zyl 2007; van Zyl and Clayton 2007; Cassa et al. 2010; Ferrante et al. 2011; Massari et al. 2012; van Zyl and Malde 2017). Table 1, adapted from Wu et al. (2011), summarizes the leakage exponent values from the laboratory and field tests carried out in different countries under varying test conditions.

Table 1: Leakage exponent values from laboratory and field tests (Wu et al. 2011)

References	**Test types**	**N1 values**	**Test conditions**
Parry (1881)	Laboratory	0.61 to 1.26	Defective taps
Hikki (1981)	Laboratory	0.36 to 0.70	Drilled holes on 60-180mm metal pipes
Ashcroft and Taylor (1983)	Laboratory	1.39 to 1.72	10 mm slit Class D PE pipes
	Laboratory	1.23 to 1.97	20 mm slit Class D PE pipes
Greyvenstein and van Zyl (2007)	Laboratory	0.50 to 0.52	Round hole
	Laboratory	1.38 to 1.85	Longitudinal PVC
	Laboratory	0.79 to 1.04	Longitudinal AC
	Laboratory	0.41 to 0.53	Circumferential

	Laboratory	0.67 to 2.30	Corrosion steel
Walski et al. (2006, 2009)	Laboratory	0.51 to 0.67	25-50 mm slit on PVC pipes
	Laboratory	0.47 to 0.54	2.7 mm holes on PVC pipes
Ogura (1979)	Field	0.65 to 2.12	Japan field tests (1979)
Farley and Throw (2003)	Field	0.70 to 1.68	UK field test on 17 zones (1977)
	Field	0.52 to 2.79	Brazil field test on 13 zones (1998)
Thornton et al (2008)	Field	0.36 to 2.95	UK field test on 75 zones (2003)
	Field	0.64 to 2.83	Cyprus field test on 15 zones (2005)
	Field	0.73 to 2.42	Brazil field test on 17 zones (2006)
Van Zyl and Malde (2017)	Laboratory	0.499 to 0.501	Round holes of 12mm diameter on uPVC, mPVC, HDPE and steel pipes
	Laboratory	0.500 to 1.041	Longitudinal slits with width of 1mm and lengths between

			50mm to 100mm, on uPVC, mPVC, HDPE and steel pipes
	Laboratory	0.490 to 0.798	Spiral slits with width of 1mm and lengths between 50mm to 105mm, on uPVC, mPVC, HDPE and steel pipes
	Laboratory	-0.262 to 0.499	Circumferential slits with width of 1mm and diameter between 50mm to 100mm, on uPVC, mPVC, HDPE and steel pipes

Possible reasons for the observed range of leakage exponents have been explored. They include: leakage hydraulics, pipe material (van Zyl and Clayton 2007), soil-leak interaction (Walski et al. 2006; van Zyl et al. 2013) and the distribution of leaks in a network (Schwaller and van Zyl 2015).

The dominant cause of the divergence of the leakage exponent was, however, found to be that leak areas are not fixed, but vary with system pressure (May 1994; van Zyl and Clayton 2007; Cassa et al. 2010; Ferrante et al. 2011; Massari et al. 2012; De Marchis et al. 2016; Fox et al. 2016; Fox et al. 2017).

Because the orifice equation cannot explain the above range of leakage exponents, practitioners proposed an empirically derived equation to model leakage flow rate (Gebhardt 1975; Ogura 1979; Hiki 1981; Lambert 2000; Trow and Farley 2003; Al-Ghamdi 2011):

$$Q = Ch^{N1} \tag{12}$$

Equation (12) is known as the conventional power leakage equation (also simply known as the $N1$ equation). The $N1$ and C in the above equation are the leakage exponent and coefficient respectively. The exponent $N1$ is sometimes replaced by the symbol α.

As the exponent $N1$ in equation (12) has a bigger impact on the leakage flow rate than the coefficient C, the $N1$ is used by practitioners to describe the pressure-leakage relationship in water distribution networks.

The exponent $N1$ is estimated from the leakage flow rates and pressure heads that are obtained by reducing system pressure during minimum night flow conditions. Equation (13) is used to estimate the$N1$, where Q_1 and Q_2 are the leakage flow rates before and after the pressure drop, while h_1 and h_2 are the corresponding pressure heads, respectively.

$$\frac{\mathrm{Q_2}}{\mathrm{Q_1}} = \left(\frac{\mathrm{h_2}}{\mathrm{h_1}}\right)^{N1}$$

$$\mathrm{N1} = \frac{\log\left(\frac{\mathrm{Q_2}}{\mathrm{Q_1}}\right)}{\log\left(\frac{\mathrm{h_2}}{\mathrm{h_1}}\right)} \tag{13}$$

With the leakage exponent known, the leakage coefficient is then calculated using either Q_1 and h_1 or Q_2 and h_2 in the equation below:

$$\mathrm{C} = \frac{\mathrm{Q}}{\mathrm{h}^{\mathrm{N1}}} \tag{14}$$

Although the leakage exponent $N1$ is used by practitioners to characterise leakage in water distribution networks and therefore to predict the likely effect of the implementation of pressure management, van Zyl and Cassa (2014) have shown that the conventional power leakage equation is flawed because:

- It is a generalised form of the orifice equation, and this generalisation severs the equation from the fundamental hydraulic principles on which the orifice equation is based.
- It is simply an empirical equation that should be applied to a range of data set for which it has been calibrated. Use of the equation outside this range is likely to result in significant modelling error (van Zyl et al. 2017).
- The leakage exponent approaches infinity under certain conditions (van Zyl et al. 2017).
- It does not explicitly take into consideration the variation of the leak area with pressure.
- Its parameters, i.e. the leakage exponent and coefficient, are not constant for a given system; instead they change with pressure.
- It is dimensionally awkward as the dimensions of the leakage coefficient include those of the variable leakage exponent.

The power leakage equation is popular with practitioners in the field of water distribution pipe networks and is therefore incorporated into most standard hydraulic modelling tools. In the widely used Epanet software it is called an emitter that is used to model pressure-dependent outflows that include leakage. The next subsection describes how the conventional power leakage equation is incorporated into the algorithm of the hydraulic network solver of the Epanet software package.

2.2.4. Implementation of the conventional power leakage equation into standard hydraulic modelling

A set of nodes and links (a graph) characterizes a water distribution network topology. A link corresponds to pipes, valves and pumps, while a node corresponds to a collection of junctions, tanks and reservoirs.

Steady state system equations in the hydraulic network solver are formulated by applying principles of conservation of energy (also known as head loss equations) and conservation of mass (also known as continuity equations) at each link and node respectively. These equations are solved simultaneously to obtain pressure heads at the junctions and flow rates in the links (Rossman 1996; Rossman 2000).

The standard model for pressure-dependent outflows used for leakage flow rate is an emitter function which is modelled as a fictional pipe connected to a fictional reservoir. The same energy and mass conservation principles are applied to the fictional pipes and reservoirs (Rossman 1996; Rossman 2004).

Figure 4 presents a summarised layout of the hydraulic network solver of Epanet with the conventional power leakage equation. The paragraphs that follow explain how the steady state system equations in the hydraulic network solver are solved.

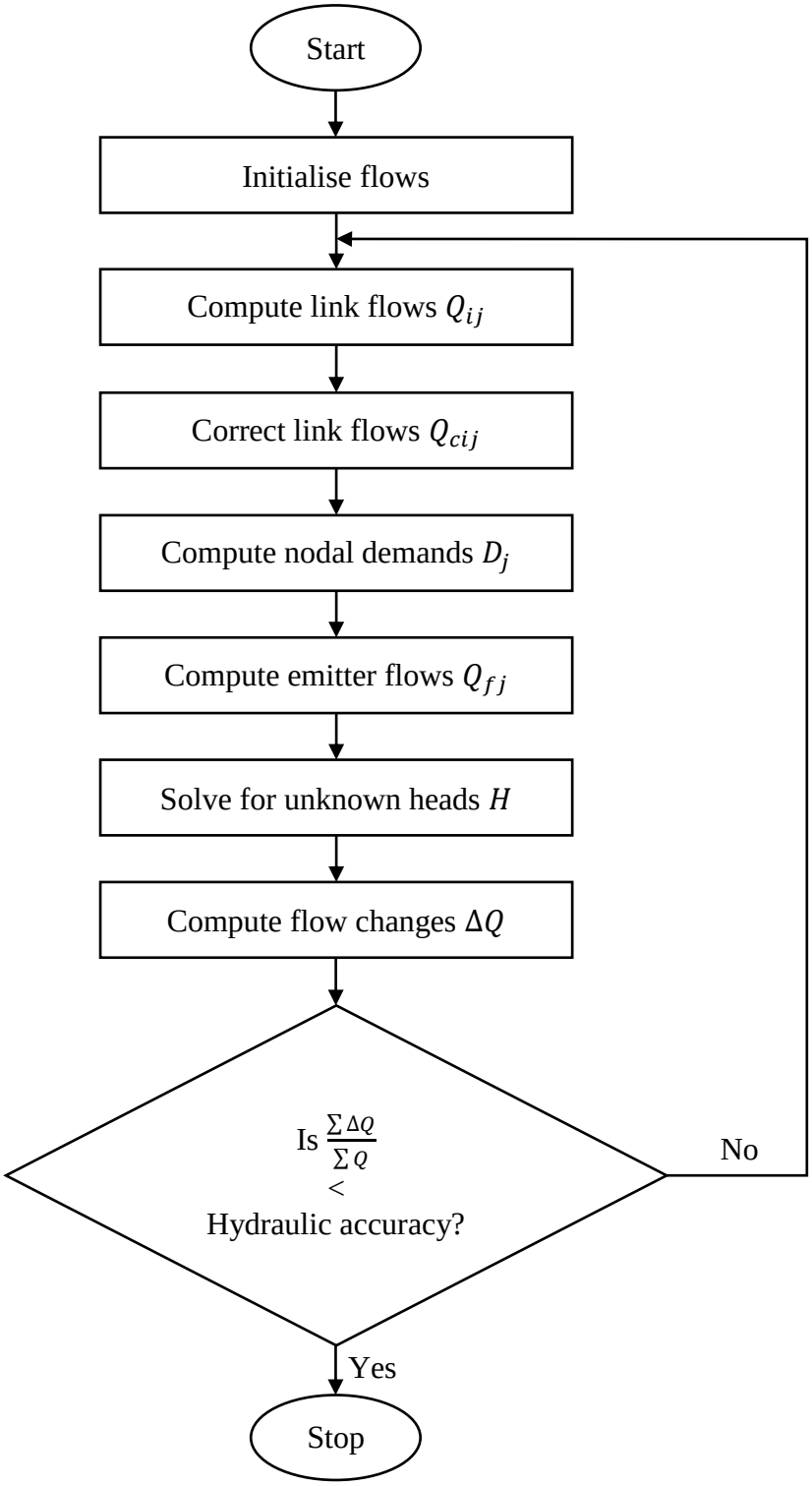

Figure 4: Process layout of the hydraulic network solver of Epanet with the conventional power equation (Rossman 1996)

The process starts with an initial estimate of flows in the links for the first iteration that may not necessarily satisfy flow continuity. For the pipes, a flow with a velocity of $1\,ft/sec$ is chosen, while for pumps the flow is equal to the design flow indicated for a specific pump (Rossman 2000).

Head loss equation

The flow-head loss relationship in a pipe between nodes i and j is given as:

$$\mathrm{h_{ij}} = \mathrm{H_i} - \mathrm{H_j} = \mathrm{rQ_{ij}^n} + \mathrm{kQ_{ij}^2} \tag{15}$$

In the above equation, H is the nodal head, Q_{ij} is the flow rate through the pipe, h is the head loss along the pipe, r is the resistance coefficient, n is the head loss exponent, and k is the minor loss coefficient.

Because of the non-linear nature of the equation, the flow rate in a pipe is corrected using the Newton–Raphson method through an iterative scheme, by first writing equation (15) in the form of $f(Q) = 0$.

$$\mathrm{f(Q)} = \mathrm{rQ_{ij}^n} + \mathrm{kQ_{ij}^2} - \left(\mathrm{H_i} - \mathrm{H_j}\right) \tag{16}$$

$$\mathrm{f'(Q)} = \mathrm{nrQ_{ij}^{n-1}} + \mathrm{2kQ_{ij}} \tag{17}$$

If equation (16) is not satisfied, the corrected flow rate Q_c is calculated using the formula:

$$\mathrm{Q_{cij}} = \mathrm{Q_{ij}} - \frac{\mathrm{f\left(Q_{ij}\right)}}{\mathrm{f'\left(Q_{ij}\right)}} \tag{18}$$

In equation (18), if the function of flow rate and its derivatives are substituted, then the corrected flow rate will be:

$$Q_{cij} = Q_{ij} - y_{ij} + p_{ij}H_i - p_{ij}H_j \tag{19}$$

$$\text{with} \quad p_{ij} = \frac{1}{nrQ_{ij}^{n-1} + 2kQ_{ij}} \quad \text{and} \quad y_{ij} = p_{ij}\left(rQ_{ij}^{n} + kQ_{ij}^{2}\right) = p_{ij}h_{ij}$$

The term p_{ij} is an inverse of the derivative of the head loss equation for the link between nodes *i* and *j*, while y_{ij} is a flow correction factor.

Continuity equation

The second set of equations that must be satisfied are the continuity equations. At any non-storage node in a water distribution network, the net inflow to the node should be equal to zero. User demands are combined at network junctions which consist of both the fixed and pressure-dependent outflows, for example leakage. If there are *N* non-storage nodes in the network, then *N* continuity equations are set up as:

$$\sum_{i=1}^{l} Q_{ij} - D_j = 0 \tag{20}$$

For $j = 1, 2, 3 \ \ldots \ N$

In this equation, l is the number of links connected to the node, Q_{ij} is the flow rate towards node j in the link connecting nodes i and j, and D_j is a known external demand at node j.

Substituting equation (19) into (20) results in:

$$\sum_{i=1}^{l} (Q_{ij} - y_{ij} + p_{ij}H_i - p_{ij}H_j) - D_j = 0 \tag{21}$$

This equation can be simplified and unknowns separated as:

$$\left[\sum_{i=1}^{l} p_{ij}\right] H_j - \left[\sum_{i=1}^{l} p_{ij}\right] H_i = \sum_{i=1}^{l} Q_{ij} - D_j - \sum_{i=1}^{l} y_{ij} \quad (22)$$

Fixed head node

A fixed head node in water distribution network is either a reservoir or tank. In case the node under consideration is connected to a fixed head node *f*, equation (22) becomes:

$$\left[\sum_{i=1}^{l} p_{ij}\right] H_j - \left[\sum_{i=1;i\neq f}^{l} p_{ij}\right] H_i = \sum_{i=1}^{l} Q_{ij} + Q_{fj} - D_j - \sum_{i=1}^{l} y_{ij} - y_{fj} + p_{fj} H_f \quad (23)$$

Emitter function

The standard model for pressure-dependent outflows used for leakage flow rate is a power function:

$$\mu_i = c_i (H_i - z_i)^{\alpha}, \text{if } H_i \geq z_i \quad (24)$$

In this equation, μ_i is the lumped nodal leakage flow rate, c_i is the leakage coefficient, z_i is the elevation of node i and α is the leakage exponent.

Equation (15), when rewritten for a fictional pipe without the minor loss component, becomes:

$$h = r Q_{fj}^{n} \quad (25)$$

In this equation, h is the headloss along the fictional pipe, r is the resistance coefficient along the fictional pipe, Q_{fj} is the flow rate through the fictional pipe and n is the head loss exponent.

Rearranging equation (25) to make flow rate the subject of the formula becomes:

$$Q_{fj} = \left[\frac{1}{r}\right]^{\frac{1}{n}} [h]^{\frac{1}{n}} \tag{26}$$

By equating equation (24) to (26), the head loss exponent n and corresponding resistance coefficient r are given by:

$$n = \frac{1}{\propto} \tag{27}$$

$$r = \frac{1}{c_i^{\frac{1}{\propto}}} = c_i^{-\frac{1}{\propto}} \tag{28}$$

The terms for the emitter function are then added to equation (22) as follows:

$$\left[p_{fj} + \sum_{i=1}^{l} p_{ij}\right] H_j - \left[\sum_{i=1}^{l} p_{ij}\right] H_i = \sum_{i=1}^{l} Q_{ij} + Q_{fj} - D_j - \sum_{i=1}^{l} y_{ij} - y_{fj} + p_{fj} Z_j \tag{29}$$

where

$$p_{fj} = \propto \left(c_i^{\frac{1}{\propto}}\right)\left(Q_{fj}^{1-\frac{1}{\propto}}\right) \qquad \text{and} \qquad y_{fj} = p_{fj}\left(c_i^{-\frac{1}{\propto}}\right)\left(Q_{fj}^{\frac{1}{\propto}}\right) = \propto Q_{fj}$$

The elevation of the fictional reservoir is the same as the elevation of the node with the emitter.

For a set of known heads at the fixed head nodes, a solution is sought for all unknown nodal heads and pipe flows that satisfy equations (15) and (20).

The calculations are repeated and at each iteration the unknown nodal heads are found by solving equation (29) in a matrix form:

$$\mathbf{AH} = \mathbf{F} \tag{30}$$

For a network with N unknown heads:

A = an (N × N) matrix of gradient coefficients,

H = an (N × 1) vector of unknown nodal heads,

F = an (N × 1) vector of right-hand side terms.

Each row i (or column j) in the matrix (**A**) corresponds to a node with unknown head. The diagonal elements of the matrix (**A**) are obtained by summing up the inverse of the first derivative of the head loss in all the links connecting the node under consideration to other nodes ($i.e.\ A_{ii} = \sum_{i=1}^{l} p_{ij}$). The non-zero (off-diagonal) terms are obtained by taking the negative value of the inverse of first derivative of head loss in the link connecting nodes i to j ($i.e.\ A_{ij} = A_{ji} = -p_{ij}$). The matrix **A** is both symmetric and sparse (i.e. most of the elements are zero). Each right-hand side term (**F**) consists of the net flow imbalance at the node and the flow correction factor from equation (29).

While the elements of the coefficient matrix **A** and those of the right-hand side terms (**F**) are deduced from the head loss and continuity equations, the elements of the nodal heads (**H**) are unknown. Determining these is the purpose for computation of the matrix equation (30).

After new nodal heads are computed by solving equation (30), new flows are found from equation (19). In case the total change in flow ($\sum \Delta Q$) relative to the total flow in the systems ($\sum Q$), is larger than a hydraulic accuracy (HACC) value (for example 0.001), the process is then repeated until convergence is achieved.

2.2.5. The modified orifice equation

Based on measurements in a water distribution network, May (1994) suggested that the total leakage flow rate has two terms, i.e. one that is related to leaks with a constant area (N1= 0.5), and another one that is related to joints and leaks that expand with pressure (N1= 1.5), see equation (31) below. In his analysis, May (1994) assumed a linear relationship between the pressure and the leak area because pipe stresses and resultant strains are a linear function of pressure.

$$\mathrm{Q_l} = \mathrm{A_0 C_d}\sqrt{2\mathrm{g}}(\mathrm{h}^{0.5}) + \mathrm{SC_d}\sqrt{2\mathrm{g}}(\mathrm{h}^{1.5}) \quad (31)$$

In the above equation, Q_l is the leakage flow rate (m^3/s), A_0 is the area of the fixed leakage paths (m^2), C_d is the dimensionless discharge coefficient, g the acceleration due to gravity, h the AZNP of the system, and S is the system expansion coefficient.

Cassa et al. (2010) and van Zyl and Cassa (2014) using finite element analysis, investigated the behaviour of longitudinal, spiral and circumferential cracks on pressurized pipes with different pipe materials, i.e. uPVC, steel, cast iron and asbestos cement. Linear elastic behaviour was assumed. It was found that the areas of all leak openings A increased linearly with pressure head h, irrespective of the type of leak opening or material (figure 5).

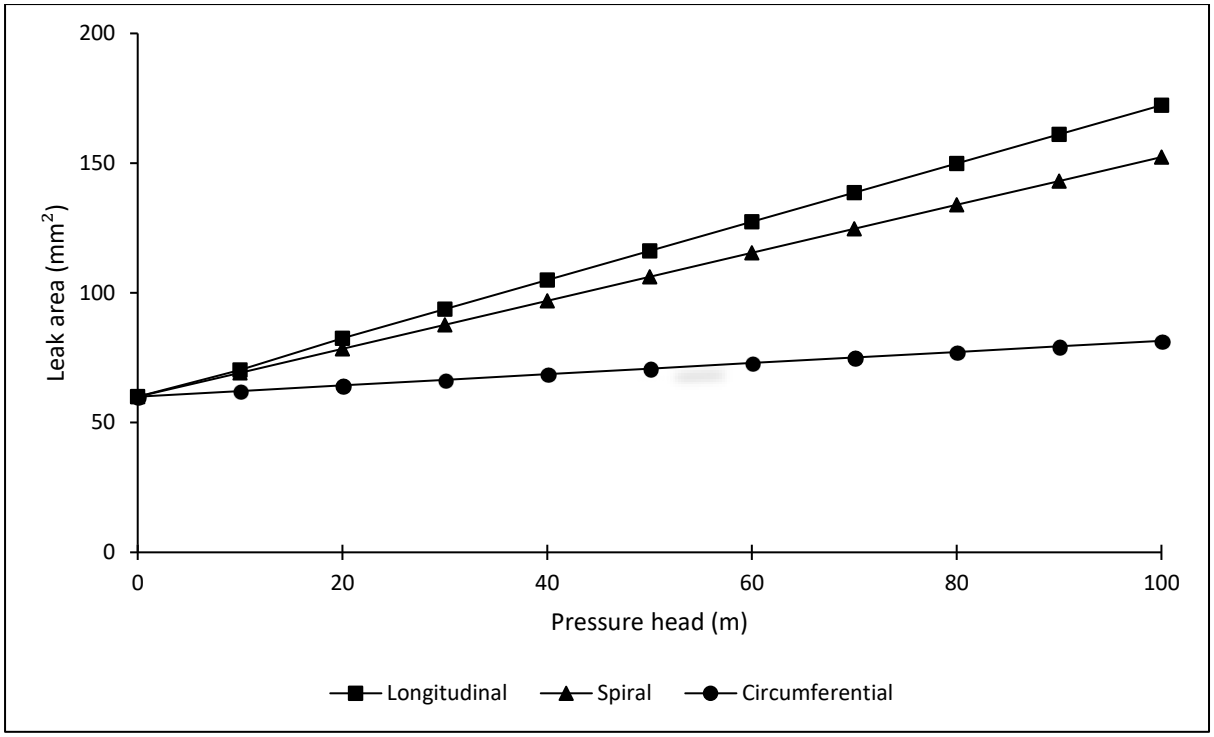

Figure 5: Relationship between leak area and pressure head (Van Zyl and Cassa 2014)

The relationship between leak area and pressure head in the above figure can be expressed as:

$$A = A_0 + mh \tag{32}$$

This shows that the leak response to pressure of any type of leak can be characterized by its initial area A_0 and head-area slope m. The parameter m depends on the material of the pipe, and the shape and geometry of the leak orifice. Experimental studies by Ferrante (2012), Ferrante et al. (2013a), Ferrante et al. (2013b) and Malde (2015), as well as a finite element study under viscoelastic conditions by Ssozi et al. (2016) also confirmed the linear relationship between the leak area and the pressure head.

The variations in leak areas where plastic deformation and fractures occur cannot be assumed to be linear. Van Zyl et al. (2017) argue that these mechanisms are unlikely to dominate the pressure-leakage response of distribution pipe networks because they are a) irreversible and b) only occur when pressures are increased and not when they are decreased. This study therefore assumed that all leaks vary linearly with pressure head.

Cassa et al. (2010) then substituted the leak area and pressure-head relationship (32) into the orifice equation (11) to get:

$$Q = C_d\sqrt{2g}(A_0 h^{0.5} + m h^{1.5}) \quad (33)$$

The above equation is the modified orifice equation known in practice as the Fixed Area Variable Areas Discharges (FAVAD) equation.

Whereas May (1994) maintained that some leak areas in a system varied with pressure while others were constant, Cassa et al. (2010) argued that all leak areas vary with pressure. It is the rate of variation that differs as defined by the head-area slope m. For example, in figure 5 for the same initial crack area of 60 mm^2, the head-area slope of the circumferential leak opening is smaller than that of the longitudinal and spiral leak openings. This means that the circumferential crack has a lower rate of expansion than the spiral and longitudinal openings.

Through a finite element analysis, Cassa and van Zyl (2011) investigated parameters that influence the head-area slope m for a leak area in a pipe. Longitudinal, spiral and circumferential cracks were considered. It was found that the crack length has the dominant effect on the head-area slope, followed by the wall thickness for all three types of cracks.

System leakage modelling using the modified orifice equation

Schwaller et al. (2015) explored the application of the modified orifice equation to several leaks in a system. Three hundred water distribution network models were developed using Microsoft Excel spreadsheets. Of the 300 network models, 100 had 100 randomly distributed leaks, another 100 had 1000 leaks, and the remaining 100 had 10000 leaks.

Leakage flow rates and average zone night pressures before and after the reduction of system pressure head were used to estimate the modified orifice parameters (i.e. m_s and A_{0s}) for a water distribution system. The same is done in practice to estimate the system leakage exponent $N1$. To do this the modified orifice equation was first written in this form:

$$\mathrm{Q} = \mathrm{C_{ds}}\sqrt{2\mathrm{g}}(\mathrm{A_{0s}h^{0.5}} + \mathrm{m_s h^{1.5}}) \tag{34}$$

Where C_{ds} is the system discharge coefficient, A_{0s} the system initial leak area, and m_s the system head-area slope. The system discharge coefficient was assumed to be 0.65, which then allowed the system's initial leak area A_{0s} and head-area slope m_s to be estimated from:

$$\mathrm{A_{0S}} = \frac{\mathrm{Q_1}}{\mathrm{C_{dS}}\sqrt{2\mathrm{gh_1}}} - \mathrm{m_S h_1} \tag{35}$$

$$\mathrm{m_S} = \frac{\mathrm{h_2^{0,5}Q_1} - \mathrm{h_1^{0,5}Q_2}}{\mathrm{C_{dS}}\sqrt{2\mathrm{g}}\left(\mathrm{h_1}^{1.5}\mathrm{h_2^{0,5}} - \mathrm{h_2}^{1.5}\mathrm{h_1^{0,5}}\right)} \tag{36}$$

In the above equations Q_1 and Q_2 are the leakage flow rates before and after the pressure drop while h_1 and h_2 are the corresponding system average zone night pressures. This is the same data set that is required to calculate the power leakage equation's exponent and coefficient using equations 13 and 14 respectively.

The estimated modified orifice parameters were found to provide a good correlation with the sum of the individual leakage parameters as follows:

- The system's initial leak area A_{0s} was found to be approximately equal to the sum of the individual initial leak areas as shown in figure 6.
- The system head-area slope m_s was found to be approximately equal to the sum of the individual head-area slopes as shown in figure 7.

The results demonstrated that pressure management data (i.e. Q_1 and h_1 plus Q_2 and h_2) can be used in the modified orifice equation to provide useful insights on the physical properties of the leaks in the system. The system's initial leak area provides a meaningful measure of the physical integrity of the system. Also, since Cassa and van Zyl (2013) demonstrated that the head-area slope of a leak can be linked to the properties of the pipe (diameter, material and wall thickness) and leak (type and size), the system head-area slope provides an understanding into the type of leaks present.

The practical application of the modified orifice equation to systems was thus found to be feasible since no additional data are required beyond the ones currently used to estimate the system leakage exponent $N1$ in the power leakage equation. The benefit of the modified orifice equation is that the system's initial leak area and the head-area slope provide physically meaningful properties which are independent of system pressure.

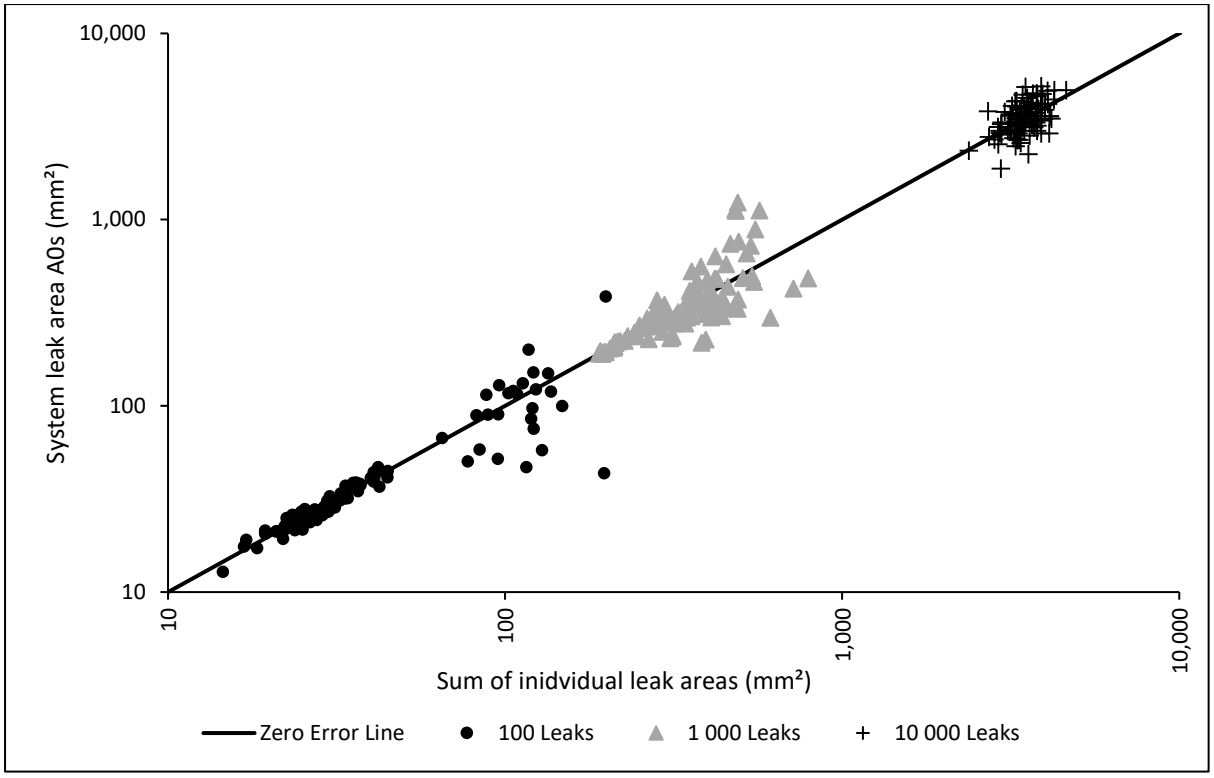

Figure 6: Comparison of system initial leak area and the sum of individual leak areas – logarithmic scale (Schwaller et al. 2015)

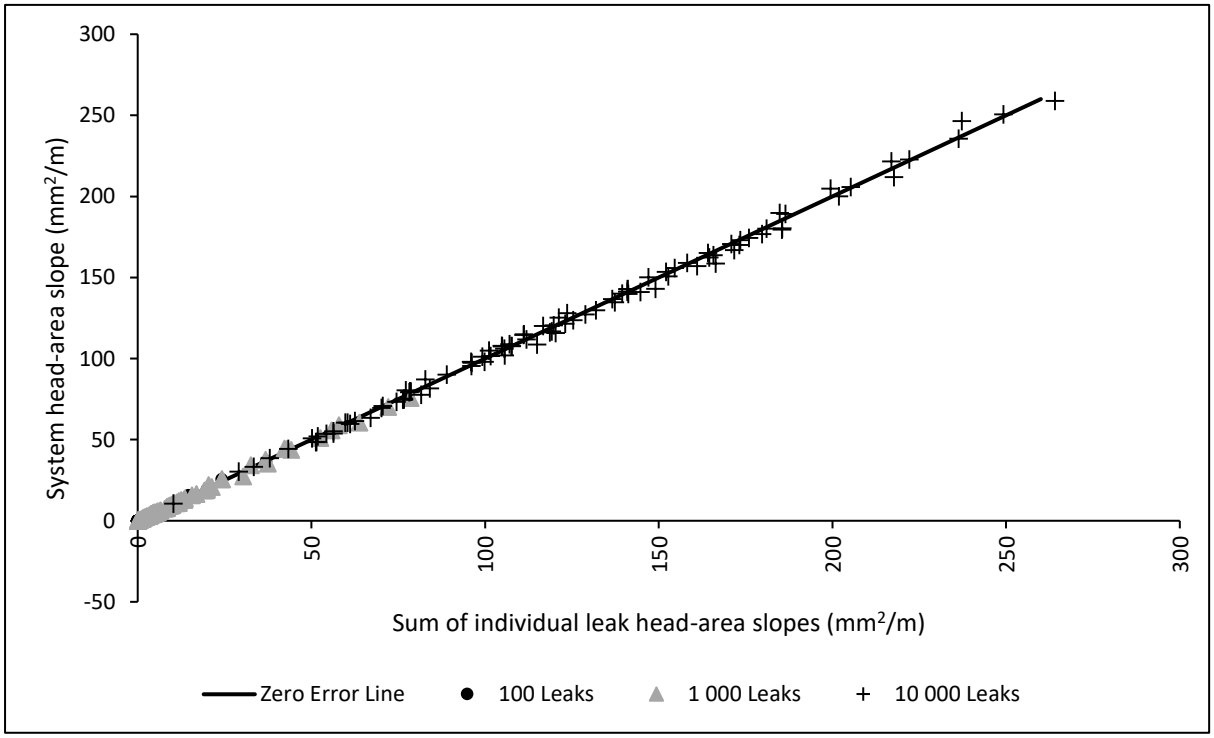

Figure 7: Comparison of system head-area slope and the sum of individual head-area slopes (Schwaller et al. 2015).

2.2.6. Link between the modified orifice equation and power equation

Through analytical exploration, van Zyl and Cassa (2014) found a relationship between the modified orifice equation and the power equation. Equation (12) was equated to equation (33) and both sides were divided by equation (11):

$$C'h^{N1-0.5} = 1 + L_N \tag{37}$$

where $C' = \frac{C}{C_d A_0 \sqrt{2g}}$ and $L_N = \frac{mh}{A_0}$

The term L_N is a dimensionless number known as the leakage number. It is the ratio of the variable to the fixed portions of the leakage as defined by the modified orifice equation (33).

Further analytical exploration of equation (37) resulted in:

$$L_N = \frac{N1 - 0.5}{1.5 - N1}$$
$$N1 = \frac{1.5L_N + 0.5}{L_N + 1} \tag{38}$$

Van Zyl et al (2017) provided a mathematical proof of the same relationship. Equation (38) describes a hyperbolic function with asymptotes $L_N = -1$ and $N1 = 1.5$ as shown graphically in figure 8.

Equation (38) shows that when the leakage exponent is equal to one, the leakage number is also equal to one. Van Zyl and Cassa (2014) also showed that in practice the leakage exponent is 1.5 when the leakage number is 100, and 0.5 when the leakage number is less than 0.01 but greater than 0.

The relationship between the leakage number and the leakage exponent is significant in the following way: when leakage is modelled using the power equation, the variation of the leakage exponent due to the pressure may be estimated by converting the leakage exponent to a leakage number, using equation (38). Then the leakage number for the new pressure is proportionally adjusted using equation (37) since m and A_0 are known. Finally, the adjusted leakage number is converted back to a leakage exponent, again using equation (38).

The relationship between the leakage number L_N and the leakage exponent $N1$ is shown in figure 8 and was found valid for both individual (van Zyl and Cassa 2014) and system leaks (Schwaller et al. 2015).

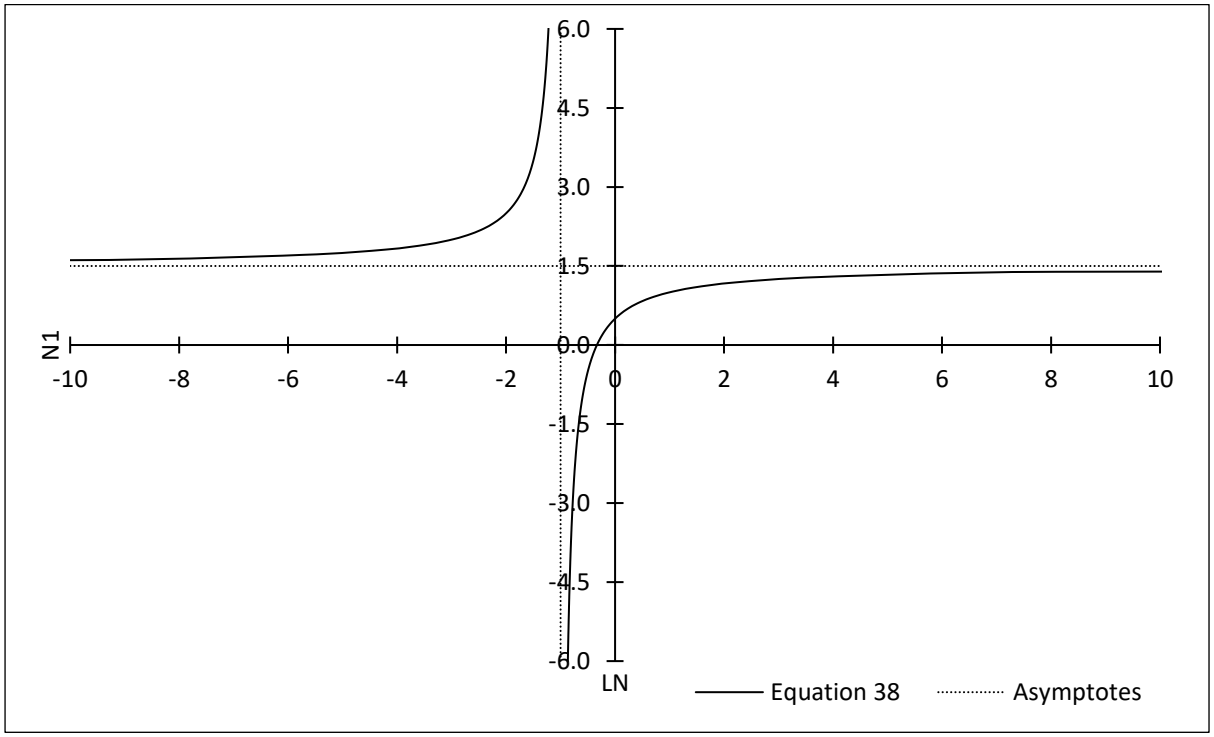

Figure 8: Relationship between leakage number L_N and leakage exponent $N1$.

2.3. Leakage management and benchmarking concepts

Leakage in water distribution networks does not only affect service delivery or cause financial loss to water utilities, but it also contributes to the depletion of a scarce resource – water (European Commision 2015). McKenzie et al. (2012) report non-revenue water in South Africa in 2010 to be 36.8%, of which 25.4% is through physical leakage. Similar figures are reported in many parts of the world (Kingdom et al. 2006; Mutikanga et al. 2009).

It is crucial to understand prevailing scenarios in order to manage leakage effectively. Over the past two decades, concepts were developed to do reconnaissance of leakage in water distribution pipe networks. This section presents some of these concepts and introduces internationally accepted water loss terminology that is relevant to this study.

2.3.1.The water balance

Establishing a water balance for a network is one of the approaches used by water utilities to account for every drop put into a water distribution network. The International Water Association (IWA) has produced a standard approach for calculating water balance (Lambert and Hirner 2000; Alegre et al. 2000 as cited in Lambert 2002; Lambert 2014). Table 2 shows the International Water Association's water balance chart (as first published), detailing the Water Loss Task Force and the Performance Indicators Task Force.

Table 2: The International Water Association' s water balance (Lambert 2014)

<table>
<tr><td rowspan="7">System Input Volume</td><td rowspan="3">Authorised Consumption</td><td rowspan="2">Billed Authorised Consumption</td><td>Billed Metered Consumption (including water exported)</td><td rowspan="2">Revenue Water (RW)</td></tr>
<tr><td>Billed Unmetered Consumption</td></tr>
<tr><td rowspan="2">Unbilled Authorised Consumption</td><td>Unbilled Metered Consumption</td><td rowspan="5">Non – Revenue Water (NRW)</td></tr>
<tr><td>Unbilled Unmetered Consumption</td></tr>
<tr><td rowspan="4">Water Losses</td><td rowspan="2">Apparent Losses</td><td>Unauthorized Consumption</td></tr>
<tr><td>Metering Inaccuracies</td></tr>
<tr><td rowspan="3">Real Losses</td><td>Leakage on Transmission and/or Distribution Mains</td></tr>
<tr><td>Leakage and Overflows at Utilities Storage Tanks</td></tr>
<tr><td>Leakage on Service Connections up to the measurement point</td></tr>
</table>

Definitions of the International Water Association’s water balance terminology (Lambert 2014):

- **System Input Volume**: This is the volume of water input into a transmission or a distribution network.
- **Authorised Consumption**: The volume of metered and/or unmetered water taken by registered customers, the water supplier and others who are implicitly or explicitly authorized to do so by the water supplier, for domestic, commercial and industrial purposes. Authorised consumption includes water that is exported.

- **Water Loss**: The water losses of a system are calculated as the difference between System Input Volume and Authorised Consumption. The water losses consist of real and apparent losses.
- **Real losses**: Also, known as leakages, these are the physical losses from a pressurised system, up to the point of consumer metering. The volume of water lost through all types of leaks, bursts and overflows depends on frequencies, flow rates and average duration of individual leaks.
- **Apparent losses**: These consist of unauthorized consumption (theft or illegal use) and all types of inaccuracies associated with bulk metering and customer metering.
- **Non-Revenue Water**: This is the difference between the System Input Volume and Billed Authorized Consumption.

It should be noted that different water utilities, technical organizations and international funding agencies in different parts of the world have applied the IWA water balance chart with minor modifications. For example, in some parts of the ASEAN region, the terms *commercial* instead of *apparent* and *physical* instead of *real* are used (Lambert 2014).

When the volumetric quantity of leakage is known to the water utility, it may then be necessary to understand the type of leaks based on their classifications. The next subsection reviews how leaks in water distribution networks are classified.

2.3.2. Classification of leaks in water distribution networks

Leaks in water distribution networks may be classified as either potentially detectable (PD) or background (BG) leaks. While the potentially detectable leaks (which include bursts) sometimes show up on the ground, or are detected using conventional methods like the acoustic, the background leaks cannot be detected visually or acoustically. In a reticulation

network, the background leaks are very small and mostly found at pipe joints and service connections.

Some studies consider the boundary between the potentially detectable and background leakage flow rate to be 250 litres/hr (Hamilton and Krywyj 2012; McKenzie 2014) . This means that leaks whose flow rate is above 250 litres/hr are generally considered to be potentially detectable, while those whose flow rate is below 250 litres/hr are undetectable (background leaks).

This boundary was initially selected because it was the typical level at which leaks could be detected using conventional leakage detection equipment. With more modern equipment available today, the actual level at which a leak is considered detectable or undetectable can be argued.

Potentially detectable leaks are further classified as reported or unreported (Lambert et al. 1999; Lambert and Hirner 2000; Alegre et al. 2006). The reported potentially detectable leaks normally have high flow rates and often appear at the surface, depending on the water pressure. On the other hand, the unreported leaks are not visible on the surface and this is often due to surrounding conditions such as a leak occurring in a flooded area or a swamp. Unreported potentially detectable leaks can only be found through active leakage control or by analysing water consumption. The reported potentially detectable leaks normally have a shorter runtime than the unreported leaks because when they are reported, they are more likely to be repaired.

Potentially detectable leaks are further classified based on their locations, i.e. either on mains or service pipes. Lambert (2009) states that potentially detectable leaks on main pipes have less runtime than those on service pipes because they are more likely to be found and repaired.

All water distribution networks, old or new, experience leakage. It is the level of leakage that differs from one network to another. New networks normally have less leakage than old ones. The next subsection discusses some of the methods that may be used to assess leakage in a water distribution network for effective control.

2.3.3. Leakage assessment

Leakage assessment basically refers to the use of tools and methods to quantify the volume of leakage in a water distribution network. These methods include:

- annual water balance
- night flow analysis
- component analysis.

2.3.3.1. Annual water balance

In this method, which is also referred to as the *top-down* approach, the water balance (table 2) is used to estimate real losses. The real loss is the volume that remains after the authorized consumption and apparent losses have been deducted from the system input volume. This analysis does not distinguish real losses due to either background or potentially detectable leaks or bursts, and it should therefore be used in combination with other methods.

2.3.3.2. Night flow analysis

This method is also referred to as the *bottom-up* approach. It is used to assess real losses based on night flows, preferably in small zones of a water distribution network called district metered areas (DMAs). Lambert (2013) defines a district metered area as “an area defined by the closure of valves or other physical constraints where distribution losses and pressures are managed”. A district metered area should preferably be supplied with water through a single metered supply point so that if required the inlet pressure can be controlled. The flows are measured

during the minimum night flow (MNF) period which is normally between 2:00 and 5:00 in the morning, although the exact time varies from between zones depending on their characteristics. It is considered that during the minimum night flow period, a significant portion of the measured flow is likely to be leakage since consumption is lowest and pressure values are relatively high. The estimate of the real loss component at minimum night flow is obtained after the subtraction of the legitimate night consumption (assessed and measured for the customers in the zone) from the measured flow rate into the zone. The night leakage information is converted into daily leakage using a night day factor (NDF) (Lambert 2017).

2.3.3.3. Component analysis

Component analysis is also known as the Burst and Background Estimate (BABE). Annual real losses can also be estimated through an analysis of components. This approach uses the number of service connections, average flow rates and average runtimes of different types of leaks and bursts (background, reported and unreported), on different parts of distribution infrastructures (mains and service pipes). A component analysis model breaks down the overall volume of real losses into its constituent components, i.e. background leaks as well as reported and unreported potentially detectable leaks.

Unavoidable annual real losses (UARLs)

Unavoidable annual real losses (in L/day) represent the theoretical low limit of leakage flow rate that could be achieved in a specific network at a given operating pressure (Lambert 2009; AWWA 2016). The unavoidable annual real losses are estimated using the formula:

$$\mathrm{UARL} = (18\mathrm{L_m} + 0.8\mathrm{N_c} + 25\mathrm{L_s})\mathrm{P_{av}} \quad (39)$$

Where L_m is the length of mains (in km), N_c the number of service connections, L_s the length of service lines between the property boundary and the water meter (in km), and P_{av} the average

zonal pressure head (in m). The length of service lines L_s is only included in equation (39) when consumer meters are installed within the property boundary, otherwise it is set to zero.

Technically the unavoidable annual real losses (UARL) consist of the unavoidable background leakage (UBL) plus physical water losses from potentially detectable leaks and bursts (reported and unreported). Table 3 presents the components of unavoidable annual real losses in metric units calculated at the 50m pressure head (Lambert 2009).

Table 3: Components of the UARL at pressure of 50m (Lambert 2009)

Infrastructure Component	**Unavoidable Background Leakage (UBL)**	**Reported PD Leaks**	**Unreported PD Leaks**	**Unavoidable Annual Real Losses (UARL)**	
Mains	480 L/km/day	290 L/km/day	130 L/km/day	900 L/km/day	18 L/km/day/ m of pressure
Service connections (main to curb-stop)	30 L/conn/day	2 L/conn/day	8 L/conn/day	40 L/conn/day	0.80 L/conn/day/ m of pressure
Service connections (curb-stop to meter)	800 L/km/day	95 L/km/day	355 L/km/day	1250 L/km/day	25 L/km/day/ m of pressure

Unavoidable background leakage (UBL)

The unavoidable background leakage (in L/h) can be estimated using either the data in table 3 or an empirically derived equation (40), if the number of consumer connections and length of pipes for a give system are known (Lambert 2009).

$$\mathrm{UBL} = 20\mathrm{L_m} + 1.25\mathrm{N_c}) * (\mathrm{AZNP}/50)^{1.5} \quad (40)$$

In the above equation, L_m is the length of mains (in km), N_c the number of service connections (main to property line), and AZNP the average zonal night pressure (in metres).

Both the UARL and UBL will vary with the pressure head and therefore the empirically derived parameters used for the calculation of the two concepts were initially specified at a standard pressure of 50 metres.

The Infrastructure Leakage Index (ILI)

The level of leakage in a district metered area is assessed using the Infrastructure Leakage Index (ILI) concept, which is defined as the ratio of the current annual real losses (CARL) to the unavoidable annual real losses (UARL):

$$\mathrm{ILI} = \frac{\mathrm{CARL}}{\mathrm{UARL}} \quad (41)$$

Whereas the unavoidable annual real losses (UARL) are estimated using equation (39), the current annual real losses (CARL) are normally estimated through the night flow analysis.

The infrastructure leakage index remains a widely-applied concept to assess the level of leakage across countries using different units as it is a dimensionless number. When leakage in a water distribution network has been assessed and the level of leakage is known, there is a need to identify the location of the leaks for repair. The next subsection provides an overview of the methods that may be used to detect leaks in a water network.

2.3.4. Leak detection

Leak detection is the application of techniques to narrow down the position of a leak to a section of a pipe network. Leakages in a water network can be reduced by increasing the efficiency of leak detection to shorten the time required for awareness, location and repair.

Below are some of the methods used to detect leaks in water distribution networks. These methods can be applied individually or in combination for affirmative results:

- **Passive observation and surveillance:** The water utility uses patrol vehicles or staff who walk the whole length of the pipelines looking for visible leaks, though these could possibly be hidden by vegetation. This is a simple but slow method to apply and not effective on its own (Mutikanga et al. 2009).
- **Acoustic methods:** These are methods that rely on sound and vibration signals induced by leaks impacting the soil from pipelines under pressure. Acoustic devices include listening rods, stethoscopes, ground microphones, noise loggers and leak noise correlators (Mutikanga 2012).
- **Hydraulic leak detection methods:** Hydraulic characteristics like flow and pressure are used to detect, locate and quantify leaks in pressurised pipelines. These methods are based on the principle that the presence of a leak in a pipeline will induce a reaction on the pressure. The methods may be further classified as either hydrostatic or transient. The hydrostatic methods are based on the premise that if there is a leak in a pipeline, the pressure will drop. The transient methods on the other hand are based on the principle that a leak or a burst in a pipeline will induce a negative pressure wave (a transient) which then travels in the opposite direction from the break point. The location and size of the leak are then analysed from the leak-induced wave.

When leakage is assessed and measures are established to detect and locate leaks, the water utility then implements techniques to control the level of leakage. The next subsection reviews some of the techniques that may be applied to control the leakage level in a water distribution network.

2.3.5. Leakage control

Leakage control is the application of techniques to reduce and control the level of leakage in water pipe networks (Mutikanga et al. 2011). Generally, such techniques may be reactive (where action is taken after a leak has occurred, for example increasing the speed to repair leaks) or proactive (where action is taken before a leak occurs, for example application of system pressure management), or both.

Figure 9 shows the International Water Association's suggested four components of an integrated effective approach to control leakage. These components are thereafter discussed.

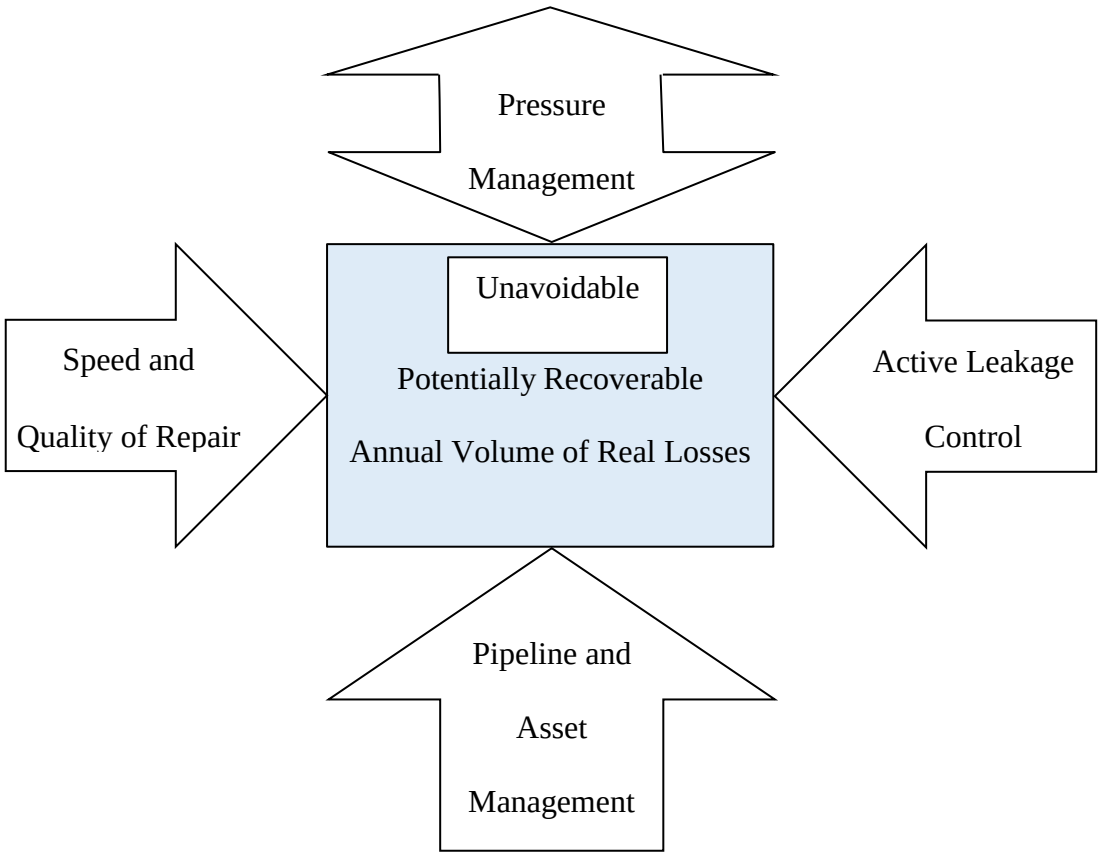

Figure 9: The IWA's water loss task force four basic leakage management techniques (Lambert 2000).

Pipeline and asset management: This component includes management of the water network rehabilitation through selection, installation, maintenance and replacement of pipes and other infrastructures. It is done in an economical way to reduce the need for corrective maintenance.

Active leakage control: This involves the monitoring of network flows on a regular basis for the early identification of new leaks which are then repaired as soon as possible. Active leakage control is done through the demarcation of district meter areas, where night flow is analysed to ascertain excess flow beyond customer usage. An increase in night flow is a likely indicator of either a new leak or the expansion of an existing leak.

Speed and quality of repairs: This addresses the repair of leaks in a timely and efficient way. It necessitates systematic working practices of the utility, stock keeping of repair materials and well trained and dedicated technicians.

Pressure management: This is about regulating pressure in the network through careful use of pressure reducing valves or break tanks in gravity systems or pumps in pumped systems. Effective pressure management is vital for effective leakage control.

If each of the above components is implemented effectively, the utility will be able to develop a successful leakage reduction strategy (Mutikanga et al. 2013).

2.4. Estimation of average pressures in water distribution networks

One of the factors that influences leakage in water distribution networks is pressure. For a given district metered area, the average system pressure (Pav) and the average zone night pressure (AZNP) can be estimated.

Lambert (2013) defines average system pressure (Pav) as the pressure in a system or zone that is either calculated or measured at a surrogate point. It is deemed the weighted average of all the pressures in that system or zone. The average system pressure is used to estimate the unavoidable annual real losses, applying equation (39).

The average zone night pressure (AZNP) is defined as the measured or calculated weighted average pressure during night hours, normally between 2:00 and 5:00 in the morning. If measured, the measurements are done at the average zone pressure (AZP) point. The AZP point is a physical location, usually a hydrant, where the pressure variations are considered representative in the zone as inflows to the zone vary on an hourly, daily and seasonal basis (Lambert 2013). The AZNP is an important parameter in modelling leaks as it is used in the estimation of the unavoidable background leakage using equation (40).

Several guidelines have been suggested to estimate the average system pressure and the average zone night pressure. Some of these guidelines are discussed in the following subsections.

2.4.1. The International Water Association guidelines to estimate average system pressure and average zone night pressure

The International Water Association (IWA) has drawn up guidelines to estimate average system pressure (Pav) and average zone night pressure (AZNP).

For the calculation of average pressures and analysis of night flows in large water networks, it is important to split the network into zones and identify the average zone pressure (AZP) point in each zone (Lambert 2013). The average system pressure and the average zone night pressure are then calculated from the pressures measured at the AZP point.

The IWA suggests the following steps in the measurement and calculation of the average pressures for a network that is divided into zones:

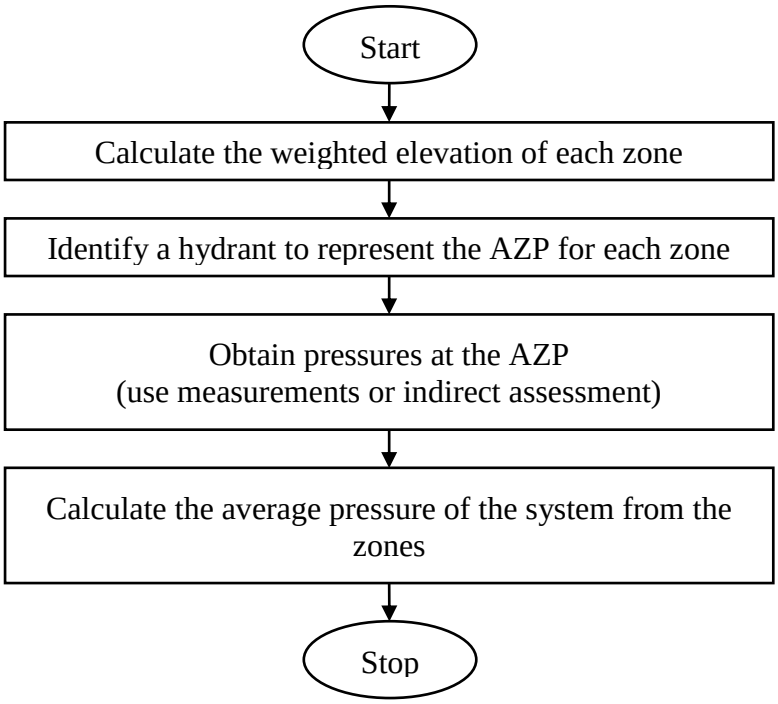

Figure 10: The IWA's recommended steps to calculate average system pressure and average zone night pressures (Lambert 2013).

Step 1: Calculate the weighted average elevation of each zone

Elevations of customer service connections and/or hydrants are identified using geographic information systems (GIS). The elevations are then weighted using one of these weighting parameters: the number of service connections if the density of connections is 20 per km or more, or the length of mains if the density of connections is less than 20 per km.

In conditions where it is difficult to obtain GIS data, average elevations may be obtained by superimposing a contour map and a plan of the distribution network in the zone. In that case, the number of service connections (or number of hydrants) bounded between the two contour lines are counted and multiplied by the average elevation of the two curves. The weighted average elevation of the chosen type of infrastructure (fire hydrants in this case) is then calculated using:

$$\mathrm{WA} = \frac{\sum_{i=1}^{c}(\mathrm{NH} \times \mathrm{MP})}{\sum_{i=1}^{c} \mathrm{NH}} \tag{42}$$

Where WA is the weighted average elevation, NH the number of hydrants, MP the midpoints of the contour bands and c the number of contour bands in the specific zone.

Step 2: Identify a hydrant to represent the average zone pressure (AZP) point

The selected hydrant should ideally be located near the centre of the zone. The elevation of the hydrant should be reasonably close to the weighted average elevation calculated in step 1. The location of this hydrant is the average zone pressure (AZP) point. In cases where such a hydrant does not exist, one that is close to the average should be selected. Pressure values should then be adjusted by the difference in elevation.

Step 3: Obtain pressures at the AZP point by either measurement or indirect assessment

Some of the methods that may be used to obtain pressures at the AZP point are:

- *Continuously taken direct pressure measurements at the AZP point*. This method gives the most accurate zone pressure estimates.
- *Measured adjustments to the inlet and/or critical point pressures*. The pressures at the inlet, the AZP point and the critical point are measured concurrently for 7 days. The average differences between the average pressure at the inlet and the AZP (ΔPi), and

the critical point and the AZP (ΔPc) are calculated. Then the average pressure at the AZP point is assessed by adjusting continually recorded inlet and/or critical point pressure by the appropriate average differences (ΔPi) or (ΔPc).

- *Estimated "small head loss" adjustments to inlet pressures*. Sometimes the pressures at the AZP point are not continually recorded. If the mains in the small zones are generously sized, an appropriate small frictional head loss between the inlet point and the AZP point can be assumed. To estimate the average pressure (Pav), the average measured inlet pressure is reduced by this small head loss, and the difference between the ground levels at the inlet point and the AZP point is corrected.
- *Using hydraulic network models*. A calibrated hydraulic network model may provide average pressures. In that case, the calculations of the weighted average pressures may be based on the number of properties or consumptions rather than on the number of service connections at a limited number of nodes.

Step 4: Calculate the average pressure of the system from the zones

The average pressure (Pav) of the whole system will then be considered equal to the weighted average pressure of all zones in that system. The proposed weights are the same as in the calculation of the weighted average elevation (step 1) and use the same criteria.

The average zone night pressure (AZNP) is the pressure obtained during minimum night flow conditions (normally between 2:00 and 5:00 in the morning) at the average zone pressure (AZP) point determined in the above steps.

2.4.2. Additional methods used to estimate average system pressure and average zone night pressure

The IWA guidelines described above are designed for systems with demarcated zones and systematically apply the definition of an average zone pressure point. This, however, is not always applicable and therefore Renaud et al. (2015) suggested other methods that do not necessarily apply the notion of the average zone pressure point. These methods are:

- the topographic method
- the hydraulic method
- the measurement method.

In the above methods, hydraulic modelling pipe nodes are selected as the basic entity and three schemes at node i are considered for weighting. These include: uniform weight ($w_i = 1$), daily average consumption at node ($w_i = c_i$), and the pipe length of the node, which is half the sum of the pipe length attached to the node in question ($w_i = l_i$).

The topographic method

This method is based on the topographic approach and ignores pressure variations due to head loss. The weighted average static pressure (PS_w) of a system is obtained by calculating the difference between the head (HS) of an infrastructure or device feeding that system (which may be a tank, a reservoir or a pump) and the weighted average ground level ($WAGL_w$).

$$\mathrm{PS_w} = \mathrm{HS} - \mathrm{WAGL_w}$$
$$\mathrm{WAGL_w} = \frac{\sum_{i=1}^{n}(\mathrm{GL_i} \times \mathrm{w_i})}{\sum_{i=1}^{n} \mathrm{w_i}} \quad (43)$$

The GL_i is the Ground Level (Elevation) of node i, and n is the number of nodes. In this method, the average system pressure is the same as the average zone night pressure (AZNP), which is equal to the weighted average static pressure (PS_w).

Hydraulic method

The hydraulic method uses a hydraulic model. It considers the hourly changes of pressure during a typical day and the head losses that are simulated by the model. The hourly dynamic pressure PD_i is calculated for each node i. This is then used to calculate the weighted hourly average dynamic pressure of the system. The n is the number of nodes.

$$\mathrm{PD}_{\mathrm{w}}^{\mathrm{h}} = \frac{\sum_{\mathrm{i}=1}^{\mathrm{n}}(\mathrm{PD}_{\mathrm{i}}^{\mathrm{h}} \times \mathrm{w}_{\mathrm{i}})}{\sum_{\mathrm{i}=1}^{\mathrm{n}} \mathrm{w}_{\mathrm{i}}} \tag{44}$$

The estimated average system pressure is the weighted daily average dynamic pressure defined in the following equation:

$$\mathrm{PD}_{\mathrm{w}} = \frac{\sum_{\mathrm{h}=0}^{23} \mathrm{PD}_{\mathrm{w}}^{\mathrm{h}}}{24} \tag{45}$$

The average zone night pressure (AZNP) is then estimated using equation (46) as the maximum weighted average pressure between 2:00 and 5:00 in the morning, when most of the demand in the system is likely to be leakage.

$$\mathrm{PDN}_{\mathrm{w}} = \mathrm{Max}_{\mathrm{h}=2}^{5}(\mathrm{PD}_{\mathrm{w}}^{\mathrm{h}}) \tag{46}$$

Measurement method

This method is based on the measurements of pressure taken at a point that represents an average for the system, i.e. the equivalent of the AZP point. Pressure is measured at a point k

considered to represent the system and whose ground level GL_k is close to the weighted average ground level $WAGL_w$.

If PM_k^h is the measured pressure at the point k at time h, the time-weighted average pressure of the system is calculated using the following equation:

$$\mathrm{PMw_k^h} = \mathrm{PM_k^h} + \mathrm{GL_k} - \mathrm{WAGL_w} \tag{47}$$

The average system pressure is then calculated from:

$$\mathrm{PMw_k} = \frac{\sum_{h=0}^{23} \mathrm{PMw_k^h}}{24} \tag{48}$$

The average zone night pressure (AZNP) is estimated using:

$$\mathrm{PMNw_k} = \mathrm{Max_{h=2}^{5}(PMw_k^h)} \tag{49}$$

Choice of the method used in this study

The IWA guidelines to estimate average system pressures are best applied in practice, whereas the methods suggested by Renaud et al. (2015) are robust and suitable for modelling.

In this study, the hydraulic method suggested by Renaud et al. (2015) was used to estimate the average system pressure (Pav) and the average zone night pressure (AZNP). The lengths of pipes connecting the junctions were used as weights.

3. Incorporating the modified orifice equation into standard hydraulic modelling

3.1. Introduction

This chapter aims to explain the approach and methodology that were applied to integrate the modified orifice equation into a standard hydraulic modelling tool.

Current standard hydraulic modelling tools apply the conventional power leakage equation (12) to model pressure dependent demands like leakage. As explained in Chapters 1 and 2, recent research has shown that the power leakage equation is flawed under certain circumstances (Cassa and van Zyl 2013; van Zyl et al. 2017). In contrast, the modified orifice equation (33) was found to be more accurate than the power equation in modelling the pressure and leakage relationship, because the modified orifice equation explicitly incorporates a linear relationship between leak area and pressure head that was reported in Cassa et al. (2010), van Zyl and Cassa (2014), and Ssozi et al. (2016).

The Epanet hydraulic modelling package Rossman (2000), which is in the public domain (i.e. freely available) and widely used, was chosen as a standard software whose algorithm of the hydraulic network solver was modified to integrate the modified orifice equation.

In section 3.2., the reasons for choosing the Epanet hydraulic modelling package are discussed.

The procedure that was followed to integrate the modified orifice equation into the algorithm of Epanet's hydraulic network solver is described in section 3.3.

Thereafter, in section 3.4., two verification tests which were conducted to ensure that the process of incorporating the modified orifice equation was successful, are explained. These

tests were conducted using a simple standard water distribution network, the properties of which are also presented. The results of the verification tests are discussed.

Finally, a summary of the chapter is presented in section 3.5.

3.2. Selection of a standard hydraulic modelling tool - Epanet

There are numerous standard hydraulic modelling tools that are used by water distribution network practitioners and researchers to model the pressure and leakage relationship. Examples of these tools are: WaterCad and WaterGems by Bentley systems (USA), MIKE-URBAN by DHI (Denmark), Pipe2016 by KYPipe (USA), PipeFlow Expert by PipeFlow (United Kingdom), WADISO by GLS (South Africa) and Epanet by the United States Environmental Protection Agency (USA), to mention but a few.

A decision to select Epanet from among the many other available tools was based on the following factors:

a) Public domain

Epanet is public domain software and therefore freely available. Partly because of this, it has a very wide range of users among water distribution networks researchers and practitioners. The integration of the modified orifice equation into the network solver of Epanet provides many researchers and practitioners with the opportunity to model the leakage and pressure relationship more accurately.

b) Robust hydraulic simulation capability

Epanet is a robust hydraulic modelling tool that can be used to model any size of a standard water distribution network. There is no limit to the number of physical and hydraulic network properties that Epanet is capable of modelling. Therefore, the

modified orifice equation was integrated into the algorithm of Epanet's hydraulic network solver to model leakage and pressure relationship correctly in any sized standard water distribution network.

c) Software architecture

The architecture of the algorithm of Epanet's hydraulic network solver, especially the procedure to model the leakage and pressure relationship, makes it possible to integrate the modified orifice equation.

The leakage flow rate is modelled at junctions and each junction has an emitter function. Because the modified orifice equation (33) describes leakage flow rate as having two components, namely leakage through a fixed area of the leak and leakage through the expanding part of the leak, a second emitter function was added to each junction.

With this approach, the first (original) emitter function models the leakage flow rate through the fixed area of the leak, while the second (added) emitter function models the leakage flow rate through the expanding part of the leak. The total leakage flow rate at each junction is the sum of leakage flow rates obtained from both emitter functions.

3.3. The procedure to incorporate the modified orifice equation into the network solver of Epanet

The Epanet hydraulic modelling package consists of two main modules: a network solver that performs hydraulic and water quality simulations, and a graphical user interface (GUI) which is used to provide input data to the network solver and to display simulation results.

Source code files are text files that contain computer programming functions. Epanet's source code files of both the network solver and the graphical user interface are freely available. They are written in C/C++ and Delphi computer programming languages respectively.

The provision of Epanet source code files has provided opportunities to many researchers to improve some of Epanet's features or even add new ones, and in this study, the modified orifice equation (33) for realistic leakage modelling was integrated.

Only the source code files of the network solver were modified for this study. It was not necessary to modify source code files of the graphical user interface because the network solver can be used as a standalone (i.e. without the graphical user interface). In that case, the network solver receives input data from a text file and writes the results to a formatted text-report file or an unformatted binary output file.

Modification of the graphical user interface to read and write the data of the two emitter functions is recommended in future studies. Using the network solver as a standalone requires some knowledge of computer programming languages. It would therefore be important to practitioners and researchers with less knowledge on computer programming for the graphical user interface to be modified to cater for added emitter function.

To keep a minimum level of modification and thereby maintain the ease and convenience of using Epanet, specific and relevant source code files plus their corresponding computer

programming functions were identified. Modifications were then limited to the identified files and their corresponding programming functions.

An open source and freely available Integrated Development Environment (IDE) for C/C++ programming language known as CodeBlocks (2011) was used to modify the Epanet hydraulic network solver.

The next subsection describes the method that was used to integrate the modified orifice equation into the algorithm of Epanet's hydraulic network solver. The modifications that were made to the algorithm are discussed.

A description of how the method to incorporate the modified orifice equation was implemented is then given. This involved identifying a list of source code files and corresponding computer programming functions that were then modified.

3.3.1. The method used to incorporate the modified orifice equation

In Chapter 2 the steady state hydraulic equations that are formulated for a system, when the leakage modelling tool that incorporates the conventional power equation is used, were described. The steps taken to solve these equations were also explained. This subsection refers to the discussions on the formulation of leakage modelling that incorporates the conventional power equation as described in Chapter 2.

The formulation of the leakage modelling which incorporates the modified orifice equation is different from the one that incorporates the power leakage equation in the following ways:

i. it has two fictional pipes connected to two fictional reservoirs at each junction to simulate the two terms in equation (33).
ii. the exponents of the two terms in equation (33) are fixed at 0.5 and 1.5.

Following on from Chapter 2, the following equation (50) which combines the continuity and head loss equations is solved in the formulation that incorporates the power leakage equation:

$$\left[p_{fj} + \sum_{i=1}^{l} p_{ij}\right] H_j - \left[\sum_{i=1}^{l} p_{ij}\right] H_i = \sum_{i=1}^{l} Q_{ij} + Q_{fj} - D_j - \sum_{i=1}^{l} y_{ij} - y_{fj} + p_{fj} Z_j \quad (50)$$

In the above equation, i and j are nodes connected to a pipe, l is the number of links connected to the node j, f is a fictional tank, H is the head at the node, Q is the flow rate through the link, and D is the external demand known at the specific node. The terms p_{ij} and p_{fj} are inverse of the derivatives of the head loss equations for the links between nodes i and j, and f and j respectively. The terms y_{ij} and y_{fj} are flow correction factors.

With the modified orifice equation incorporated into the algorithm of the hydraulic network solver of Epanet, the only change in the process layout presented in figure 4 in Chapter 2 is the computation of emitter flow rates, in which $Q_{f_1 j}$ and $Q_{f_2 j}$ are computed for the respective first and second emitter functions.

In Chapter 2 it was shown that the model for pressure-dependent outflow that is used for leakage flow rate is as follows:

$$\mu_i = c_i (H_i - z_i)^{\alpha}, \text{if } H_i \geq z_i \quad (51)$$

In the above equation, μ_i is the lumped nodal leakage flow rate, c_i is the leakage coefficient, z_i is the elevation of node i and α is the leakage exponent.

For the modified orifice formulation, equation (51) is written as equation (52):

$$\mu_i = \mu_{1i} + \mu_{2i} = c_{1i} (H_i - z_i)^{0.5} + c_{2i} (H_i - z_i)^{1.5}, \text{if } H \geq z_i \quad (52)$$

In the above equation, c_{1i} is equal to the sum of $\sqrt{2g}C_dA_0$ and c_{2i} is equal to the sum of $\sqrt{2g}C_dm$ of all the individual leaks lumped to node *i*. The other terms remain as earlier defined.

Adding terms of the second emitter function to equation (50) gives:

$$\left[p_{f_1 j} + p_{f_2 j} + \sum_{i=1}^{l} p_{ij}\right] H_j - \left[\sum_{i=1}^{l} p_{ij}\right] H_i = \sum_{i=1}^{l} Q_{ij} + Q_{f_1 j} + Q_{f_2 j} - D_j - \sum_{i=1}^{l} y_{ij} - y_{f_1 j} - y_{f_2 j} + p_{f_1 j} Z_j + p_{f_2 j} Z_j \quad (53)$$

where $p_{f_1 j} = \frac{C_{1i}^2}{2Q_{f_1 j}}$; $p_{f_2 j} = \frac{3}{2}\left(c_{2i}^{\frac{2}{3}}\right)\left(Q_{f_2 j}^{\frac{1}{3}}\right)$

$y_{f_1 j} = \frac{Q_{f_1 j}}{2}$; $y_{f_2 j} = \frac{3}{2} Q_{f_2 j}$

Equation (53) is then transformed into a matrix format (i.e. equation 30) and thereafter solved following the same procedure as described in Chapter 2 for the case of the formulation that incorporates the conventional power leakage equation.

3.3.2. Implementation of the method used to incorporate the modified orifice equation in Epanet

The modified orifice equation was implemented into the network solver of the Epanet software package through identification and modification of source code files and computer programming functions.

A list of these source code files and their corresponding programming functions is presented in table 4. The purpose of the programming functions and the exact modifications that were made are also shown.

Table 4: Epanet's source code files and functions that were modified

Source file	Name of function	Purpose of function	Modifications made
Epanet.c	int ENsetoption (int code, float v)	Sets value for a parameter in the OPTIONS section	A statement that sets a value for the second emitter exponent was added
	int ENgetoption (int code, float *value)	Retrieves a value for a parameter in the OPTIONS section	A statement that retrieves a value for the second emitter exponent was added
	int ENsetnodevalue (int index, int code, float v)	Sets input parameter value for a node	A statement that sets a coefficient for the second emitter was added
	int ENgetnodevalue (int index, int code, float *value)	Retrieves parameter value for a node	A statement that retrieves a coefficient for the second emitter was added
Epanet2.h	Define Epanet toolkit constants (Node Parameters)	Declares Epanet toolkit constants for a node	A constant for the second emitter was added to the node parameters
	Define Epanet toolkit constants (OPTIONS section)	Declares Epanet toolkit constants of the OPTIONS section	A constant for the second emitters was added to the OPTIONS section
Funcs.h	Function prototypes for Epanet Program	Declares function prototypes for the Epanet program	A declaration of a prototype for a function that computes flow from

			the second emitter was added
Hydraul.c	void inithyd (int initflag)	Initializes the hydraulics solver	An initialization statement for the second emitter flow was added
	int allocmatrix ()	Allocates memory used for the solution matrix coefficients	A statement to allocate memory for the solution matrix coefficients of the second emitter was added
	void freematrix ()	Frees memory used for solution matrix coefficients	A statement to free memory for the solution matrix coefficients of the second emitter was added
	int netsolve (int *iter, double *relerr)	Solves equations for heads and flows using Todini's Gradient Algorithm	A statement that adds emitter flows (both first and second) to the junction demand was modified
	double newflows ()	Updates link flows after new nodal heads are computed	A statement that updates link flows after new nodal heads were computed was modified to include second emitter flows
	void emittercoeffs ()	Computes matrix coefficient for emitters	A statement that computes matrix coefficient for the second emitter was added

	double emitflowchange (int i)	Computes flow change at an emitter node	A function that computes flow rate change at the second emitter was added
Inpfile.c	int saveinpfile (char *fname)	Saves data describing a piping network to a formatted text file	A statement that writes the second emitter input data to a text file was added
Input1.c	void setdefaults ()	Assigns default values to global variables	A default exponent for the second emitter was added
	void convertunits ()	Converts units of input data	A statement that converts emitter coefficients to head loss coefficients for the second emitter was added
Input3.c	int juncdata ()	Processes junction data	A statement for processing of the second emitter at a junction was added
	int tankdata ()	Processes tank and reservoir data	The function was modified to add the second emitter
	int emitterdata ()	Processes junction emitter data	The function was modified to process data of the second emitter
	int optionvalue (int n)	Processes numerical value of the OPTIONS data	The function was modified to add a statement

			assigning a value to the second emitter
Text.h	string constants for Epanet Program (Keyword Dictionary).	Provides string constants for the Epanet program	A string constant for the second emitter was added
Toolkit.h	define Epanet toolkit constants (Node Parameters)	Defines Epanet toolkit constants for the node parameters	A statement to define the toolkit constant for the second emitter at the node was added
	define Epanet toolkit constants (Misc Options)	Defines Epanet toolkit constants for the OPTIONS section	A statement to define the toolkit constant for the second emitter in the OPTIONS section was added
Type.h	Global Data Structures (NODE OBJECT)	Defines the global constants and data types for Epanet	A statement to define a global constant for the second emitter was added
Vars.h	Global variables for Epanet Program	Defines global variables for Epanet	A statement to define a global variable for the second emitter was added

3.4. Verification of the procedure that was used to incorporate the modified orifice equation into Epanet

The procedure that was used to incorporate the modified orifice equation into the network solver of Epanet was verified using two tests. The main purpose of the tests was to make sure that the added emitter function was working in the same way as the original one.

The next subsection presents the physical properties of the water distribution network that was used in the two tests. The procedure that was followed to perform the tests and the results that were obtained are discussed thereafter.

3.4.1. Physical properties of the network used in verification tests

A schematic layout of the network that was used in the verification tests is shown in figure 11. This network was adapted from Net1, an example network from the Epanet software package. The network has 9 junctions, 1 storage tank, 1 reservoir, 1 pump and 12 pipes with diameter range from $200 - 500mm$. The total length of the pipes is $19.4km$.

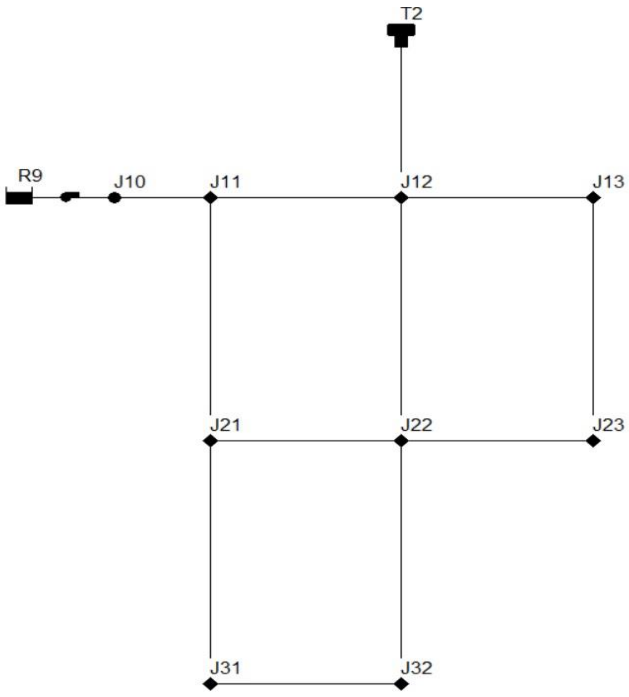

Figure 11: Layout of the network that was used in the verification test

3.4.2. Procedure and results of the verification tests

The following tests were performed, namely the exchange of emitter parameters and the sum of emitter flow rates.

Test 1: Exchange of emitter parameters

The emitter parameters, namely the coefficient and the exponent of the pressure head, were swapped between the two emitter functions. This means that the emitter parameters of the original emitter function were replaced with those of the added emitter function and vice versa as presented in equations (54) and (55);

$$\mathrm{Q_b} = \mathrm{Q_{b\_o}} + \mathrm{Q_{b\_a}} = \mathrm{C_1 h^{0.5}} + \mathrm{C_2 h^{1.5}} \quad (54)$$

$$\mathrm{Q_a} = \mathrm{Q_{a\_o}} + \mathrm{Q_{a\_a}} = \mathrm{C_2 h^{1.5}} + \mathrm{C_1 h^{0.5}} \quad (55)$$

In these equations, Q_b, Q_{b_o}, and Q_{b_a} are the total, original, and added emitter flow rates respectively before the parameters were swapped, while Q_a, Q_{a_o} and Q_{a_a} are the respective corresponding values after the emitter parameters had been swapped.

Flow rates Q_{b_o} and Q_{b_a} were first obtained from each of the two emitter functions for an extended period of hydraulic simulation (24 hours). In this case, C_1 and 0.5 were the respective coefficient and pressure head exponent for the original emitter function, while, C_2 and 1.5 were the corresponding values for the added emitter function.

The emitter parameters were then swapped between the two emitter functions. This means that C_1 and 0.5 were now allocated to the added emitter function, while C_2 and 1.5 were allocated to the original emitter function. A hydraulic simulation with extended period was conducted again and flow rates Q_{a_o} and Q_{a_a} were obtained.

The hypothesis for this test was that, if the two emitter functions work the same way, the flow rate through the original emitter function before swapping the parameters Q_{b_o} should be equal to the flow rate through the added emitter function after swapping the parameters Q_{a_a}. The same should apply to Q_{b_a} and Q_{a_o}.

Figure 12 presents the emitter flow rates (l/s) at each of the junctions in the system, before and after the emitter parameters were swapped during the first period of simulation.

The flow rate obtained from the original emitter function before swapping of the parameters was found to be equal to the flow rate obtained from the added emitter function after the parameters were swapped. Also, the flow rate obtained from the added emitter function before the swapping of the parameters was found to be equal to the flow rate obtained from the original emitter function after swapping of the parameters.

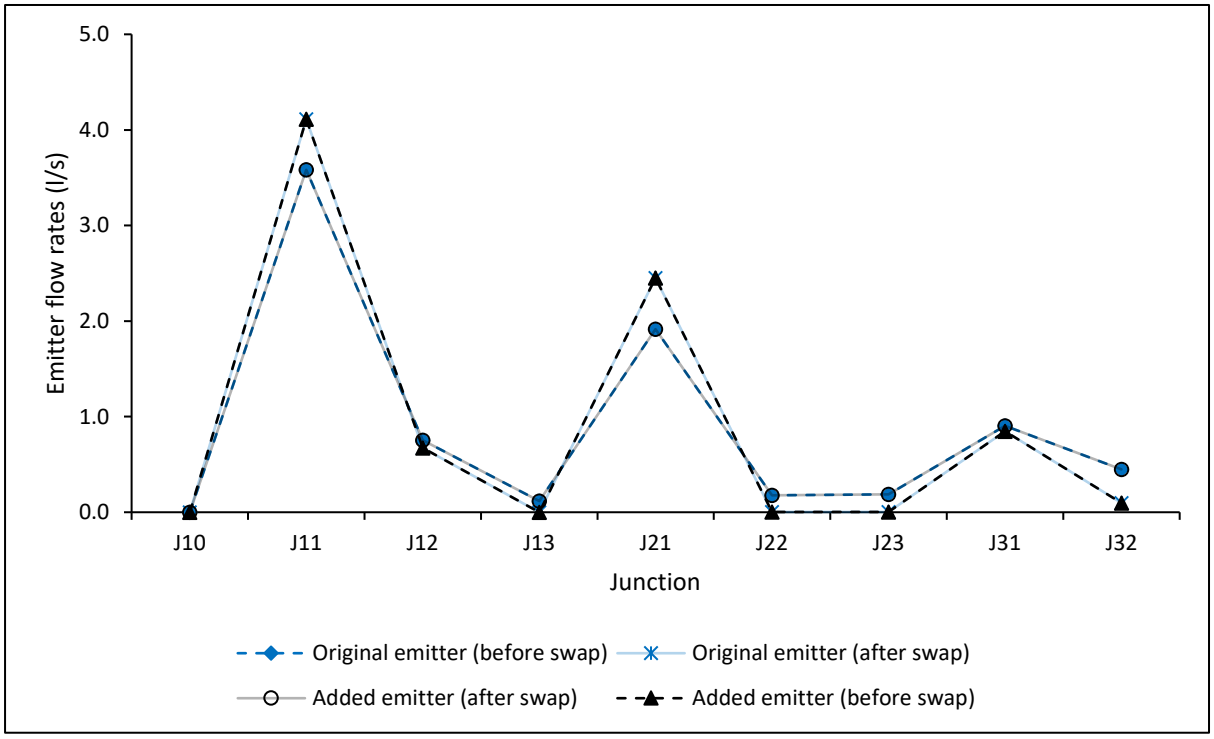

Figure 12: Comparison of emitter flow rates before and after swapping of the emitter parameters during the first hour of simulation

The emitter flow rates obtained from each junction were then added for each period of simulation. Figure 13 presents the sum of flow rates for each period of simulation before and after swapping of the parameters. The results show that for the 24-hour simulation period the flow rates obtained from the original emitter function before swapping of the parameters are equal to those of the added emitter function after the parameters were swapped. Similarly, the flow rates of the added emitter function before swapping of the parameters are equal to those of the original emitter function after swapping of the parameters.

These results show that the two emitter functions (i.e. original and added) calculate the exact emitter flow rates.

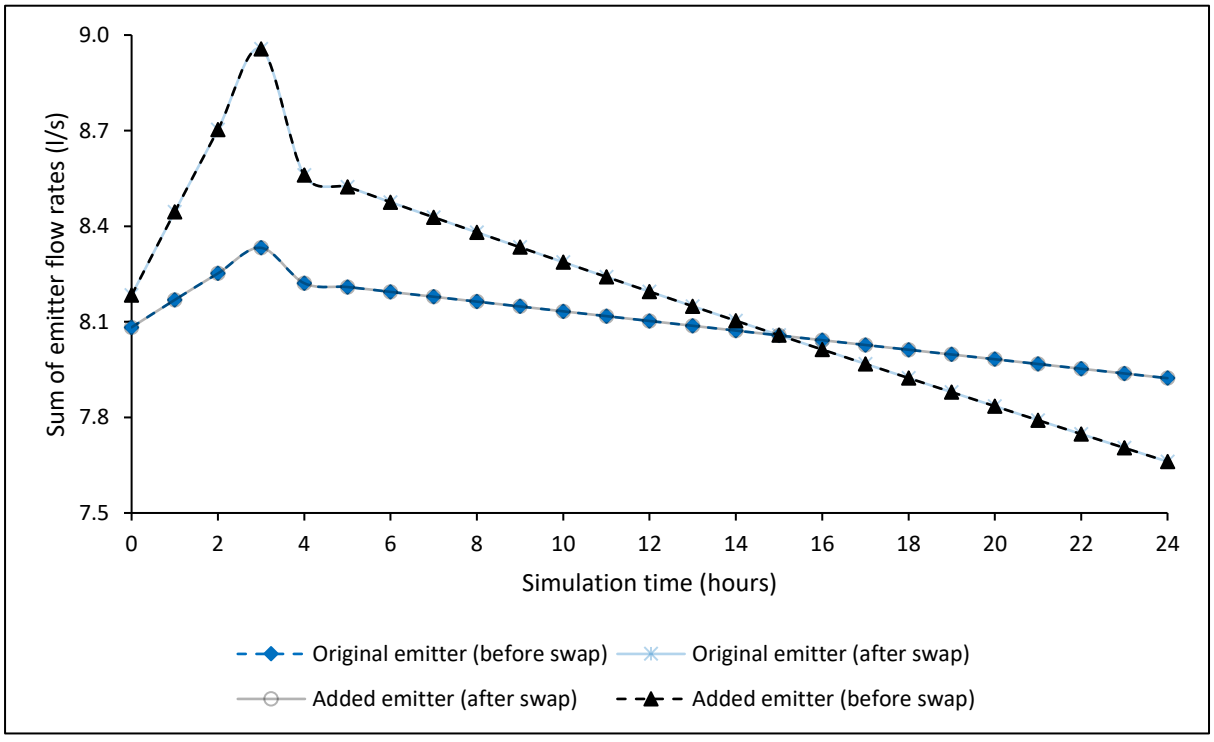

Figure 13: Comparison of emitter flow rates for 24-hour simulation period before and after swapping the emitter parameters

Test 2: Sum of emitter flow rates

The sum of flow rates at each junction from the two emitter functions in the modified Epanet tool that incorporates the modified orifice equation, was compared to the flow rate obtained from the original Epanet that has only one emitter function.

The emitter coefficient in the original Epanet tool with one emitter function, was equal to the algebraic sum of the emitter coefficients at the same node in the modified Epanet tool with two emitter functions as shown in equations (56) and (57).

The pressure head exponents of the two emitter functions in the modified Epanet were maintained equally i.e. 0.5, while the corresponding coefficients were different. The pressure head exponent in the original Epanet was also maintained as 0.5.

$$\mathrm{Q_{E1}} = \mathrm{K_{e1}h^{0.5}} + \mathrm{K_{e2}h^{0.5}} \quad (56)$$

$$\mathrm{Q_{E2}} = (\mathrm{K_{e1}} + \mathrm{K_{e2}})\mathrm{h^{0.5}} \quad (57)$$

In the above equations, Q_{E1} is the sum of emitter flows obtained from the modified Epanet with the two emitter functions, Q_{E2} is the emitter flow rate obtained from the original Epanet with one emitter function, K_{e1} is the emitter coefficient for the original emitter function, K_{e2} is the emitter coefficient for the added emitter function, and h is the pressure head at the specific junction.

An extended period of hydraulic simulation was first conducted using the modified Epanet hydraulic modelling tool that has two emitter functions. The total emitter flow rate (Q_{E1}) at each junction was obtained by adding the flow rates from each emitter function as shown in equation (56).

The emitter coefficients K_{e1} and K_{e2} were then added together and their sum used as a coefficient in the original Epanet hydraulic modelling package that has only one emitter

function. An extended period of hydraulic simulation was again conducted and the flow rate Q_{E2} at each junction obtained as shown in equation (57).

The underlying hypothesis for this test was that since the pressure head (h) at a given junction is the same, the emitter flow rates Q_{E1} and Q_{E2} should be equal if the procedure of adding a second emitter function was correctly implemented.

Figure 14 presents the emitter flow rates modelled by both the modified and the original Epanet hydraulic modelling tools at each junction for the first hour of simulation. The graph shows that the sum of the flow rates obtained from the modified Epanet are equal to the flow rate obtained from the original Epanet with one emitter function.

The emitter flow rates modelled by both the modified and original Epanet hydraulic modelling tools at all junctions in the system were then added during each period of simulation.

Figure 15 presents the total emitter flow rates (l/s) per period of simulation modelled with both the modified and the original Epanet. The graph illustrates that for each period of simulation the sums of the emitter flow rates are equal for both the modified and original Epanet models.

The results obtained from the two verification tests indicate that the process of adding the second emitter function to the network solver of Epanet was correctly implemented.

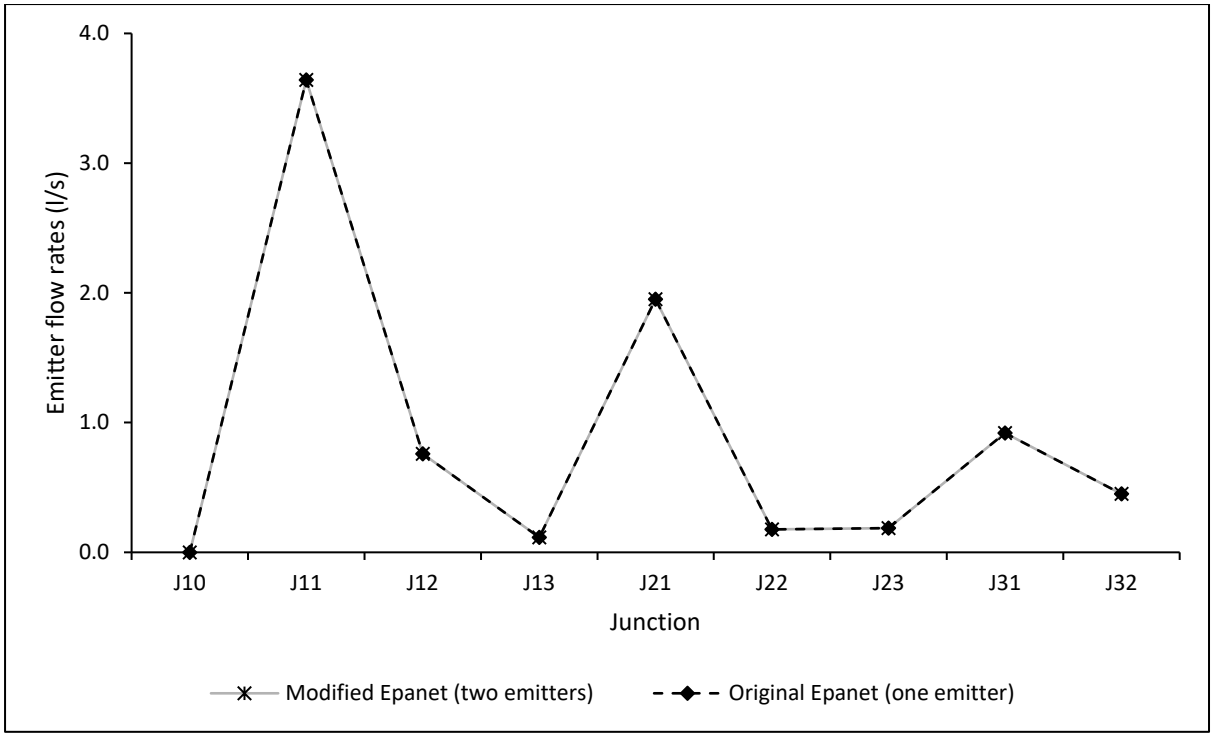

Figure 14: Comparison of emitter flow rate at each junction from the modified and the original Epanet tools during the first hour of simulation

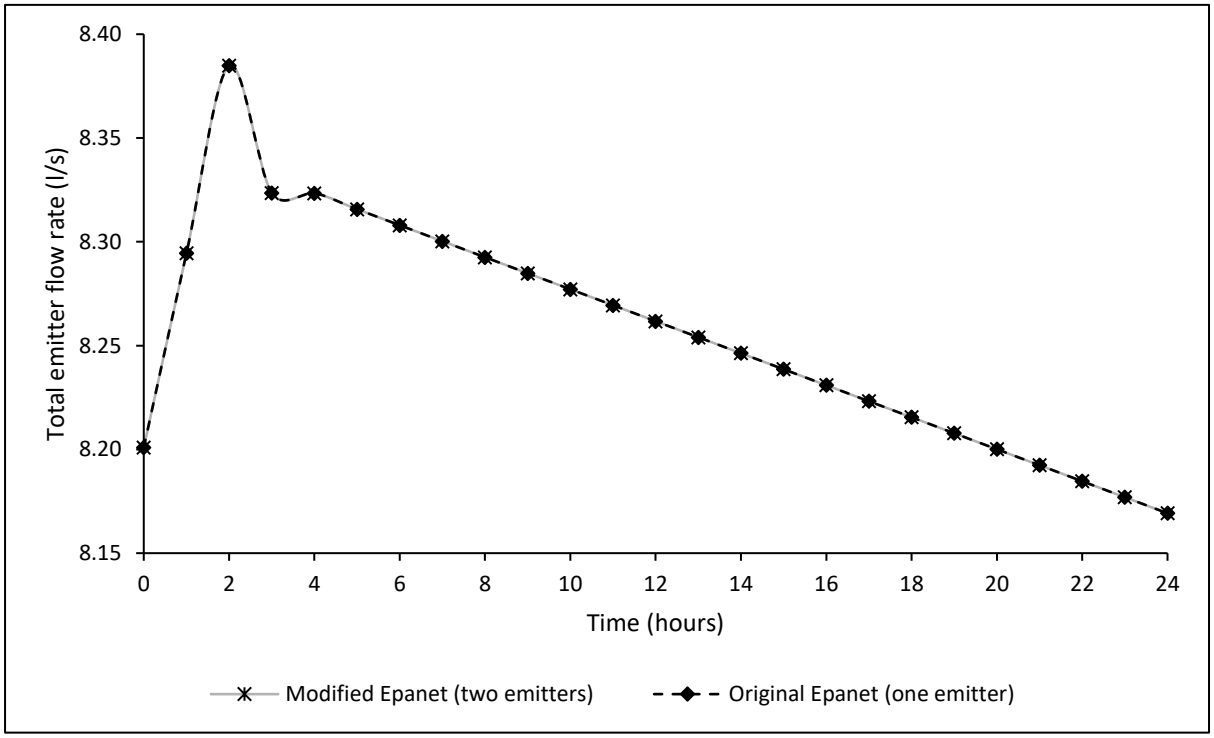

Figure 15: Comparison of system emitter flow rates obtained from both the modified and the original Epanet tools during a 24-hour simulation period

3.5. Summary of the chapter

This chapter described the method and procedure that were applied to incorporate the modified orifice equation for leakage modelling into the algorithm of the hydraulic network solver of Epanet.

First the method was described which involved adding a second emitter function to the algorithm of the hydraulic network solver of Epanet, and thereafter a description was given of the procedures that were followed in the implementation process.

Two verification tests were carried out to ensure that the added emitter function was working in the same way as the original one. The results of the verification tests confirmed that the method and the procedure that were followed to incorporate the modified orifice equation into the algorithm of the hydraulic network of Epanet were implemented correctly.

4. A stochastic model for generation and distribution of leaks

4.1. Introduction

Based on the available literature and expertise on leakage behaviour in water distribution networks, Schwaller and van Zyl (2015) first suggested a stochastic model that generates leaks realistically. Their model was built in Microsoft Excel and assumes a network with no head losses along pipelines. Physical properties of a typical water distribution network like links and nodes cannot be incorporated into the model.

This study has adapted Schwaller and van Zyl's (2015) model and expanded it to include a realistic distribution of leaks into any standard water distribution network.

Unlike Schwaller and van Zyl's (2015) model, this study considers the physical and hydraulic properties of the water distribution networks. Head losses along links and pressure heads at junctions are considered in the generation of leakage volume, while the number of consumer connections along pipelines is considered during the distribution of leaks.

The model developed in this study is built in C/C++ computer programming language. This facilitates easy interaction with some hydraulic modelling tools like the standard Epanet, whose source code of the hydraulic network solver is built in the same programming language.

The Infrastructure Leakage Index (ILI), which is an internationally accepted water loss benchmarking concept (Lambert and Hirner 2000; Lambert and McKenzie 2002; Winarni 2009 and AWWA 2016), was incorporated into the leaks generation and distribution model to appraise the level of leakage.

The Schwaller and van Zyl (2015) model is first discussed in section 4.2.. Thereafter in section 4.3. a description is provided of how it was adapted for this study.

Section 4.4. compares the range of leak parameters generated in this study with the Schwaller and van Zyl's (2015) model. The equivalent leakage exponents of the power equation are analysed first, followed by the discharge coefficients. Then the initial leak areas and head-area slopes of the modified orifice equation are compared as well.

The chapter ends with a summary in section 4.5.

4.2. Leak generation model

This section describes how the discharge coefficient C_d, the leak parameters, i.e. the initial leak area A_0, the head-area slope m and the pressure head h were modelled.

While the pressure head, the discharge coefficients and the initial leak areas for both background (BG) and potentially detectable (PD) leaks were stochastically generated, the head-area slopes were calculated using equations that are described later in the chapter.

Statistical distribution parameters (i.e. mean μ and standard deviation σ) were calculated for the discharge coefficients and the initial leak areas of both background and potentially detectable leaks.

Figure 16 summarizes the procedure used to generate a single leak. All the steps involved are explained in the following subsections. Apart from the calculation of the statistical parameters, these steps can be repeated to generate as many leaks as required.

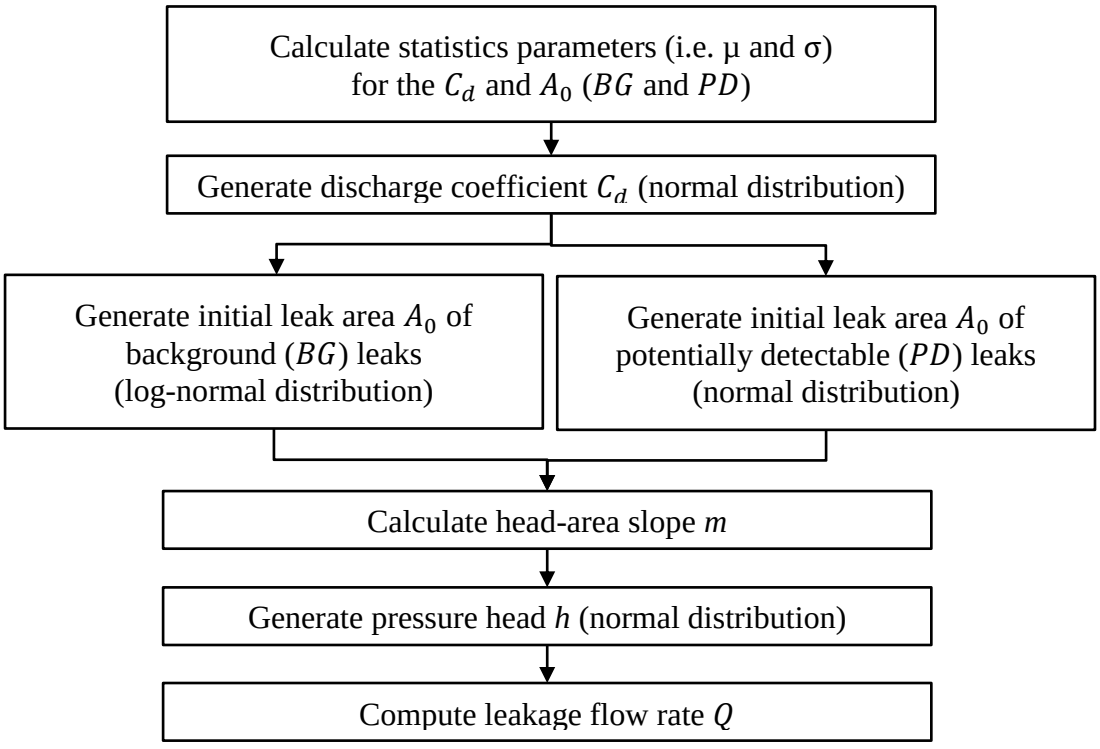

Figure 16: Layout of the process to generate a single leak (Schwaller and van Zyl 2015).

4.2.1. Calculating statistical parameters

The procedure to calculate statistical parameters, i.e. the mean μ and the standard deviation σ, is described below. These statistical parameters were calculated for the discharge coefficient and the initial leak areas.

For the initial leak areas, two classifications of leaks were considered, namely background (BG) leaks – which are very small and cannot be detected and thus repaired, and potentially detectable (PD) leaks – which are normally discovered through efforts of leak detection and therefore be reported and repaired.

The boundary between the background and potentially detectable leaks in terms of flow rate was $250\ L/h$ Hamilton and Krywyj (2012), as cited in Schwaller and van Zyl (2015). This flow rate is equivalent to a leak area of $3.41\ mm^2$ if a pressure head of $50m$ is used in the Torricelli equation (11).

The calculation of the statistical parameters of the discharge coefficients is described first, followed by that of the background leaks and thereafter the potentially detectable leaks.

4.2.1.1. Discharge coefficient

Studies have found that the coefficients of discharge are functions of different parameters like the shape of the leak opening, the material and curvature of the pipe and the pressure head (Brater et al. 1996; Lambert 2000). Lea (1942) as cited in Brater et al. (1996) found a discharge coefficient of 0.6 for a completely turbulent flow on circular openings.

As the discharge coefficient for a lamina flow regime can be lower than the above value, while the discharge coefficient of transitional flows can be higher, the average coefficient of discharge varied between 0.5 and 0.8.

The discharge coefficients were considered to demonstrate a normal distribution. A mean μ of 0.65 was assumed for the distribution. The standard deviation σ of 0.0304 was calculated based on the assumption that 95% of the discharge coefficients could be smaller than 0.7 (i.e. $P(C_d < 0.7) = 0.95$).

4.2.1.2. Background leaks

Because background leaks are not easily found, very little specific information about their numbers is obtainable in the literature. The concept of the unavoidable background leakage (UBL) within the unavoidable annual real losses (UARL) was used.

The International Water Association water loss task force proposed an unavoidable background leakage of 20 L/h/km of the main pipes plus 1.25 L/h/service connection (main pipe to property line) at a standard pressure head of $50m$ (Lambert et al. 1999).

A typical district metered area (DMA) was assumed to have $40\ km$ of mains and 2500 service connections (Lambert 2012). This results in unavoidable background leakage of about $64\ mm^2$ of the total background leak area when the orifice equation (11) is used. Further assumption was made that a typical DMA would have 550 background leaks (Lambert 2012). The figures assumed above result in an average background leak area of about $0.12\ mm^2$ in a typical DMA.

Background leaks were assumed to be distributed lognormally, with 2.5% of the leaks being larger than $3.41\ mm^2$. The assumption of lognormal distribution was because background leaks are generally difficult to find and fix as compared to the potentially detectable leaks. Also, lognormal (skewed) distributions are generally assumed when mean values are low and variances are large Diwakar (2017), which seems to match observations in small leaks than large leaks in distribution systems. The mean μ of the lognormal distribution and standard deviation σ were thus obtained through a trial and error method, by varying either the mean or

the standard deviation, until the overall average background leak area was $0.12\ mm^2$ for any number of background leaks generated.

4.2.1.3. Potentially detectable leaks

To model leakage realistically, the potentially detectable leaks were further categorized based on their location and their status. Potentially detectable leaks may be either on the service or the main pipes and either reported or unreported.

The categorisation was necessary because potentially detectable leak events have different discharges based on their location and their status. For example, while reported potentially detectable leaks are usually repaired in approximately three to eight days depending on their location, the unreported leaks have a longer run time which is mostly determined by the interval between two active leakage detections.

The above categorisation resulted into four types of potentially detectable leaks, namely service reported SR, service unreported SU, mains reported MR and mains unreported MU. The statistical parameters (μ and σ) were calculated for each of these categories.

Because potentially detectable leaks can be generally found easily and fixed, they were modelled using a normal distribution. The mean leakage flow rates in table 5 for the four categories of potentially detectable leaks, as suggested by Lambert (2012), were used to calculate the corresponding mean initial leak areas.

Table 5: Mean leakage flow rates of potentially detectable leaks (Lambert 2012)

	Service pipes		**Mains**	
	Unreported	**Reported**	**Unreported**	**Reported**
	Service Unreported (SU)	Service Reported (SR)	Mains Unreported (MU)	Mains Reported (MR)
Mean leakage flow rate (m^3/h)	0.5	1.6	6.0	12
Coefficient of Variation, cv	0.3			

The orifice equation (11) was used to calculate the mean initial leak area μ, given that the discharge coefficient and average pressure were known.

The standard deviation σ was then calculated for each of the categories from the mean and coefficient of variation cv, using equation (58). Schwaller (2012) found through a trial and error method that a coefficient of a variation of 0.3 gave reasonable results.

$$\sigma = \mu \times \mathrm{cv} \tag{58}$$

4.2.2. Generating leakage

In this subsection, the procedure to generate the discharge coefficients, the initial leak areas of background and potentially detectable leaks, plus the calculation of the head-area slope are described. The subsection ends with a discussion of the generation of the pressure heads and the computation of leakage flow rate from the leak parameters.

Discharge coefficient and initial leak areas of background leaks

The calculated mean μ and standard deviation σ of discharge coefficients are used to generate random discharge coefficient values, one at a time, using the probability distribution function of the normal distribution.

Similarly, the mean μ and standard deviation σ of background leaks are used to generate their random initial area, one at a time.

The discharge coefficients assume a normal distribution while the initial leak areas of background leaks assume a lognormal distribution.

Potentially detectable leaks

Potentially detectable leaks are categorised as described in table 5 above. Therefore, the frequency of events and runtimes in each of the four categories guides the selection of the category of the leak that the model generates.

The following four steps are followed to establish a criterion for the selection of the category of the leak that the model generates at a time:

- establishing the frequency of events for each category
- establishing the runtimes for each category
- applying weights (i.e. the runtimes) to the frequency of events in each category
- expressing the potentially detectable leaks in each category as a fraction of the total potentially detectable leaks.

a) Frequency of events

The categorized frequency of potentially detectable events on both service and main pipes was based on the World Bank Institute banding system for developed countries. This banding system provides performance categories i.e. bands from A to D, for a water utility and suggests priorities for activities to reduce leakage (Liemberger and McKenzie 2005; Liemberger et al 2007). The Infrastructure Leakage Index (ILI) concept was used in the

grading of leakage levels. These potentially detectable frequency events (table 6) are specified for drinking water systems with leakage level grading from “very low” to “very high” (Lambert 2012).

Table 6: Potentially detectable leak frequency of events for leakage level gradings based on World Bank Institute's banding system for developed countries (Lambert 2012)

	Service pipes (per 1000 connections/year)	**Mains (per 100 km/ year)**
Very low (ILI = 1)	2.25	13
Low (ILI = 2)	4.5	26
Typical	6.75	32.5
High (ILI = 4)	9	39
Very high (ILI = 8)	18	104

Based on the above data, the frequency of potentially detectable events for a specific system can be calculated. A typical DMA with 40 km of main pipes and 2500 service connections was considered and the corresponding frequency of events per year for each category is shown in table 7. Lambert (2009) indicated that 5% and 25% of the potentially detectable events that are located on mains and service pipes respectively are unreported. These fractions were applied to the data in table 7. Schwaller and van Zyl (2015) chose the frequency of events for a “Typical” leakage level for their analysis.

Table 7: Potentially detectable leak frequency of events (f) per year for a typical DMA

	Potentially detectable leaks per year on service pipes			**Potentially detectable leaks per year on mains**		
	Total	**Unreported (SU)**	**Reported (SR)**	**Total**	**Unreported (MU)**	**Reported (MR)**
Fraction of PD events		0.25	0.75		0.05	0.95
Very low	5.63	1.41	4.22	5.2	0.26	4.94
Low	11.25	2.81	8.44	10.4	0.52	9.88
Typical	16.88	4.22	12.66	13	0.65	12.35
High	22.50	5.63	16.88	15.6	0.78	14.82
Very high	45.00	11.25	33.75	41.6	2.08	39.52

b) Runtimes of leak events

Potentially detectable leaks that are reported are usually found and repaired quickly, while the unreported leaks have a longer runtime. Table 8 presents the average runtime of potentially detectable leaks calculated for a typical DMA (40 km mains and 2500 service connections). The average duration (in days) for the unreported potentially detectable leaks on both service pipes and mains was estimated as half of the time interval between two active leakage controls (ALC). The average duration of reported leaks was estimated to be 8 and 3 days for leaks on the service pipes and main pipes respectively (Lambert 2012). Schwaller and van Zyl (2015) chose the runtime for a "Typical" leakage level for their analysis.

Table 8: Runtime of potentially detectable leak events per year for a typical DMA

	Interval between ALC interventions (years)	**Average duration of potentially detectable leaks (days)**			
		Service pipes		**Mains**	
		Unreported	**Reported**	**Unreported**	**Reported**
Very low	0.5	91.25	8	91.25	3
Low	1	182.5	12	182.5	4.5
Typical	2	365	16	365	6
High	5	730	20	730	7.5
Very high	10	1,095	24	1,095	9

c) Weighted frequency of potentially detectable events

The frequency of the potentially detectable leak events f is weighted with the runtime because the actual leakage flow is influenced by how long the leak has been running before it is fixed. It is often assumed that large potentially detectable leaks are the largest contributors to leakage but these leaks are visible above ground and thus they are normally found and fixed although the rate of response depends on the utility's capacity. On the other hand, small leaks have a profound impact over a long period because they often remain unobserved and thus unfixed. The weighted number of potentially detectable leak events N_w at any time t (number of days in a year) was calculated using the following formula:

$$\mathrm{N_w} = \mathrm{f} \times \frac{\mathrm{t}}{365} \tag{59}$$

d) Fraction of PD events in each category

The weighted number of leaks for each category is then expressed as a fraction of the total number of potentially detectable leaks in the network as follows:

$$f_r = \frac{W_c}{T_c} \tag{60}$$

In the above equation, f_r is the fraction of potentially detectable events, W_c is the weighted number of potentially detectable events in a category, and T_c is the total weighted number of all potentially detectable events.

Cumulative fractions of the weighted leaks, which must add up to 1, are then calculated and systematically arranged from 0 to 1. Each range represents a potentially detectable leak category. The type of the potentially detectable leak that is to be generated at a time is thus determined by generating a random number between 0 and 1; this is then associated with one of the categories.

The head-area slope

In real water pipe networks, the leakage exponent $N1$ of background leakage is often found to be close to 1.5 (Lambert 2002; Thornton and Lambert 2005) . To replicate this, Schwaller and van Zyl (2015), assumed about 20% of the background leaks generated to constitute this type of background leaks. Their head-area slope m is then calculated using equation (61). In this equation, the average zone night pressure (AZNP) is known and the leakage number L_N of 100 is used. This is because van Zyl and Cassa (2014) found that when the leakage exponent is close to 1.5 the leakage number will be 100.

$$m = \frac{L_N \times A_0}{AZNP} \tag{61}$$

For the potentially detectable leaks and background leaks whose leakage exponent is not close to 1.5, the head-area slope m is calculated using an initial leak area power equation (62), that was developed by Schwaller and van Zyl (2015) using data from Cassa et al. (2010).

$$\mathrm{m} = 2 \times 10^{6} \times \mathrm{A_0}^{2.9102} \tag{62}$$

Pressure heads

Schwaller and van Zyl (2015), assumed a uniform distribution for the pressure head h. In practice, pressure reduction tests are carried out during morning hours when consumption is at its minimum. This means that the pressure head at any point in the system is determined by the static head. The same principle is assumed in the Schwaller and van Zyl's (2015) model, where the head losses due to pipe friction are assumed to be very negligible.

The average pressure head for a DMA is measured at the average zone pressure (AZP) point. Ranges of average pressure heads that were reported for different countries were used, from which a typical average pressure head of $45m$ was assumed (Lambert 2012). A range of pressure heads in a typical DMA was assumed to be $\pm 10m$. This therefore allowed for a random pressure head to be generated within the above range.

Computation of the leakage flow rate

After the generation and calculation of the leak parameters, leak coefficients C_1 and C_2 were obtained from equations (63) and (64) in which g is the acceleration due to gravity:

$$\mathrm{C_1} = \mathrm{C_d A_0}\sqrt{2\mathrm{g}} \tag{63}$$

$$\mathrm{C_2} = \mathrm{C_d m}\sqrt{2\mathrm{g}} \tag{64}$$

The leakage flow rate Q was then computed using the equation below, in which h is the pressure head:

$$\mathrm{Q} = \mathrm{C_1 h^{0.5}} + \mathrm{C_2 h^{1.5}} \tag{65}$$

4.3. Improvements to the leak generation model

This section describes the improvements that were made to Schwaller and van Zyl's (2015) leak generation model. They include:

- incorporating the hydraulic properties (like the pressure head) of the pipe network for which the leaks are to be generated and distributed
- introducing the use of Infrastructure Leakage Index (ILI) concept to appraise leakage level while generating leaks
- introducing the distribution of leaks to pipes, considering the physical properties of the pipe network.

In addition to the above improvements, the leak generation model was written in the C/C++ computer programming language. This facilitates linking the model with hydraulic modelling tools, for example Epanet, of which the source code of the algorithm of the hydraulic network solver is written in the same programming language.

The subsections that follow describe each of the improvements to the leak generation model.

4.3.1. Incorporating hydraulic properties of the pipe network

The hydraulic properties of the system in which the leaks are to be distributed were incorporated into the model by requesting the user of the model to supply an input file in the format of the Epanet hydraulic modelling tool. The input file is supplied without any leak parameters.

The supplied input file is run in the Epanet hydraulic model to obtain pressure heads at the junctions; these are then weighted using the number of consumer connections. The pressure heads are weighted because they are significantly influenced by consumer demands. The procedure used in the weighting of the pressure heads assumes that the length of pipes

corresponds to the number of consumer connections. A detailed description of the pressure head weighting procedure is discussed in Chapter 2.

The average system pressure P_{av} and the average zone night pressure (AZNP) of the input water distribution network are then calculated from the weighted junction pressure heads using the hydraulic method that was proposed by Renaud et al. (2015) and discussed earlier in Chapter 2. See equations (45) and (46) respectively.

The unavoidable annual real losses (UARL) for the input water distribution network is then calculated; from this the unavoidable background leakage (UBL) is estimated as being 69% (Lambert 2009).

4.3.2. Incorporating the ILI in the generation of leaks

The level of leakage to be generated by the model (expressed as the ILI) is supplied by the user. Because the process of generating leaks is random, the input ILI is essentially a target value, providing a range within which the model should generate leaks. The actual system ILI is calculated from the leaks that have been generated.

4.3.2.1. Calculate statistical parameters

The process of generating leaks starts with the calculation of the statistical parameters, i.e. the mean μ and the standard deviation σ, of the discharge coefficients and the initial leak areas of both background and potentially detectable leaks. The procedure described by Schwaller and van Zyl (2015) is generally applied.

For the background leaks, a trial and error method was used to establish a mean μ and standard deviation σ, that resulted in an overall average background initial leak area of $0.12mm^2$.

For potentially detectable leaks, data for a system with a typical leakage level as defined in Schwaller and van Zyl (2015) was used to calculate the weighted number of potentially detectable leak events for each of the four categories. This data is presented in table 9.

Table 9: Data to estimate potentially detectable leak events

	Service pipes		**Mains**	
	Unreported	**Reported**	**Unreported**	**Reported**
Average runtimes of PD leaks (days)	365	16	365	6
Ratio of reporting PD leaks	0.25	0.75	0.05	0.95
Frequency of events for PD leaks (system with typical leakage level)	6.75 per 1000 connections per year		32.5 per 100 km per year	

With the weighted number of potentially detectable events, fractions are calculated for each category. The cumulative fractions of the weighted leaks, which must add up to 1, are then calculated and systematically presented as described by Schwaller and van Zyl (2015).

After the statistical parameters (μ and σ) have been calculated, the next step is to generate the discharge coefficient and the initial leak area and then calculate the head-area slope for each initial leak area that is generated.

4.3.2.2. Generating leak parameters

Using the statistical parameters i.e. μ and σ, probability distribution functions were used to generate the discharge coefficient (normal distribution) and initial leak areas (normal and lognormal distributions).

Leakage equivalent to the unavoidable background leakage (UBL) is generated first. This is 69% of the system's unavoidable annual real losses (UARL) as per the description of the UARL concept by Lambert (2009).

In practice, background leakage in water distribution networks is more than the unavoidable background leakage described in the theory. However, there was no available literature to establish the exact level of background leakage in a water distribution network. The model thus takes the unavoidable background leakage to be the only background leakage in the networks.

After all background leakage has been generated, potentially detectable leakage is then generated and added to the background leakage until the system's level of leakage, i.e. the calculated ILI, is within 0.001% of the target ILI. A strict condition of 0.001% permitted a very negligible deviation of the calculated ILI from the desired or target ILI.

Background leaks

To realistically model background leaks, two categories are considered, namely background leaks whose $N1$ is close to 1.5, and those whose $N1$ is not. The procedure to generate background leaks whose $N1$ is close to 1.5 is described first, followed by the procedure to generate background leaks whose $N1$ is not close to 1.5.

Background leaks whose N1 is close to 1.5

This category of background leaks is generated first as presented in the figure below:

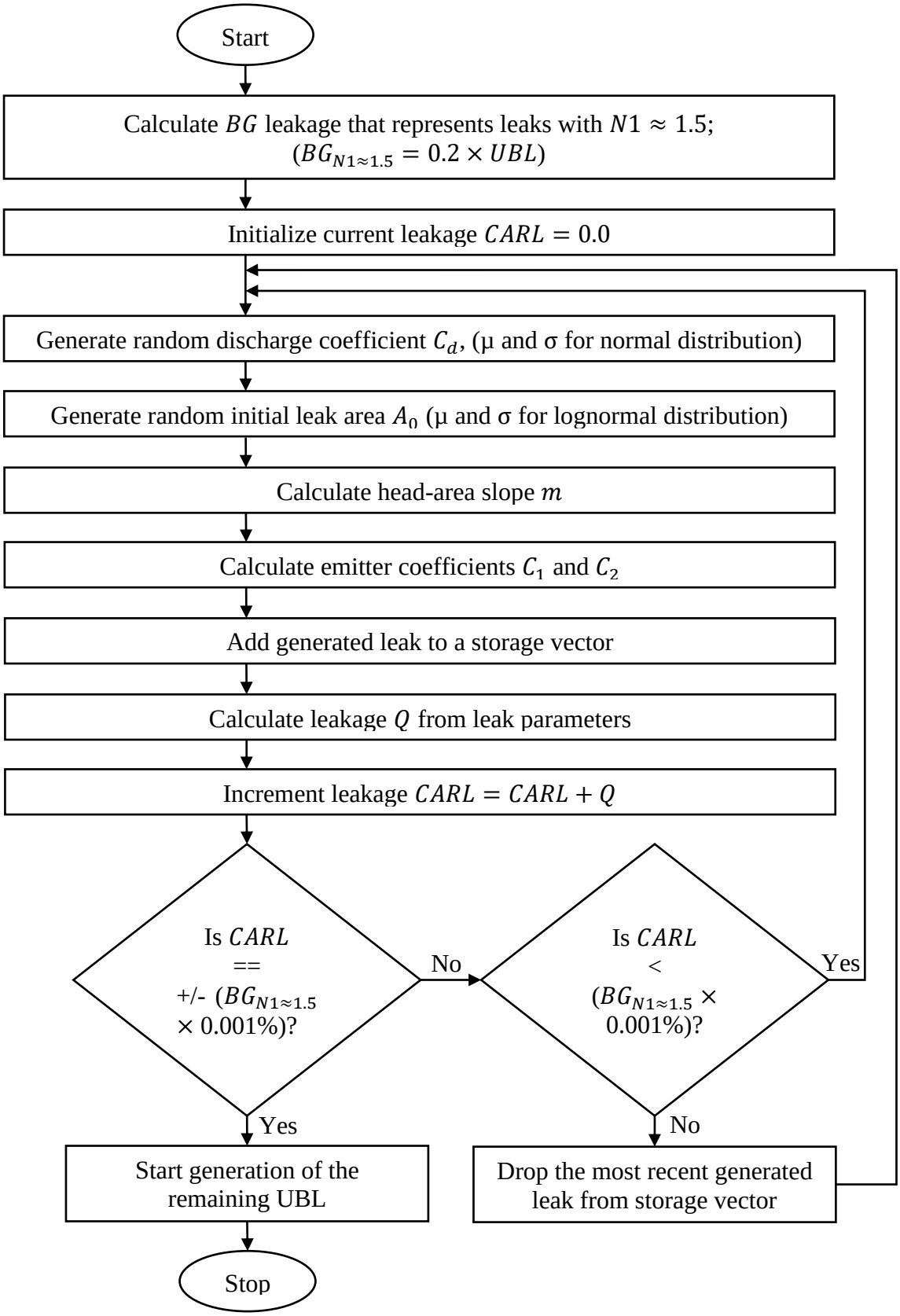

Figure 17: Layout of process to generate background leaks with a leakage exponent $N1$ close to 1.5

The model starts by calculating the leakage flow rate equivalent to leaks with $N1$ close to 1.5. This was considered as 20% of the UBL.

The current leakage flow rate which is referred to as the current annual real losses (CARL) to be consistent with the IWA's internationally recognised terminologies (Lambert and Hirner 2000), is then initialised.

Using mean μ and standard deviation σ of a normal distribution, a discharge coefficient is generated randomly.

The initial leak area A_0 is then generated using mean μ and standard deviation σ of a lognormal distribution for background leaks.

Considering leakage number L_N of 100, equation (61) is used to calculate the head-area slope m, since the average zone night pressure (AZNP) which was calculated during minimum night flow conditions is known.

The emitter coefficients C_1 and C_2 are then calculated using equations (63) and (64) respectively.

These coefficients are then stored in a storage vector created in the computer's memory.

The leakage flow rate Q of the most recent generated leak parameters is calculated using equation (65).

The leakage flow rate is then incremented and the updated current annual real losses (CARL) obtained.

Because the process of generating leaks is random, it is possible that the flow rate of the generated leakage might be below or above a target value. With that in mind, the current

leakage is tested to ensure that it is within 0.001% of the background leakage whose $N1$ is close to 1.5, i.e. $CARL = +/-0.001\% \times BG_{N1\approx1.5}$.

If the current leakage is less than 0.001% of the background leakage with N_1 close to 1.5, a new leak is generated and added to the storage vector. If it is more, then the most recently generated leak is dropped from the storage vector and a new leak generated until the desired condition is satisfied.

Background leaks whose N1 is not close to 1.5

When the generation of background leaks whose $N1$ is close to 1.5 is complete, leaks equivalent to the remaining background leakage, i.e. whose $N1$ is not close to 1.5, are generated.

There are three differences between the process for generating background leaks whose $N1$ is close to 1.5, and those whose $N1$ is not close to 1.5, as presented below:

- the current annual real losses (CARL) are not initialized when generating background leaks whose $N1$ is not close to 1.5; instead, the new leaks are accumulated to those that were generated previously
- the head-area slope m is calculated using an initial leak area (A_0) power equation (62)
- to maintain the level of leakage generated in the desired range, the current annual real losses (CARL) are checked against the unavoidable background leakage (UBL).

Potentially detectable leaks

The generation of the potentially detectable leaks commences when all the background leaks have been generated. The potentially detectable leaks are generated one at a time and added to the background leaks until the calculated ILI is within 0.001% of the target ILI. Figure 18 presents a layout of the process that is used to generate potentially detectable leaks.

Background leakage that was generated earlier becomes the current annual real losses (CARL) at the beginning of the process to generate potentially detectable leaks.

A discharge coefficient is generated randomly using the statistical parameters mean μ and standard deviation σ for a normal distribution.

A random number r between 0 and 1 is generated. A range is established in the systematically arranged cumulative fractions (C_{SU}, C_{SR}, C_{MU}, C_{MR}) to which r is found. This may be:

- between 0 and C_{SU}, for which an unreported leak on a service pipe (SU) is generated or
- between C_{SU} and C_{SR}, for which a reported leak on a service pipe (SR) is generated or
- between C_{SR} and C_{MU}, for which an unreported leak on main pipes (MU) is generated or
- between C_{MU} and C_{MR}, for which a reported leak on main pipes (MR) is generated.

Depending on the category of the potentially detectable leaks that has been selected, an initial leak area A_0 is then generated using corresponding mean and standard deviations for a normal distribution.

The head-area slope m is then calculated using the initial leak area power equation (62).

The emitter coefficients C_1 and C_2 are calculated using equations (63) and (64) respectively, and the generated leak parameters are added to the storage vector.

Using equation (65), the leakage flow rate Q of the most recently generated leak is calculated and added to the (CARL). The infrastructure leakage index (ILI) is then calculated.

The calculated ILI is tested whether it is within 0.001% of the target ILI. If the calculated ILI is less than 0.001% of the target ILI, a new potentially detectable leak is generated and added to the storage vector. If it is more, then the most recently generated leak is dropped from the storage vector and a new leak is generated until the desired condition is satisfied.

The process to generate potentially detectable leaks stops when the calculated ILI is within 0.001% of the target ILI.

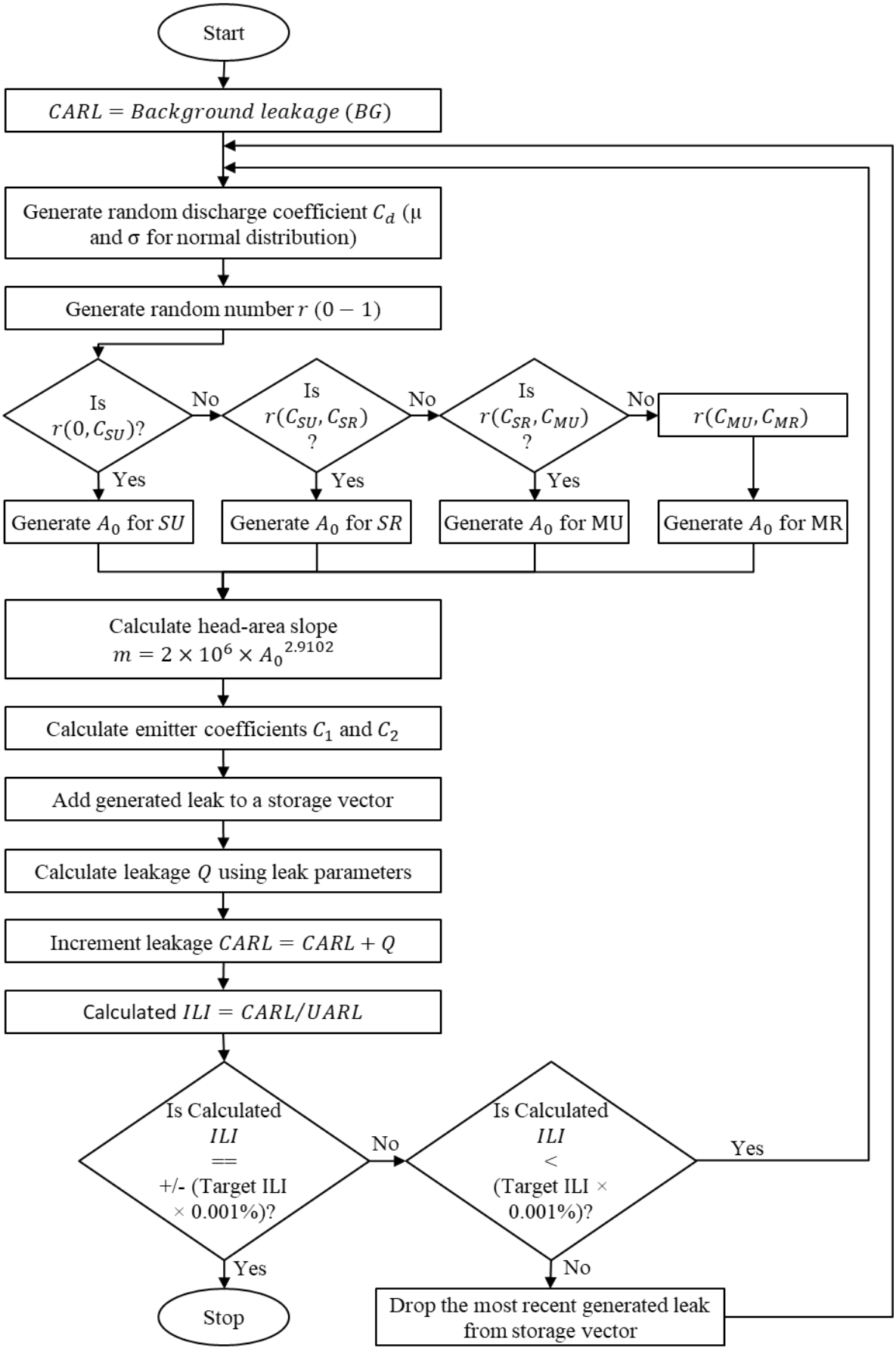

Figure 18: Layout of the process to generate potentially detectable leaks

4.3.3. Distribution of leaks

The model distributes leaks initially stored in the storage vector as per the procedure presented in figure 19 and described below:

a) A leak, which basically consists of two emitter coefficients $C_1 = C_d A_0 \sqrt{2g}$ and $C_2 = C_d m \sqrt{2g}$, is picked from the storage vector.

b) A random number R between 0 and 1 is then generated. This number is later used to distribute the leak to the two junctions that connect the pipe, if both junctions have emitters.

c) Another random number R_p between 0 and the total cumulative pipe length (TC_{pl}) is generated. R_p is later used to select a pipe to which the leak that was picked from the storage vector is allocated.

d) The next step is to select a pipe to which the leak will be allocated. The cumulative length of pipes is systematically arranged as shown in table 10. For example, if the random number R_p is 2500, then pipe $P3$ is selected and the leak is distributed between junctions $J21$ and $J22$. With this approach, the longest pipe in the pipe network is most likely being assigned a leak.

e) In the next step, the number of emitter junctions connected to the selected pipe are established. A pipe in a water distribution network could be connected to either two emitter junctions, or two non-emitter nodes (for example a reservoir and a tank), or one emitter junction. The selected pipe is then tested for the three scenarios.

   In the case where the selected pipe is connected to two emitter junctions, the random number R (generated in step b) above) is used to distribute the leak. Using the example of pipe $P3$ that was selected in step d), RC_1 and $(1 - R)C_1$ are added to the coefficients of the emitter with pressure head exponent 0.5 of junctions $J21$ and $J22$ respectively.

Similarly, the terms RC_2 and $(1-R)C_2$ are added to the coefficients of the emitter with pressure head exponent 1.5 of the two junctions $J21$ and $J22$ respectively.

In the case where the selected pipe is connected to one emitter junction, the entire leak is allocated to that junction. Using the example data in table 10, if the selected pipe is $P1$ which is connected to a tank and an emitter junction $J11$, then C_1 and C_2 are added to the coefficients of the junction $J11$ with pressure head exponents of 0.5 and 1.5 respectively.

If the selected pipe is not connected to any emitter junctions, for example if it is connected to two tanks, then another pipe is selected by generating a new random number R_p, in which case steps c) to e) are repeated.

f) The leak that was selected and distributed is then removed from the storage vector to ensure that each leak is distributed only once.

g) The model then checks whether all the leaks that were generated are distributed. If some leaks have not been distributed, then the model picks another leak and repeats steps a) to g), until all the leaks in the storage vector are distributed.

Table 10: Example of pipe length cumulative calculation

Pipe ID	Node 1	Node 2	Length (m)	Cumulative length (m)	Cumulative length range
P1	Tank	J11	200	200	0 – 200
P2	J11	J12	800	1,000	> 200 – 1,000
P3	J21	J22	2,000	3,000	> 1,000 – 3,000
P4	J11	J21	1,000	4,000	> 3,000 – 4,000

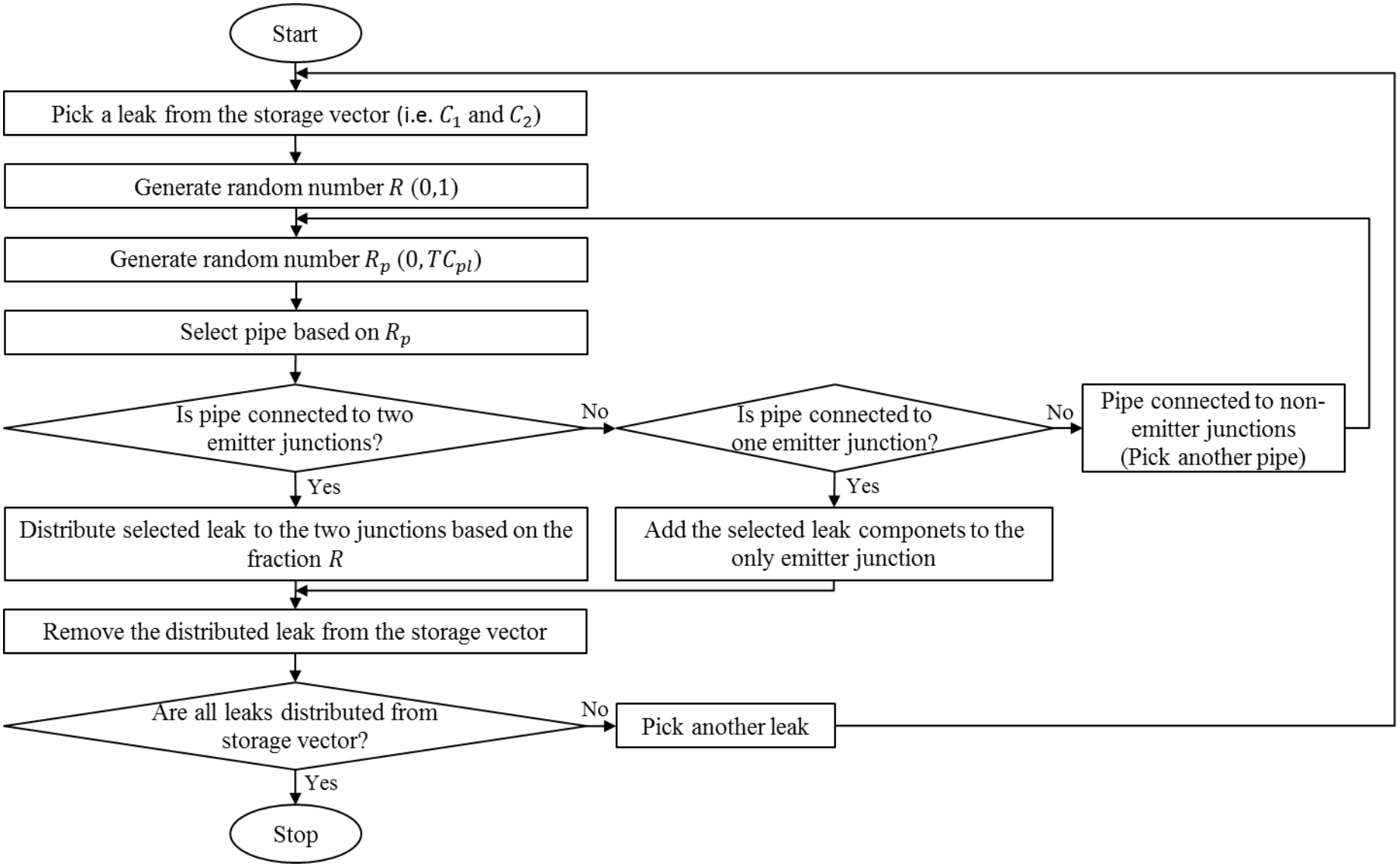

Figure 19: Layout of the process to distribute leaks in water distribution pipe network

4.4. Analysis of the generated leaks

This section analyses and compares the generated leaks to the study by Schwaller and van Zyl (2015). Leak parameters, i.e. the power equation's leakage exponents $N1$, the discharge coefficients C_d, the initial leak areas A_0 and the head-area slopes m are compared.

Three hundred systems with stochastically generated and distributed leaks as in Schwaller and van Zyl (2015) are considered. The systems are divided into three groups; each group has 100 systems. Each system in the first group has 100 leaks, in the second group it has 1000 leaks and in the third group it has 10,000 leaks.

The range of the power equation's system leakage exponents $N1$ for the 300 systems is compared first.

The range of discharge coefficients, initial leak areas and head-area slopes of the $10{,}000$ leaks are thereafter compared in the subsection that follows.

4.4.1. The power equation's leakage exponents

Figure 20 compares ranges of the power equation's leakage exponents $N1$ that were found in the Schwaller and van Zyl (2015) and in this study. The solid lines indicate the Schwaller and van Zyl's (2015) study results, while the dotted lines show the results of this study.

The range of leakage exponents show reasonably acceptable differences to the study by Schwaller and van Zyl (2015). These differences may be attributed to the impact of head losses due to pipe friction and the variation of pressure heads at the locations of leaks.

Schwaller and van Zyl (2015) study assumed a pipe network without head losses while this study incorporates all pipe network components, thus considering frictional head losses.

System leakage exponents also vary due to system pressure heads. Although the number of leaks generated in both studies were the same (i.e. 100, 1000, and 10000), the pressure heads at the leak locations are different.

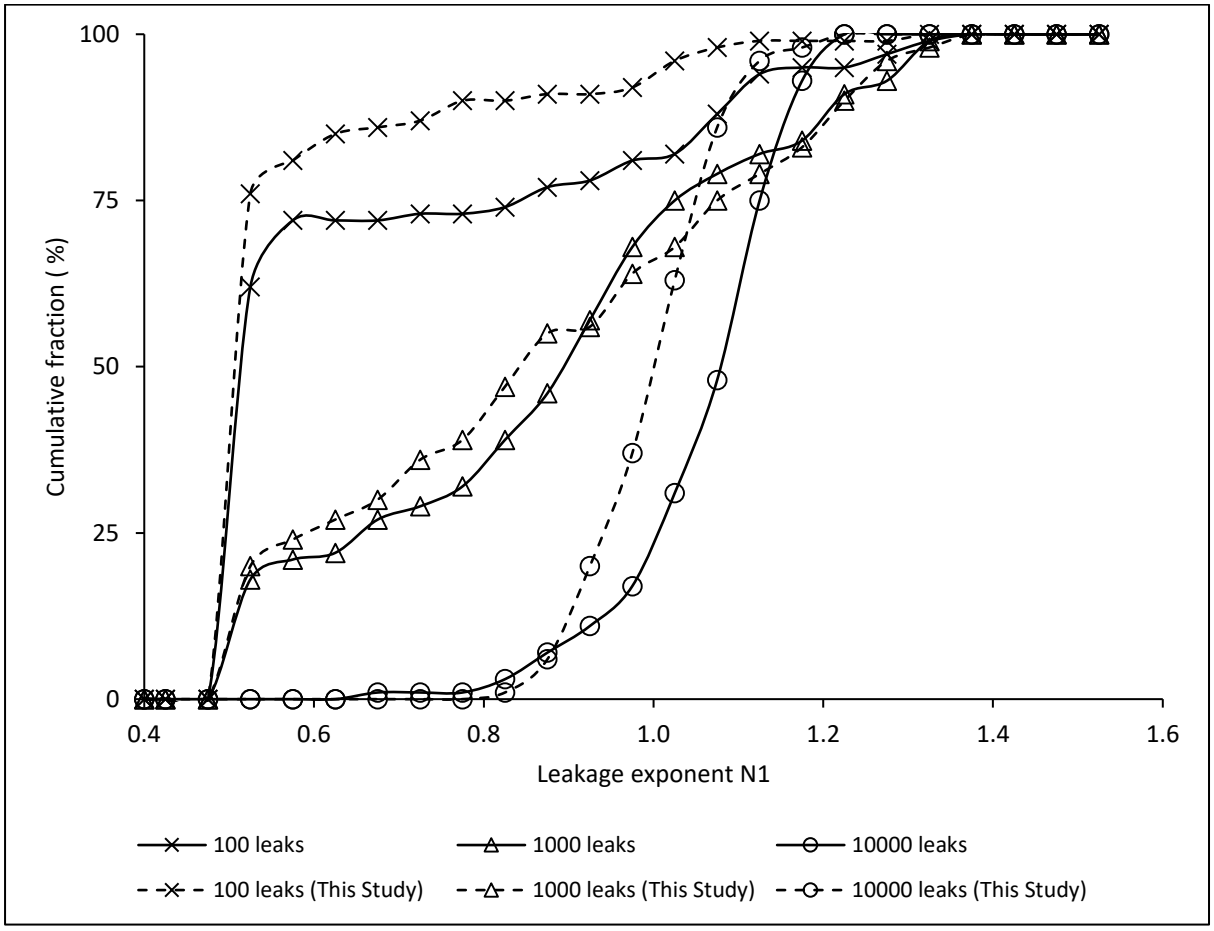

Figure 20: The range of leakage exponents of 300 systems as compared to the study by Schwaller and van Zyl (2015)

4.4.2. The modified orifice equation's leak parameters

The range of discharge coefficients C_d, the initial leak areas A_0 and the head-areas slopes m of 10,000 stochastically generated leaks are compared to Schwaller and van Zyl's (2015) study.

Figure 21 shows a comparison of the discharge coefficients. The values are sorted in ascending order to have a smoothly plotted graph. The range of values observed in both studies are very similar.

Figure 22 shows a comparison of the initial leak areas. Like the discharge coefficients, the initial leak areas have also been sorted in ascending order to have a smoothly plotted graph. The horizontal axis is a logarithmic scale because of a broader spectrum of initial leak areas, (lowest: $2.14 \times 10^{-08}\ mm^2$ and highest: $205.69\ mm^2$). A very similar range of initial leak areas is observed in both studies.

Figure 23 shows the comparison of the head-area slopes. For the same reasons as for the initial leak areas, the head-area slopes have been sorted in ascending order and the horizontal axis is a logarithmic scale. Again, a very similar range of head-area slopes is observed in both studies.

Overall, the comparisons of the discharge coefficients, the initial leak areas, and the head-area slopes as presented in figures 21, 22 and 23 respectively, were good enough to use Schwaller and van Zyl's (2015) study as a benchmark for the leak generation process.

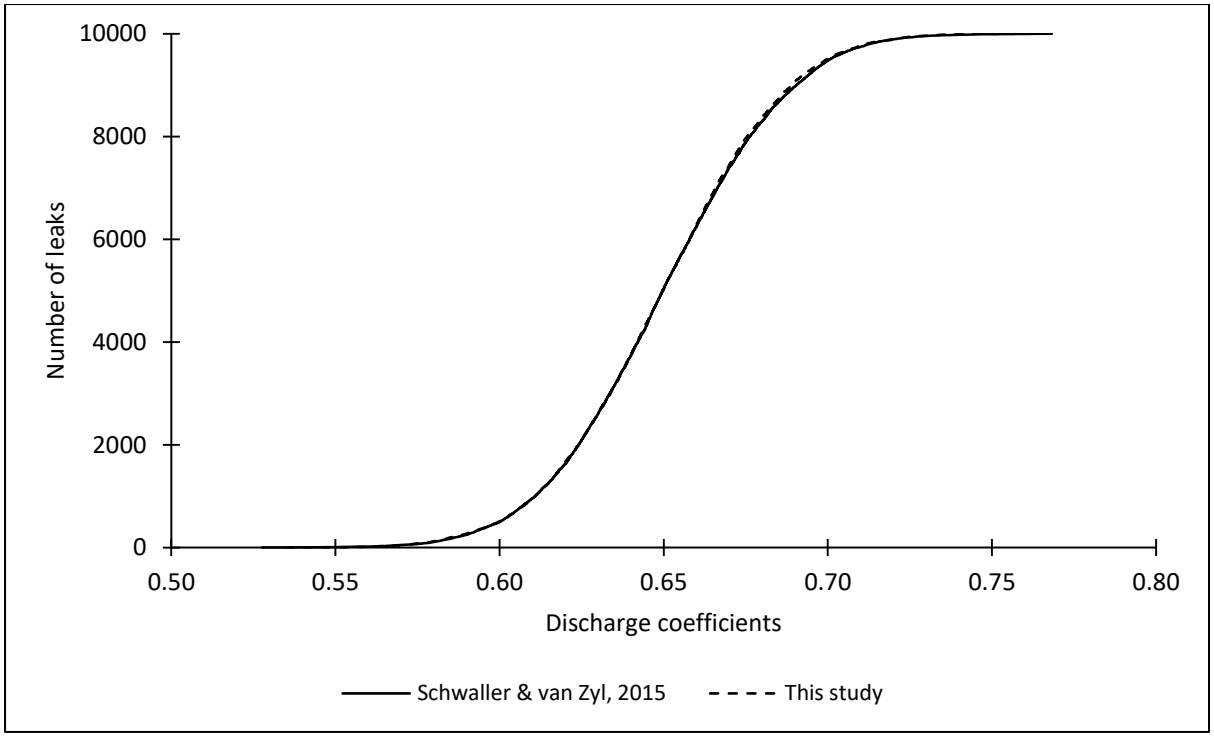

Figure 21: The range of discharge coefficients as compared to the study by Schwaller and van Zyl (2015)

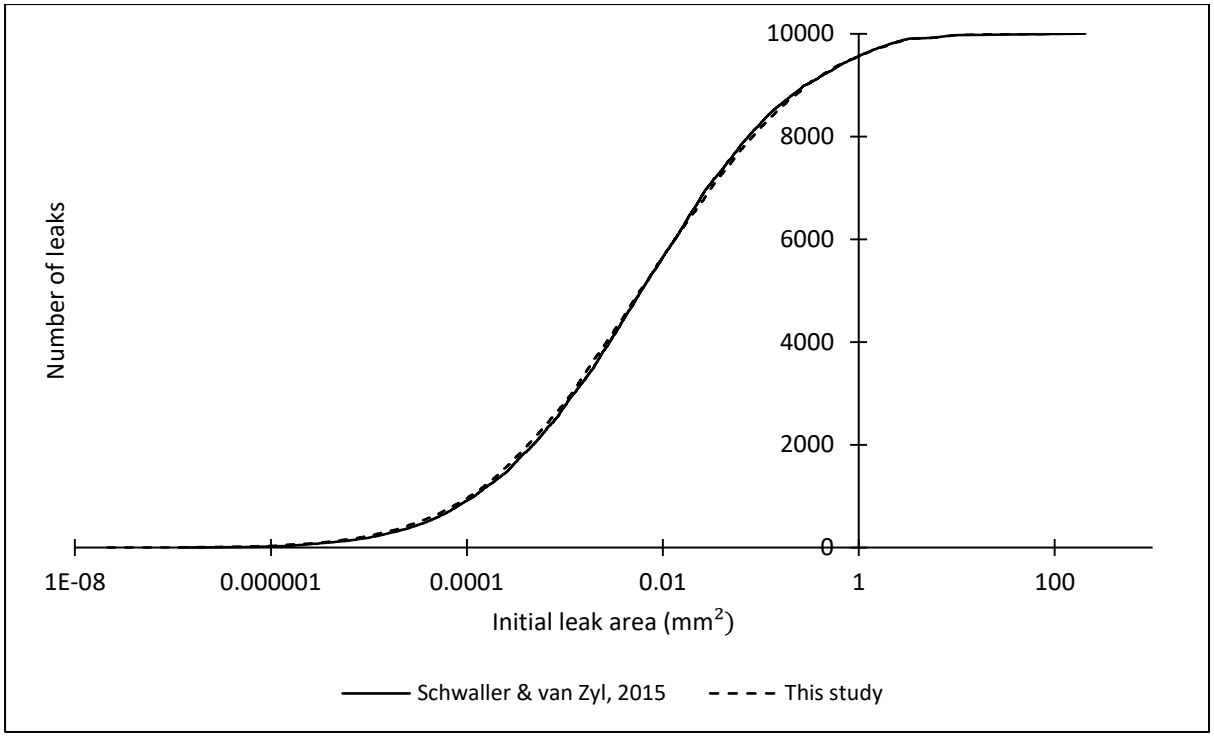

Figure 22: The range of the initial leak areas as compared to the study by Schwaller and van Zyl (2015)

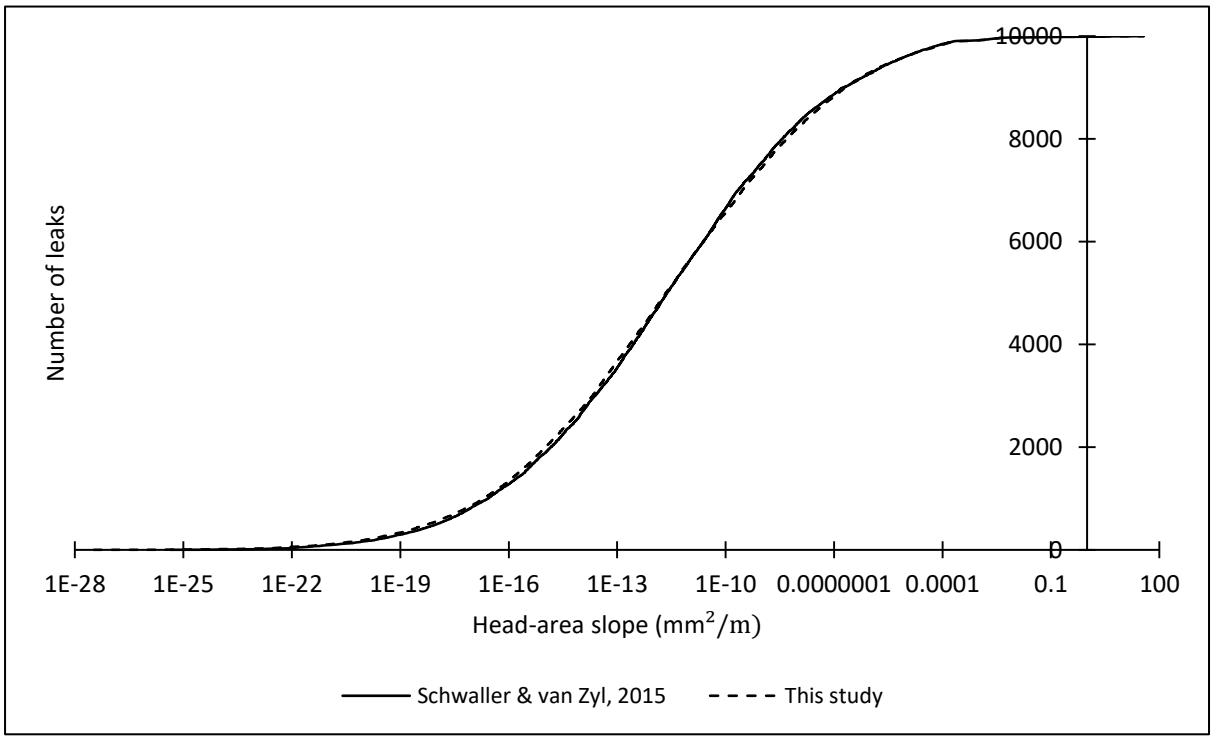

Figure 23: The range of head-area slopes as compared to the study by Schwaller and van Zyl (2015)

4.5. Summary of the chapter

This chapter has described a stochastic model for leak generation and distribution that was developed based on the model that was suggested by Schwaller and van Zyl (2015).

First, the Schwaller and van Zyl's model was described and thereafter the improvements made were discussed. The improvements include the integration of the hydraulic properties of the pipe network for which the leaks are to be generated and distributed, the introduction of the Infrastructure Leakage Index (ILI) concept to appraise leakage level, and the distribution of leaks to the pipes which considers the physical properties of the network.

The range of parameters of the generated leaks (i.e. the leakage exponents, discharge coefficients, initial leak areas and head-area slope) were then compared to those in the Schwaller and van Zyl's study. The comparison found very close ranges for each of the leak parameters.

5. Impact of leakage equations on modelling results

5.1. Introduction

This chapter presents an evaluation of the impact of using the modified orifice equation instead of the power equation for pressure and leakage modelling in water distribution pipe networks. It is important to understand the impact of the leakage equations on simulation accuracy and convergence to decide whether and when, in hydraulic simulations, the modified orifice equation should be used instead of the power equation.

The analysis assumes that the modified orifice equation simulates the true behaviour of leaks in water distribution pipe networks. This assumption is made because the modified orifice equation is based on fundamental hydraulic principles. Furthermore, recent research has verified that a leak area expands linearly with an increase in pressure (Cassa et al. 2010; van Zyl and Cassa 2014). This linearity is explicitly incorporated into the modified orifice equation. On the other hand, the power equation is simply an empirical formulation as described earlier in Chapter 2. The study, therefore, aims to identify under what conditions the power equation produces adequate results, and when the simulation errors are large enough to necessitate a change of simulation approach to the modified orifice equation.

The evaluation was based on three water distribution networks (small, medium and large) and four levels of leakage equivalent to infrastructure leakage indices (ILIs) of 1, 4, 16 and 64. ILIs of 1 and 64 were used to model the lowest and the highest system leakage levels respectively, while ILIs of 4 and 16 modelled moderate and typical leakage levels respectively. Although systems with leakage levels higher than the equivalent ILI of 64 have been reported in practice (Seago et al. 2005), in this research it was deemed sufficient to use ILI of 64 as the highest system leakage level in all three differently sized networks.

Two hundred (200) individual systems with stochastic leakage distributions were generated for each combination of the standard network and leakage level. In total, 2400 stochastic distributions (i.e. three different size networks times four leakage levels per network, times two hundred systems per combination of network and leakage level) were generated and analysed.

Each system was simulated at two input pressures: a high initial pressure representing normal operating conditions and a reduced pressure representing a system with pressure management implemented. A large pressure difference between the initial and the pressure managed conditions was used to allow differences in simulation results to be enhanced for evaluation purposes.

Section 5.2 describes the three water distribution pipe networks used in the study as examples. Their physical and some hydraulic properties are presented to illustrate the uniqueness of each network.

A description of the methodology used to evaluate the impact of leakage equations on modelling results is subsequently presented in section 5.3. First a generalized flow chart is given, and then each step is explained in the paragraphs that follow.

Thereafter, a detailed analysis of diurnal simulation results of a typical individual system and a typical set of 200 stochastically generated systems (medium network with an infrastructure leakage index of 16) is presented in section 5.4. Two nodes were considered in analysing pressure head and leakage flow rate variation during the 24-hour simulation period: the average zone pressure (AZP) node which is representative of the system's average pressure head and the critical node at which the pressure head is at its minimum during peak demand conditions. This analysis shows explicitly the investigations conducted and detailed results of all the 2400

individual systems (i.e. 12 sets of 200 systems each that have the same example network and leakage level), are presented in Appendix A.

An evaluation of the impact of different leakage levels on each of the three example networks follows in section 5.6. The results of the medium network's leak distribution, picked randomly, are discussed here in detail, while the results of all the networks (small, medium and large) are presented in Appendix B.

The impact of network size on simulation results was also investigated and the results are discussed in detail in section 5.7. All three networks are compared for the same leakage level. The results of leakage level equivalent to infrastructure leakage index of 16, picked randomly, are discussed in this section. The results of all other simulations are presented in Appendix C.

Finally, the overall trends and noteworthy results are pointed out and discussed in the last section of this chapter.

5.2. Example networks

Three different sized (i.e. small, medium and large) water pipe networks were used to evaluate the modified orifice equation through hydraulic modelling. Table 11 summarizes the physical properties of these networks and figures 24, 25 and 26 show their respective schematic layouts.

The small and medium networks were both adapted from example networks of Epanet, i.e. Net1 and Net3 respectively. Adjustments were made to both networks to ensure that they operate under gravity and that each one is supplied from a single point thereby enabling control of system pressure.

The original Epanet's Net1 network has a reservoir and a storage tank. It also operates under pumping, with the pump connected to the reservoir. To have a single system input point where system pressure can be controlled, the storage tank was removed from the adapted network. In addition to this, the pump was eliminated to make the system operate under gravity and therefore more feasible for the implementation of pressure management. With the elimination of the pump the head at the single water supply point was adjusted to maintain the system pressure heads close enough to their state before network modification.

The original Epanet's Net3 network has two water supply points, i.e. a river and a lake, and three storage tanks. Both sources (river and lake) have pumps connected to them, pumping water directly into the system. To have a single water supply point, the lake and the three storage tanks were removed. In addition, both pumps were eliminated and the head at the remaining supply point was adjusted to reasonably maintain the same range of system pressure to what it was before network modification. Also, Net3 network may be skeletonised but this was not considered when leaks were distributed. It was assumed that the fact that the network was skeletonised would not significantly affect the distribution of leaks.

The large network was adapted from a water distribution network model of the central business district of Durban, a coastal city and part of the eThekwini Metropolitan Municipality in South Africa. The municipality spans in an area of approximately 2,297 km^2 with a population of approximately three and a half million people according to the Statistics South Africa (2011 Census). The adapted district metered area (DMA) has a mixed consumption pattern as shown in

table 12. A single water supply point to the adapted DMA was considered to make the implementation of pressure management feasible.

It should be noted that the modifications made to the example networks were only intended to define and control pressure heads, and that Epanet software with the modified orifice equation can be used on any network size with any complexity like multiple pumps and sources.

Table 11: Physical properties of networks used in evaluation of the impact of leakage equations on modelling results

Network	**Number of junctions**	**Pipe length (km)**	**Pipe diameter range (mm)**
Small	8	19.3	150 - 450
Medium	85	60.0	200 - 750
Large	747	103.8	25 - 800

Table 12: Consumption data for the large network (eThekwini Municipality)

Demand category	**Average consumption (m^3/conn/day)**	**Number of connections**	**Total consumption (m^3/day)**
Domestic	1.10	2389	2628
Industrial	19.62	124	2433
Commercial	8.90	917	8161

Institutional	10.69	21	224

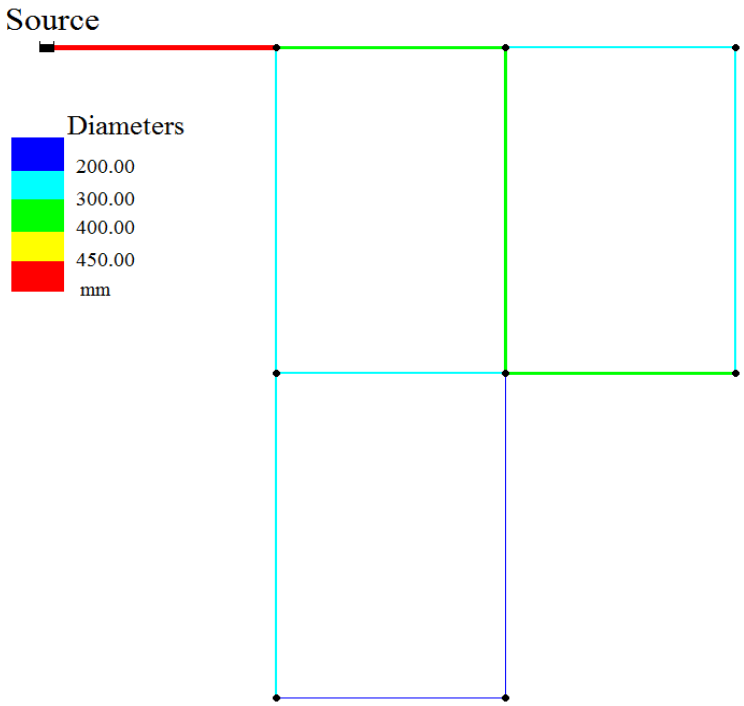

Figure 24: Schematic pipe layout of the small network adapted from Net1 of the Epanet example networks

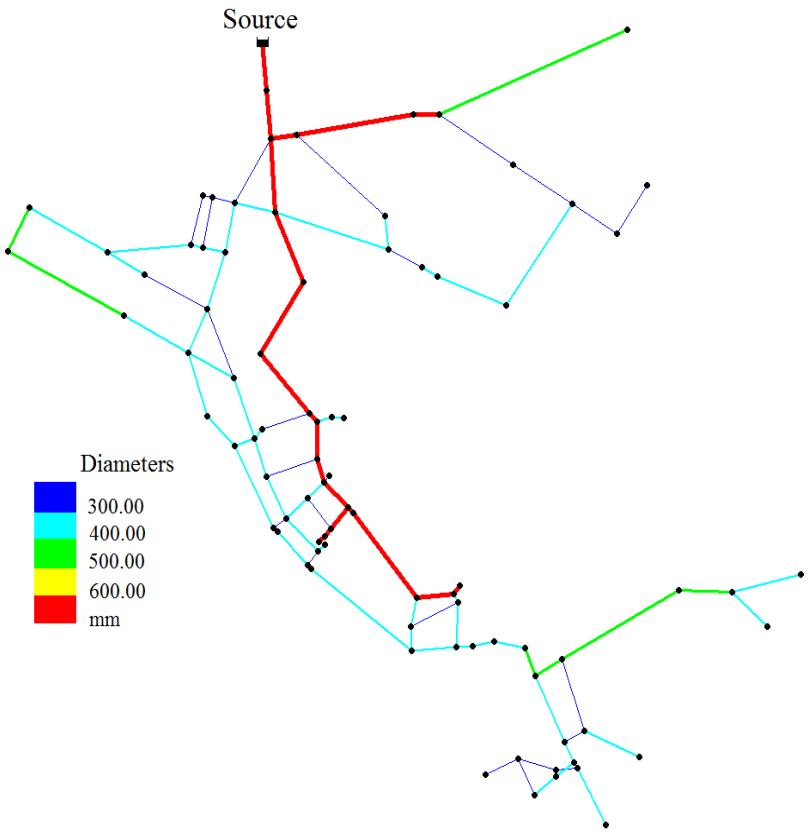

Figure 25: Schematic layout of the medium network adapted from Net3 of the Epanet example networks

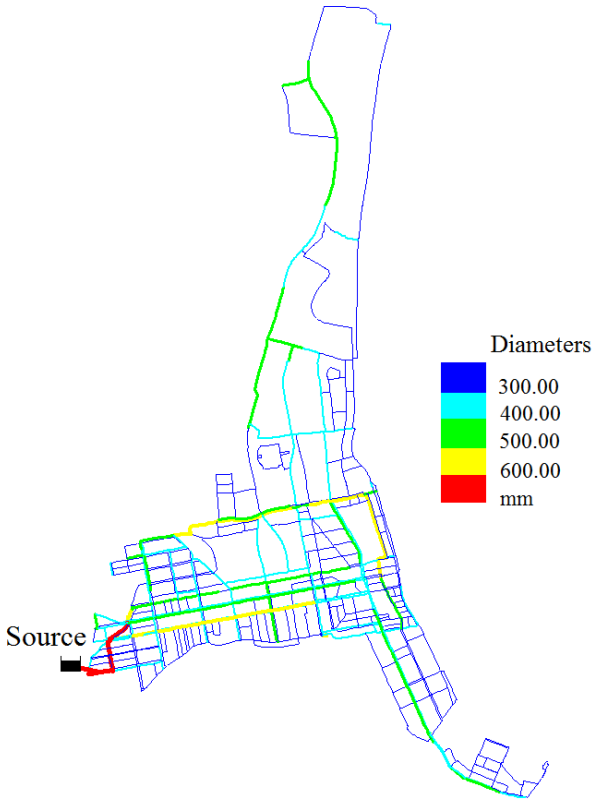

Figure 26: Schematic layout of the large network which was adapted from a water distribution system in the City of Durban, South Africa

Table 13 presents some hydraulic properties of these example networks for the lowest and highest leakage levels (i.e. ILIs of 1 and 64). The pressure heads at the AZP node and system consumer demands during both MNF and peak demand conditions are presented. Scenarios of before and after the implementation of pressure management are considered for the pressure heads.

The difference between the pressure heads before and after the implementation of pressure management was deliberately made large to allow simulation errors to be studied. These models are therefore not meant to represent a typical distribution pipe network. Nevertheless, such cases are not unrealistic, and examples can be found in real pipe networks. The level of the reservoirs is maintained constant during the extended period simulation.

As expected, the system with an ILI of 1 showed higher AZP pressure heads than the one with an ILI of 64. During minimum night flow the system with an ILI of 1 was found to have 3.4%, 13.1% and 2.4% more initial AZP pressure heads than the one with an ILI of 64, for the small, medium and large systems respectively. Likewise, during peak demand conditions, the differences were 12.1%, 19.1% and 7.6% for the small, medium and large networks respectively.

Table 13: Hydraulic properties of the example networks used to evaluate the modified orifice equation

		ILI of 1			**ILI of 64**		
		Small	**Medium**	**Large**	**Small**	**Medium**	**Large**
MNF	Initial AZP node pressure head (m)	86.5	105.9	113.4	83.6	93.6	110.7
	AZP node pressure head after pressure management (m)	26.5	56.0	33.6	26.2	50.1	33.1
	Consumer demand (m^3/h)	3.5	1581.6	965.6	3.5	1581.6	965.6
Peak demand	Initial AZP node pressure head (m)	77.0	72.4	99.0	68.7	60.8	92.0
	AZP node pressure head after pressure management (m)	17.0	22.6	19.2	15.4	18.8	18.0
	Consumer demand (m^3/h)	385.5	3003.1	7133.1	385.5	3003.1	7133.1

5.3. Methodology

The procedure used in investigating the impact of the leakage equations on simulation results is presented in figure 27 and described in detail thereafter.

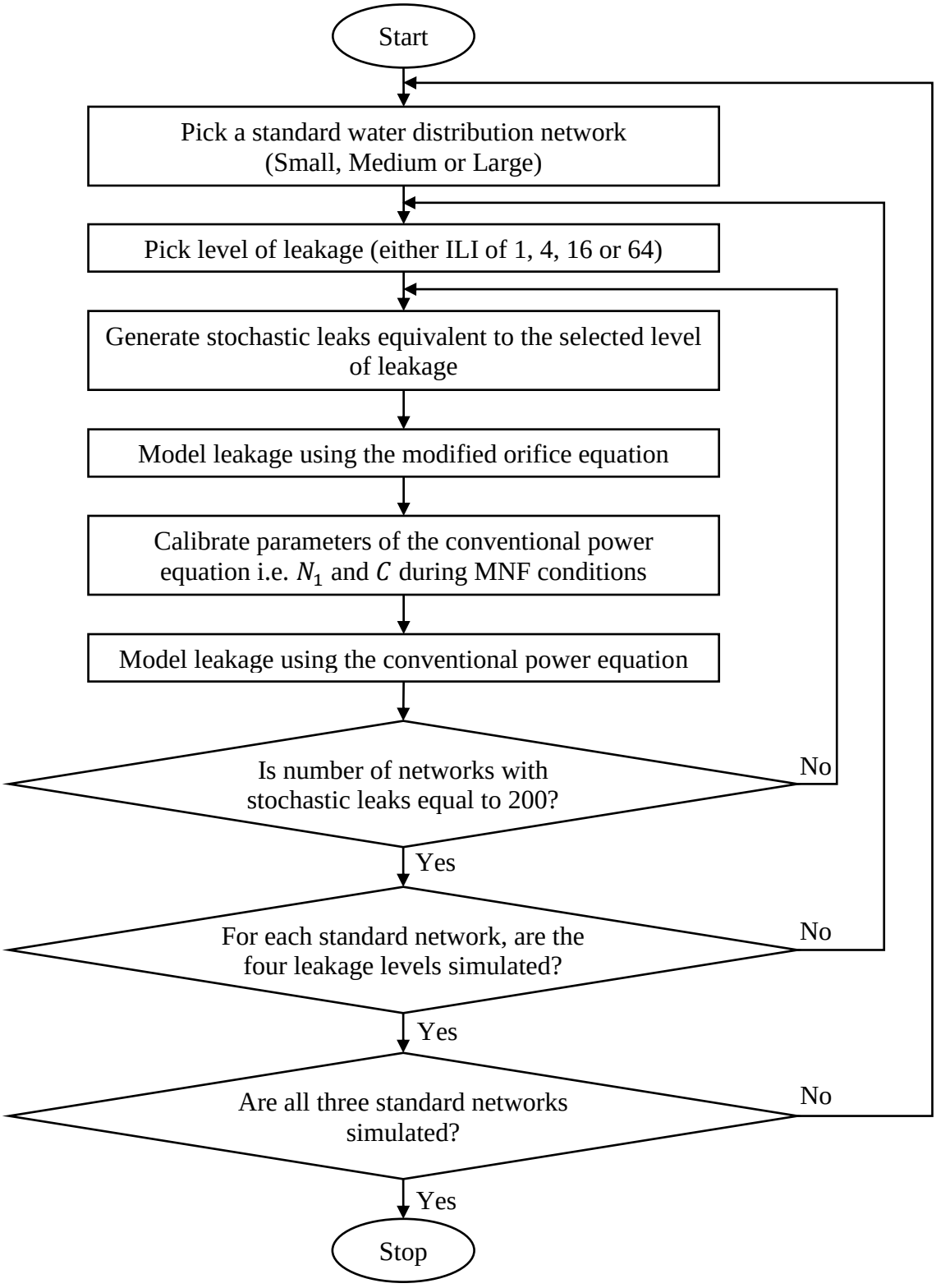

Figure 27: Procedure to evaluate the impact of leakage equations on modelling results

a) The procedure commences with a sequential selection of small, medium and large water distribution networks. A static hydraulic simulation (without leakage in the pipe networks) is conducted to establish the average zone pressure (AZP) node as well as the critical node for that network. Identifying these two nodes is crucial because hydraulically simulated parameters like pressure head and leakage flow rate variations are analysed on both nodes during the 24-hour simulation period.

b) For the network selected in a) above, a leakage level is chosen that has an equivalent infrastructure leakage index (ILI) of 1, 4, 16 or 64. The infrastructure leakage index of 1 represents a system with the lowest possible leakage level while an ILI of 64 represents a system with a very high leakage level. The ILIs of 4 and 16 are typical of most real water distribution pipe networks in many parts of the world especially developing countries (Liemberger and McKenzie 2005).

c) Stochastic leaks equivalent to the leakage level chosen in b) are then generated and distributed as explained in Chapter 4.

d) Subsequently, leakage is modelled using the modified orifice equation. The selected water distribution network, with leaks distributed, is then simulated as follows:

    i. Under normal conditions (i.e. before pressure management implementation).

    A hydraulic simulation is performed. Individual nodal pressures and leakage flows are obtained from which the total system leakage is calculated. The number of iterations required for the system to converge to a hydraulic solution is also recorded.

    ii. After implementation of pressure management.

    The hydraulic head at the single supply point is then reduced to a lower value to model the implementation of pressure management. A hydraulic simulation

is run again and the individual nodal pressure heads and leakage flows are obtained. The total system leakage flow rates are also calculated.

e) The next step is to calibrate the parameters of the conventional power leakage equation which are equivalent to the generated system leakage flow rates. The following two steps were followed for this process:

   i. Estimating the equivalent system leakage exponent $N1$ of the power equation.

   With a 5m head differential at the supply point, two (i.e. before and after pressure reduction) average night zonal pressure (AZNPs) points and their respective system leakage flows during minimum night flow (MNF) are applied to estimate the system leakage exponent $N1$ using equation (13).

   ii. Estimating junction leakage coefficients.

   The format of the input file is then converted from that of the modified orifice equation to that of the conventional power equation. This is done by estimating the leakage coefficients for identical nodal leakage flows of each junction during minimum night flow conditions. Equation (14) is used in estimating each junction's leakage coefficient since the system leakage exponent $N1$ and the flow rate Q are already known.

f) Thereafter, leakage is modelled using the conventional power leakage equation. With the input file in the format of the conventional power leakage equation, hydraulic simulations are performed both before and after the implementation of pressure management. The same procedure as explained in step d) above is repeated for the conventional power formulation. Individual nodal pressures and leakage flow rates are obtained, from which the total system leakage flow rates are calculated. The number of iterations required for the systems to convergence to a hydraulic solution are also recorded.

g) For the chosen network and leakage level, steps c, d, e and f are repeated until 200 systems with stochastic leak distributions are generated.

h) Then the next leakage level is selected. This is repeated until all the four equivalent leakage levels have been simulated for each network size.

i) In the last step of the model, the next network size is selected. This is repeated until all three water distribution pipe networks have been simulated with the four leakage levels. In total, 2400 individual systems (i.e. three different size networks times four leakage levels times two hundred systems) with stochastic leak distributions are generated.

5.4. Simulation results for a typical individual system

5.4.1. Introduction

Presented here are diurnal simulation results of an individual system with stochastically generated and distributed leaks. Because all networks are analysed in the same way, one of the networks, which is the medium network with an infrastructure leakage index of 16, is discussed in detail in this section. The rest of all network simulation results are given in Appendix A.

In the subsection 5.4.2 an analysis of nodal pressure variations is presented at the two vital points in the system, namely the average zone pressure (AZP) node and the critical node.

This is followed by an analysis of the diurnal leakage flow rate variations in subsection 5.4.3, first at all the nodes in the system and thereafter at the critical node.

Finally, in subsection 5.4.4 the number of iterations that the global gradient algorithm (GGA) in Epanet requires to converge, thereby finding a hydraulic solution, is presented for both the modified orifice and the power equation approaches.

5.4.2. Nodal pressure heads

5.4.2.1. Pressure head variation at the average zone pressure (AZP) node

The variation of pressure head at the AZP node is presented in table 14 and figure 28. Before leaks were distributed to the system, the arithmetic mean pressure head over a 24-hour simulation was $88.62m$. This reduced to $84.99m$ for the modified orifice equation and to $85.01m$ for the conventional orifice equation after the distribution of leaks. The minimum and maximum pressure heads were $72.69m$ and $106.08m$ respectively before the distribution of leaks. With leaks distributed, the minimum pressure heads were $69.16m$ and $69.21m$ for the modified orifice equation and the power equation respectively. The maximum pressure heads

for both equations were $102.78m$ after the distribution of leaks. These results show that in practical terms it makes no difference in the system pressure heads whether the modified orifice equation or the power equation is used.

Pressure management was then implemented and the arithmetic mean pressure was found to be $37.11m$ and $37.29m$ for the modified orifice equation and the power leakage equation respectively. The minimum pressure heads were $21.52m$ and $21.80m$ for the modified orifice and the power equation respectively, while the corresponding maximum values were $54.48m$ and $54.55m$ respectively. These results show that irrespective of the equation used, the system pressure heads will be practically the same even after the implementation of pressure management.

Generally, irrespective of whether pressure heads are modelled before or after the implementation of pressure management, the results show clearly that the pressure heads at the AZP node are influenced very little by the level of leakage and hardly at all by the equation used. The reason for this could be that the leakage flow rate in the model is relatively small compared to the actual consumer demand and therefore has less impact on the pressure head. The percentage error in estimating pressure head by the conventional power equation is presented later in subsection 5.6.4.

Table 14: Pressure head variation at AZP node before and after pressure management

		Pressure head (m)			
		Minimum	**Arithmetic Mean**	**Median**	**Maximum**
Before pressure management	Without leaks	72.69	88.62	90.24	106.08
	Modified orifice equation	69.16	84.99	86.53	102.78
	Power equation	69.21	85.01	86.54	102.78
After pressure management	Modified orifice equation	21.52	37.11	38.65	54.48
	Power equation	21.80	37.29	38.81	54.55

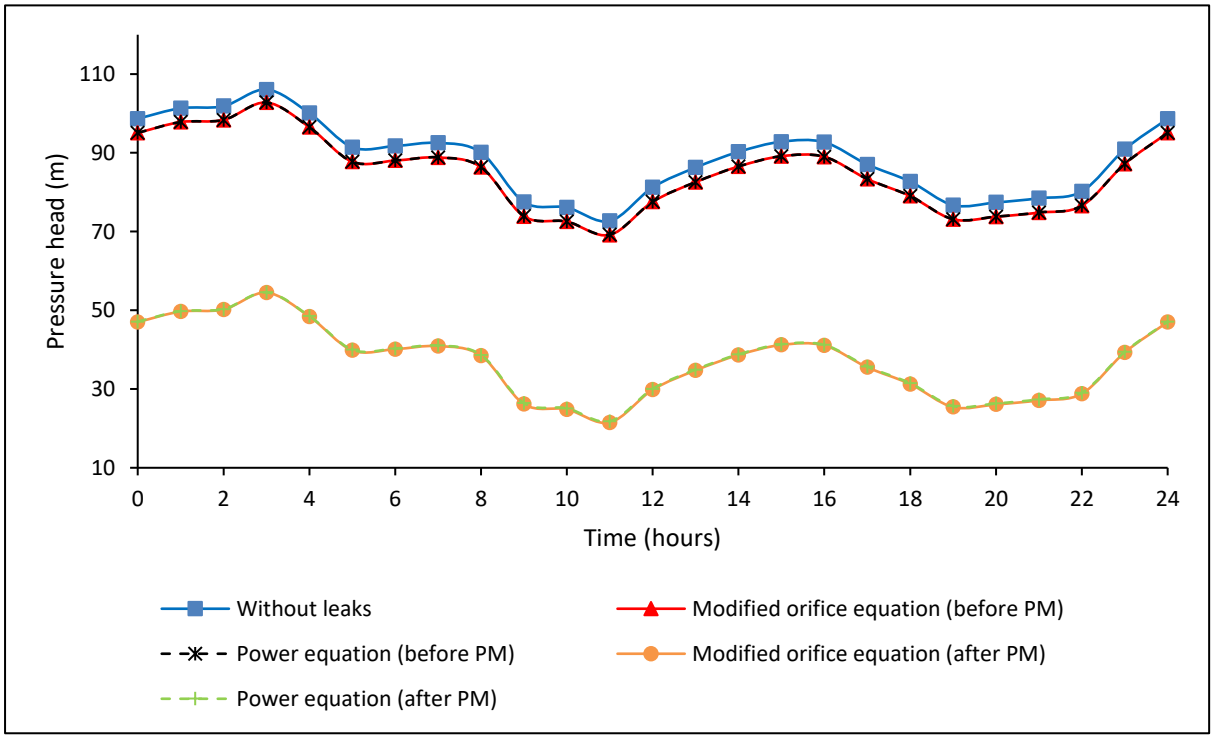

Figure 28: Pressure variation at AZP node before and after pressure management

5.4.2.2. Pressure head variation at the critical node

Pressure head variation at the critical node is presented in table 15 and figure 29. Before leaks were distributed, the arithmetic mean pressure head was $75.09m$, while the minimum and maximum values were $60.21m$ and $90.93m$ respectively.

With leaks distributed, the arithmetic mean pressure head was $71.77m$ and $71.78m$ for the modified orifice equation and the conventional power equation respectively. The minimum and maximum pressure heads were very close in both approaches. These results show that this level of leakage had little influence on the pressure head at the critical node, and practically no impact of the type of leakage modelling equation used.

Pressure management was then implemented and the arithmetic mean pressure head was found to be $23.71m$ and $23.87m$ for the modified orifice and power equations respectively. The minimum pressure heads were $9.13m$ and $9.39m$, with corresponding maximum values $39.46m$ and $39.53m$ respectively. Again, the same behaviour observed before implementation of pressure management was observed after implementation, in that the two approaches showed practically no differences in the pressure heads.

As was the case for the pressure head analysis at the AZP node, the above results clearly show that the pressure heads at the critical node were generally very close for both the modified orifice and power equation tools, both before and after the implementation of pressure management.

Table 15: Pressure head variation at critical node before and after pressure management

		Pressure head (m)			
		Minimum	**Arithmetic Mean**	**Median**	**Maximum**
Before pressure management	Without leaks	60.21	75.09	76.77	90.93
	Modified orifice equation	56.97	71.77	73.36	87.90
	Power equation	57.02	71.78	73.37	87.90
After pressure management	Modified orifice equation	9.13	23.71	25.30	39.46
	Power equation	9.39	23.87	25.45	39.53

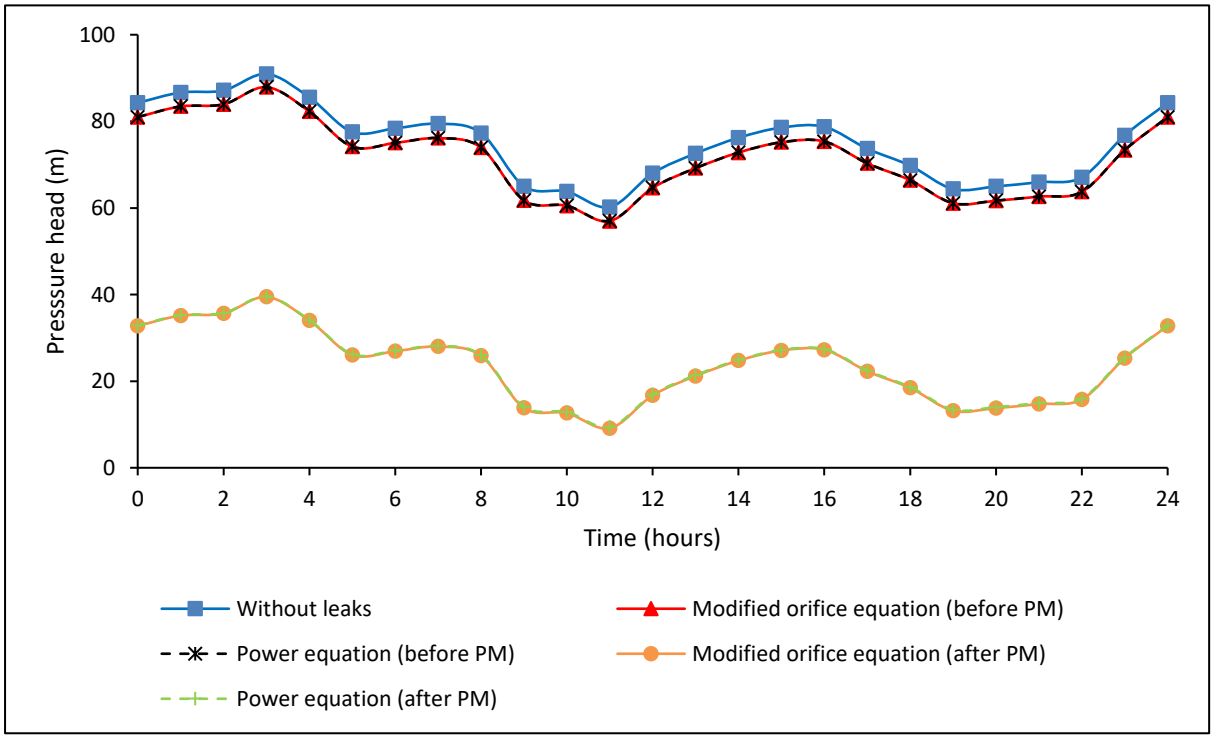

Figure 29: Pressure variation at critical node before and after pressure management

5.4.3. Leakage flow rate

5.4.3.1. System leakage flow rate variation

System leakage flow rate is the sum of leakage flow rates at all junctions in the system during the entire period of simulation; in this study, it is 24 hours. Variation in system leakage flow rates before and after the implementation of pressure management is presented in table 16, figures 30 and 31.

Before the implementation of pressure management, the leakage flow rate modelled in both approaches, i.e. the modified orifice and power equations, was practically the same. The arithmetic mean of the leakage was $144.78 m^3/h$ and $144.22 m^3/h$ for the modified orifice equation and the conventional power equation respectively. On average the conventional power equation underestimated leakage by 0.4%, which is an insignificant error in practical terms. The minimum leakage flow rates were $115.15 m^3/h$ and $113.44 m^3/h$ respectively, while both formulations showed the same maximum value of $179.23 m^3/h$.

The calibration of system leakage exponent $N1$ and therefore the approximation of the expansion of leaks in the power equation was done during minimum night flow, before the implementation of pressure management. This is the reason why the two formulations show the same leakage flow rate results during minimum night flow. Relative differences in the leakage flow rates are observed as pressure heads become different from the ones observed during minimum night flow conditions. These results further confirm that the power equation will give realistic results only under the conditions under which it has been calibrated.

After the implementation of pressure management, the arithmetic average of the leakage flow rates was $61.98 m^3/h$ and $55.22 m^3/h$ for the modified orifice and power equations respectively. It was found that on average the power equation underestimated system leakage

flow rate by almost 11%. The highest error was 24.07% during period 11, which was the time when the pressure head was the furthest from the one during minimum night flow, when the power equation parameters were calibrated.

Generally, the error in estimating leakage by the power equation was greater after the implementation of pressure management than before. It is also evident from these results that the error in leakage modelling by the power equation increases as the pressure difference, from the one at which the power equation parameters were calibrated, increases. This is shown in both figures 30 and 31, during periods 11 and 19 when the error is highest.

Table 16: System leakage variation before and after pressure management

		Leakage flow rate (m^3/h)			
		Minimum	**Arithmetic Mean**	**Median**	**Maximum**
Before pressure management	Modified orifice equation	115.15	144.78	147.42	179.23
	Power equation	113.44	144.22	147.06	179.23
After pressure management	Modified orifice equation	38.76	61.98	64.00	89.07
	Power equation	29.43	55.22	57.50	85.15

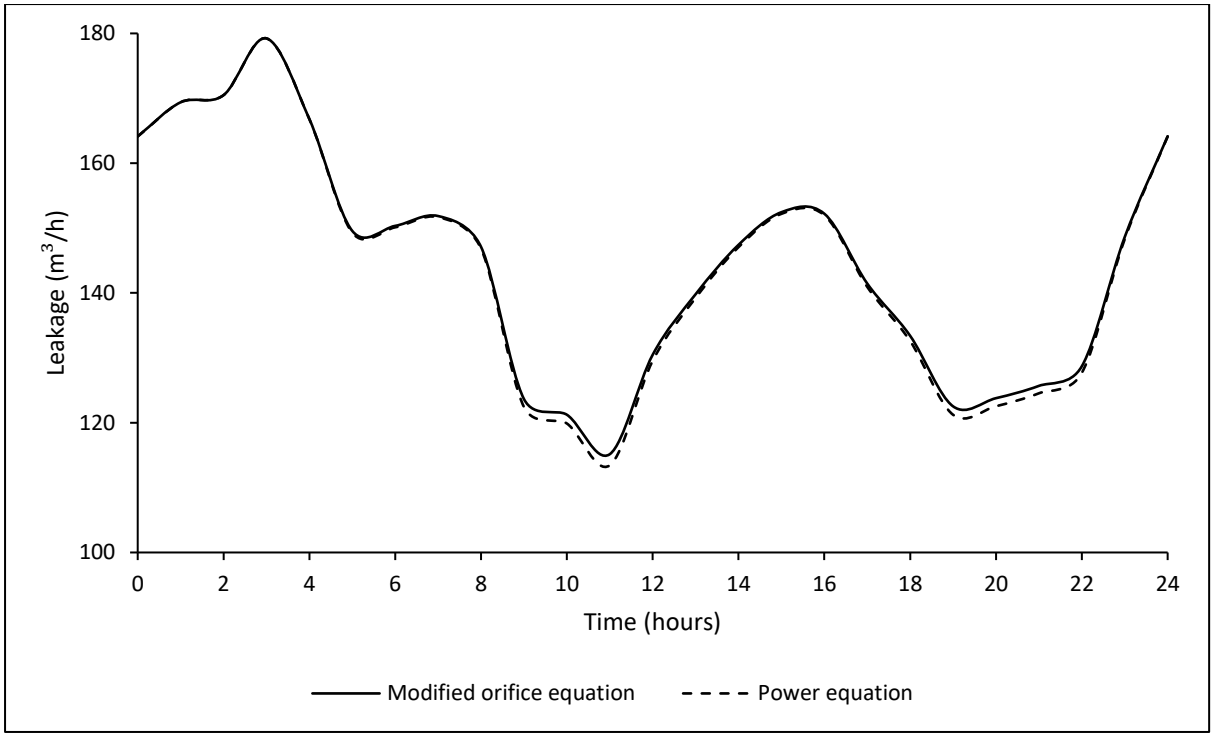

Figure 30: System leakage flow rate variation before pressure management

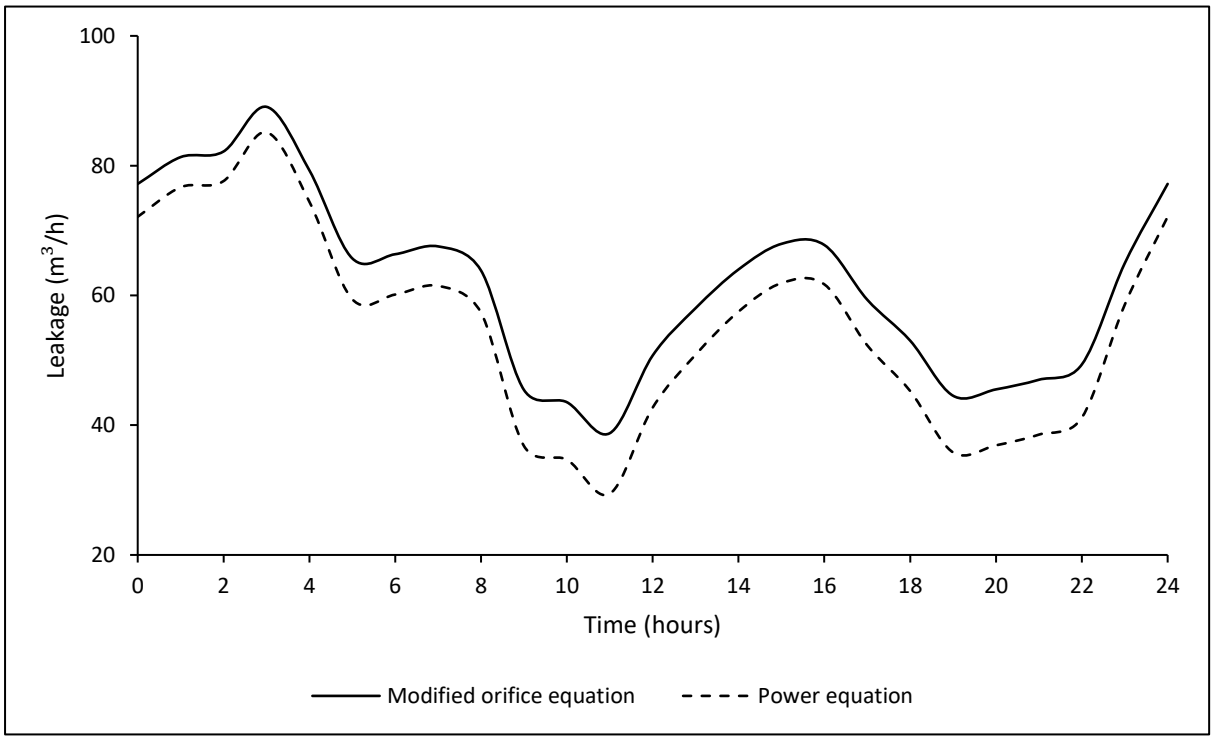

Figure 31: System leakage flow rate variation after pressure management

5.4.3.2. Leakage flow rate variation at the critical node

Leakage flow rate variation at the critical node is shown in table 17, and figures 32 and 33. Although the error in estimating system leakage was insignificant before the implementation of pressure management, results at the individual node show that it is big enough to make an impact on simulation results.

Before the implementation of pressure management, the arithmetic average of the leakage flow rates was $0.15m^3/h$ and $0.13m^3/h$ for the modified orifice and power equations respectively. This converts to 13.3% underestimation of leakage by the conventional power equation, on average. The minimum flow rate for the modified orifice equation was $0.13m^3/h$ while that of the power equation was $0.10m^3/h$. The maximum leakage flow rate for both approaches was $0.16m^3/h$.

As explained earlier, in the case of system leakage flow rate, the power equation parameters were calibrated during the third hour of simulation, before pressure management was implemented. It is the reason why leakage flow rates modelled by both approaches during this time are close enough, compared to the other times of simulation in figure 32. The highest percentage error was 32.65% during period 11, which is also the period when the pressure head is further away from the one at which power equation parameters were calibrated. This again demonstrates that the power equation will realistically model leakage behaviour only under the conditions in which it has been calibrated.

With pressure management implemented, the arithmetic mean of leakage flow rates was $0.08m^3/h$ and $0.04m^3/h$ for the modified orifice and conventional power equations respectively. The highest percentage error was 76.9% during period 11, while on average the conventional power equation underestimated leakage flow rate by 50%. Results in table 17

further show that the minimum and maximum flow rates also differ significantly in both approaches.

Generally, the error in estimating leakage flow rate by the power equation is quite well observed when analysing individual node leakage flow rate rather than the system leakage flow rate. It was also observed that the error increases as the pressure is further away from the one during which the power equation parameters were calibrated.

Table 17: Leakage variation at the critical node before and after pressure management

		Leakage flow rate (m^3/h)			
		Minimum	**Arithmetic Mean**	**Median**	**Maximum**
Before pressure management	Modified orifice equation	0.13	0.15	0.15	0.16
	Power equation	0.10	0.13	0.13	0.16
After pressure management	Modified orifice equation	0.05	0.08	0.09	0.11
	Power equation	0.01	0.04	0.04	0.06

Figure 32: Leakage flow rate variation at the critical node before pressure management

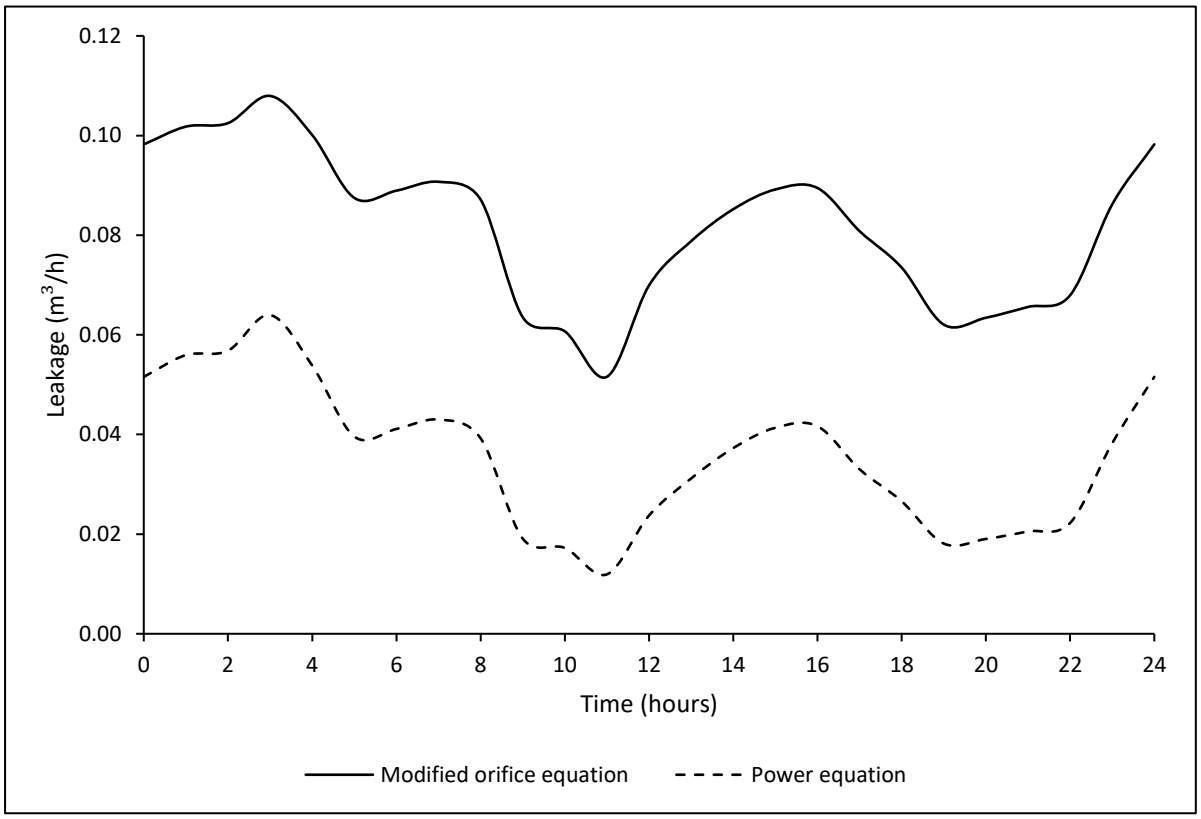

Figure 33: Leakage flow rate variation at the critical node after pressure management

5.4.4. Simulation convergence

System convergence occurs when a solution is found to the nonlinear hydraulic equations that govern system hydraulics as earlier discussed in Chapter 2. During a given simulation period, the global gradient algorithm (GGA) repeatedly performs a hydraulic analysis to find a solution. The number of iterations or trials depends on the system's hydraulic features.

Adding a second emitter function to the hydraulic solver of Epanet had some impact on the convergence to the hydraulic solution of the nonlinear equations that govern system hydraulics. This is shown in figure 34, where at the start of the simulation, i.e. at time = 0, the modified orifice and power equations took 25 and 10 iterations respectively to converge to a hydraulic solution. However, it was noted that after the first period, both approaches required practically the same number of iterations to converge. The difference in the number of iterations required for the first period of simulation is attributed to the added term in the modified orifice equation (33) which models leakage from an expanding part of the leak.

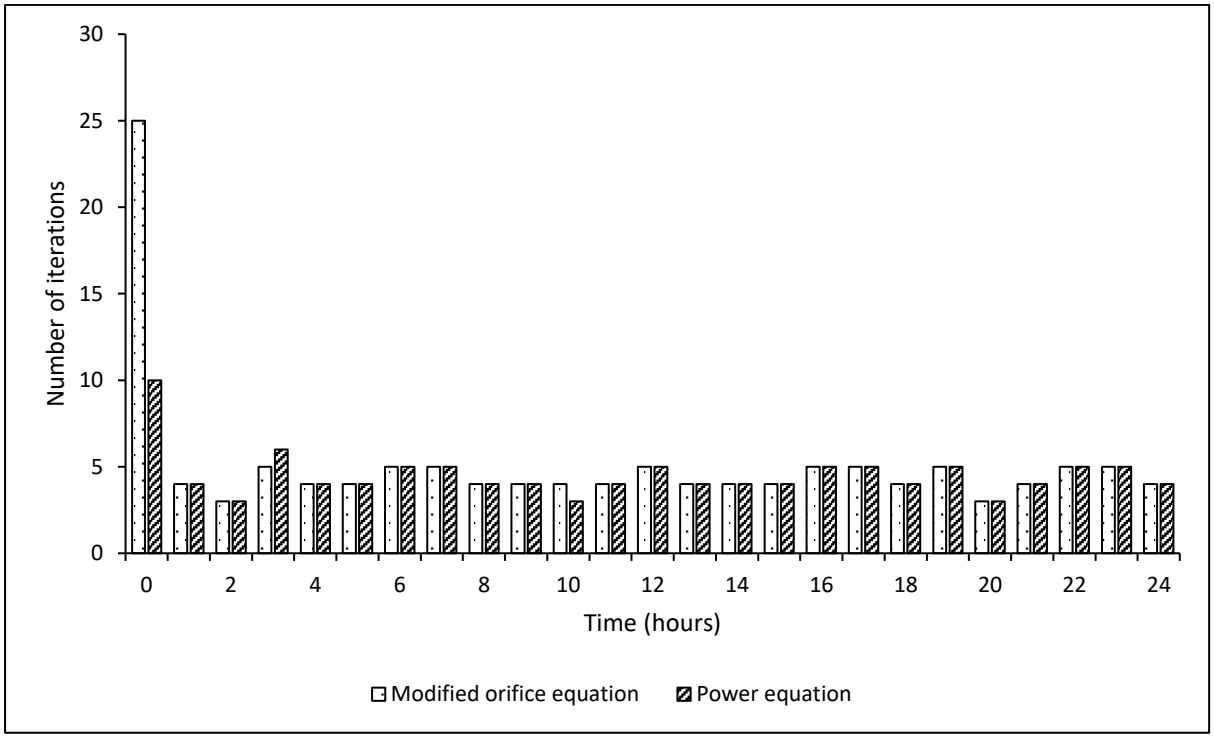

Figure 34: Number of iterations required by both the modified orifice and power equations before convergence

5.5. Simulation results for a typical set of two hundred systems

5.5.1. Introduction

In this section, simulation results for a set of 200 medium-sized water distribution systems with infrastructure leakage index (ILI) of 16 are presented. Each of these systems has random but realistically generated and distributed leaks following the method described in Chapter 4.

A total number of 12 sets were generated, consisting of small, medium or large pipe networks and infrastructure leakage indices of 1, 4, 16 or 64. Because all 12 sets are analysed in a similar way, the medium-sized set with the infrastructure leakage index of 16 was selected for discussion in this section. The rest of the analysis results are documented in Appendix A.

In subsection 5.5.2, system leakage parameters adhering to the modified orifice equation, i.e. the initial leak area A_0 and head-area slope m, are discussed. Also, presented here are parameters that adhere to the conventional power equation, i.e. the system leakage exponent $N1$ and leakage coefficient C.

This is followed in subsection 5.5.3 by an analysis of the performance of systems modelled using both the modified orifice and conventional power equation approaches. The average number of iterations required for a system to converge to a hydraulic solution is presented and analysed. Furthermore, the impact of leakage on pressure head simulation results as well as the estimated error in leakage flow rates and pressure heads on an individual node and in the whole system are discussed.

5.5.2. System leak parameters

For each of the 200 systems, the leaks were stochastically generated in the format of the modified orifice equation. The exact same leaks were calibrated into the format of the conventional power equation. This section presents statistical distributions of the leak parameters in the format of the modified orifice equation and their equivalent in the format of the conventional power equation. These leak parameters are essentially the system leakage exponent $N1$ and leakage coefficient C for the conventional power equation, and the initial leak area A_0 and head-area slope m for the modified orifice equation. The parameters equivalent to the power equation were calibrated during minimum night flow, through a two-step simulation where the average zonal pressures and system leakage flow rates were estimated. Equations (13) and (12) were used to calculate these parameters.

Van Zyl and Cassa (2014) suggested a dimensionless leakage number L_N, which is the ratio of the second to the first term in the modified orifice equation (33). They also propose an empirical formulation, (i.e. equation 38), to link the leakage number to the power equation's leakage exponent. The last part of this subsection presents how, for the 200 stochastic distributions, the leaks associate between the leakage numbers and corresponding leakage exponents.

5.5.2.1. Power equation

Table 18 presents a statistical range of the leakage exponent $N1$ and leakage coefficient C for the simulated systems. The leakage exponents varied between 0.81 and 1.35, with the arithmetic mean and median value of 1.07. The probability distribution function of leakage exponents was almost symmetrical, as can be seen from the arithmetic mean and median.

The leakage coefficients varied between $9.2E-05$ and $1.2E-03$, with arithmetic mean value of $3.9E-04$. As was the case with the leakage exponent, the probability distribution function

for the leakage coefficients also seems nearly symmetrical, although there is some difference between the arithmetic mean and median values. Figures 35 and 36 present a normalized cumulative distribution of the leakage exponents and coefficients respectively.

Table 18: System parameters of the power equation for the medium network with an ILI of 16

	Minimum	**Arithmetic Mean**	**Median**	**Maximum**
Leakage exponent N1	0.81	1.07	1.07	1.35
Leakage coefficient C	9.2E-05	3.9E-04	3.6E-04	1.2E-03

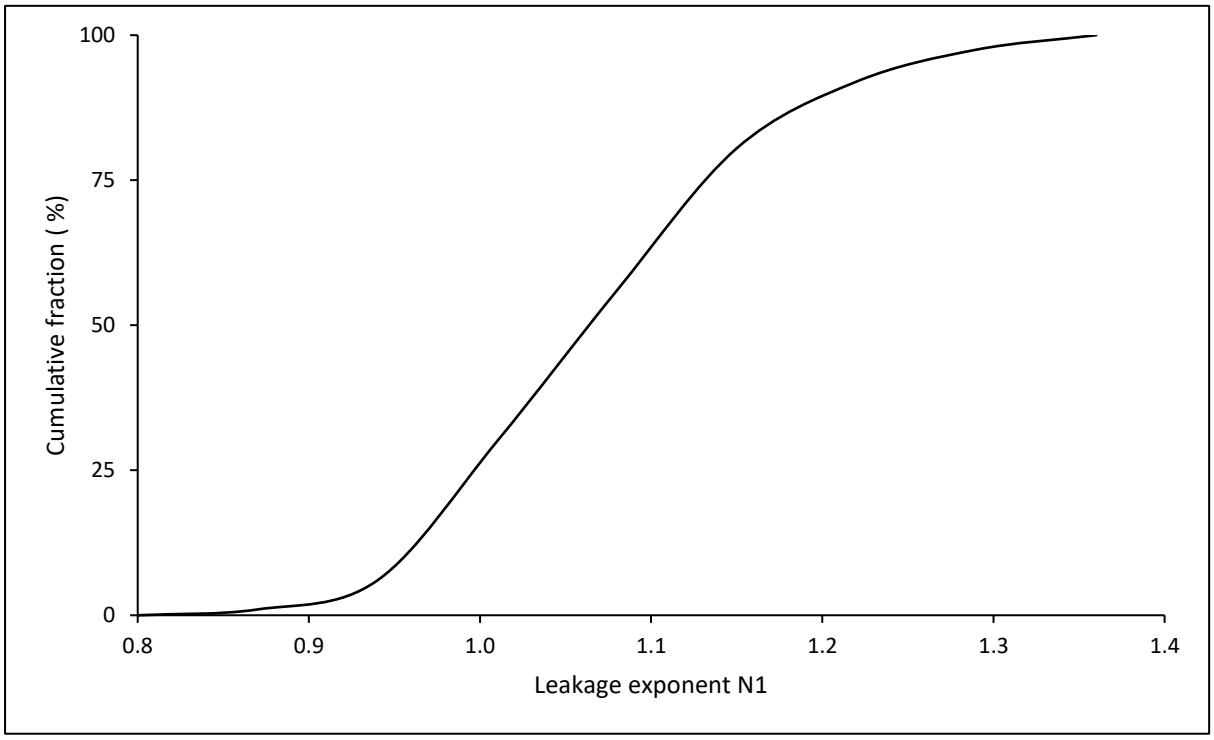

Figure 35: Cumulative fraction of system N1 for the medium network with an ILI of 16

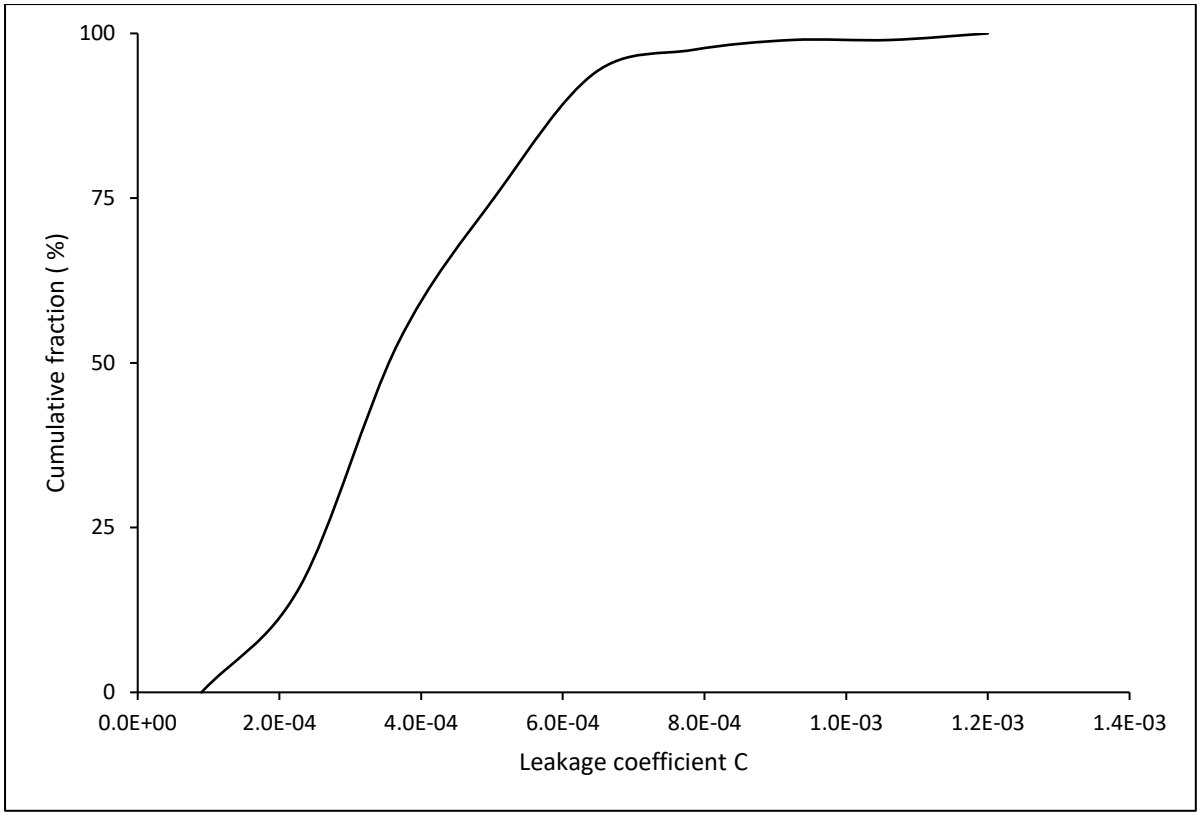

Figure 36: Cumulative fraction of system C for the medium network with an ILI of 16

5.5.2.2. Modified orifice equation

System parameters of the modified orifice equation, i.e. the initial leak area and head-area slope, plus the leakage number are presented in table 19. Schwaller et al. (2015) suggests that to improve the accuracy of estimation of the modified orifice parameters, the unknown discharge coefficient can be included in the parameter estimation. Equations (35) and (36) show that when the initial leak area A_0 and head area slope m are respectively multiplied by the discharge coefficient, their corresponding effective values $A_0{}'$ and m' are obtained as shown in the equations below:

$$\mathrm{A_0'} = (\mathrm{C_d A_0}) = \frac{\mathrm{Q_1}}{\sqrt{2\mathrm{g h_1}}} - \mathrm{m' h_1} \tag{66}$$

$$\mathrm{m'} = (\mathrm{C_d m}) = \frac{\mathrm{h_2^{0.5} Q_1 - h_1^{0.5} Q_2}}{\sqrt{2\mathrm{g}}(\mathrm{h_1^{1.5} h_2^{0.5} - h_2^{1.5} h_1^{0.5}})} \tag{67}$$

Schwaller et al. (2015) recommends of the use of the effective initial leak areas ($A_0{}'$) and head-area slopes (m') were applied to avoid any errors that could have been introduced by assuming a discharge coefficient.

The effective initial leak areas were found to be in the range of $158.20mm^2$ to $781.98mm^2$, while the effective head-area slopes varied from $3.52mm^2/m$ to $9.17mm^2/m$. The arithmetic mean of the effective initial leak area was $472.64mm^2$ and the median of the range was $475.04mm^2$. The arithmetic mean and median of the head area slope were the same at $6.2mm^2/m$. The statistical distribution of the effective initial leak areas and head-area slopes were almost systematic, given that their respective arithmetic mean and median values were close enough.

The leakage numbers varied from 0.45 to 5.54, with an arithmetic mean value of 1.49 and a median of 1.32. A slight level of skewness was observed in the distribution of system leakage numbers as compared to the initial leak areas and head-area slopes.

Figures 37, 38 and 39 show the normalized cumulative fraction of the effective initial the leak area, effective head-area slope, and the leakage number respectively.

Table 19: System parameters of the modified orifice equation for the medium network with an ILI of 16

	Minimum	**Arithmetic Mean**	**Median**	**Maximum**
Effective initial leak area C_dA0 (mm^2)	158.20	472.64	475.04	781.98
Effective head-area slope C_dm (mm^2/m)	3.52	6.20	6.20	9.17
Leakage number LN	0.45	1.49	1.32	5.54

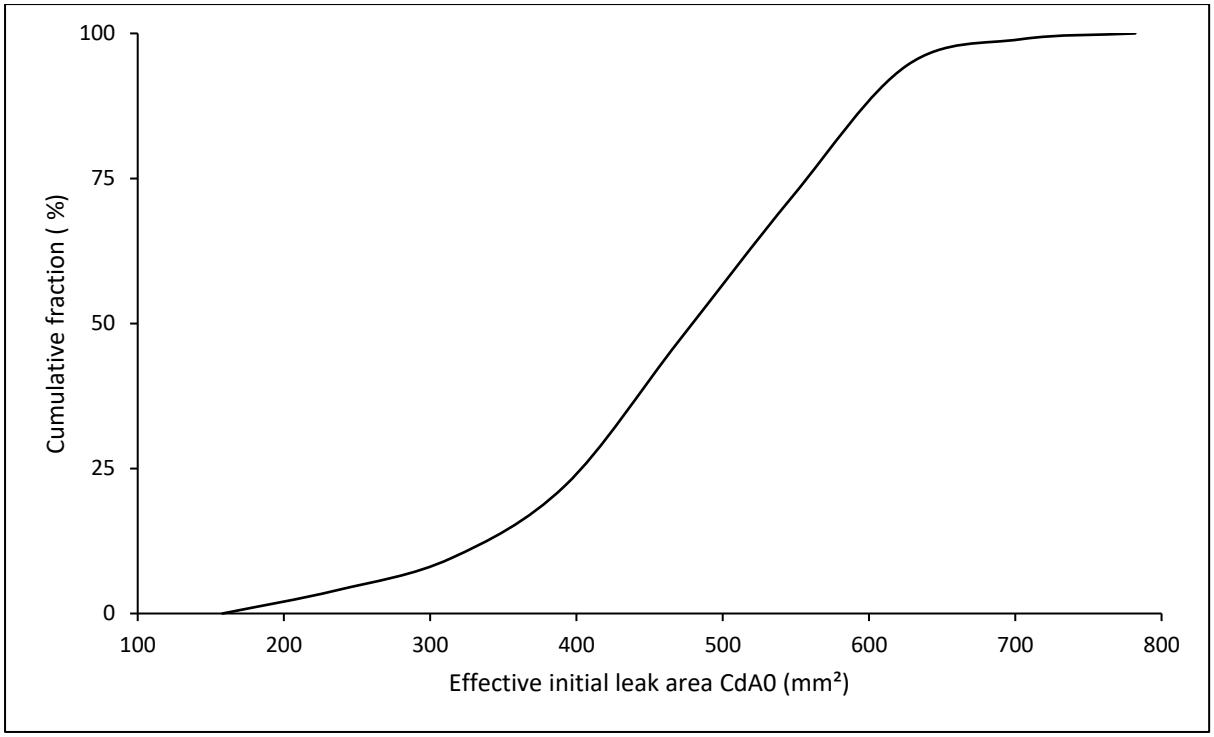

Figure 37: Cumulative fraction of the effective initial leak area for the medium network with an ILI of 16

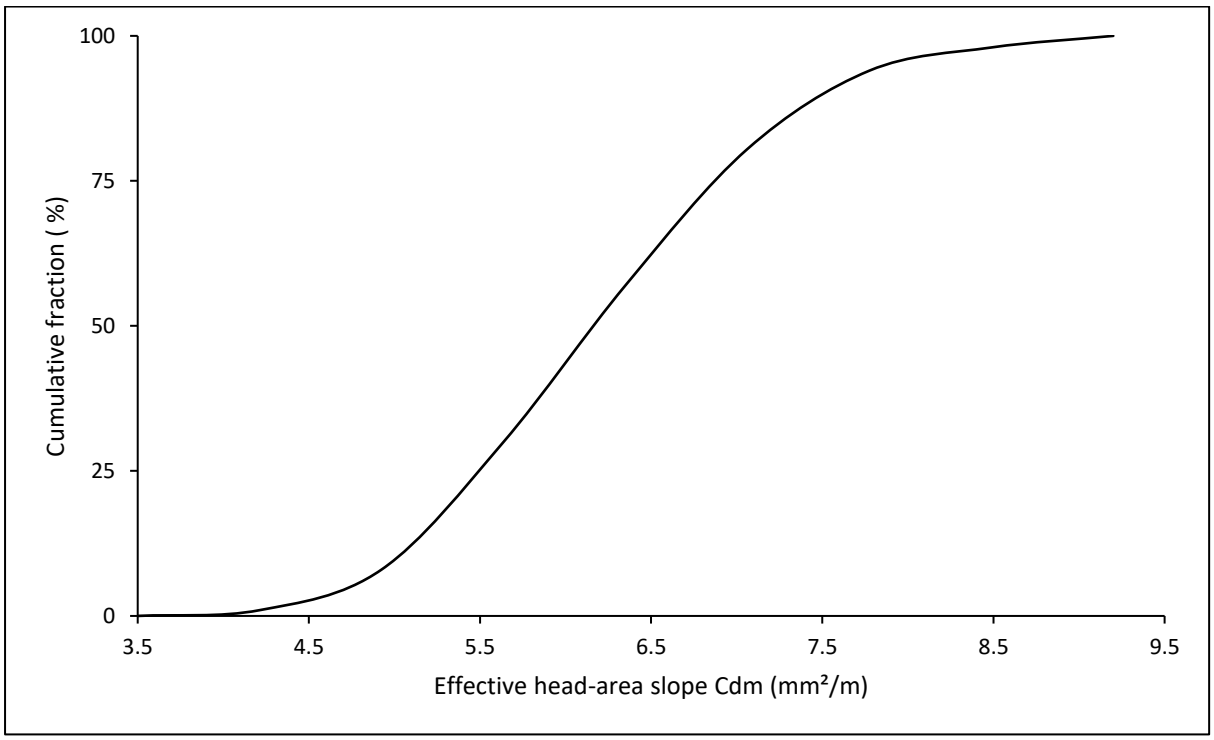

Figure 38: Cumulative fraction of the effective head-area slope for the medium network with an ILI of 16

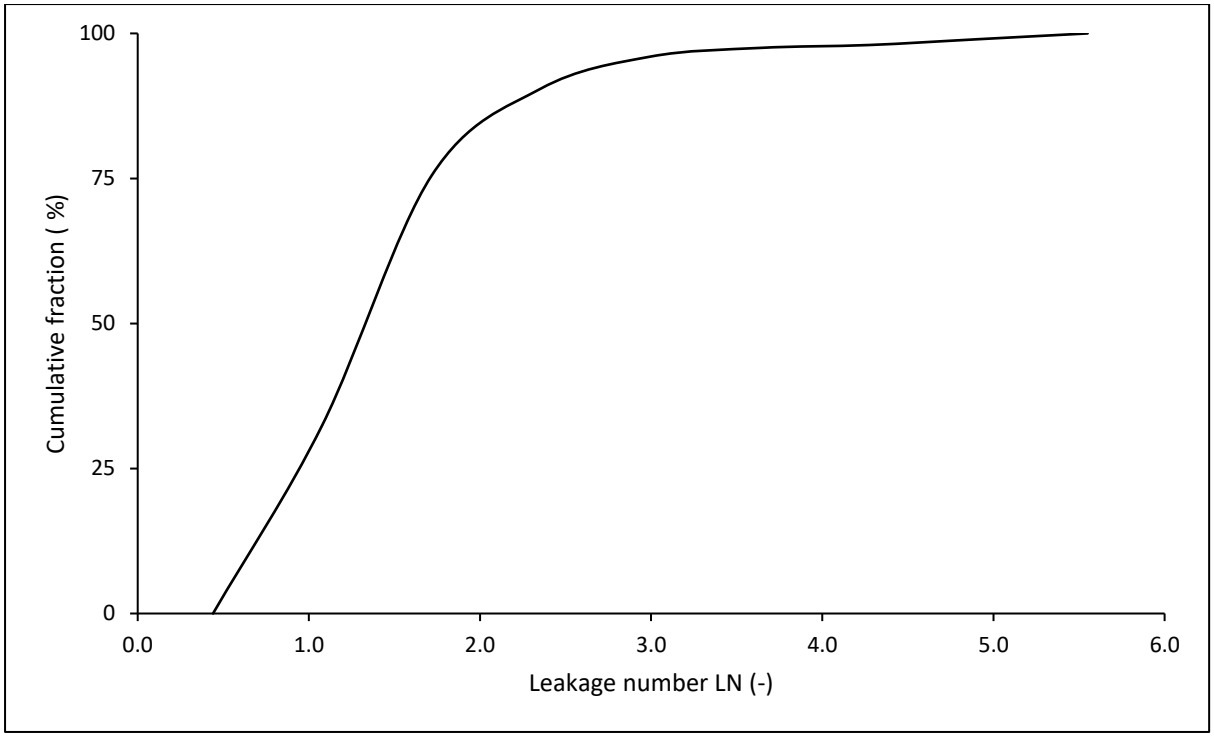

Figure 39: Cumulative fraction of system leakage numbers for the medium network with an ILI of 16

5.5.2.3. Predicting system leak parameters of the modified orifice equation

Schwaller et al. (2015) found that the modified orifice equation can be applied to both individual and system leaks. As earlier explained in Chapter 2, the initial leak area and head-area slope in a system can be predicted quite accurately from the sum of the respective individual parameters.

In this study, therefore, the sum of effective initial leak areas of individual leaks in each system was plotted against the corresponding system effective initial leak areas. The results are presented in figure 40 and show a strong correlation. The plotted points are positioned around a zero-error line; this implies that the system's initial leak area can be reasonably accurately predicted from the sum of individual leak areas for a given system, as was suggested by Schwaller et al. (2015).

The system's head-area slopes and the sum of individual head-area slopes are also plotted closely on the zero-error line, as is shown in figure 41. This means that the system head-area slope can be predicted quite accurately from the sum of individual head-area slopes for a given water distribution system.

The correlation between the sum of individual and system leak parameters shows the feasibility of using the modified orifice equation in pressure management. The sum of the individual initial leak areas provides an explicit measure of the physical integrity of the system. The head-area slope provides an understanding into the type of leaks present since it can be linked to the type and size of a leak (Cassa and van Zyl 2013).

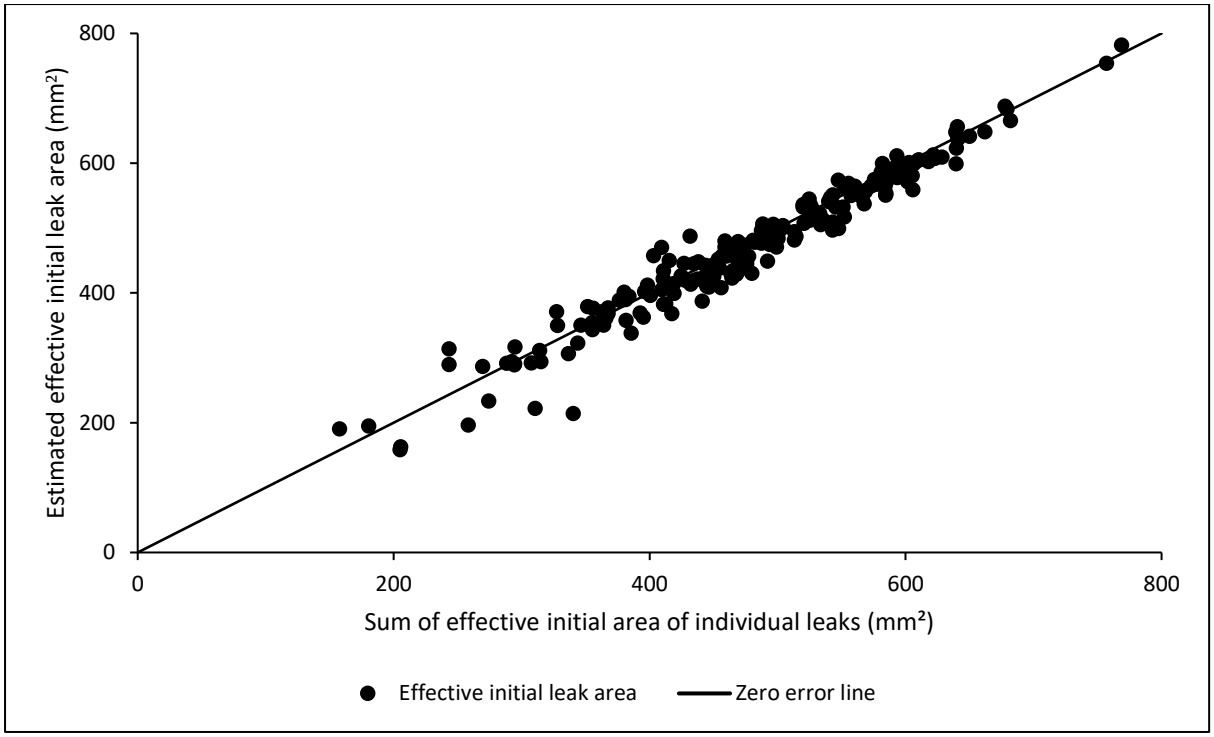

Figure 40: Plot of the estimated effective initial leak areas of systems against the sum of effective initial areas of individual leaks

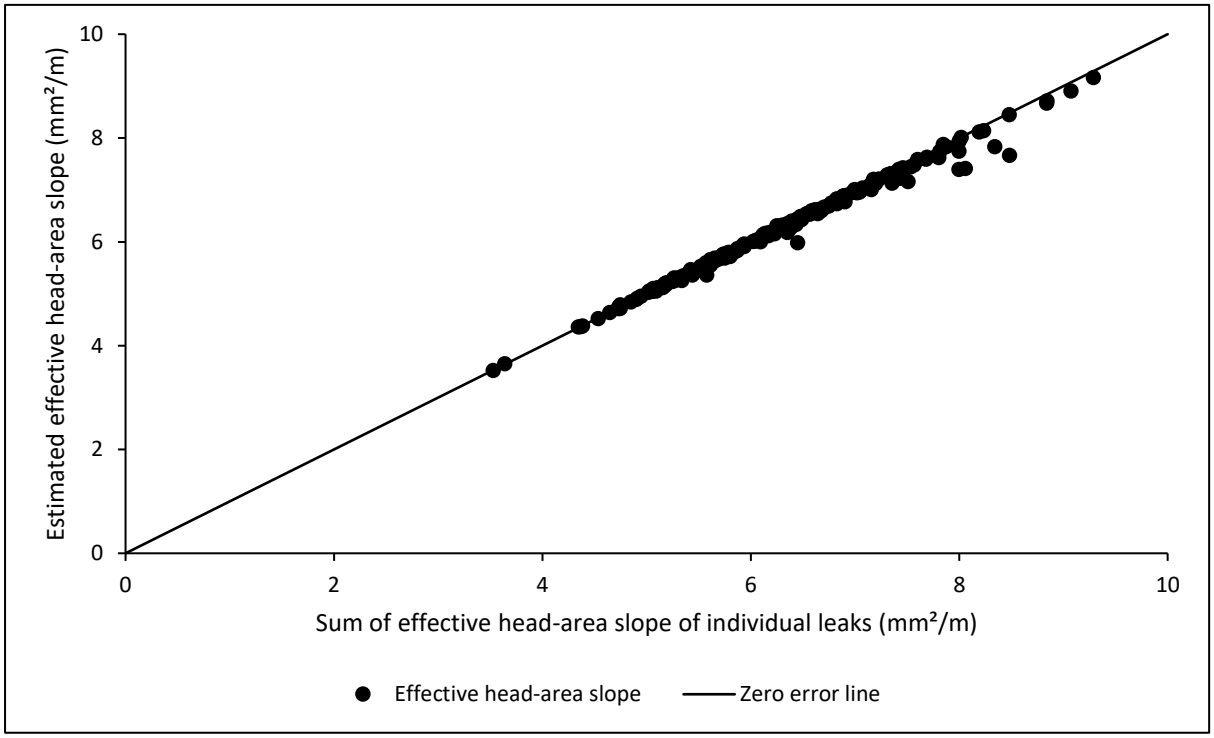

Figure 41: Plot of the estimated effective head-area slope of systems against the sum of effective head-area slopes of individual leaks

5.5.2.4. Linking the modified orifice equation to the conventional power equation

The leakage number L_N is used to link the modified orifice equation to the conventional power equation as explained in section 2.2.6.

A plot of leakage exponents against corresponding leakage numbers (see figure 42) shows the theoretical relationship described by equation (38) and figure 8.This means that conversion from one form of equation to the other is possible.

This relationship is significant for many practitioners with water distribution system data in the format of the conventional power equation, as they can easily convert from this format to the modified orifice equation and therefore model leakage in a more realistic approach.

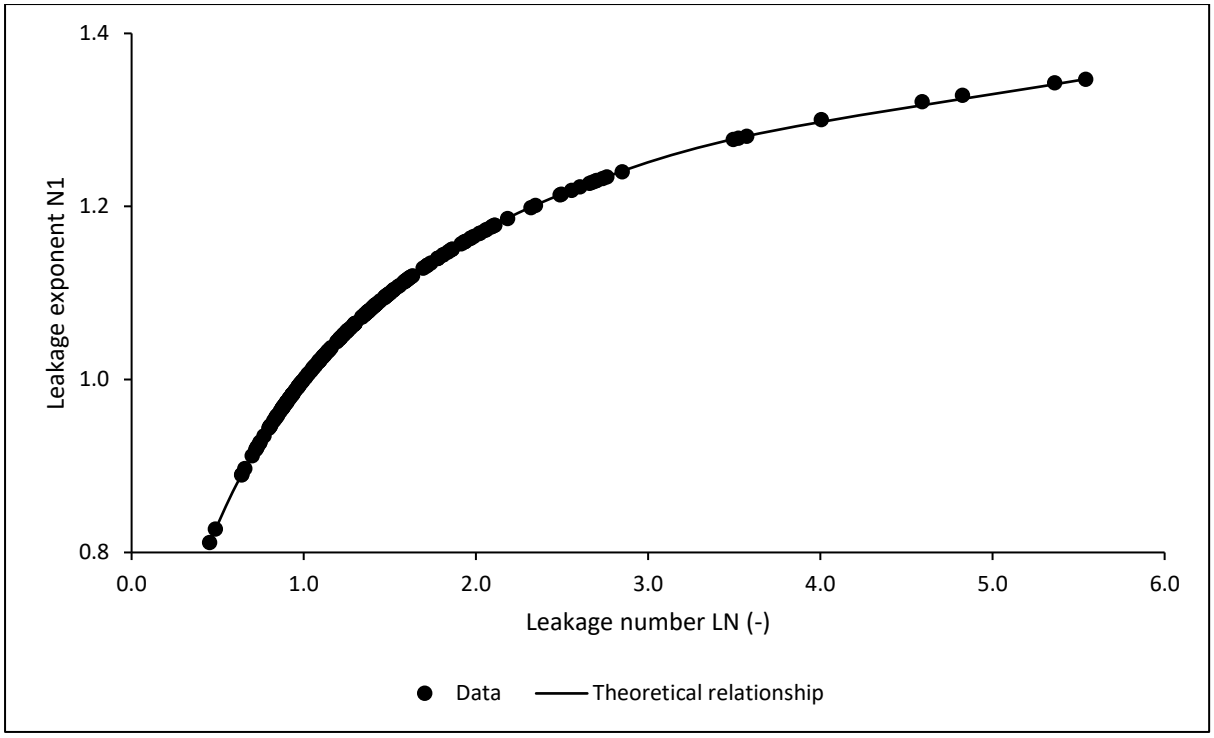

Figure 42: Relationship between leakage exponent and leakage number for the medium network with an ILI of 16

5.5.3. Hydraulic performance of systems

In this section a comparison of the hydraulic performance of both the modified orifice and power equations is made. First, the arithmetic mean of the number of iterations required for the global gradient algorithm to converge to a hydraulic solution is presented.

The effect of leakage on pressure when modelled using either of the two equations is presented during minimum night flow (MNF) and peak demand conditions. The average zone pressure node and the critical node are considered in this analysis.

Thereafter an investigation is presented into the error made when nodal pressure heads are modelled using the conventional power equation instead of the more realistic modified orifice equation. The average zone pressure node and the critical node are again considered during minimum night flow and peak demand conditions.

To conclude this section, the leakage estimate error occurring with the use of the conventional power equation is analysed. An analysis is carried out for system leakage and for an individual node, which in this case is the critical node. Two scenarios are considered, i.e. when the system pressure head is at normal operating conditions and when it has been reduced to model the implementation of pressure management.

5.5.3.1. System simulation convergence

The average number of iterations reported for all 200 systems and the 24-hour simulation period are calculated and presented in table 20, indicating the minimum, arithmetic mean, median and maximum values.

Overall, the conventional power equation was found to converge to a hydraulic solution at slightly lower average number of iterations than the modified orifice equation, as shown in

table 20 and figure 43. However, the difference in the number of iterations was on average less than 1 for all the simulated systems.

The slight increase in the average number of iterations required for the modified orifice equation to converge to a hydraulic solution is attributed to the added emitter function at each junction with leakage.

Table 20: Average number of iterations to achieve a hydraulic solution

	Minimum	**Arithmetic Mean**	**Median**	**Maximum**
Modified orifice equation	4.92	5.12	5.12	5.24
Power equation	4.20	4.43	4.40	4.72

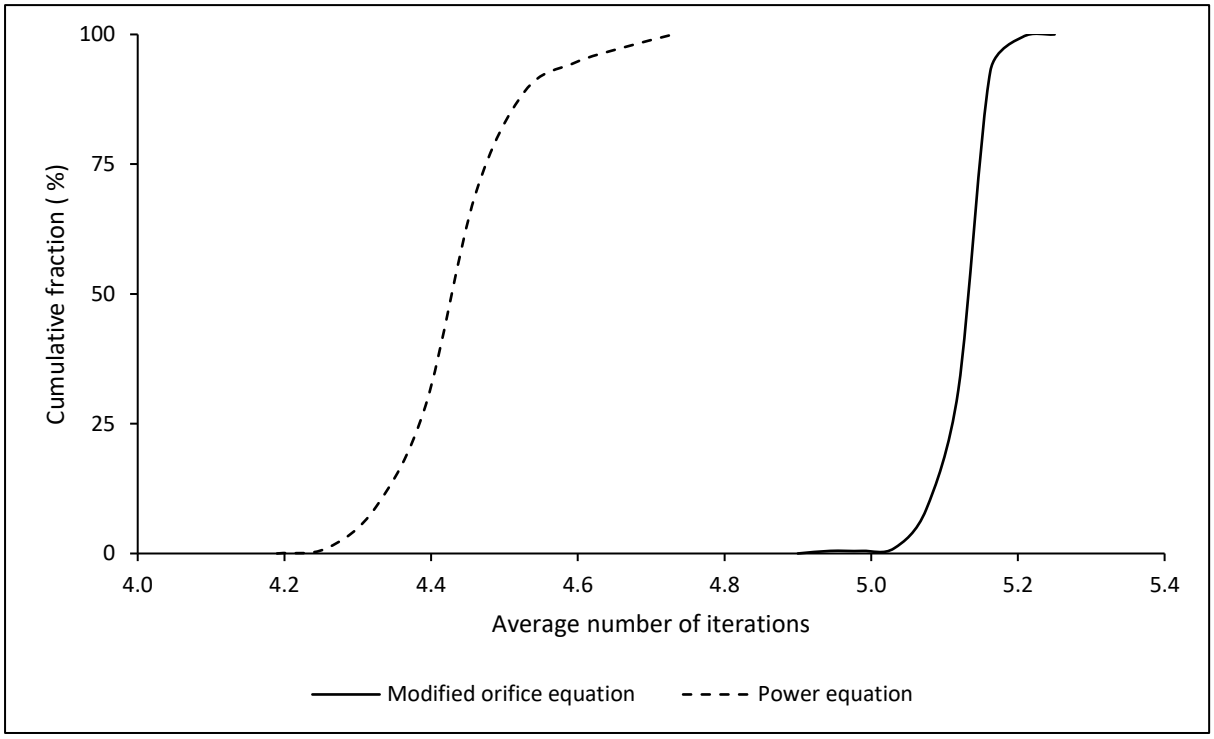

Figure 43: Cumulative fraction of average number of iterations required for network to converge

5.5.3.2. Effect of leakage on pressure

At the average zone pressure (AZP) node

The effect of leakage on pressure was analysed at the average zone pressure (AZP) node, which is a point in a system at which the pressure head is representative of the system pressure. Two conditions that characterize a diurnal demand were considered: the minimum night flow (MNF) when system pressure is highest, and peak demand when system pressure is lowest.

Leakage influence was estimated by subtracting the pressure head when there is no leakage in the system from the pressure head when the system has leakage. As leakage lowers system pressure, the difference must be a negative value.

The results show that largely, the effect of leakage on pressure is almost the same for the modified orifice and power equations during both minimum night flow and peak demand conditions as presented in table 21, figures 44 and 45.

In almost 75% of the simulated systems the effect was found to be in the range of $-3.4m\ to -3.1m$ during minimum night flow, and $-4.0m\ to -3.5m$ during peak demand conditions, as shown in figures 44 and 45 respectively.

Table 21: Effect of leakage on pressure at the AZP node

	During MNF conditions				**During peak demand conditions**			
	Min (m)	**Mean (m)**	**Median (m)**	**Max (m)**	**Min (m)**	**Mean (m)**	**Median (m)**	**Max (m)**
Modified orifice equation	-3.86	-3.31	-3.30	-2.73	-4.13	-3.66	-3.68	-2.85
Power equation	-3.86	-3.31	-3.30	-2.73	-4.07	-3.60	-3.61	-2.73

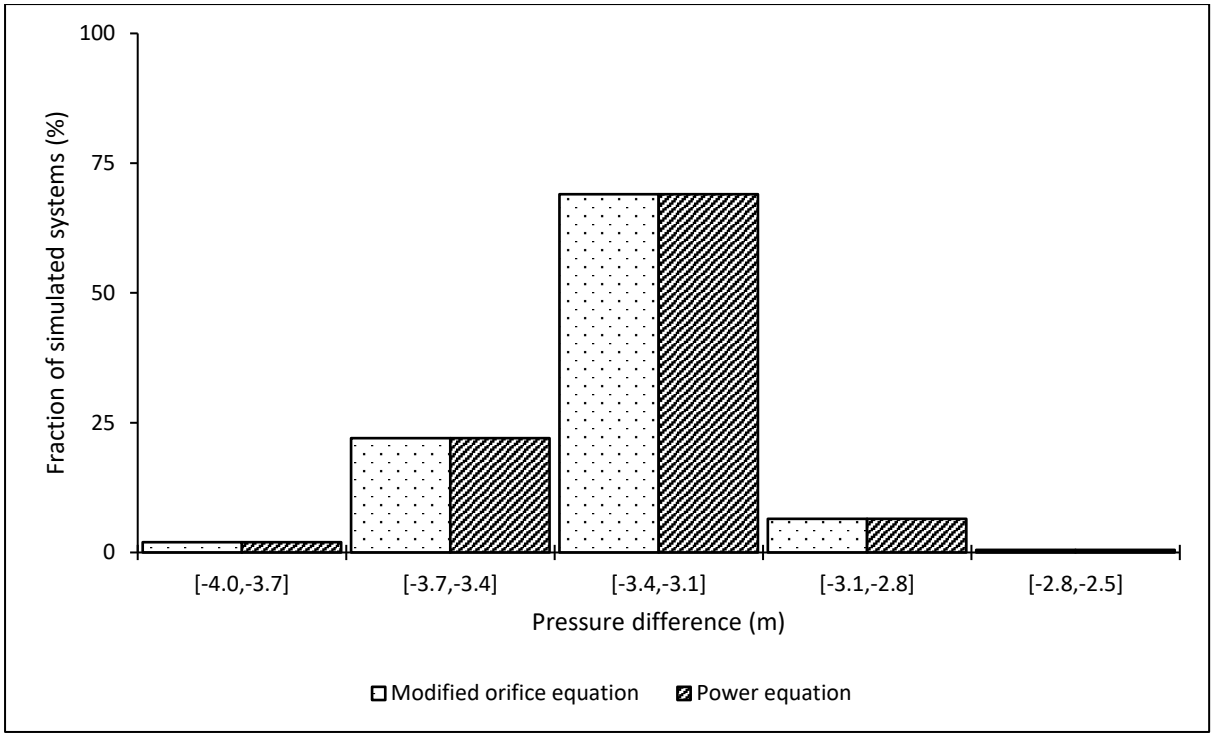

Figure 44: Effect of leakage on pressure at the AZP node during minimum night flow

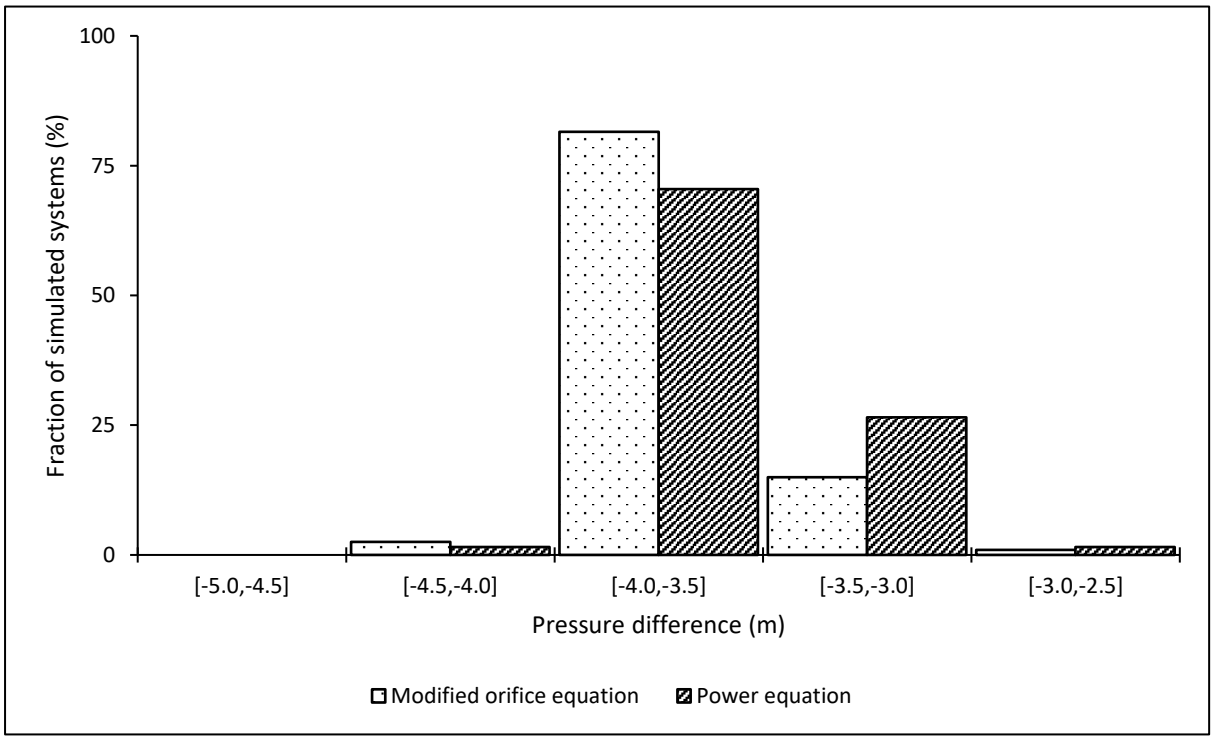

Figure 45: Effect of leakage on pressure at the AZP node during peak demand

At the critical node

The critical node has the lowest pressure in the system during peak demand. As was the case at the AZP node, two diurnal demand conditions, i.e. the minimum night flow and peak demand, were considered in this analysis.

The influence of leakage on pressure for both the modified orifice and power equations was generally the same and insignificant at the critical node as evident in table 22. The results show that for 85% of the simulated systems, the influence is in the range $-3.2m\ to\ -2.8m$ during minimum night flow as shown in figure 46.

On the other hand, during peak demand almost 60% of the simulated system show that the influence is in the range $-3.7m\ to\ -3.4m$ as shown in figure 47.

Table 22: Effect of leakage on pressure at the critical node

	During MNF conditions				**During peak demand conditions**			
	Min (m)	**Mean (m)**	**Median (m)**	**Max (m)**	**Min (m)**	**Mean (m)**	**Median (m)**	**Max (m)**
Modified orifice equation	-3.82	-3.10	-3.08	-2.72	-3.91	-3.44	-3.48	-2.61
Power equation	-3.82	-3.10	-3.08	-2.72	-3.86	-3.38	-3.41	-2.51

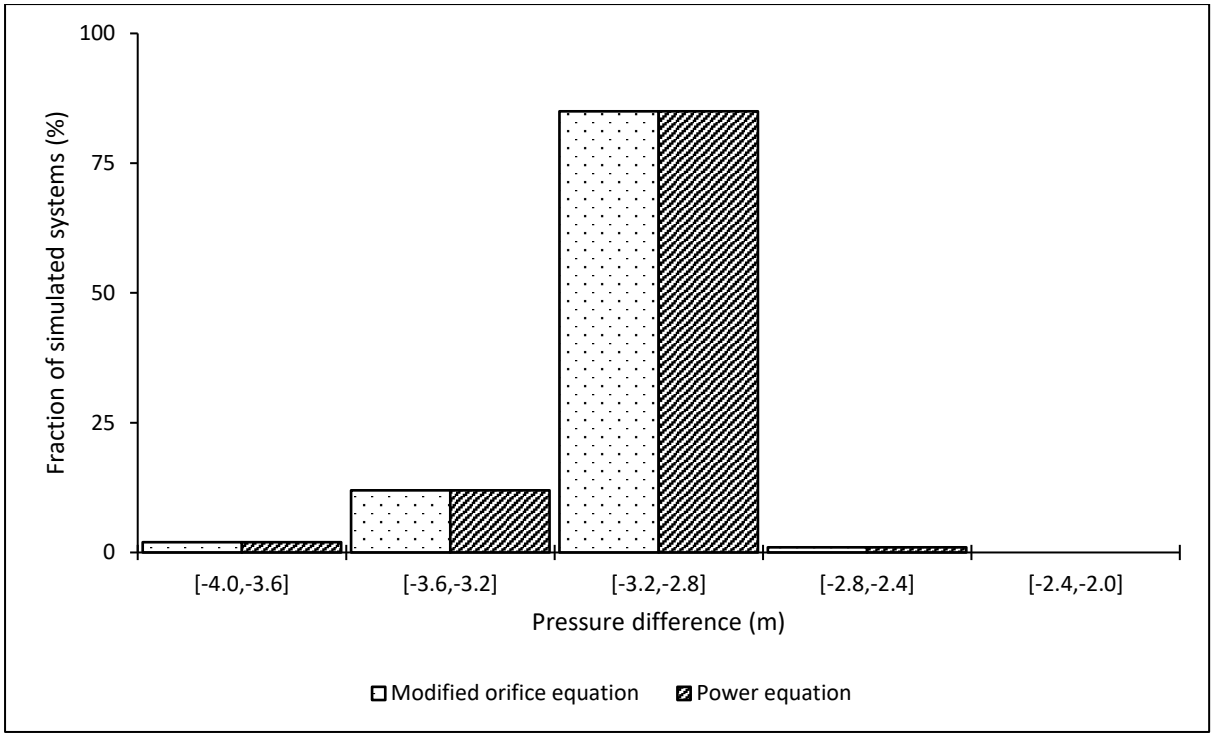

Figure 46: Effect of leakage on pressure at the critical node during minimum night flow

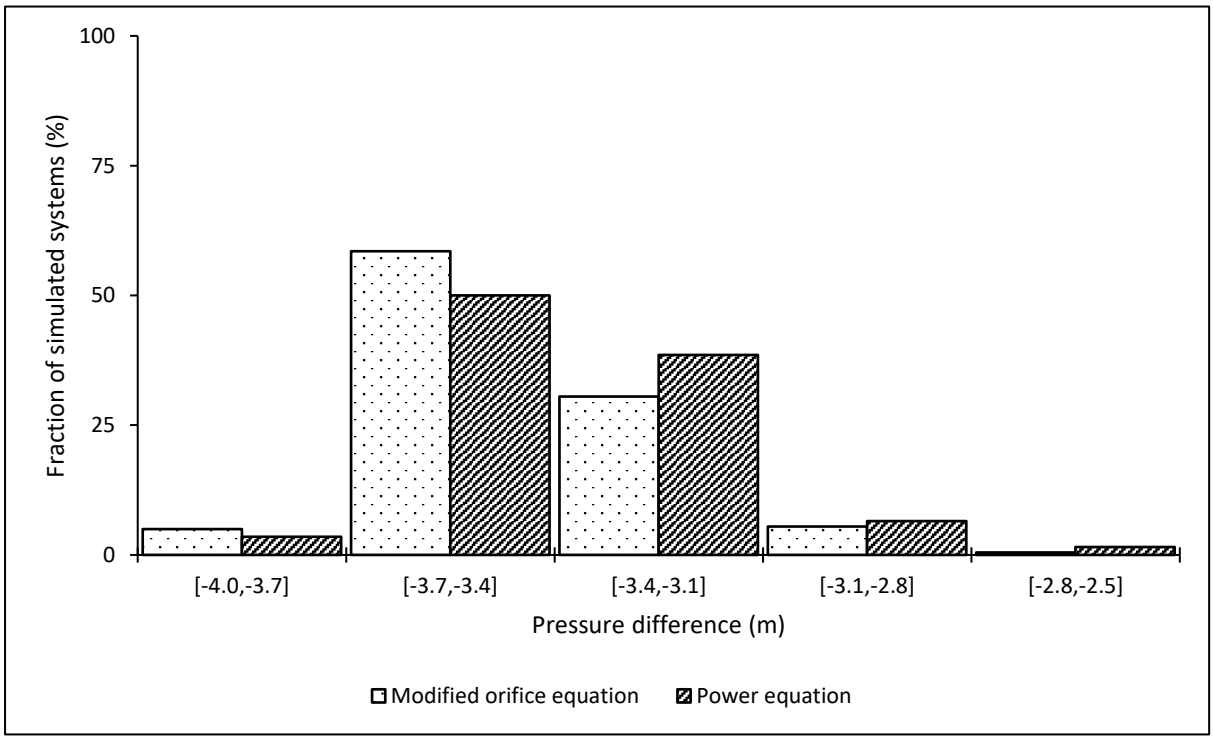

Figure 47: Effect of leakage on pressure at critical node during peak demand

5.5.3.3. Pressure head estimation error

The percentage error in estimating pressure head by the conventional power equation was calculated using equation (68). A negative value implies that the power equation underestimated the pressure head while a positive value shows overestimation.

$$E_p = \frac{P_1 - P_0}{P_0} * 100 \quad (68)$$

Where:

E_p = Pressure head error (%)

P_1= Pressure head obtained from the power equation

P_0= Pressure head obtained from the modified orifice equation.

Two investigations were conducted, one on the average zone pressure (AZP) node and the other on the critical node. In each investigation, the minimum night flow (MNF) and peak demand conditions, were considered.

As presented in table 23, the results show that during minimum night flow there was almost no error in estimating the pressure head by the power equation at both the AZP and critical nodes. These results are attributed to the fact that the power equation's equivalent system leakage exponent $N1$ and leakage coefficient C are calibrated during minimum night flow.

Results further show that during peak demand there was some error, namely the arithmetic mean of 0.09% and 0.11% at the AZP and critical nodes respectively. However, this size of error is very insignificant and will not have big effect on hydraulic simulation results.

Figure 48 shows that 58% of the systems simulated indicated errors in the range $-0.1\% \; to \; 0.1\%$ during peak demand at the AZP node. Figure 49 shows very similar results at

the critical node during peak demand, with more than 80% of the simulated systems indicating errors in the range $0.1\%\ to\ 0.2\%$.

Table 23: Pressure head estimation error at the AZP and critical nodes using the power equation.

	During MNF conditions				During peak demand conditions			
	Min (%)	**Mean (%)**	**Median (%)**	**Max (%)**	**Min (%)**	**Mean (%)**	**Median (%)**	**Max (%)**
At the AZP node	0.00	0.00	0.00	0.00	-0.03	0.09	0.09	0.26
At the critical node	0.00	0.00	0.00	0.00	-0.06	0.11	0.11	0.27

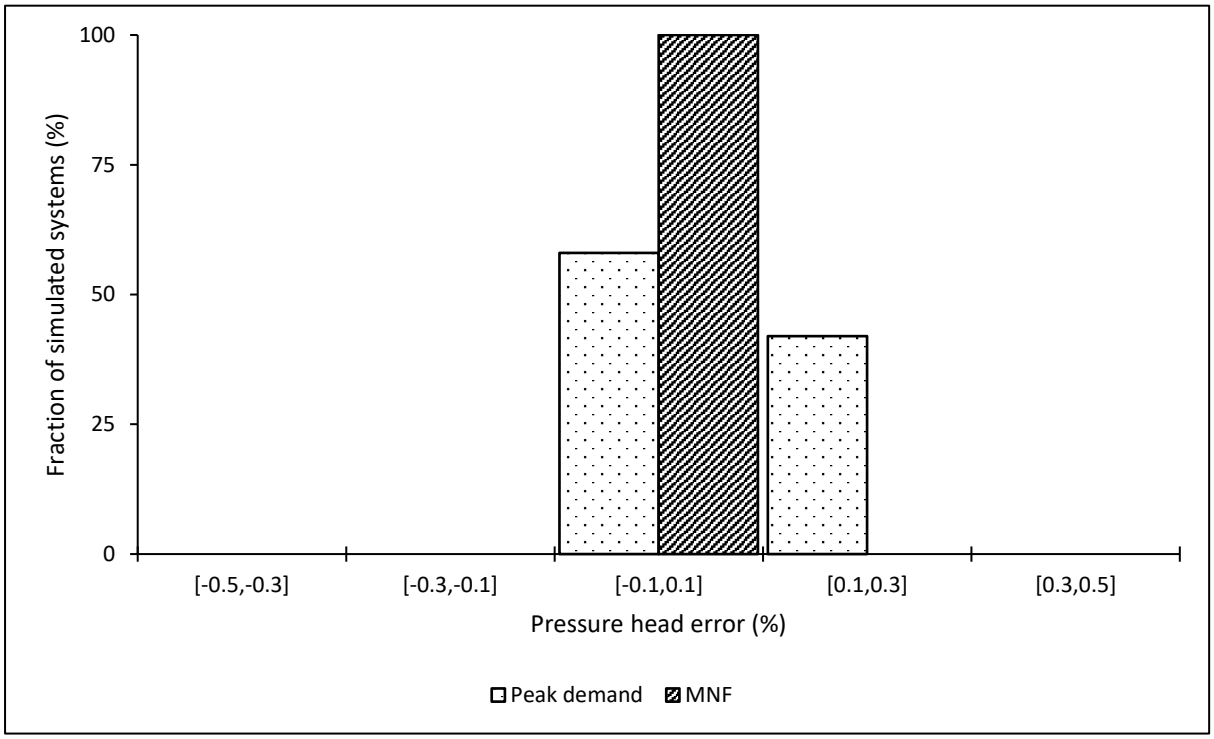

Figure 48: Pressure estimation error using the power equation at the AZP node

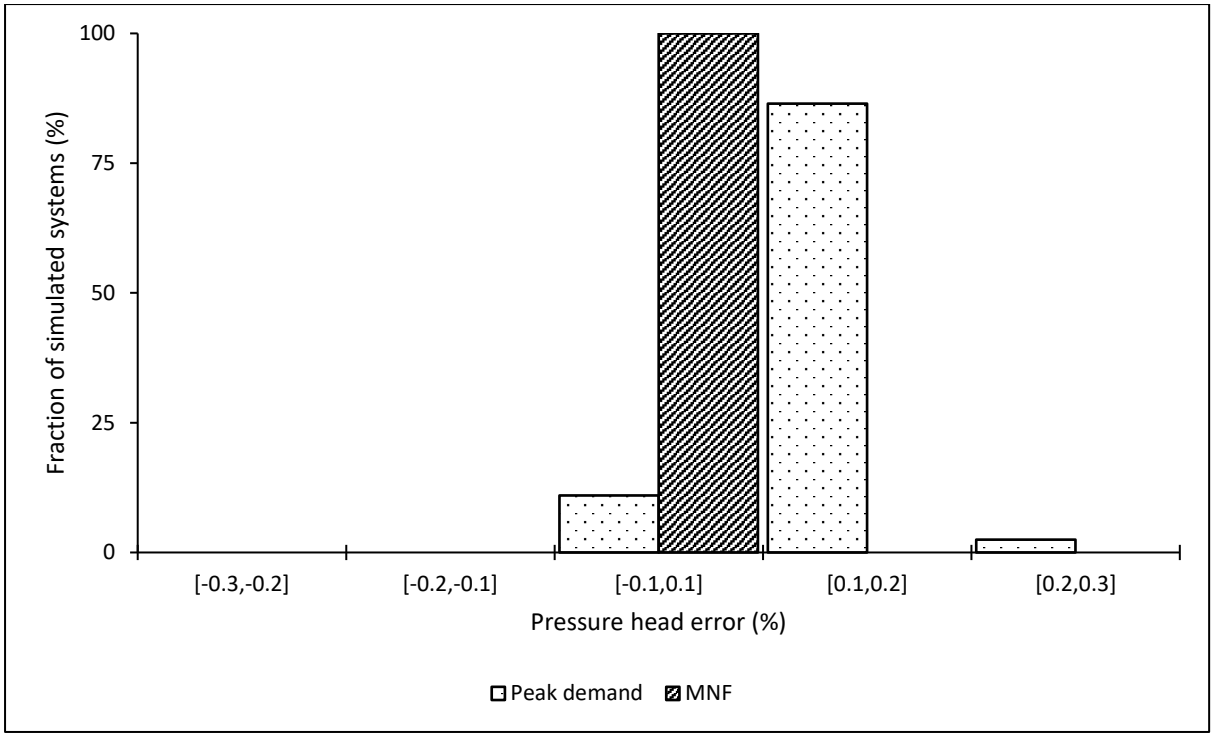

Figure 49: Pressure estimation error using the power equation at the critical node

5.5.3.4. Leakage flow rate estimation error

System leakage

Equation (69) was used to estimate the percentage error in the diurnal system leakage modelling by the conventional power equation before and after implementation of pressure management. Negative values imply that the conventional power equation underestimated system leakage while positive values imply that it was overestimated.

$$E_l = \frac{L_1 - L_0}{L_0} * 100 \quad (69)$$

Where:

E_l = Leakage flow rate error (%)

L_1= Leakage flow rate obtained from the power equation

L_0= Leakage flow rate obtained from the modified orifice equation.

The results in table 24 show that before the implementation of pressure management the arithmetic mean of the percentage error in system leakage modelling was -0.51%. There was both underestimation and overestimation of up to -2.32% and 0.50% respectively.

Figure 50 shows that 90% of the simulated systems indicated that the percentage error in system leakage flow rate modelling by the power equation is in the range of $-1\% \; to \; 0$ %.

In general, the percentage error in modelling system leakage flow rate by the power equation before the implementation of pressure management is small. The reason is that the approximation of the leak expansion in the power equation, also known as the calibration of the leakage exponent $N1$, is done before the implementation of pressure management.

After implementation of pressure management, the arithmetic mean of the percentage error in estimating system leakage by the power equation was found to be -11.04%, with almost 75% of the simulated systems indicating underestimation in the range of $-15\%\ to-10\%$. The results presented in table 24 further show that system leakage was underestimated up to -23.6% and that no cases of overestimation were observed.

Generally, the difference in the total daily system leakage volumes, modelled with the two approaches, is negligibly small for the system operating under normal conditions without pressure management being implemented.

However, after the implementation of pressure management the percentage error observed when using the conventional power equation becomes significant. This is because the conventional power equation is simply an empirical formulation that can be applied safely within a given calibrated pressure range. This observation is vital to consider for estimations of probable savings from the implementation of pressure management activities.

Table 24: System leakage estimation error using the power equation before and after pressure management

	Leakage estimate error (%)			
	Minimum	**Arithmetic Mean**	**Median**	**Maximum**
Before implementing pressure management	-2.32	-0.51	-0.48	0.50
After implementing pressure management	-23.60	-11.04	-10.91	-2.40

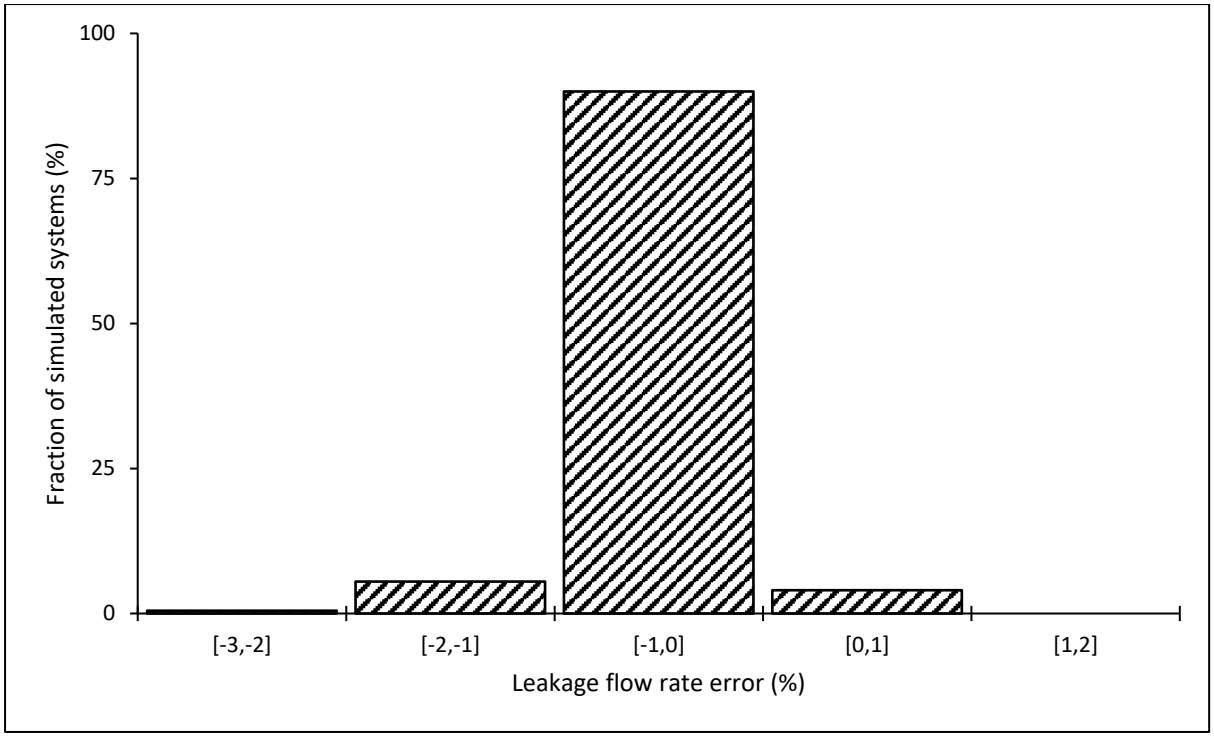

Figure 50: System leakage estimation error using the power equation before the implementation of pressure management

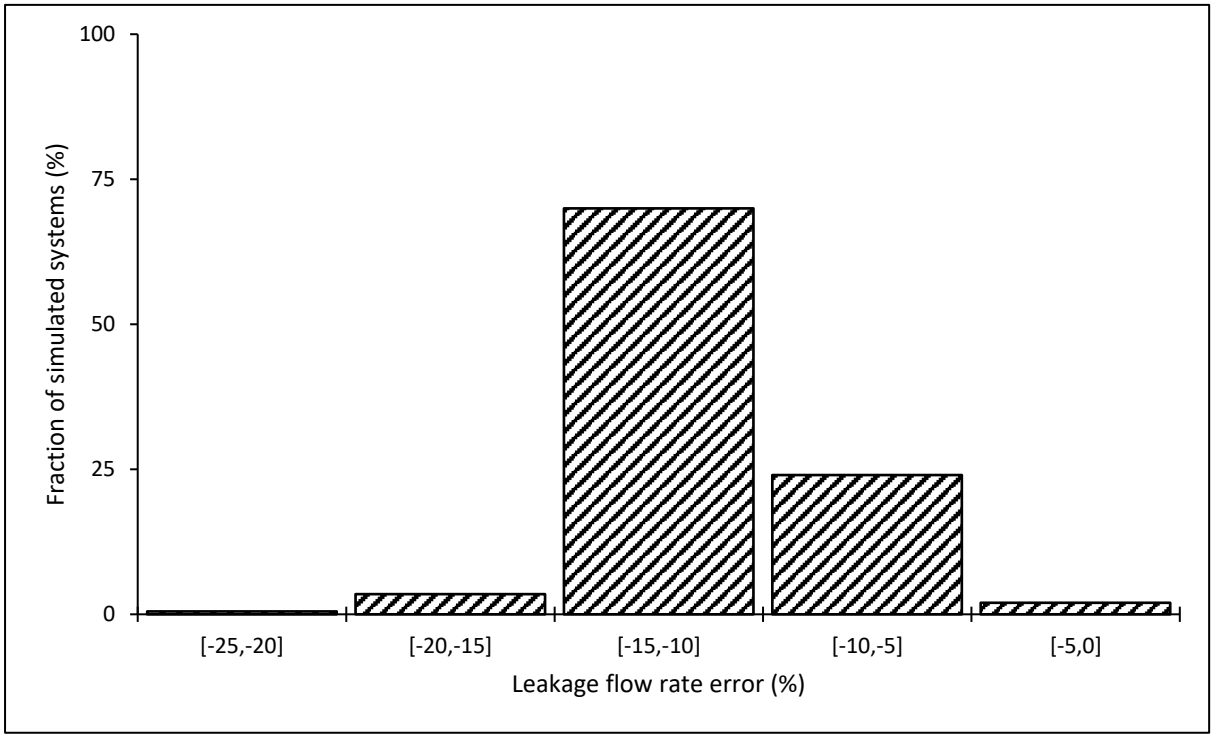

Figure 51: System leakage estimation error using the power equation after the implementation of pressure management

Individual node

A critical node with the lowest pressure in the system during peak demand was used to analyse the size of error when the conventional power equation is used to model diurnal leakage flow rate on an individual node.

Equation (69) was applied to estimate the percentage error in leakage flow rate, before and after the implementation of pressure management.

Although results for the diurnal system leakage flow rate before pressure management indicated that the error in leakage estimation was virtually negligible, the same cannot be said for an individual node. As presented in table 25, there was up to -14.95% underestimation and up to 5.29% overestimation of leakage by the power equation before implementation of pressure management.

Figure 52 illustrates that in 43% of the simulated systems the power equation underestimated leakage flow rate at the critical node is in the range $-10\% \; to \; -5\%$, and that in 36.5% of the systems there was underestimation in the range $-15\% \; to \; -10\%$. Furthermore, 91% of the simulated systems showed underestimation while only 9% showed overestimation.

After the implementation of pressure management, there was up to -64.43% underestimation of leakage flow rate by the power equation at the critical node and up to 26% overestimation; this is shown in table 25.

Table 25 indicates that on average, after the implementation of pressure management, the power equation underestimated leakage by -41.27%. Figure 53 shows that in 80% of the simulated systems the power equation underestimated leakage by more than -30%.

The leakage simulation results before and after the implementation of pressure management as presented in this section emphasize further that the conventional power equation is simply an empirical formulation that should only be used within a range of data for which it has been calibrated.

Table 25: Leakage estimate error at critical node using the power equation

	Leakage estimate error (%)			
	Minimum	**Arithmetic Mean**	**Median**	**Maximum**
Before implementing pressure management	-14.95	-7.74	-9.04	5.29
After implementing pressure management	-64.43	-41.27	-46.11	26.00

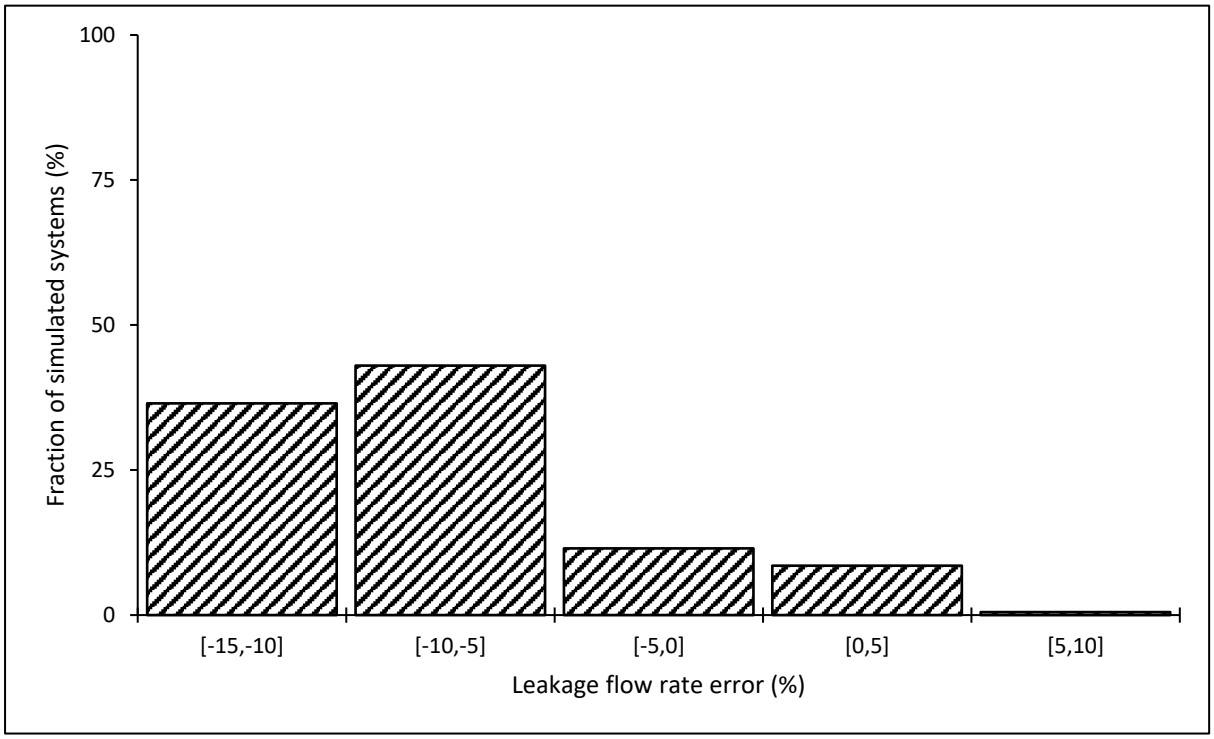

Figure 52: Leakage estimation error when using the power equation at the critical node before the implementation of pressure management

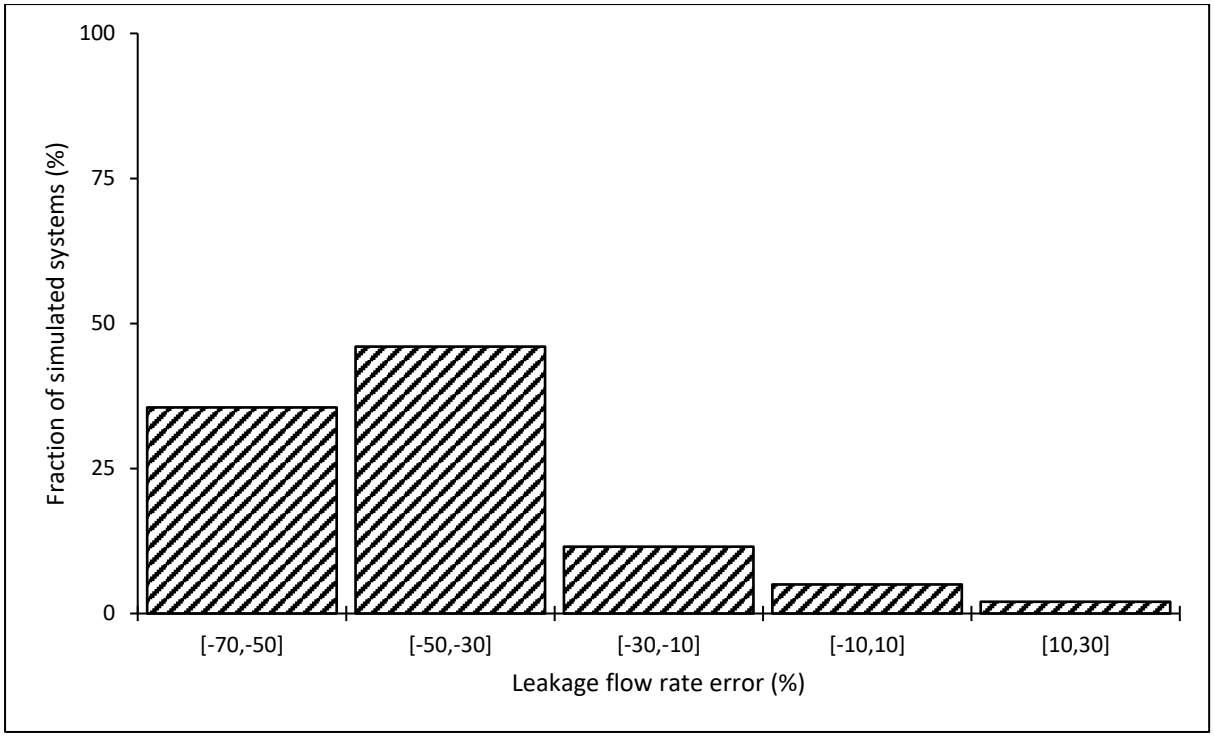

Figure 53: Leakage estimation error using the power equation at the critical node after the implementation of pressure management

5.6. Impact of leakage level on simulation results

5.6.1. Introduction

This section presents an evaluation of the impact of different leakage levels in water distribution pipe networks, on the hydraulic simulation results obtained from the modified orifice and conventional power equations.

Instances of the medium network with leakage levels equivalent to the infrastructure leakage indices (ILIs) of 1, 4, 16 and 64 were randomly chosen for presentation in this section. Simulation results of small and large networks are analysed in the same way and documented in Appendix B.

First, the impact on the power equation's system leakage exponent is presented, followed by the impact on predicting the modified orifice equation's system parameters from individual leaks. Then the effect of leakage level on the power equation's error in estimating pressure head is presented. This is followed by a description of the impact on the error in estimating the leakage flow rate for both the entire system and individual nodes.

5.6.2. Leakage exponent of the power equation

A key parameter in the power equation is the leakage exponent $N1$. Given that it is an exponent of the pressure head, it has much influence on the magnitude of the leakage flow rate when compared to the corresponding leakage coefficient C. Statistical distributions of the equivalent leakage exponents obtained for the medium network with the four leakage levels (ILIs) of 1, 4, 16 and 64 are presented in table 26.

Generally, leakage exponents increased with the level of leakage in the systems. The lowest leakage exponent was 0.57, observed in a system with an ILI of 4, and the highest was 1.40, observed in the system with an ILI of 64.

For all four leakage levels, the distribution of leakage exponents can be regarded as almost symmetrical since the arithmetic mean values are very close to the corresponding median values.

Figure 54 presents normalized cumulative fractions of simulated systems when plotted against corresponding system leakage exponents. The plot shows that the observed leakage exponents are in the range of values that have been found in many other field and experimental studies (Ogura 1979; Lambert 2000; Trow and Farley 2003; Cassa and van Zyl 2013 and Schwaller et al. 2015) . Noticeably for the ILI of 16 which models a typical leakage level in most water distribution pipe networks around the world, about 70% of the simulated systems showed a leakage exponent of about 1.1. This value has been found in many field studies as reported in Trow and Farley (2003).

Table 26: System leakage exponents for medium network with ILI of 1, 4, 16 and 64

Infrastructure Leakage Index (ILI)	**System leakage exponents (N1)**			
	Minimum	**Arithmetic Mean**	**Median**	**Maximum**
1	0.64	0.68	0.67	0.83
4	0.57	0.83	0.84	1.10
16	0.81	1.07	1.07	1.35
64	1.06	1.18	1.18	1.40

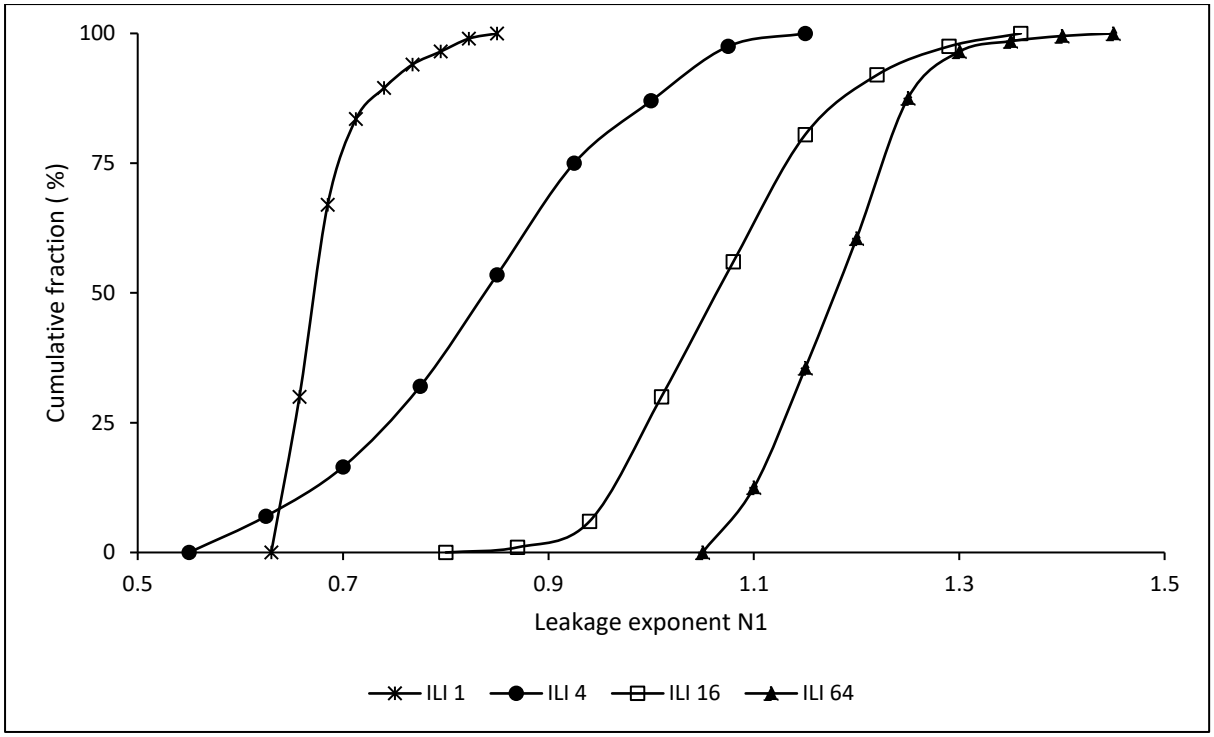

Figure 54: Cumulative fractions of system leakage exponents for the medium network with an ILI of 1, 4, 16 and 64.

5.6.3. System leak parameters in the modified orifice equation

The leak parameters in the modified orifice equation are the initial leak area A_0 and the head-area slope *m*, from which the corresponding effective values are obtained using equations (66) and (67).

Figure 55 shows how the system's estimated effective initial leak areas and the sum of the effective individual initial leak areas approximate to the zero-error line. This indicates that irrespective of the level of leakage, the system's initial leak area can be estimated reasonably accurately from the sum of the individual initial leak areas. These results conform to the findings in Schwaller et al. (2015).

Figure 56 shows that the system's estimated effective head-area slopes and the sum of effective individual head-area slopes also plot around the zero-error line for low leakage levels equivalent to ILIs of 1, 4 and 16. For a high leakage level, equivalent to an ILI of 64, some points are below the zero-error line while none is above the line. These results indicate that the accuracy with which system head-area slopes can be predicted from the sum of individual head-area slopes is reduced with an increase in the system leakage flow rates.

In conclusion, a system's initial leak areas can be predicted quite accurately from the sum of individual initial leak areas irrespective of the level of system leakage, while the prediction of a system's head-area slope is influenced by the leakage level.

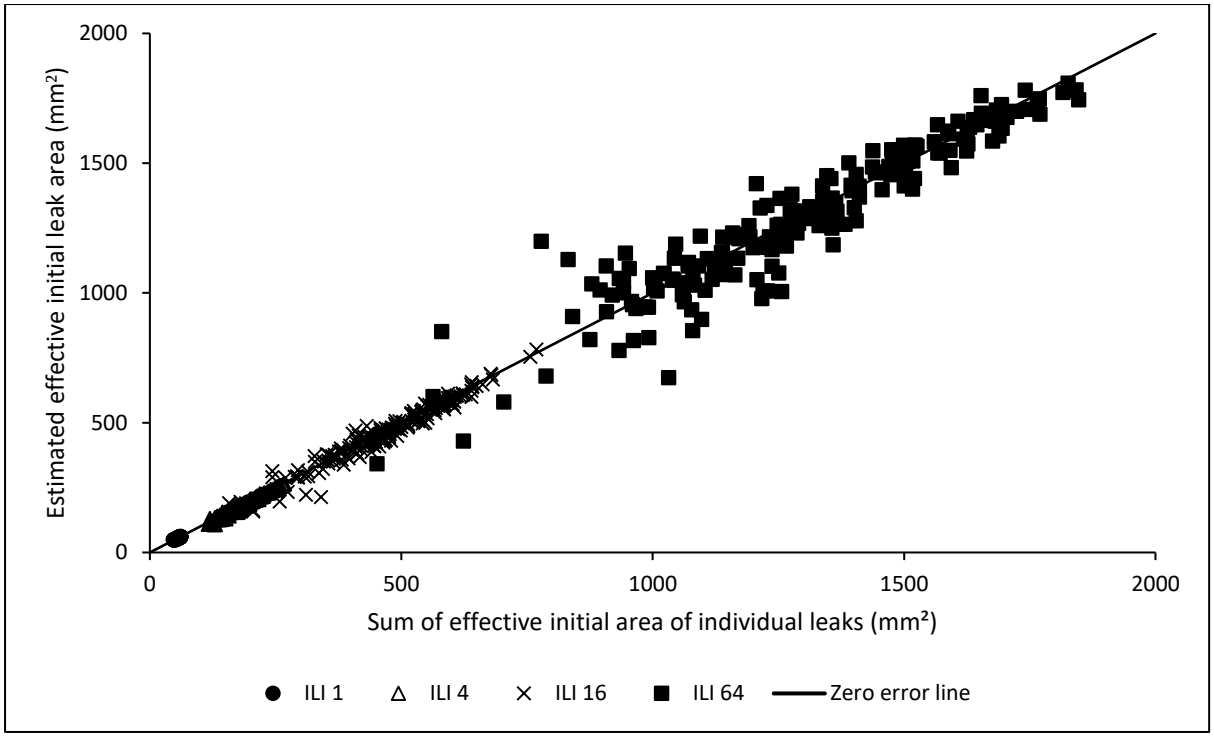

Figure 55: Predicting a system's initial leak area from the sum of individual leaks for networks with an ILI of 1, 4, 16 and 64

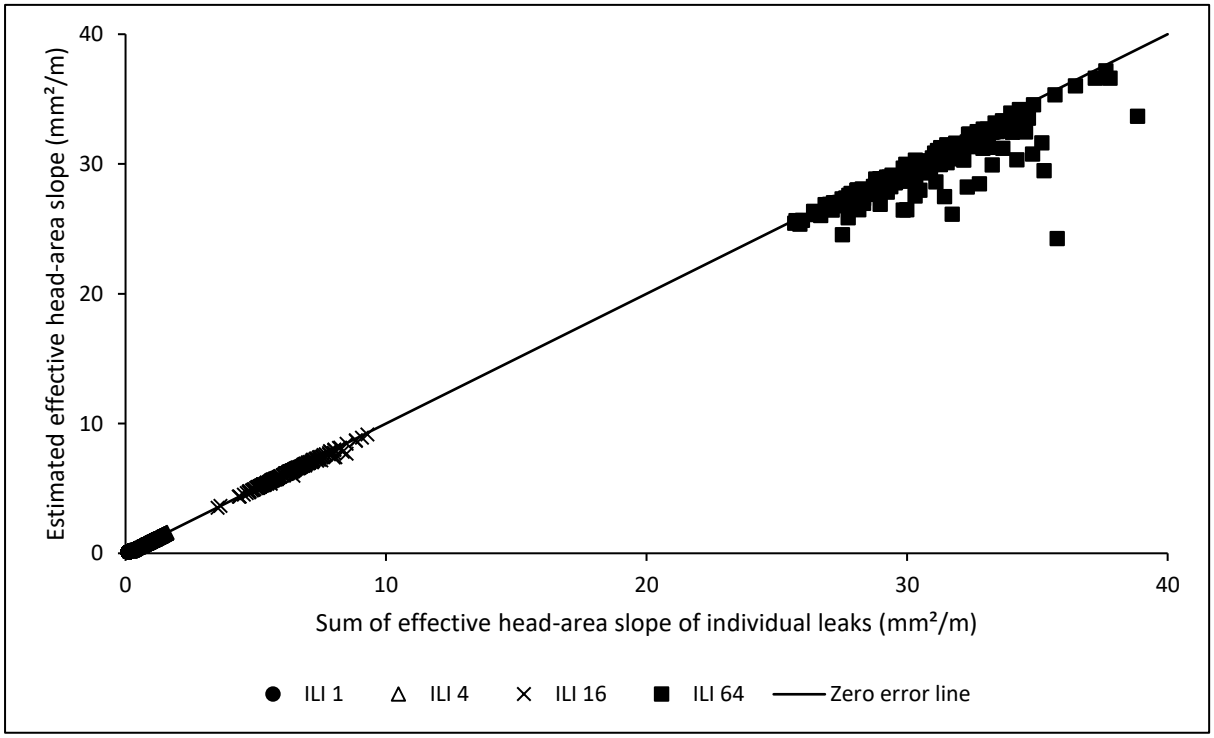

Figure 56: Predicting a system's head-area slope from the sum of individual leaks for networks with an ILI of 1, 4, 16 and 64

5.6.4. Pressure head estimation error in the use of the power equation

It was assumed that leakage levels have an impact on the error that occurs when the conventional power equation is used to estimate the pressure head. This was investigated at the average zone pressure (AZP) node during the minimum night flow (MNF) and at peak demand conditions.

Overall, the results show that the leakage levels had no effect on the pressure head estimation error for the power equation, both during minimum night flow and at peak demand. As shown in figures 57 and 58, all the simulated systems with leakage levels equivalent to ILIs of 1, 4, and 16 showed that the error was in the range $-0.0001\%\ to\ 0.0001\%$ during minimum night flow and $-0.3\%\ to\ 0.3\%$ during peak demand.

Systems with a leakage level equivalent to an ILI of 64 showed a very slight increase in the percentage error, both during the minimum night flow and peak demand. However, this increase is too insignificant to be regarded as having any effect in practice.

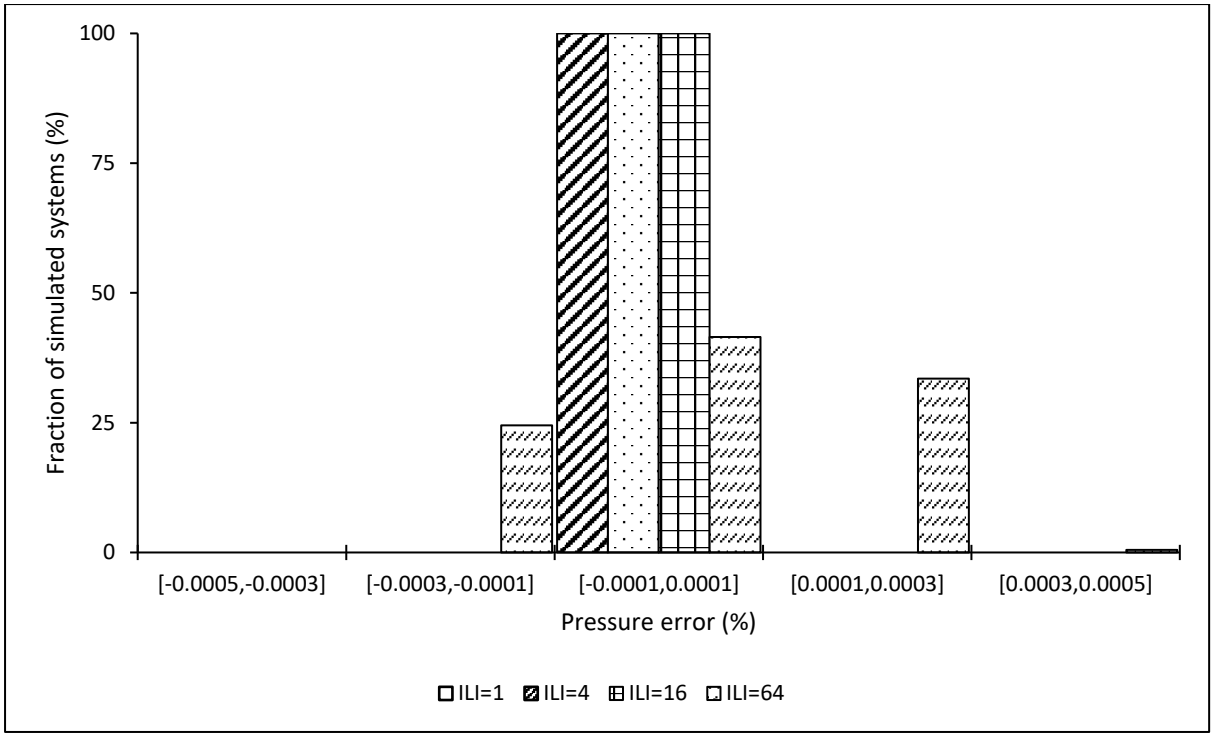

Figure 57: Pressure estimation error in the use of the power equation at AZP node during MNF for networks with an ILI of 1, 4, 16 and 64

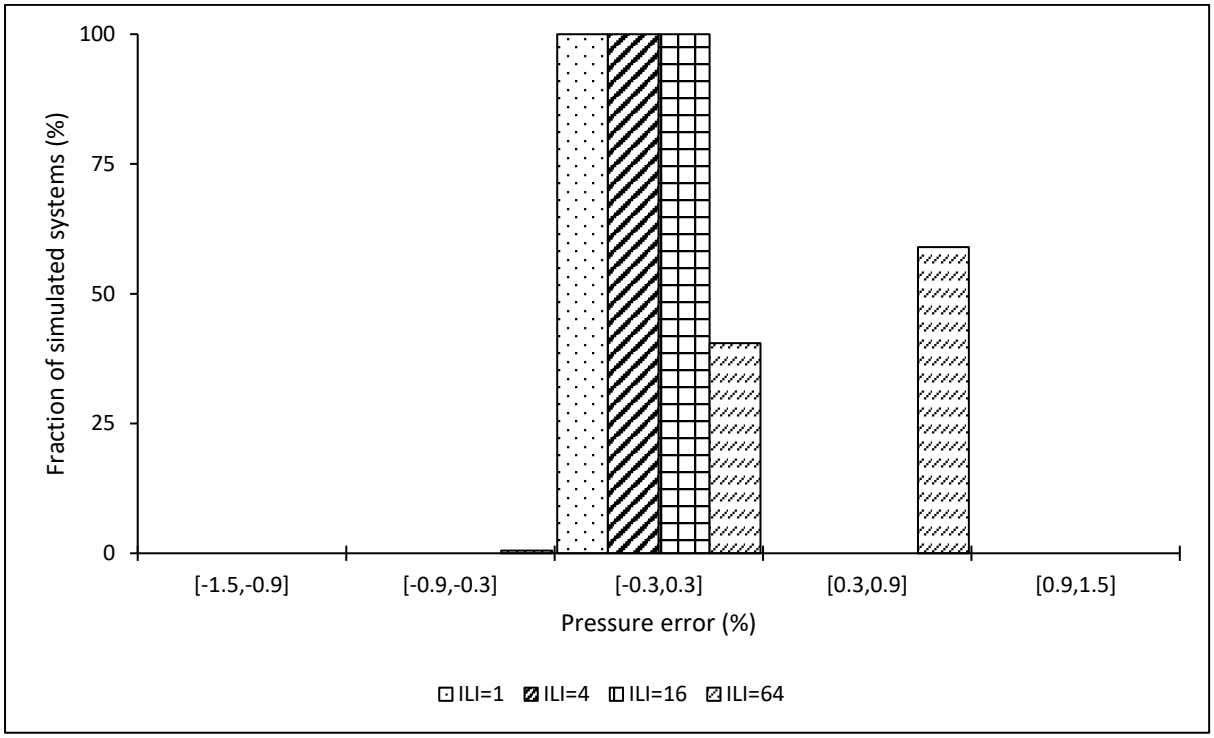

Figure 58: Pressure estimation error in the use of the power equation at AZP node during peak demand for networks with an ILI of 1, 4, 16 and 64

5.6.5. System leakage estimation error in the use of the power equation

The impact of the leakage level on the error occurring when the power equation is used to model system leakage flow rate was analysed for systems with leakage levels equivalent to an ILI of 1, 4, 16 and 64. The analyses were conducted both before and after the implementation of pressure management.

Figure 59 shows the results before the implementation of pressure management. These results indicate that for each leakage level in more than 80% of the simulated systems the percentage error in the system leakage estimated by the power equation was in the range $-0.9\% \; to \; -0.1\%$. The results further show that there were cases of both underestimation and overestimation irrespective of the leakage level.

Figure 60 illustrates that after the implementation of pressure management more than 60% of the simulated systems with leakage levels equivalent to an ILI of 4, 16 and 64 showed that the power equation underestimated system leakage flow rate in the range $-13\% \; to \; -7\%$. Also, at least 84% of simulated systems with an ILI of 1 showed that the error was in the range $-7\% \; to \; -1\%$. Only 1% of the simulated systems with an ILI of 64 showed that the power equation overestimated the leakage flow rate.

Generally, as presented in the results, the analyses found that the leakage level in the water distribution systems did not greatly influence the leakage flow rate error in system leakage modelling using the power equation, both before and after the implementation of pressure management.

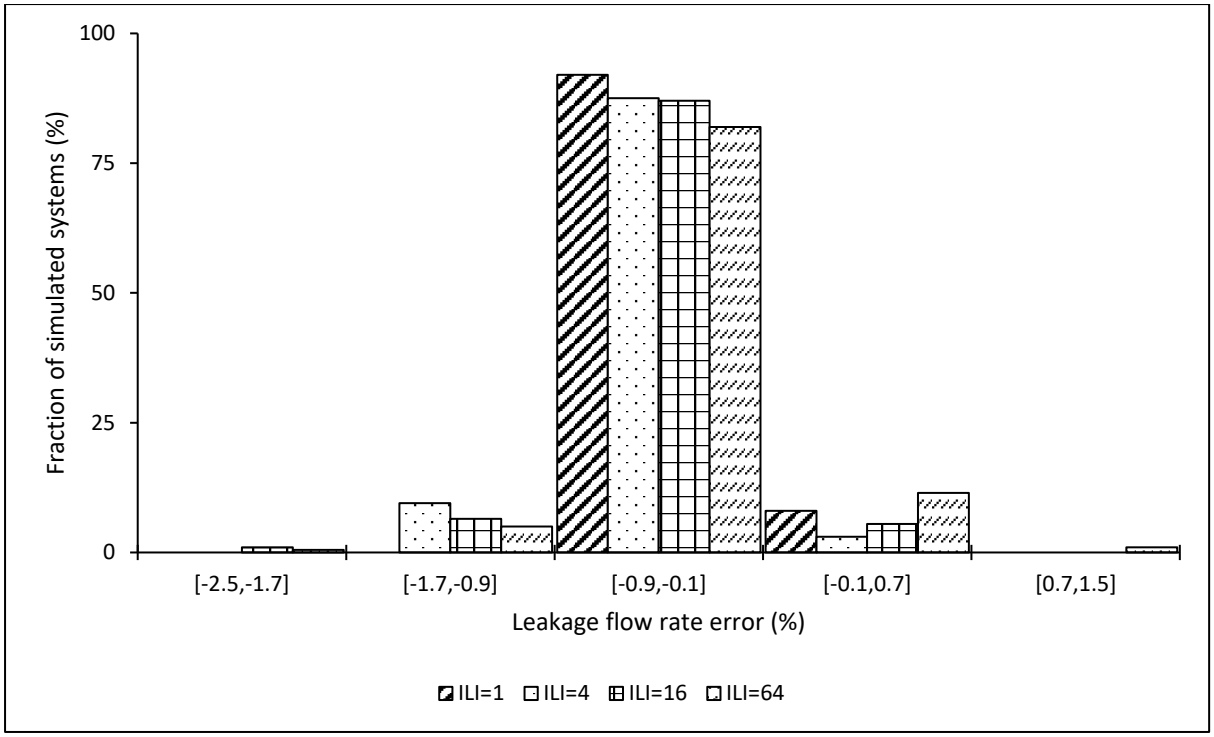

Figure 59: System leakage estimation error in the use of the power equation for networks with an ILI of 1, 4, 16 and 64 before the implementation of pressure management

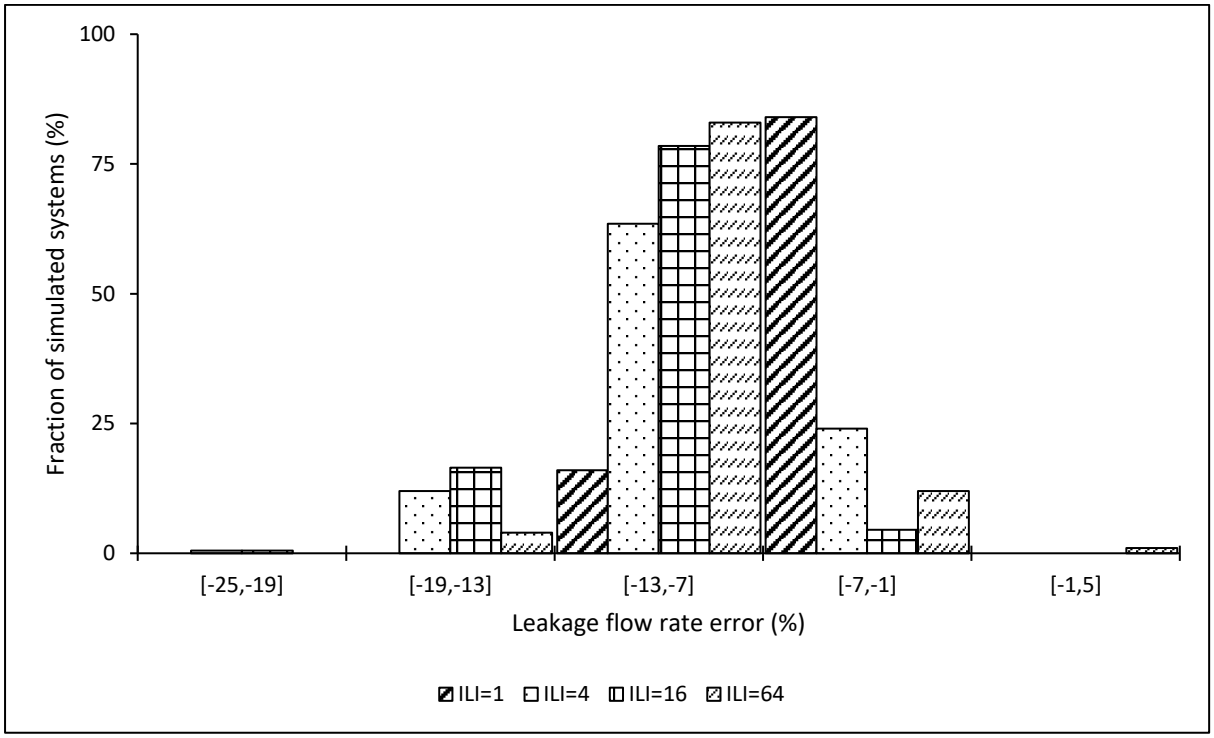

Figure 60: System leakage estimation error in the use of the power equation for networks with an ILI of 1, 4, 16 and 64 after the implementation of pressure management

5.6.6. Individual node leakage estimation error in the use of the power equation

This section presents the impact of the leakage level on the error occurring when the power equation is used to model the leakage flow rate at an individual node, both before and after the implementation of pressure management. A critical node which has the minimum pressure in the system during peak demand was used in the analysis.

Figure 61 shows the results before the implementation of pressure management. These results indicate that for an ILI of 1 the use of the power equation led to a leakage flow rate error in the range $-5\%\ to\ 5\%$ in more than 80% of the simulated systems. For ILIs of 16 and 64, the error was in the range $-15\%\ to\ -5\%$ in more than 60% of the simulated systems. For systems with an ILI of 4, 51% showed an error in the range $-15\%\ to\ -5\%$, while for 47% and 2% it was in the range of $-5\%\ to\ 5\%$ and $5\%\ to\ 15\%$ respectively.

After the implementation of pressure management, the leakage flow rate error occurring with the use of the power equation in estimating leakage flow rate increased enormously; this is shown in figure 62. More than 60% of the simulated systems with an ILI of 1 and 4 showed that the error was in the range $-40\%\ to\ 20\%$, while the same percentage of systems with an ILI of 16 and 64 showed that it was in the range $-100\%\ to\ -40\%$. For systems with an ILI of 1, about 1.5% showed that the error was in the range $140\%\ to\ 200\%$ and about 0.5% showed that it was in the range $-100\%\ to\ -40\%$.

Generally, the leakage flow rate error that occurred with the use of the power equation increased with the leakage level of the system, both before and after the implementation of pressure management.

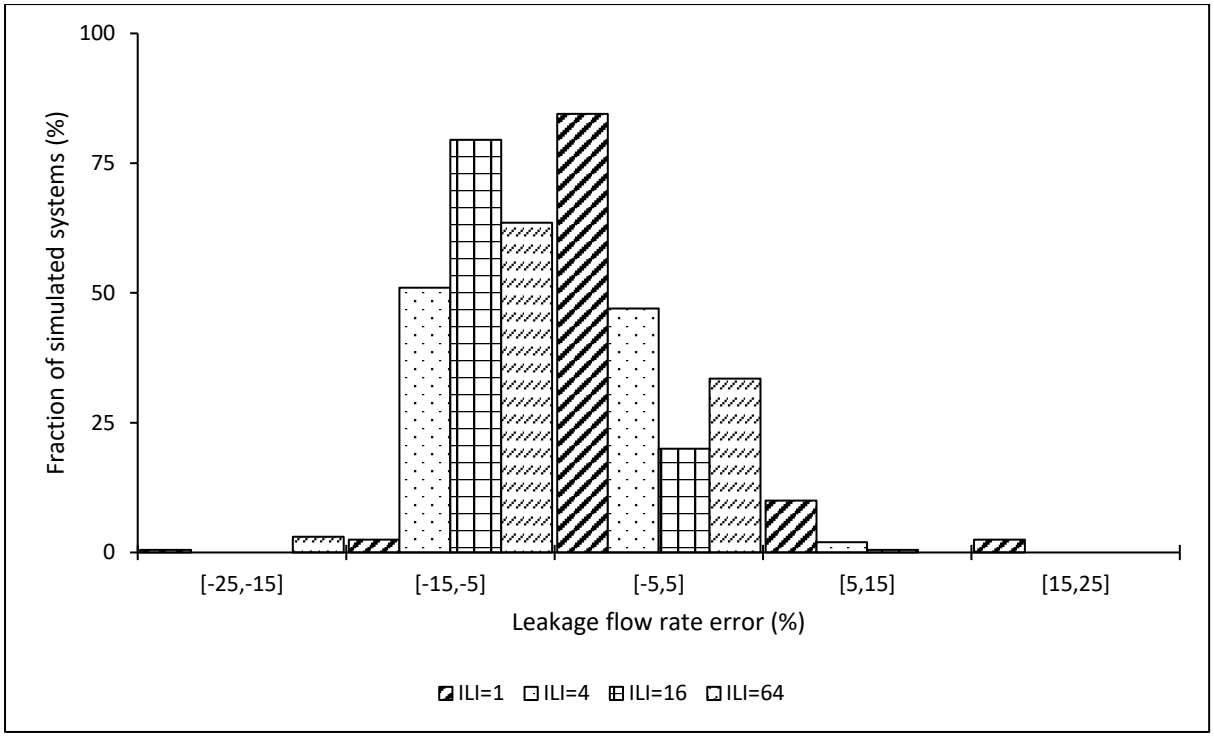

Figure 61: Leakage estimation error with the use of the power equation at the critical node before the implementation of pressure management

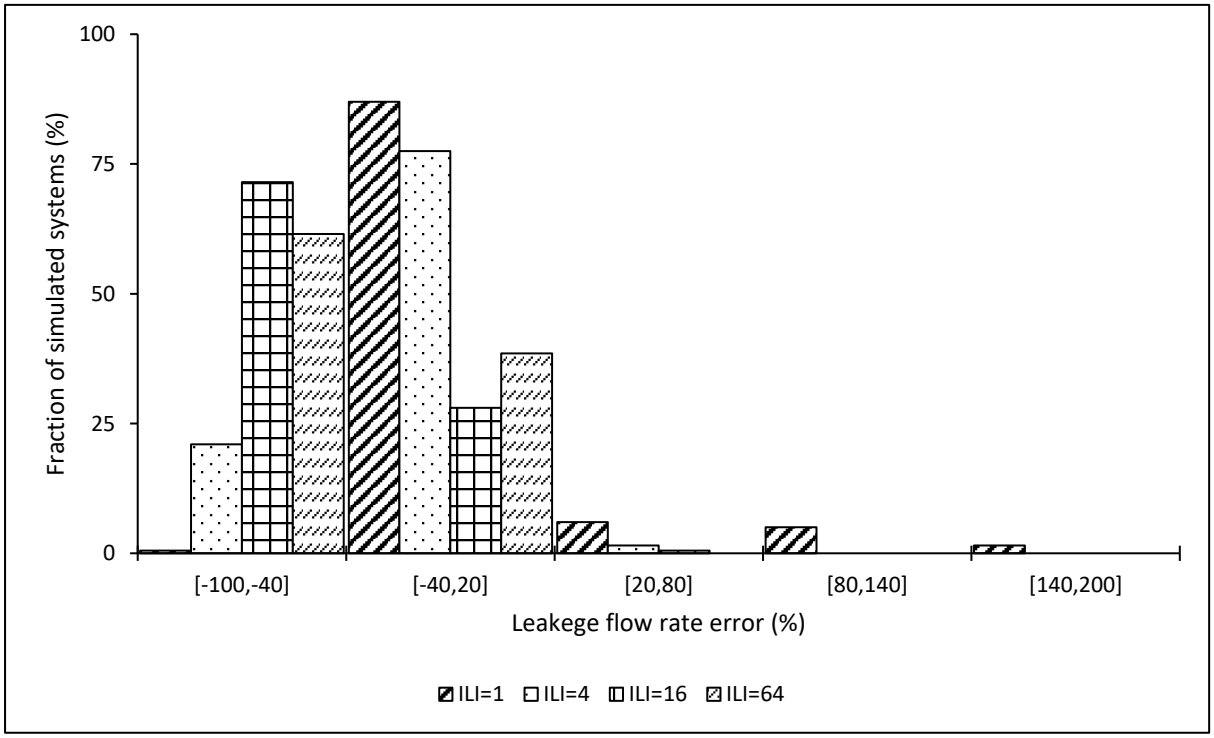

Figure 62: Leakage estimation error with the use of the power equation at the critical node after implementation of pressure management

5.7. Impact of network size on simulation results

5.7.1. Introduction

This section describes the impact of the physical size of a water distribution network on hydraulic simulation results in the modelling of the leakage and pressure relationship. Three differently sized pipe networks, i.e. small, medium and large, were analysed for the same leakage level, i.e. either 1, 4, 16 or 64. Because the analysis of each of the leakage levels for the three networks was the same, only results for an ILI of 16 were selected for presentation in this section. All the other results are documented in Appendix C.

First, the influence of network size on the power equation's leakage exponent is evaluated, followed by a prediction of the system parameters of the modified orifice equation from the sum of individual leaks.

A description is then given of the impact that the power equation has on the pressure head estimation error, as well as of the impact on the error when both system and individual node leakage flow rates are modelled.

The section concludes with an investigation of the impact of network size on the average number of iterations required for the global gradient algorithm (GGA) to converge to a hydraulic solution in the simulated systems for both the modified orifice and power equations.

5.7.2. System leakage exponents of the power equation

In this section, the impact of network size on the system leakage exponents of the power equation is analysed. Statistical distribution parameters of the leakage exponents for small, medium and large networks are presented in table 27. A plot of the cumulative fractions of the systems that were simulated against the system leakage exponents is shown in figure 63.

The results show the overall minimum and maximum leakage exponent values of 0.65 and 1.37 that were observed in small and large systems respectively. All the leakage exponents observed were in the range of pressure head exponents described by the modified orifice formulation, i.e. between 0.5 and 1.5.

The arithmetic mean values were found to be 0.92, 1.07, and 1.16 for the small, medium and large networks respectively. This indicates that generally system leakage exponents increased with the increase in the network size. It should be noted that a large network will have more leaks than a small network of the same ILI. These results conform with the findings in a study by Schwaller et al. (2015), in which they studied distributions of $N1$ values for sets of 10,000, 1,000 and 100 leaks. High $N1$ values were observed in the 10,000 leaks set as compared to the other two sets.

Finally, the results show that a statistical distribution of the leakage exponents was practically symmetrical since the arithmetic mean values were very close to their corresponding median values. It is however noticeable that the medium and large networks were relatively more symmetrical than the small ones.

Table 27: System leakage exponents for small, medium and large networks with an ILI of 16

	System leakage exponents (N1)			
	Minimum	**Arithmetic Mean**	**Median**	**Maximum**
Small	0.65	0.92	0.91	1.25
Medium	0.81	1.07	1.07	1.35
Large	0.99	1.16	1.16	1.37

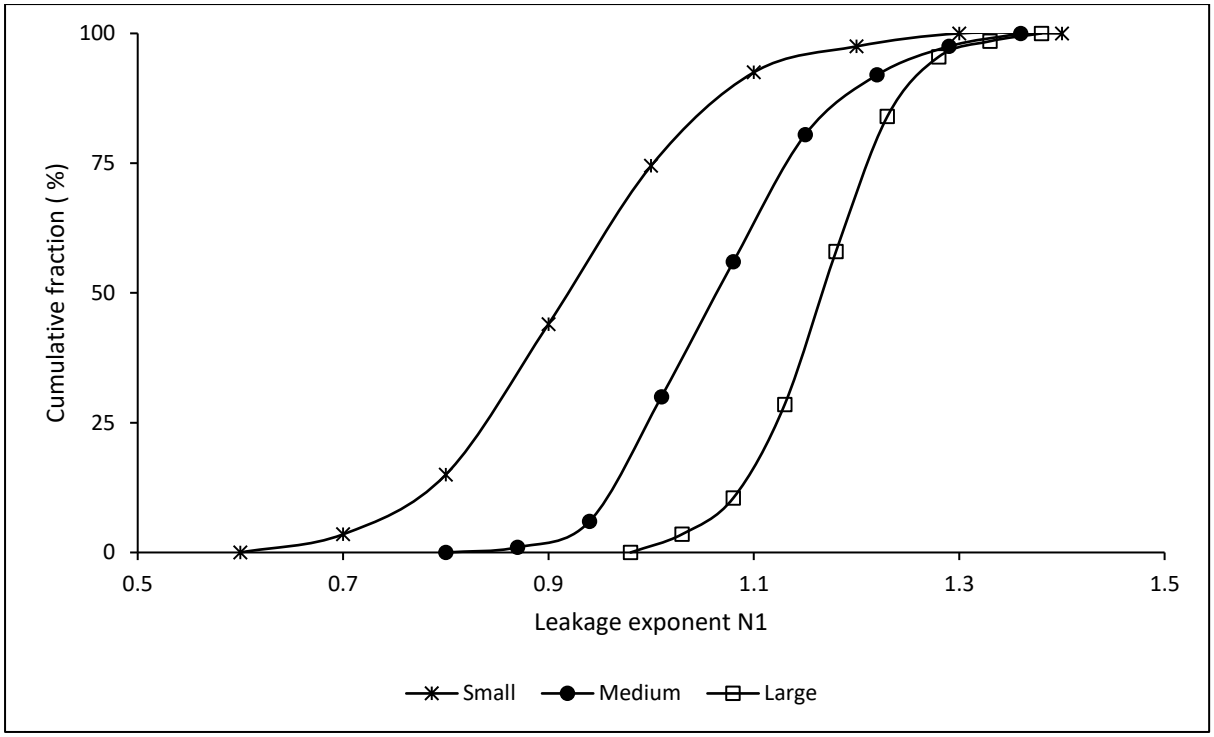

Figure 63: System leakage exponents for small, medium and large networks with an ILI of 16

5.7.3. System leakage parameters of the modified orifice equation

This section describes the effect of network size on the prediction of a system's initial leak area and head-area slope with the use of the modified orifice equation from the sum of respective individual leak parameters. The estimated effective system leak parameters are plotted against the sum of individual leaks effective parameters, on the same scale as a zero-error line.

Figure 64 shows that the plotted points are quite close to the zero-error line; this means that irrespective of the size of the network the system's initial leak areas can be predicted quite accurately from the sum of the individual leak initial areas.

For the head-area slope, figure 65 shows that in small networks, the system head-area slope and the sum of the individual head-area slopes plot quite closely along the zero-error line. However, as the size of the network increases, the plotted points tend to move away from the zero-error line. More plotted points lie below the zero-error line as the pipe network size increases.

The results indicate that a system's initial leak areas can generally be predicted quite accurately irrespective of the size of the network, whereas the degree of accuracy in predicting system head-area slope decreases with an increase in the size of the network.

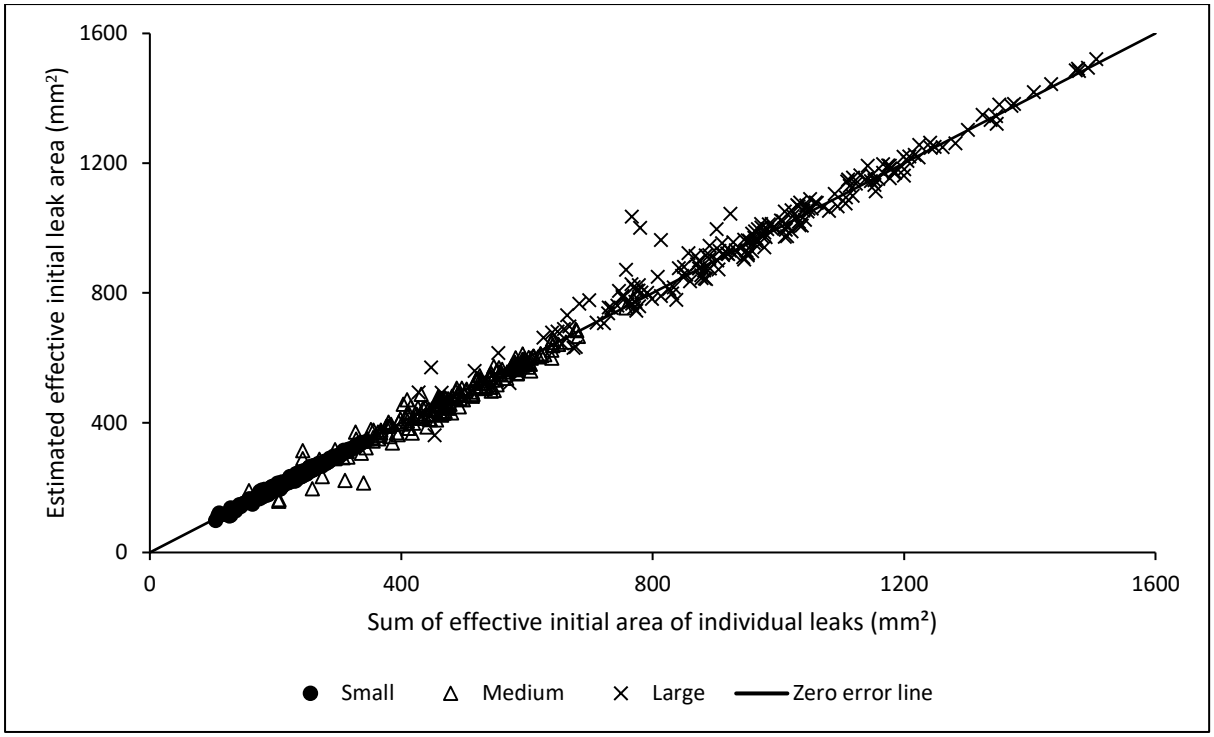

Figure 64: Predicting a system's initial leak area from the sum of individual leaks for small, medium and large networks

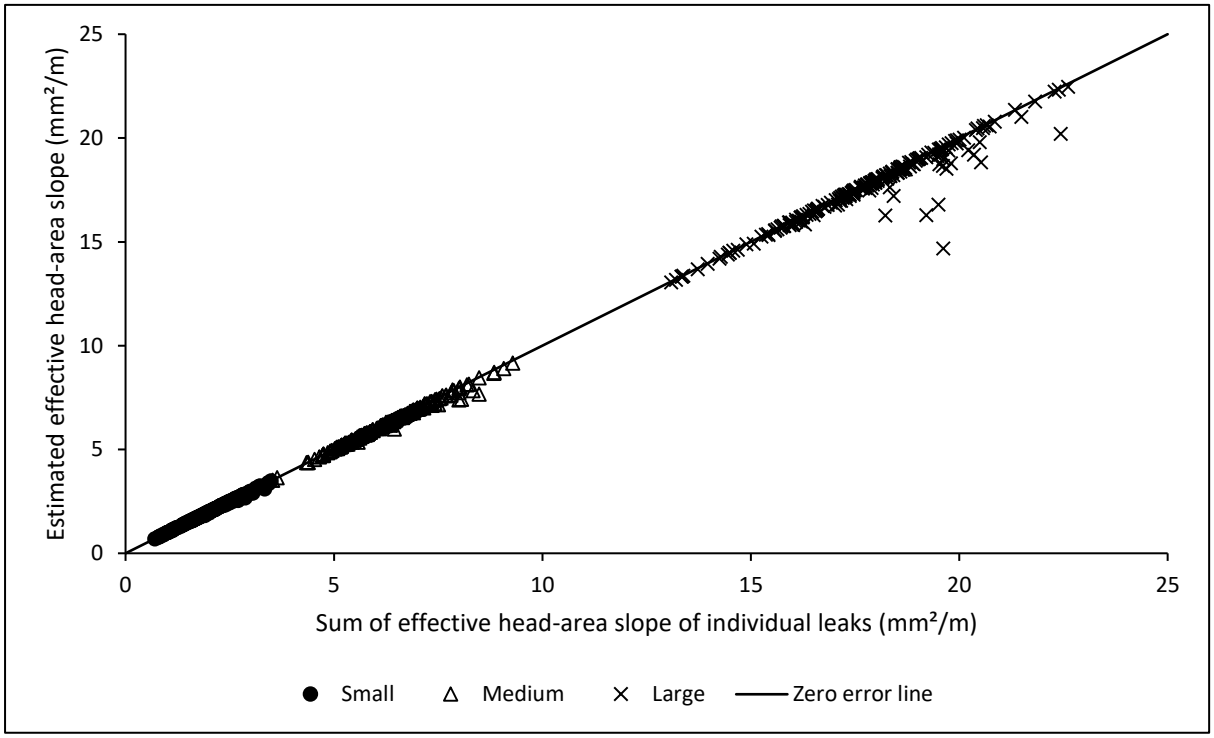

Figure 65: Predicting a system's head-area slope from the sum of individual leaks for small, medium and large networks

5.7.4. Pressure head estimation error for the power equation

In this section, the impact of network size on the pressure head estimation error that occurs with the use of the power equation when modelling leakage, is investigated. The average zone pressure (AZP) node, which is considered to have a pressure head representative of the system pressure, was used. The errors were calculated during minimum night flow (MNF) condition, a period when system pressure head is believed to be the highest, and at peak demand when system pressure head is the lowest.

The results show that, irrespective of the size of network, during minimum night flow the pressure estimation error was very insignificant, in the range $-0.01\% \; to \; 0.01\%$ as shown in figure 66.

During peak demand conditions, 42% of the simulated medium networks showed the error to be in the range $0.1\% \; to \; 0.3\%$, while the rest of the systems showed a pressure head estimation error in the range $-0.1\% \; to \; 0.1\%$ This is shown in figure 67.

Overall, results show that the size of network did not have an influence on the pressure head estimation error when the power equation is used to model the pressure and leakage relationship in water distribution networks.

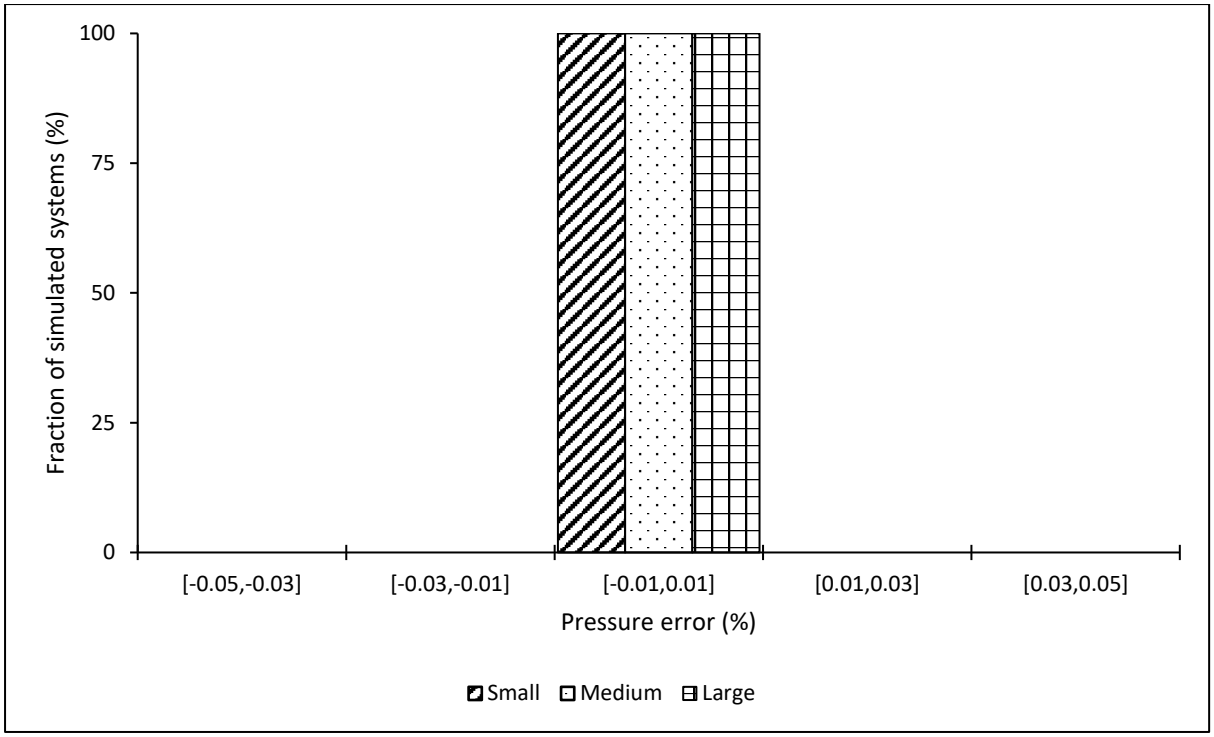

Figure 66: Pressure estimation error with use of the power equation for small, medium and large networks during MNF

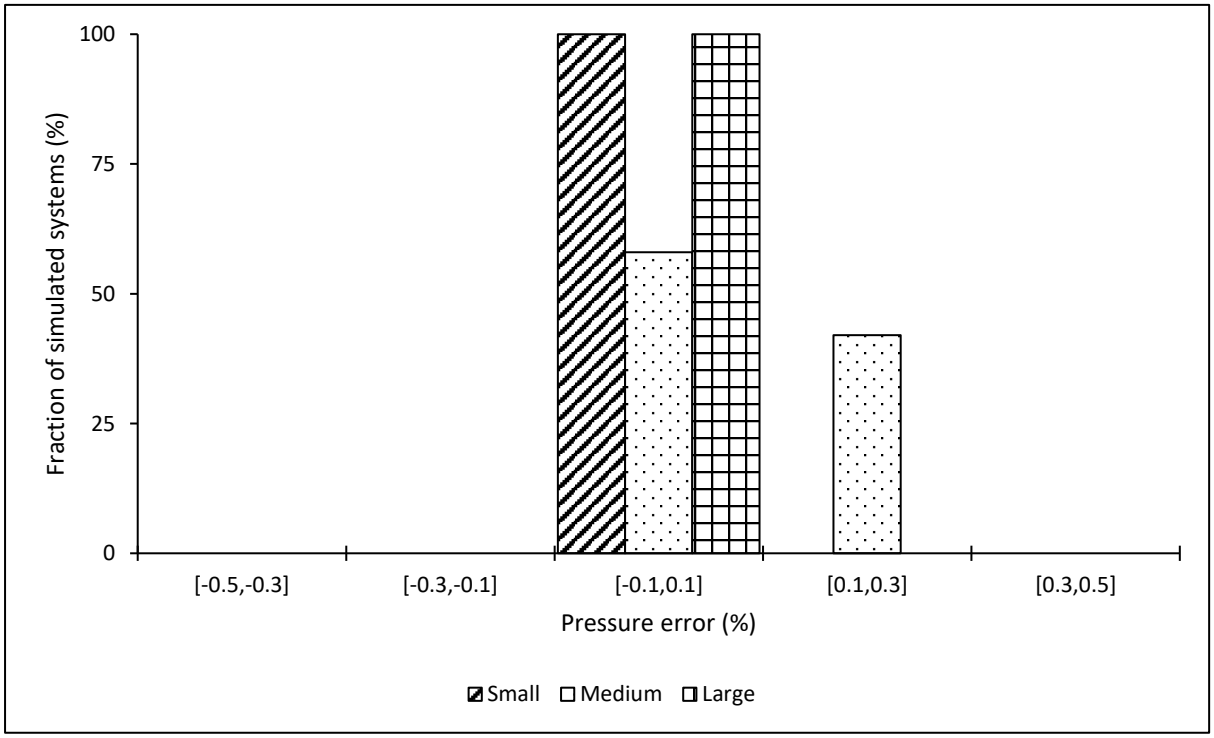

Figure 67: Pressure estimation error with use of the power equation for small, medium and large networks during peak demand

5.7.5. System leakage estimation error for the power equation

This section describes the impact of network size on the error occurring with the use of the power equation in modelling system leakage flow rate, both before and after the implementation of pressure management.

The study found that before implementation of pressure management, regardless of the size of the network, the error in the estimation of system leakage was practically insignificant; this is shown in figure 68. It was found that 100%, 53%, and 99.5% of small, medium and large networks respectively showed the estimation error to be in the range $-0.5\%\ to\ 0.5\%$. About 1% of medium systems showed the biggest underestimation in the range $-2.5\%\ to\ -1.5\%$. About 0.5% of large systems showed the overestimation leakage flow rate to be in the range $0.5\%\ to\ 1.5\%$. There was no system in the medium or small size networks that showed that the power equation was overestimating system leakage. Also, after the implementation of pressure management, none of the simulated systems (small, medium and large) showed system leakage overestimation.

After the implementation of pressure management, results showed that the error in estimating system leakage increased considerably irrespective of the size of the network. This is shown in figure 69. For the medium networks, 70% showed underestimation of leakage flow rate in the range $-15\%\ to\ -10\%$, while for the large and small systems 62% and 56% respectively showed underestimation in the range $-20\%\ to\ -15\%$. It is noted that the results did not show any systems in which leakage flow rate was overestimated.

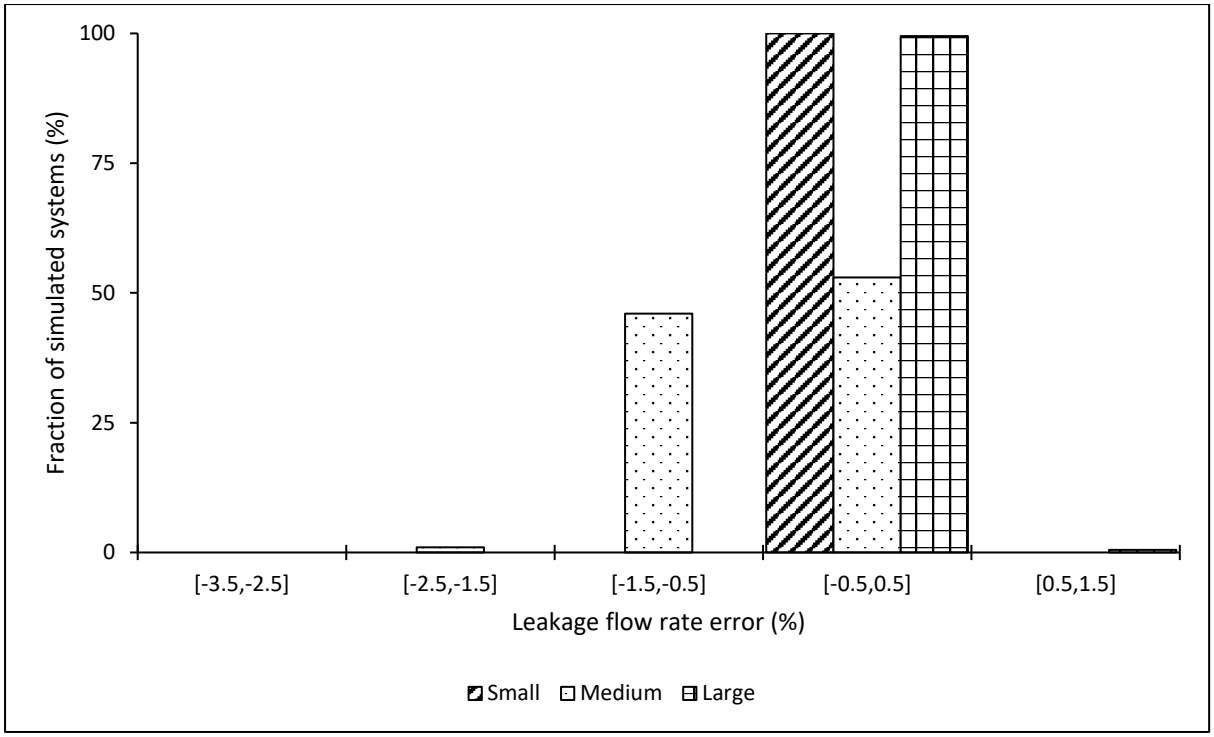

Figure 68: System leakage estimation error in the power equation for small, medium and large networks, before implementation of pressure management

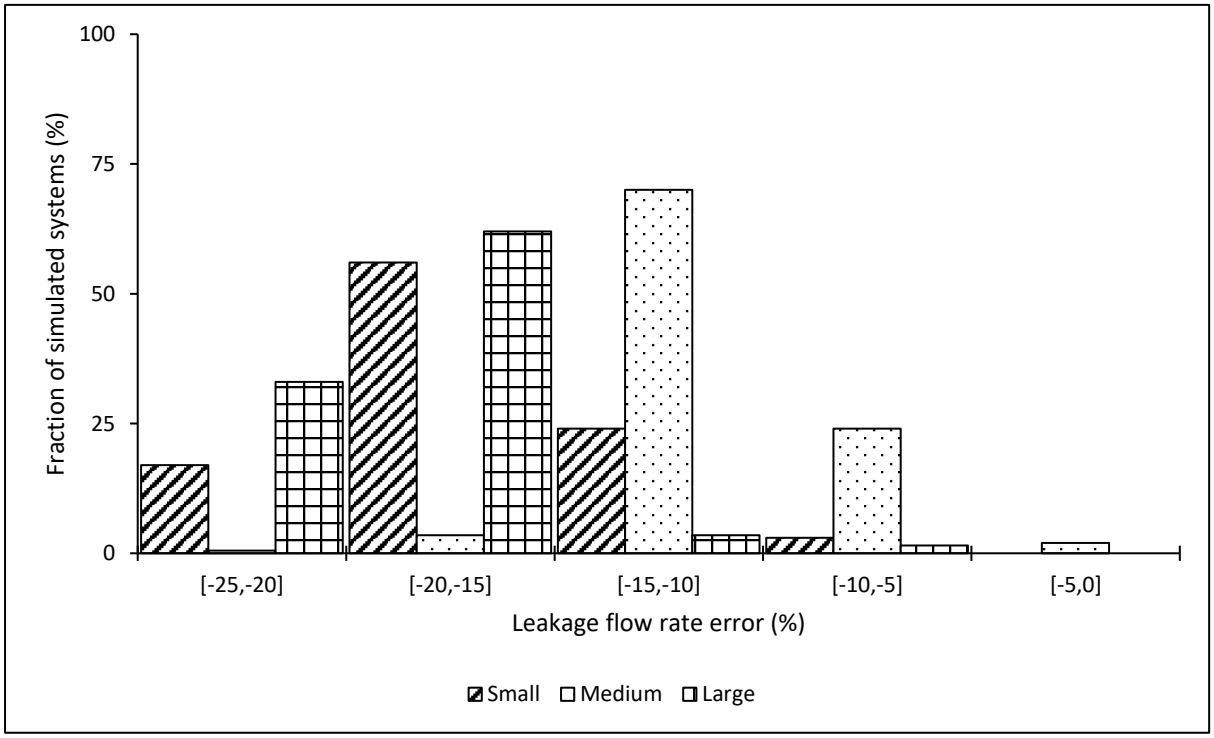

Figure 69: System leakage estimation error in the power equation for small, medium and large networks, after the implementation of pressure management

5.7.6. Leakage estimation error at the individual node for the power equation

A critical node was used in investigating the impact of network size on the leakage estimation error, when the power equation is used to model leakage flow rate at an individual node. The investigations were made both before and after the implementation of pressure management.

The results presented in figure 70 show that 89.5% and 67.5% of the large and small networks respectively underestimated leakage flow rate in the range $-5\%\ to\ 0\%$. Most of the medium networks showed an estimation error in the range $-15\%\ to\ -10\%$ and $-10\%\ to\ -5\%$. It is noticeable that most of the simulated systems indicated that the leakage flow rate was underestimated, although a few showed overestimation, irrespective of the network sizes.

After the implementation of pressure management, the results shown in figure 71 indicate that in most of the simulated systems the estimation error was in the range $-80\%\ to\ -50\%$ and $-50\%\ to\ -20\%$, regardless of the network sizes. A few cases of overestimation of individual leakage flow rates were observed in all three different sized networks.

Generally, the results showed that both before and after the implementation of pressure management, the size of the network did not have an impact on the leakage flow rate estimation error with the use of the power equation to model leakage at an individual node.

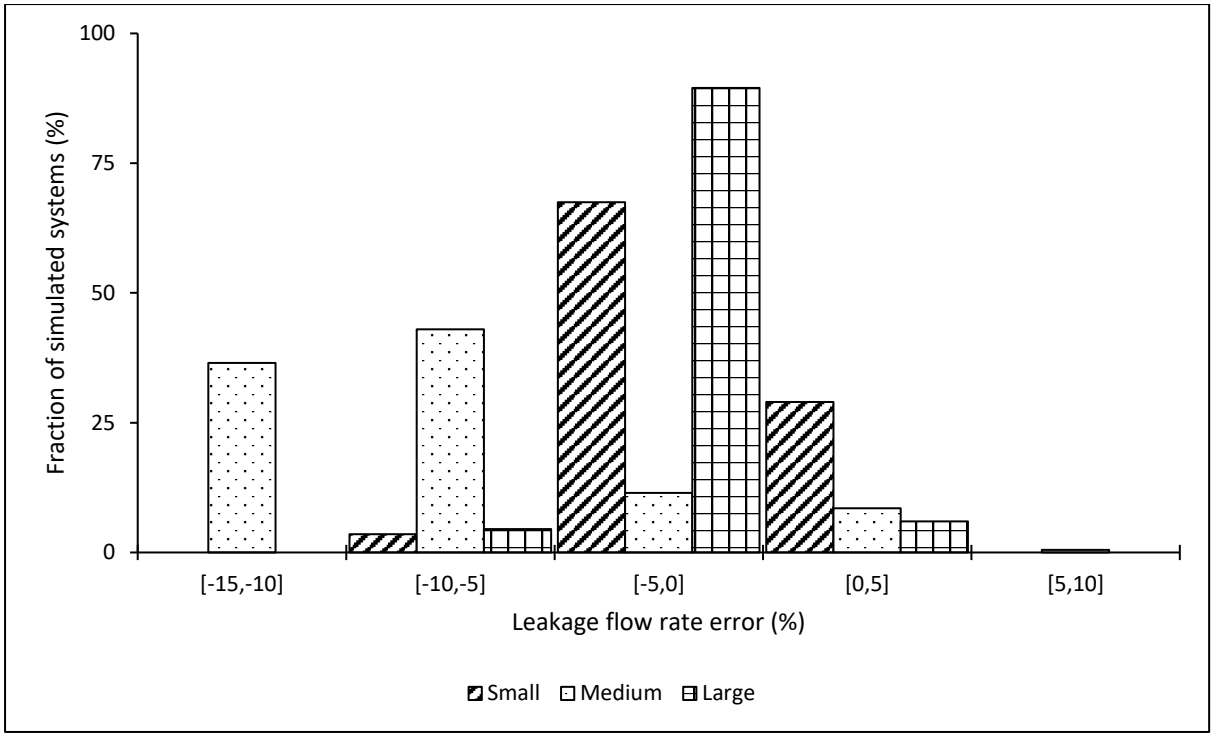

Figure 70: Leakage estimation error for the power equation at the critical node for small, medium and large networks before the implementation of pressure management

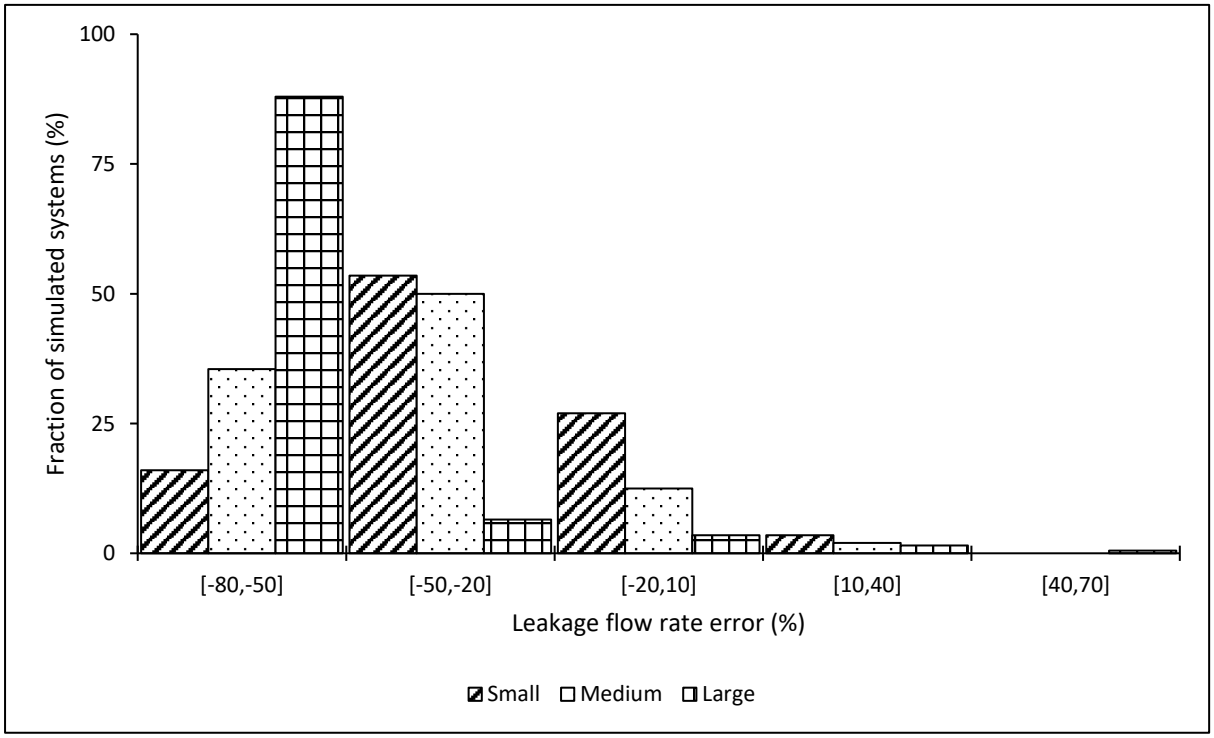

Figure 71: Leakage estimation error for the power equation at the critical node for small, medium and large networks after the implementation of pressure management

5.7.7. System convergence to a hydraulic solution

The impact of network size on the average number of iterations required for a system to converge to a hydraulic solution is presented in figure 72.

As expected, the small pipe networks required the lowest average number of iterations as compared to the medium and large networks. In all three differently sized networks the modified orifice equation required more iterations than the conventional power equation. This was because of the added second emitter function in the modified orifice equation that models leakage flow rate through the expanding part of the leak.

For the large networks, the number of iterations required when there is no leakage in the network was generally higher than when there is leakage. In small and medium networks, this was not the case. This could have been due to the physical properties of the large network shown earlier in table 11, where there are many small diameter pipes, some as small as 25mm. Small diameter pipes with low flow rates will require many iterations for the global gradient algorithm of Epanet to converge to a hydraulic solution.

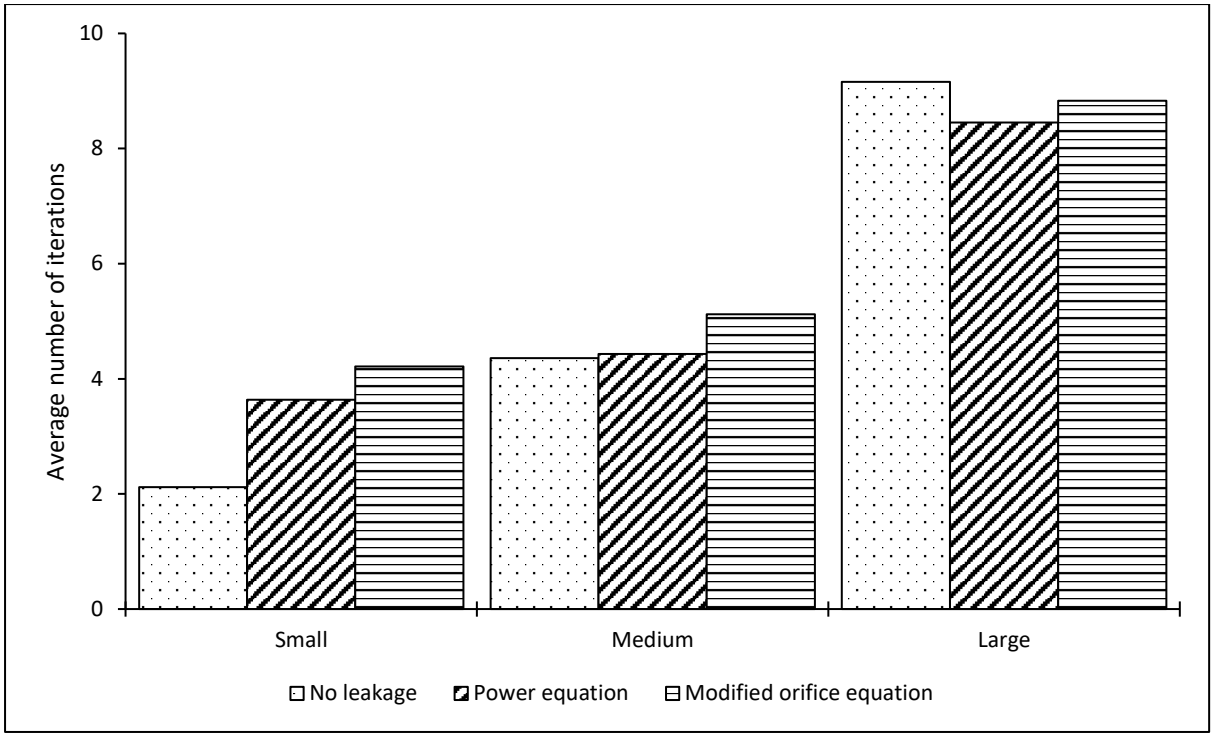

Figure 72: Average number of iterations required for small, medium and large networks to converge to a hydraulic solution, with no leaks in the network and when the leaks are modelled using the power and modified orifice equations

5.8. Discussion

5.8.1. Introduction

This section presents a general discussion on some of the results that were presented in this chapter. First, the effect of the leakage modelling approach (using either the modified orifice or the power equation) on junction pressure heads is discussed. This is followed by a discussion of the effect of the modelling approach on the leakage flow rates both in the entire system and at an individual node.

Statistical distributions of the leakage exponents in the power equations are then discussed for all the different sized pipe networks (small, medium and large) and leakage levels (ILIs of 1, 4, 16 and 64) that were considered in this study.

A discussion on how the system parameters of the modified orifice equation may be predicted from the individual leak parameters, for all the different sized networks and leakage levels follows.

The section ends with a discussion on the convergence properties of the both the power leakage and modified orifice equations.

5.8.2. Effect of leakage modelling approach on the pressure head

The effect of the leakage modelling approach, i.e. either the modified orifice or the conventional power equation, on pressure head at pipe network junctions is discussed here.

Two junctions, namely the average zone pressure (AZP) node and the critical node, were considered in this analysis. Although the variation in pressure head was observed for the 24-hour simulation period, pressure head values during two crucial periods, i.e. minimum night flow (MNF) and peak demand, are discussed.

During minimum night flow, the same pressure heads were observed for both approaches at both the average zone pressure and critical nodes. This was the case for all the simulated systems with the different network sizes and leakage levels.

However, during peak demand conditions the results showed a very small difference in the pressure heads modelled by the two approaches. For example, for 200 medium-sized networks with stochastically generated leaks that are equivalent to an ILI of 16, the arithmetic average of the pressure head error was found to be 0.09% and 0.11% at the average zone pressure and critical nodes respectively. These small differences may be generally considered to be very insignificant in practice.

It must be noted that calibration of the power equation's leakage parameters was done during the minimum night flow conditions and thus the reason why the pressure heads during that period were observed to be the same for the two approaches.

5.8.3. Effect of leakage modelling approach on the leakage flow rate

Although there was practically no significant difference in the effect of the leakage modelling approach on the pressure heads, the same cannot be said for the effect on the flow rates. This analysis was conducted on both the system and individual leakage flow rates before and after the implementation of pressure management.

For the system leakage flow rates, the results showed that before the implementation of pressure management the power equation underestimated leakage, but not as much as after pressure management was implemented. For 200 medium-sized systems with stochastically generated leaks that are equivalent to an ILI of 16, the arithmetic average of the error in leakage modelling was found to be -0.51% and -11.04% before and after the implementation of pressure management respectively.

The percentage errors in modelling leakage flow rates were found to be more during the analysis of individual nodes flow rates, than during the analysis of the entire system flow rates. For example, for the same 200 systems with an ILI of 16, the arithmetic averages of individual leakage flow rates were found to be -7.74% and -41.27% before and after the implementation of pressure management respectively.

Generally, the error in leakage modelling with the power equation approach increased as the pressure head was further away from the one during which the power equation parameters had been calibrated. This was further demonstrated by the increase in leakage error after the implementation of pressure management for both the system and individual node analyses. The results were similar for all the three different sized networks and the four leakage levels.

These results demonstrated that the power equation models leakage accurately only if it is used under the same pressure head during which it has been calibrated.

5.8.4. System leakage exponents for the power equation

The power equation's equivalent system leakage exponents for the three different size networks are presented in table 28 (ILIs of 1 and 4) and table 29 (ILIs of 16 and 64). The cumulative fractions of these leakage exponents (i.e. all the three networks and the four ILIs) are graphically presented in figure 73.

As expected for a given network size, the system leakage exponents generally increased with increase in the level of leakage. It was only in the small-sized network that the arithmetic average of the system leakage exponent reduced from 0.65 to 0.62 when the leakage level was increased from an ILI of 1 to 4. Also, for a given level of leakage, the system leakage exponents increased with an increase in the size of the network. This is the case because with an increase in network size the number of leaks that are generated and distributed also increases, even for the same ILI.

It is noticeable that all the system leakage exponents observed in the analyses (i.e. all network sizes and leakage levels) are in the range of the pressure head exponents described in the modified orifice equation, i.e. between 0.5 and 1.5.

For the leakage level equivalent to an ILI of 16, the arithmetic average system leakage exponent is generally close to 1.1, a value that was found in many field and experimental studies as reported in Trow and Farley (2003). It should be noted that in this study a typical system leakage level was modelled using an ILI of 16.

Table 28: System leakage exponents for small, medium and large networks with an ILI of 1 and 4

	ILI 1				**ILI 4**			
	Min	Mean	Median	Max	Min	Mean	Median	Max
Small	0.63	0.65	0.64	0.72	0.54	0.62	0.58	0.96
Medium	0.64	0.68	0.67	0.83	0.57	0.83	0.84	1.10
Large	0.65	0.72	0.70	0.97	0.76	0.98	0.98	1.26

Table 29: System leakage exponents for small, medium and large networks with an ILI of 16 and 64

	ILI 16				**ILI 64**			
	Min	Mean	Median	Max	Min	Mean	Median	Max
Small	0.65	0.92	0.91	1.25	0.89	1.08	1.07	1.37
Medium	0.81	1.07	1.07	1.35	1.06	1.18	1.18	1.40
Large	0.99	1.16	1.16	1.37	1.08	1.21	1.21	1.31

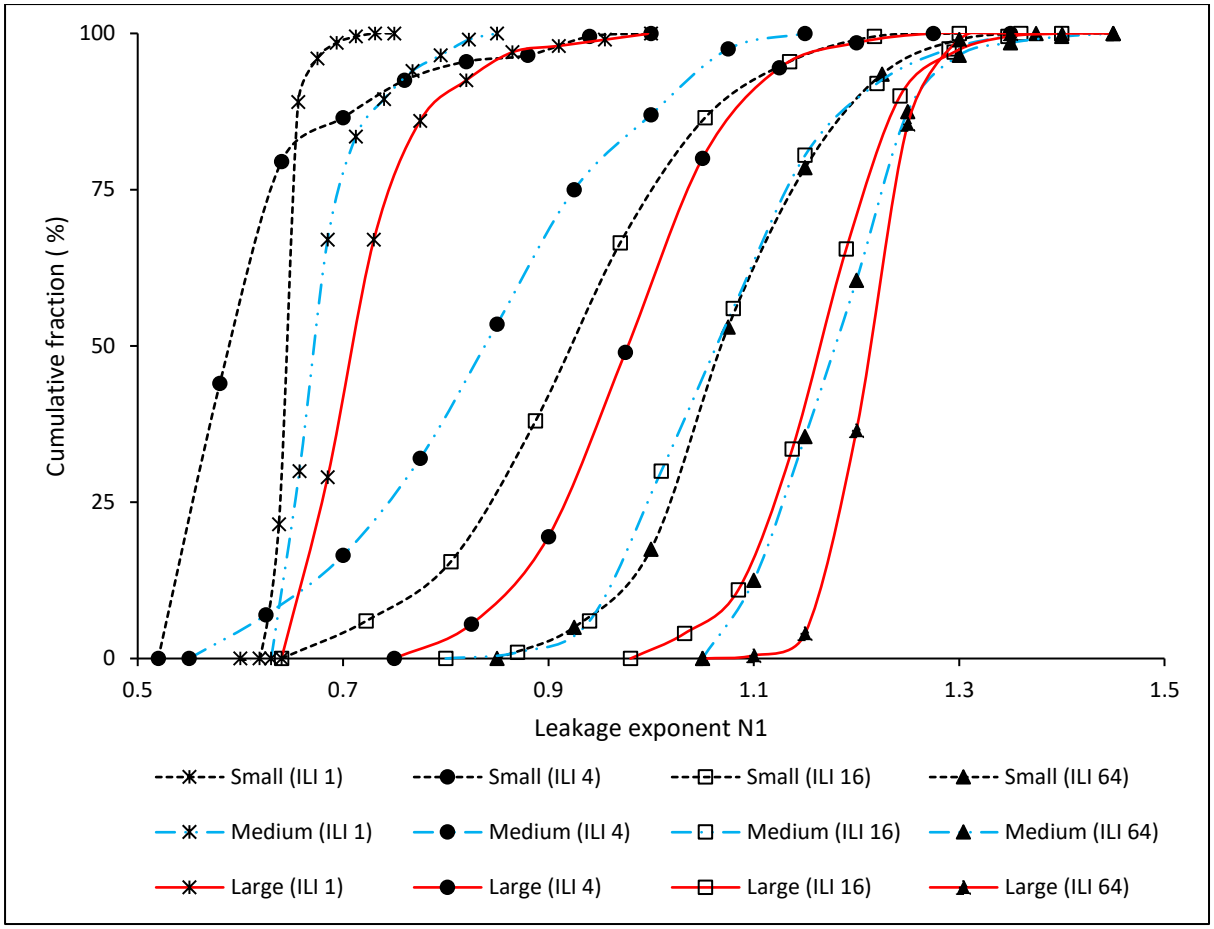

Figure 73: Leakage exponents for small, medium and large networks with varying leakage levels (an ILI of 1, 4, 16 and 64)

5.8.5. Predicting the system leak parameters of the modified orifice equation

The combined impact of both network size and level of system leakage on the accuracy of predicting the leak parameters of the modified orifice equation (i.e. the system's initial leak area and head-area slope) is described here.

Figure 74 shows that irrespective of the size of the network and level of leakage, the system's initial leak area can be predicted quite accurately from the sum of individual leaks' initial areas.

However, the results presented in figure 75 show that a system's head-area slope is predicted quite accurately for small, medium and large networks with an ILI of 1 and 4. Results of networks with leakage level equivalent to an ILI of 16 and 64 show many plotted points below the zero-error line. The dispersion below the zero-error line increases as the size of the network and the leakage level increase.

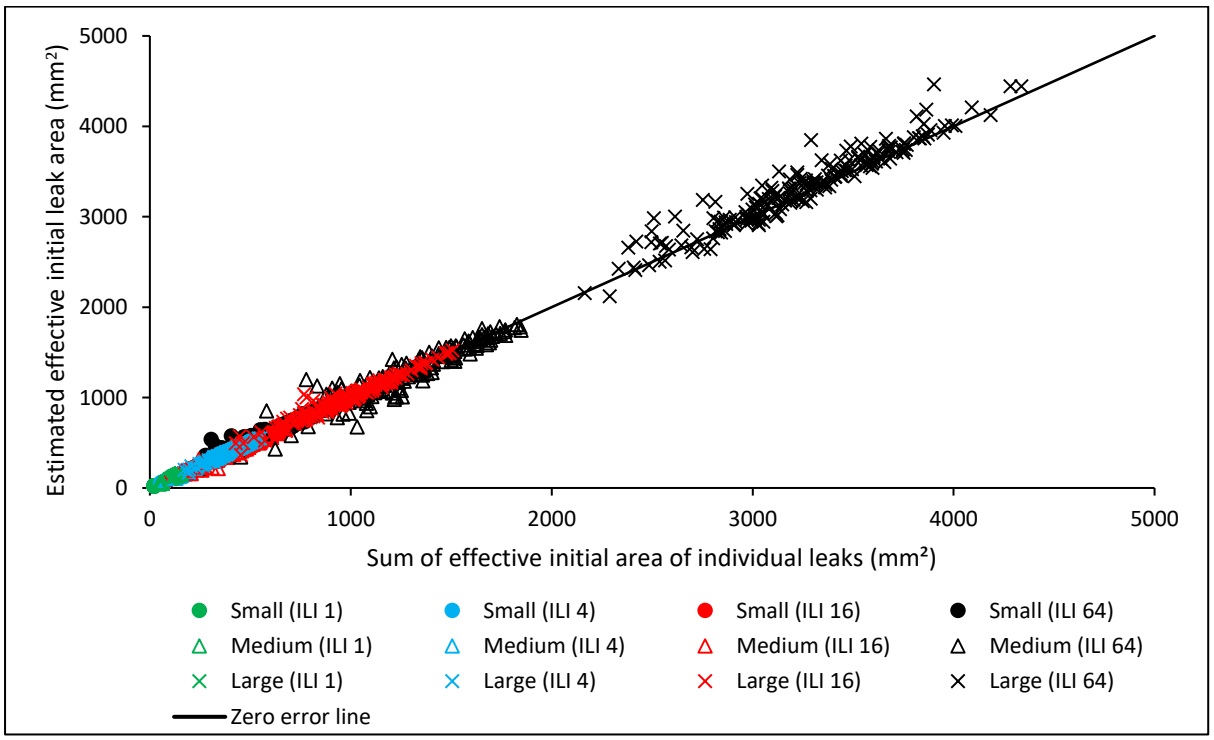

Figure 74: Predicting system initial leak area from the sum of individual leak areas for small, medium and large networks with ILI of 1, 4, 16 and 64

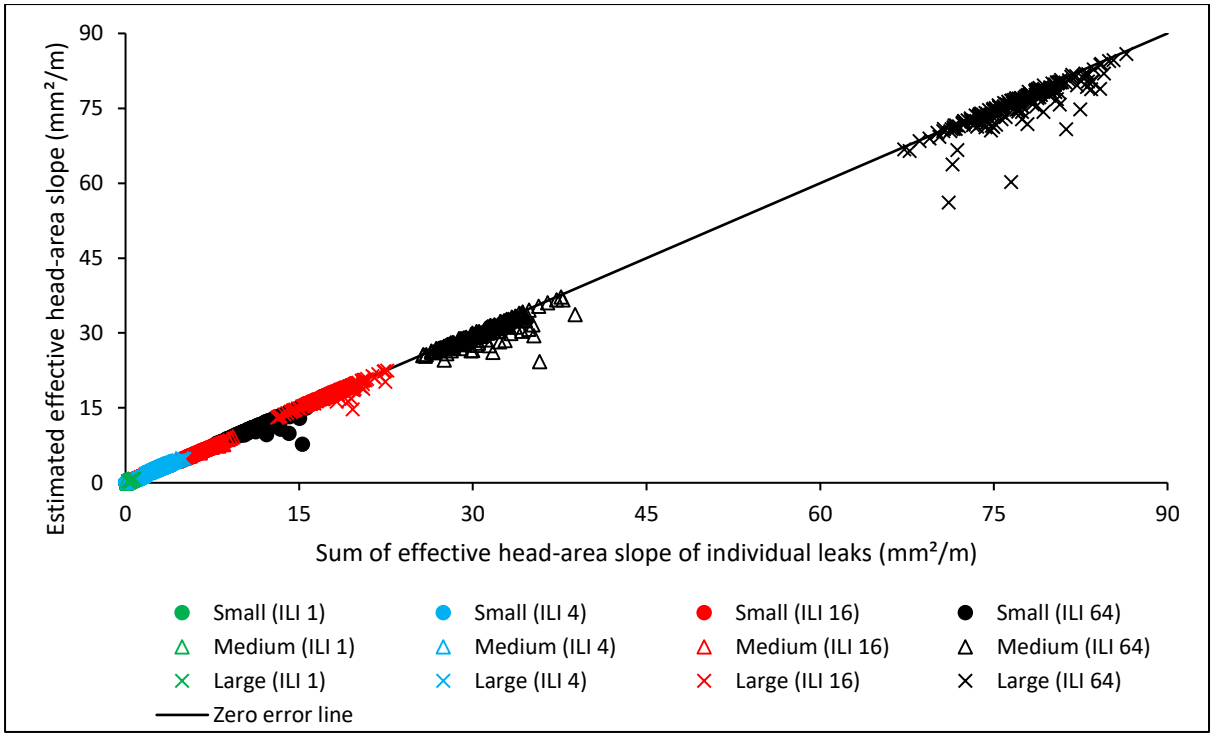

Figure 75: Predicting system head-area slope from the sum of individual head-area slopes for small, medium and large networks with ILI of 1, 4, 16 and 64

5.8.6. Convergence properties

The modified orifice equation required slightly more iterations to converge compared to the power equation for all three pipe networks and four leakage levels that were considered in this study. This increase is attributed to the increased number of unknowns in the modified orifice equation because of the second emitter that was added to each node.

The global gradient method is known to have convergence problems under certain conditions. Kabaasha et al. (2018) argues that some of these problems that are due to ill-conditioned Jacobian matrices, badly chosen initial solutions, or a large range of link resistances will be experienced with both the power and modified orifice equations.

However, it was found that for the power leakage equation, the standard global gradient algorithm failed to converge if the equivalent leakage exponent was greater than two. Since the

modified orifice equation exponents are fixed at 0.5 and 1.5, this problem cannot be experienced.

The leakage exponents above two sometimes occurred when generating stochastic system leaks with high ILI values. These large leakage exponents are not unrealistic and have been observed in field and laboratory studies as discussed in Chapter 2. This problem was addressed in Kabaasha et al. (2018), by suggesting to introduce a damping factor into the algorithm.

6. Correction of the conventional power leakage equation

6.1. Introduction

Although studies have found that under certain conditions the power equation that is used to model leakage is flawed, the equation is still entrenched in practice and used by many researchers. The aim of this chapter is to present methods that were developed based on the current knowledge of leakage behaviour, to correct the power leakage equation by adjusting its parameters, i.e. the leakage exponent $N1$ and coefficient C.

Given that most hydraulic modelling softwares apply the conventional power equation for leakage modelling, these methods are of importance to many researchers and practitioners wanting to model leakage realistically without change to a software that has the modified orifice equation.

Section 6.2 presents the methods that were developed, while section 6.3 shows how their performance is influenced by pre-defined factors.

Section 6.4 discusses how each of the developed methods would improve the performance of an existing study (Berglund et al. 2017). Berglund et al developed successive linear approximation methods for leakage detection. They used the power equation to model leakage flow rates. The results show a significant improvement in the performance of the leak detection methods when the leakage equation parameters are corrected.

The chapter ends with a summary in section 6.5.

6.2. The correction methods

The errors in the conventional power leakage parameters may be due to the nodal elevation differences between the AZP node (where the leak is thought to be when the power equation is used to model leakage) and the actual node with the leak. They may also be due to the variation of the nodal pressure because of the diurnal variation in consumer demand patterns.

Three methods have been developed to correct the power leakage equation by adjusting its parameters. The correction of errors due to the nodal elevation differences are discussed first, followed by the correction of additional errors due to the diurnal nodal pressure variation.

A limitation of all three methods is that parameters of only one leak can be adjusted at a time. The reason is that currently the Epanet hydraulic modelling tool uses one emitter exponent for the entire system. If each node in the network model had a separate emitter exponent, the parameters at each node would be corrected.

6.2.1. Correction of errors due to the nodal elevation differences

The power leakage equation parameters are estimated from data obtained in a pressure reduction test. This test is conducted during minimum night flow conditions by reducing system pressure and measuring leakage flow rates before and after the pressure reduction. The corresponding average zone night pressures (AZNPs), are also obtained at the AZP node.

Modelling leakage using the power equation assumes that the leak is located at the AZP node. Because of that assumption, the leakage exponent $N1$ is estimated from the average zone night pressures (AZNPs) and the leakage flow rates using equation (13). The corresponding leakage coefficient C is thus estimated using equation (14) since the leakage flow rate Q and pressure head h are known.

The pressure head at the node with the leak may differ significantly from the pressure head at the AZP node. In that case, using the average zone night pressure (AZNP) will result into an incorrect estimation of the leakage exponent, and hence an incorrect leakage coefficient.

Two of the three methods that have been developed can be used to correct the leakage exponent error due only to the elevation differences between the AZP node and the node where the leak is located. They are:

- the nodal pressure ratio method and
- the nodal pressure resimulation method.

The third method: the time-varying pressure correction method, has the added advantage of correcting errors due to the variation with time of the nodal pressure heads.

The nodal pressure ratio method

Schwaller and van Zyl (2015) developed a model that performed a sensitivity analysis on the average zone night pressure (AZNP) and the leakage exponent $N1$. The model assumed a system with very insignificant head losses. The results showed a proportional relationship between errors in the AZNP and the $N1$ as shown in figure 76. This implies that if there is an error of 20% in the AZNP, will result in the same percentage error in the $N1$ estimate.

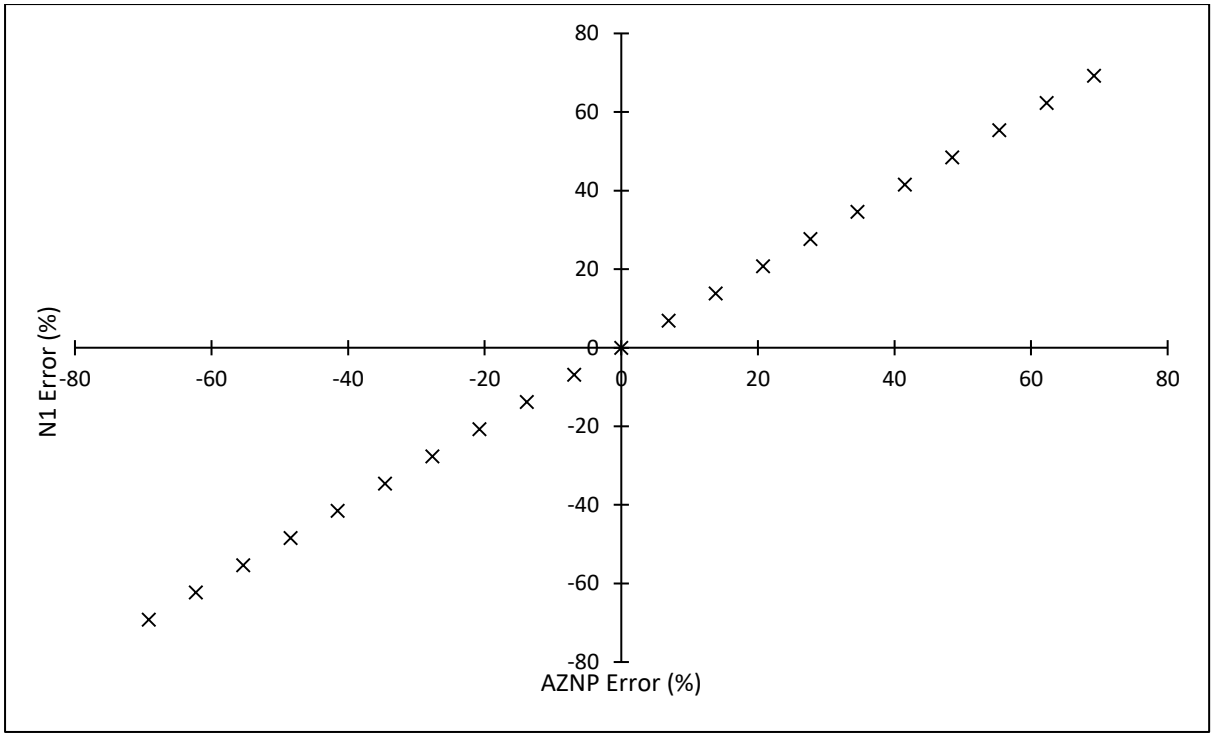

Figure 76: Impact of the error in the AZNP on the error in the estimation of N1 (Schwaller and van Zyl 2015).

In form of an equation, the relationship between the AZNP and the $N1$ in the above figure can be written as:

$$\frac{\mathrm{N1_i} - \mathrm{N1_c}}{\mathrm{N1_c}} = \frac{\mathrm{AZNP_i} - \mathrm{AZNP_c}}{\mathrm{AZNP_c}} \tag{70}$$

The $N1_i$ and $N1_c$ are the incorrect and correct leakage exponents respectively, while the $AZNP_i$ and $AZNP_c$ are the corresponding average zone night pressures.

The $N1_i$ and the $AZNP_i$ in equation (70) are determined from the pressure reduction test.

The leakage flow rate is well known from the pressure reduction test, but the location of the leak and thus the elevation of the point where the leak is located are unknown. The known leakage flow rate can therefore be used to estimate the different $N1$ values at different nodes with leaks.

If the pressure head at the node with the leak is h_c, the nodal pressure ratio method is written as:

$$\mathrm{N1_c} = \left(\frac{\mathrm{h_c}}{\mathrm{AZNP_i}}\right)\mathrm{N1_i} \tag{71}$$

The corresponding leakage coefficient C_c is estimated as follows:

$$\mathrm{C_c} = \frac{\mathrm{Q}}{\mathrm{h_c}^{\mathrm{N1_c}}} \tag{72}$$

In the above equation Q is the leakage flow rate determined from the field data during minimum night flow conditions.

The main limitation of the nodal pressures ratio method is that it assumes that there are no head losses in the system. While it may seem reasonable to assume static conditions under minimum night flow conditions, this is not necessarily the case, especially at higher night consumption or leakage levels.

The nodal pressure resimulation method

Figure 77 presents the process layout of the nodal pressure resimulation method.

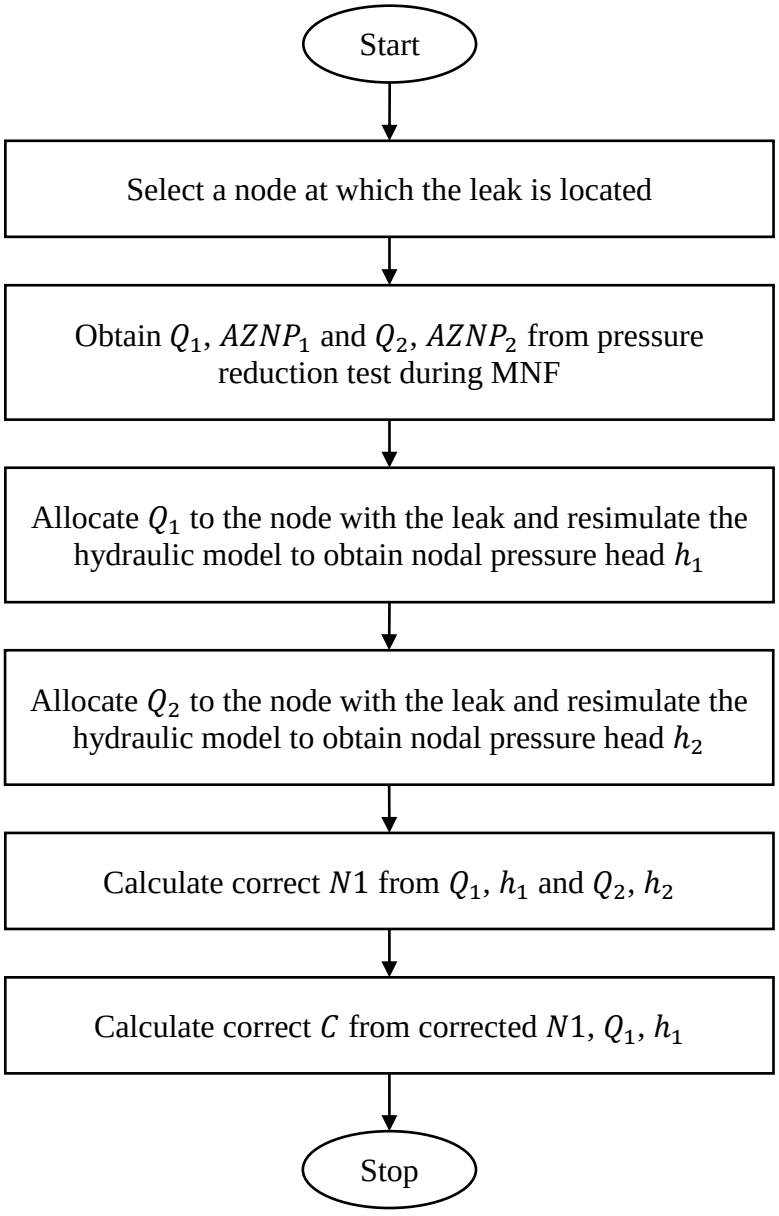

Figure 77: Process layout of the nodal pressure resimulation method.

The procedure begins with the selection of a node at which the leak is to be located. Leakage flow rates Q_1 and Q_2 plus the corresponding average zone night pressures $AZNP_1$ and $AZNP_2$ are known from the pressure reduction test performed during minimum night flow conditions.

Leakage flow rate Q_1 is then allocated to the selected node with the leak, and the model resimulated to obtain the nodal pressure head h_1. Similarly, leakage flow rate Q_2 is allocated to the selected node with the leak and the nodal pressure head h_2 obtained.

The correct leakage exponent $N1$ is calculated from the flow rates Q_1 and Q_2 plus their corresponding actual nodal pressure heads h_1 and h_2, from:

$$\mathrm{N1} = \frac{\log\left(\frac{\mathrm{Q_2}}{\mathrm{Q_1}}\right)}{\log\left(\frac{\mathrm{h_2}}{\mathrm{h_1}}\right)} \tag{73}$$

Thereafter, the correct leakage coefficient C is estimated from:

$$\mathrm{C} = \frac{\mathrm{Q_1}}{\mathrm{h_1}^{\mathrm{N1}}} \tag{74}$$

6.2.2. Correction of additional error due to diurnal time-varying pressure

A typical water distribution system has diurnal time-varying pressure, normally with high pressure during the minimum night flow conditions and low pressure during peak demand conditions. As discussed in Chapter 2, recent studies have shown that the N_1 will vary with pressure and that therefore for the same leak the N_1 will be different during each diurnal period.

In addition to the errors due to the elevation difference between the AZP node and the node with the leak, the third method (i.e. the time-varying pressure correction method) has the added advantage that it can be used to adjust additional errors in the leakage parameters. The additional errors are due to the diurnal variation with time of the nodal pressure heads.

Figure 78 presents the procedure to apply the time-varying pressure correction method and each step is thereafter discussed.

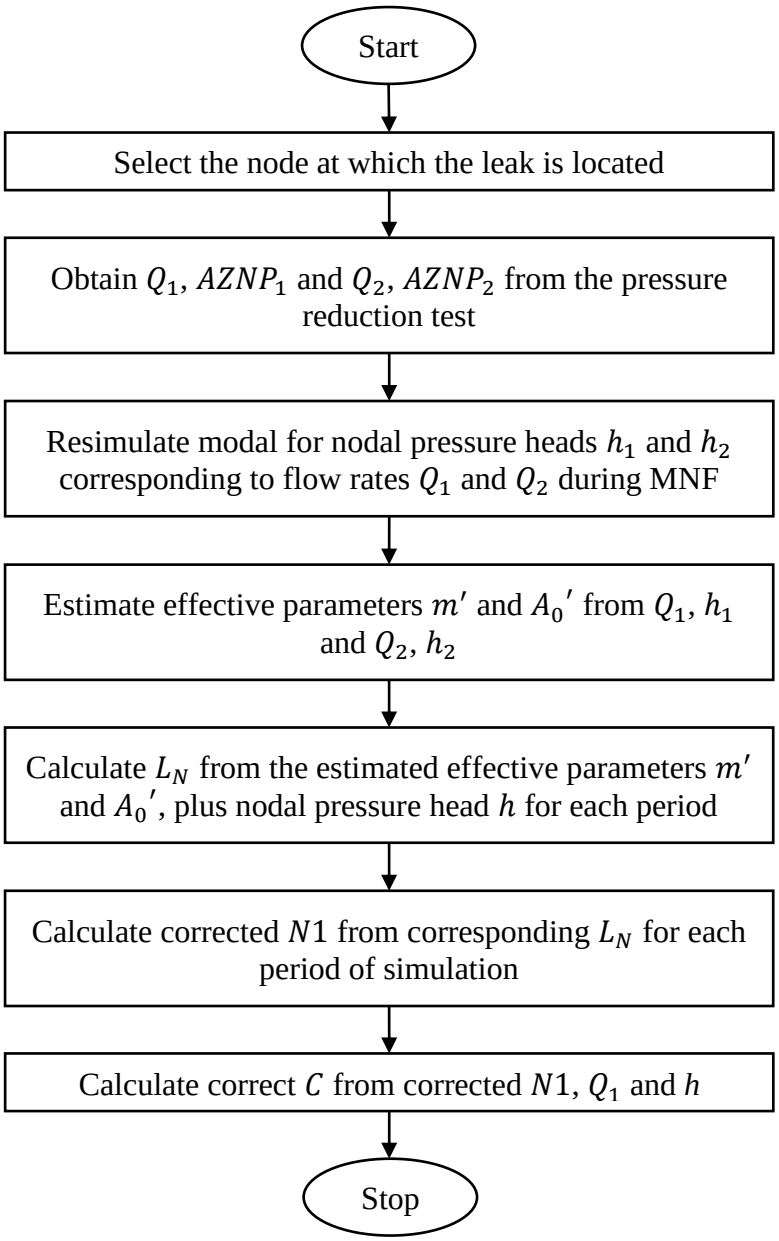

Figure 78: Process layout of the method to correct the power leakage equation for both elevation differences and time-varying pressures.

The process begins with the selection of a node where the leak is to be located.

The leakage flow rates Q_1 and Q_2 plus corresponding average zone night pressures $AZNP_1$ and $AZNP_2$ are obtained from the pressure reduction test during the minimum night flow.

As stated before, while the values of the flow rates are known, the location and thus the pressure head at the node with the leak are unknown. The nodal pressure heads h_1 and h_2 corresponding to the flow rates Q_1 and Q_2 respectively are obtained during the minimum night flow conditions after a resimulation of the hydraulic model. This step corrects the error in the $N1$ value which occurs due to the difference in the elevation between the AZP node and the node with the leak.

To correct the error due to time-varying pressure variations, the leakage number concept is applied. The pressure heads obtained at the node with the leak (h_1 and h_2) and the leakage flow rates (Q_1 and Q_2) are thus used to estimate the effective initial leak area A_0' and effective head-area slope m' using equations (66) and (67).

The leakage number L_N is then estimated for each period using equation (75), where h is the nodal pressure head for the specific period.

$$\mathrm{L_N} = \frac{\mathrm{m'h}}{\mathrm{A_0'}} \tag{75}$$

The correct leakage exponent $N1$ for the specific period is then calculated from:

$$\mathrm{N1} = \frac{1.5\mathrm{L_N} + 0.5}{\mathrm{L_N} + 1} \tag{76}$$

The corresponding leakage coefficient C is calculated from:

$$\mathrm{C} = \frac{\mathrm{Q_1}}{\mathrm{h^{N1}}} \tag{77}$$

6.3. Performance of the power equation correction methods

An investigation was conducted to evaluate the performance of the power leakage equation correction methods that were developed. The following pre-defined factors were considered:

- system head losses during minimum night flow conditions
- system head losses due to nodal pressure head variation with time.

The effect of the system head losses during minimum night flow conditions is presented first, followed by effect of the system head losses due to time-varying pressure variations.

6.3.1. Effect of system head losses during minimum night flow conditions

As the power leakage equation parameters are estimated during minimum night flow conditions, an investigation was conducted to evaluate the effect of the system head losses on the performance of the correction methods during that period.

This was achieved through observation of pressure heads during minimum night flow conditions at chosen nodes for different leakage levels. The AZP node and the node with the leak were considered.

The large system, whose physical and hydraulic properties are described in Chapter 5, section 5.2, was used in this analysis. Leakage levels equivalent to ILIs of 64, 16 and 4 were considered. All the leakage was assigned to a single node in the system that was not the AZP node. Although it may not be realistic in practice to have such huge leakage flow rate at a single node, it was intended to allow for the effect of head losses to be studied.

The head at the system supply point was reduced by a Δh of $15m$. The differences in the pressure heads (i.e. before and after the head reduction at the supply point) were calculated at both the AZP node and the node with the leak.

Figure 79 presents the pressure head difference Δh (m) at: the supply point, the AZP node and the node with the leak. Figure 80 provides the pressure head differences at the AZP node and the node with the leak expressed as a percentage of the pressure head difference at the supply point. This percentage difference indicates by how much the pressure head at a specific node reduces relative to the reduction at the system supply point, for a given level of leakage.

For the three levels of leakage, the reduction of the pressure head at the supply point was the same (i.e. $15m$).

When the level of leakage was very high (i.e. an ILI of 64), the pressure head difference at the AZP node was $14.71m$, which is equivalent to 98.1% of the Δh at the supply point. For the same leakage level, the pressure head difference at the node with the leak was $8.14m$, that is equivalent to 54.3% of the Δh at the supply point.

The leakage level was then reduced to an ILI of 16, and the pressure head difference at the AZP node was found to be $14.89m$. This is equivalent to 99.3% of the Δh at the supply point. For the same leakage level, the pressure head difference at the node with the leak was found to be $13.66m$. This is equivalent to 91.1% of the supply point pressure head difference.

As the leakage level was further reduced to an ILI of 4, the difference in the head at the AZP node was found to be $14.96m$, which is equivalent to 99.7% of the Δh at the supply point. For the same leakage level, the difference at the node with the leak was found to be $14.85m$, which is equivalent to 98.9% of the supply point pressure head difference.

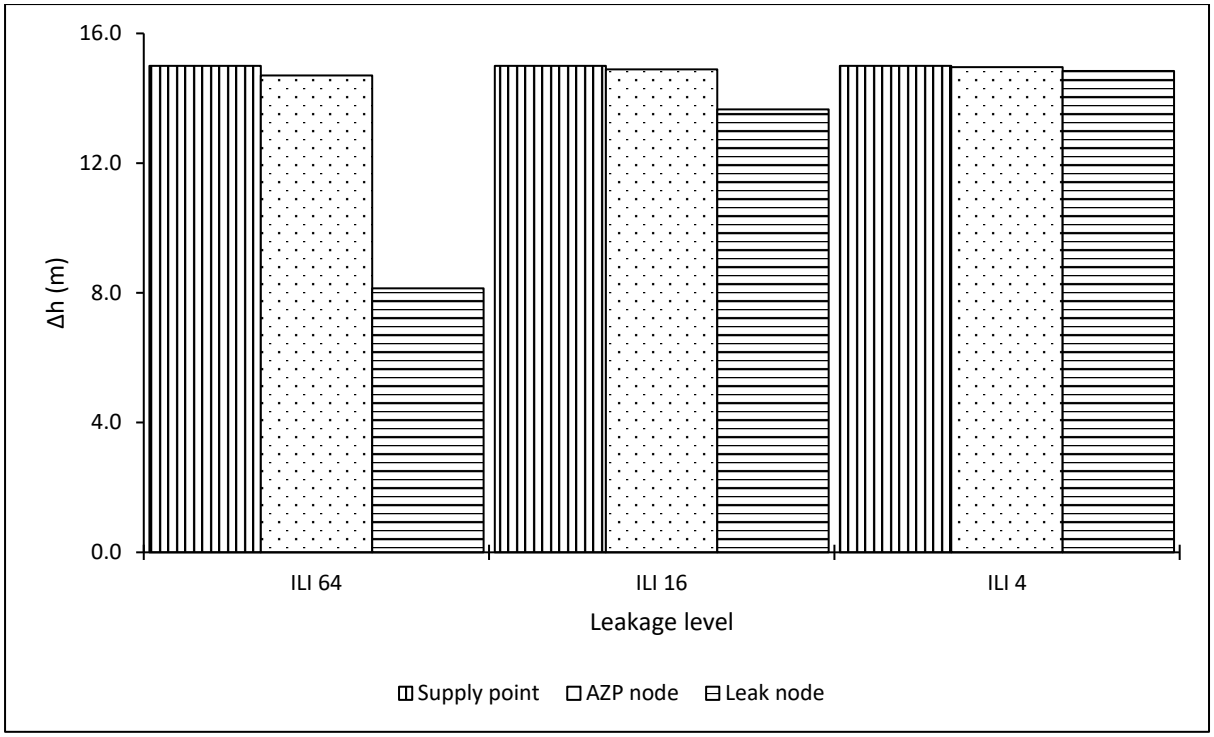

Figure 79: Comparison of pressure variation at the AZP node and the critical node with the variation at the source.

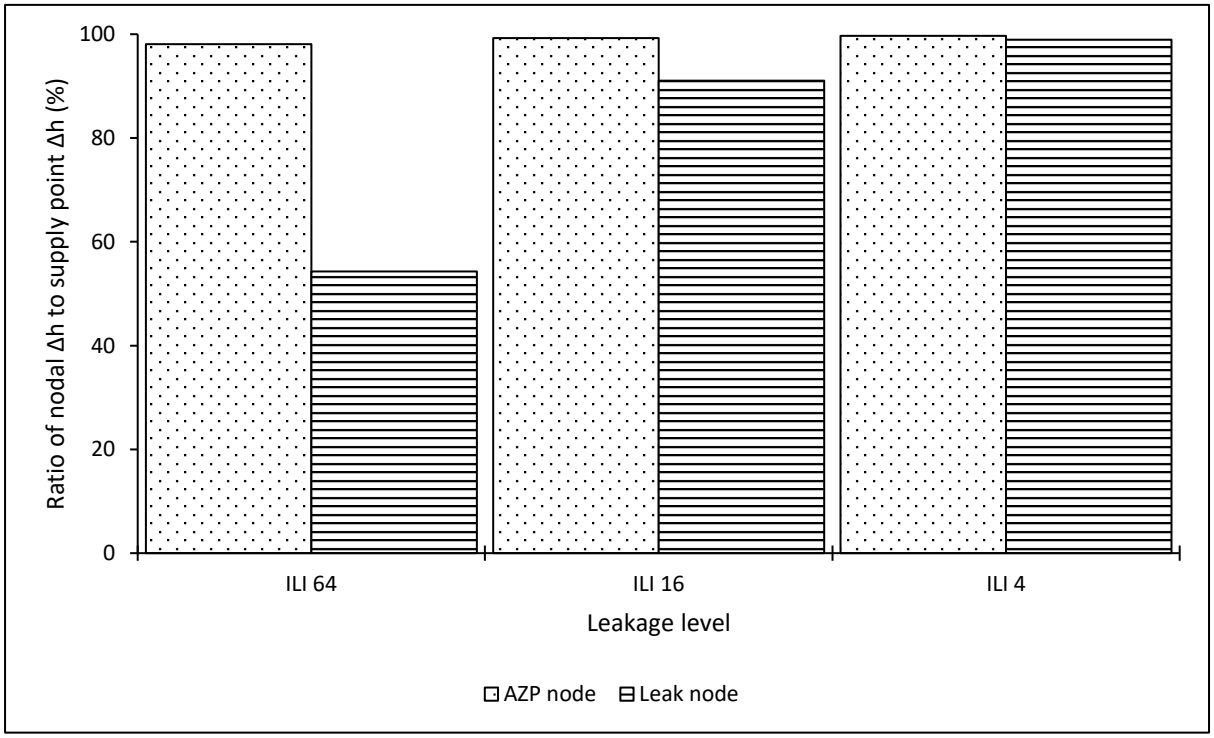

Figure 80: Fractions of pressure head variations at the AZP node and the node with the leak, relative to the pressure head difference at system supply point.

In their study, Schwaller and van Zyl (2015) assumed that the effect of head losses in the system during minimum night flow conditions was very insignificant and that therefore a pressure head reduction (Δh) at the system supply point would result in the same reduction at any node in the system.

Although this assumption may be valid in some cases, it may at times not be true as demonstrated in figures 79 and 80. For example, for the leakage level equivalent to an ILI of 4, the pressure head reductions at the AZP node and the node with the leak were very close to that at the supply point (i.e. 99.7% and 98.9% respectively). For an ILI of 64, the reduction at the AZP node was 98.1%, whereas at the node with the leak it was 54.3% of the reduction at the system supply point.

These results show that the reduction in the pressure heads at the AZP node and the node with the leak moved closer to the reduction at the system supply point as the leakage level was reduced. This occurred because a reduction in the pressure head at the supply point reduces the leakage flow rate, hence reducing the head losses in the pipes. This in turn increases the pressure at the node with the leak. The leakage level equivalent to an ILI of 64 is big enough to demonstrate an influence on the simulation results compared to the leakage level equivalent to an ILI of 4.

The nodal pressure ratio method would thus give realistic results in the system with an ILI of 4 rather than in the system with an ILI of 64.

The nodal pressure resimulation and the time-varying pressure correction methods were found to consider the effect of head losses during minimum night flow conditions, as they use nodal pressure heads after head losses have been considered.

6.3.2. Effect of system head losses due to the time-varying pressure variations

In a water distribution system, as pressure varies due to variation in the diurnal demand pattern, the system head losses either increase or decrease. An investigation was conducted to establish the effect of increased system head losses on the correction methods that were developed.

The large system was used with leakage levels equivalent to ILIs of 64, 16 and 4. Head losses were increased from 0m (during minimum night flow conditions) to 50m in intervals of 10m. The increment in headloss was modelled synthetically using Microsoft Excel by reducing the pressure head during MNF. It is considered that similar effects would result from a decrease of the head losses.

Leakage flow rates were then calculated using:

- the modified orifice equation,
- the power leakage equation with $N1$ and C values that are not corrected,
- the power leakage equation with $N1$ and C values that have been corrected using the nodal pressure correction method, and finally
- the power leakage equation with $N1$ and C values that have been corrected using the time-varying pressure correction method.

Leakage flow rates were modelled using both the modified orifice and power leakage equations and the difference was calculated for each of the cases, i.e. uncorrected, corrected with the nodal pressure resimulation method and corrected with the time-varying pressure variations method. Given that the modified orifice equation expresses the true behaviour of leakage, the difference in the two equations is described as an error in the power leakage equation.

Figures 81 and 82 show the leakage flow rate errors before and after the power leakage equation parameters were corrected, using the nodal pressure resimulation method and the time-varying pressure correction method respectively.

For the nodal pressure resimulation method (figure 81) an increase in the head losses leads to an increase in the leakage flow rate error after correction. When the leakage level was equivalent to an ILI of 64 and the head losses were 50m, the leakage flow rate error increased to 13%. On the other hand, when the leakage level was equivalent to ILIs of 16 and 4, the leakage flow rate error was about 4% for head losses of 50m.

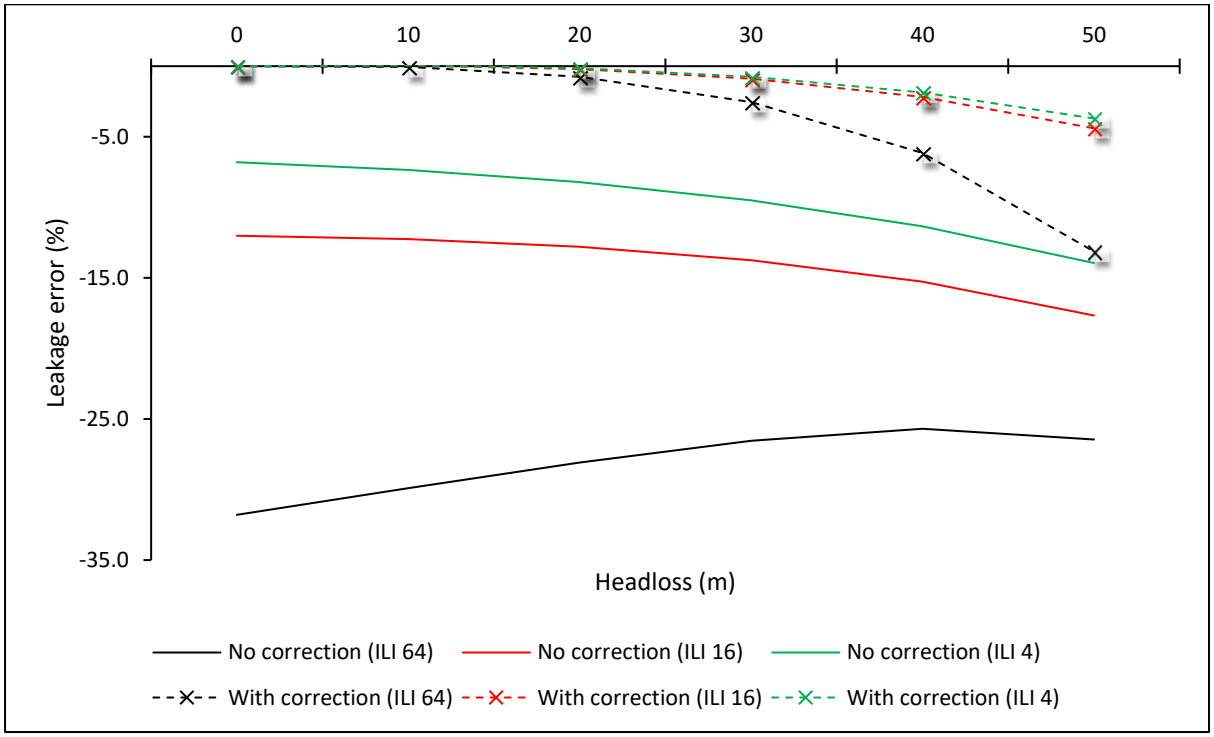

Figure 81: Leakage flow rate error using the power leakage equation before and after the equation parameters were corrected using the nodal pressure resimulation method.

For the time-varying pressure correction method (figure 82), the leakage flow rate errors are seen to be eliminated completely even when there are head losses in the system. The method allows correction of the power leakage equation parameters to adjust for both the elevation differences and the system head losses.

These results demonstrate the ability of the time-varying pressure correction method to fully correct the leakage flow rate error made by the power leakage equation, irrespective of the level of leakage or the presence of head losses in the system.

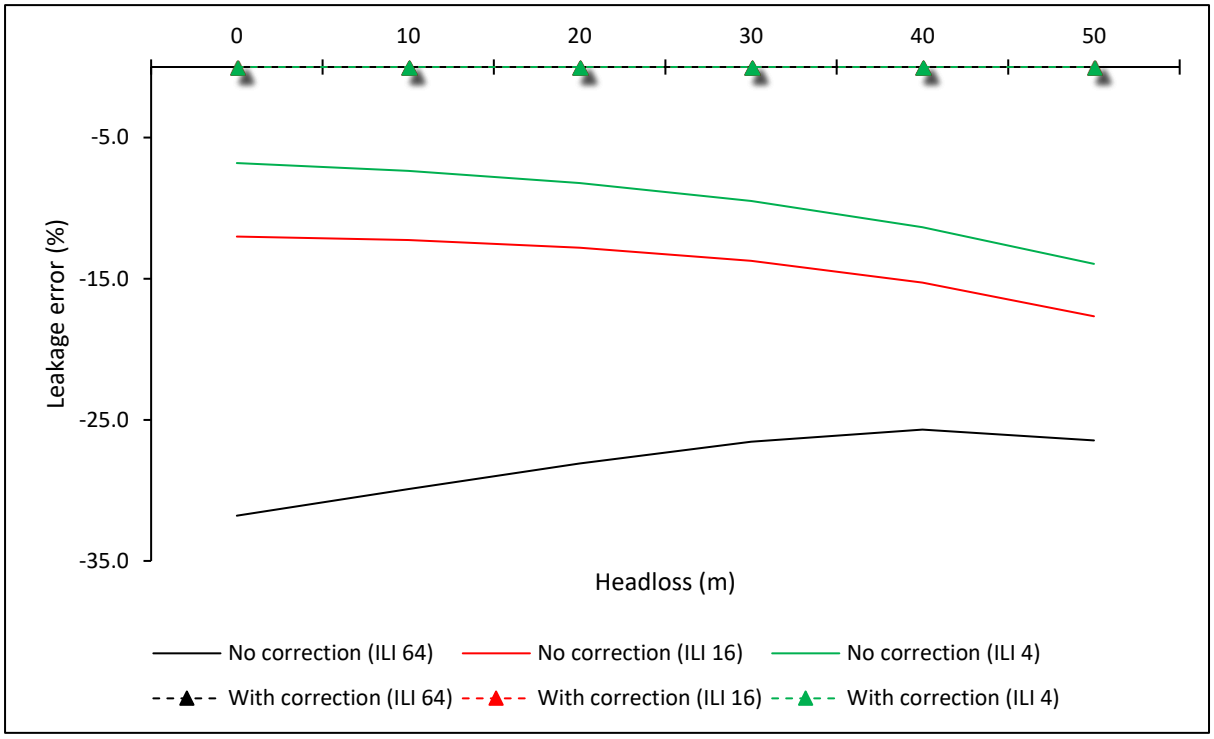

Figure 82: Leakage flow rate error using the power leakage equation before and after the equation parameters were corrected using the time-varying pressure correction method.

6.4. Application of the power leakage equation correction methods

The application of the power leakage equation correction methods was tested. This section discusses the procedure and the results of the tests. Two of the three correction methods were tested, namely the nodal pressure resimulation and the time-varying pressure correction methods.

Application of the nodal pressure ratio method was not tested because the modelled water network had head losses during minimum night flow conditions. In section 6.3, it was shown that head losses during minimum night flow influence the performance of the nodal pressure ratio method.

A study by Berglund et al. (2017) was chosen for the tests. Berglund et al. applies successive linear approximation methods to detect leaks in water distribution systems. Their methods use the conventional power equation (12) to model the relationship between leakage and pressure. The leakage coefficient C is assumed to represent the size of the leak orifice and thus used to define the magnitude of the leak.

Based on pressure measurements, the methods seek to determine the leakage coefficient C since the leakage exponent $N1$ is known. The methods are therefore likely to work better when the pressure data and the leakage exponent represent true operational behaviour.

The next subsection discusses Berglund's et al. successive linear approximation methods for leak detection. Thereafter, the procedure to test the application of the correction methods is presented. This is followed by a discussion of the results of the application tests.

6.4.1. The successive linear approximation methods for leak detection in water distribution pipe networks

Berglund et al. (2017) applies successive linear approximation methods (based on linear programming (LP) and mixed integer linear programming (MILP)) in a simulation-optimization framework to detect both the location and magnitude of leaks in water distribution networks.

A sensitivity analysis was first performed by Berglund et al. (2017). The results showed that an approximately linear relationship exists between pressure change and leak magnitude. In addition, the analysis demonstrated that the interaction of multiple leaks in a water distribution pipe network which might have a complex nonlinear effect, can be approximated as linear.

The Berglund et al. methods seek to minimize the sum of the absolute differences between the observed and the simulated pressure values to determine the magnitudes of leaks (i.e. the leak coefficients) at candidate nodes that approximate closely to the observed pressures.

The observed pressure values measured at pressure sensor nodes are provided. In addition, pressure data without leaks (i.e. the no-leak case) and with leaks (i.e. the leak case) are generated from the modelled network. The no-leak and the leak cases respectively reflect the normal operations of a water distribution network before and after the introduction of leaks.

At regular intervals, hydraulic simulations are conducted to obtain pressure data at pressure sensor nodes.

When leaks are introduced, the change in pressure does not explicitly disclose the location or magnitude of the introduced leaks. Determining the leak location and magnitude is an inverse problem. It needs a model to select candidate leaks that produce a pressure change signature close to the one introduced by leaks in the observed case.

The linear programming (LP) model

A linear programming (LP) model (78) was built and optimized to determine the linear combination of single simulated leaks that best match the change in pressure between the no-leaks case and the observed case.

$$\mathrm{P_{sim}(x)} = \mathrm{Ax} + \mathrm{P_{sim}(0)} \tag{78}$$

Where $P_{sim}\ (x)$ is the simulated pressure with leaks, A the leak sensitivity matrix, x the vector of leak coefficients, and $P_{sim}\ (0)$ the simulated pressure with no leaks. The leak sensitivity matrix A is given by:

$$\mathrm{A} = \left[\mathrm{a_1} \ldots \mathrm{a_j} \ldots \mathrm{a_m}\right]_{\mathrm{n\times m}}$$

Where, $\mathrm{a_j} = \mathrm{j^{th}}$ column of A(n x 1 vector) $= \frac{\mathrm{P_{sim}(C_j) - P_{sim}(0)}}{\mathrm{C_j}}$

$\mathrm{C_j}$ = leak magnitude at node j

$\mathrm{P_{sim}(C_j)}$ = simulated pressures for leak magnitude $\mathrm{C_j}$ at node j and no leaks elsewhere (n × 1 vector)

$\mathrm{P_{sim}(0)}$ = simulated pressures for no leaks (n × 1 vector)

n = number of sensors

m = number of candidate nodes

The LP selects a combination of leaks that minimize the objective function, i.e. the sum of the absolute difference between the simulated and observed pressures (79).

$$\underset{\mathrm{x}}{\mathrm{minimize}} \ \| \mathrm{Ax} - \mathrm{b} \|_1 \tag{79}$$

$\mathrm{b} = \mathrm{P_{obs}} - \mathrm{P_{sim}(0)}$; $\mathrm{P_{obs}}$ is the observed pressure.

Figure 83 presents the algorithm of the LP iterative approach. The sensitivity matrix A is recalculated using updated values of the C_j based on the previous solutions of x_j. The calculation of the sensitivity matrix A (step 2) requires the execution of Epanet simulations, while solving the LP problem (step 3) requires the execution of the MATLAB LP solver. An optimal solution to the LP is passed back to the simulation and used to update the assumed magnitude (coefficient) of the simulated leak. The updated simulation results in new constraint values for the LP and the model is optimized again. The stopping criterion is either the maximum allowable iterations or when there is no improvement in the objective value, whichever comes first.

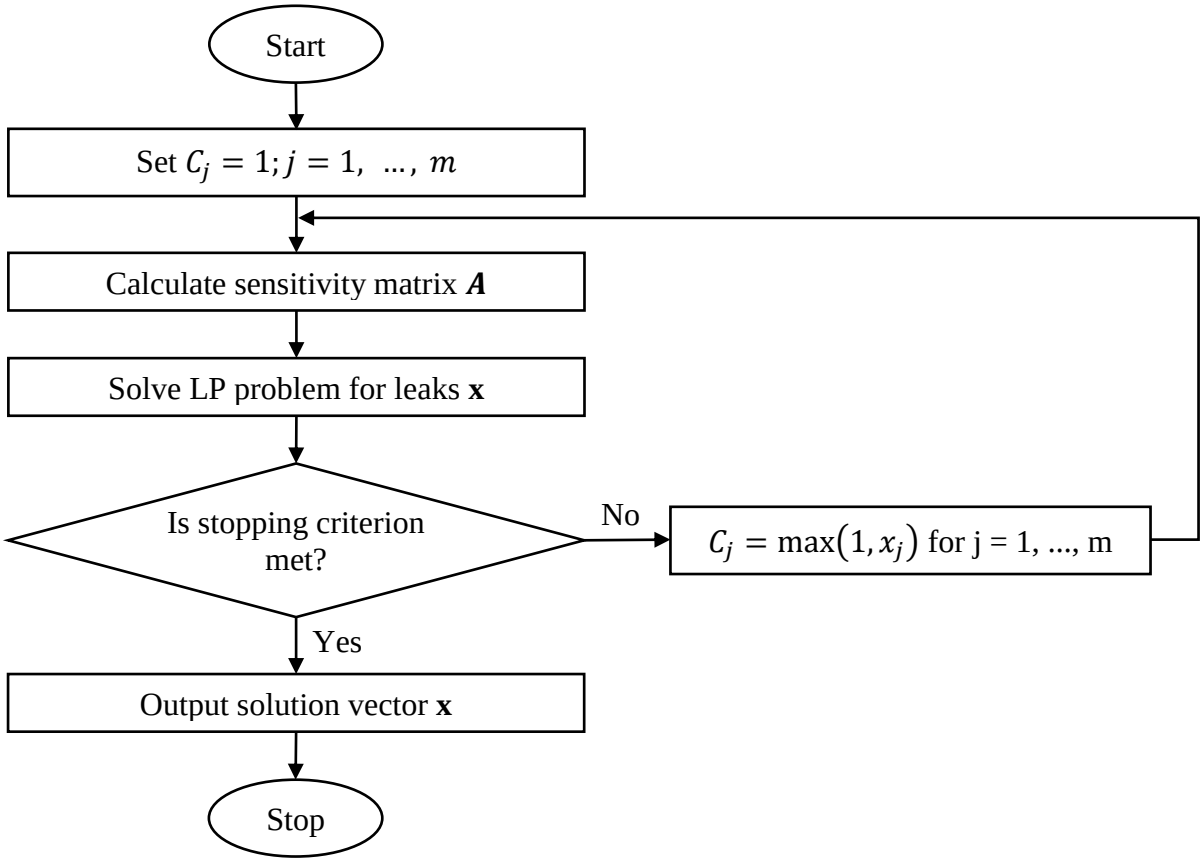

Figure 83: The LP iterative approach algorithm.

The mixed integer linear programming (MILP) model

In this model, the LP and the MILP are solved successively in each iteration - this is referred to as the LP-MILP iterative approach. Its algorithm is presented in figure 84.

Steps 1, 2 and 3 are the same as in the LP algorithm. The number of estimated leaks (N) in the LP solution with a C value greater than a preselected parameter threshold value (δ) is counted. This number is then used in a polishing step in which additional binary constraints are added in the mixed integer linear programming (MILP) model. The threshold δ is readily adjustable and can be tuned if additional system information is known, or by observing how solutions respond as the number of searched-for leaks is changed. Once the MILP is constructed, it is solved iteratively as the LP. The stopping criterion is the same as in the LP iterative approach.

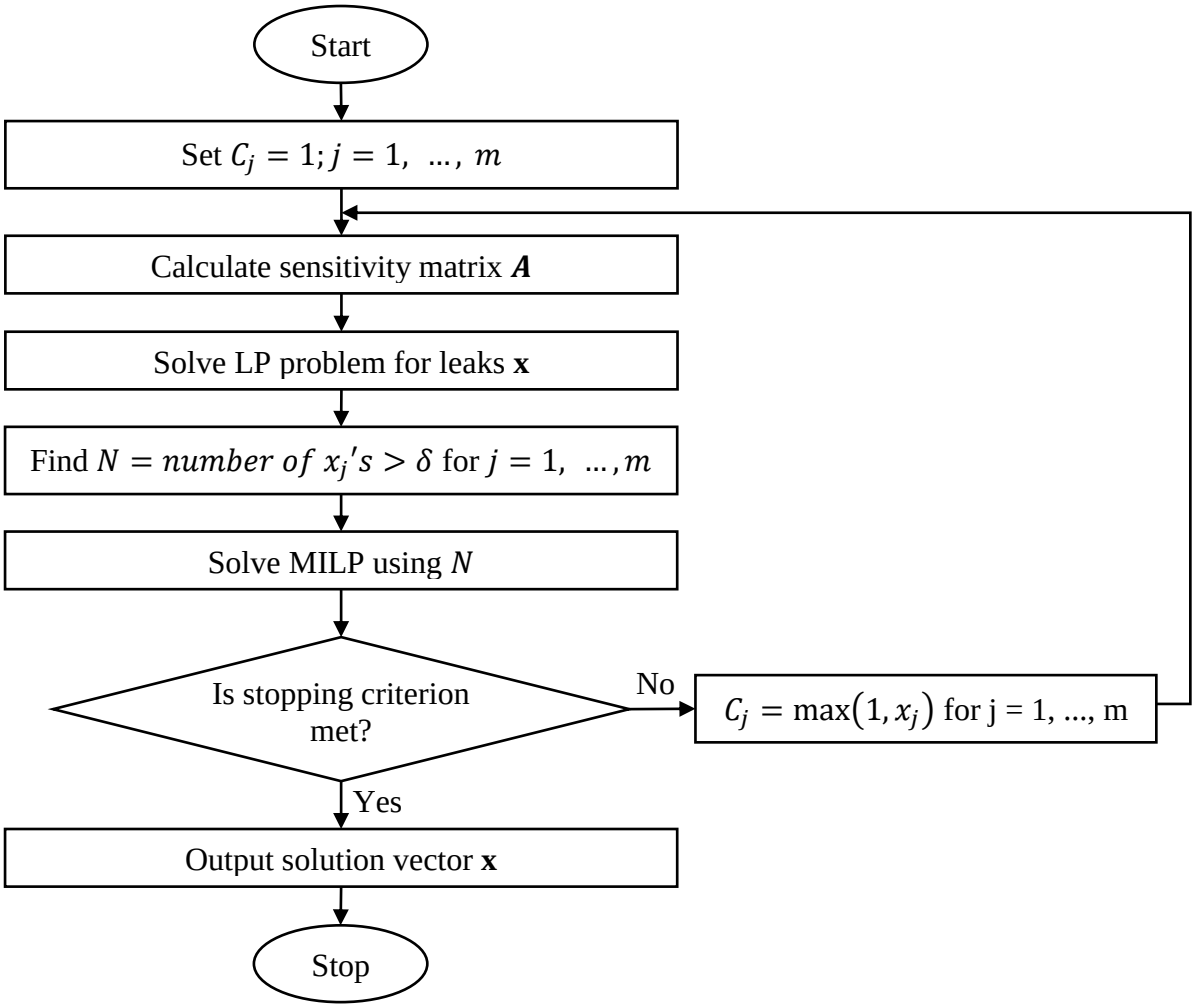

Figure 84: The LP-MILP iterative approach algorithm.

The simulation-optimization framework

The LP-based simulation-optimization framework uses the Epanet Programmer's Toolkit functions together with the MATLAB Optimization Toolbox. All hydraulic simulations are performed using Epanet's hydraulic simulation capability. A single Epanet simulation is required to obtain the pressure values for the no-leaks case at all sensor nodes. True leak locations and magnitudes for the hypothetical leak cases are selected. Information regarding the true leaks is used for assessment of LP and MILP-generated solutions. The model is otherwise run as if this information were unavailable.

The MATLAB Epanet toolkit utility functions are used. The Epanet functions are invoked from MATLAB to construct the sensitivity matrix and any additional calculations as needed. The MATLAB toolbox functions 'linprog' and 'intlinprog' are respectively used as the LP and MILP solvers.

Key assumptions

The methods described above were developed based on the following key assumptions:

- The methods try to find leaks that occur after the modelled network has been calibrated.
- The leak orifices do not expand or contract due to pressure, i.e. the leakage coefficient in equation (12) remains constant.
- There are no measurement errors in the observed pressures.

6.4.2. Procedure to test the application of the correction methods

The procedure to test the application of the power leakage correction methods is described. The large network, whose physical and hydraulic properties are described in Chapter 5 section 5.2 was used. The following steps were followed:

Step 1: Leaks equivalent to the ILIs of 8 and 4 were generated. All the leaks were allocated to one node in the network.

Step 2: The equivalent leakage exponent $N1$ and leakage coefficient C were calibrated during minimum night flow conditions.

Step 3: Three cases were then considered to identify the leak size C and corresponding location using the LP-MILP iterative approach, namely:

- when the power leakage equation parameters (i.e. N_1 and C) are uncorrected
- when the parameters are corrected using the nodal pressure resimulation method and
- when the parameters are corrected using the time-varying pressure correction method.

In the above cases, the *observed* pressure data were synthetically generated using the modified orifice equation, which is assumed to model the true behaviour of leaks. Also, sixteen sensor nodes and thirty-two candidate nodes were distributed in the network as shown in figure 85.

Case 1: Using the LP-MILP iterative method, the size of the leak and the corresponding location were determined. The true leak size (obtained in step 2) was then compared to the one obtained using the LP-MILP approach.

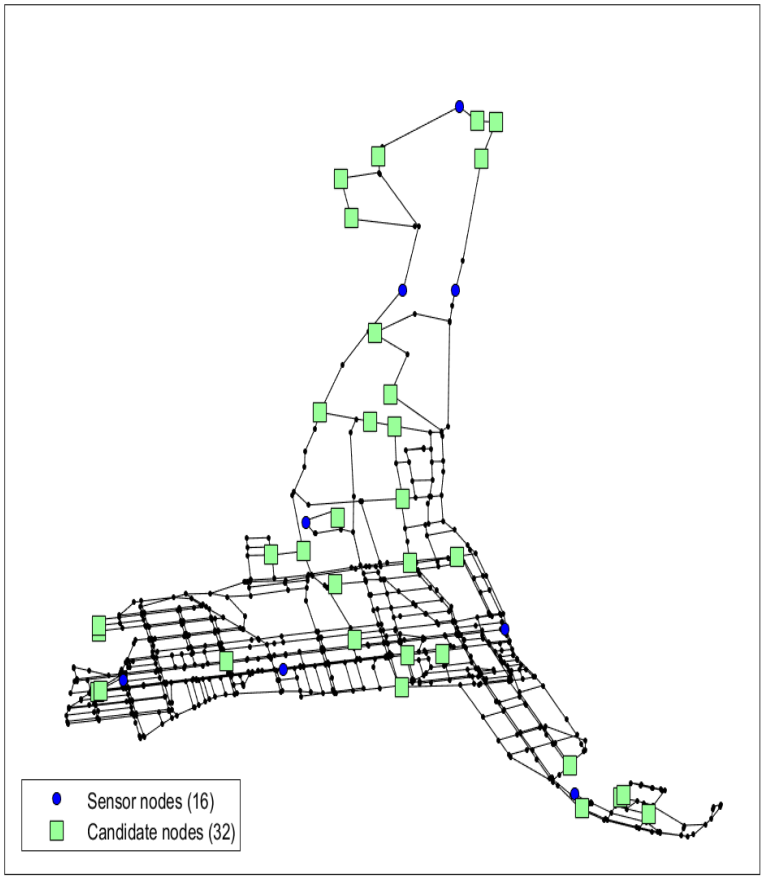

Figure 85: Distribution of sensor and candidate nodes.

Case 2: The parameters that were calibrated in step 2 were corrected using the nodal pressure resimulation method. The LP-MILP iterative method was again used to identify the size of the leak and corresponding location. The true leak size (obtained after correction) was then compared to the one that was obtained using the LP-MILP approach.

Case 3: The procedure described in case 2 was repeated for the time-varying pressure correction method.

Figure 86 summarises the above procedures.

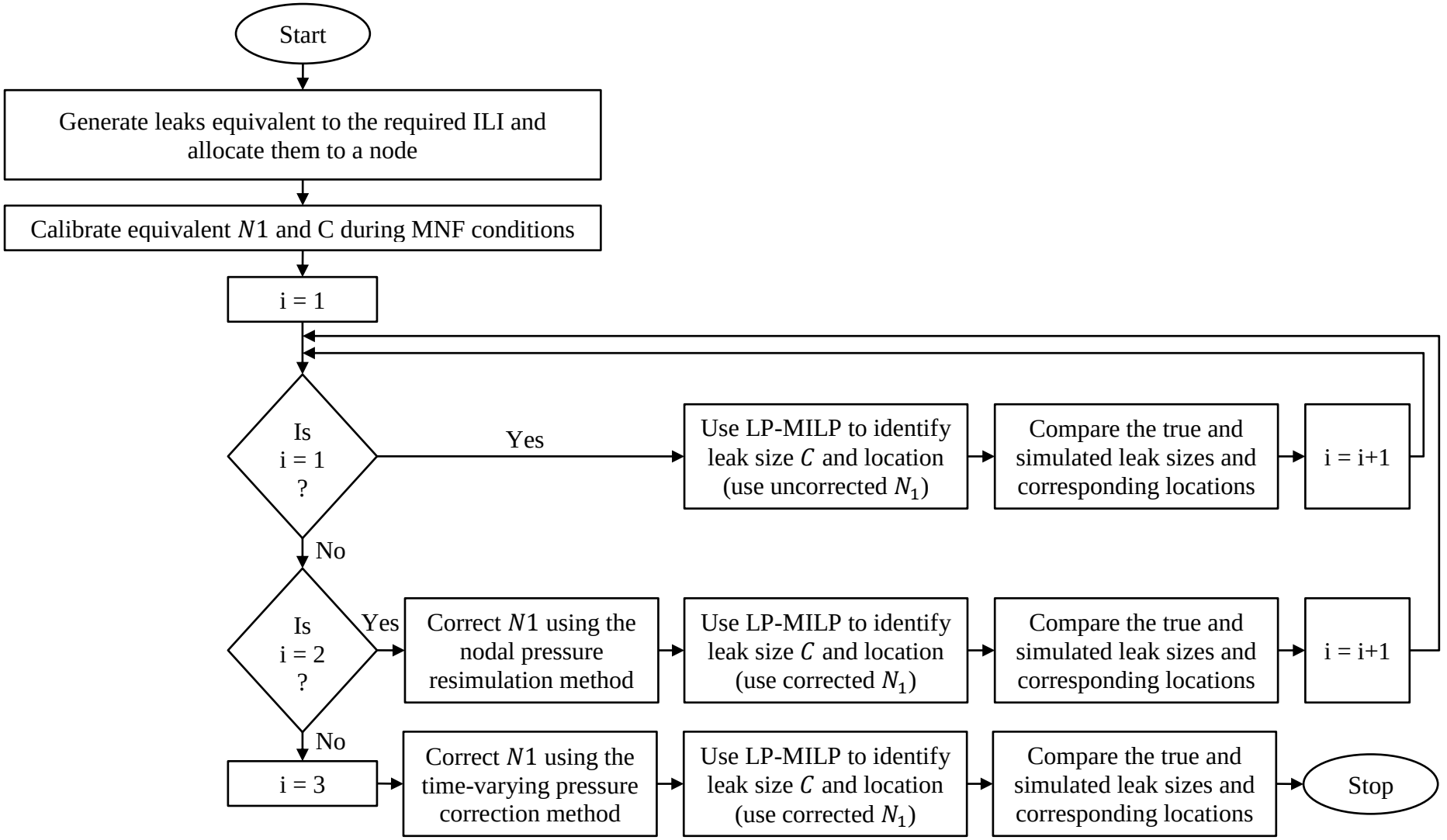

Figure 86: Procedure to test the application of the power equation correction methods

6.4.3. Results of the application tests of the correction methods

For the three cases, the true and the LP-MILP simulated leak sizes and corresponding locations were compared during minimum night flow and peak demand. The two periods were considered because they represent extreme pressures in a pipe network. Under normal operating conditions, pressure in a water distribution network is maximum during minimum night flow and the minimum during peak demand conditions.

The results show a comparison of the accuracy of the LP-MILP iterative method, before and after the correction of parameters of the power leakage equation. This section discusses results for a system with an ILI of 8, analysed during peak demand conditions. The results of all other simulations are analysed in a similar way and are presented in Appendix D.

Figure 87 shows results before the leakage exponents were adjusted. The true leak node is 25, and the results show that the model reports some false positive leak nodes at nodes 2, 3, 4, 7, 14, 19, 20 and 22. The LP-MILP model also miscalculated the leak coefficient at the true node (node 25) by 41.5% as presented in figure 90.

Figure 88 presents results after the leakage exponent was adjusted, using the nodal pressure resimulation method. The candidate nodes with no leaks yielded zero magnitudes as there were no false positives. The difference in the leak magnitude between the true leak and the LP-MILP simulated one is 5.6% as presented in figure 90.

Finally, figure 89 presents results after the leakage exponent was adjusted, using the time-varying pressures correction method. Also, the candidate nodes with no leaks yielded zero magnitudes and there were no false positives. The difference between the true leak magnitude and the LP-MILP simulated one is 4.9% as presented in figure 90.

These results show that by adjusting the leakage exponent, the variation of the leak area with pressure is implicitly considered. The relationship between pressure and leakage is therefore realistically modelled. The performance of the LP-MILP iterative model is augmented.

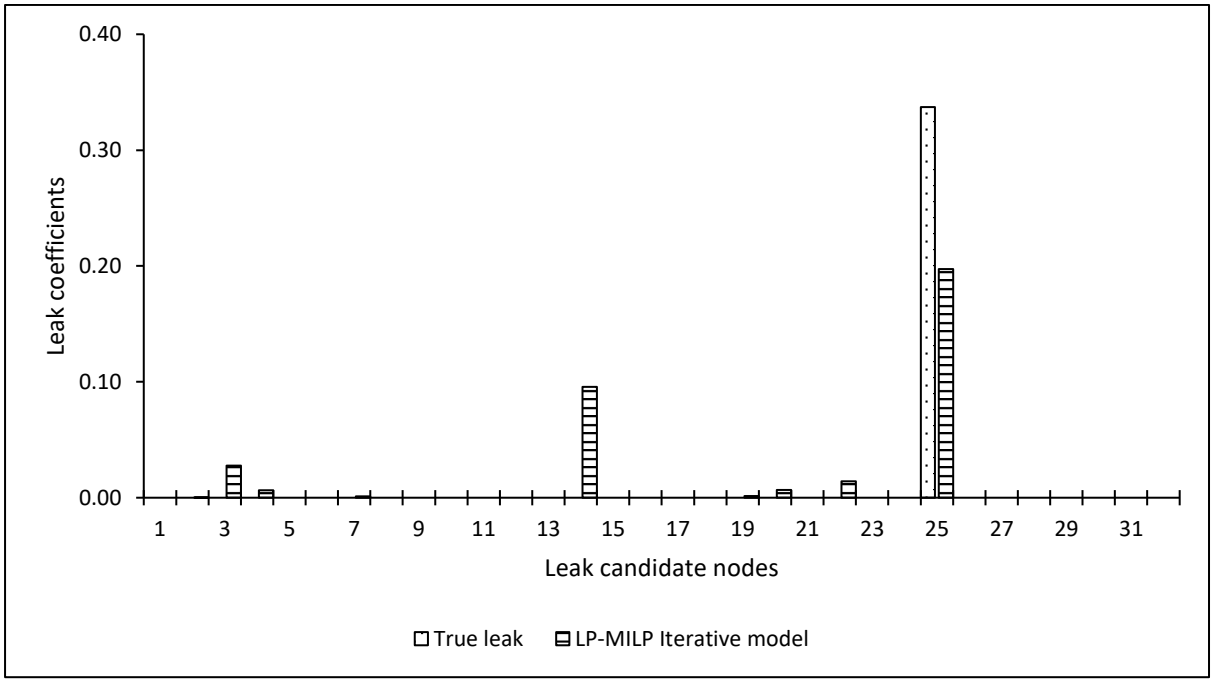

Figure 87: Leak detection by the LP-MILP method before correction of the leakage exponent during peak demand conditions.

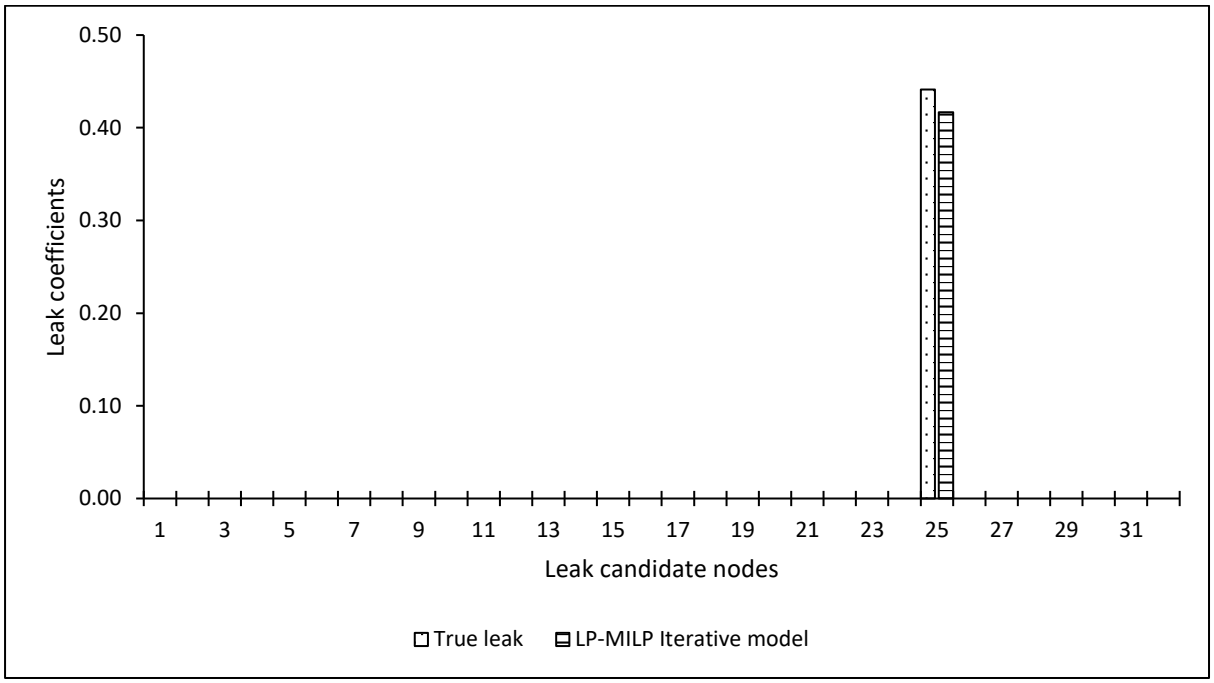

Figure 88: Leak detection by the LP-MILP method during peak demand condition after the leakage exponent was adjusted using the nodal pressure resimulation method.

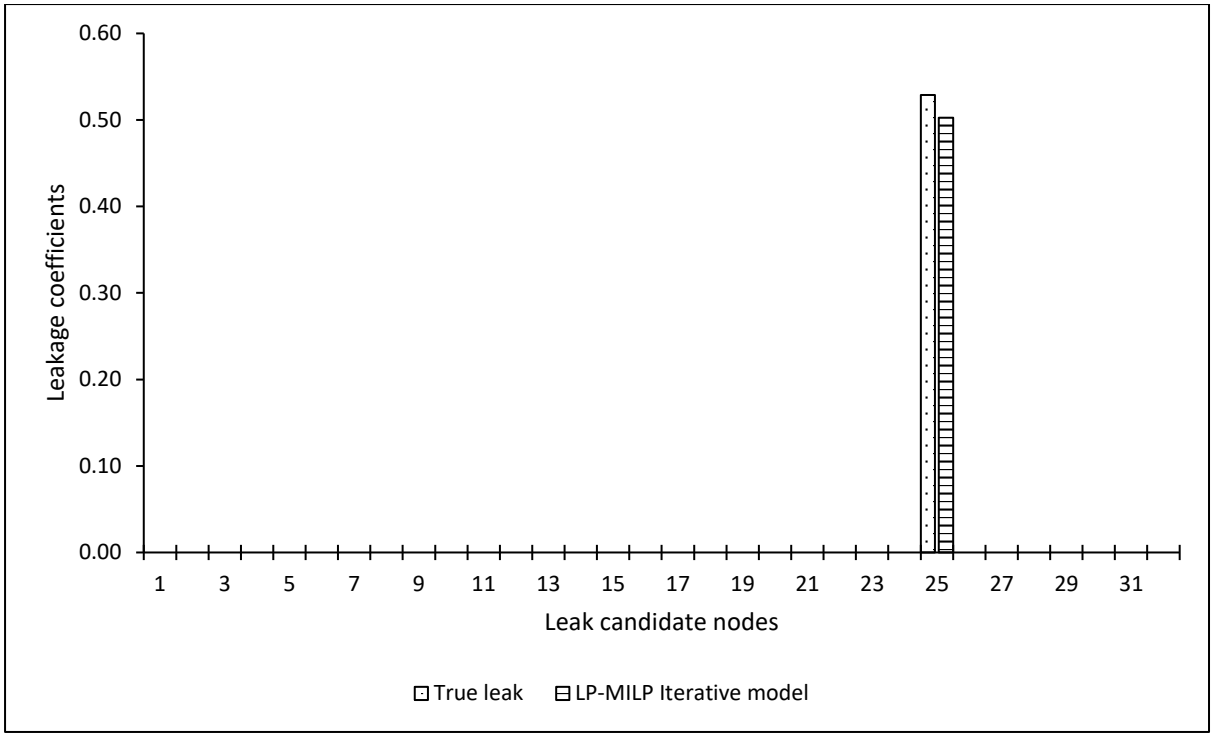

Figure 89: Leak detection by the LP-MILP method during peak demand condition after the leakage exponent was adjusted using the time-varying pressure correction method.

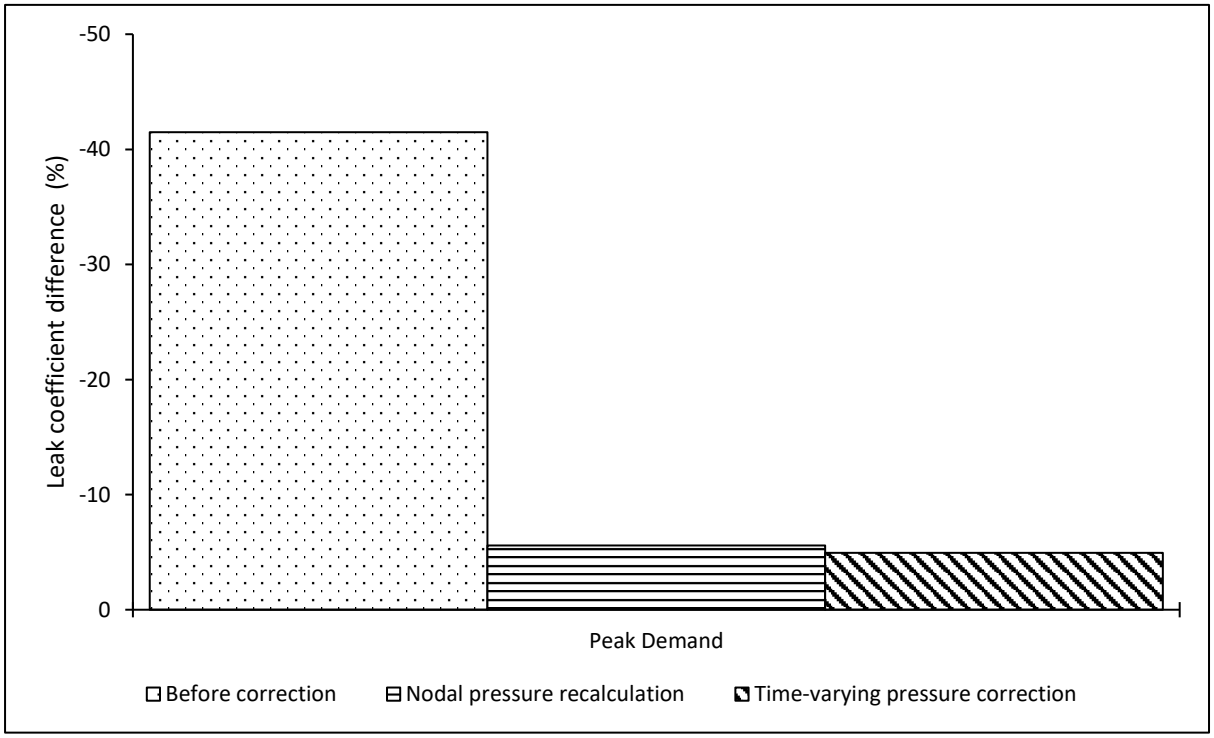

Figure 90: Percentage difference between the true leak coefficient and the LP-MILP modelled leak coefficient for a network with an ILI of 8 during peak demand.

6.5. Summary of the chapter

This chapter presented methods that were developed to correct the power leakage equation parameters, with the aim of modelling leakage without change of the software to one that uses the modified orifice equation. Three methods were discussed: the nodal pressure ratio, the nodal pressure resimulation, and the time-varying pressure correction methods.

The performance of these methods was discussed under pre-defined conditions. The nodal pressure ratio method was found to be generally influenced by head losses in the system during minimum night flow conditions. It was suggested that this method can be used only in systems where head losses are very insignificant. The nodal pressure resimulation method was found to be influenced by the head losses which result from diurnal pressure variations. The time-varying pressure correction method was found to be the most accurate, as it could fully correct the power leakage equation errors resulting from any head losses.

Finally, the correction methods were tested using an existing study Berglund et al. (2017) to investigate how they would improve the study's performance. The study that was chosen uses the power leakage equation in the detection of leaks through successive linear approximation methods. It was found that by correcting the power leakage equation parameters, false positives in the detection of the nodes with leaks were eliminated. Also, the error made to determine the magnitude of the leak was reduced from 41.5% before applying corrections to 4.9% after the corrections were applied.

7. Conclusion and recommendations

This chapter presents the main conclusions of this study and makes recommendations for future work. Section 7.1. summarises each of the results obtained and points out possible implications for research and practice. A future perspective is offered in section 7.2.

7.1. Conclusion

This study investigated the integration of the latest findings on leakage behaviour into a hydraulic modelling software for realistic leakage modelling in water distribution pipe networks. This was achieved by incorporating the modified orifice equation into the standard hydraulic network solver of the Epanet software package. The implications of this process were then investigated.

A stochastic model that generates and distributes leaks in a realistic way in a water distribution system was developed.

A methodology that may be used to correct the power leakage equation to model leakage flow rates and volumes realistically was also developed.

Concluding remarks on these results are presented in the following subsections and the implications of each one of them are discussed.

7.1.1. The integration of the modified orifice equation into a standard hydraulic modelling software

Currently, known hydraulic modelling software packages use an empirical power equation to model leakage in water distribution pipe networks. The motivation for this study was that recent research has shown that the power leakage equation is flawed under certain conditions and that, if its parameters are extrapolated beyond the pressure range for which they were calibrated,

this could result into significant leakage flow rate errors. In addition, research has shown that leak areas vary linearly with pressure heads. The power leakage equation does not consider this.

There is thus a need for a modelling tool for leakage flow rates in water distribution networks that considers the linear relationship between leak area and pressure head. This study has filled this gap by integrating the modified orifice equation into the widely used Epanet hydraulic modelling software package.

The integration of the modified orifice equation into hydraulic modelling may have implications for the performance of leakage modelling applications, the characterization of the pressure-leakage response, the convergence properties of simulated pipe networks, and the implementation of pressure management in pipe networks. These implications are discussed below:

a) Leakage modelling applications

The integration of the modified orifice equation into Epanet could be of interest to both researchers and practitioners who use leakage modelling in various applications in water distribution networks. Applications such as leaks detection and pipe network optimisation models ought to improve when the modelled leakage flow rates are realistic.

b) Characterization of the pressure-leakage response of pipe networks with many leaks

Schwaller et al. (2015) found that the total initial areas of all leaks in a system as well the sum of all the head-area slopes can be estimated using the modified orifice equation. Their model assumed a system with no head losses.

The results of this study contribute to the findings of Schwaller et al. (2015) for situations where system head losses are considered. This could be of interest to practitioners managing

water distribution networks. Because the parameters of the modified orifice equation in systems do not change with pressure, they can be used to evaluate and monitor the extent and type of leaks present in the system. The initial leak area provides a meaningful measure of the physical integrity of the system, while the head-area slope can be linked to the properties of the pipe (diameter, material and wall thickness) and leak (type and size). The head-area slope thus provides insights into the type of leaks present in the system.

c) Convergence properties of simulated pipe networks

The modified orifice equation in the global gradient algorithm was found to converge, on average, one more iteration compared to the power leakage equation. This was because of the added emitter in the modified orifice equation.

The use of the power leakage equation also resulted in non-convergence for leakage exponents greater than two. This was identified in some systems with high leakage levels. Although a stochastic model was used for the generation and distribution of leaks, large leakage exponents are not unrealistic and have been observed in both field and laboratory studies (Trow and Farley 2003; Greyvenstein and van Zyl 2007) .

Use of the modified orifice equation has the advantage of not presenting the problem of non-convergence due to large leakage exponents, because here the pressure head exponents are fixed at 0.5 and 1.5.

d) Implementation of pressure management

Using a stochastic model that assumed no head losses in the system, Schwaller and van Zyl (2015) suggested that the modified orifice equation should be used in the implementation of pressure management. This is because the same data is required for the use of the modified orifice equation as for the power leakage equation, and the modified orifice equation has many

advantages. The evidence from this study which considered head losses in the pipe networks supports Schwaller and van Zyl's recommendations.

This study's investigation also showed that in water pipe networks the use of the power and modified orifice equations produced similar results for total system leakage flow rates and volumes under normal diurnal pressure variations. The reason for this may be that pressures are both lower and higher at different nodes in the system and therefore the leakage flow rates (being functions of pressure head) cancel out.

However, the leakage flow rates at individual nodes, where elevations differed from the average zonal pressures, were found to differ significantly. In addition, it was found that simulation of systems at pressures that are significantly different from the normal diurnal range (for instance when pressure management is implemented) results in substantial errors in both leakage flow rates and volumes.

These results might be of interest to practitioners who would like to estimate the benefits that would be reaped from the implementation of pressure management. This study has clearly demonstrated that significant errors may occur if the power leakage equation is used to estimate such benefits. The power leakage equation should only be used when the pressure is within the same range as when its parameters (i.e. the $N1$ and C) were calibrated. This is not possible when pressure management is implemented.

7.1.2. Stochastic model for leaks generation and distribution

Schwaller and van Zyl (2015) developed a stochastic model that generates and distributes leaks. Their model does not consider physical and hydraulic properties of the pipe network to which the leaks are distributed. It assumes a system with no head losses.

This study has developed a stochastic model that generates and distributes leaks based on the physical and hydraulic properties of the pipe network. It therefore considers head losses in the system. In addition, the developed stochastic model applies the infrastructure leakage index to appraise the level of leakage in the pipe network.

This model would be of importance to both researchers and practitioners who want to perform pipe network diagnosis. These diagnoses may include analysis of the impact of leakage distribution on pressure heads, consumer demands and general system performance, to mention a few.

7.1.3. Methodology for correction of the power leakage equation

Because studies have shown that the power leakage equation may be flawed under certain conditions, this study has developed methods that can be used to correct the equation. The parameters of the conventional power leakage equation are adjusted to enable modelling of realistic leakage flow rates.

These methods could be especially of interest in cases where leakage modelling data is in the format of the power leakage equation.

It is also well known that the power leakage equation is still entrenched in practice and is likely to remain so for some time. This may be because the power leakage equation is integrated in most hydraulic modelling tools. Some researchers and practitioners may be reluctant to change to software that uses the modified orifice equation for leakage modelling. These methods therefore would be of importance under such circumstances.

7.2. Recommendations

The following recommendations are made for further research:

- Many laboratory and modelling studies have confirmed that all leaks adhere to the modified orifice equation. However, no field studies have been conducted to verify this assumption. May (1994) who did a field study concluded that some leak adhered to the modified orifice equation while others did not. It would therefore be of interest if a field study was conducted to investigate whether all leaks adhere to the modified orifice equation.
- The methods that were developed to correct the power leakage equation can only correct a single leak at a time because Epanet has only one emitter exponent for all the nodes in the pipe network. A modification of Epanet to have an emitter exponent for each node is recommended. This would be useful in order to apply the power equation correction method to each node in the pipe network.
- Finally, further investigations are recommended on the implications of applying the more realistic modified orifice equation to the results of modelling studies that include leakage. This study investigated the implications on some leak detection methods (Berglund et al. 2017). However, it would be of interest if similar investigations were done, for example, on the calibration of pipe networks and operational optimization studies.

References

Al-Ghamdi, A. S. (2011). "Leakage–pressure relationship and leakage detection in intermittent water distribution systems." Journal of Water Supply: Research and Technology - Aqua **60**(3): 178-183.

Alegre, H., J. M. Baptista, E. Cabrera Jr, F. Cubillo, P. Duarte, W. Hirner, W. Merkel and R. Parena (2006). Performance indicators for water supply services, IWA publishing.

Alegre, H., W. Hirner, J. M. Baptista and R. Parena (2000). Performance indicators for water supply services. IWA manual of best practice., IWA.

AWWA (2016). Water audits and loss control programs. A. W. W. Association. United States of America, American Water Works Association. **M36**.

Berglund, A., V. S. Areti, D. Brill and G. Mahinthakumar (2017). "Successive linear approximation methods for leak detection in water distribution systems." Journal of Water Resources Planning and Management **143**(8).

Brater, E. F., H. W. King, J. E. Lindell and C. Y. Wei (1996). Handbook of hydraulics, McGraw-Hill.

Cassa, A. M. and J. E. van Zyl (2011). Predicting the pressure-area slopes and leakage of cracks in pipes.

Cassa, A. M. and J. E. van Zyl (2013). "Predicting the head-leakage slope of cracks in pipes subject to elastic deformations." Journal of Water Supply: Research and Technology - Aqua **62**(4): 214-223.

Cassa, A. M. and J. E. van Zyl (2013). Predicting the leakage exponents of elastically deforming cracks in pipes. 12th International Conference on Computing and Control for the Water Industry, CCWI 2013.

Cassa, A. M., J. E. van Zyl and R. Laubscher (2010). "A numerical investigation into the effect of pressure on holes and cracks in water supply pipes." Urban Water Journal.

CodeBlocks. (2011, 28-01-2016). "CodeBlocks: The open source, cross platform and free integrated developemnt environemnt (IDE) for C, C++ and Fortran computer programming languages." Retrieved 06-07-2017, 2017, from http://www.codeblocks.org/.

De Marchis, M., C. M. Fontanazza, G. Freni, V. Notaro and V. Puleo (2016). "Experimental evidence of leaks in elastic pipes." Water Resources Management **30**(6): 2005-2019.

Diwakar, R. (2017). "An evaluation of normal versus lognormal distribution in data description and emprical analysis." Practical Assessment, Research and Evaluation **22**(13).

European Commision (2015). EU reference document: Good practices on leakage managemetn WFD CIS WG PoM. Luxembourg.

Ferrante, M. (2012). "Experimental investigation of the effects of pipe material on the leak head-discharge relationship." Journal of Hydraulic Engineering **138**(8): 736-743.

Ferrante, M., C. Massari, B. Brunone and S. Meniconi (2011). "Experimental evidence of hysteresis in the head-discharge relationship for a leak in a polyethylene pipe." Journal of Hydraulic Engineering **137**(7): 775-780.

Ferrante, M., C. Massari, B. Brunone and S. Meniconi (2013a). "Leak behaviour in pressurized PVC pipes." Water Science and Technology: Water Supply **13**(4): 987-992.

Ferrante, M., C. Massari, E. Todini, B. Brunone and S. Meniconi (2013b). "Experimental investigation of leak hydraulics." Journal of Hydroinformatics **15**(3): 666-675.

Fox, S., R. Collins and J. Boxall (2016). "Physical investigation into the significance of ground conditions on dynamic leakage behaviour." Journal of Water Supply: Research and Technology - Aqua **65**(2): 103-115.

Fox, S., R. Collins and J. Boxall (2017). "Experimental study exploring the interaction of structural and leakage dynamics." Journal of Hydraulic Engineering **143**(2): 04016080.

Gebhardt, D. (1975). "The effects of pressure on domestic water supply including observations on the effect of limited garden-watering restrictions during a period of high demand." Water SA **1**(1): 3-8.

Greyvenstein, B. and J. E. van Zyl (2007). "An experimental investigation into the pressure - leakage relationship of some failed water pipes." Journal of Water Supply: Research and Technology - AQUA.

Hamilton, S. and D. Krywyj (2012). The problem of leakage detection on large diameter mains. Proceedings of IWA Waterloss Conference 2012, Manila, Philippines.

Hiki, S. (1981). "Relationship between leakage and pressure." Journal of Japan Waterworks Association **5**: 50-54.

Kabaasha, A. M., O. Piller and J. E. van Zyl (2018). "Incorporating the modified orifice equation into pipe network solvers for more realistic leakage modeling." Journal of Hydraulic Engineering **144**(2): 04017064.

King, H. W. (1918). Handbook of hydraulics: For the solution of hydraulic problems. New York: 370 Seventh Avenue, McGraw-Hill Book Company, Inc.

Kingdom, B., R. Liemberger and P. Marin (2006). The challenge of reducing non-revenue water in developing countries-How the private sector can help : A look at performance-based service contracting. Water supply and sanitation sector board discussion paper series; no. 8. Washington, DC., World Bank.

Lambert, A. (2000). What do we know about pressure-leakage relationships in distribution systems. IWA Specialised Conference on System Approach to Leakage Control and Water Distribution Systems Management, Brno, Czech Republic, IWA.

Lambert, A. (2009). Ten years experience in using the UARL formula to calculate infrastructure leakage index. Proc. IWA Conf. Water loss, Cap Town, South Africa.

Lambert, A. (2012). Expert advice and international data on leakage in water distribution systems. J. Schwaller and J. E. van Zyl.

Lambert, A. (2013). Guidelines relating to the assessment and calculation of average pressure in water distribution systems and zones, ILMSS Ltd.

Lambert, A. (2014). "Fixed And Variable Area Discharges: Pressure influences some leaks flow rates more than others." Retrieved 05-07-2017, 2017, from http://www.leakssuite.com/concepts/favad/.

Lambert, A. (2014). "International Water Association (IWA) best practice standard water balance." Retrieved 05-07-2017, 2017, from http://www.leakssuite.com/concepts/iwa-water-balance/.

Lambert, A. (2017, 14/11/2017). "Night Day Factor (NDF)." Retrieved 29/05/2018, 2018, from http://www.leakssuite.com/night-day-factor-ndf/.

Lambert, A. and W. Hirner (2000). Losses from water supply systems: A standard terminology and recommended performance measures (The blue pages), IWA.

Lambert, A. and R. McKenzie (2002). Practical experience in using the Infrastructure Leakage Index. Proceedings of IWA Conference–Leakage Management: A Practical Approach. Lemesos, Cyprus.

Lambert, A. O. (2002). "International report: Water losses management and techniques." Water Science and Technology: Water Supply **2**(4): 1-20.

Lambert, A. O., T. G. Brown, M. Takizawa and D. Weimer (1999). "A review of performance indicators for real losses from water supply systems." Journal of Water Supply: Research and Technology - Aqua **48**(6): 227-237.

Liemberger, R. and R. McKenzie (2005). Accuracy limitations of the ILI: is it an appropriate indicator for developing countries? Conference Proceedings, IWA Leakage 2005 Conference in Halifax, Nova Scotia, Canada.

Liemberger, R., R. McKenzie, K. Brothers, A. Lambert, A. Rizzo and T. Waldron (2007). Water loss performance indicators. Proceedings of IWA Specialised Conference 'Water Loss.

Malde, R. (2015). An analysis of leakage parameters of individual leaks on a pressure pipeline through the development and application of a standard procedure Masters Dissertation, University of Cape Town.

Massari, C., M. Ferrante, B. Brunone and S. Meniconi (2012). "Is the leak head–discharge relationship in polyethylene pipes a bijective function?" Journal of Hydraulic Research **50**(4): 409-417.

May, J. (1994). "Pressure dependent leakage." World Water and Environmental Engineering.

McKenzie, R. (2014). Guidelines for reducing water losses in South African Municipalities. Gezina, South Africa, Water Research Commission.

McKenzie, R. S., Z. Siqalaba and W. Wegelin (2012). The state of non-revenue water in South Africa (2012). Gezina, Pretoria, South Africa, Water Research Commission.

Mutikanga, H. E. (2012). Water loss management: Tools and methods for developing countries. Doctorate, UNESCO-IHE Institute for Water Education and Delft University of Technology

Mutikanga, H. E., S. Sharma and K. Vairavamoorthy (2009). "Water loss management in developing countries: Challenges and prospects." American Water Works Association. Journal **101**(12): 57.

Mutikanga, H. E., S. K. Sharma and K. Vairavamoorthy (2013). "Methods and tools for managing losses in water distribution systems." Journal of Water Resources Planning and Management **139**(2): 166-174.

Mutikanga, H. E., K. Vairavamoorthy, S. K. Sharma and C. S. Akita (2011). "Operational tools for decision support in leakage control." Water Practice and Technology **6**(3).

Ogura, L. (1979). "Experiment on the relationship between leakage and pressure." Japan Water Works Association, Tokyo: 38-45.

Renaud, E., M. Sissoko, M. Clauzier, D. Gilbert, A. Sandraz and J. Pillot (2015). "Comparative study of different methods to assess average pressures in water distribution zones." Water Utility Journal(10): 25 - 35.

Rossman, L. A. (1996). A memorandum: Notes on Epanet's hydraulic solver (updated). U. S. E. P. Agency.

Rossman, L. A. (1999). Computer models/ Epanet. Water distribution systems handbook. New York, McGraw Hill.

Rossman, L. A. (2000). "Epanet 2 users manual, us environmental protection agency." Water Supply and Water Resources Division, National Risk Management Research Laboratory, Cincinnati, OH **45268**.

Schwaller, J. (2012). Modelling the effects of a large number of leaks in a water distribution netwrok using the FAVAD equation Masters of Engineering, University of Applied Sciences Karlsruhe.

Schwaller, J. and J. E. van Zyl (2015). "Modeling the pressure-leakage response of water distribution systems based on individual leak behavior." Journal of Hydraulic Engineering **141**(5).

Schwaller, J., J. E. van Zyl and A. M. Kabaasha (2015). "Characterising the pressure-leakage response of pipe networks using the FAVAD equation." Water Science and Technology: Water Supply **15**(6): 1373-1382.

Seago, C., R. McKenzie and R. Liemberger (2005). International benchmarking of leakage from water reticulation systems. Leakage 2005 Conference, Halifax.

Ssozi, E. N., B. D. Reddy and J. E. van Zyl (2016). "Numerical Investigation of the Influence of Viscoelastic Deformation on the Pressure-Leakage Behavior of Plastic Pipes." Journal of Hydraulic Engineering **142**(3).

Statistics South Africa. (2011 Census). "Statistics on the Ethekwini metropolitan municipality in the KwaZulu-Natal province of South Africa." Retrieved 12-07-2017, 2017, from http://www.statssa.gov.za/?page_id=1021&id=ethekwini-municipality.

Thornton, J. and A. Lambert (2005). Progress in practical prediction of pressure: leakage, pressure: burst frequency and pressure: consumption relationships. Paper to IWA Special Conference 'Leakage 2005', September 12-14, Halifax, Canada.

Trow, S. and M. Farley (2003). Losses in water distribution networks - A practitioner's guide to assessment, monitoring and control, IWA.

Van Zyl, J. E., M. O. A. Alsaydalani, C. R. I. Clayton, T. Bird and A. Dennis (2013). "Soil fluidisation outside leaks in water distribution pipes – preliminary observations." Proceedings of the Institution of Civil Engineers - Water Management **166**(10): 546-555.

Van Zyl, J. E. and A. M. Cassa (2014). "Modeling elastically deforming leaks in water distribution pipes." Journal of Hydraulic Engineering **140**(2): 182-189.

Van Zyl, J. E. and C. R. I. Clayton (2007). "The effect of pressure on leakage in water distribution systems." Institution of Civil Engineers (ICE)(WMO): 1-6.

Van Zyl, J. E., A. Lambert and R. Collins (2017). "Realistic modeling of leakage and intrusion flows through leak openings in pipes." Journal of Hydraulic Engineering **143**(9).

Van Zyl, J. E. and R. Malde (2017). "Evaluating the pressure-leakage behaviour of leaks in water pipes." Journal of Water Supply: Research and Technology - Aqua.

Walski, T., W. Bezts, E. T. Posluszny, M. Weir and B. E. Whitman (2006). "Modelling leakage reduction through pressure control." American Water Works Association: 147 - 155.

Wikipedia. (2017, 02-07-2017). "Torricelli's law." Retrieved 05-08-2017, 2017, from https://en.wikipedia.org/wiki/Torricelli%27s_law.

Winarni, W. (2009). "Infrastructure leakage index (ILI) as water losses indicator." Civil Engineering Dimension **11**(2): pp. 126-134.

Wu, Z. Y., M. Farley, D. Turtle, Z. Kapelan, J. Boxall, S. Mounce, S. Dahasahasra, M. Mulay and Y. Kleiner (2011). Water loss reduction.

Published work

The following work was published during the course this research:

Journal papers:

- Schwaller, J., J. E. van Zyl and **A. M. Kabaasha** (2015). "Characterising the pressure-leakage response of pipe networks using the FAVAD equation." Water Science and Technology: Water Supply 15(6): 1373-1382.

- **Kabaasha, A. M**., O. Piller and J. E. van Zyl (2018). "Incorporating the modified orifice equation into pipe network solvers for more realistic leakage modeling." Journal of Hydraulic Engineering 144(2): 04017064.

Conference paper:

- **Kabaasha, A. M.**, J. E. van Zyl and O. Piller (2016). Modelling pressure – leakage response in water distribution systems considering leak area variation. Paper presented at the 14th CCWI (Computing and Control for the Water Industry) conference, Amsterdam, Netherlands.

Appendices

Appendix A-1: Small-sized network with an ILI of 1

Results for an individual system

Pressure head at the average zone pressure (AZP) node

		Pressure head (m)			
		Minimum	**Arithmetic Mean**	**Median**	**Maximum**
Before pressure management	Without leaks	77.08	82.16	82.27	86.48
	Modified orifice equation	76.95	82.07	82.18	86.48
	Power equation	76.95	82.07	82.18	86.48
After pressure management	Modified orifice equation	17.03	22.12	22.23	26.48
	Power equation	17.03	22.12	22.23	26.48

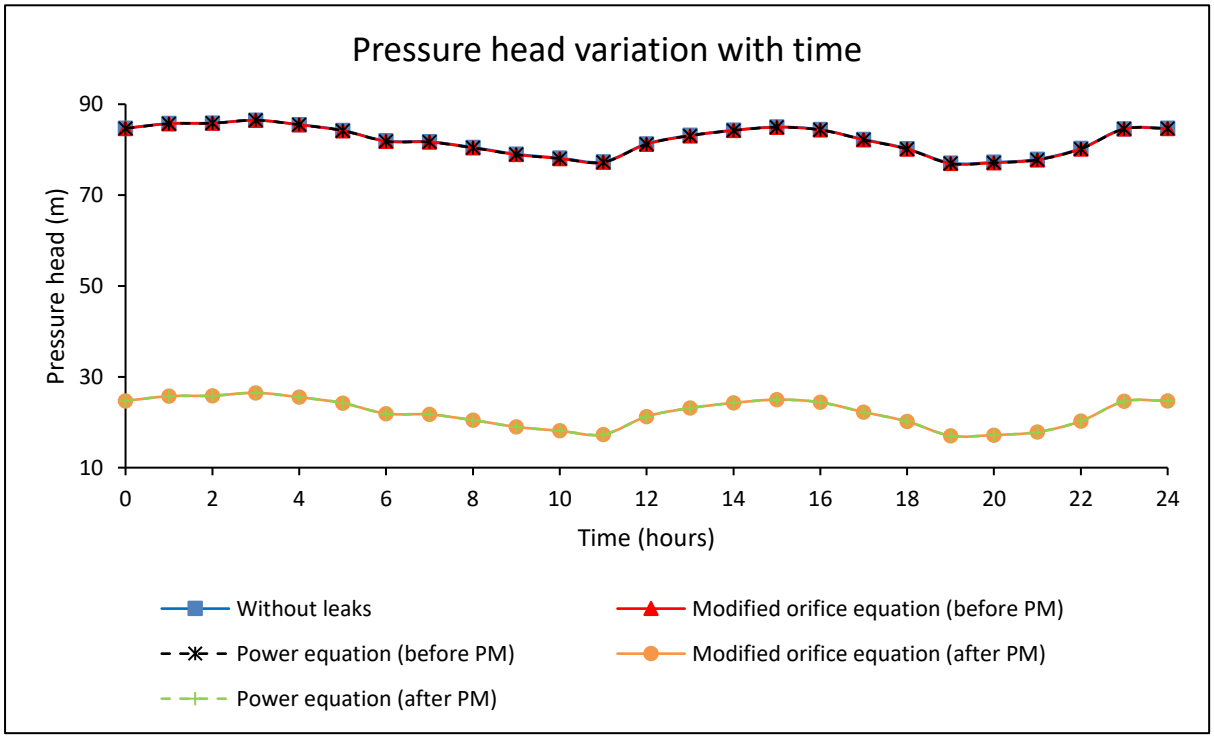

Pressure head at the critical node

		Pressure head (m)			
		Minimum	**Arithmetic Mean**	**Median**	**Maximum**
Before pressure management	Without leaks	70.86	77.65	77.80	83.43
	Modified orifice equation	70.71	77.55	77.69	83.43
	Power equation	70.71	77.55	77.69	83.43
After pressure management	Modified orifice equation	10.79	17.60	17.75	23.43
	Power equation	10.80	17.61	17.75	23.43

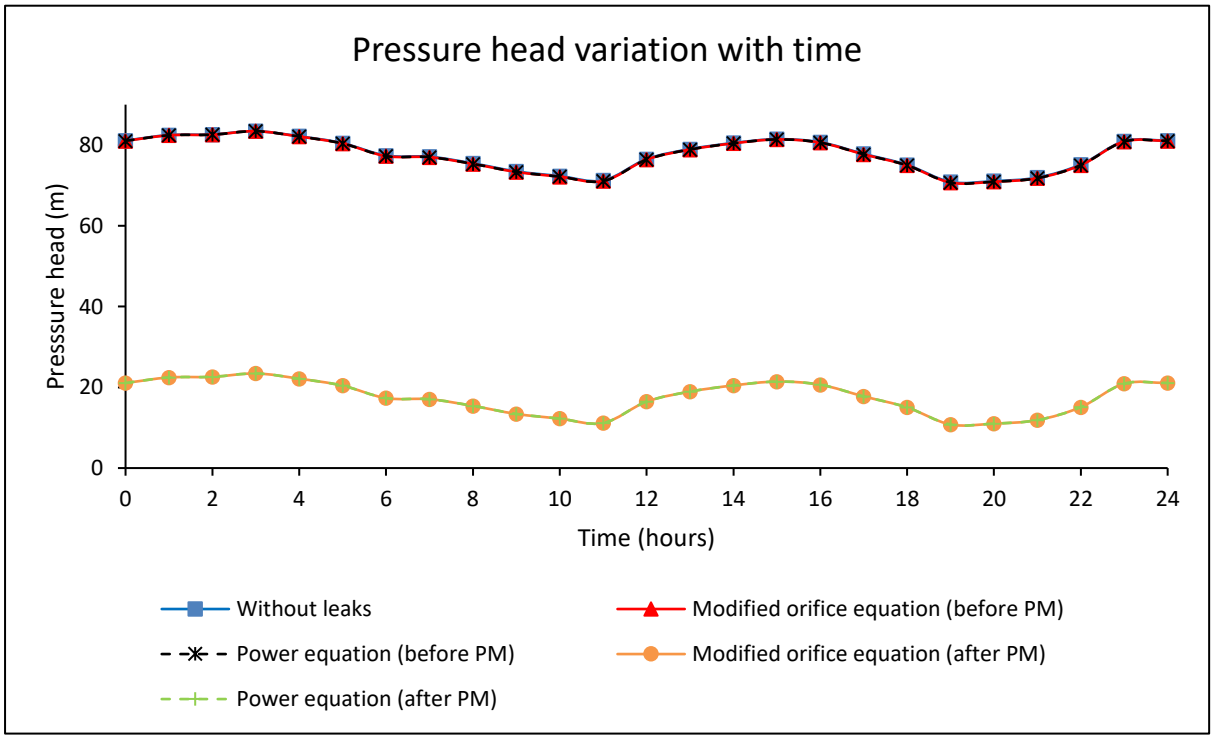

System leakage flow rate

		Leakage flow rate (m^3/h)			
		Minimum	**Arithmetic Mean**	**Median**	**Maximum**
Before pressure management	Modified orifice equation	3.52	3.63	3.64	3.73
	Power equation	3.52	3.63	3.64	3.73
After pressure management	Modified orifice equation	1.52	1.69	1.70	1.83
	Power equation	1.37	1.56	1.57	1.71

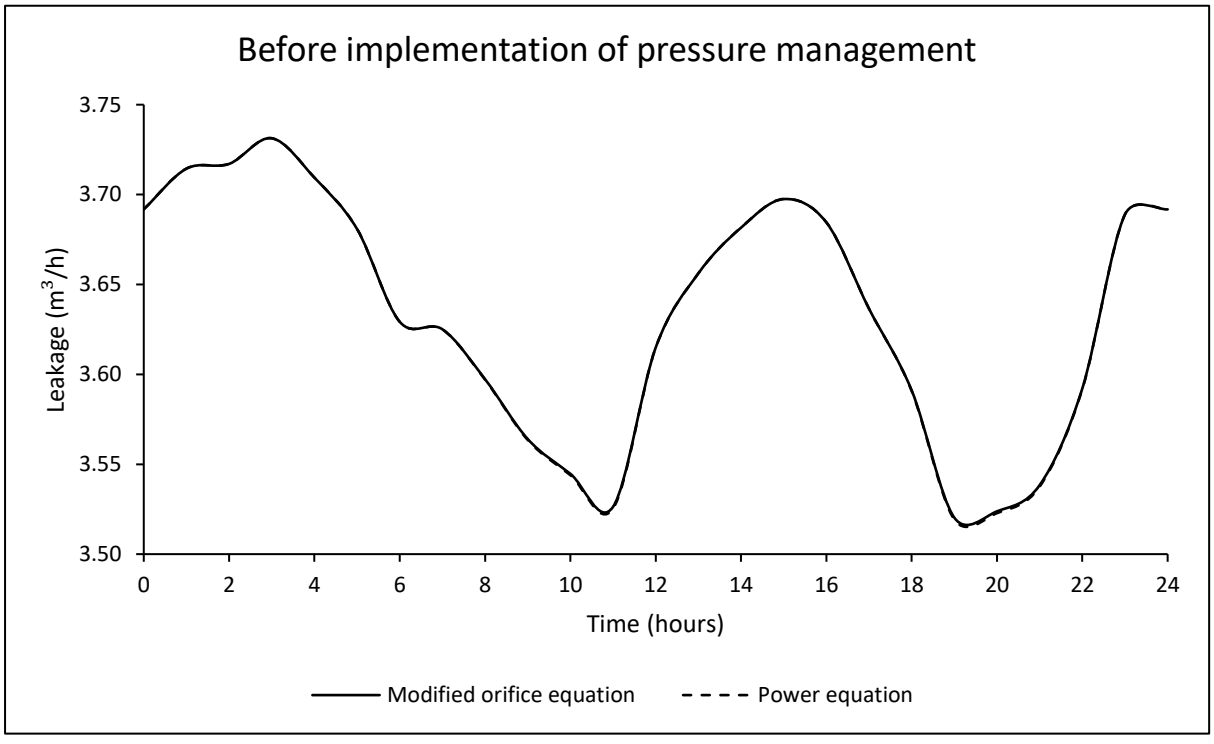

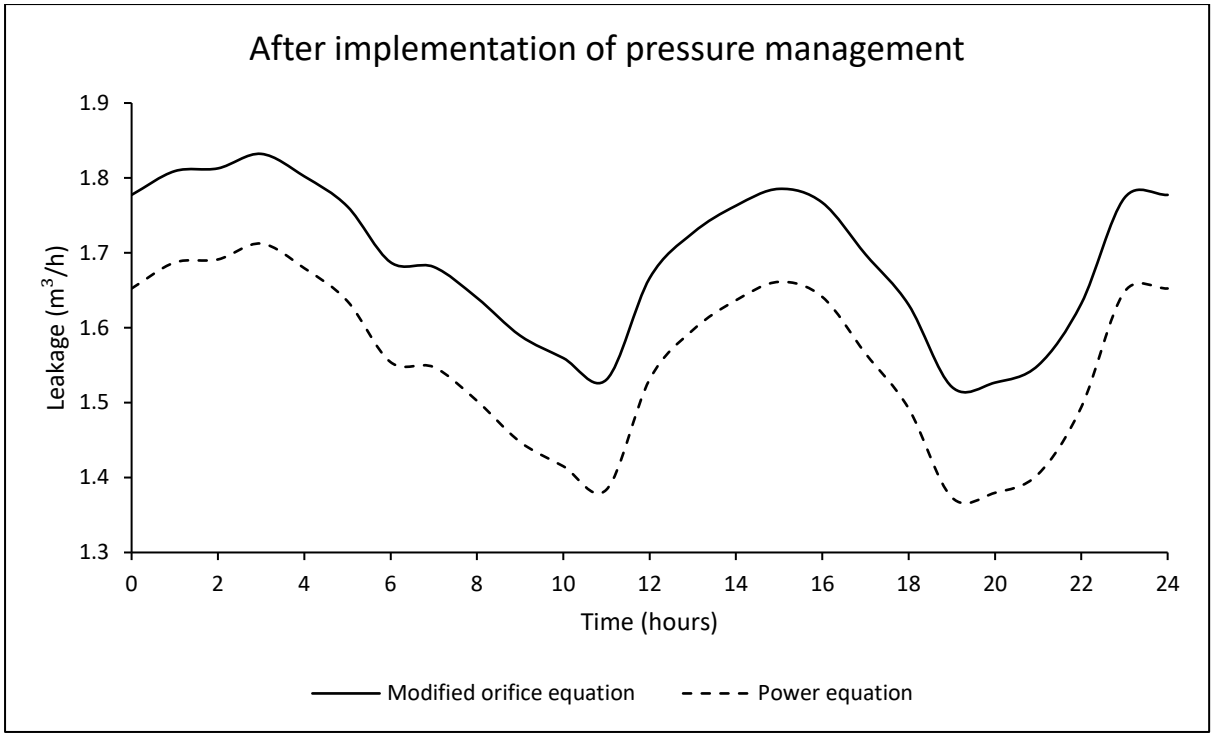
After implementation of pressure management
Leakage (m3/h)
1.9
1.8
1.7
1.6
1.5
1.4
1.3
0
2
4
6
8
10
12
14
16
18
20
22
24
Time (hours)
Modified orifice equation
Power equation

Leakage flow rate at the critical node

		Leakage flow rate (m^3/h)			
		Minimum	**Arithmetic Mean**	**Median**	**Maximum**
Before pressure management	Modified orifice equation	0.15	0.15	0.15	0.16
	Power equation	0.14	0.15	0.15	0.16
After pressure management	Modified orifice equation	0.06	0.07	0.07	0.08
	Power equation	0.04	0.06	0.06	0.07

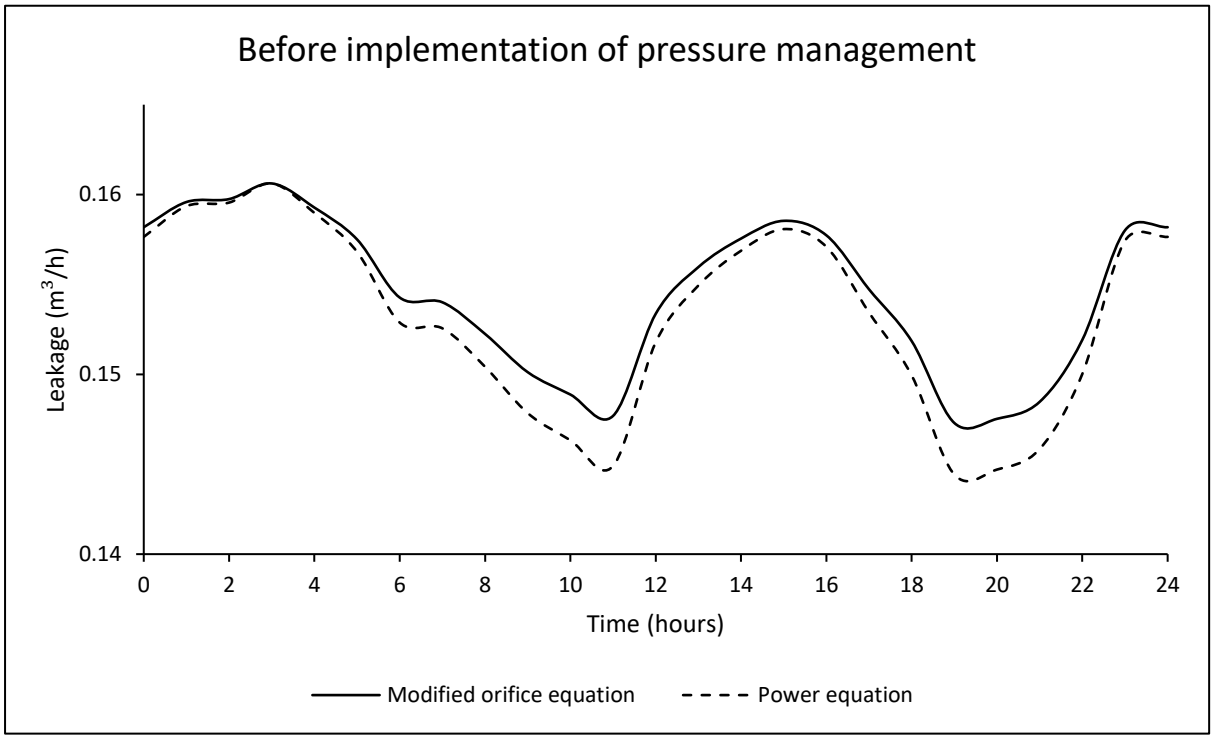

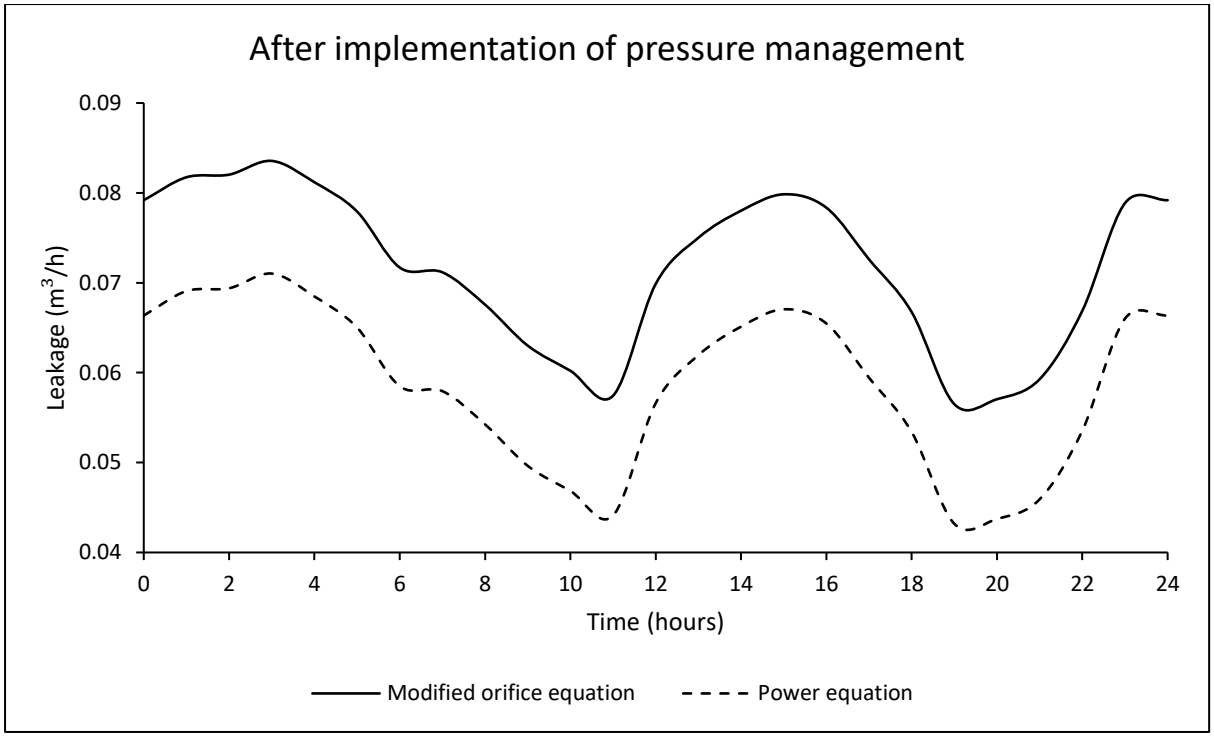
After implementation of pressure management
0.09
0.08
0.07
0.06
0.05
0.04
Leakage (m3/h)
0
2
4
6
8
10
12
14
16
18
20
22
24
Time (hours)
Modified orifice equation
Power equation

Number of iterations required for a system to converge to a hydraulic solution for both formulations

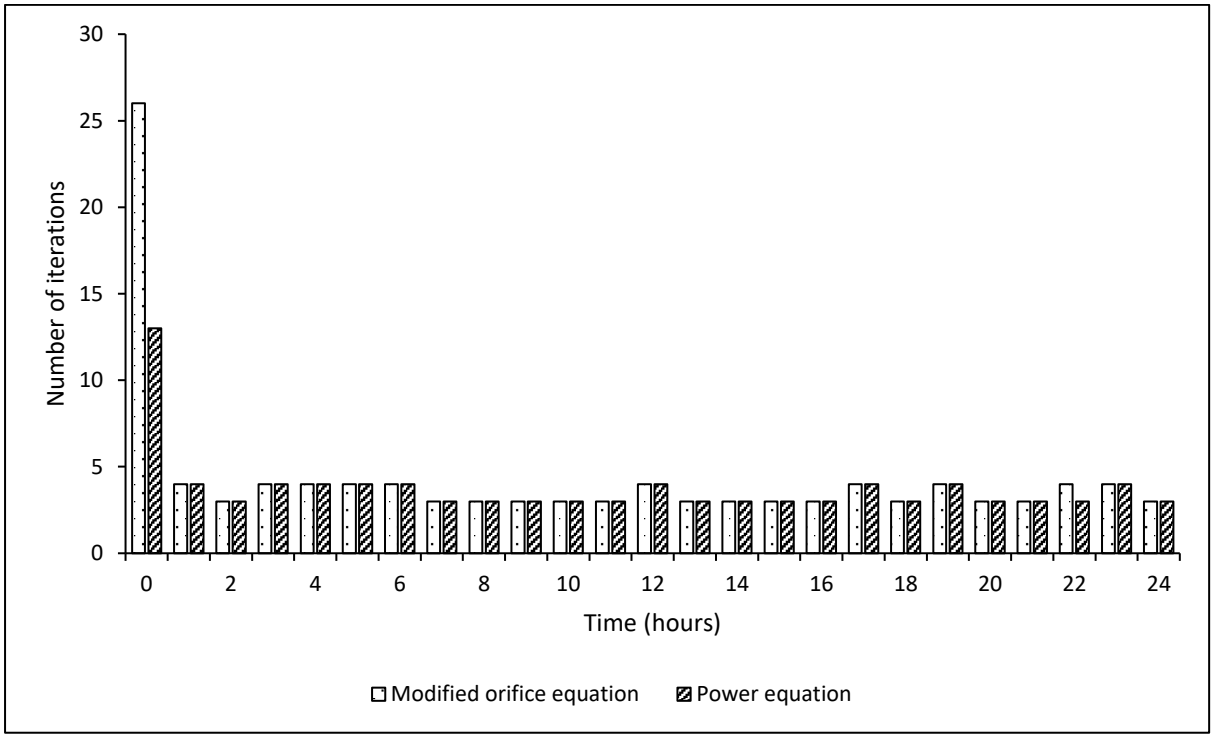

Results for combined systems

System parameters for both power and modified orifice formulations

	Minimum	Arithmetic Mean	Median	Maximum
Leakage exponent N1	0.63	0.65	0.64	0.72
Leakage coefficient C	4.1E-05	5.9E-05	6.0E-05	6.3E-05
Effective initial leak area C_dA0 (mm^2)	19.34	21.56	21.61	22.06
Effective head-area slope C_dm (mm^2/m)	0.04	0.04	0.04	0.07
Leakage number LN	0.15	0.17	0.17	0.29

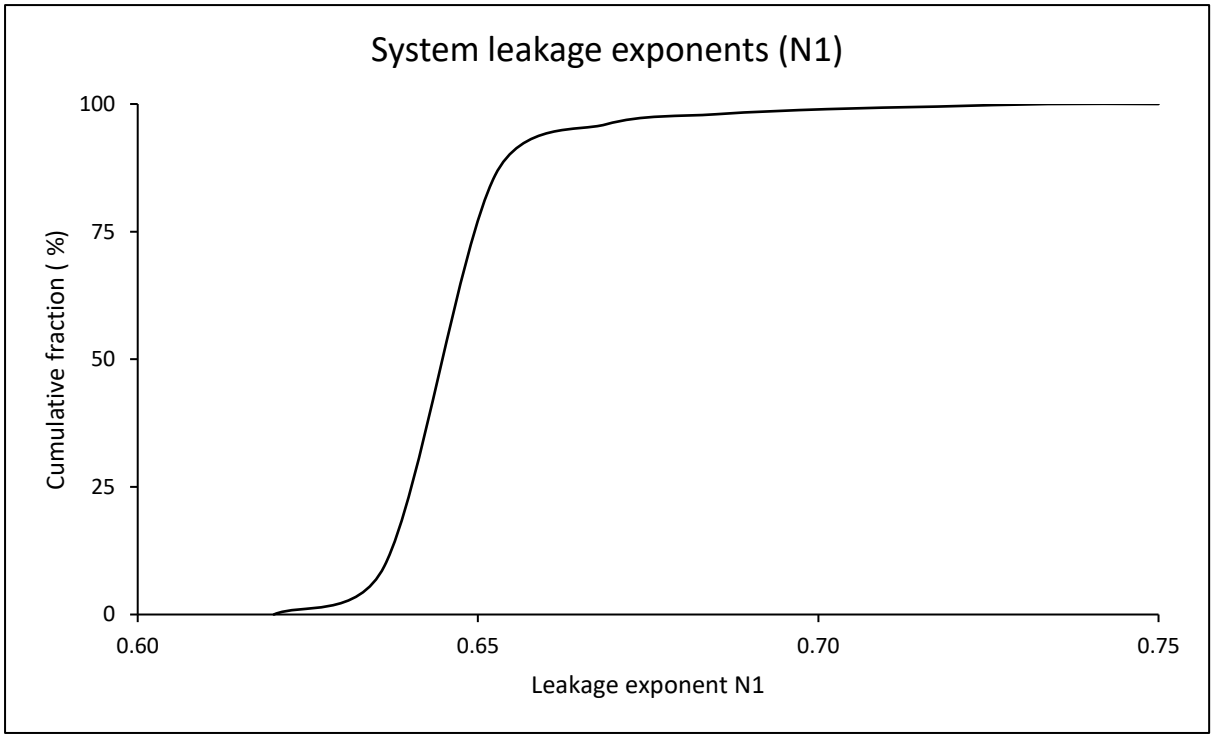

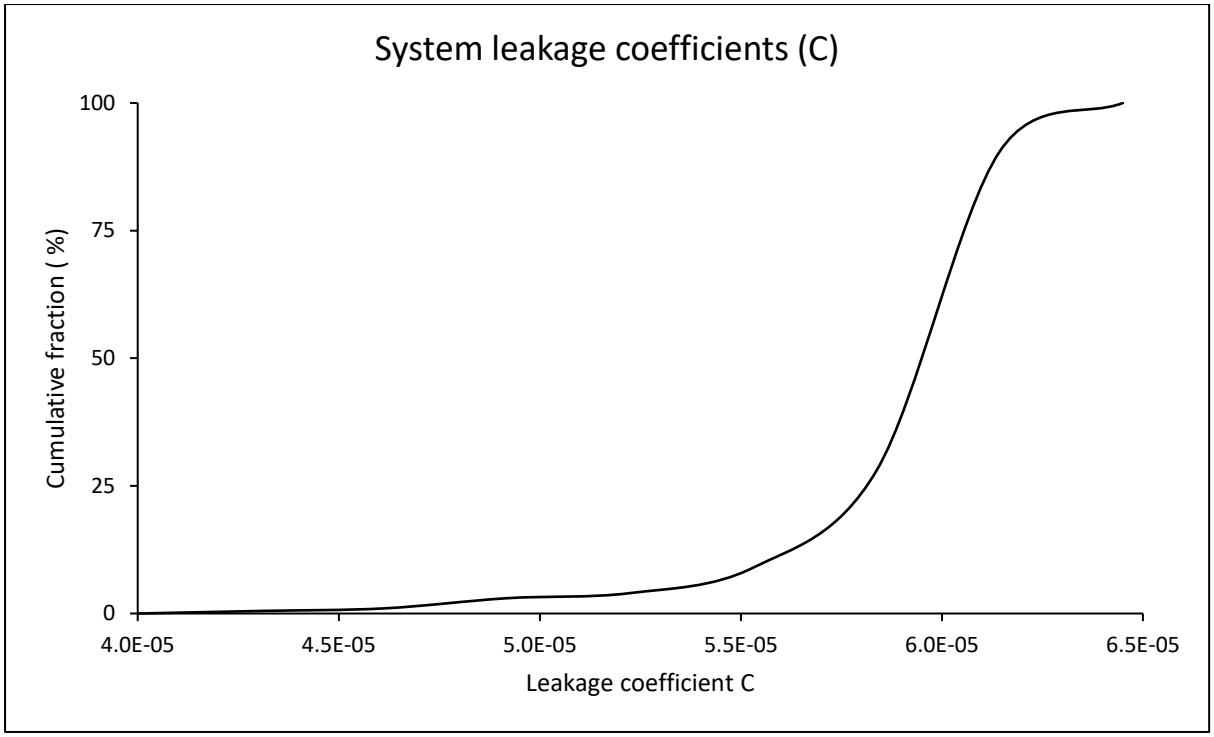
System leakage coefficients (C)
100
75
50
25
0
Cumulative fraction (%)
4.0E-05
4.5E-05
5.0E-05
5.5E-05
6.0E-05
6.5E-05
Leakage coefficient C

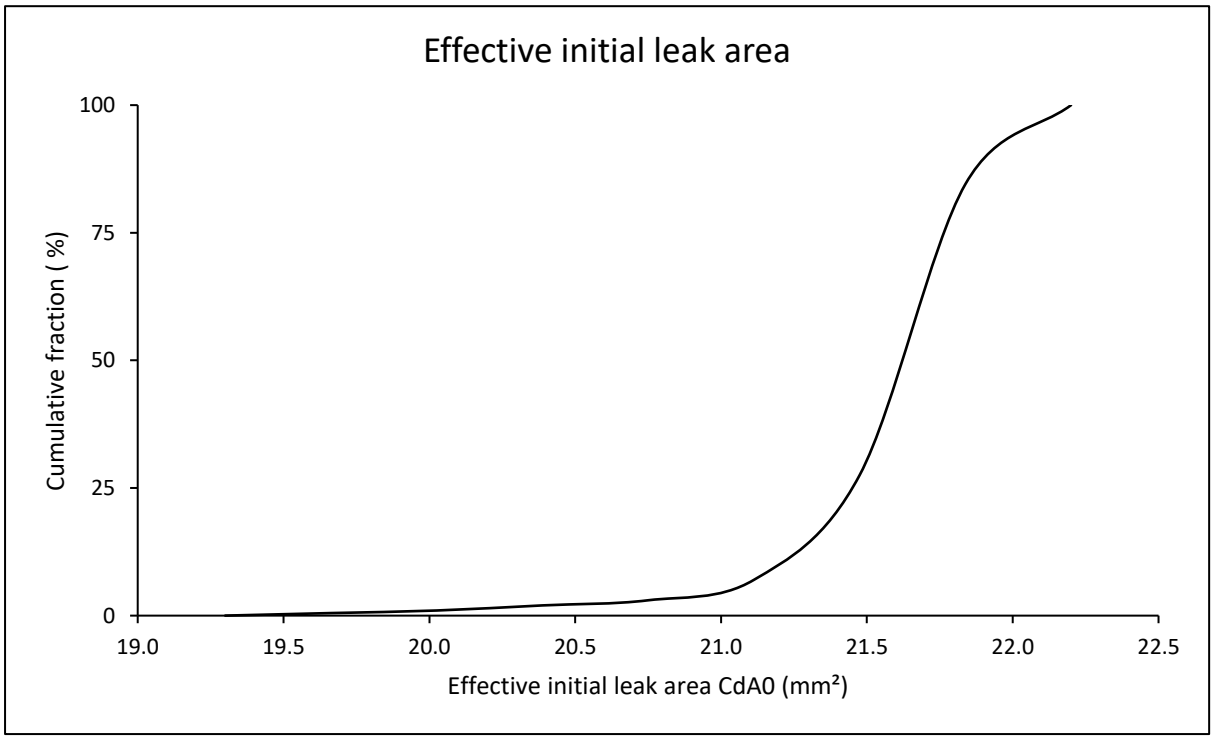
Effective initial leak area
100
75
50
25
0
Cumulative fraction (%)
19.0
19.5
20.0
20.5
21.0
21.5
22.0
22.5
Effective initial leak area CdA0 (mm²)

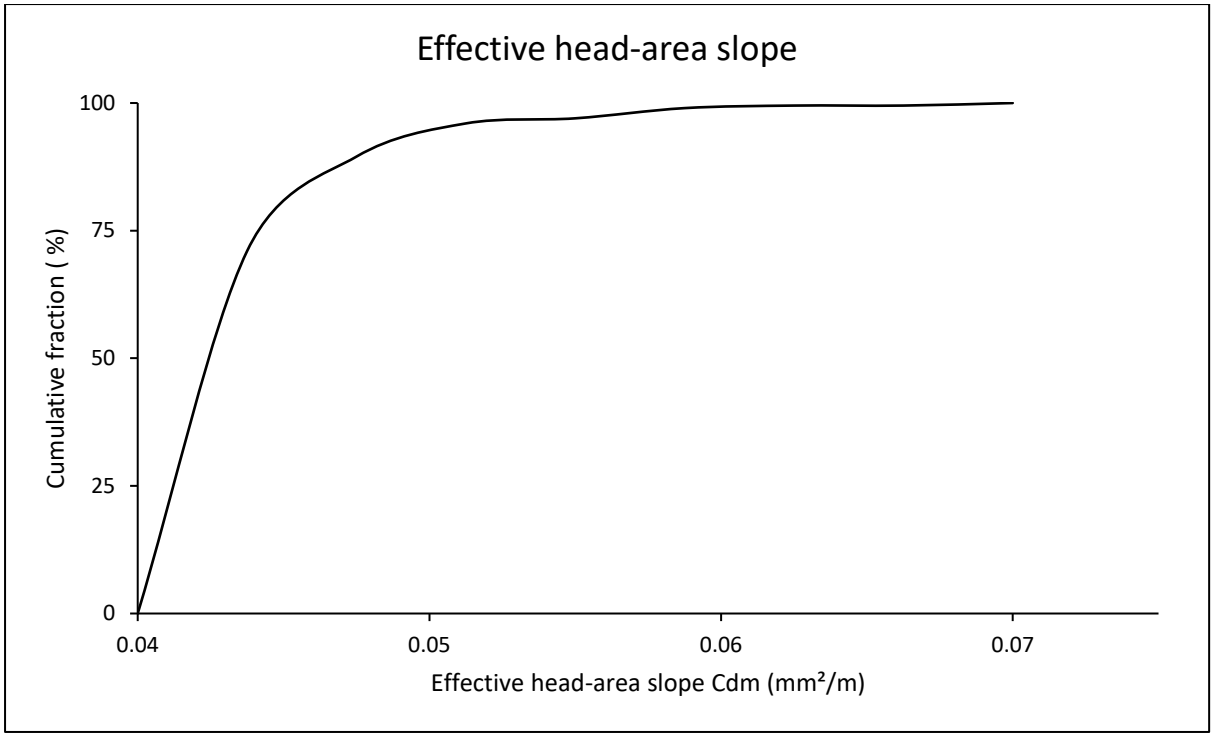
Effective head-area slope
100
75
50
25
0
Cumulative fraction (%)
0.04
0.05
0.06
0.07
Effective head-area slope Cdm (mm²/m)

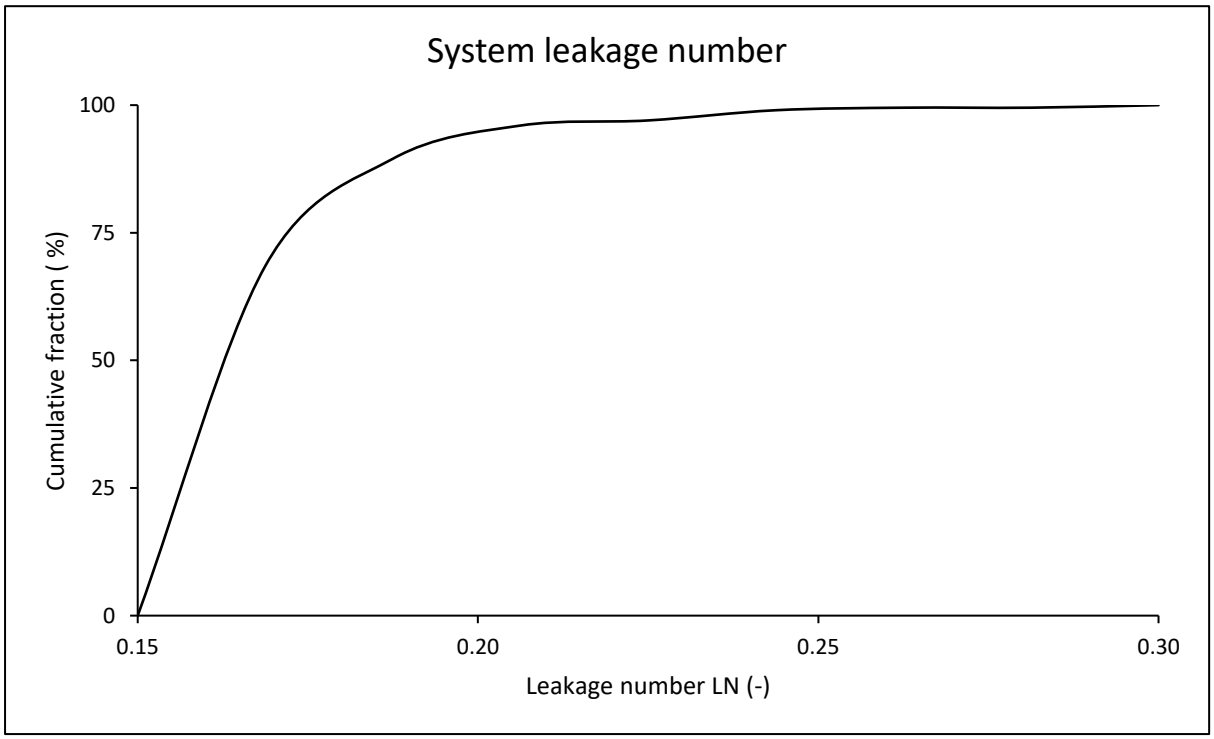
System leakage number
100
75
50
25
0
Cumulative fraction (%)
0.15
0.20
0.25
0.30
Leakage number LN (-)

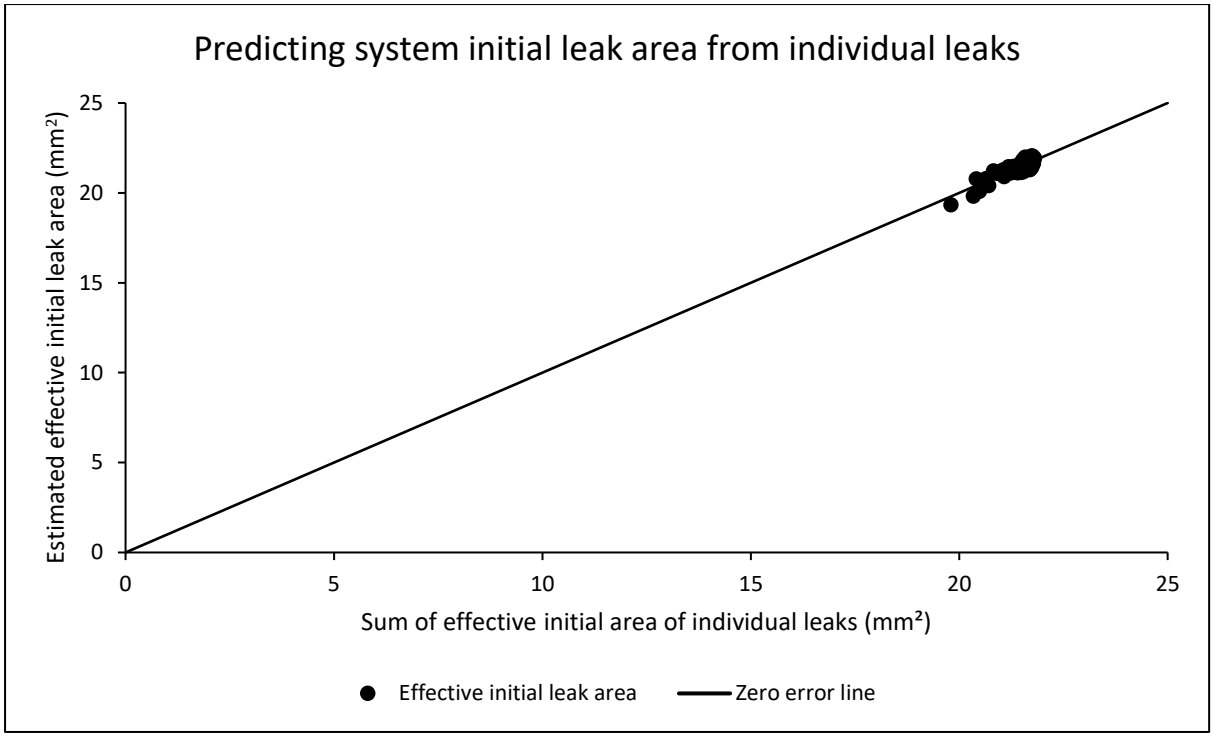
Predicting system initial leak area from individual leaks
Estimated effective initial leak area (mm²)
25
20
15
10
5
0
0
5
10
15
20
25
Sum of effective initial area of individual leaks (mm²)
Effective initial leak area
Zero error line

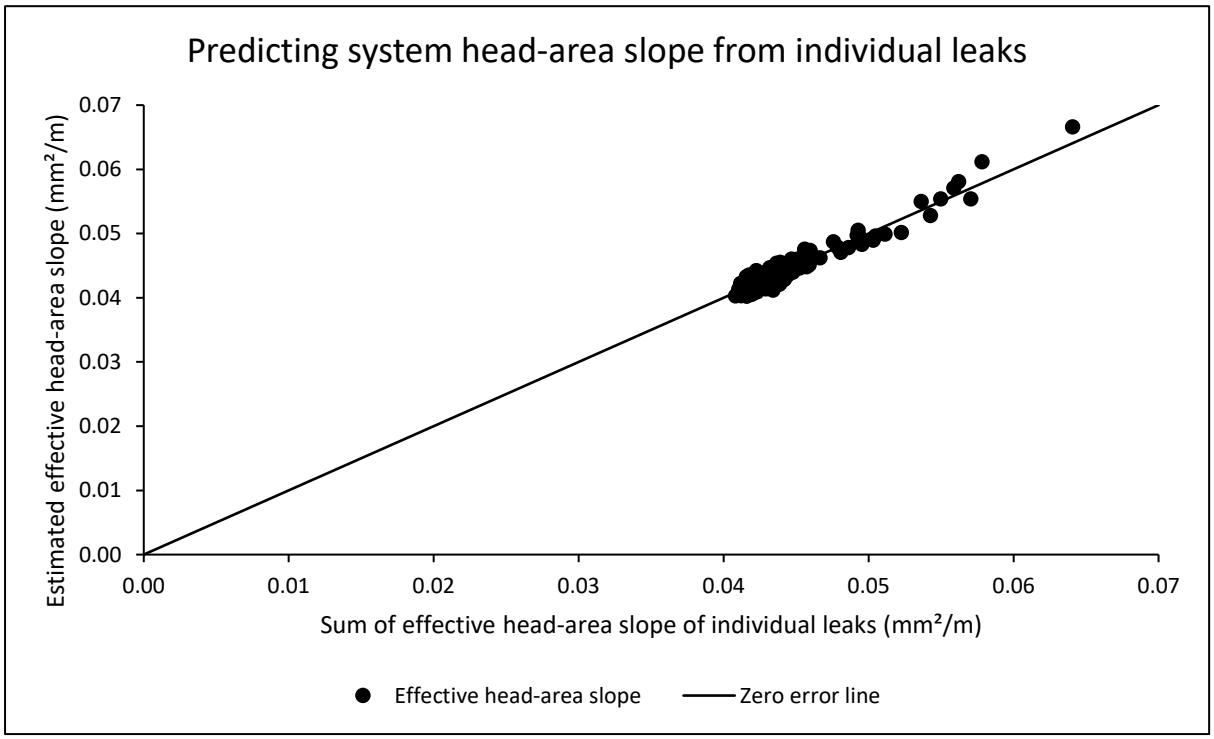
Predicting system head-area slope from individual leaks
Estimated effective head-area slope (mm²/m)
0.07
0.06
0.05
0.04
0.03
0.02
0.01
0.00
0.00
0.01
0.02
0.03
0.04
0.05
0.06
0.07
Sum of effective head-area slope of individual leaks (mm²/m)
Effective head-area slope
Zero error line

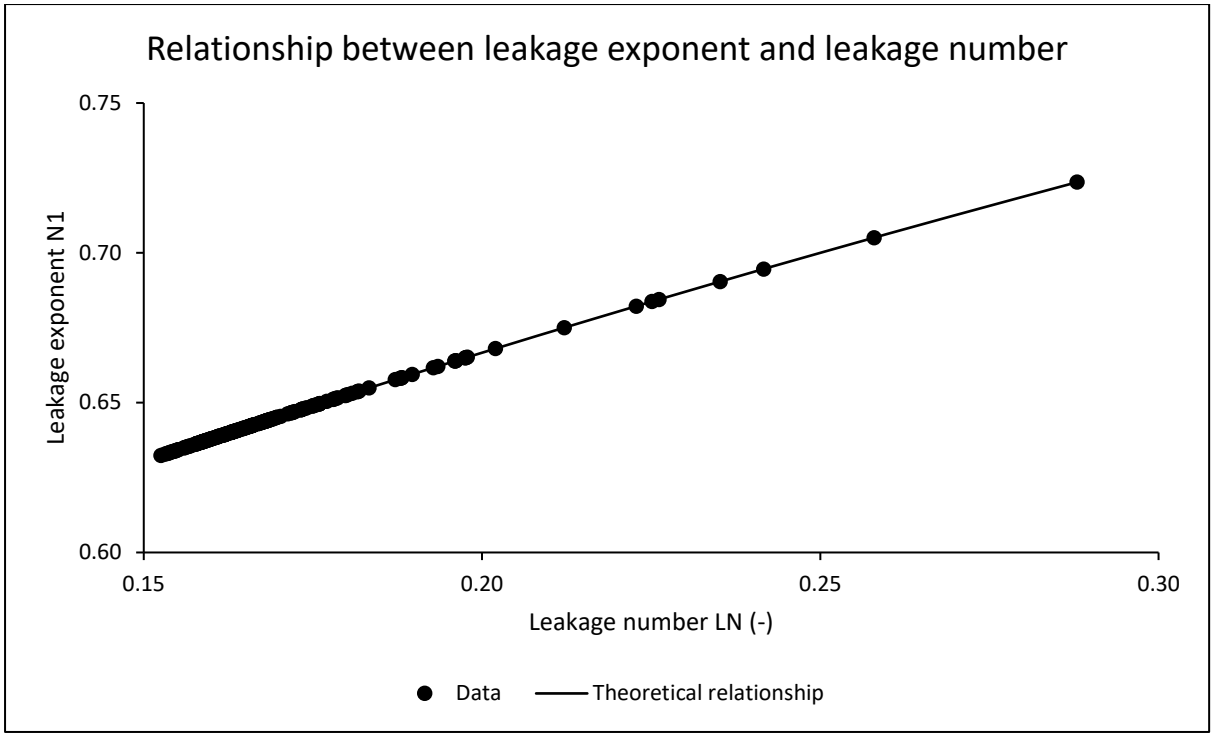
Relationship between leakage exponent and leakage number
Leakage exponent N1
0.75
0.70
0.65
0.60
0.15
0.20
0.25
0.30
Leakage number LN (-)
Data
Theoretical relationship

Average iterations required for a system to converge using both formulations

	Minimum	Arithmetic Mean	Median	Maximum
Modified orifice equation	3.76	4.16	4.16	4.44
Power equation	3.44	3.75	3.76	3.88

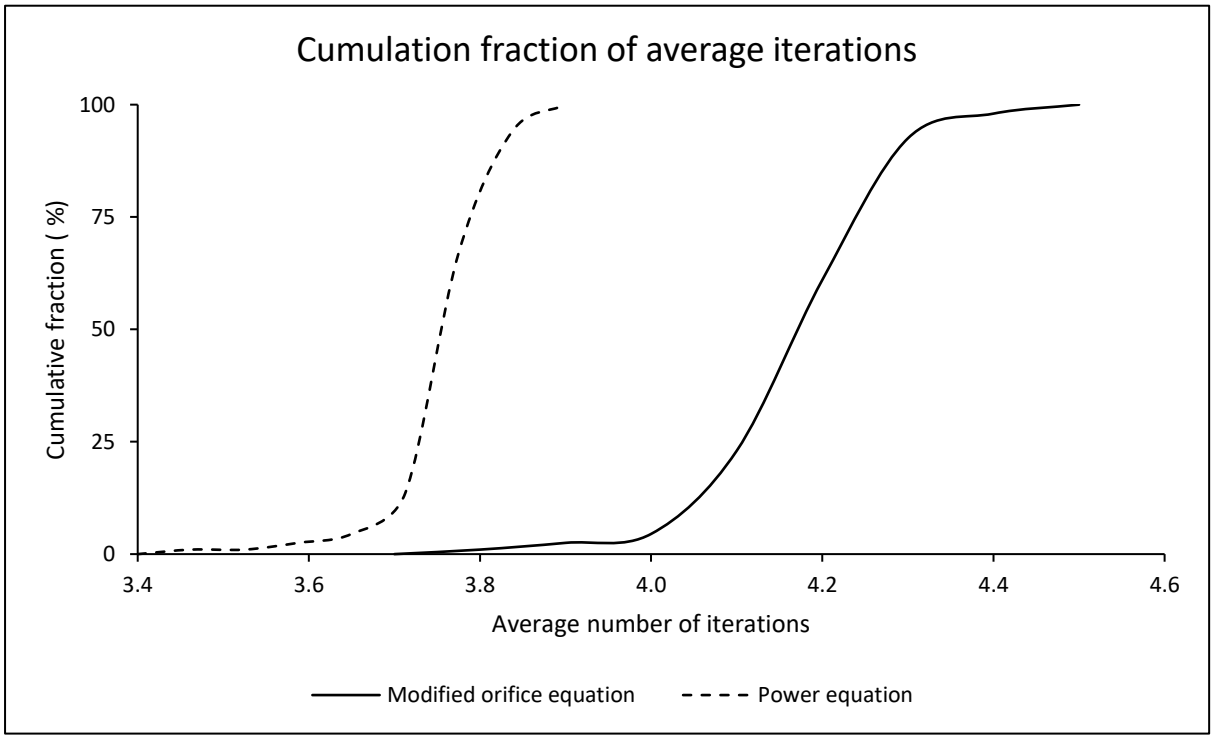

Effect of leakage on pressure at both average zone pressure (AZP) and critical nodes

AZP node								
	During MNF conditions				During peak demand conditions			
	Min (m)	Mean (m)	Median (m)	Max (m)	Min (m)	Mean (m)	Median (m)	Max (m)
Modified orifice equation	-0.01	0.00	0.00	0.00	-0.17	-0.15	-0.15	-0.10
Power equation	-0.01	0.00	0.00	0.00	-0.17	-0.15	-0.15	-0.10
Critical node								
Modified orifice equation	-0.01	-0.01	-0.01	0.00	-0.32	-0.19	-0.18	-0.11
Power equation	-0.01	-0.01	-0.01	0.00	-0.32	-0.19	-0.18	-0.11

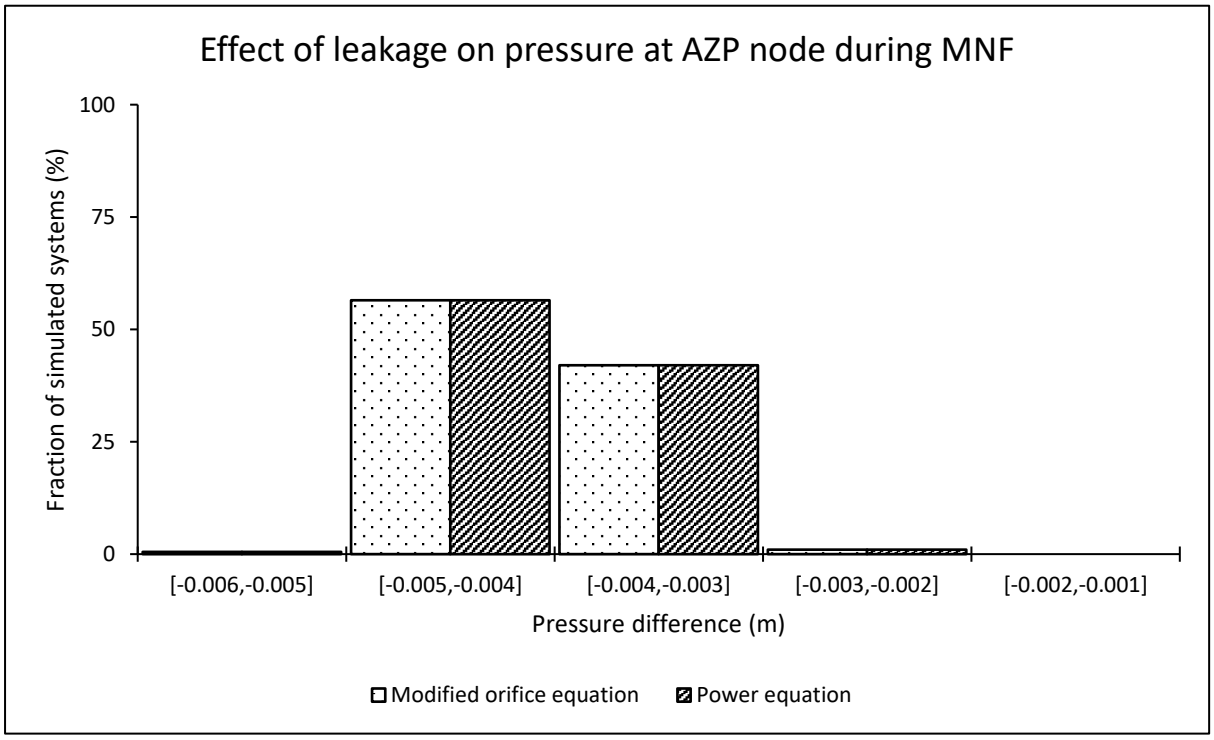

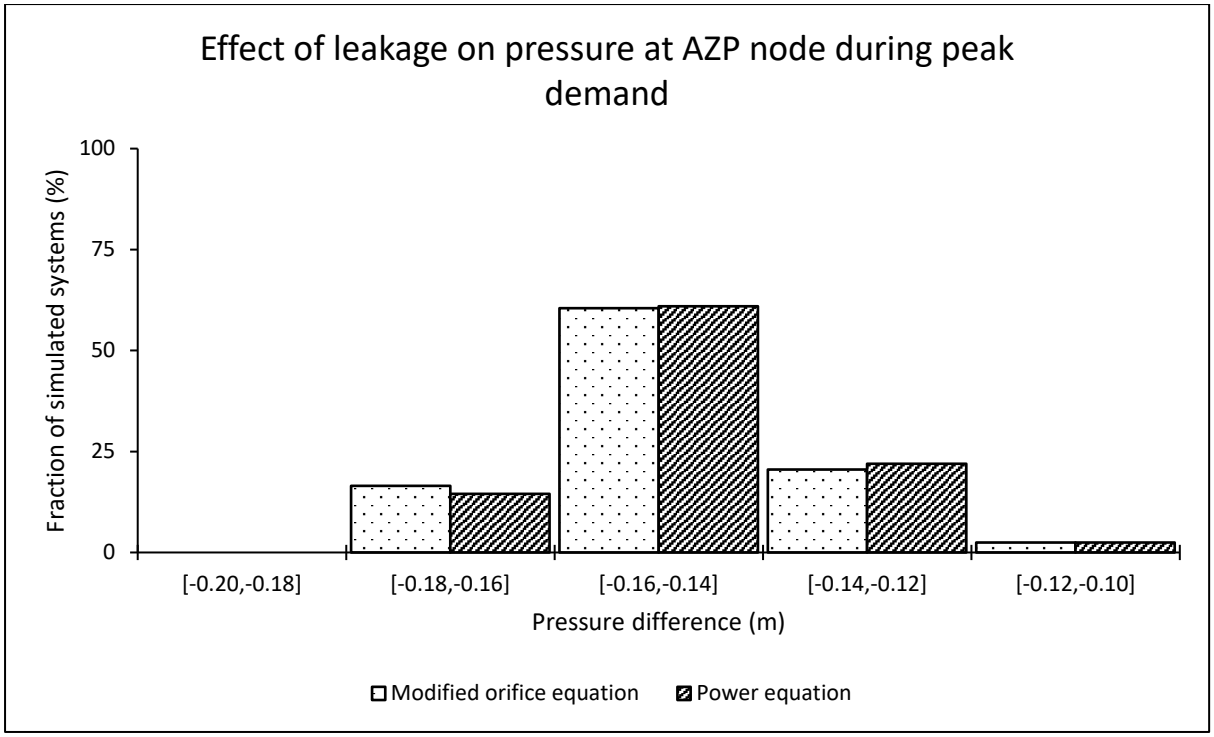
Effect of leakage on pressure at AZP node during peak demand
Fraction of simulated systems (%)
100
75
50
25
0
[-0.20,-0.18]
[-0.18,-0.16]
[-0.16,-0.14]
[-0.14,-0.12]
[-0.12,-0.10]
Pressure difference (m)
Modified orifice equation
Power equation

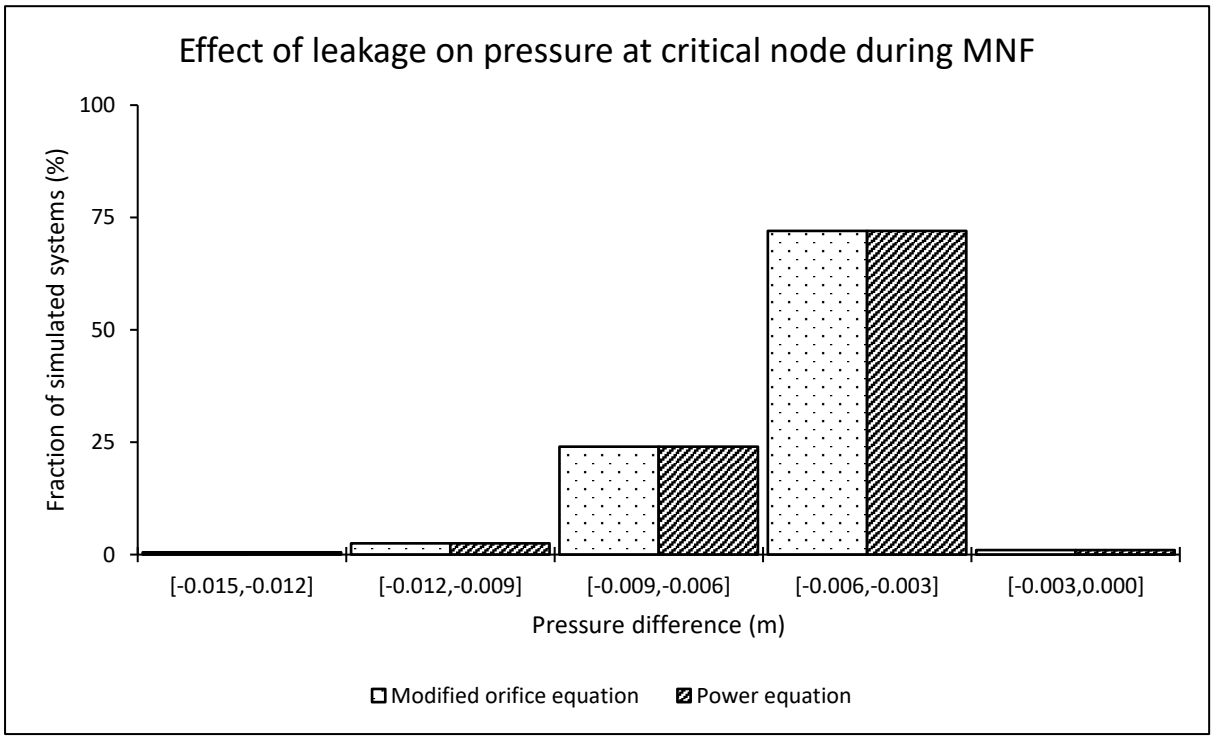
Effect of leakage on pressure at critical node during MNF
Fraction of simulated systems (%)
100
75
50
25
0
[-0.015,-0.012]
[-0.012,-0.009]
[-0.009,-0.006]
[-0.006,-0.003]
[-0.003,0.000]
Pressure difference (m)
Modified orifice equation
Power equation

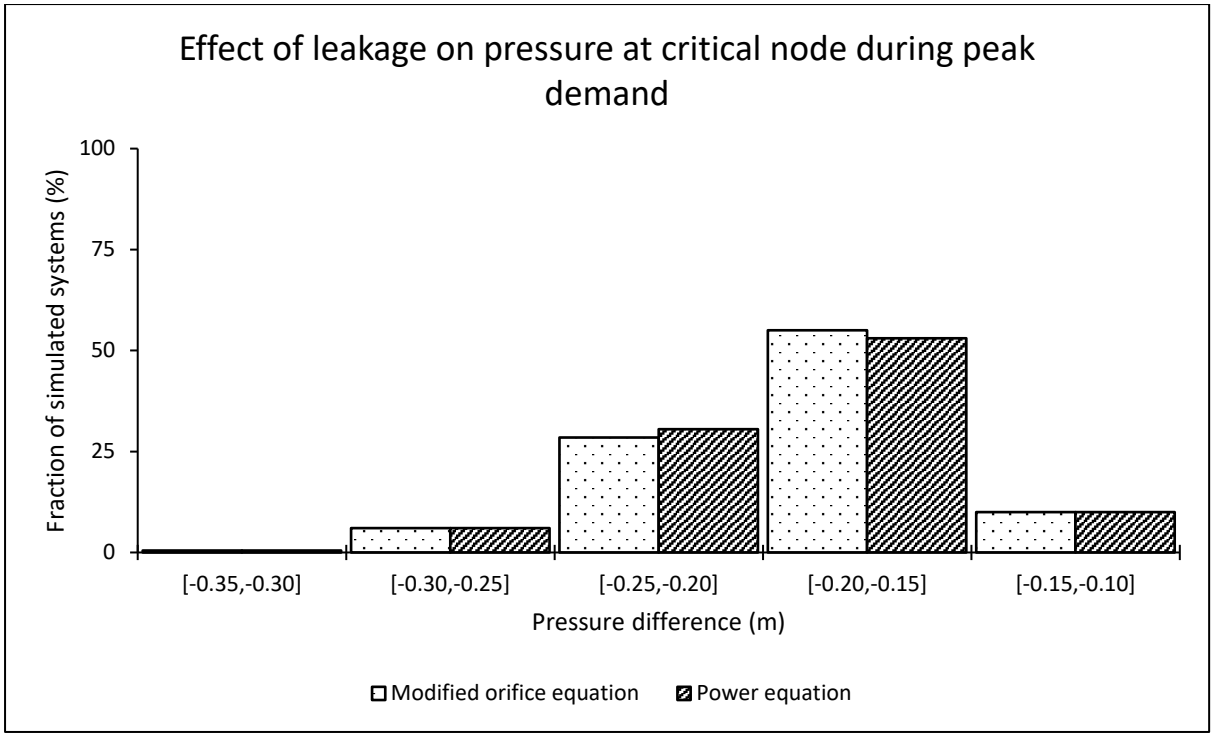
Effect of leakage on pressure at critical node during peak demand
Fraction of simulated systems (%)
100
75
50
25
0
[-0.35,-0.30]
[-0.30,-0.25]
[-0.25,-0.20]
[-0.20,-0.15]
[-0.15,-0.10]
Pressure difference (m)
Modified orifice equation
Power equation

Pressure estimation error when using the power equation at average zone pressure (AZP) and critical nodes

	During MNF conditions				During peak demand conditions			
	Min (%)	**Mean (%)**	**Median (%)**	**Max (%)**	**Min (%)**	**Mean (%)**	**Median (%)**	**Max (%)**
At the AZP node	0.00	0.00	0.00	0.00	0.00	0.00	0.00	0.00
At the critical node	0.00	0.00	0.00	0.00	-0.01	0.00	0.00	0.00

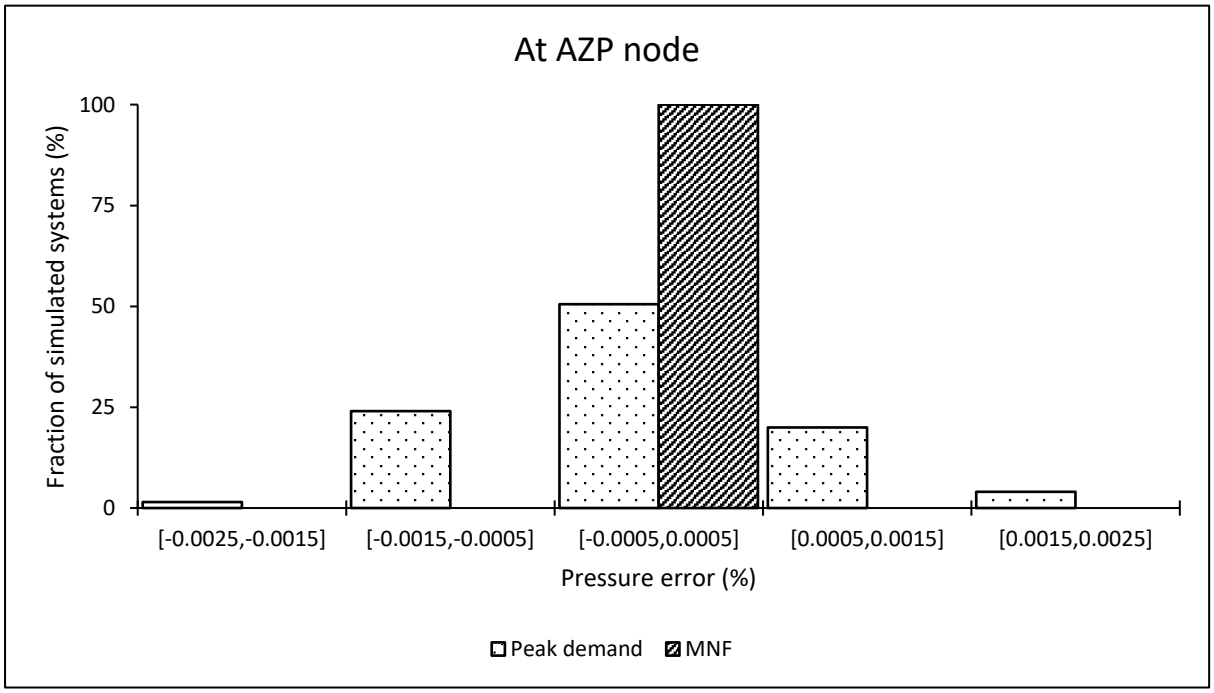

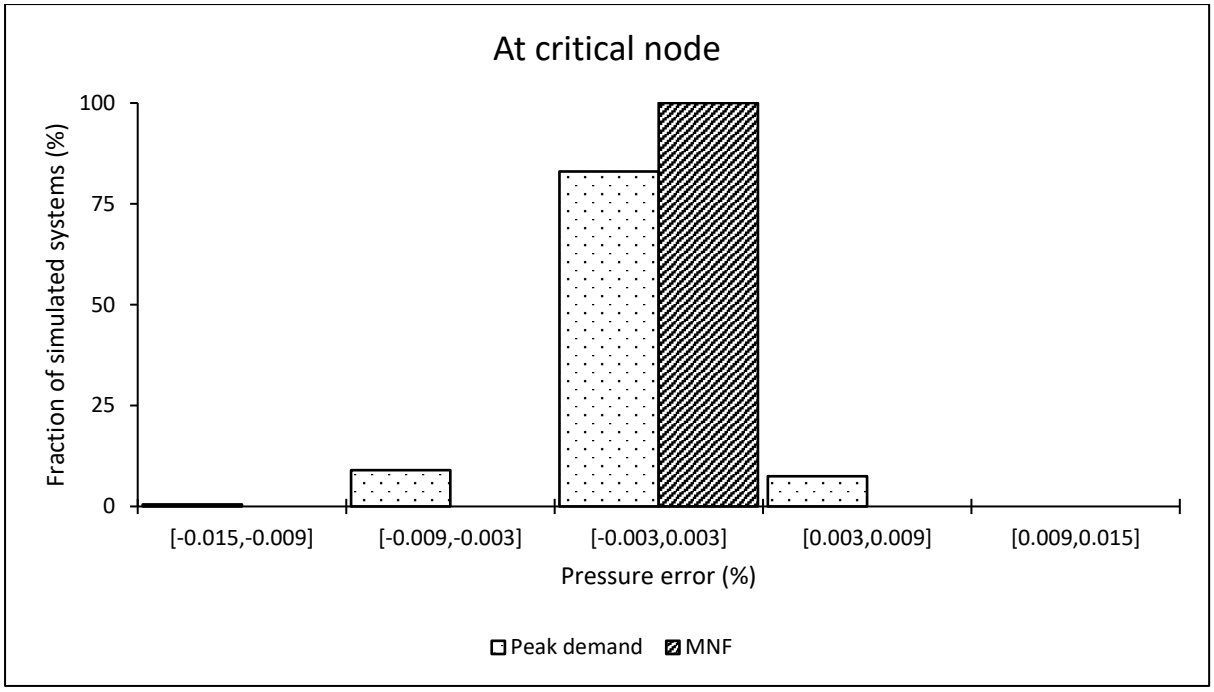
At critical node
Fraction of simulated systems (%)
100
75
50
25
0
[-0.015,-0.009]
[-0.009,-0.003]
[-0.003,0.003]
[0.003,0.009]
[0.009,0.015]
Pressure error (%)
Peak demand
MNF

System leakage estimation error when using the power equation

	Leakage estimation error (%)			
	Minimum	**Arithmetic Mean**	**Median**	**Maximum**
Before implementing pressure management	-0.29	0.00	0.01	0.26
After implementing pressure management	-11.92	-7.67	-7.61	-6.25

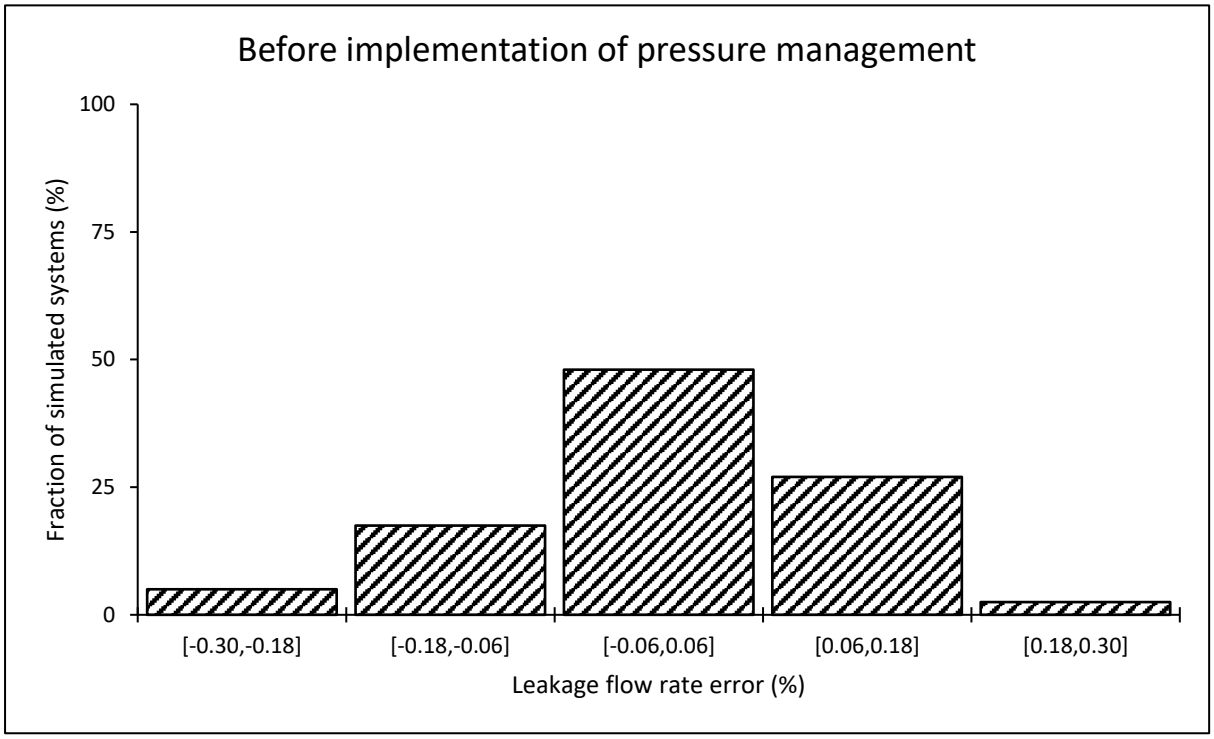

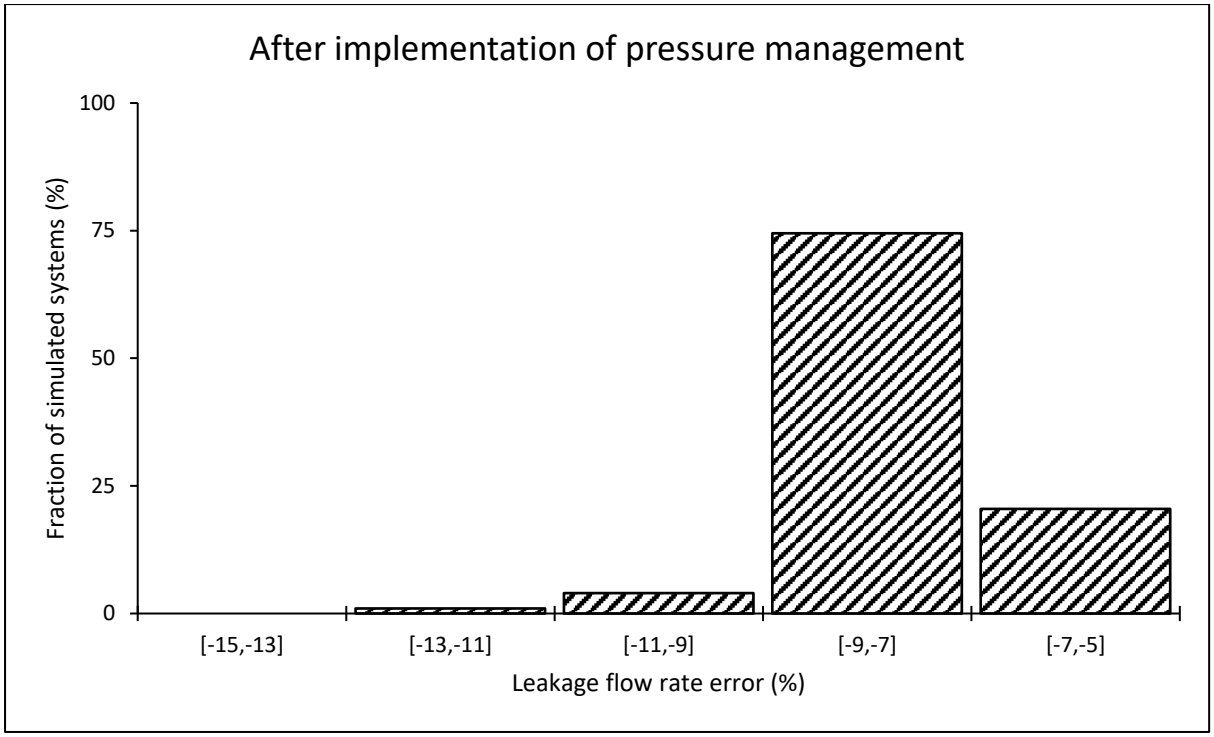
After implementation of pressure management
Fraction of simulated systems (%)
100
75
50
25
0
[-15,-13]
[-13,-11]
[-11,-9]
[-9,-7]
[-7,-5]
Leakage flow rate error (%)

Leakage estimation error when using the power equation at the critical node

	Leakage estimation error (%)			
	Minimum	**Arithmetic Mean**	**Median**	**Maximum**
Before implementing pressure management	-1.13	0.44	-0.34	5.96
After implementing pressure management	-21.66	4.88	-13.01	228.15

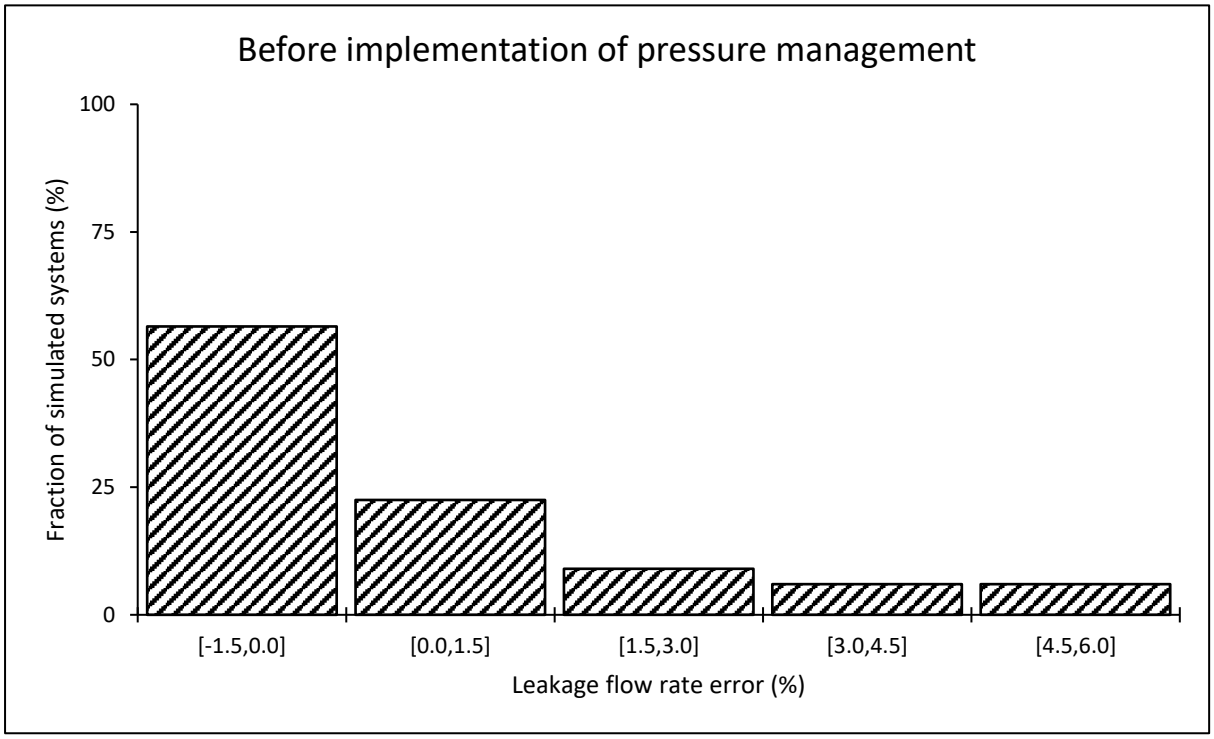

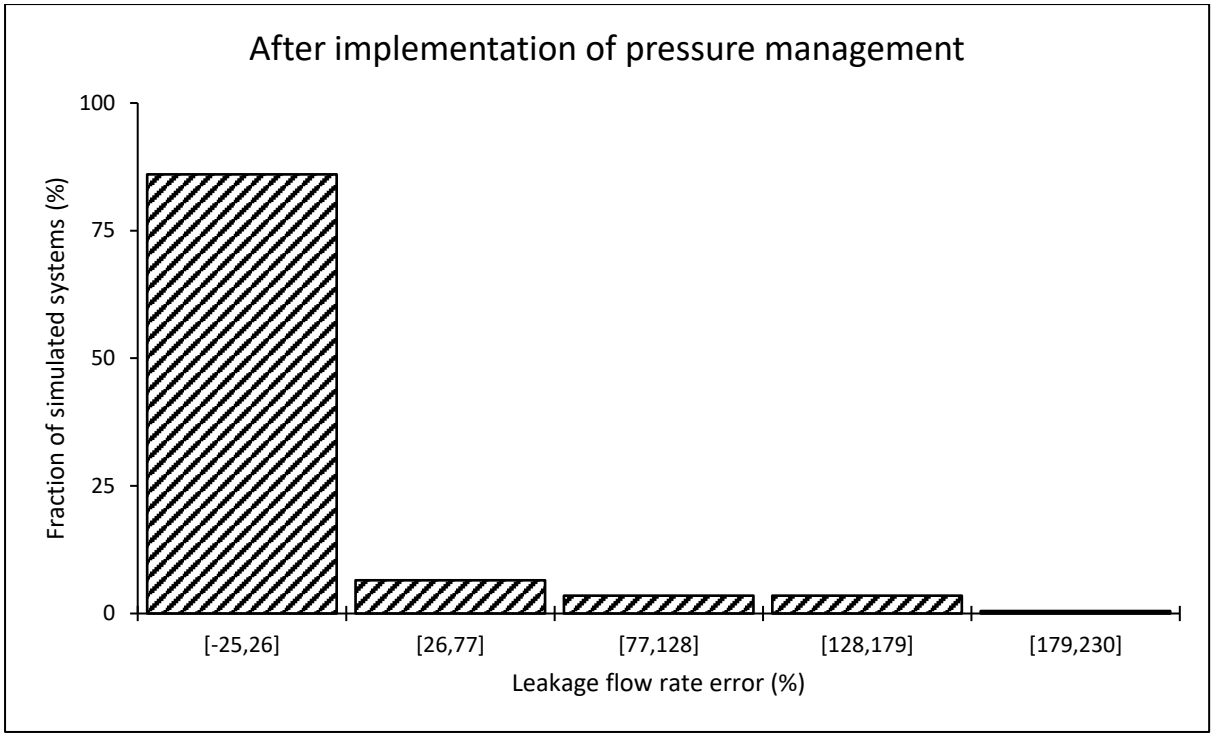
After implementation of pressure management
Fraction of simulated systems (%)
100
75
50
25
0
[-25,26]
[26,77]
[77,128]
[128,179]
[179,230]
Leakage flow rate error (%)

Appendix A-2: Small-sized network with an ILI of 4

Results for an individual system

Pressure head at the average zone pressure (AZP) node

		Pressure head (m)			
		Minimum	**Arithmetic Mean**	**Median**	**Maximum**
Before pressure management	Without leaks	77.08	82.16	82.27	86.48
	Modified orifice equation	76.52	81.78	81.87	86.45
	Power equation	76.52	81.78	81.87	86.45
After pressure management	Modified orifice equation	16.83	21.98	22.07	26.47
	Power equation	16.84	21.99	22.08	26.47

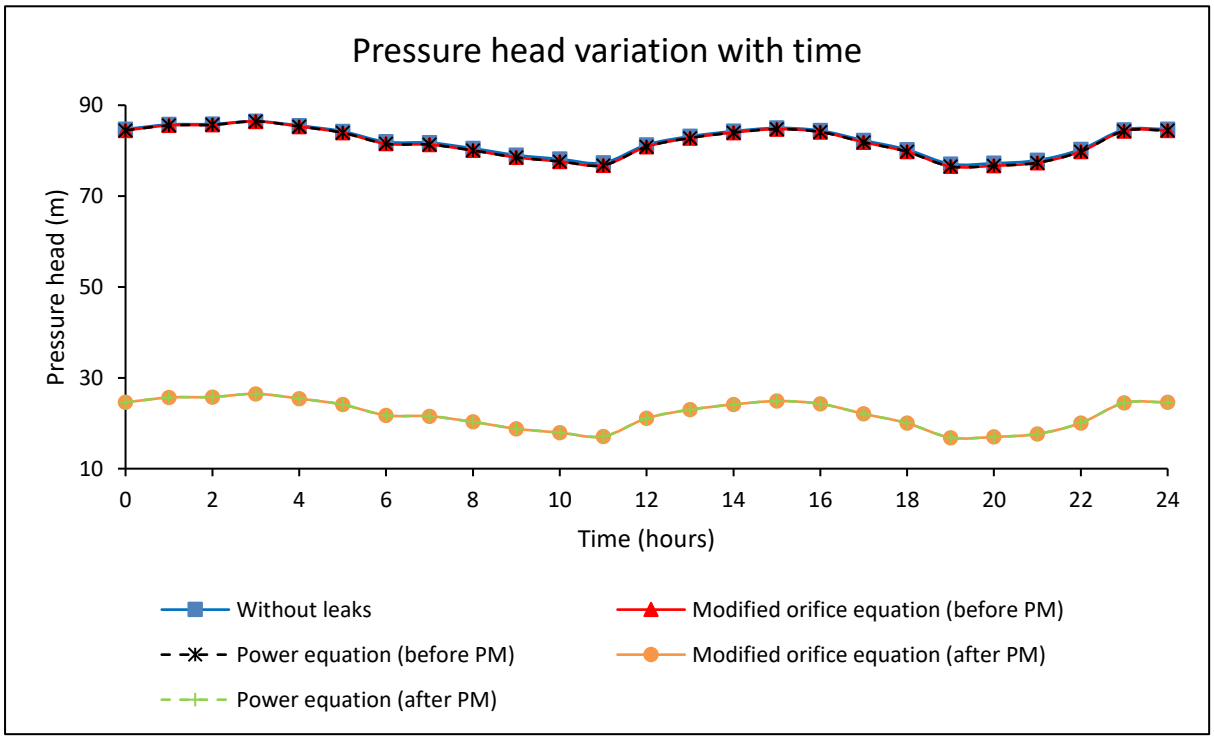

Pressure head at the critical node

		Pressure head (m)			
		Minimum	**Arithmetic Mean**	**Median**	**Maximum**
Before pressure management	Without leaks	70.86	77.65	77.80	83.43
	Modified orifice equation	70.16	77.18	77.30	83.40
	Power equation	70.16	77.18	77.30	83.40
After pressure management	Modified orifice equation	10.55	17.43	17.55	23.42
	Power equation	10.57	17.44	17.57	23.42

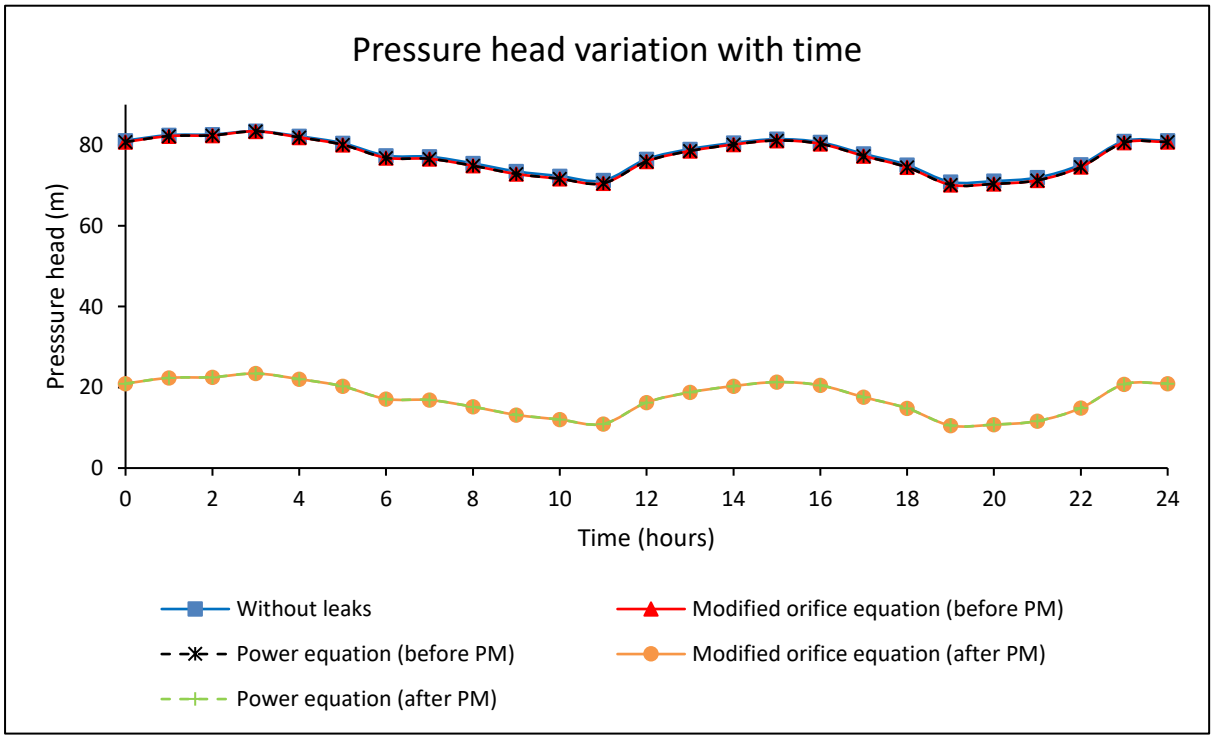

System leakage flow rate

		Leakage flow rate (m^3/h)			
		Minimum	**Arithmetic Mean**	**Median**	**Maximum**
Before pressure management	Modified orifice equation	14.12	14.57	14.58	14.97
	Power equation	14.11	14.57	14.58	14.97
After pressure management	Modified orifice equation	6.38	7.15	7.18	7.79
	Power equation	6.04	6.85	6.88	7.52

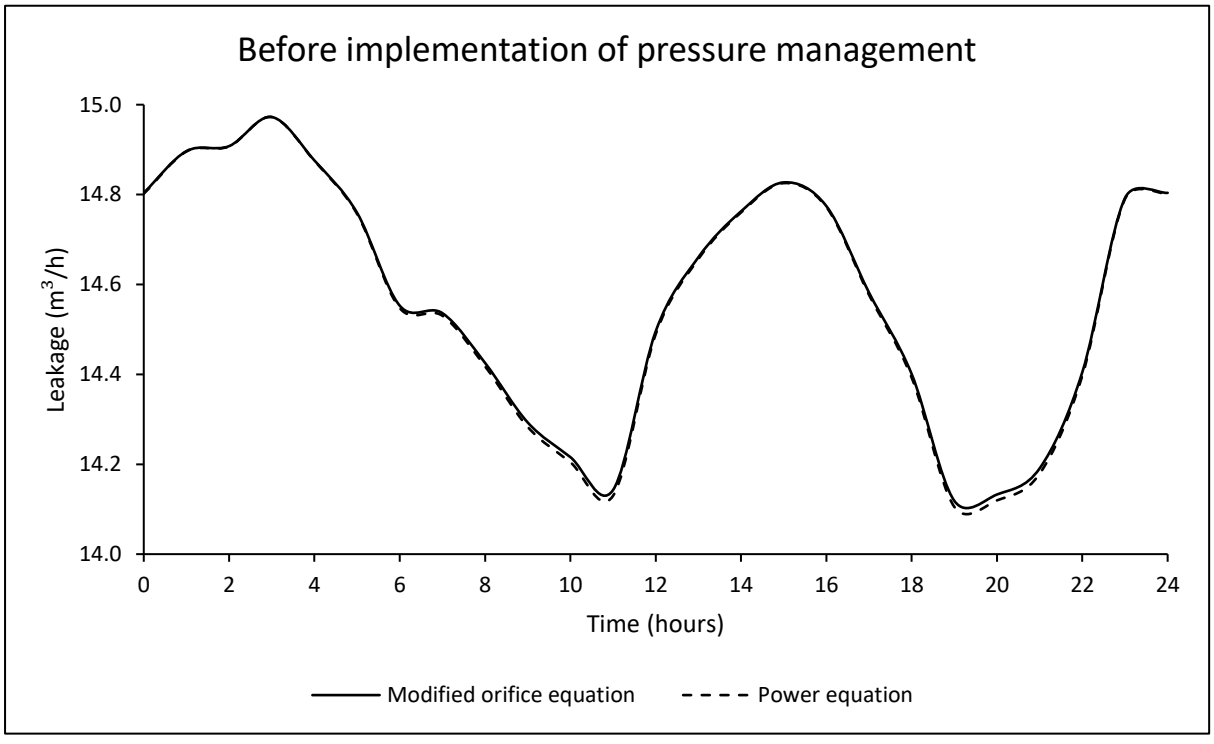

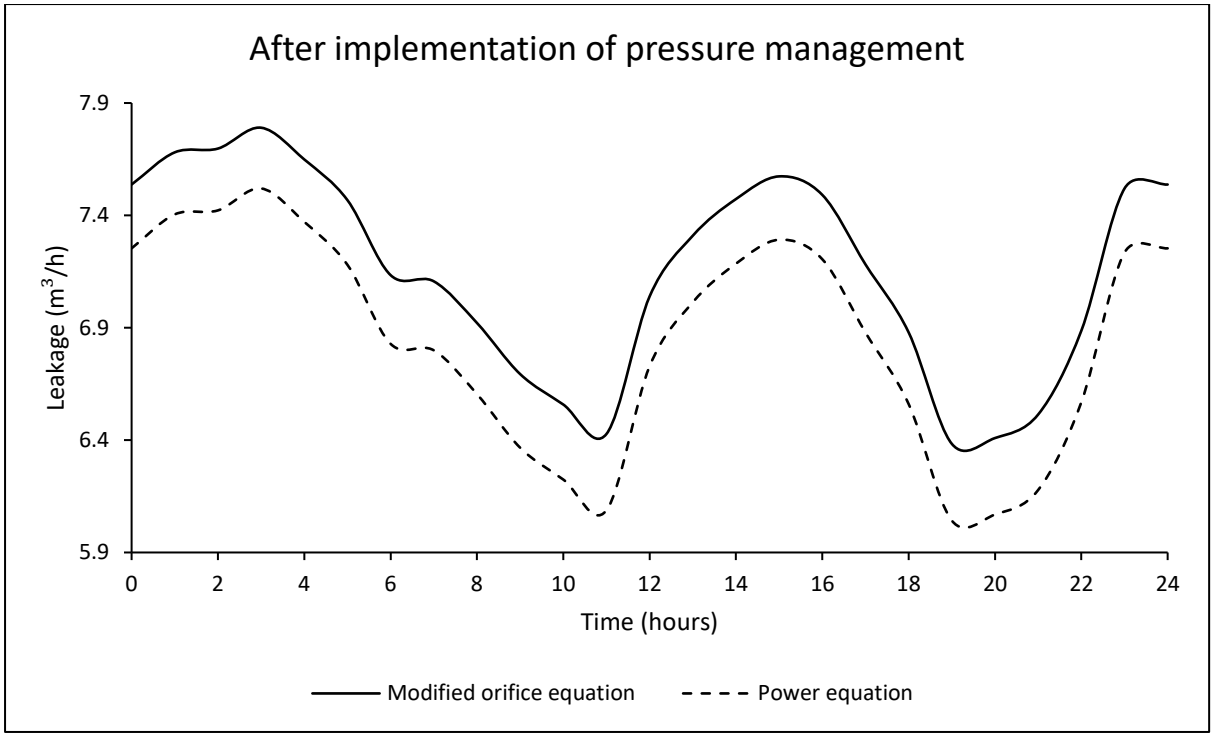
After implementation of pressure management
7.9
7.4
6.9
6.4
5.9
Leakage (m3/h)
0
2
4
6
8
10
12
14
16
18
20
22
24
Time (hours)
Modified orifice equation
Power equation

Leakage flow rate at the critical node

		Leakage flow rate (m^3/h)			
		Minimum	**Arithmetic Mean**	**Median**	**Maximum**
Before pressure management	Modified orifice equation	0.89	0.93	0.93	0.97
	Power equation	0.88	0.93	0.93	0.97
After pressure management	Modified orifice equation	0.34	0.43	0.44	0.51
	Power equation	0.30	0.39	0.40	0.47

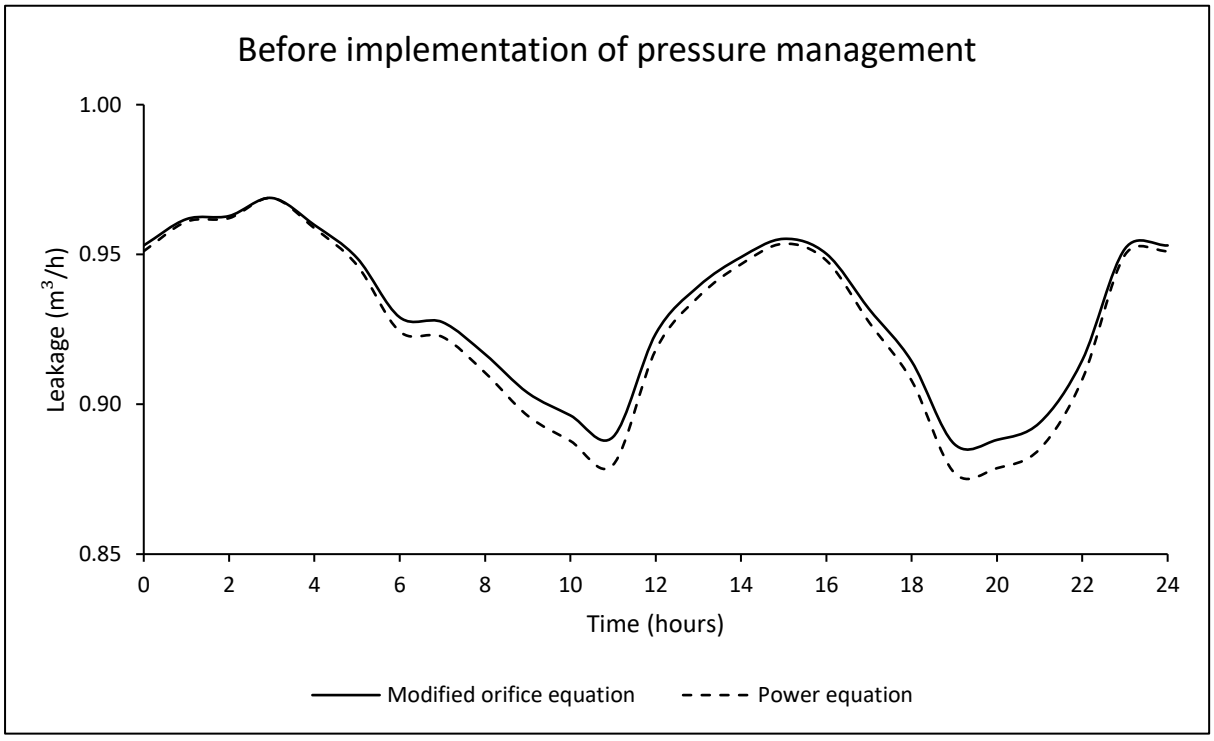

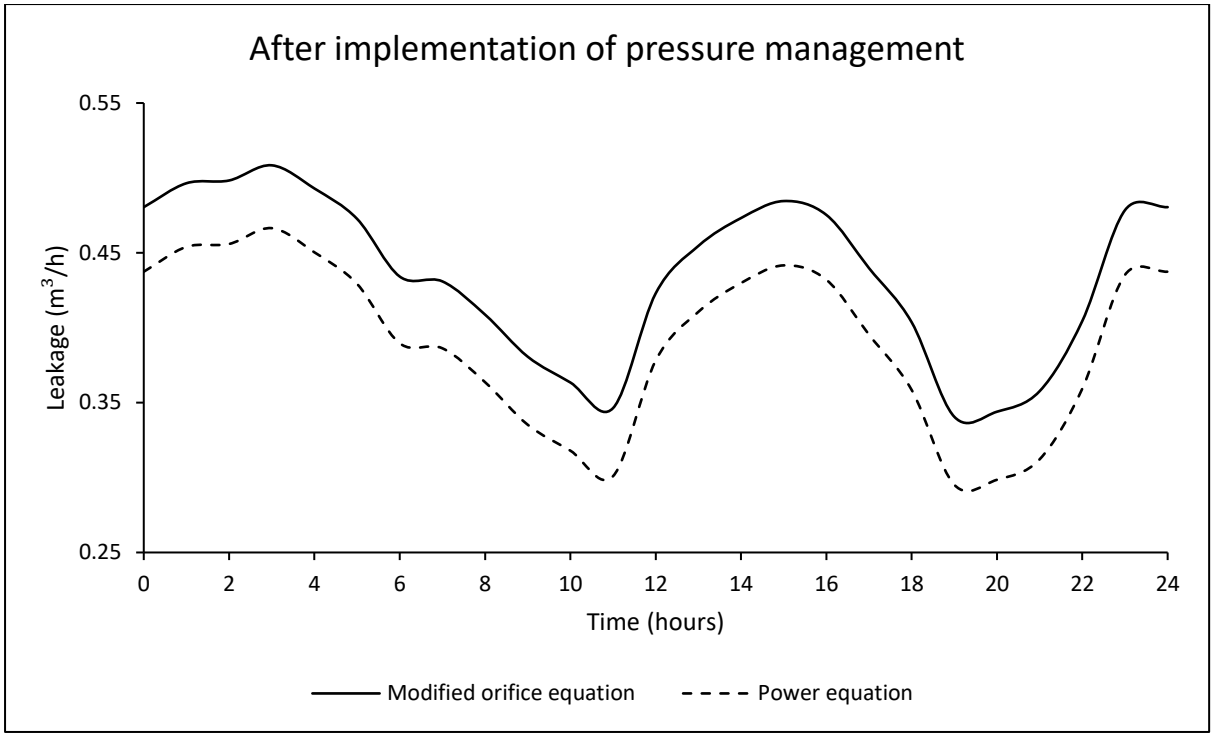
After implementation of pressure management
0.55
0.45
0.35
0.25
Leakage (m3/h)
0
2
4
6
8
10
12
14
16
18
20
22
24
Time (hours)
Modified orifice equation
Power equation

Number of iterations required for a system to converge to a hydraulic solution with both formulations

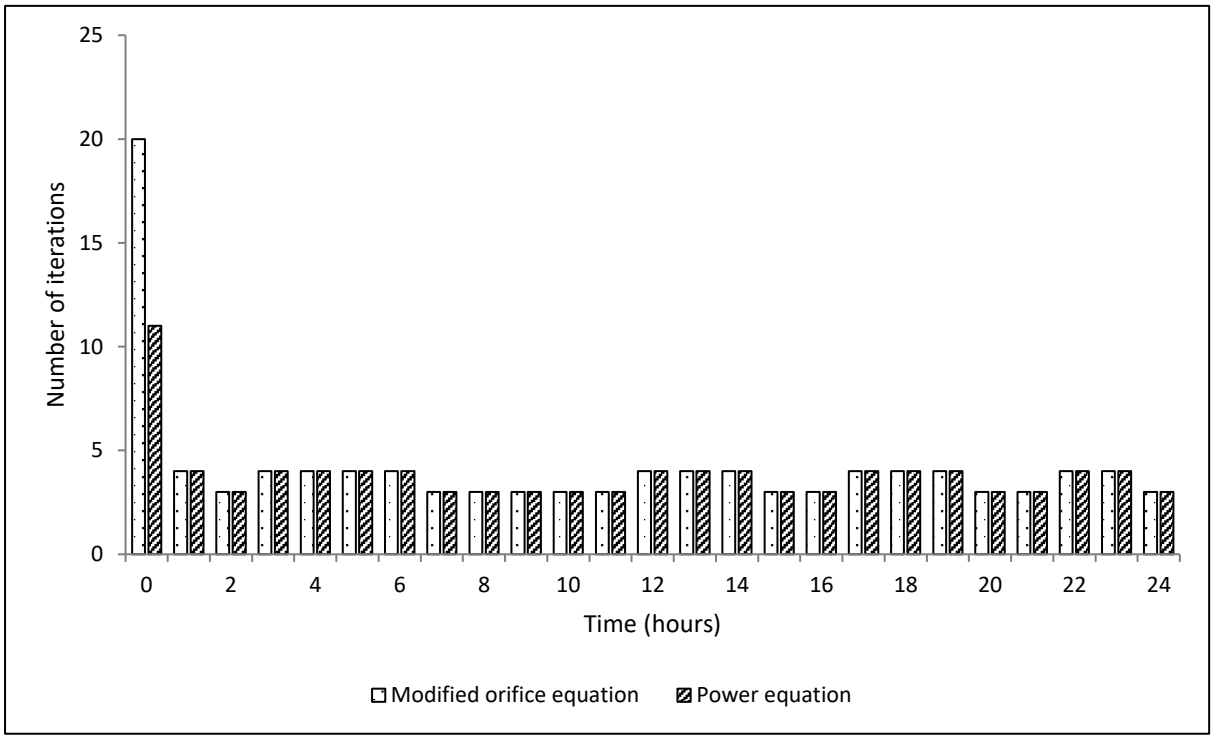

Results for combined systems

System parameters for both power and modified orifice formulations

	Minimum	Arithmetic Mean	Median	Maximum
Leakage exponent N1	0.54	0.62	0.58	0.96
Leakage coefficient C	5.6E-05	2.8E-04	3.1E-04	3.7E-04
Effective initial leak area C_dA0 (mm^2)	52.61	89.27	92.60	96.91
Effective head-area slope C_dm (mm^2/m)	0.05	0.14	0.10	0.55
Leakage number LN	0.05	0.14	0.09	0.87

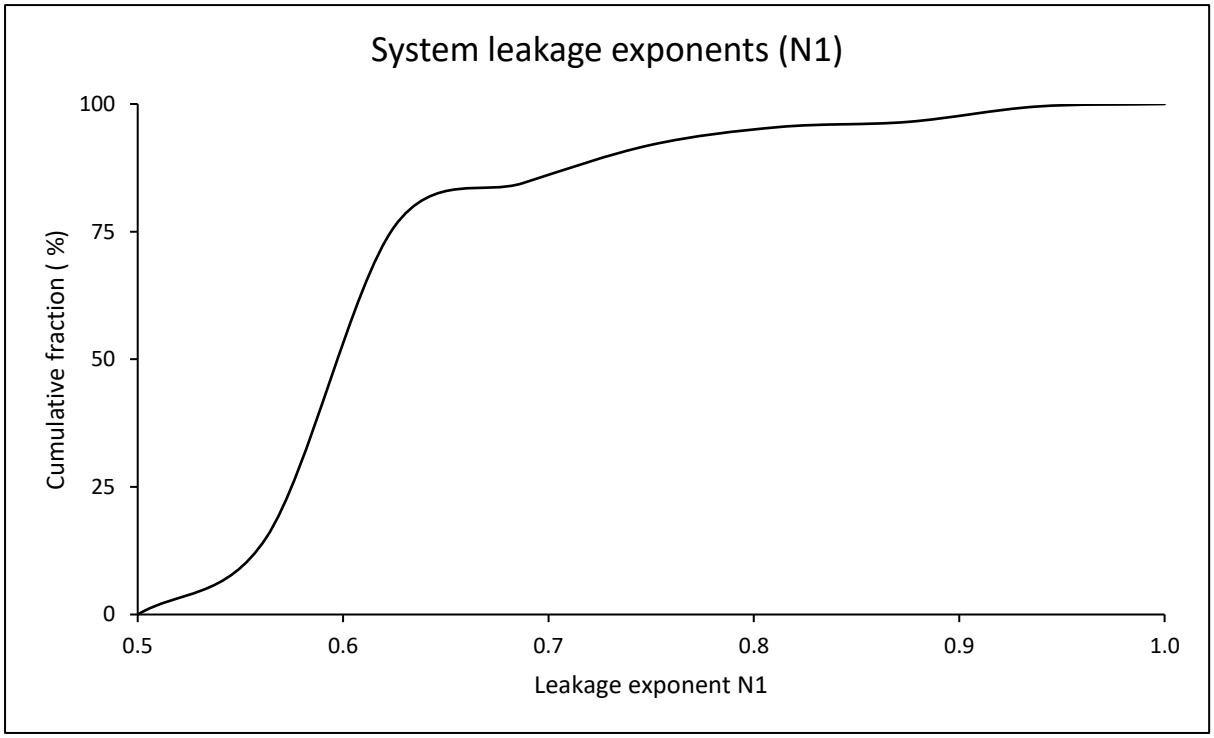

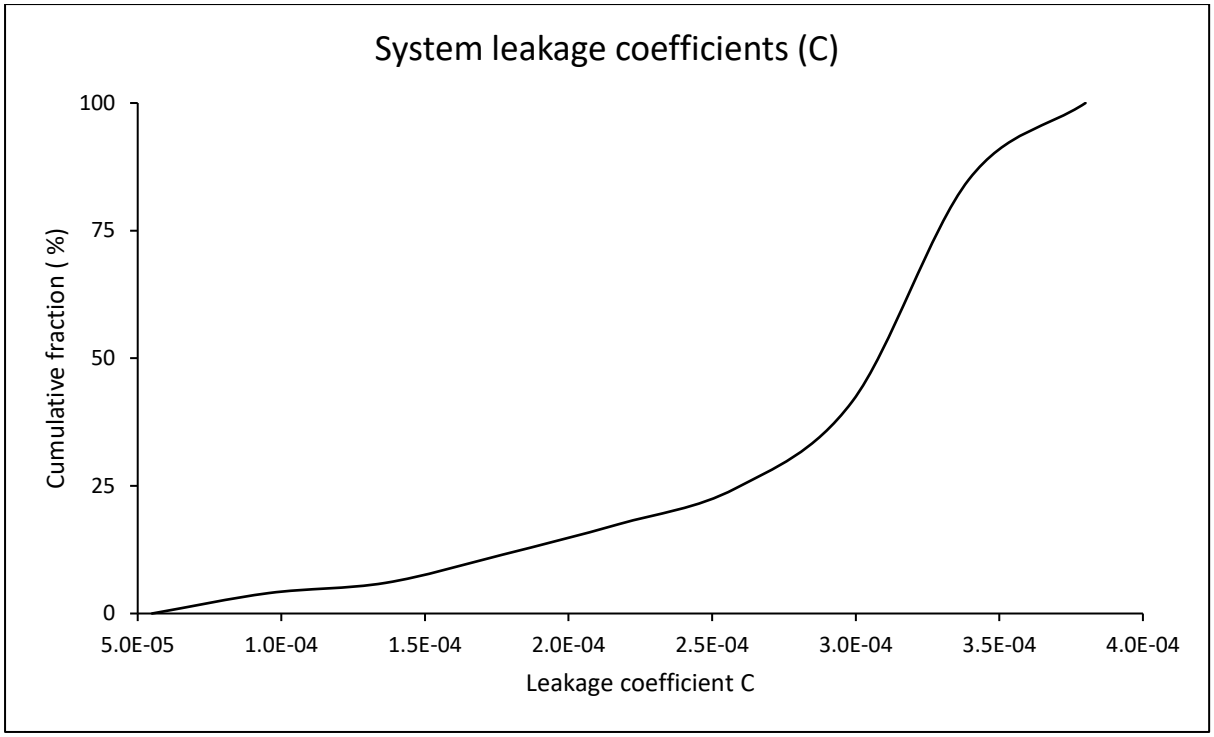
System leakage coefficients (C)
Cumulative fraction (%)
100
75
50
25
0
5.0E-05
1.0E-04
1.5E-04
2.0E-04
2.5E-04
3.0E-04
3.5E-04
4.0E-04
Leakage coefficient C

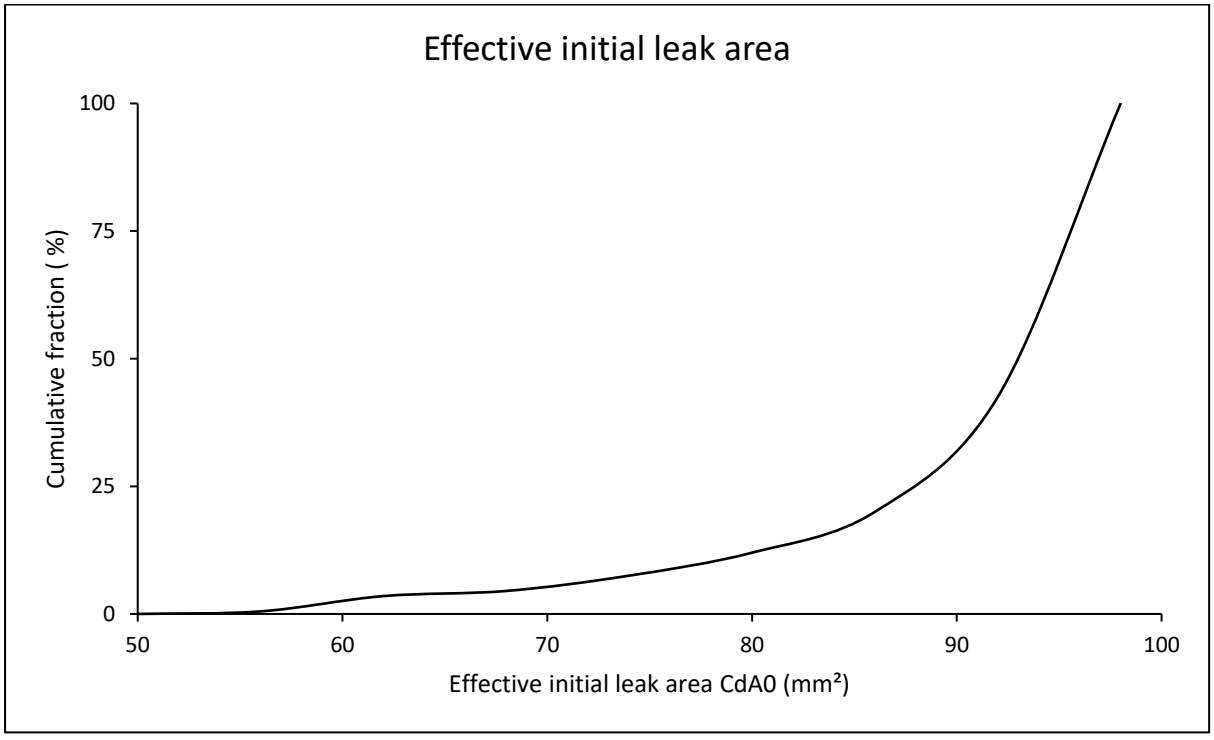
Effective initial leak area
Cumulative fraction (%)
100
75
50
25
0
50
60
70
80
90
100
Effective initial leak area CdA0 (mm²)

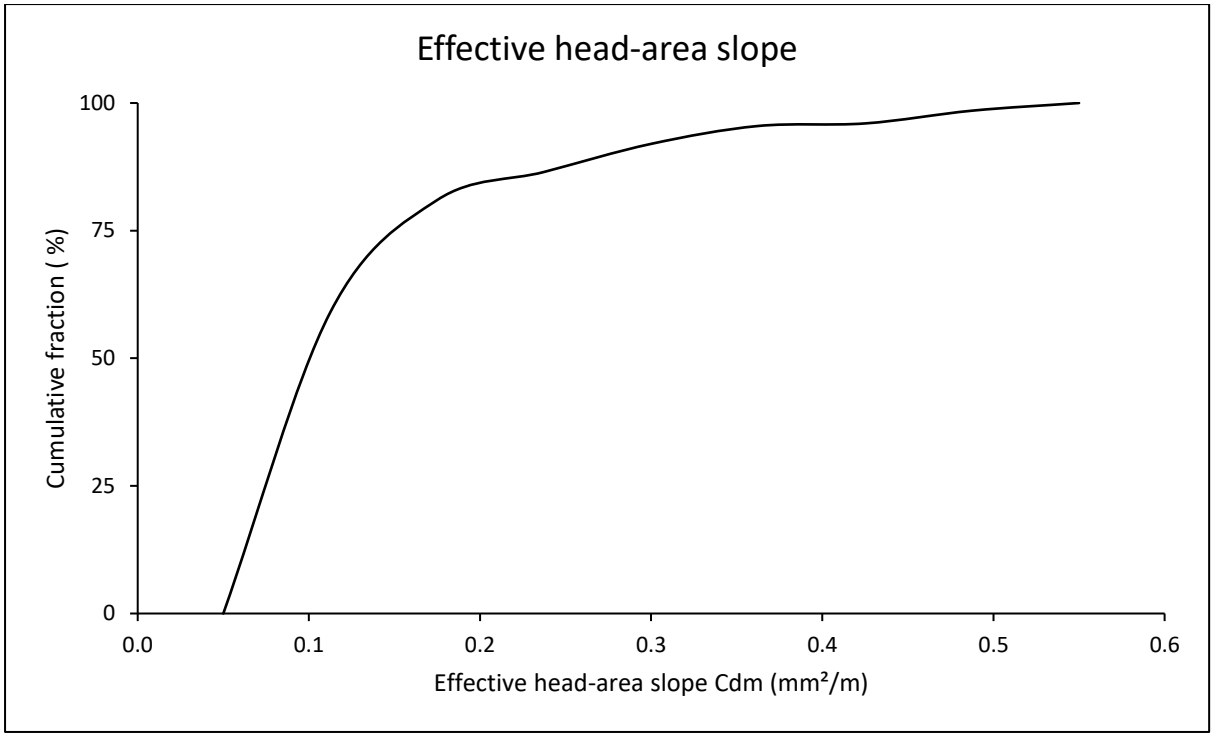
Effective head-area slope
Cumulative fraction (%)
100
75
50
25
0
0.0
0.1
0.2
0.3
0.4
0.5
0.6
Effective head-area slope Cdm (mm²/m)

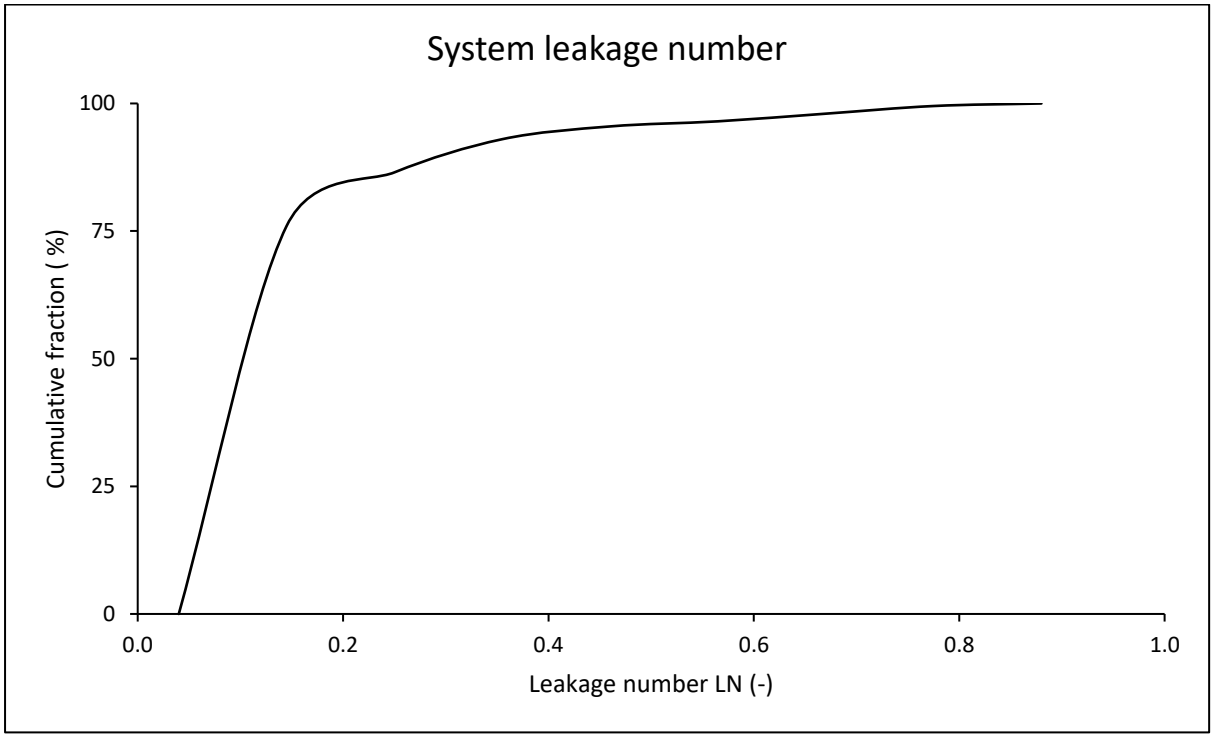
System leakage number
Cumulative fraction (%)
100
75
50
25
0
0.0
0.2
0.4
0.6
0.8
1.0
Leakage number LN (-)

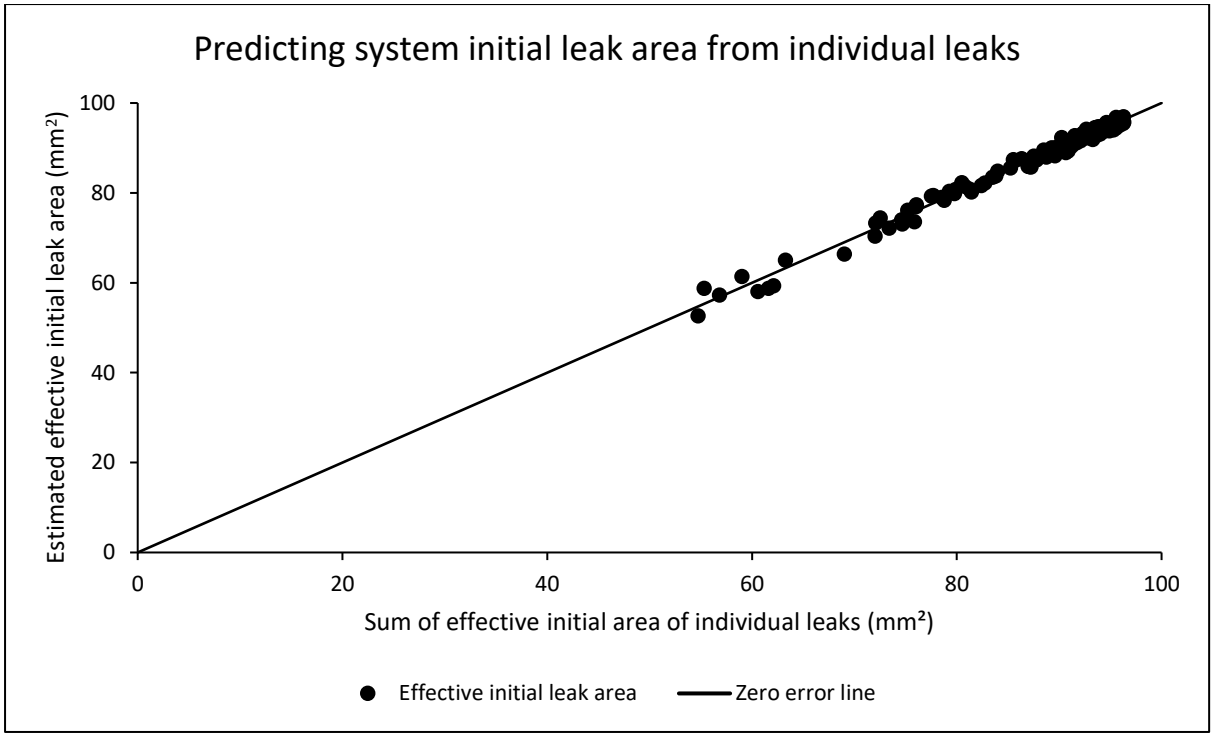
Predicting system initial leak area from individual leaks
Estimated effective initial leak area (mm²)
100
80
60
40
20
0
0
20
40
60
80
100
Sum of effective initial area of individual leaks (mm²)
Effective initial leak area
Zero error line

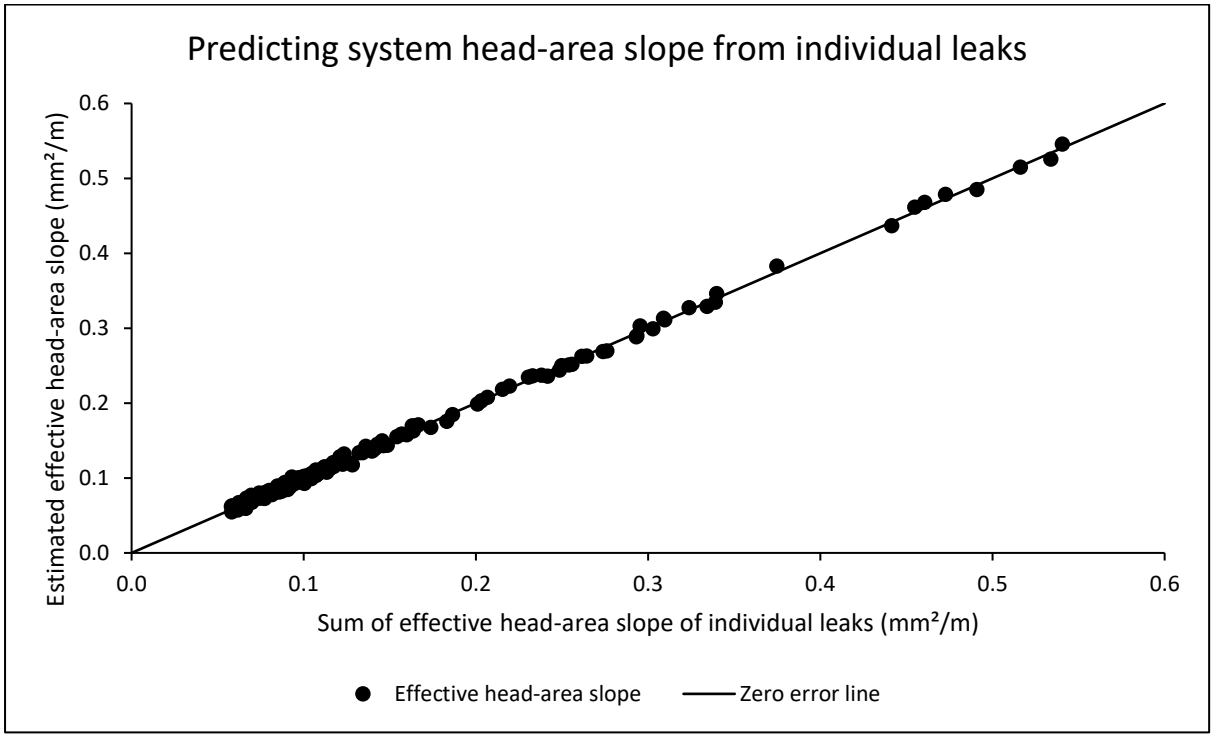
Predicting system head-area slope from individual leaks
Estimated effective head-area slope (mm²/m)
0.6
0.5
0.4
0.3
0.2
0.1
0.0
0.0
0.1
0.2
0.3
0.4
0.5
0.6
Sum of effective head-area slope of individual leaks (mm²/m)
Effective head-area slope
Zero error line

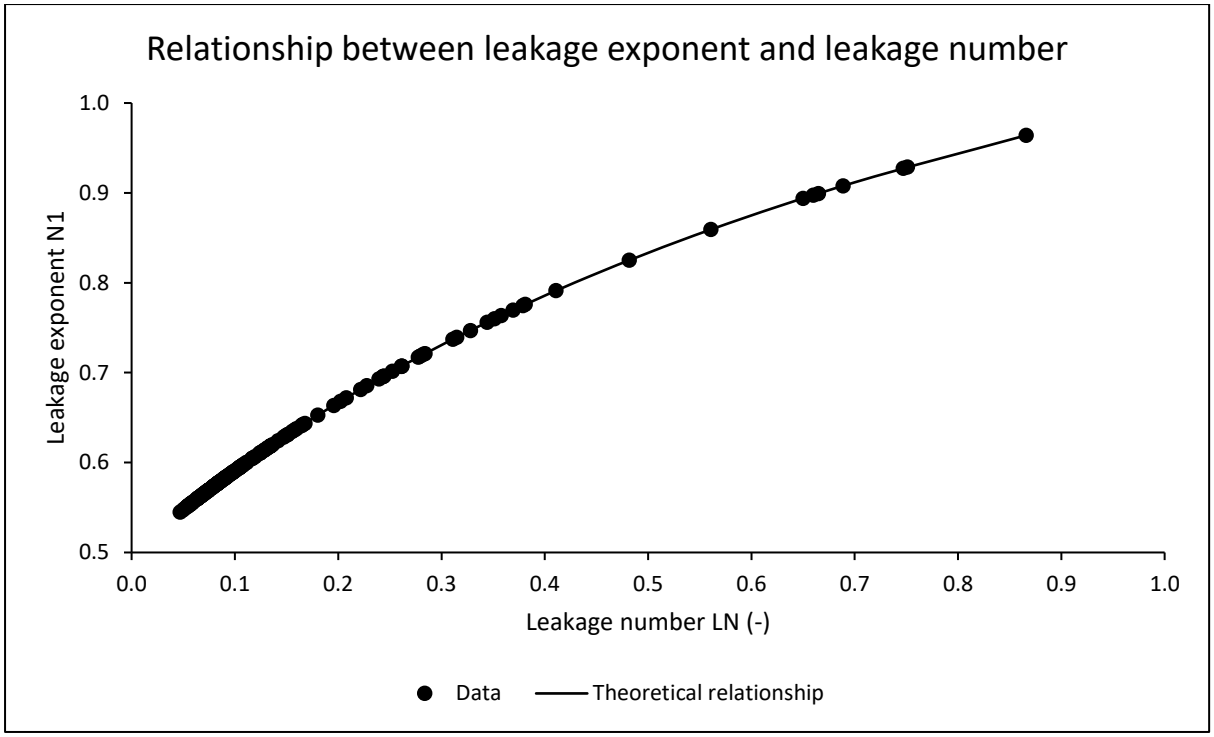
Relationship between leakage exponent and leakage number
Leakage exponent N1
1.0
0.9
0.8
0.7
0.6
0.5
0.0
0.1
0.2
0.3
0.4
0.5
0.6
0.7
0.8
0.9
1.0
Leakage number LN (-)
Data
Theoretical relationship

Average iterations required for a system to converge using both formulations

	Minimum	Arithmetic Mean	Median	Maximum
Modified orifice equation	4.08	4.19	4.16	4.44
Power equation	3.24	3.84	3.84	4.04

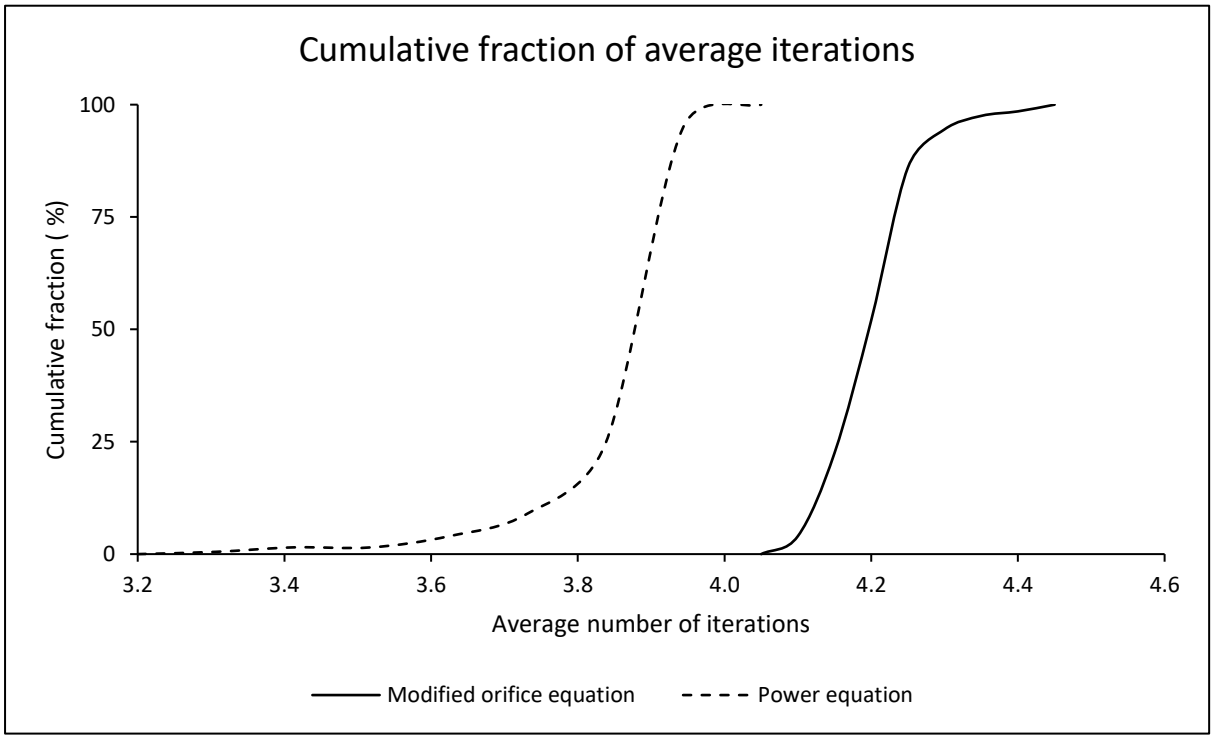

Effect of leakage on pressure at both average zone pressure (AZP) and critical nodes

AZP node								
	During MNF conditions				During peak demand conditions			
	Min (m)	Mean (m)	Median (m)	Max (m)	Min (m)	Mean (m)	Median (m)	Max (m)
Modified orifice equation	-0.05	-0.03	-0.03	-0.02	-0.71	-0.61	-0.61	-0.39
Power equation	-0.05	-0.03	-0.03	-0.02	-0.71	-0.61	-0.61	-0.39
Critical node								
Modified orifice equation	-0.11	-0.04	-0.04	-0.02	-1.29	-0.79	-0.79	-0.43
Power equation	-0.11	-0.04	-0.04	-0.02	-1.28	-0.79	-0.79	-0.44

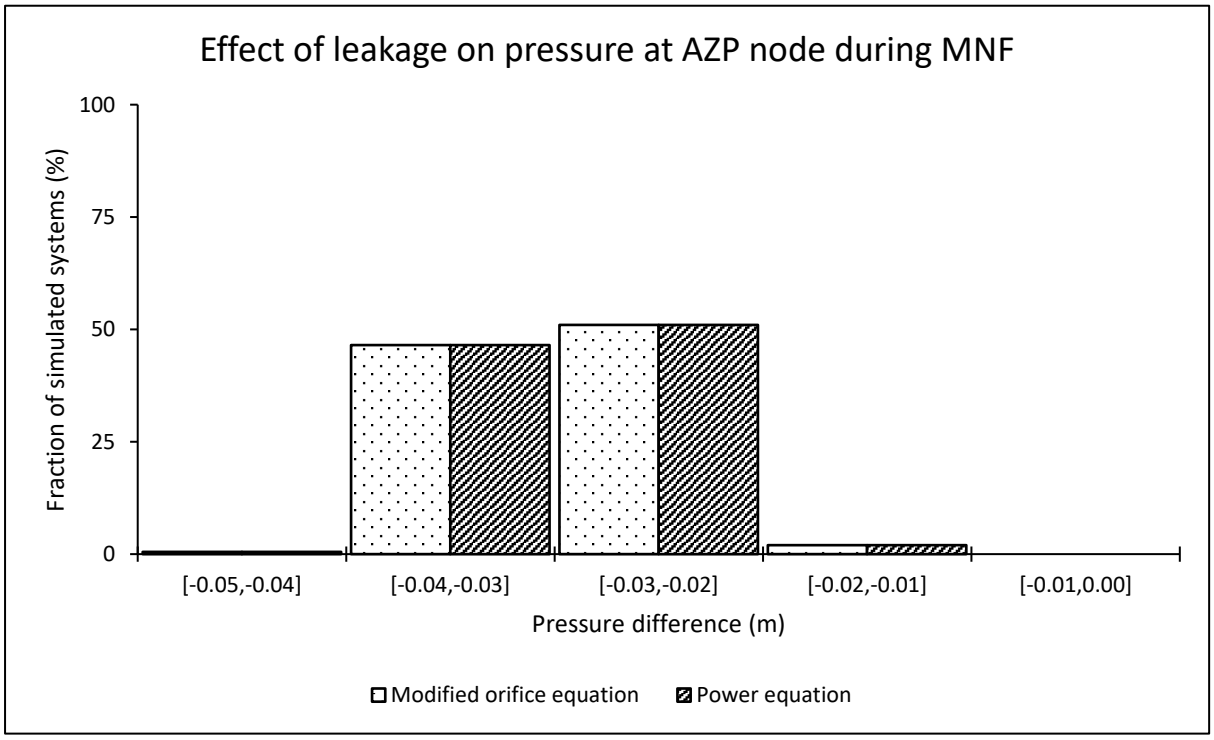

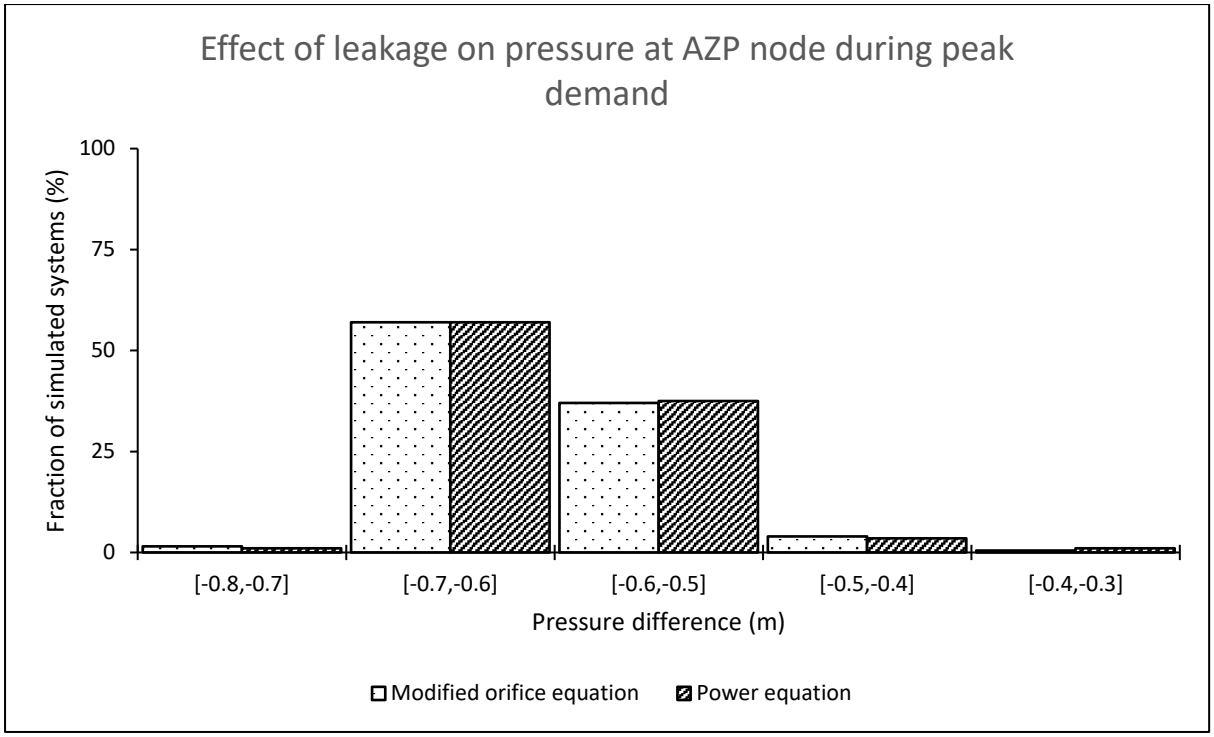
Effect of leakage on pressure at AZP node during peak demand
Fraction of simulated systems (%)
100
75
50
25
0
[-0.8,-0.7]
[-0.7,-0.6]
[-0.6,-0.5]
[-0.5,-0.4]
[-0.4,-0.3]
Pressure difference (m)
Modified orifice equation
Power equation

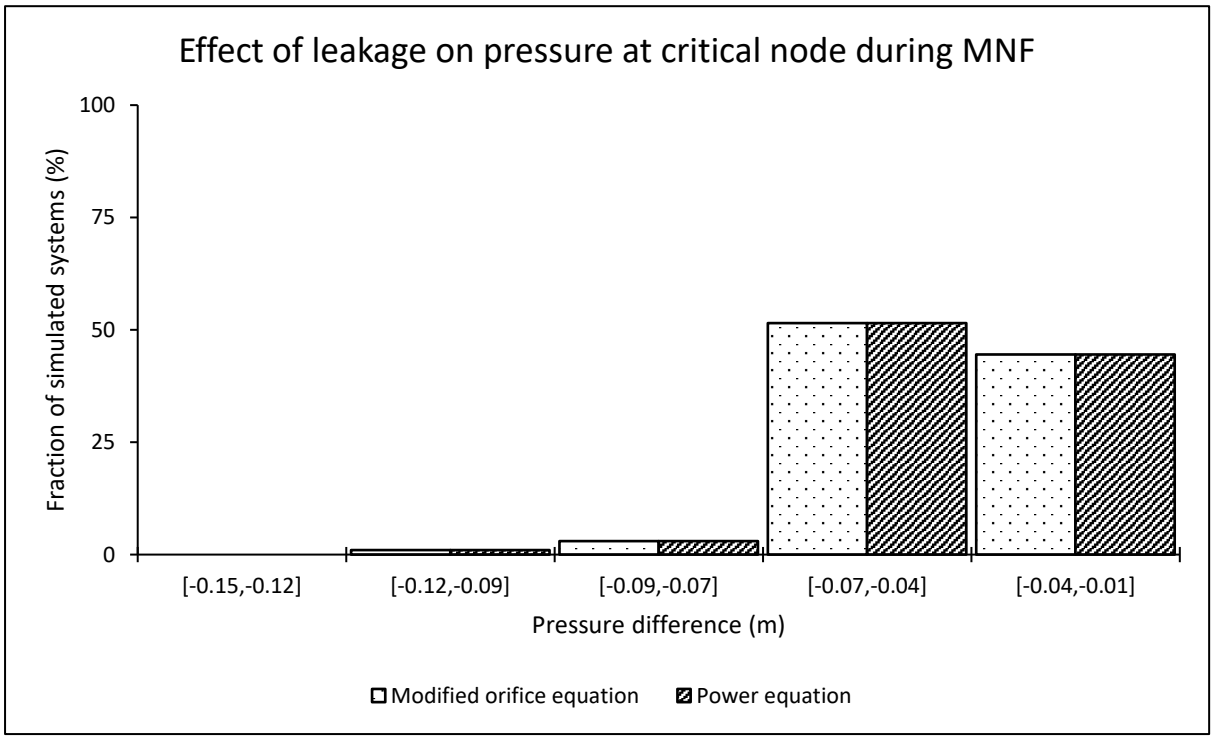
Effect of leakage on pressure at critical node during MNF
Fraction of simulated systems (%)
100
75
50
25
0
[-0.15,-0.12]
[-0.12,-0.09]
[-0.09,-0.07]
[-0.07,-0.04]
[-0.04,-0.01]
Pressure difference (m)
Modified orifice equation
Power equation

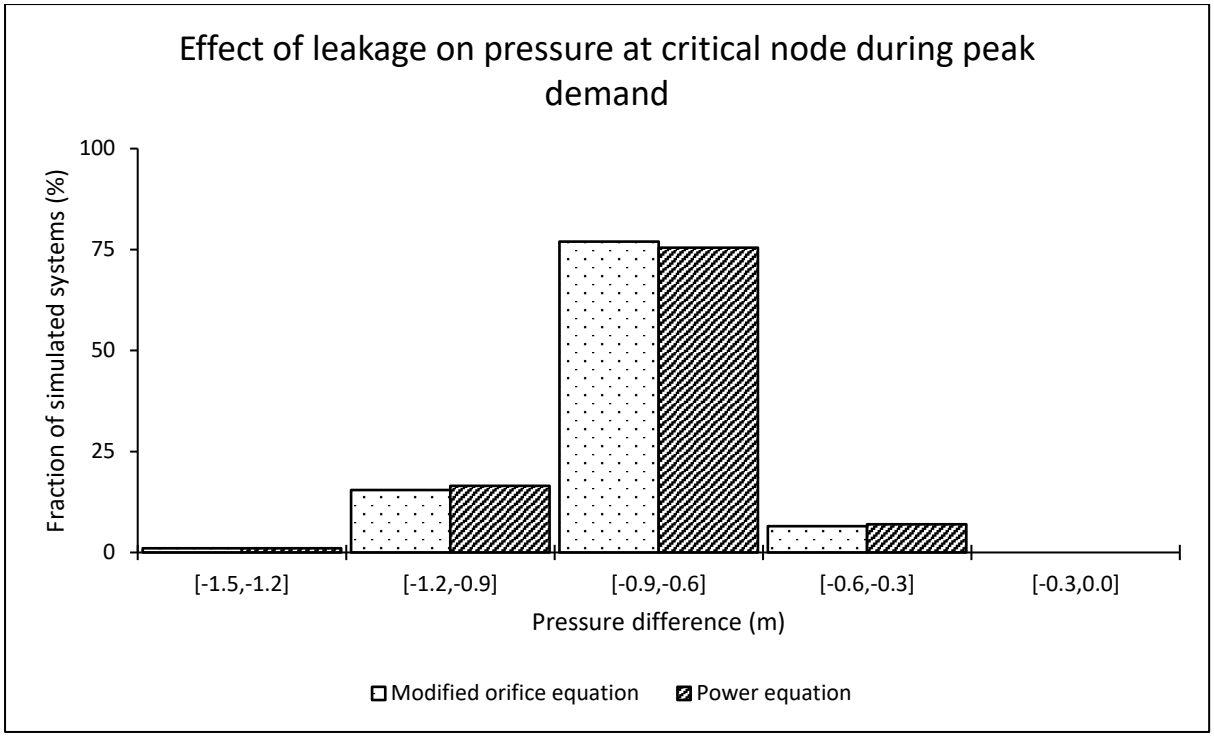
Effect of leakage on pressure at critical node during peak demand
Fraction of simulated systems (%)
100
75
50
25
0
[-1.5,-1.2]
[-1.2,-0.9]
[-0.9,-0.6]
[-0.6,-0.3]
[-0.3,0.0]
Pressure difference (m)
Modified orifice equation
Power equation

Pressure estimation error when using the power equation at average zone pressure (AZP) and critical nodes

	During MNF conditions				During peak demand conditions			
	Min (%)	**Mean (%)**	**Median (%)**	**Max (%)**	**Min (%)**	**Mean (%)**	**Median (%)**	**Max (%)**
At the AZP node	0.00	0.00	0.00	0.00	0.00	0.00	0.00	0.01
At the critical node	0.00	0.00	0.00	0.00	-0.01	0.00	0.00	0.02

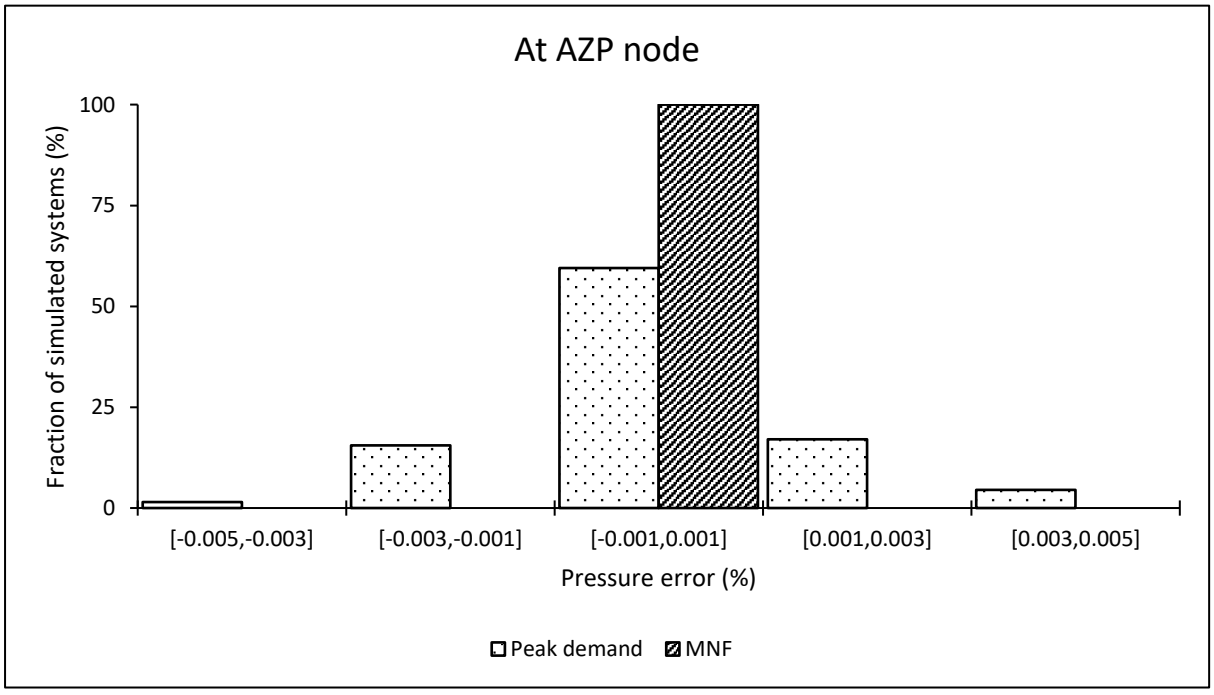

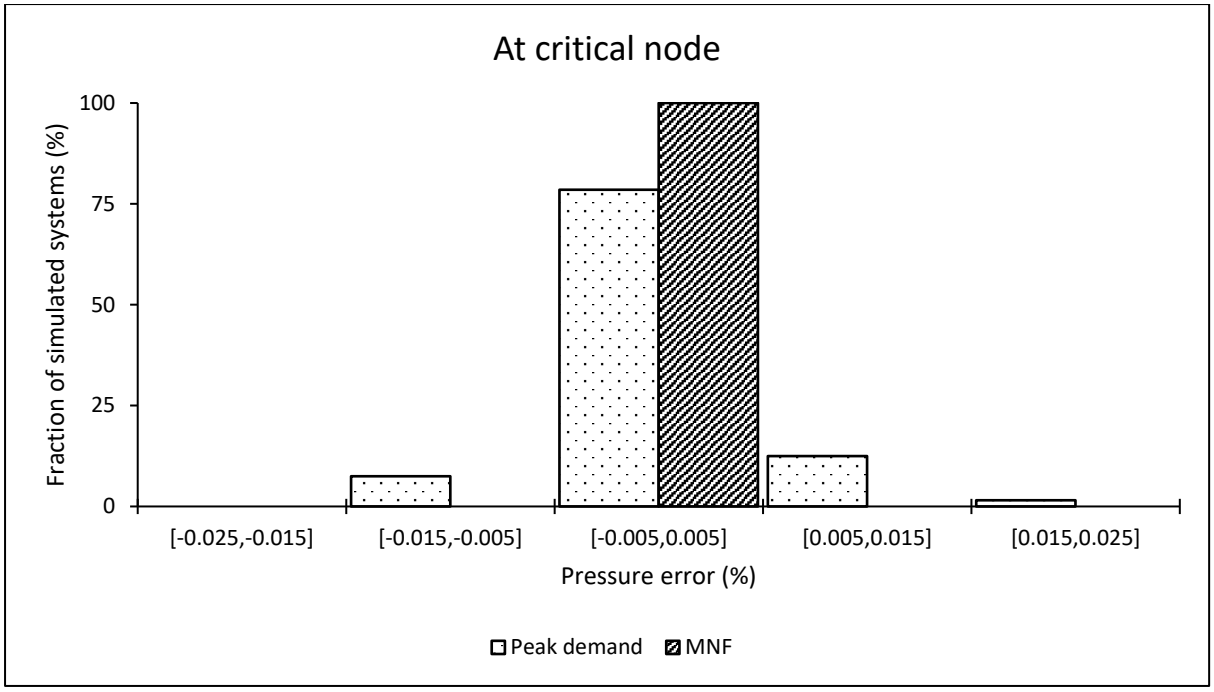
At critical node
Fraction of simulated systems (%)
100
75
50
25
0
[-0.025,-0.015]
[-0.015,-0.005]
[-0.005,0.005]
[0.005,0.015]
[0.015,0.025]
Pressure error (%)
Peak demand
MNF

System leakage estimation error when using the power equation

	Leakage estimation error (%)			
	Minimum	**Arithmetic Mean**	**Median**	**Maximum**
Before implementing pressure management	-0.32	-0.01	0.00	0.17
After implementing pressure management	-19.60	-6.00	-4.70	-2.25

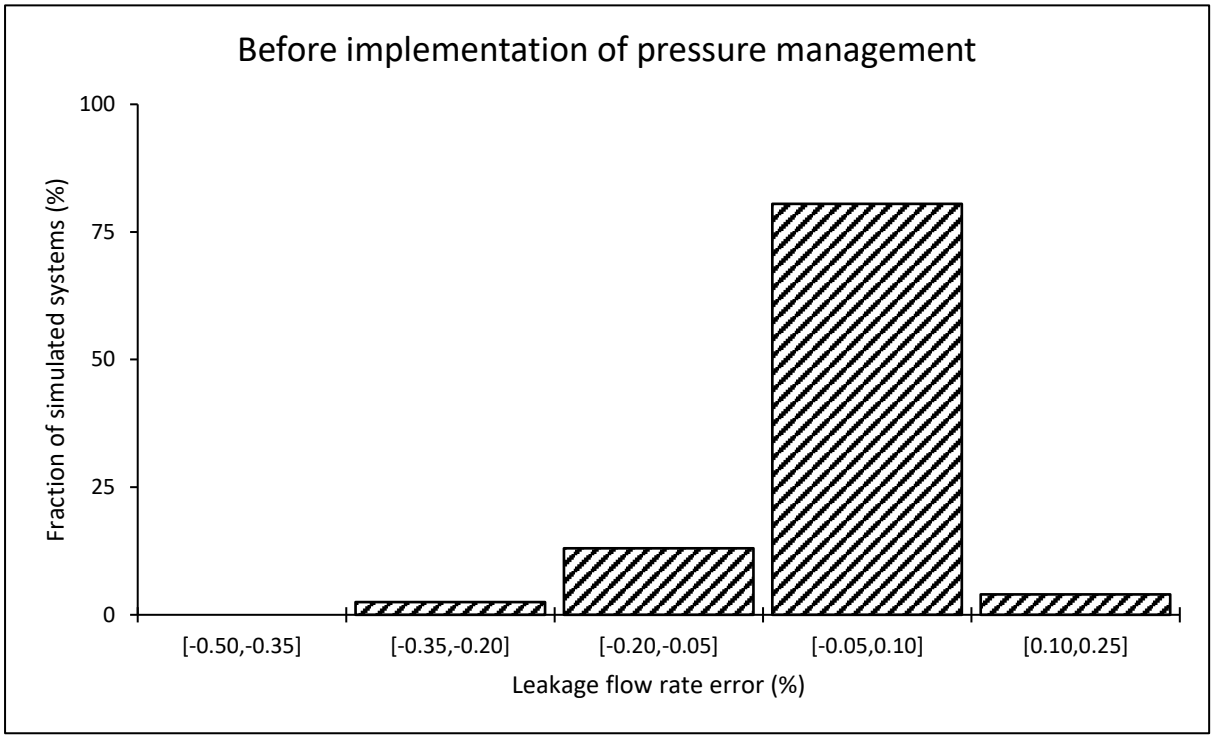

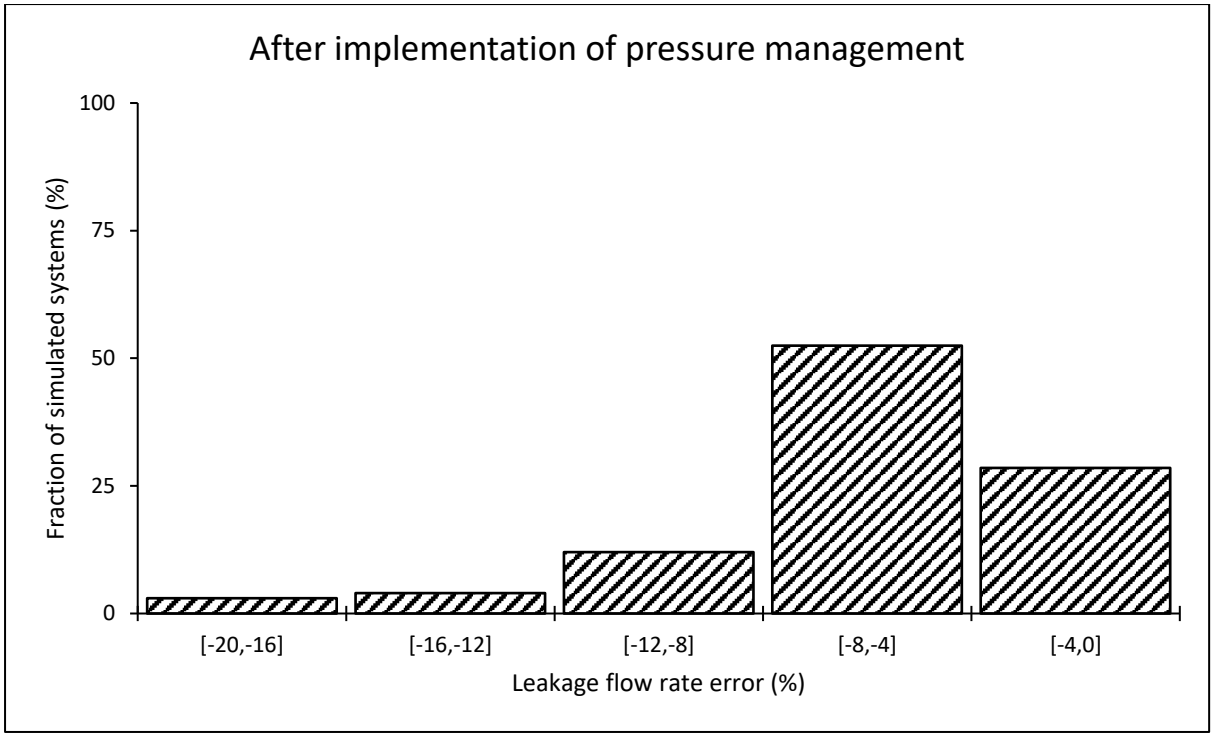
After implementation of pressure management
Fraction of simulated systems (%)
100
75
50
25
0
[-20,-16]
[-16,-12]
[-12,-8]
[-8,-4]
[-4,0]
Leakage flow rate error (%)

Leakage estimation error when using the power equation at the critical node

	Leakage estimation error (%)			
	Minimum	**Arithmetic Mean**	**Median**	**Maximum**
Before implementing pressure management	-2.99	-0.13	-0.23	6.38
After implementing pressure management	-48.65	-6.64	-8.54	196.78

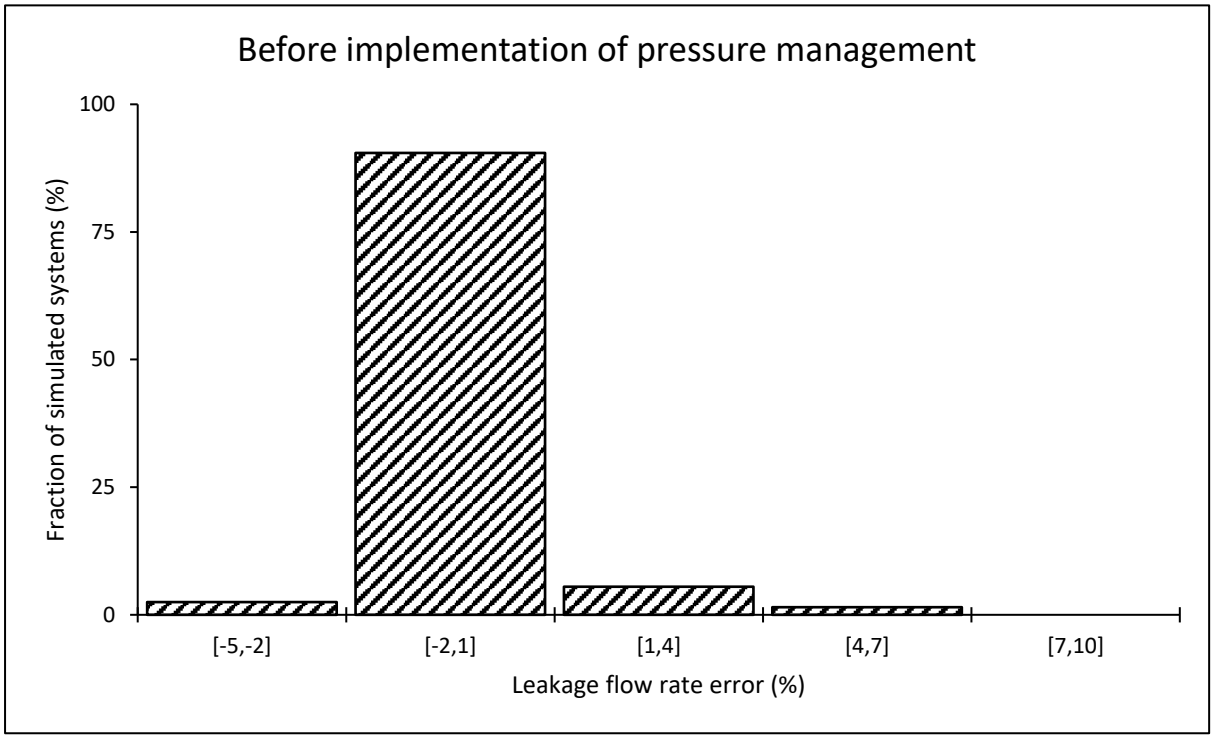

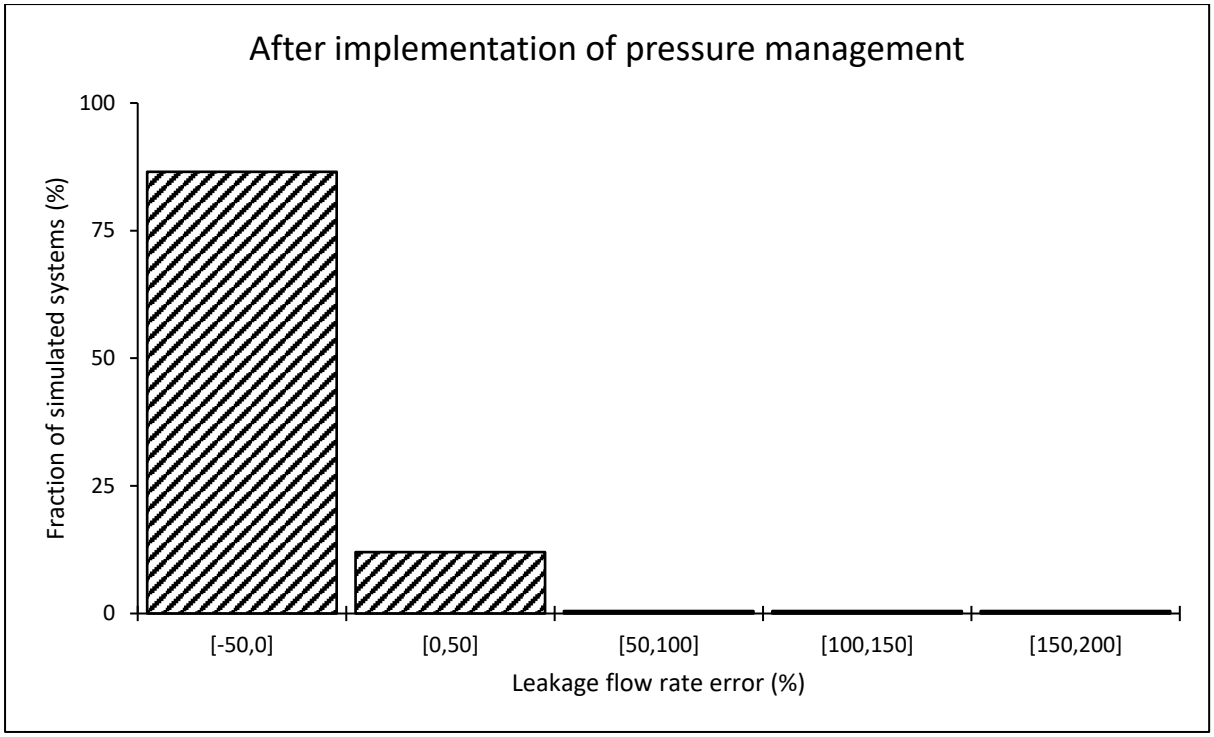
After implementation of pressure management
Fraction of simulated systems (%)
100
75
50
25
0
[-50,0]
[0,50]
[50,100]
[100,150]
[150,200]
Leakage flow rate error (%)

Appendix A-3: Small-sized network with an ILI of 16

Results for an individual system

Pressure head at the average zone pressure (AZP) node

		Pressure head (m)			
		Minimum	**Arithmetic Mean**	**Median**	**Maximum**
Before pressure management	Without leaks	77.08	82.16	82.27	86.48
	Modified orifice equation	74.97	80.68	80.68	86.22
	Power equation	74.98	80.68	80.68	86.22
After pressure management	Modified orifice equation	16.47	21.70	21.76	26.43
	Power equation	16.64	21.80	21.87	26.44

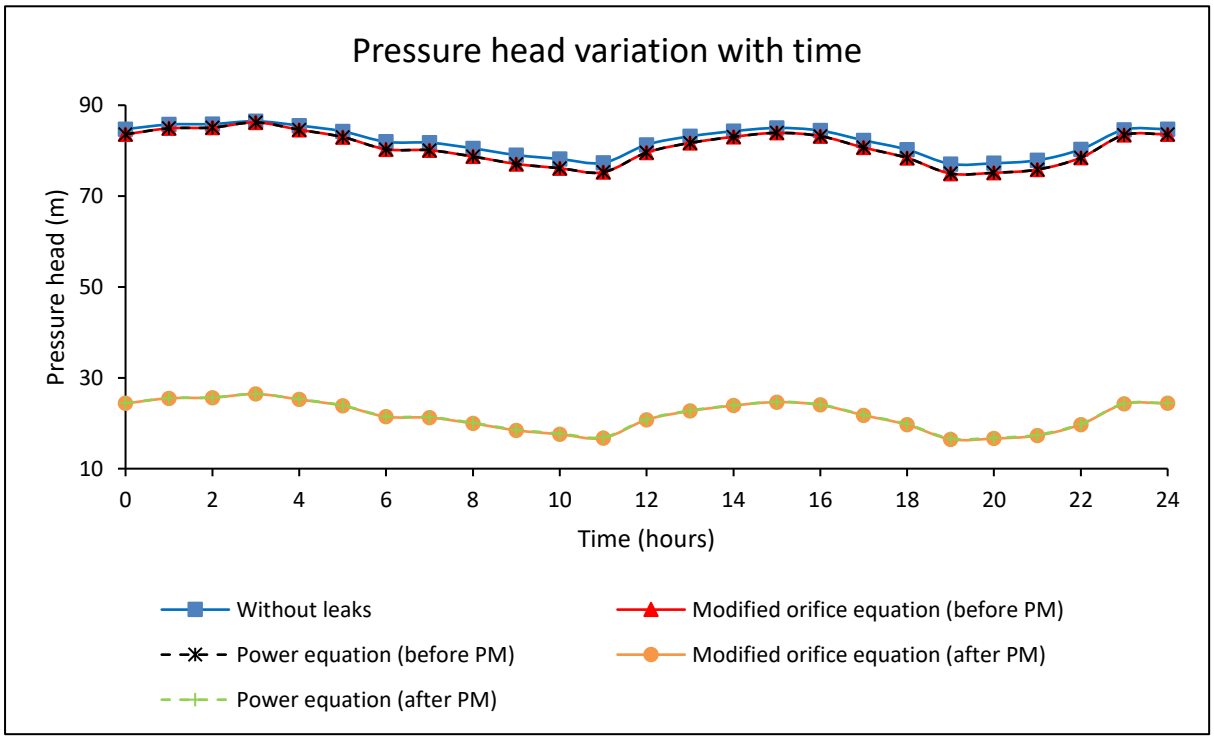

Pressure head at the critical node

		Pressure head (m)			
		Minimum	**Arithmetic Mean**	**Median**	**Maximum**
Before pressure management	Without leaks	70.86	77.65	77.80	83.43
	Modified orifice equation	68.28	75.84	75.84	83.12
	Power equation	68.31	75.85	78.85	83.12
After pressure management	Modified orifice equation	10.11	17.08	17.17	23.37
	Power equation	10.34	17.23	17.23	23.39

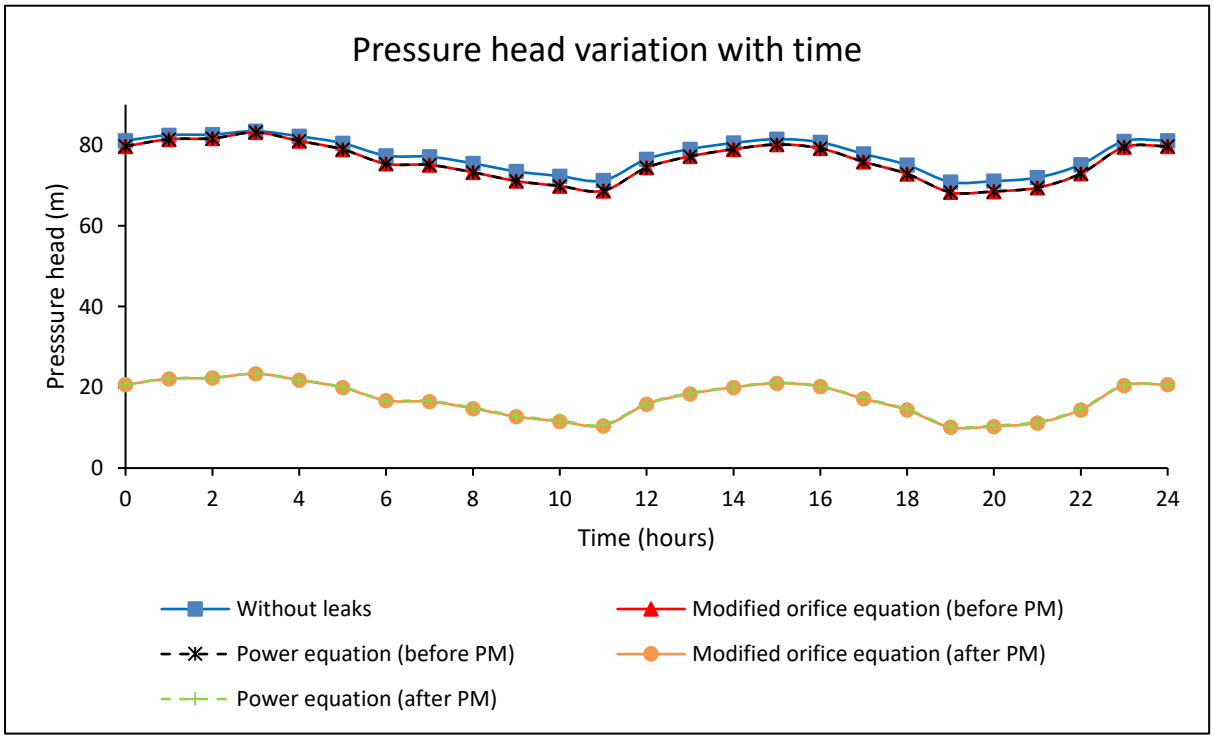

System leakage flow rate

		Leakage flow rate (m^3/h)			
		Minimum	**Arithmetic Mean**	**Median**	**Maximum**
Before pressure management	Modified orifice equation	52.82	55.93	55.92	59.00
	Power equation	52.63	55.85	55.84	59.00
After pressure management	Modified orifice equation	15.71	18.31	18.35	20.62
	Power equation	11.72	14.58	14.61	17.16

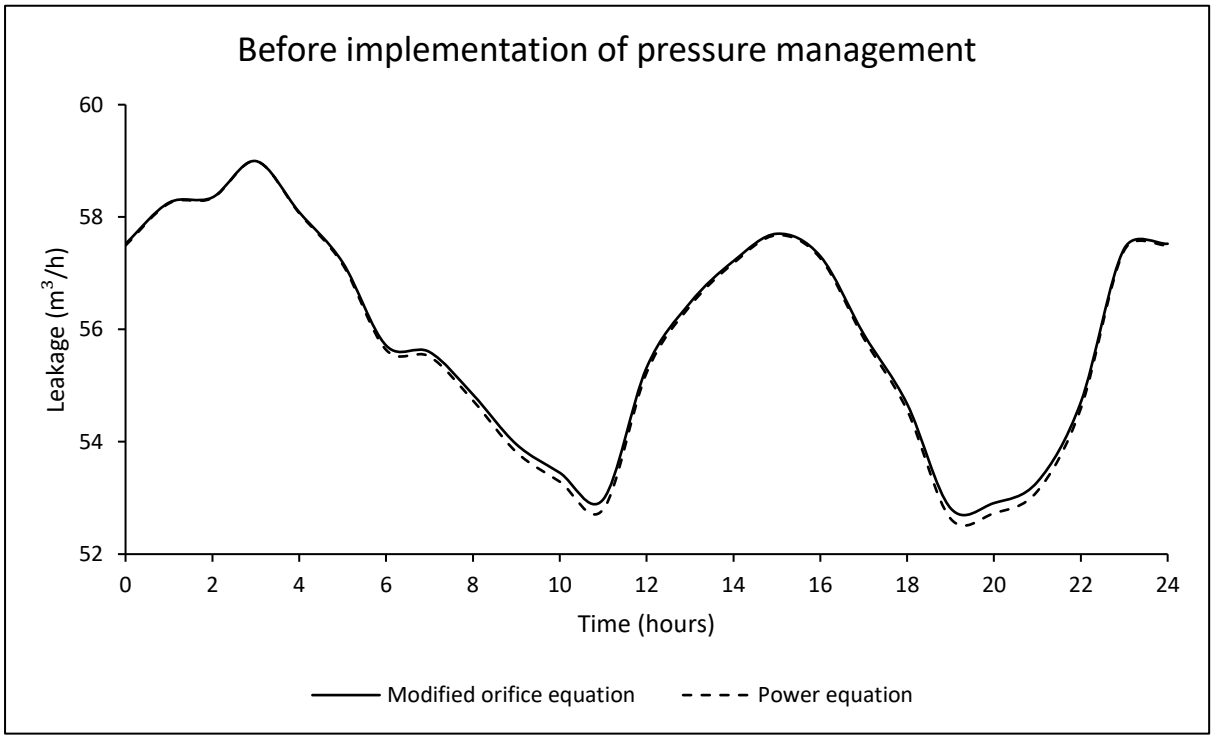

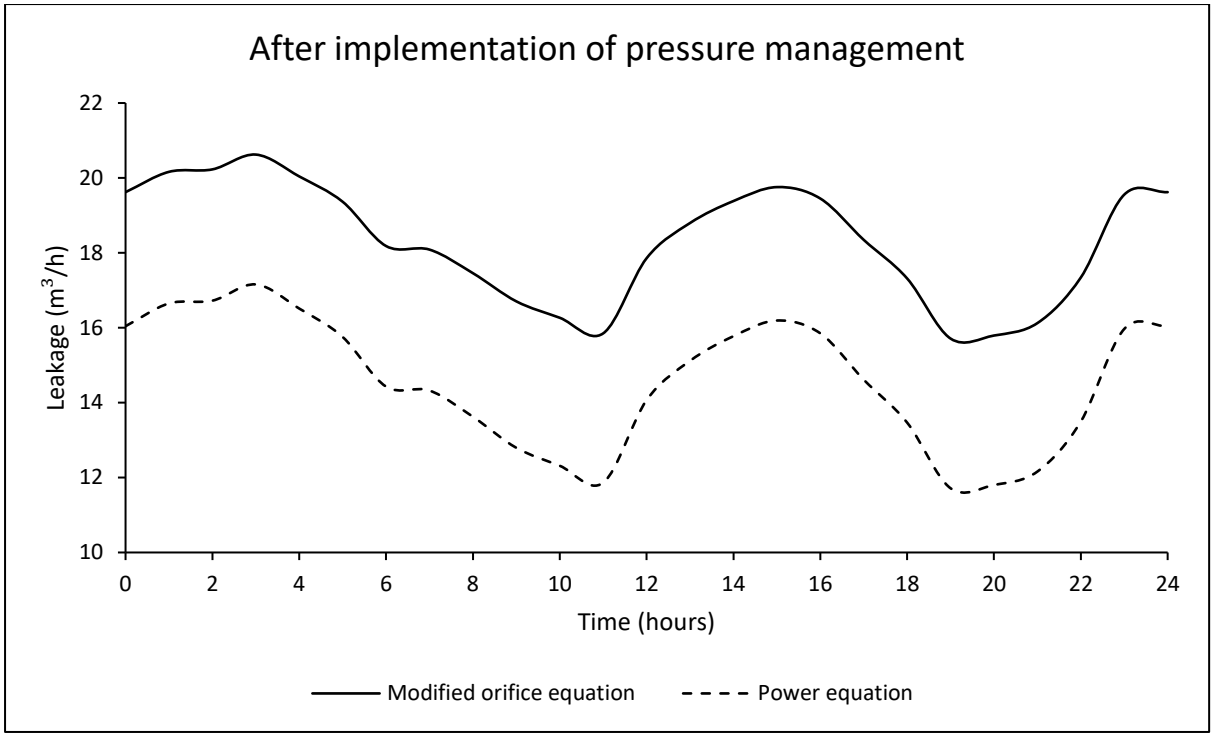
After implementation of pressure management
Leakage (m3/h)
22
20
18
16
14
12
10
0
2
4
6
8
10
12
14
16
18
20
22
24
Time (hours)
Modified orifice equation
Power equation

Leakage flow rate at the critical node

		Leakage flow rate (m^3/h)			
		Minimum	**Arithmetic Mean**	**Median**	**Maximum**
Before pressure management	Modified orifice equation	1.76	1.89	1.89	2.01
	Power equation	1.65	1.83	1.83	2.01
After pressure management	Modified orifice equation	0.59	0.77	0.78	0.93
	Power equation	0.24	0.41	0.41	0.56

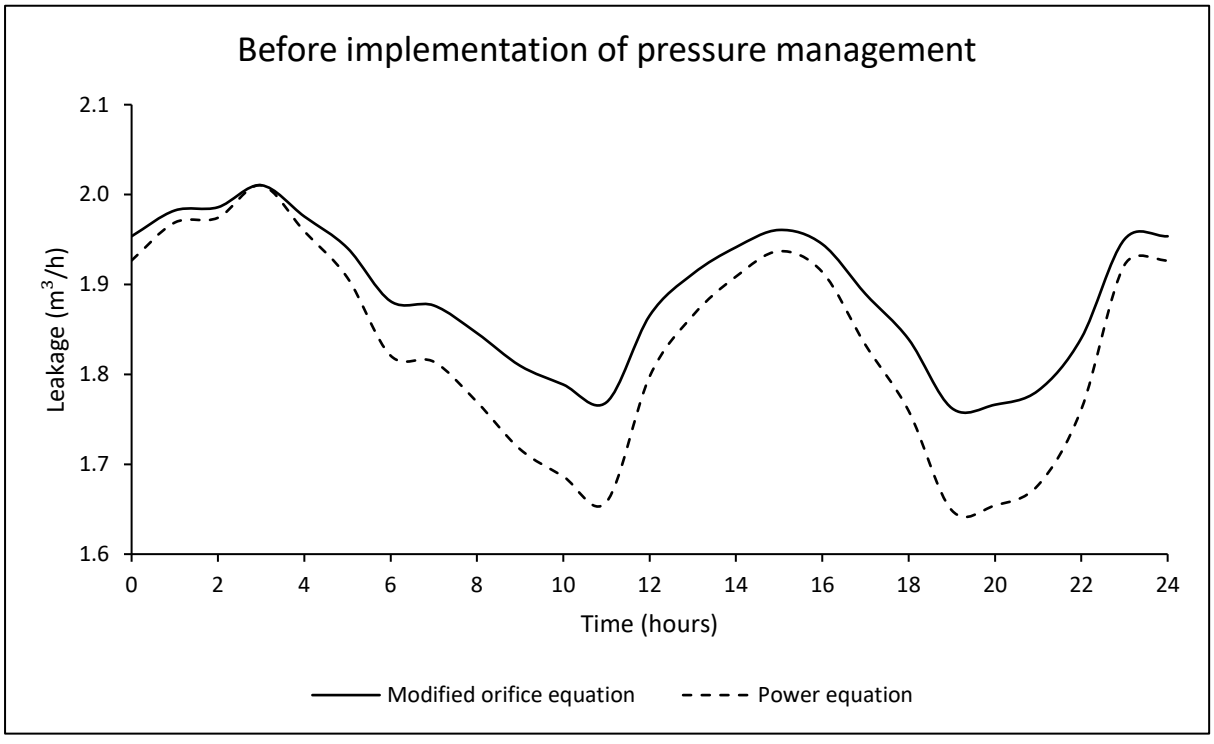

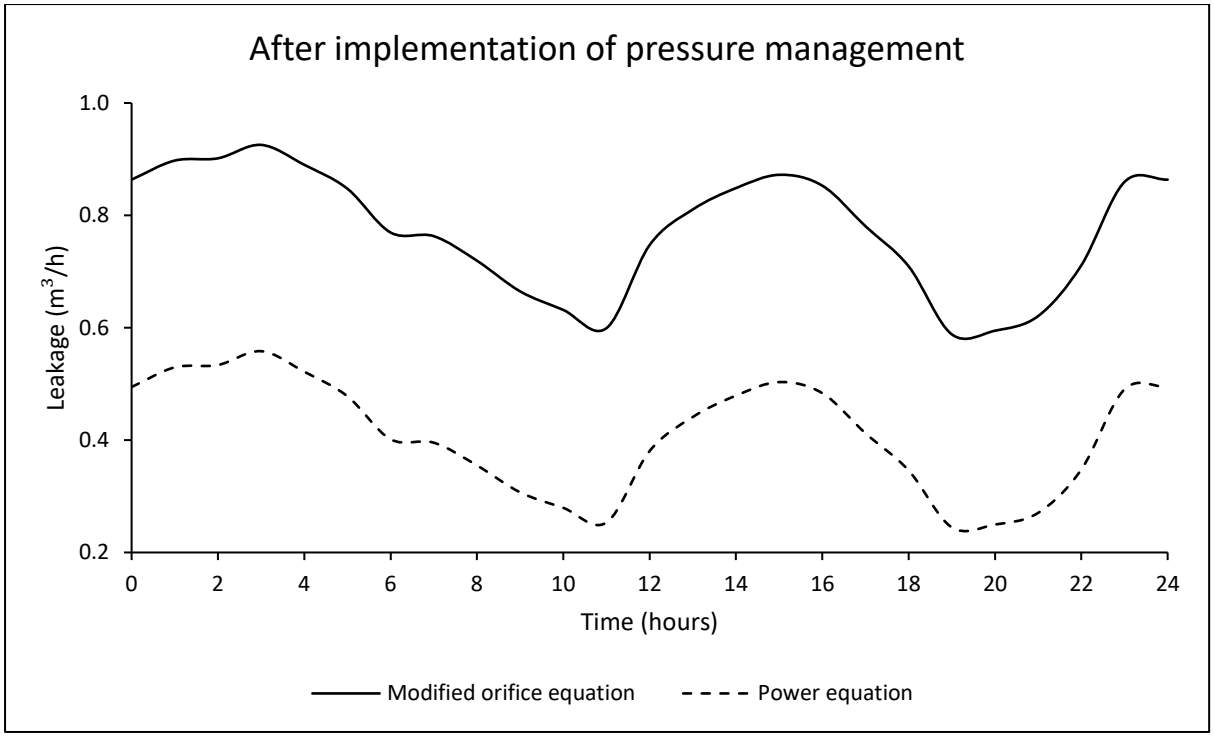
After implementation of pressure management
1.0
0.8
0.6
0.4
0.2
Leakage (m3/h)
0
2
4
6
8
10
12
14
16
18
20
22
24
Time (hours)
Modified orifice equation
Power equation

Number of iterations required for a system to converge to a hydraulic solution for both formulations

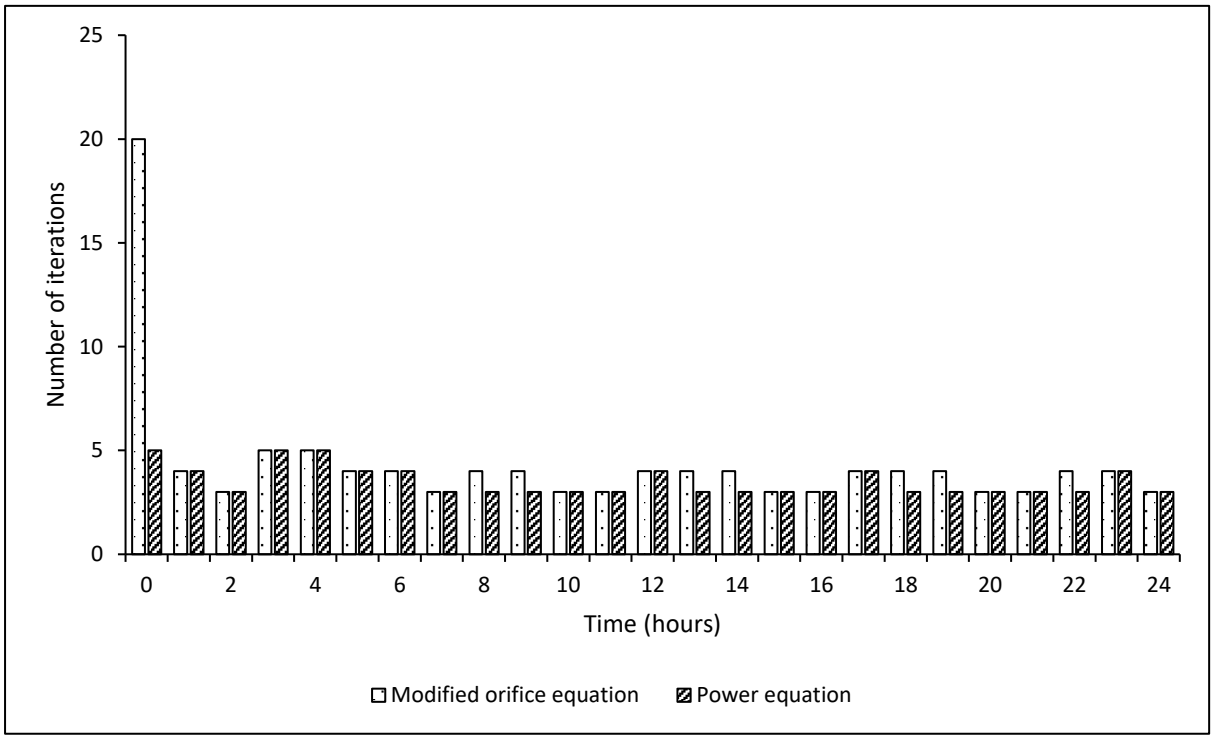

Results for combined systems

System parameters for both power and modified orifice formulations

	Minimum	Arithmetic Mean	Median	Maximum
Leakage exponent N1	0.65	0.92	0.91	1.25
Leakage coefficient C	6.3E-05	3.2E-04	2.9E-04	9.3E-04
Effective initial leak area C_dA0 (mm^2)	98.40	231.04	234.73	342.13
Effective head-area slope C_dm (mm^2/m)	0.70	2.01	1.97	3.49
Leakage number LN	0.17	0.82	0.70	2.96

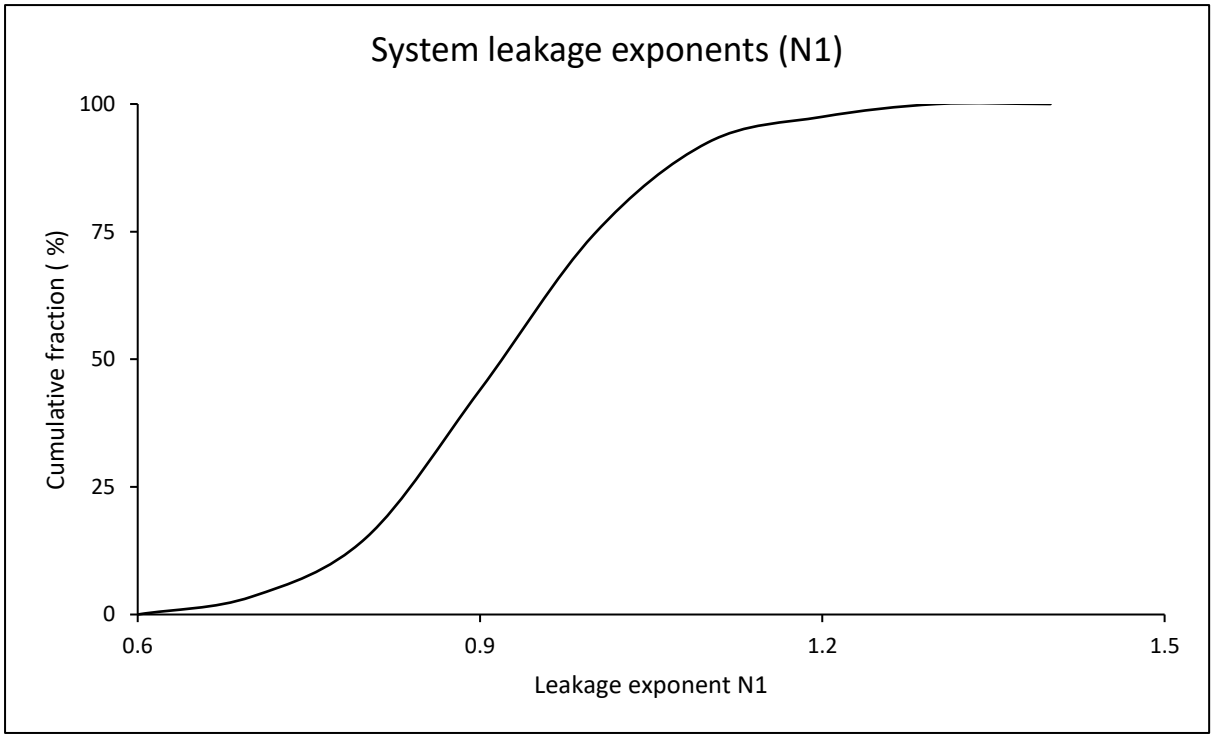

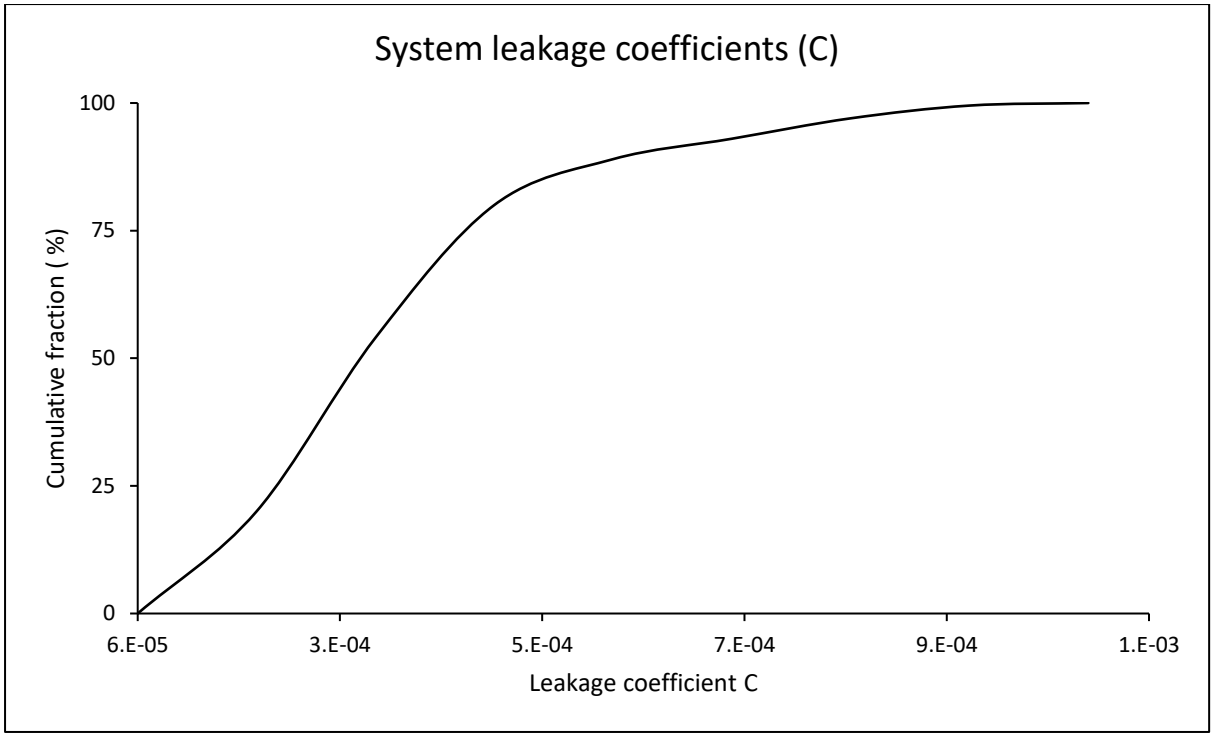
System leakage coefficients (C)
100
75
50
25
0
Cumulative fraction (%)
6.E-05
3.E-04
5.E-04
7.E-04
9.E-04
1.E-03
Leakage coefficient C

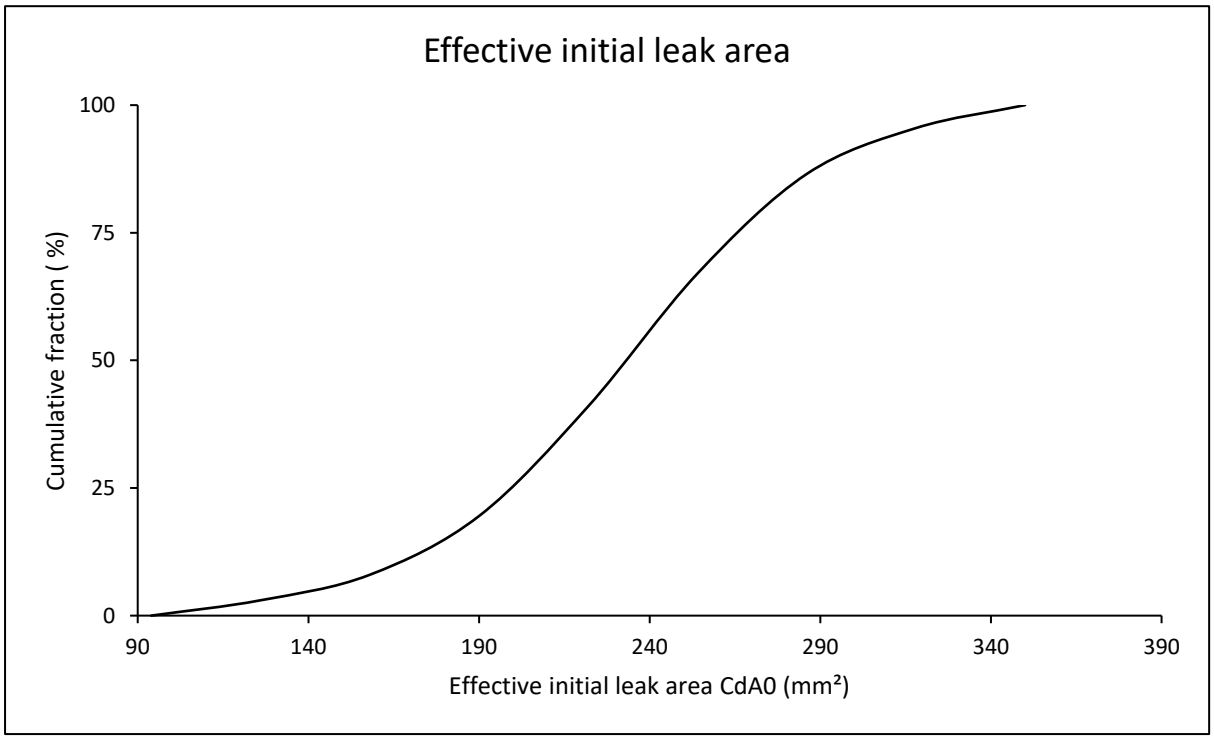
Effective initial leak area
100
75
50
25
0
Cumulative fraction (%)
90
140
190
240
290
340
390
Effective initial leak area CdA0 (mm²)

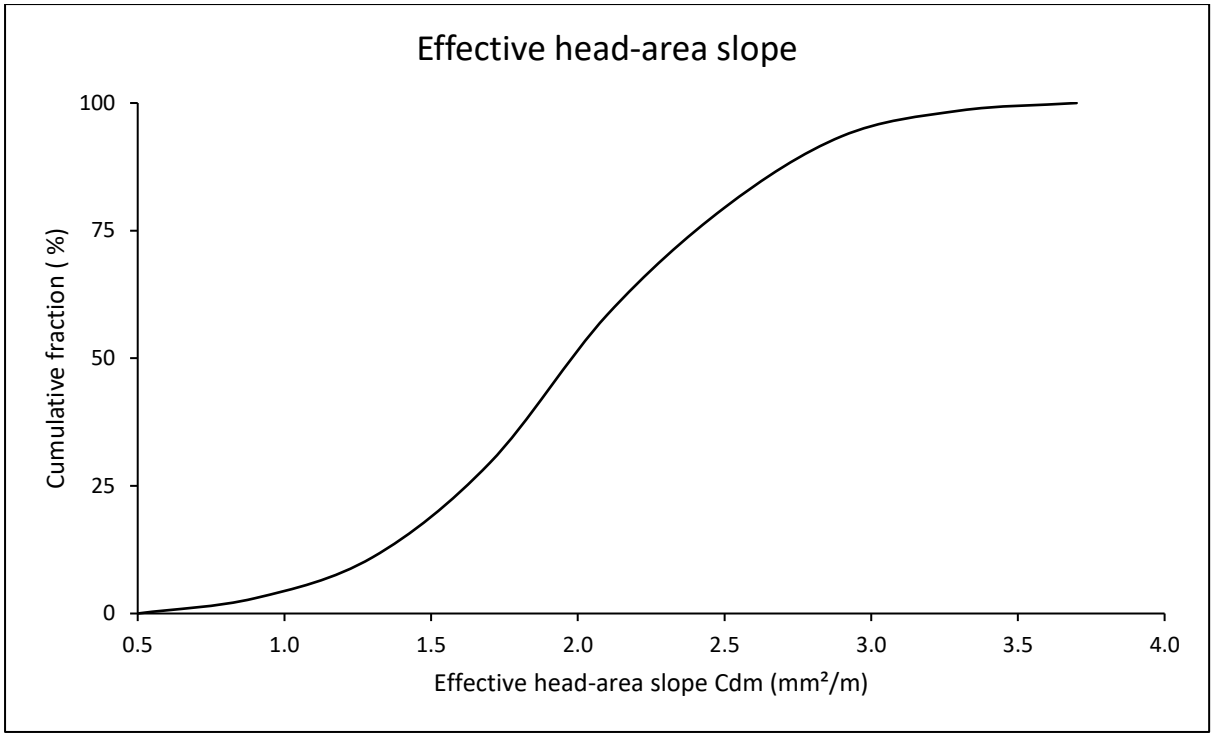
Effective head-area slope
Cumulative fraction (%)
100
75
50
25
0
0.5
1.0
1.5
2.0
2.5
3.0
3.5
4.0
Effective head-area slope Cdm (mm²/m)

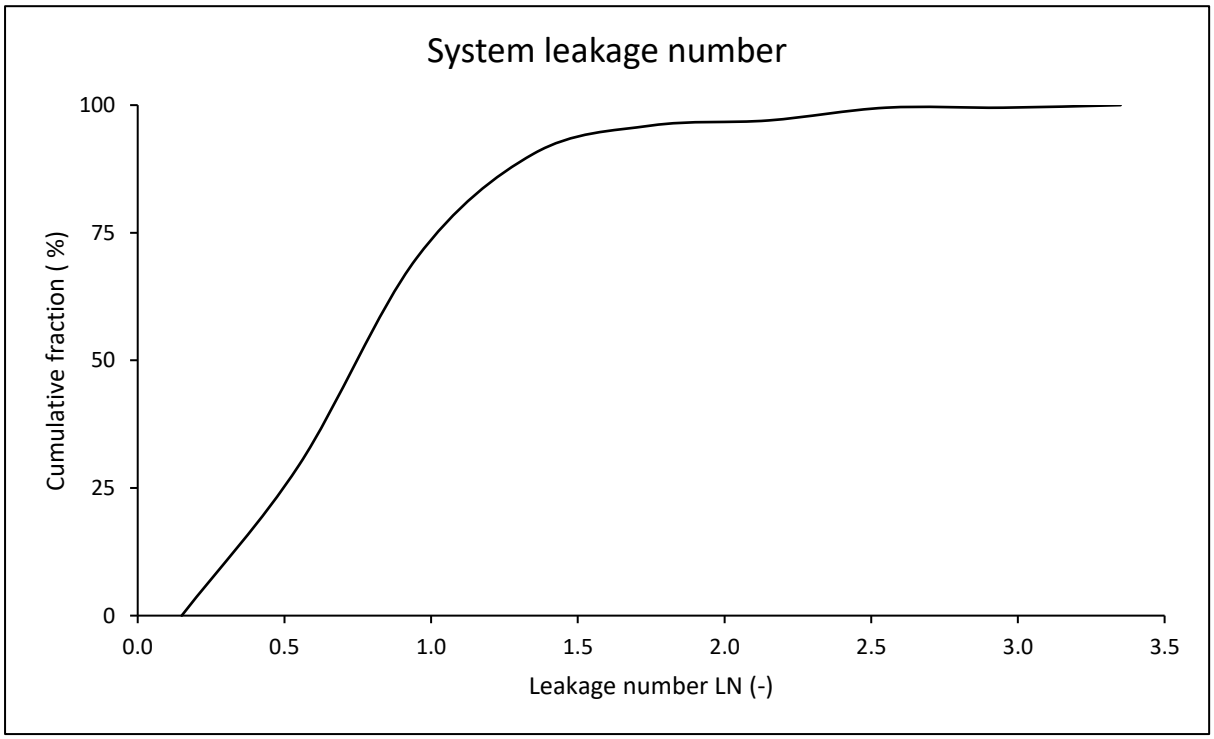
System leakage number
Cumulative fraction (%)
100
75
50
25
0
0.0
0.5
1.0
1.5
2.0
2.5
3.0
3.5
Leakage number LN (-)

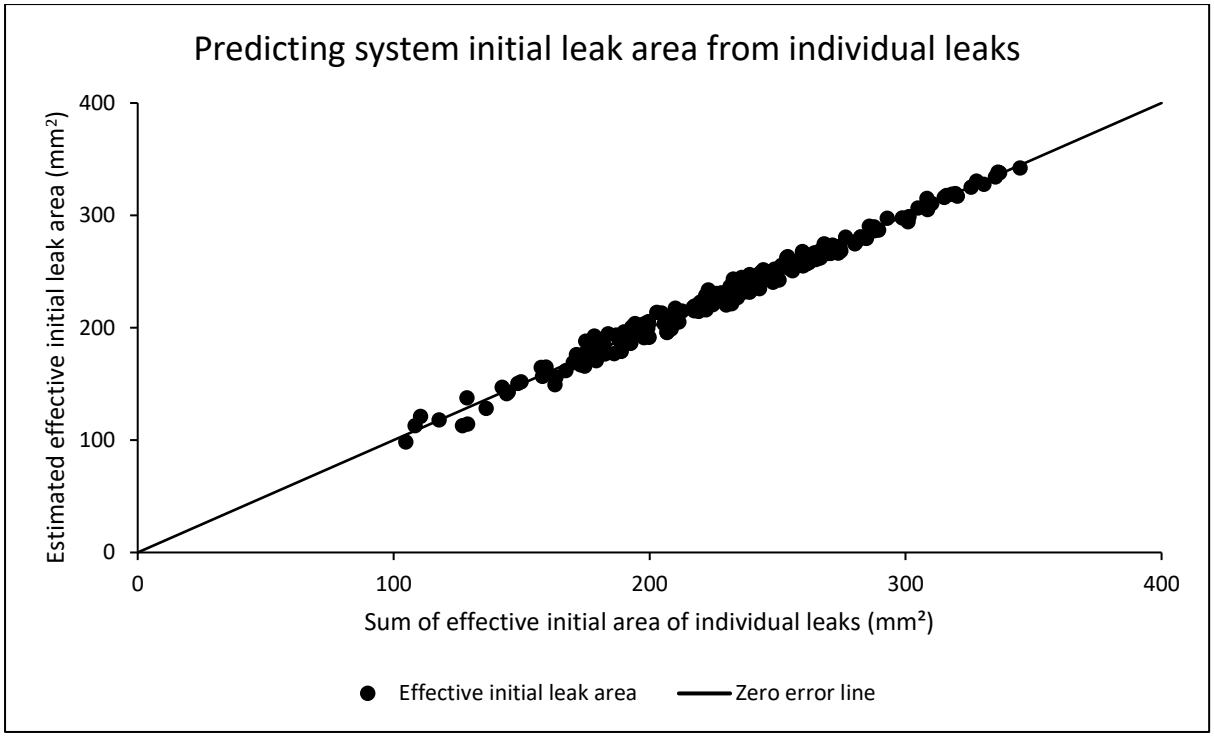
Predicting system initial leak area from individual leaks
Estimated effective initial leak area (mm²)
400
300
200
100
0
0
100
200
300
400
Sum of effective initial area of individual leaks (mm²)
Effective initial leak area
Zero error line

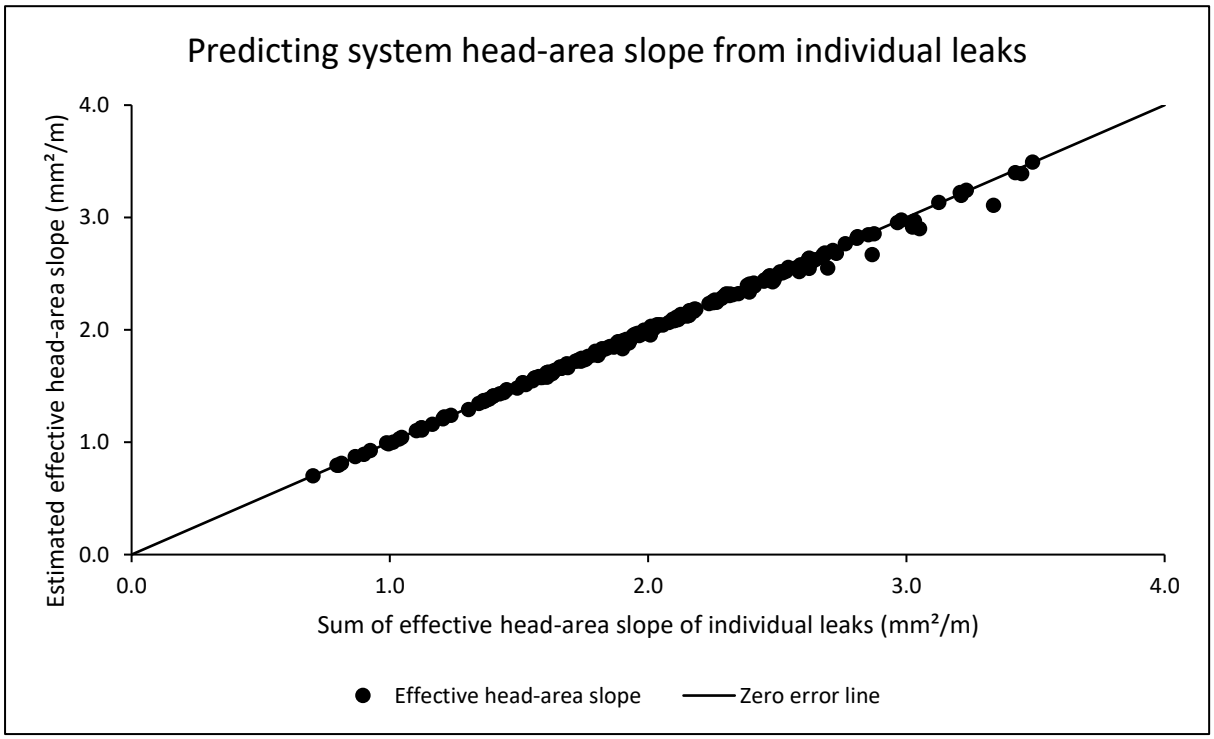
Predicting system head-area slope from individual leaks
Estimated effective head-area slope (mm²/m)
4.0
3.0
2.0
1.0
0.0
0.0
1.0
2.0
3.0
4.0
Sum of effective head-area slope of individual leaks (mm²/m)
Effective head-area slope
Zero error line

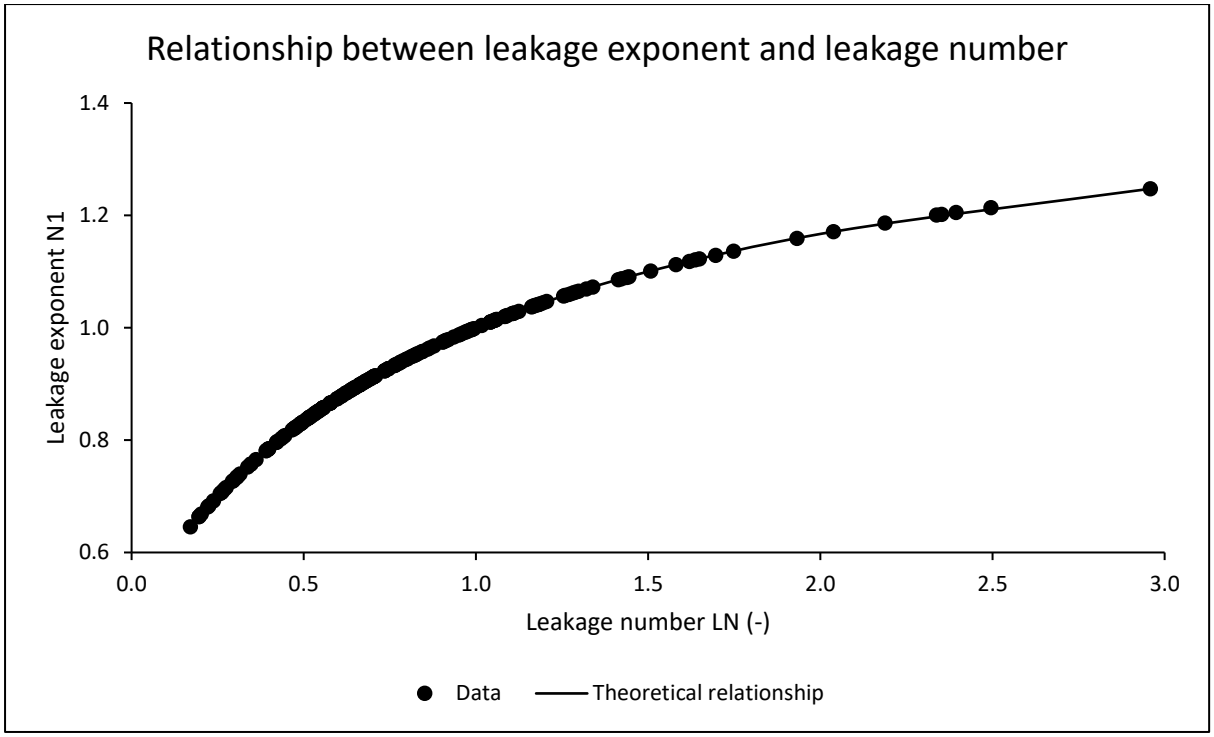
Relationship between leakage exponent and leakage number
Leakage exponent N1
1.4
1.2
1.0
0.8
0.6
0.0
0.5
1.0
1.5
2.0
2.5
3.0
Leakage number LN (-)
Data
Theoretical relationship

Average iterations required for a system to converge using both formulations

Average number of iterations	Minimum	Arithmetic Mean	Median	Maximum
Modified orifice equation	4.08	4.22	4.20	4.44
Power equation	3.20	3.64	3.64	3.92

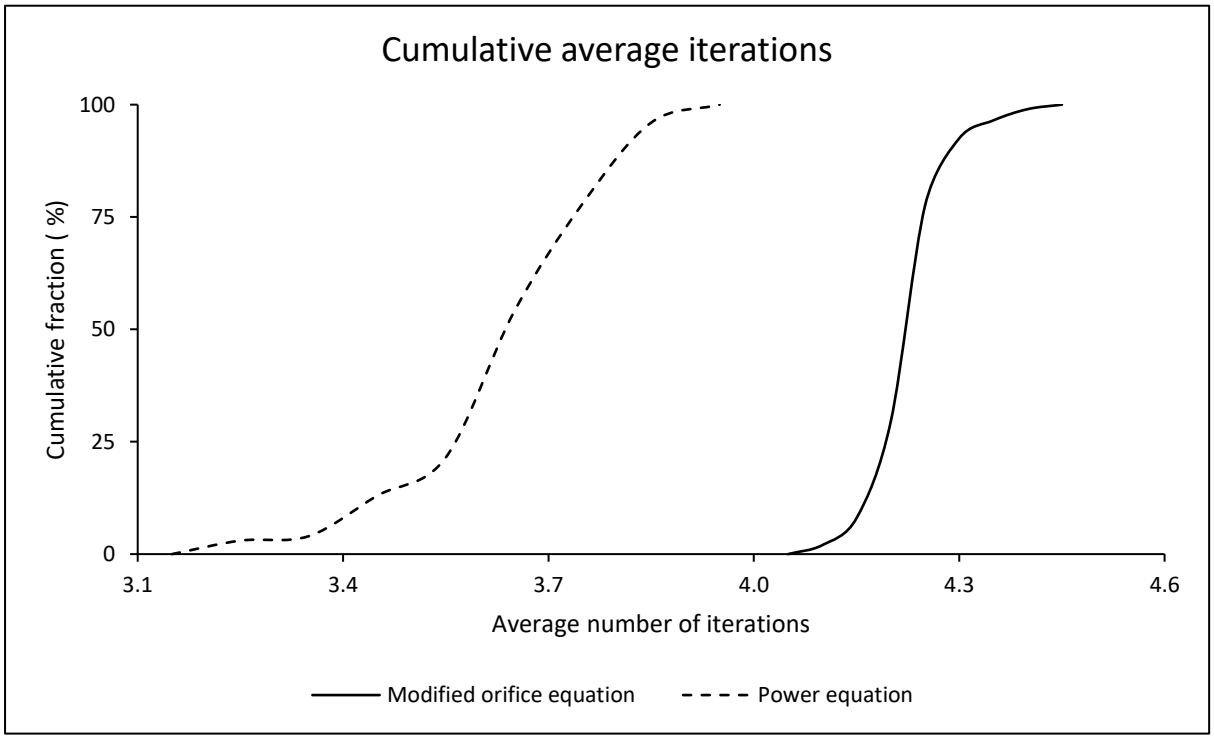

Effect of leakage on pressure at both average zone pressure (AZP) and critical nodes

AZP node								
	During MNF conditions				During peak demand conditions			
	Min (m)	Mean (m)	Median (m)	Max (m)	Min (m)	Mean (m)	Median (m)	Max (m)
Modified orifice equation	-0.52	-0.30	-0.30	-0.17	-2.81	-2.34	-2.38	-1.48
Power equation	-0.52	-0.30	-0.30	-0.17	-2.82	-2.33	-2.37	-1.46
Critical node								
Modified orifice equation	-2.74	-0.53	-0.38	-0.17	-6.92	-3.22	-2.88	-1.53
Power equation	-2.74	-0.53	-0.38	-0.17	-7.01	-3.22	-2.87	-1.51

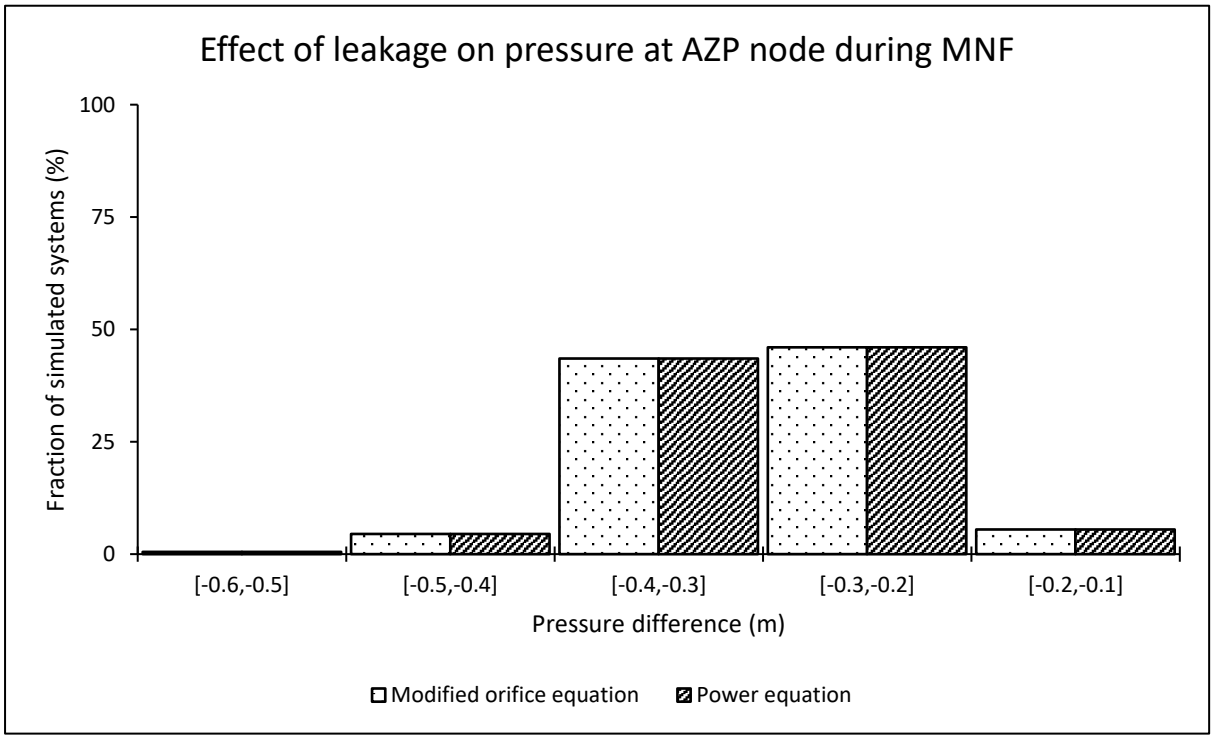

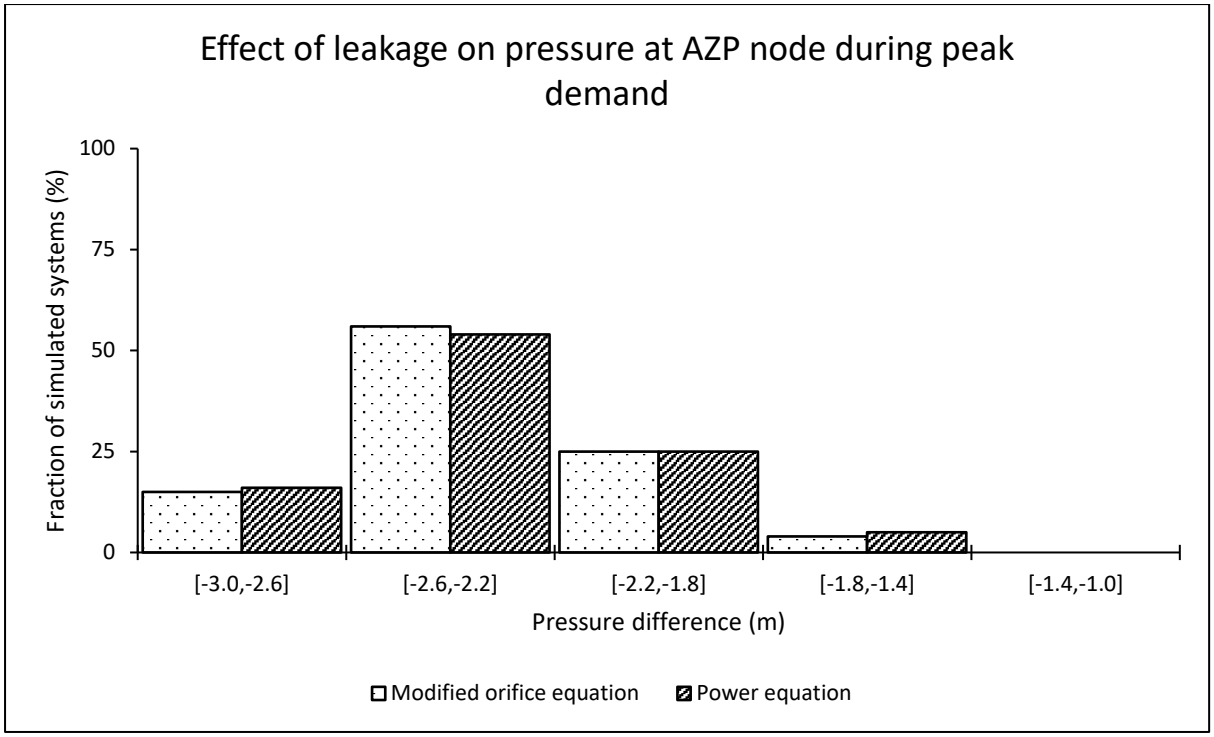
Effect of leakage on pressure at AZP node during peak demand
Fraction of simulated systems (%)
100
75
50
25
0
[-3.0,-2.6]
[-2.6,-2.2]
[-2.2,-1.8]
[-1.8,-1.4]
[-1.4,-1.0]
Pressure difference (m)
Modified orifice equation
Power equation

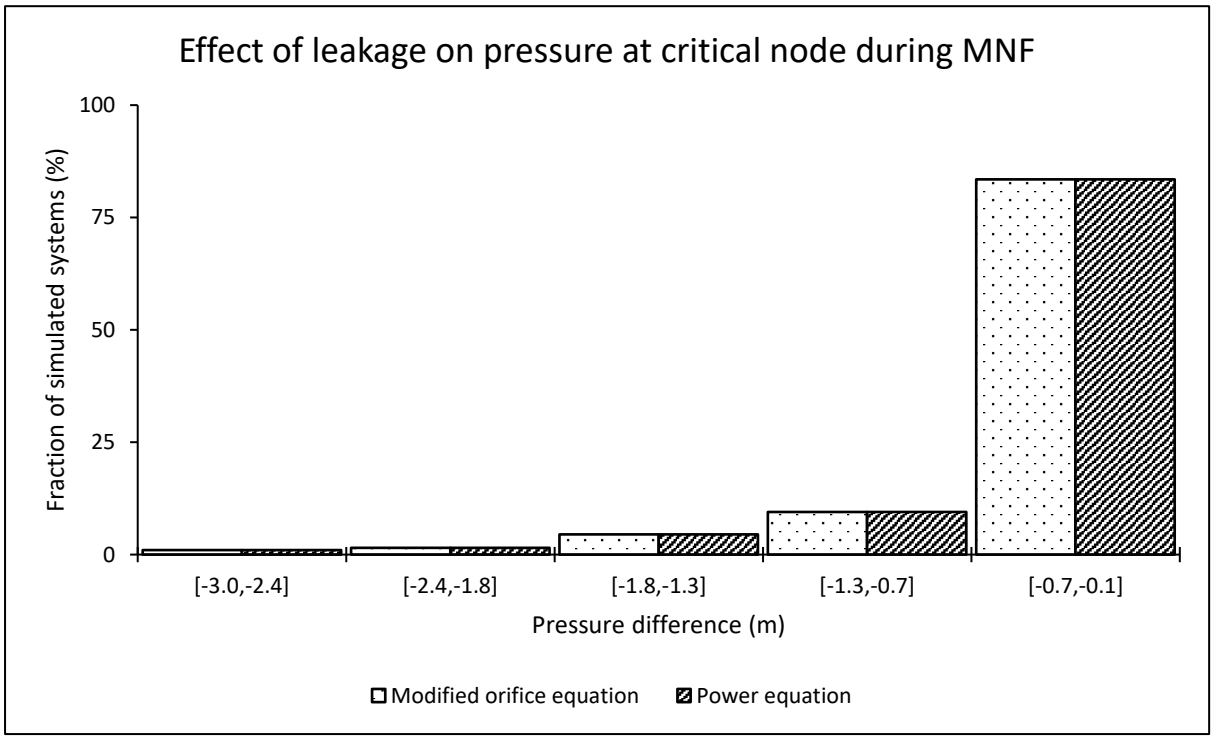
Effect of leakage on pressure at critical node during MNF
Fraction of simulated systems (%)
100
75
50
25
0
[-3.0,-2.4]
[-2.4,-1.8]
[-1.8,-1.3]
[-1.3,-0.7]
[-0.7,-0.1]
Pressure difference (m)
Modified orifice equation
Power equation

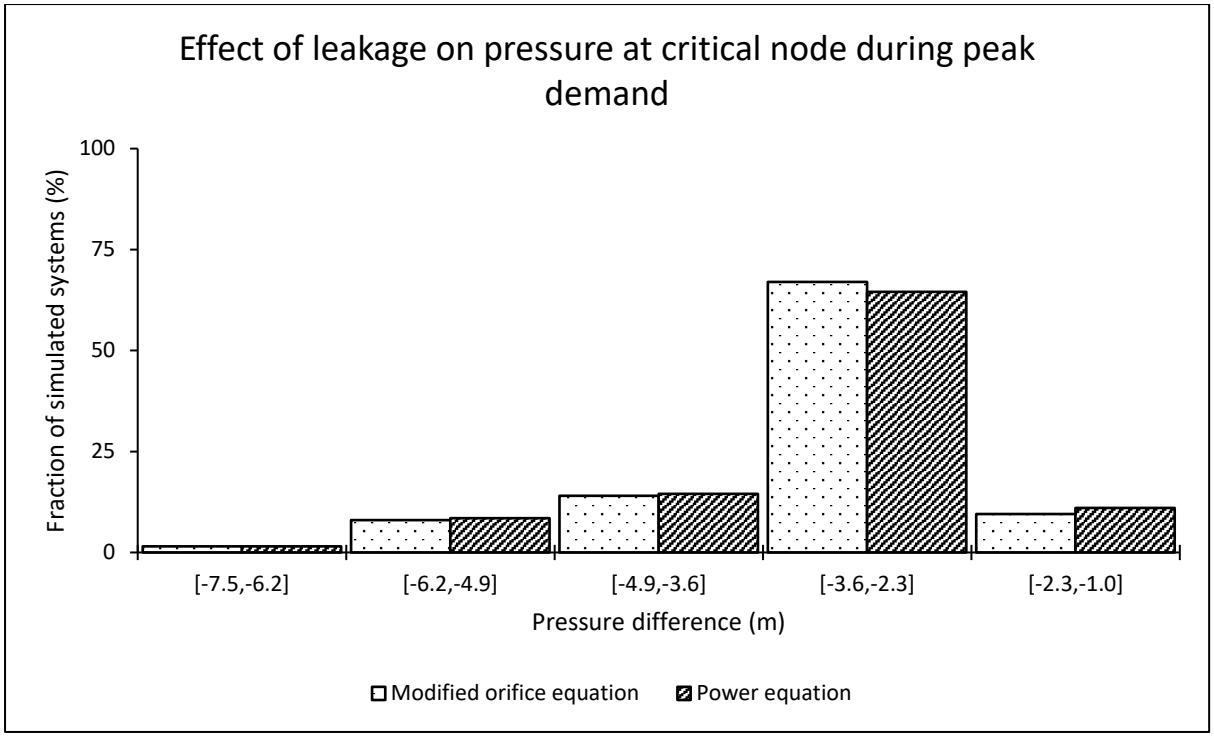
Effect of leakage on pressure at critical node during peak demand
Fraction of simulated systems (%)
100
75
50
25
0
[-7.5,-6.2]
[-6.2,-4.9]
[-4.9,-3.6]
[-3.6,-2.3]
[-2.3,-1.0]
Pressure difference (m)
Modified orifice equation
Power equation

Pressure estimation error when using the power equation at average zone pressure (AZP) and critical nodes

	During MNF conditions				During peak demand conditions			
	Min (%)	**Mean (%)**	**Median (%)**	**Max (%)**	**Min (%)**	**Mean (%)**	**Median (%)**	**Max (%)**
At the AZP node	0.00	0.00	0.00	0.00	-0.04	0.00	0.00	0.06
At the critical node	0.00	0.00	0.00	0.00	-0.29	0.00	0.02	0.11

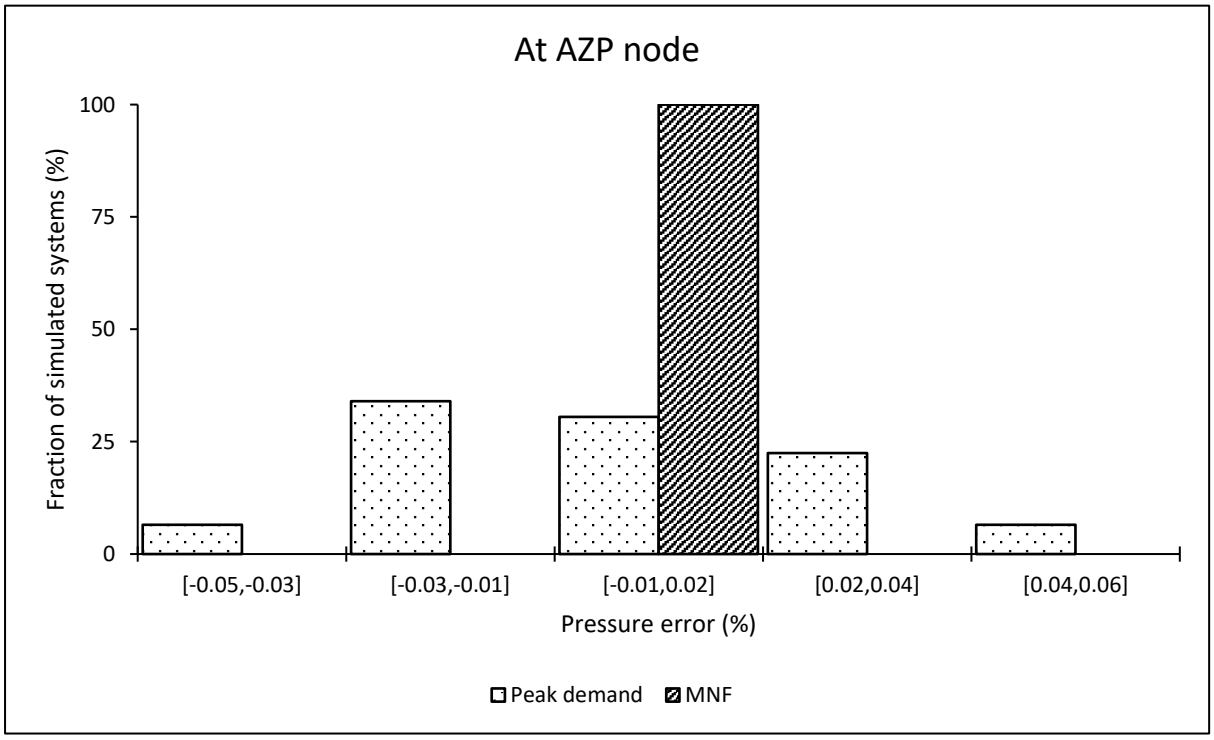

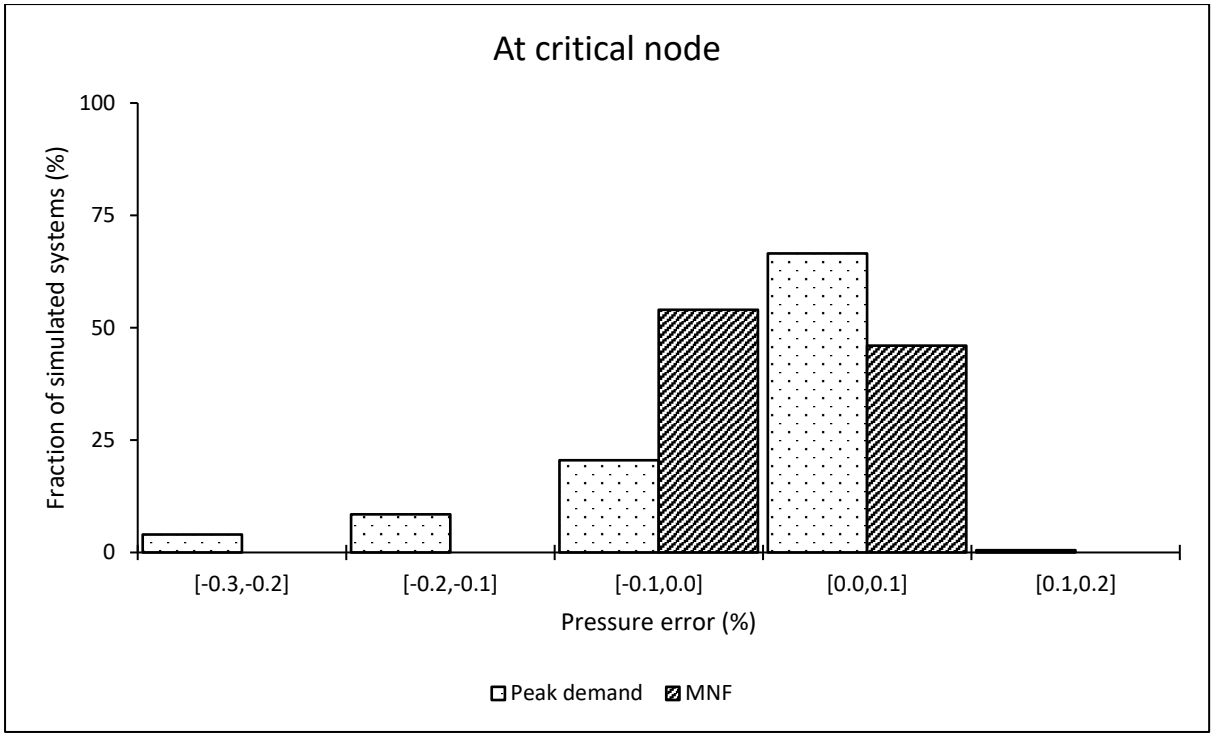
At critical node
Fraction of simulated systems (%)
100
75
50
25
0
[-0.3,-0.2]
[-0.2,-0.1]
[-0.1,0.0]
[0.0,0.1]
[0.1,0.2]
Pressure error (%)
Peak demand
MNF

System leakage estimation error when using the power equation

	Leakage estimation error (%)			
	Minimum	**Arithmetic Mean**	**Median**	**Maximum**
Before implementing pressure management	-0.45	0.00	0.03	0.40
After implementing pressure management	-23.77	-16.64	-16.61	-8.11

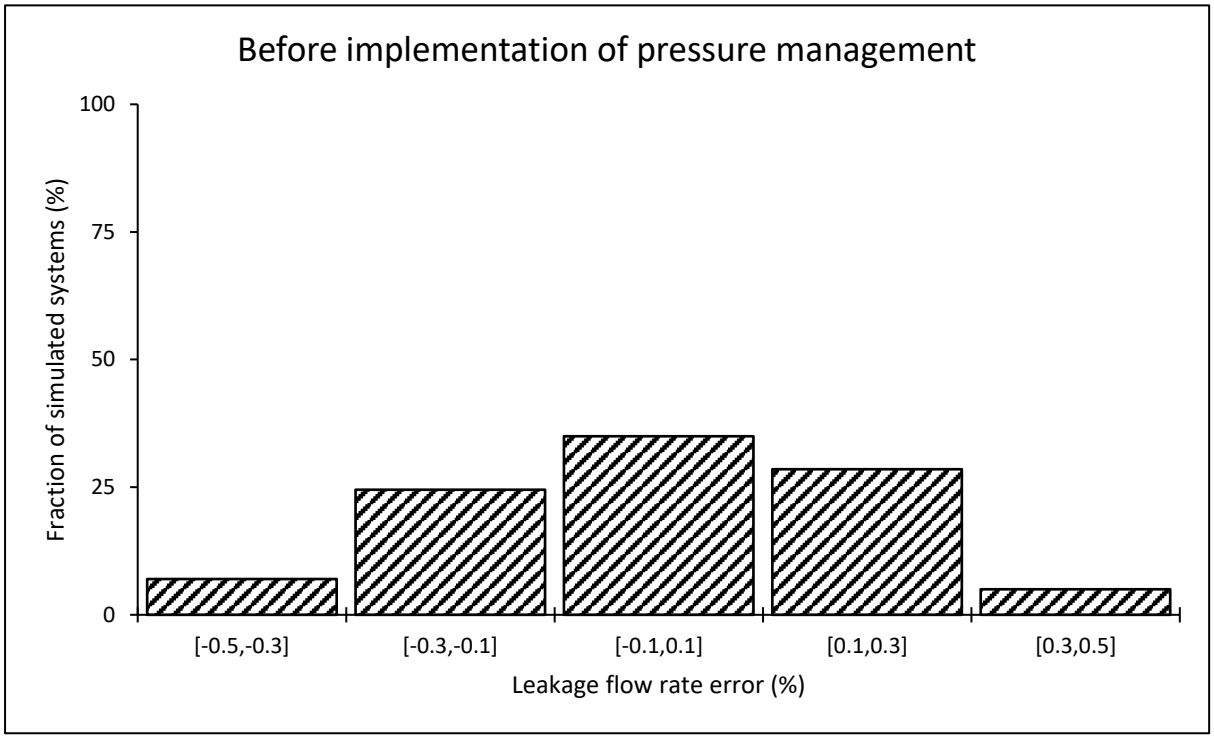

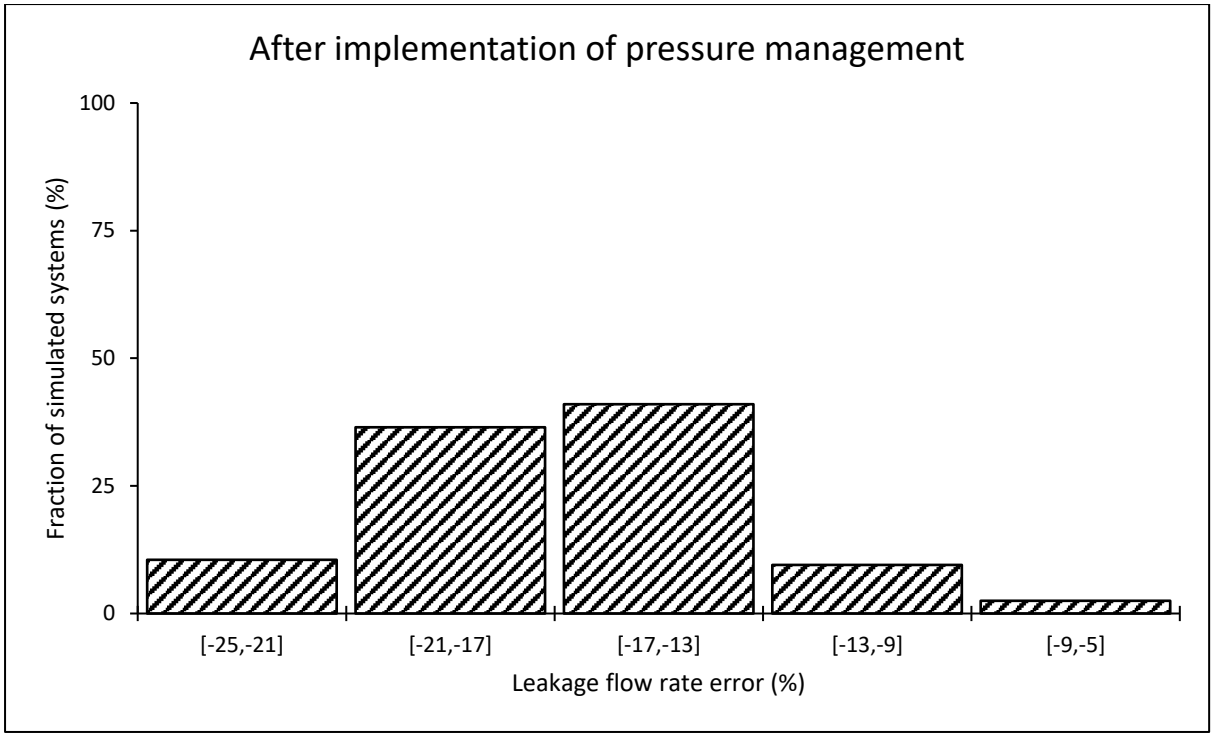
After implementation of pressure management
Fraction of simulated systems (%)
100
75
50
25
0
[-25,-21]
[-21,-17]
[-17,-13]
[-13,-9]
[-9,-5]
Leakage flow rate error (%)

Leakage estimation error when using the power equation at the critical node

	Leakage estimation error (%)			
	Minimum	**Arithmetic Mean**	**Median**	**Maximum**
Before implementing pressure management	-6.81	-1.64	-2.19	2.54
After implementing pressure management	-67.89	-30.89	-35.57	17.92

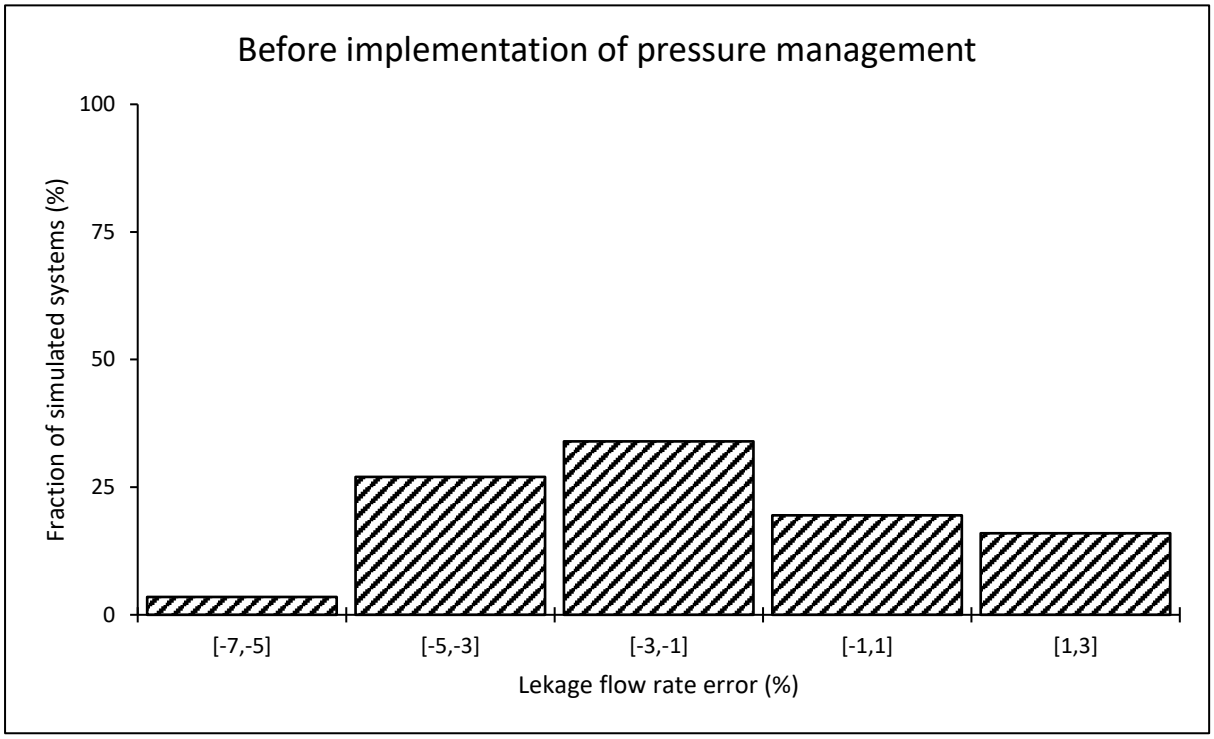

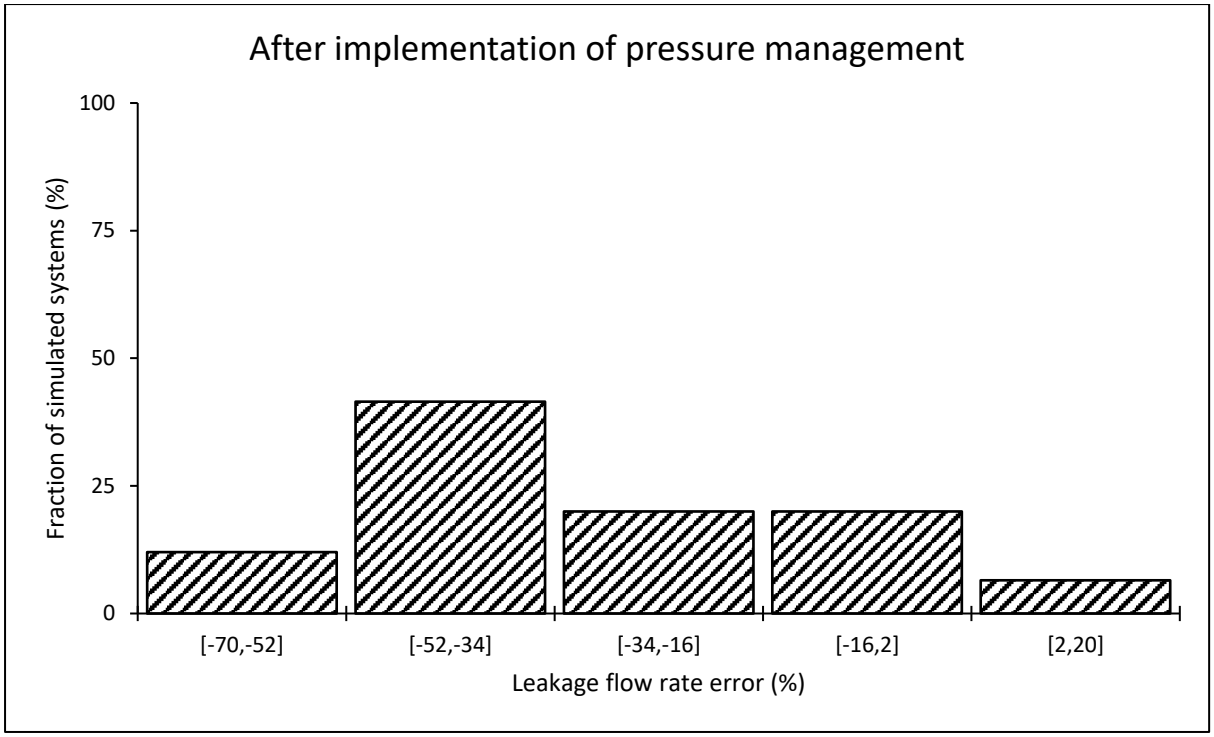
After implementation of pressure management
Fraction of simulated systems (%)
100
75
50
25
0
[-70,-52]
[-52,-34]
[-34,-16]
[-16,2]
[2,20]
Leakage flow rate error (%)

Appendix A-4: Small-sized network with an ILI of 64

Results for an individual system

Pressure head at the average zone pressure (AZP) node

		Pressure head (m)			
		Minimum	**Arithmetic Mean**	**Median**	**Maximum**
Before pressure management	Without leaks	77.08	82.16	82.27	86.48
	Modified orifice equation	68.70	75.52	75.24	83.58
	Power equation	68.83	75.58	75.30	83.58
After pressure management	Modified orifice equation	15.37	20.75	20.71	26.17
	Power equation	15.91	21.12	21.10	26.26

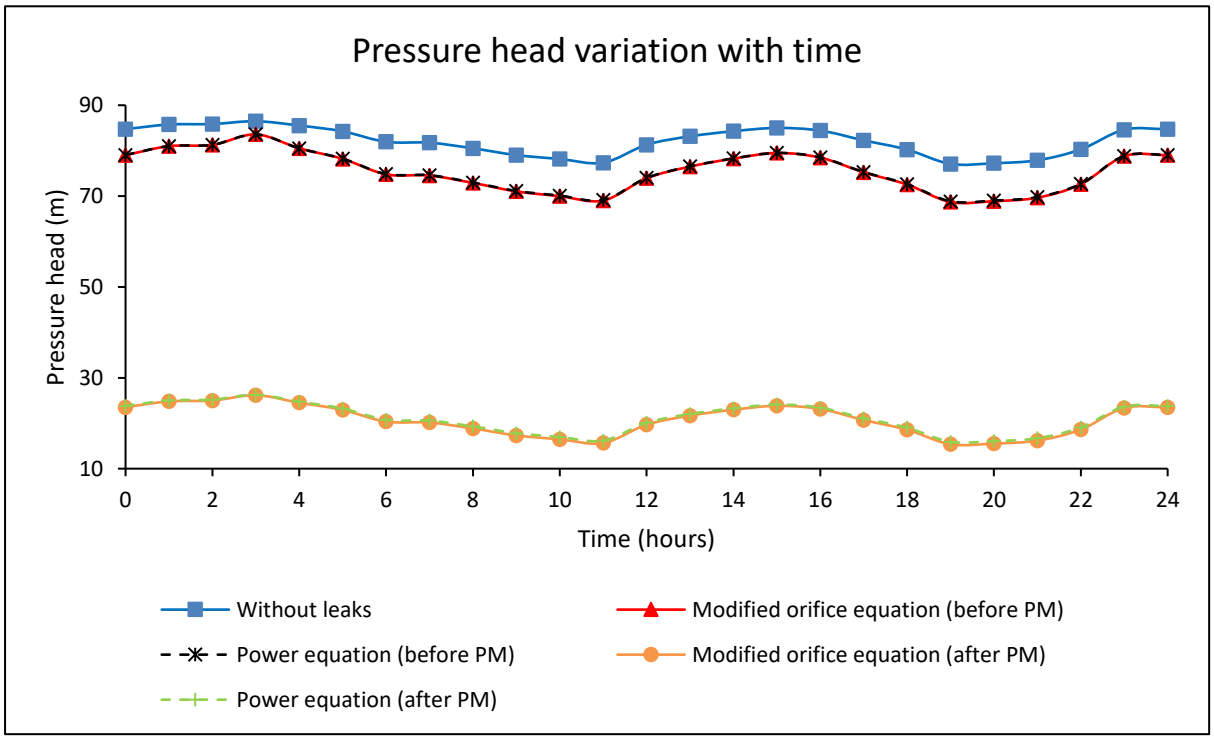

Pressure head at the critical node

		Pressure head (m)			
		Minimum	**Arithmetic Mean**	**Median**	**Maximum**
Before pressure management	Without leaks	70.86	77.65	77.80	83.43
	Modified orifice equation	59.24	68.17	67.78	79.02
	Power equation	59.51	68.30	67.90	79.02
After pressure management	Modified orifice equation	8.53	15.66	15.59	22.93
	Power equation	9.37	16.26	16.22	23.10

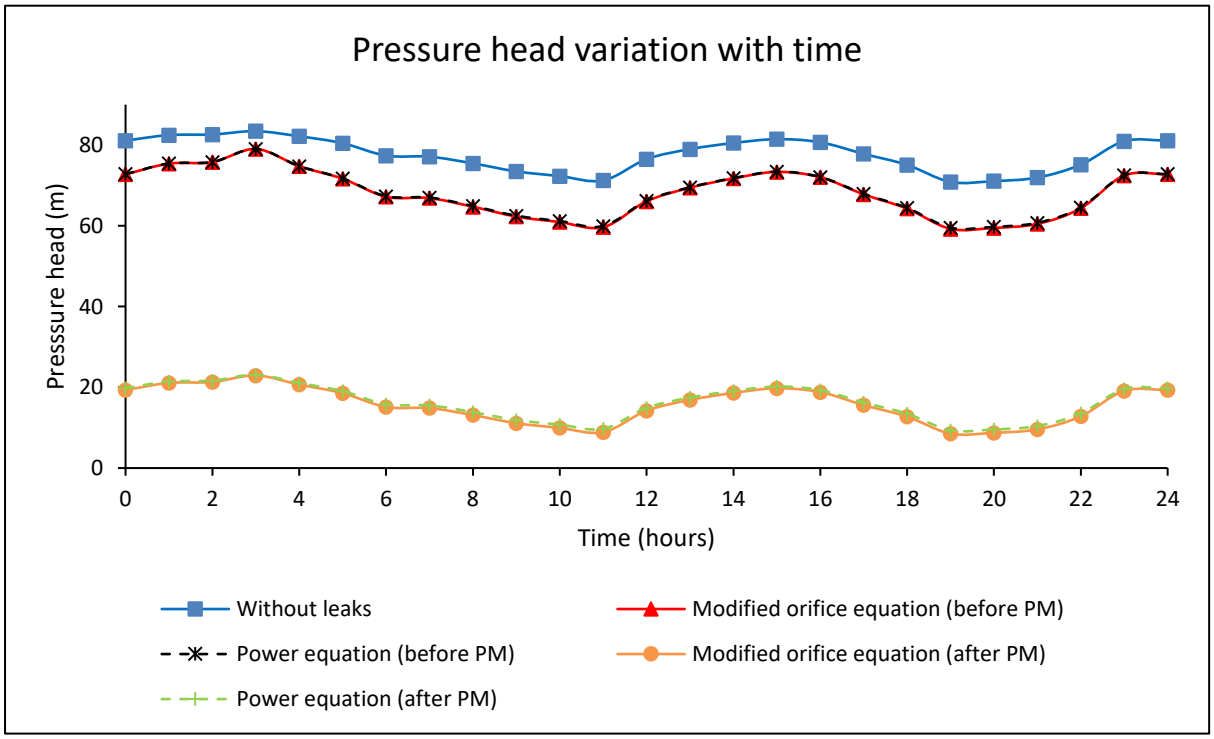

System leakage flow rate

		Leakage flow rate (m^3/h)			
		Minimum	**Arithmetic Mean**	**Median**	**Maximum**
Before pressure management	Modified orifice equation	185.69	204.08	203.12	226.77
	Power equation	184.21	203.31	202.33	226.77
After pressure management	Modified orifice equation	40.42	50.77	50.62	61.42
	Power equation	30.31	40.88	40.70	51.80

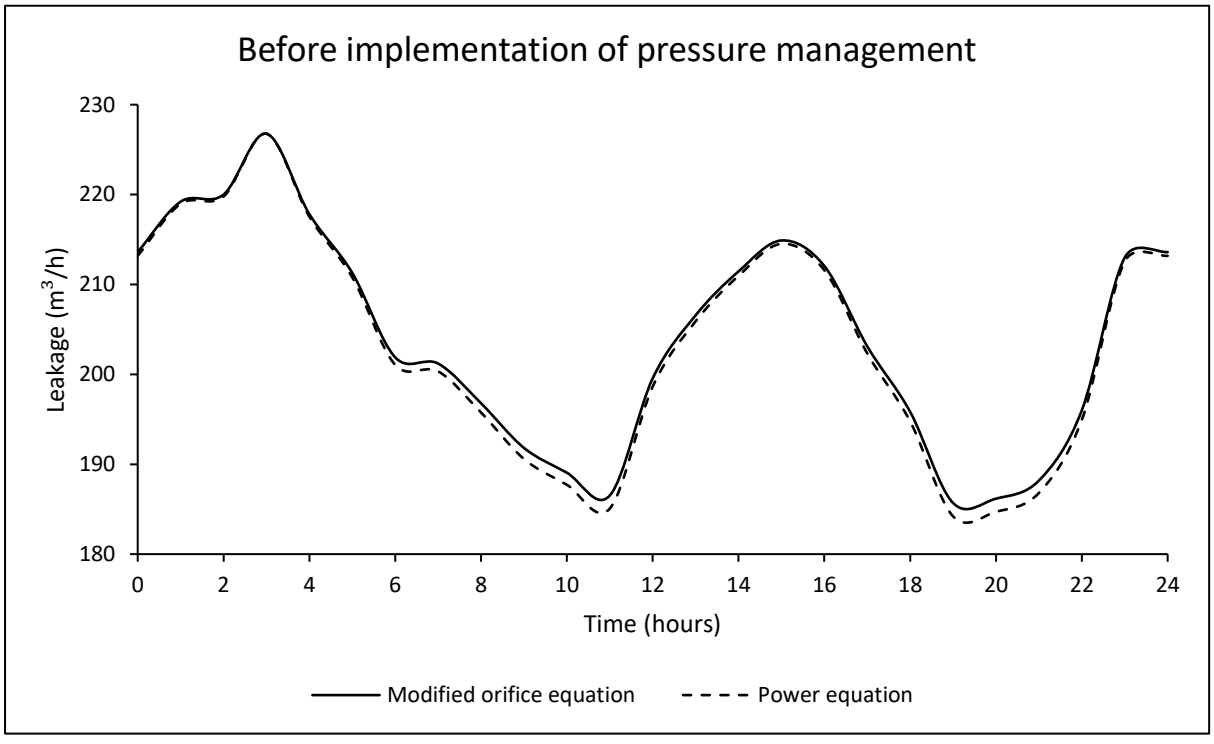

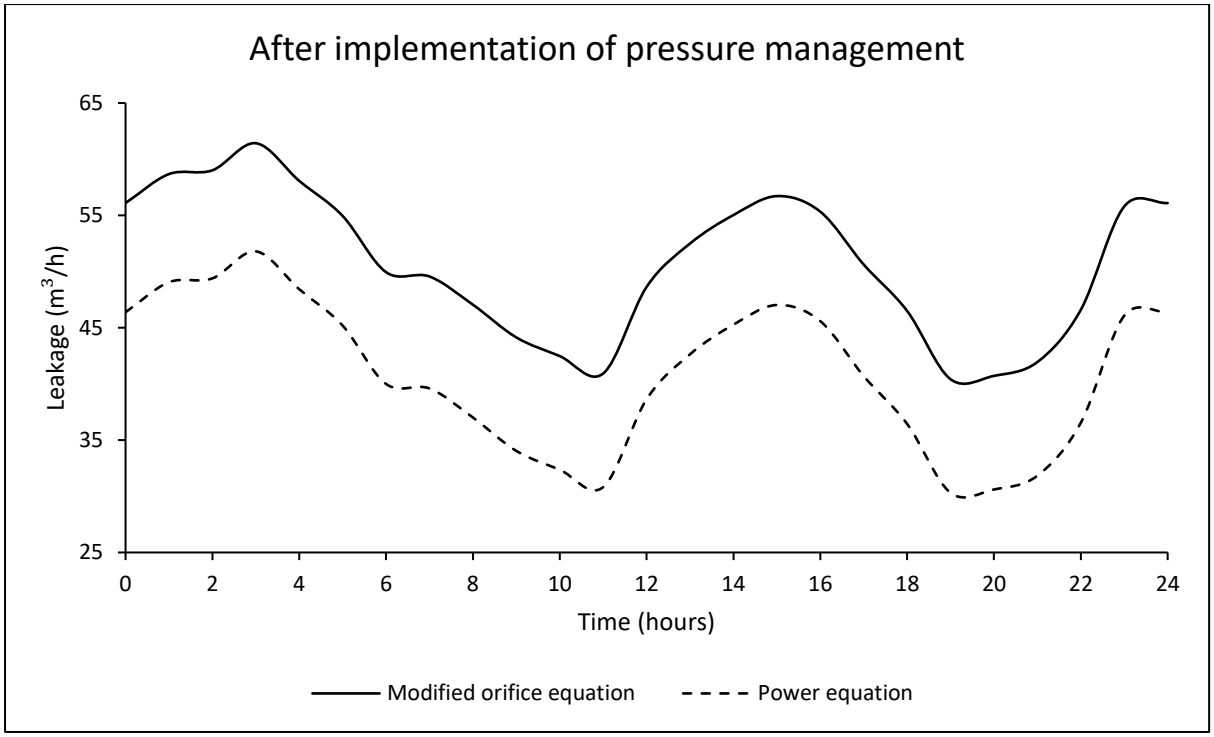
After implementation of pressure management
65
55
45
35
25
Leakage (m3/h)
0
2
4
6
8
10
12
14
16
18
20
22
24
Time (hours)
Modified orifice equation
Power equation

Leakage flow rate at the critical node

		Leakage flow rate (m^3/h)			
		Minimum	**Arithmetic Mean**	**Median**	**Maximum**
Before pressure management	Modified orifice equation	8.50	9.67	9.62	11.12
	Power equation	7.83	9.30	9.22	11.12
After pressure management	Modified orifice equation	2.13	3.08	3.08	4.00
	Power equation	0.80	1.59	1.57	2.43

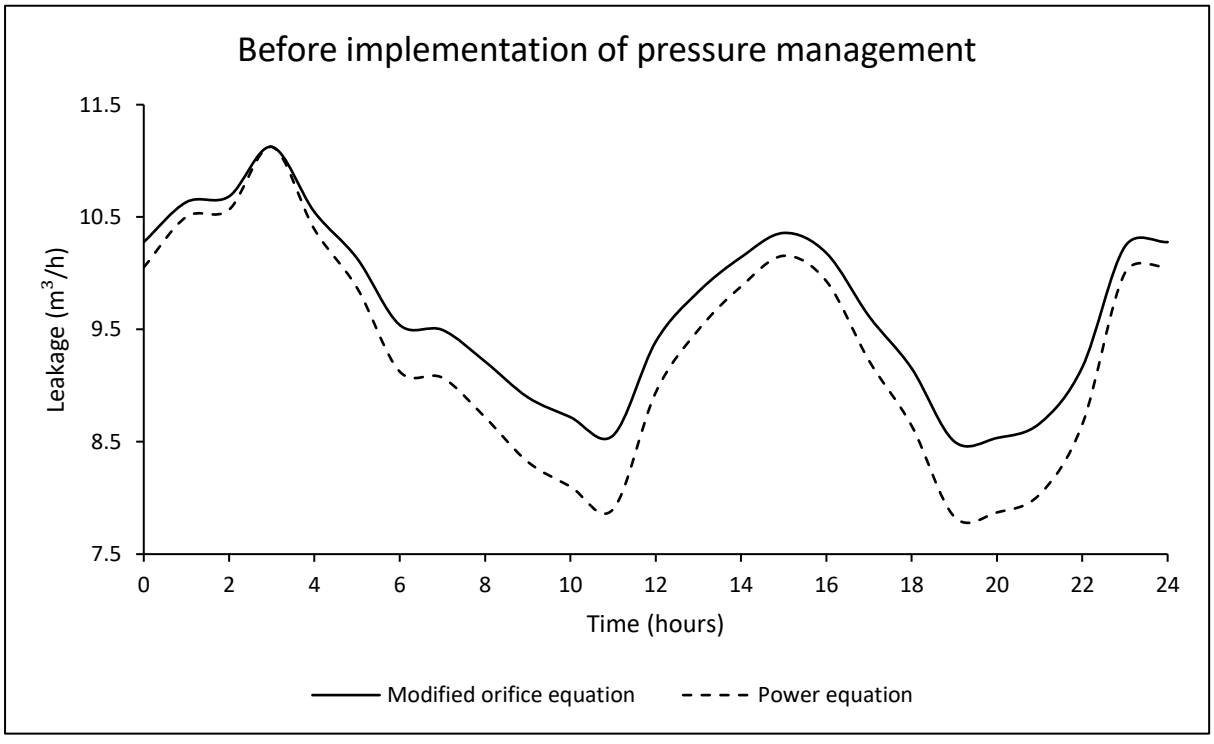

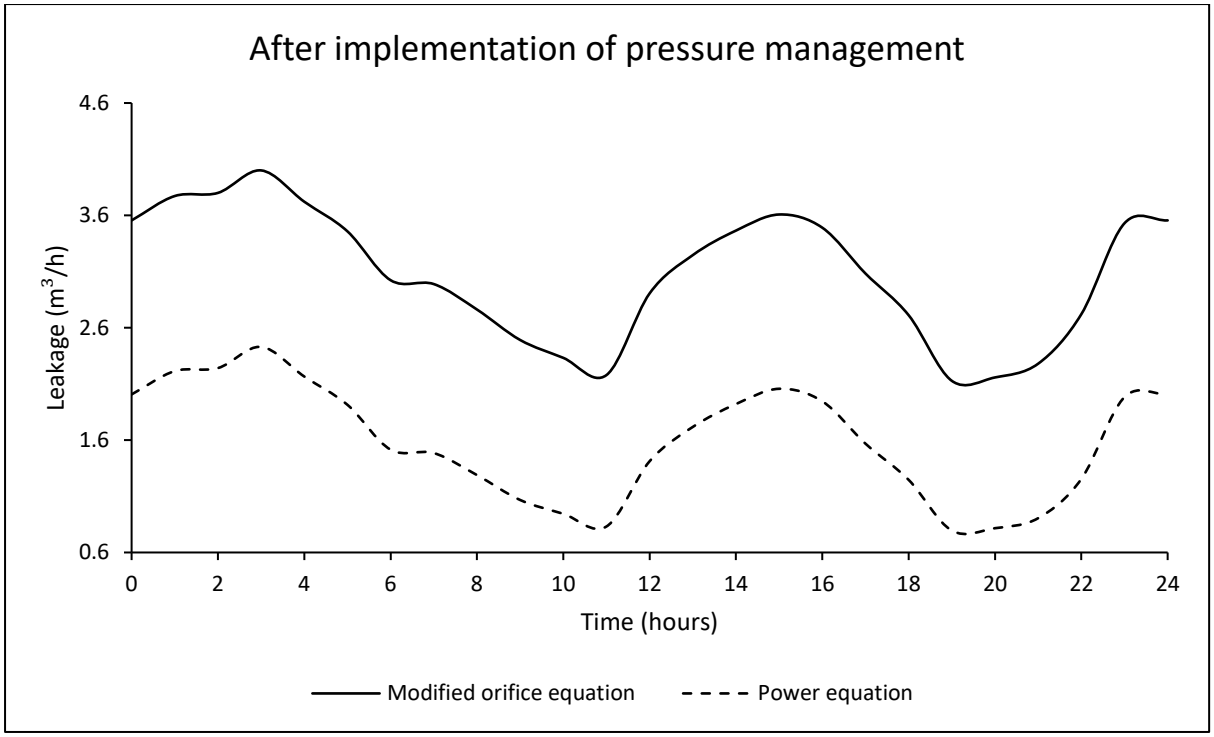
After implementation of pressure management
4.6
3.6
2.6
1.6
0.6
Leakage (m3/h)
0
2
4
6
8
10
12
14
16
18
20
22
24
Time (hours)
Modified orifice equation
Power equation

Number of iterations required for a system to converge to a hydraulic solution for both formulations

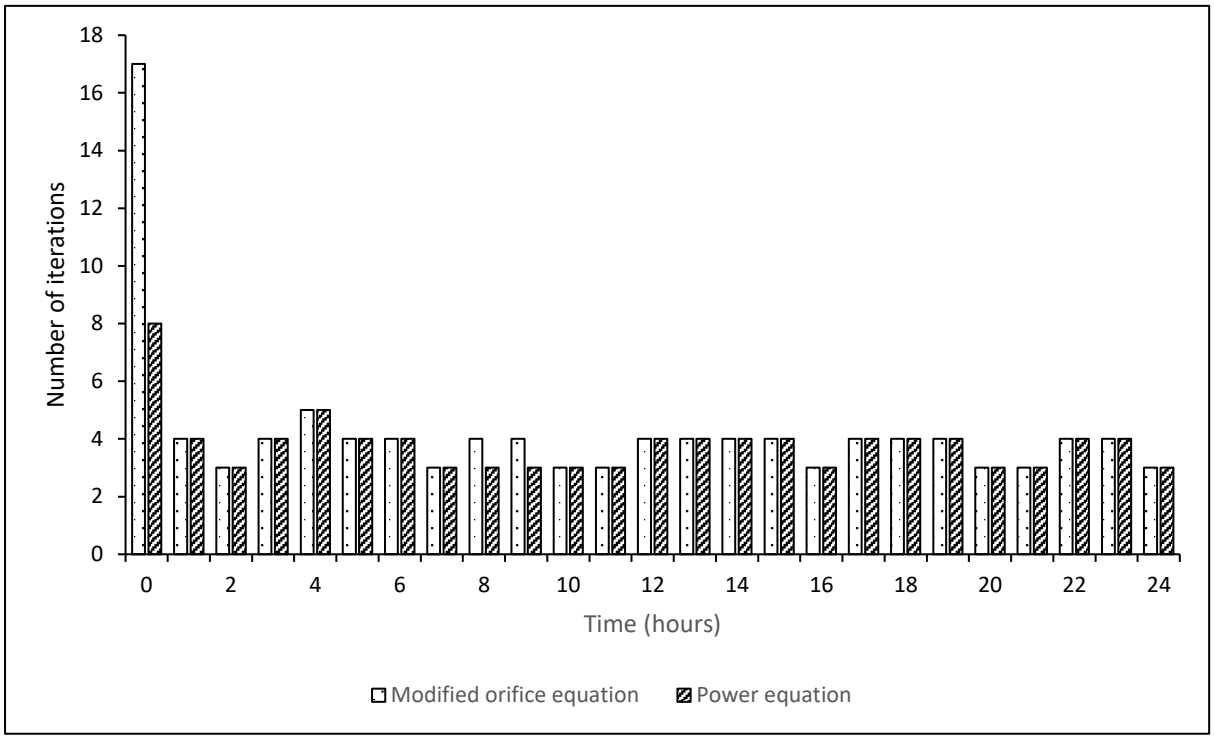

Results for combined systems

System parameters for both power and modified orifice formulations

	Minimum	Arithmetic Mean	Median	Maximum
Leakage exponent N1	0.89	1.08	1.07	1.37
Leakage coefficient C	1.5E-04	5.8E-04	5.6E-04	1.3E-03
Effective initial leak area C_dA0 (mm^2)	201.21	652.24	668.34	968.07
Effective head-area slope C_dm (mm^2/m)	7.62	11.11	10.91	15.82
Leakage number LN	0.63	1.51	1.33	6.43

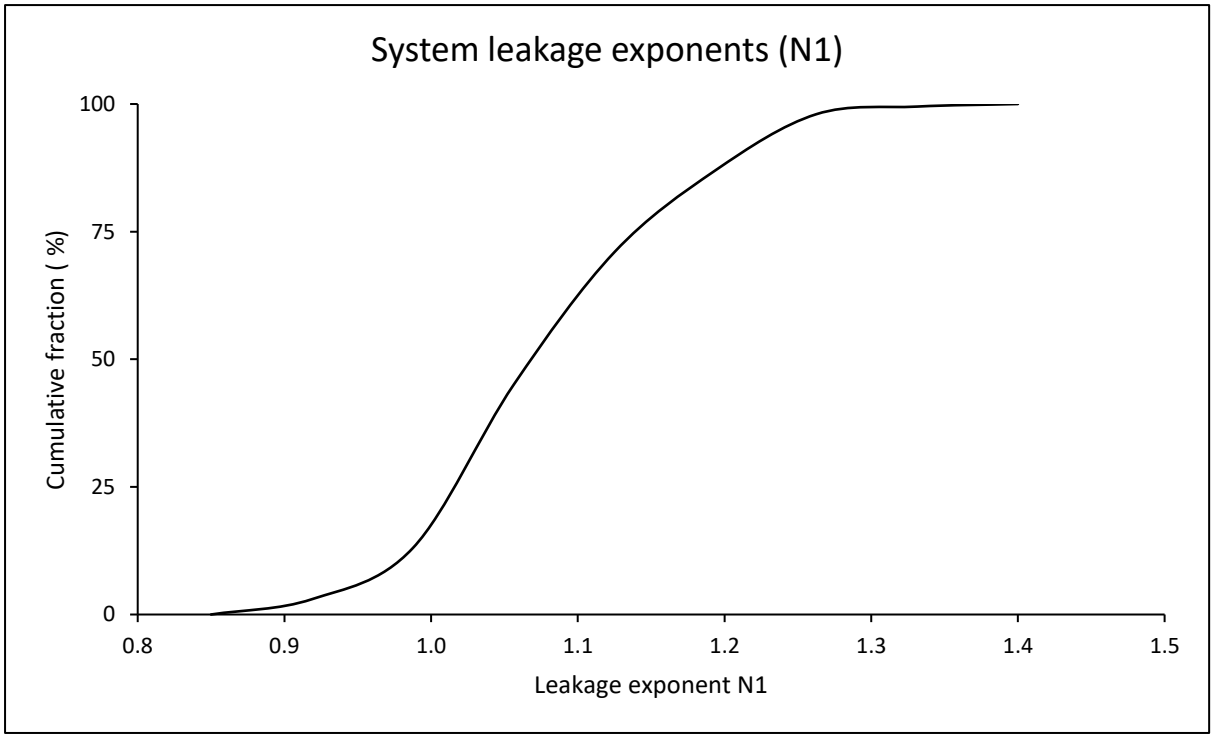

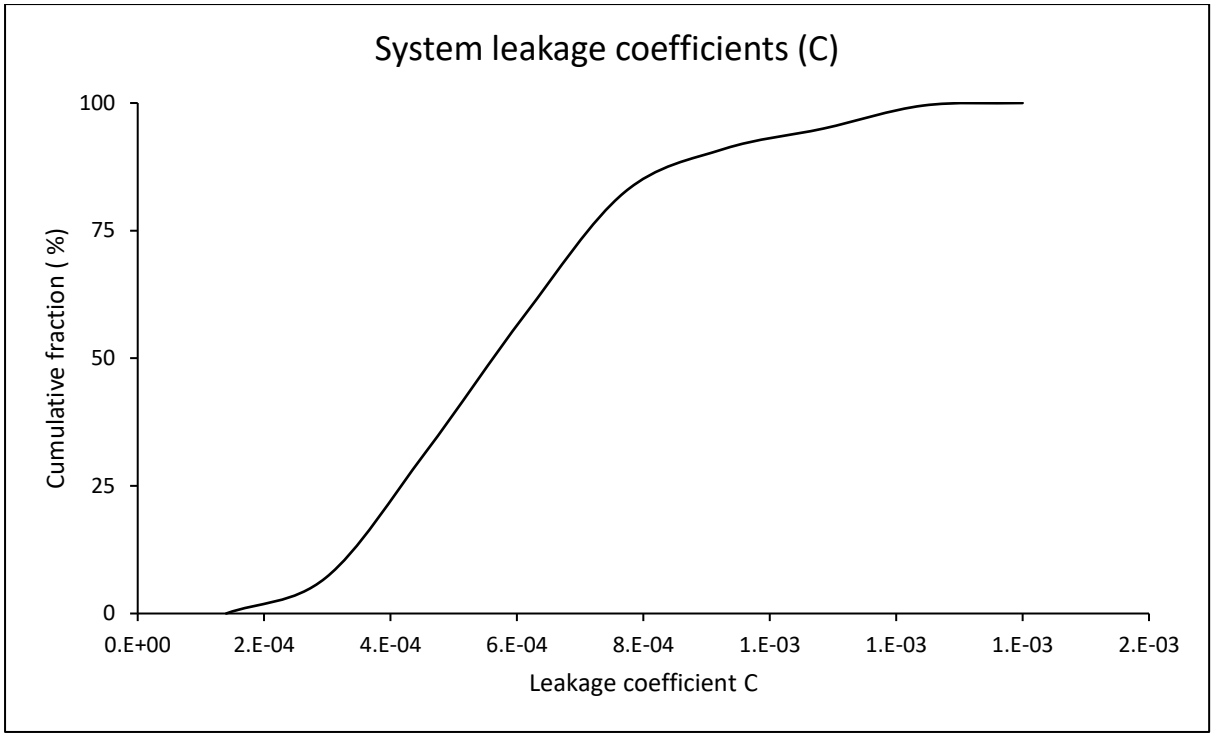
System leakage coefficients (C)
100
75
50
25
0
Cumulative fraction (%)
0.E+00
2.E-04
4.E-04
6.E-04
8.E-04
1.E-03
1.E-03
1.E-03
2.E-03
Leakage coefficient C

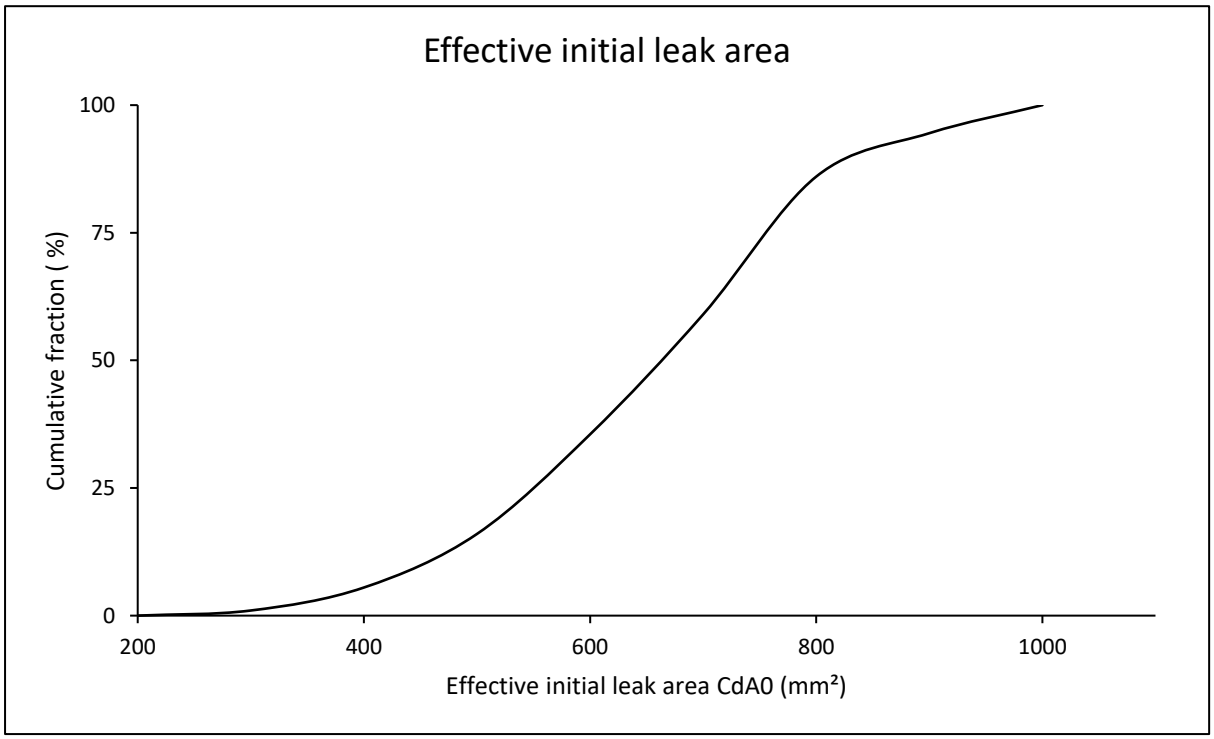
Effective initial leak area
100
75
50
25
0
Cumulative fraction (%)
200
400
600
800
1000
Effective initial leak area CdA0 (mm²)

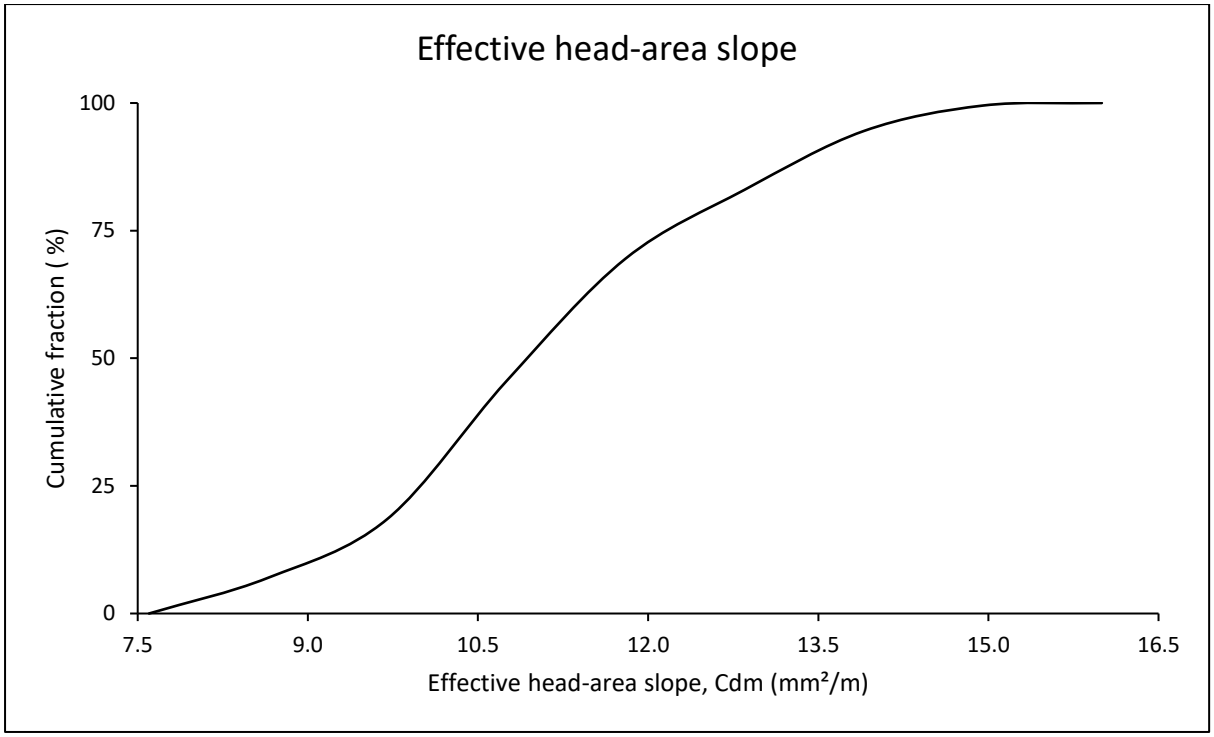
Effective head-area slope
100
75
50
25
0
Cumulative fraction (%)
7.5
9.0
10.5
12.0
13.5
15.0
16.5
Effective head-area slope, Cdm (mm²/m)

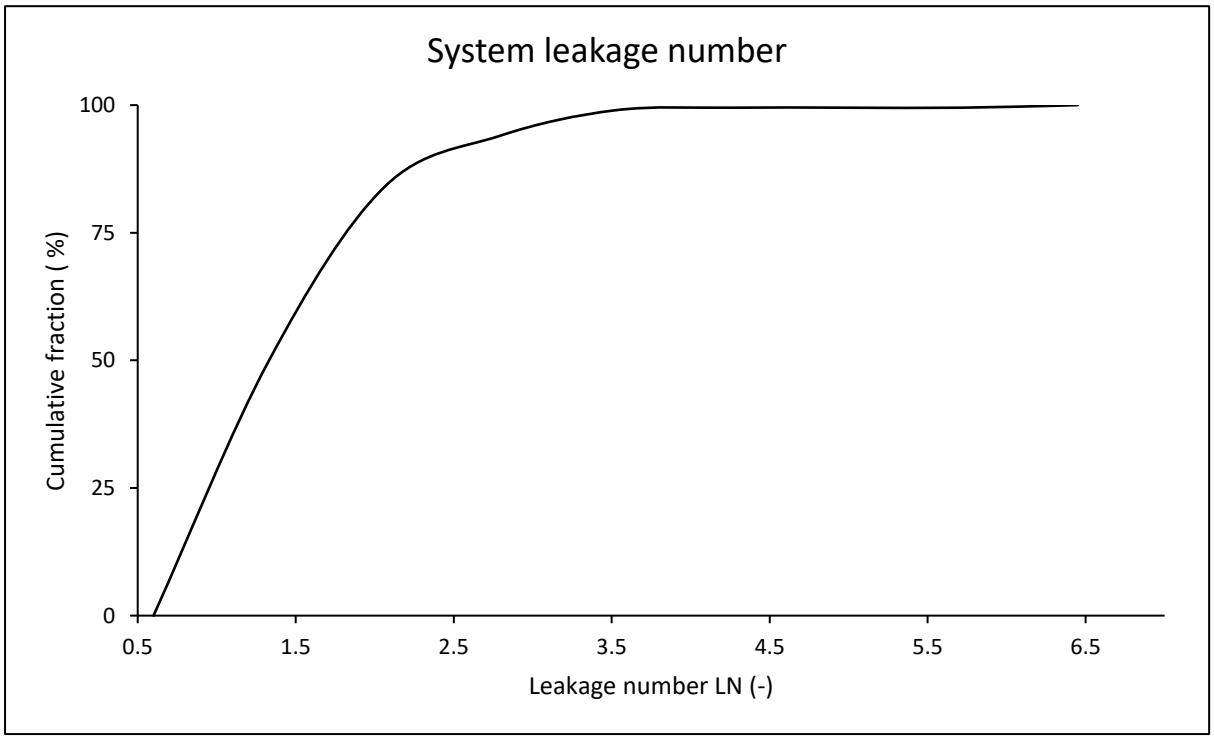
System leakage number
100
75
50
25
0
Cumulative fraction (%)
0.5
1.5
2.5
3.5
4.5
5.5
6.5
Leakage number LN (-)

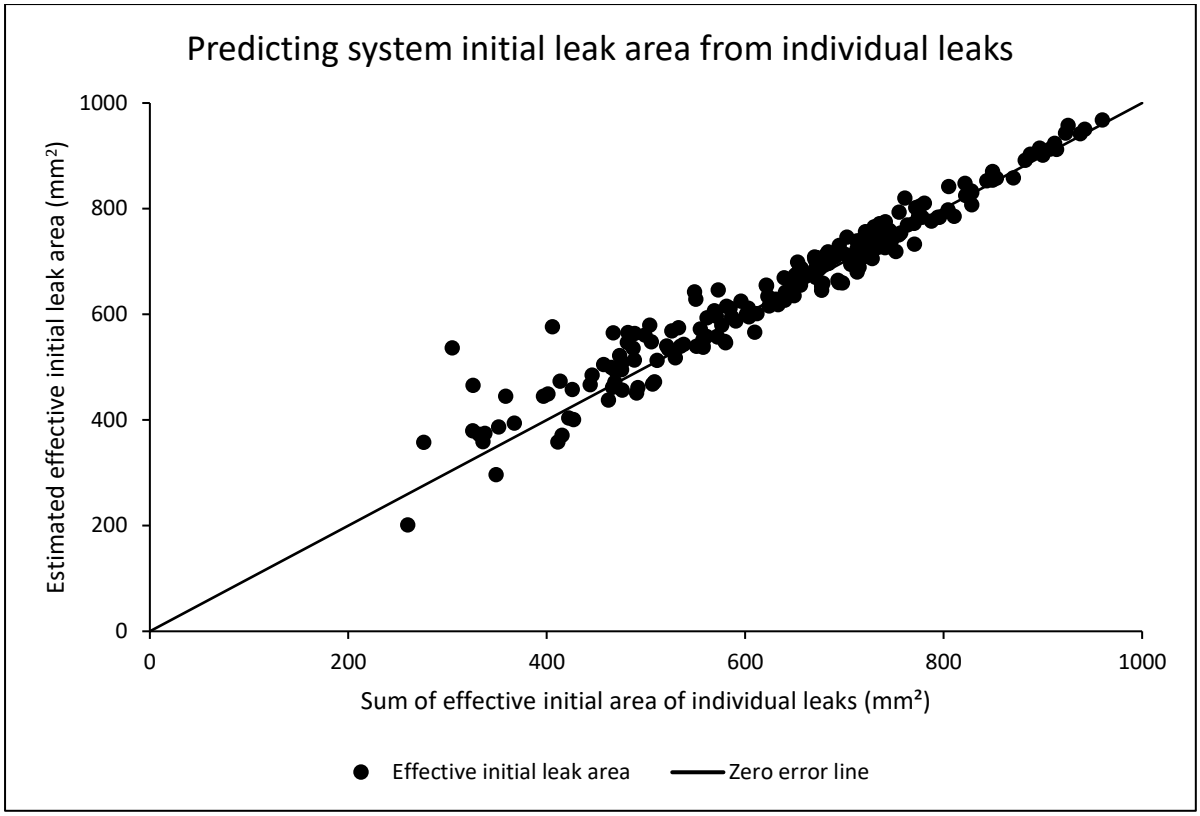
Predicting system initial leak area from individual leaks
Estimated effective initial leak area (mm²)
1000
800
600
400
200
0
0
200
400
600
800
1000
Sum of effective initial area of individual leaks (mm²)
Effective initial leak area
Zero error line

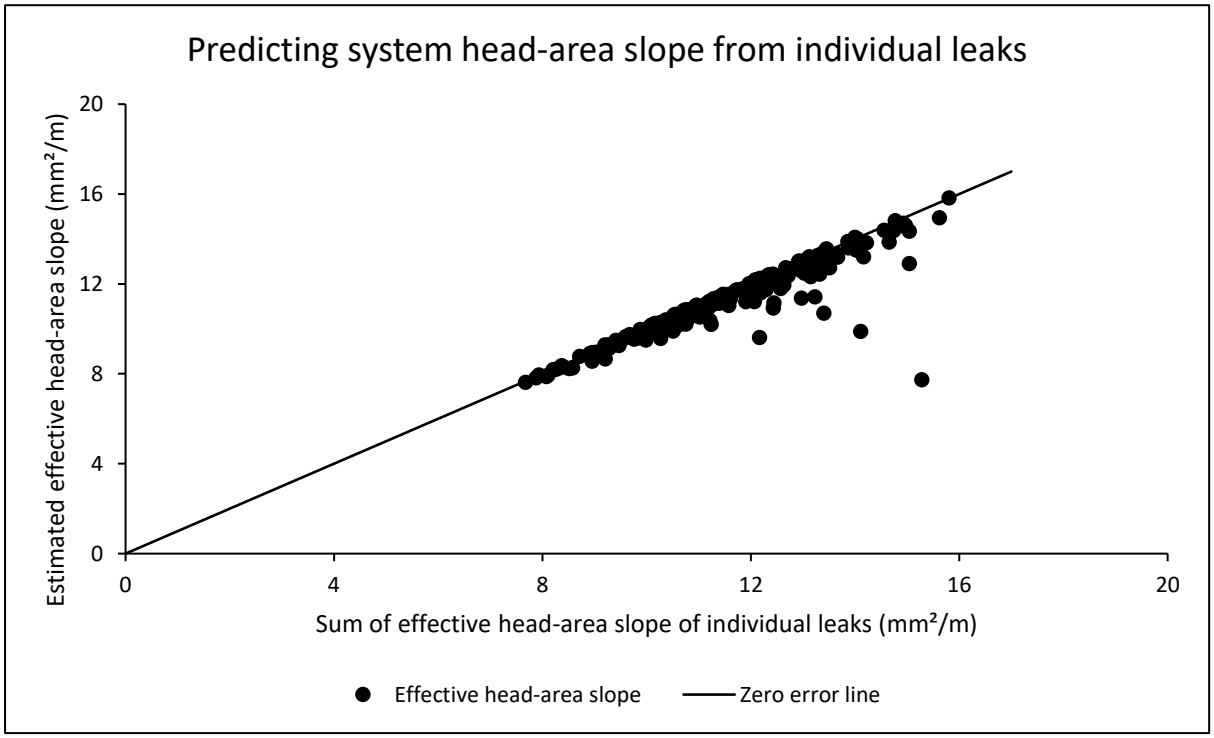
Predicting system head-area slope from individual leaks
Estimated effective head-area slope (mm²/m)
20
16
12
8
4
0
0
4
8
12
16
20
Sum of effective head-area slope of individual leaks (mm²/m)
Effective head-area slope
Zero error line

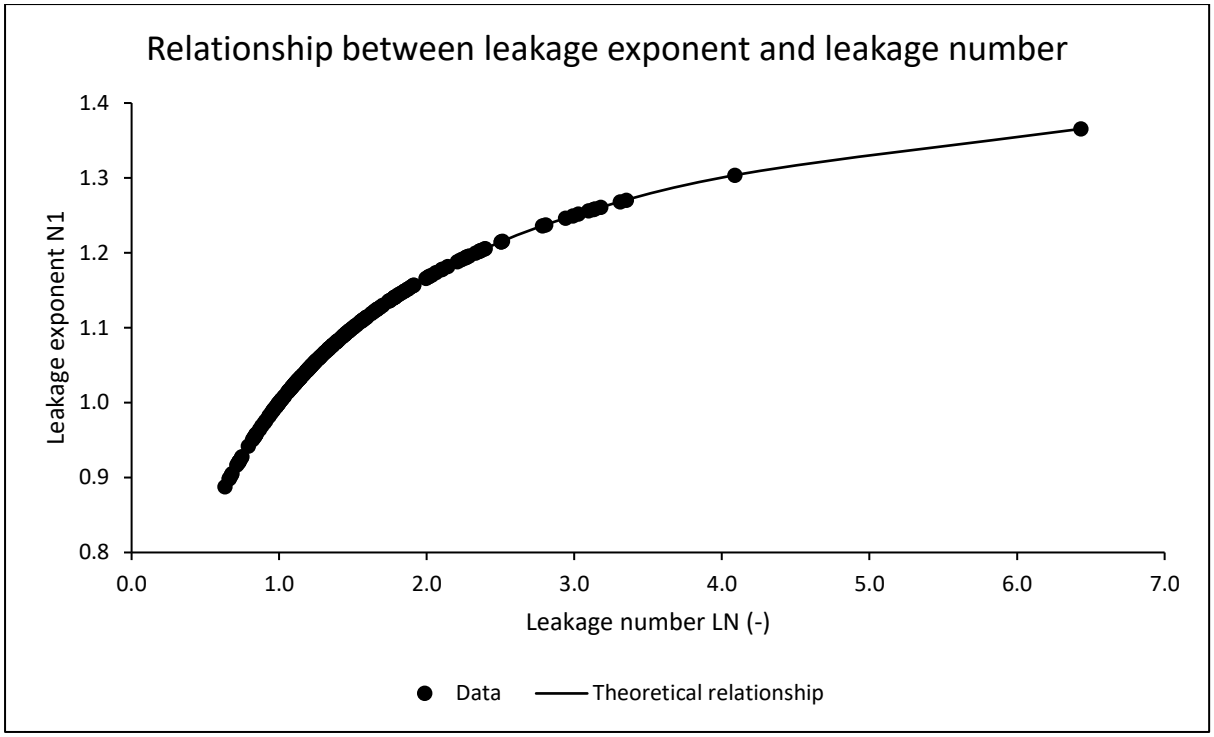
Relationship between leakage exponent and leakage number
Leakage exponent N1
1.4
1.3
1.2
1.1
1.0
0.9
0.8
0.0
1.0
2.0
3.0
4.0
5.0
6.0
7.0
Leakage number LN (-)
Data
Theoretical relationship

Average iterations required for a system to converge using both formulations

	Minimum	Arithmetic Mean	Median	Maximum
Modified orifice equation	3.92	4.15	4.16	4.52
Power equation	3.40	3.66	3.64	4.00

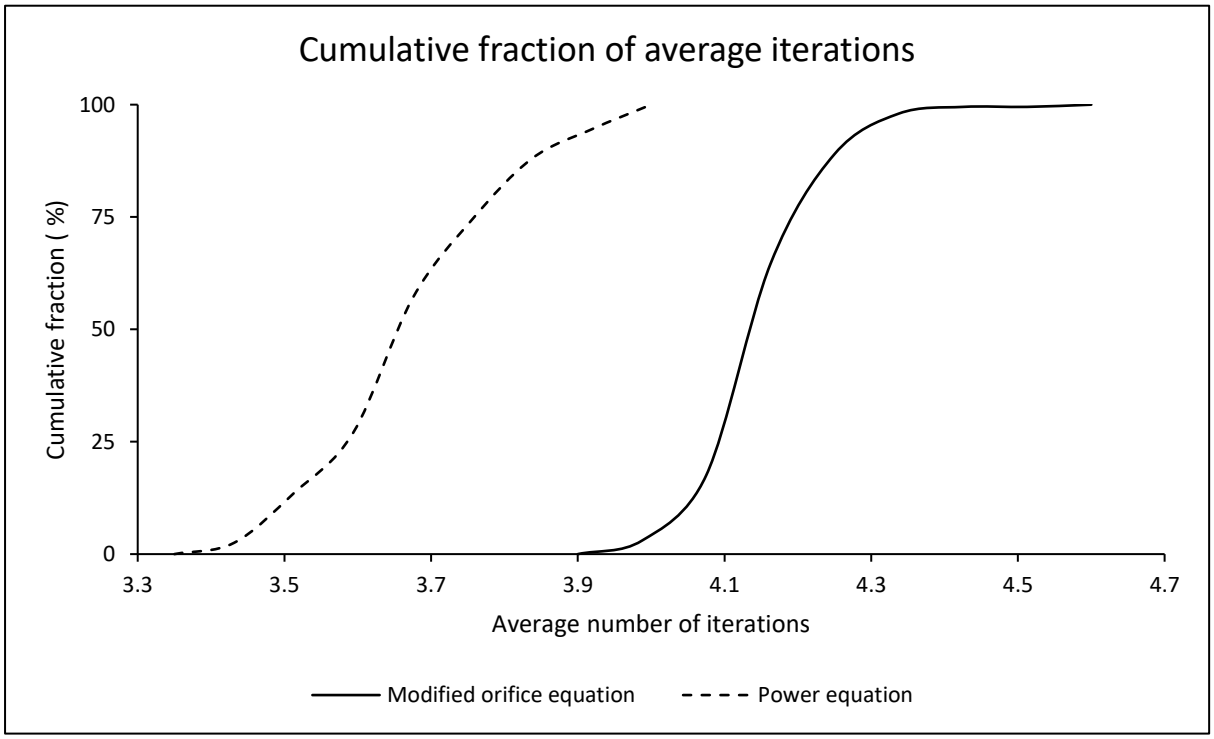

Effect of leakage on pressure at both average zone pressure (AZP) and critical node

AZP node								
	During MNF conditions				During peak demand conditions			
	Min (m)	Mean (m)	Median (m)	Max (m)	Min (m)	Mean (m)	Median (m)	Max (m)
Modified orifice equation	-5.15	-3.36	-3.36	-1.89	-10.95	-9.30	-9.40	-6.03
Power equation	-5.15	-3.36	-3.36	-1.89	-11.03	-9.29	-9.43	-5.93
Critical node								
Modified orifice equation	-21.60	-4.76	-4.23	-1.90	-24.63	-12.02	-11.69	-6.15
Power equation	-21.60	-4.76	-4.23	-1.90	-26.18	-12.00	-11.63	-6.04

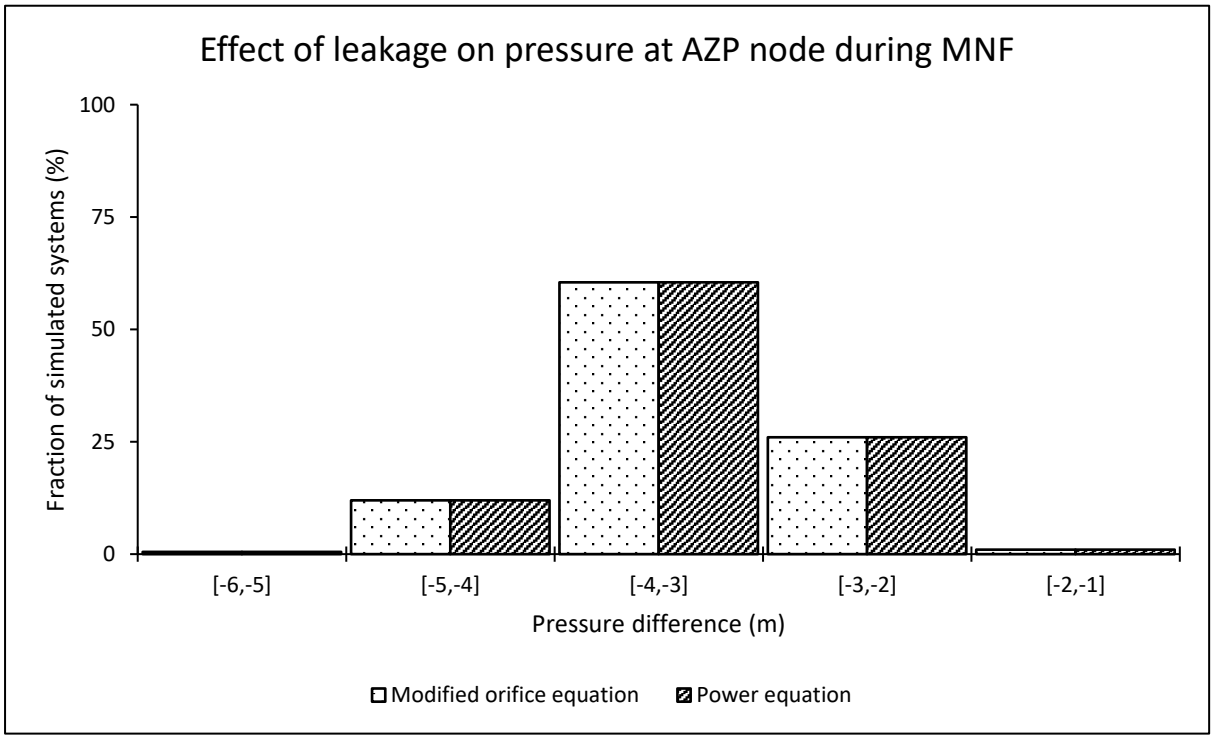

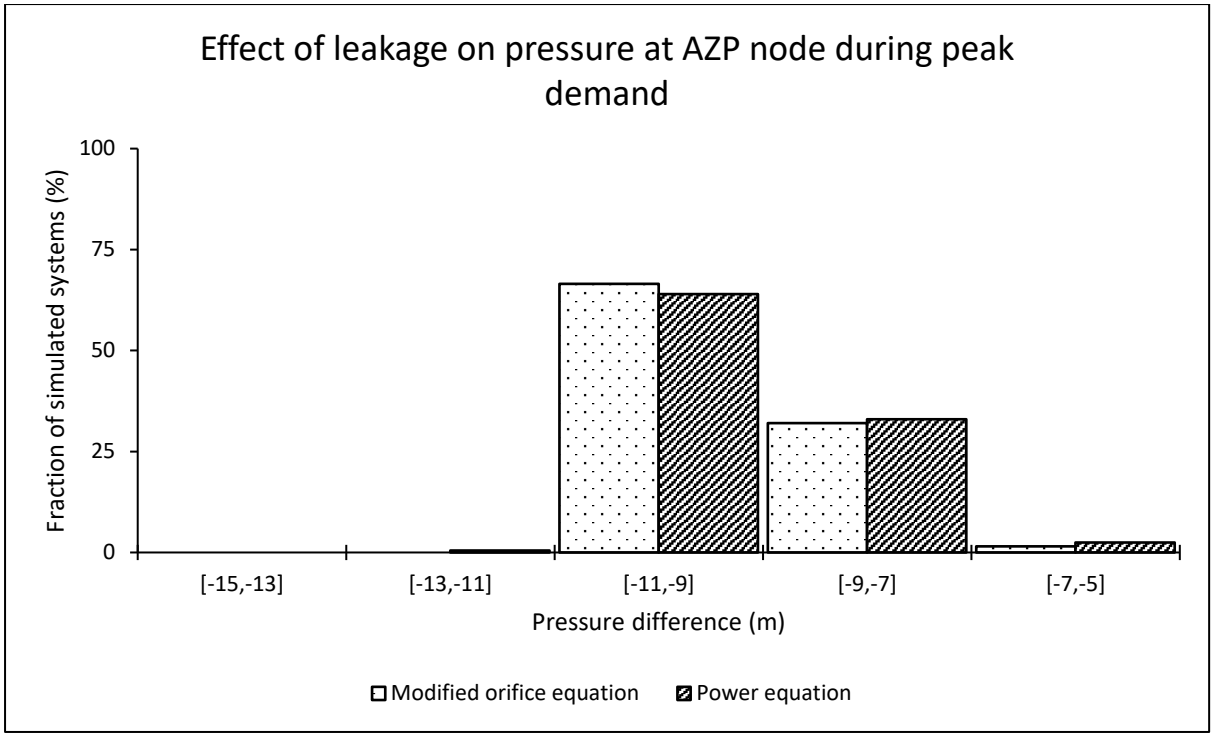
Effect of leakage on pressure at AZP node during peak demand
Fraction of simulated systems (%)
100
75
50
25
0
[-15,-13]
[-13,-11]
[-11,-9]
[-9,-7]
[-7,-5]
Pressure difference (m)
Modified orifice equation
Power equation

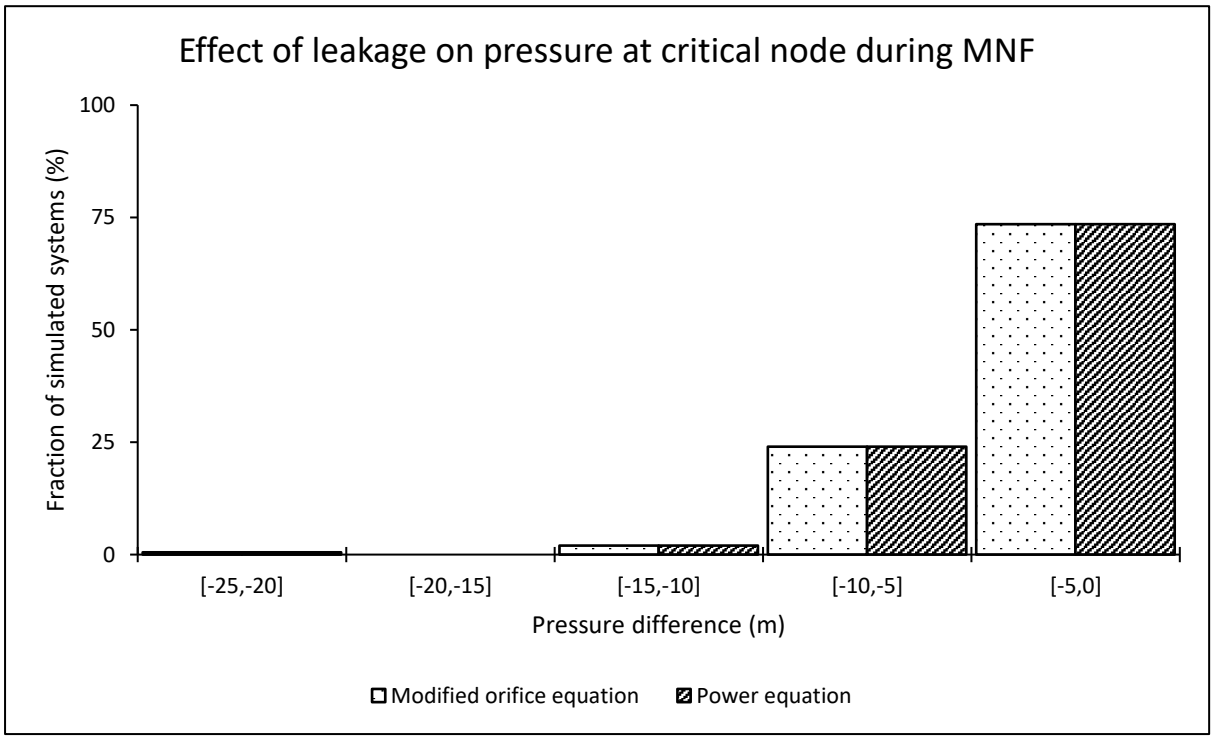
Effect of leakage on pressure at critical node during MNF
Fraction of simulated systems (%)
100
75
50
25
0
[-25,-20]
[-20,-15]
[-15,-10]
[-10,-5]
[-5,0]
Pressure difference (m)
Modified orifice equation
Power equation

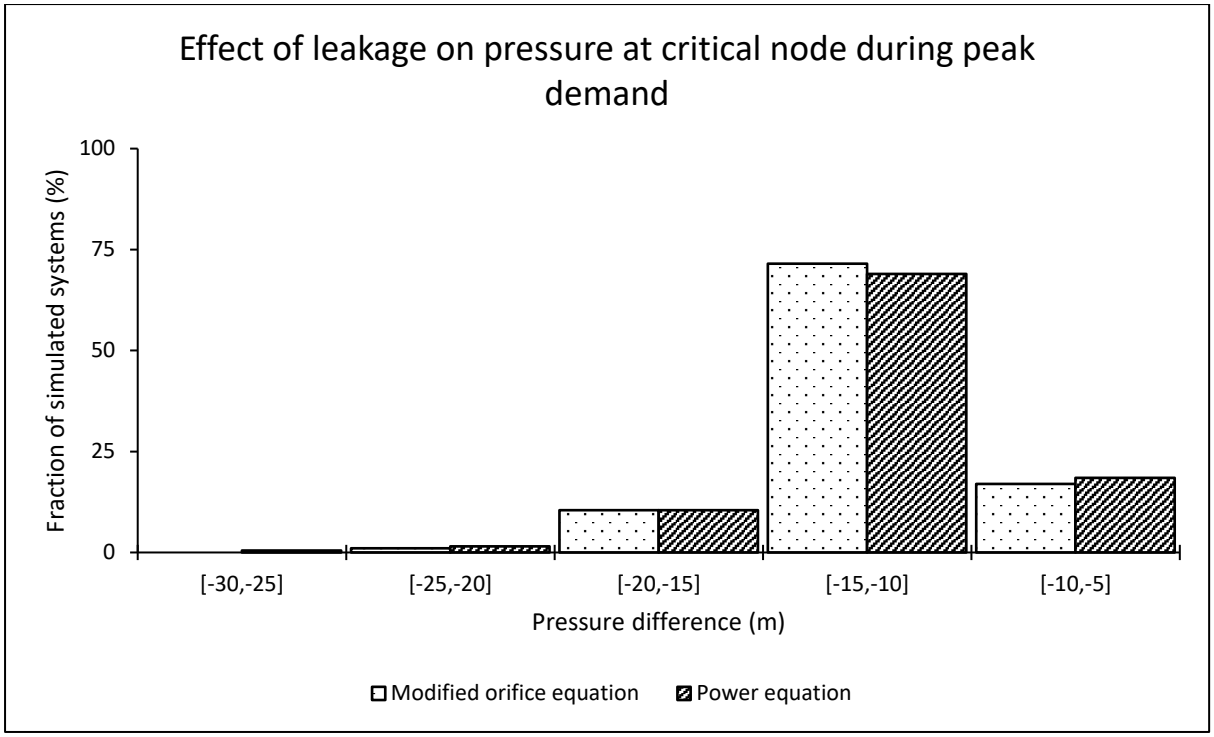
Effect of leakage on pressure at critical node during peak demand
Fraction of simulated systems (%)
100
75
50
25
0
[-30,-25]
[-25,-20]
[-20,-15]
[-15,-10]
[-10,-5]
Pressure difference (m)
Modified orifice equation
Power equation

Pressure estimation error when using the power equation at average zone pressure (AZP) and critical nodes

	During MNF conditions				During peak demand conditions			
	Min (%)	**Mean (%)**	**Median (%)**	**Max (%)**	**Min (%)**	**Mean (%)**	**Median (%)**	**Max (%)**
At the AZP node	0.00	0.00	0.00	0.00	-0.42	0.02	0.02	0.31
At the critical node	0.00	0.00	0.00	0.00	-3.36	0.01	0.08	0.58

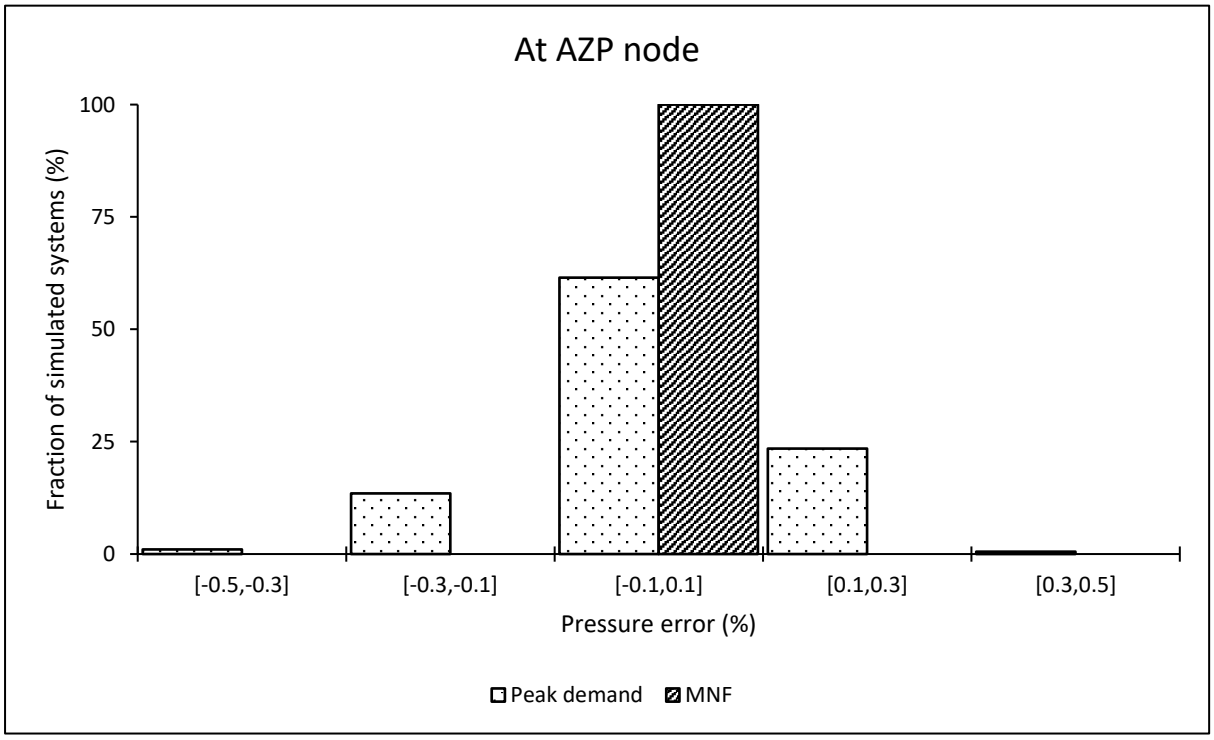

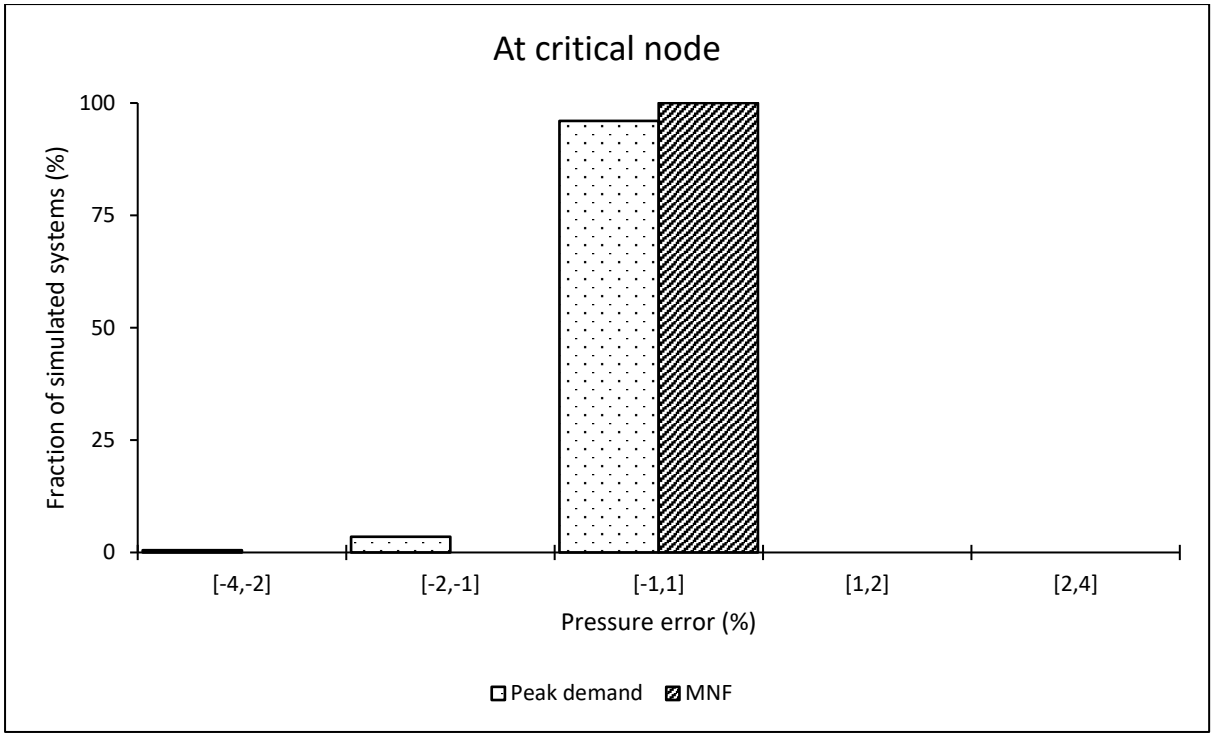
At critical node
Fraction of simulated systems (%)
100
75
50
25
0
[-4,-2]
[-2,-1]
[-1,1]
[1,2]
[2,4]
Pressure error (%)
Peak demand
MNF

System leakage estimation error when using the power equation

	Leakage estimation error (%)			
	Minimum	**Arithmetic Mean**	**Median**	**Maximum**
Before implementing pressure management	-0.55	0.03	0.02	1.89
After implementing pressure management	-22.36	-17.06	-17.46	4.44

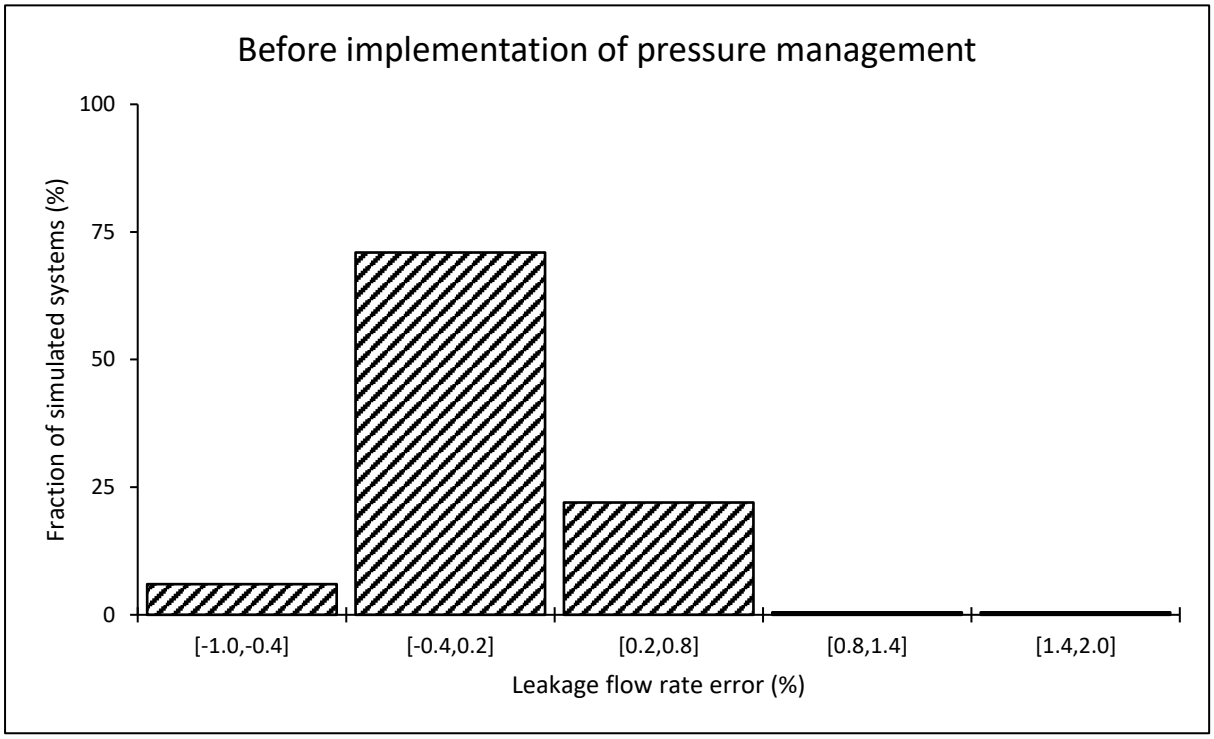

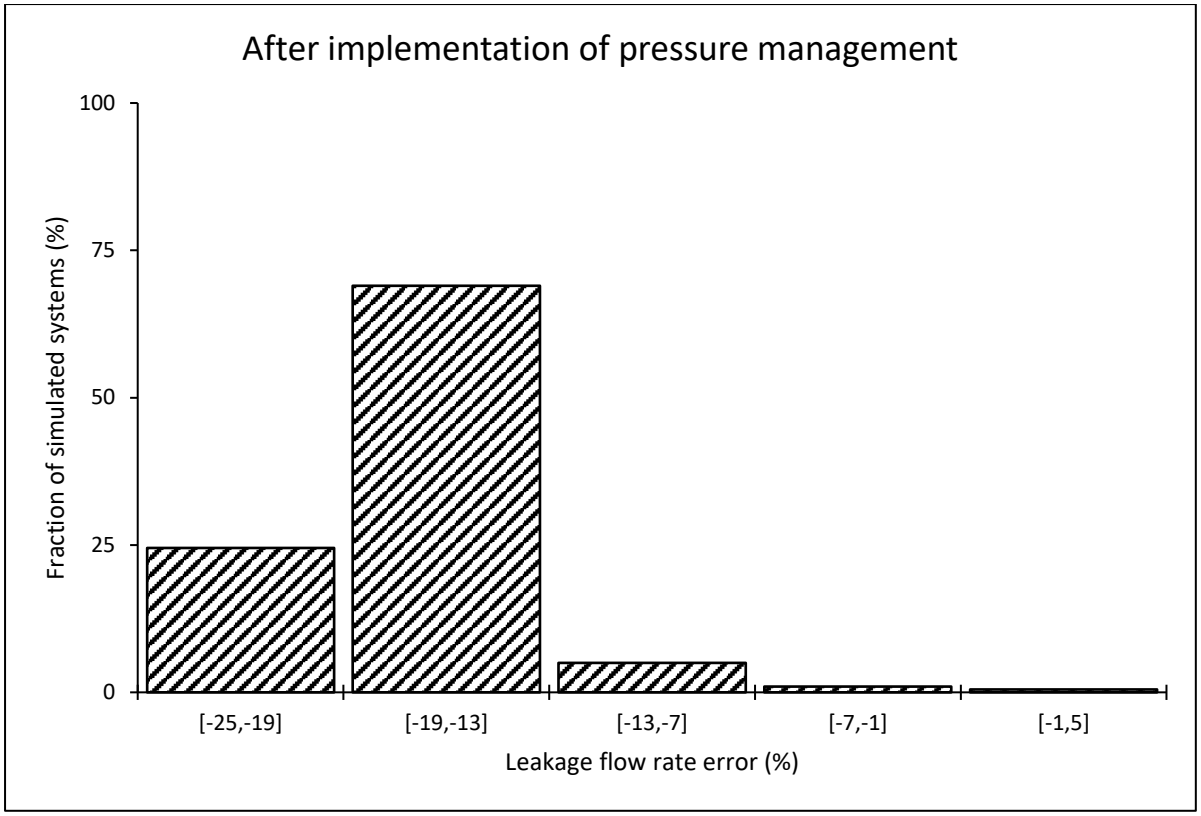
After implementation of pressure management
Fraction of simulated systems (%)
100
75
50
25
0
[-25,-19]
[-19,-13]
[-13,-7]
[-7,-1]
[-1,5]
Leakage flow rate error (%)

Leakage estimation error when using the power equation at the critical node

	Leakage estimation error (%)			
	Minimum	**Arithmetic Mean**	**Median**	**Maximum**
Before implementing pressure management	-9.78	-3.18	-2.48	2.93
After implementing pressure management	-72.21	-37.37	-38.68	21.96

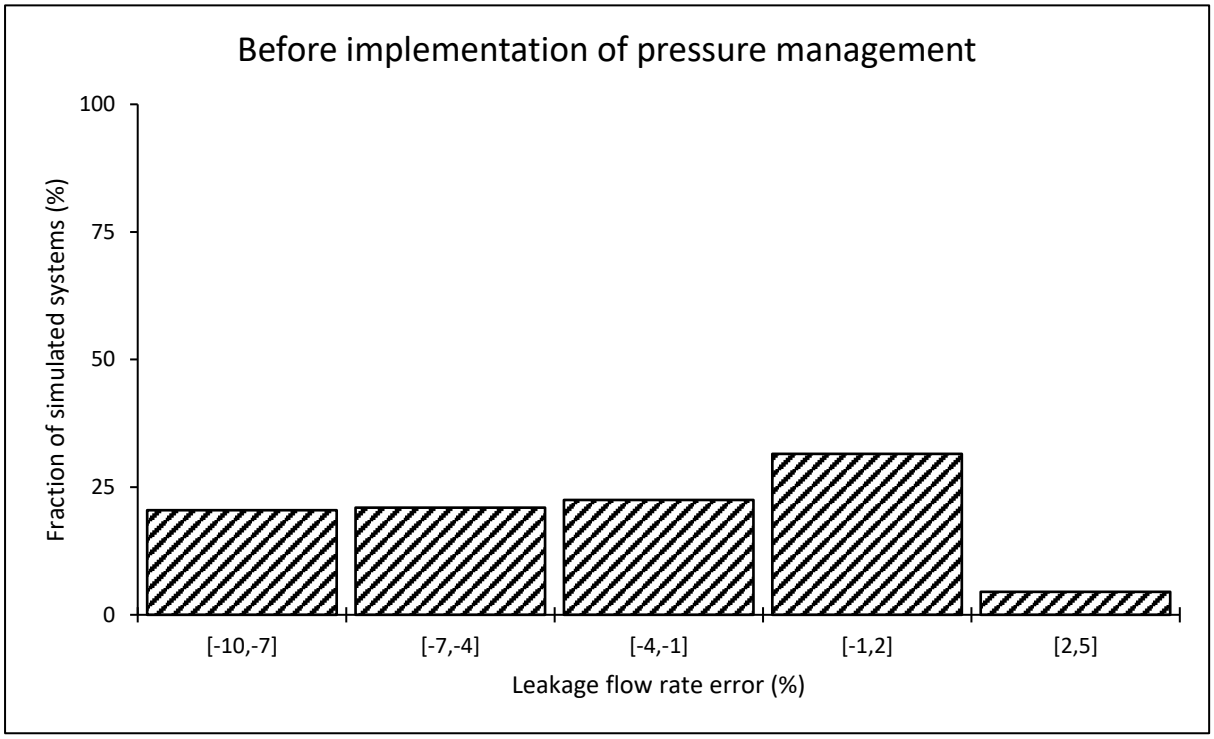

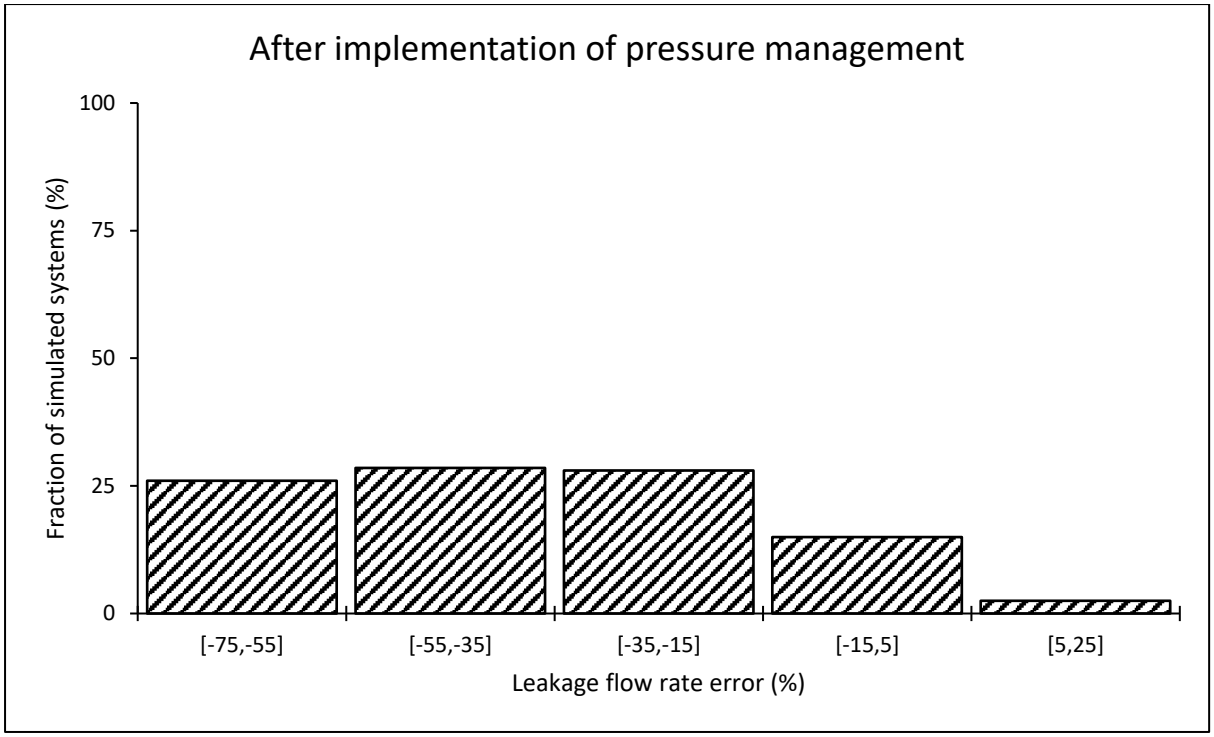
After implementation of pressure management
Fraction of simulated systems (%)
100
75
50
25
0
[-75,-55]
[-55,-35]
[-35,-15]
[-15,5]
[5,25]
Leakage flow rate error (%)

Appendix A-5: Medium-sized network with an ILI of 1

Results for an individual system

Pressure head at the average zone pressure (AZP) node

		Pressure head (m)			
		Minimum	**Arithmetic Mean**	**Median**	**Maximum**
Before pressure management	Without leaks	72.69	88.62	90.24	106.08
	Modified orifice equation	72.42	88.37	89.99	105.88
	Power equation	72.43	88.37	89.99	105.88
After pressure management	Modified orifice equation	22.56	38.48	40.09	55.95
	Power equation	22.57	38.49	40.10	55.96

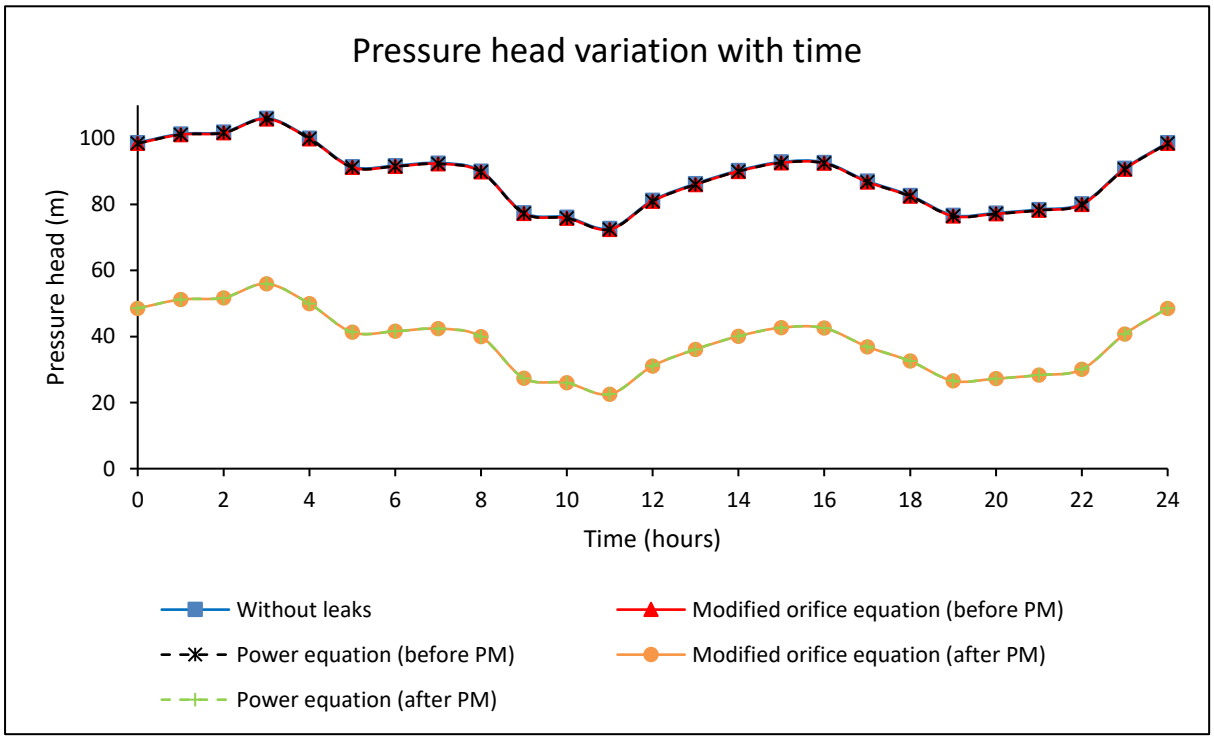

Pressure head at the critical node

		Pressure head (m)			
		Minimum	**Arithmetic Mean**	**Median**	**Maximum**
Before pressure management	Without leaks	60.21	75.09	76.77	90.93
	Modified orifice equation	59.95	74.85	76.53	90.74
	Power equation	59.96	74.85	76.54	90.74
After pressure management	Modified orifice equation	10.08	24.95	26.63	40.81
	Power equation	10.10	24.96	26.64	40.81

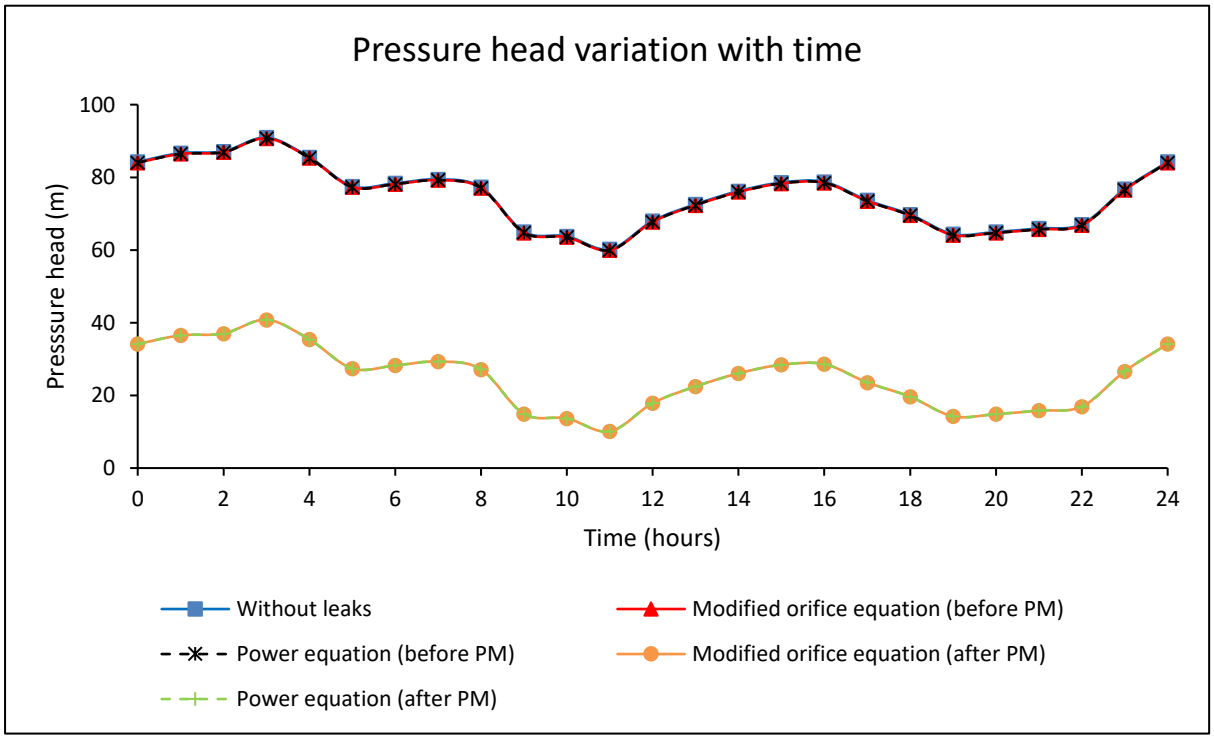

System leakage flow rate

		Leakage flow rate (m^3/h)			
		Minimum	**Arithmetic Mean**	**Median**	**Maximum**
Before pressure management	Modified orifice equation	9.06	10.28	10.43	11.58
	Power equation	8.94	10.24	10.39	11.58
After pressure management	Modified orifice equation	4.50	6.06	6.26	7.58
	Power equation	3.89	5.63	5.85	7.33

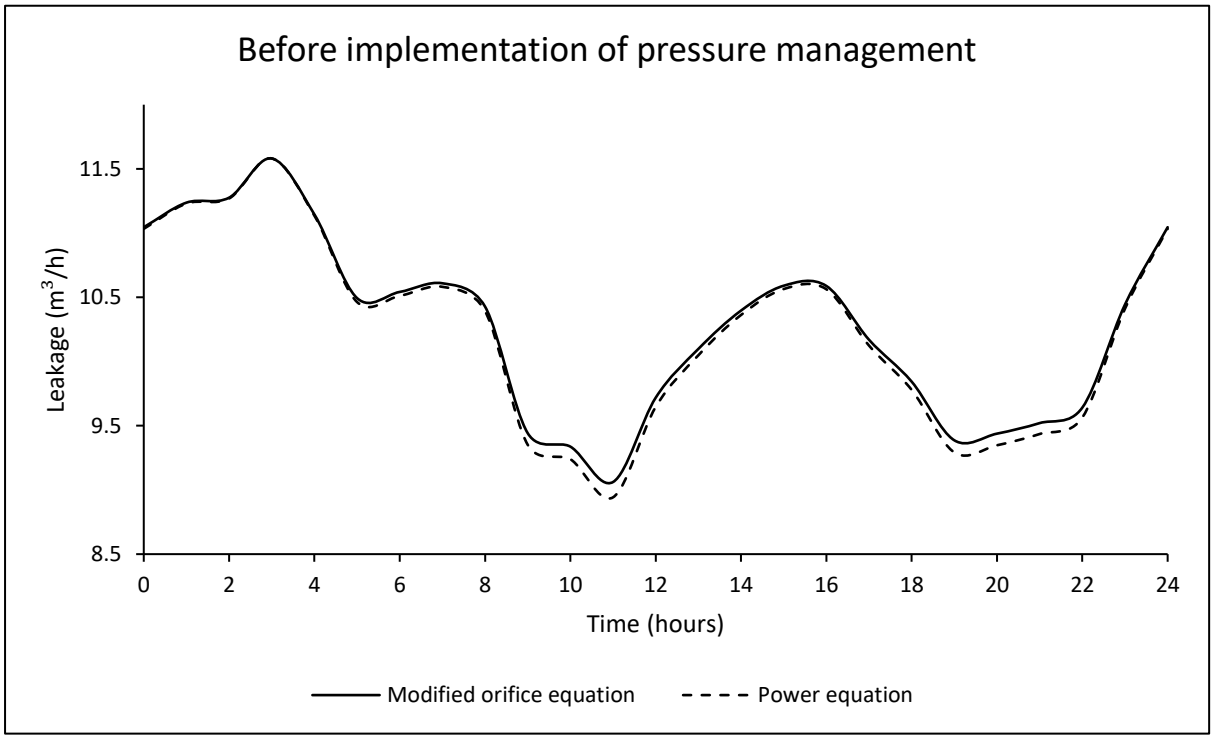

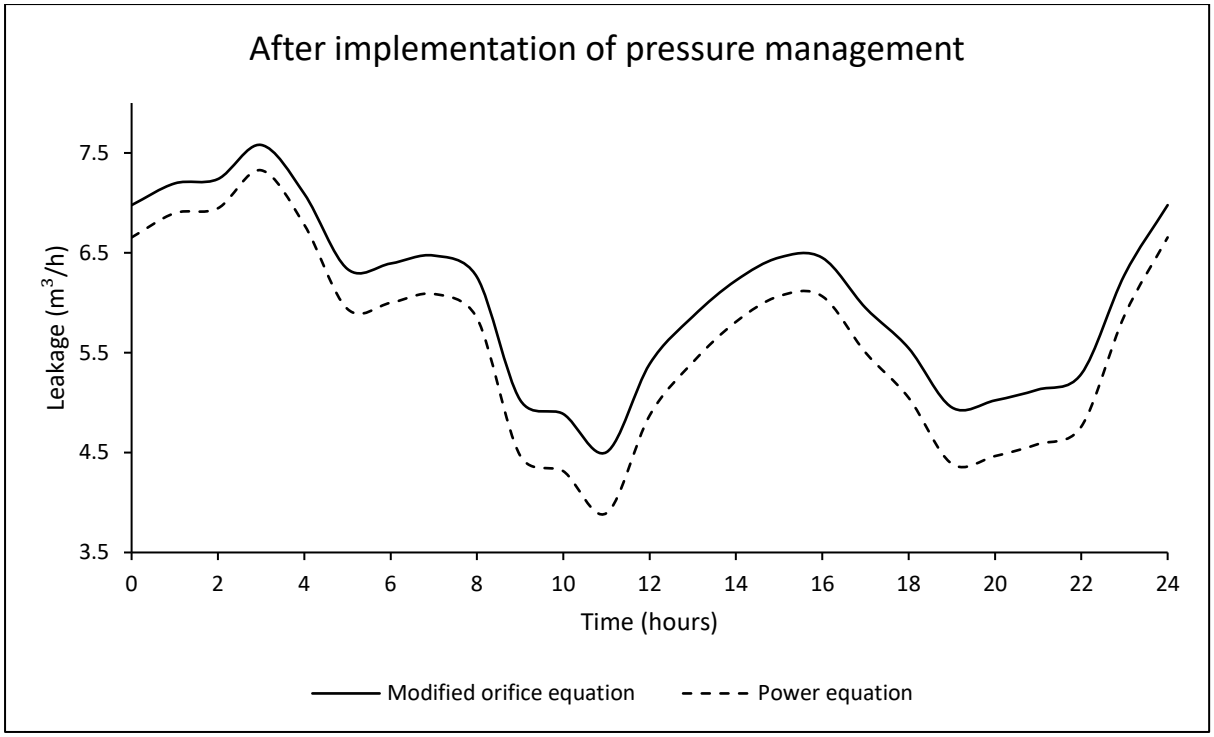
After implementation of pressure management
Leakage (m3/h)
7.5
6.5
5.5
4.5
3.5
0
2
4
6
8
10
12
14
16
18
20
22
24
Time (hours)
Modified orifice equation
Power equation

Leakage flow rate at the critical node

		Leakage flow rate (m^3/h)			
		Minimum	**Arithmetic Mean**	**Median**	**Maximum**
Before pressure management	Modified orifice equation	0.82	0.95	0.97	1.09
	Power equation	0.81	0.95	0.97	1.09
After pressure management	Modified orifice equation	0.29	0.48	0.50	0.64
	Power equation	0.23	0.43	0.46	0.62

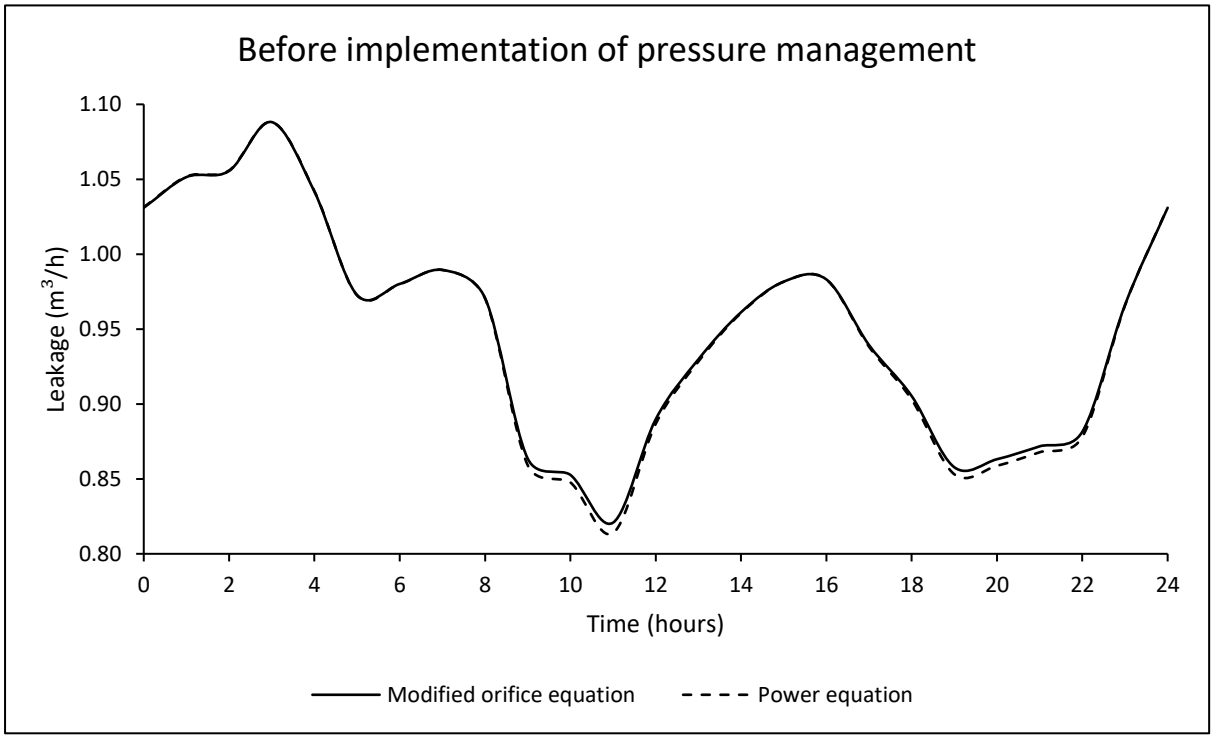

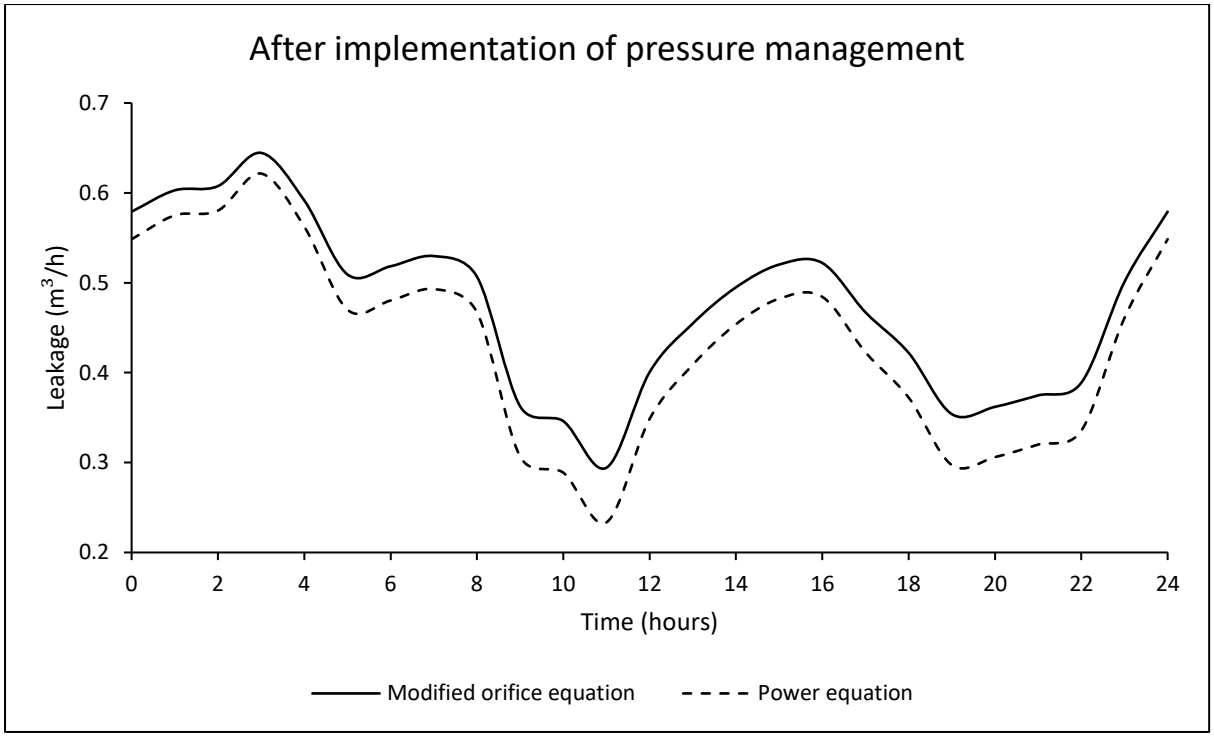
After implementation of pressure management
0.7
0.6
0.5
0.4
0.3
0.2
Leakage (m3/h)
0
2
4
6
8
10
12
14
16
18
20
22
24
Time (hours)
Modified orifice equation
Power equation

Number of iterations required for a system to converge to a hydraulic solution for both formulations

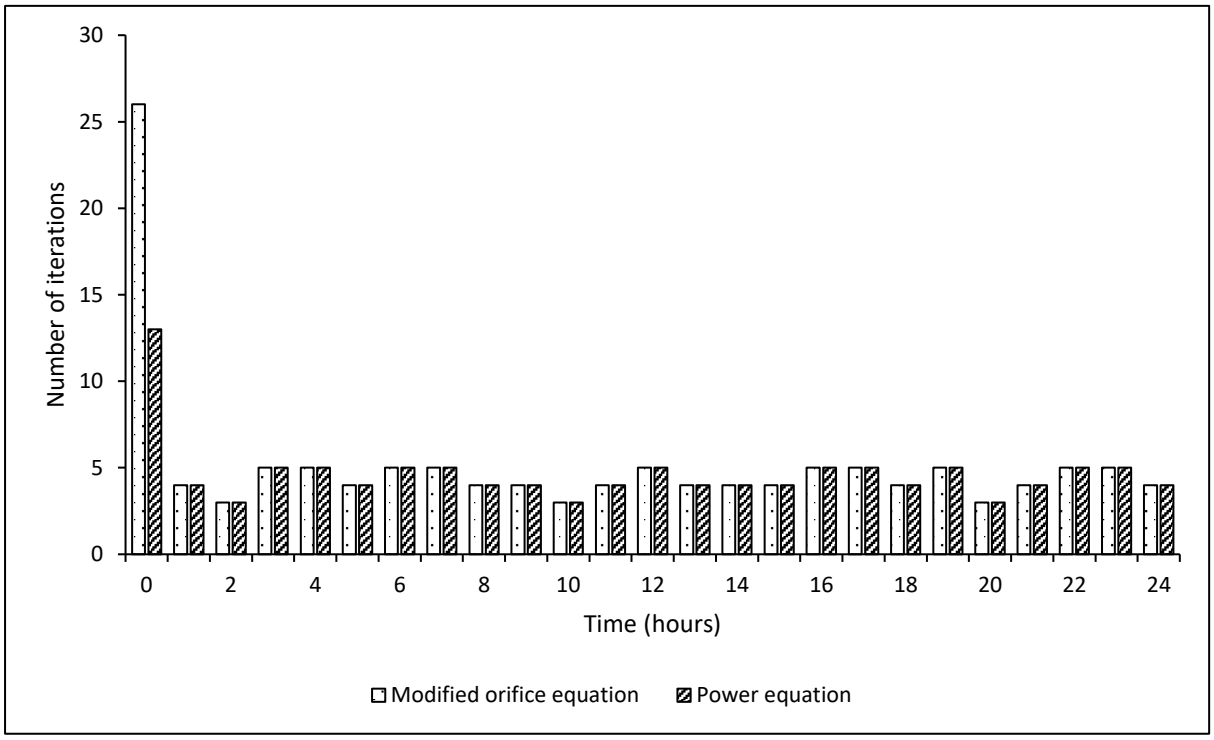

Results for combined systems

System parameters for both power and modified orifice formulations

	Minimum	Arithmetic Mean	Median	Maximum
Leakage exponent N1	0.64	0.68	0.67	0.83
Leakage coefficient C	6.9E-05	1.4E-04	1.4E-04	1.6E-04
Effective initial leak area C_dA0 (mm^2)	47.97	57.79	58.58	61.33
Effective head-area slope C_dm (mm^2/m)	0.10	0.13	0.12	0.23
Leakage number LN	0.17	0.23	0.20	0.49

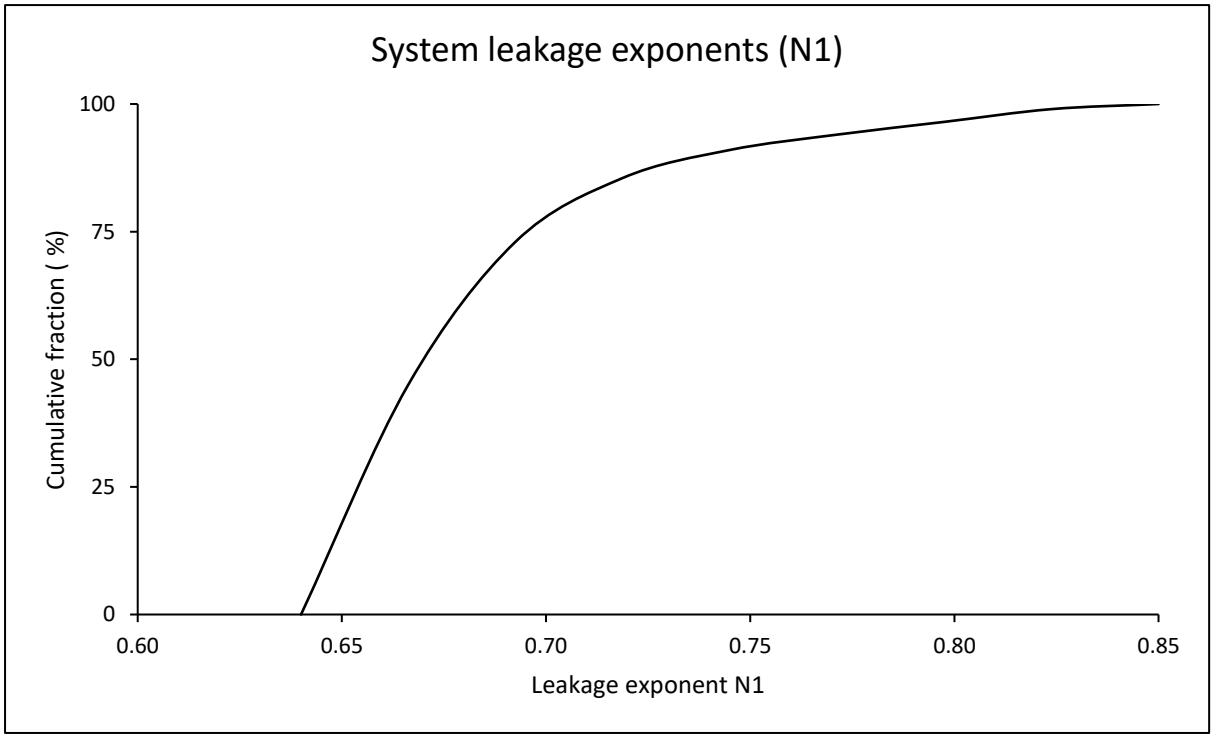

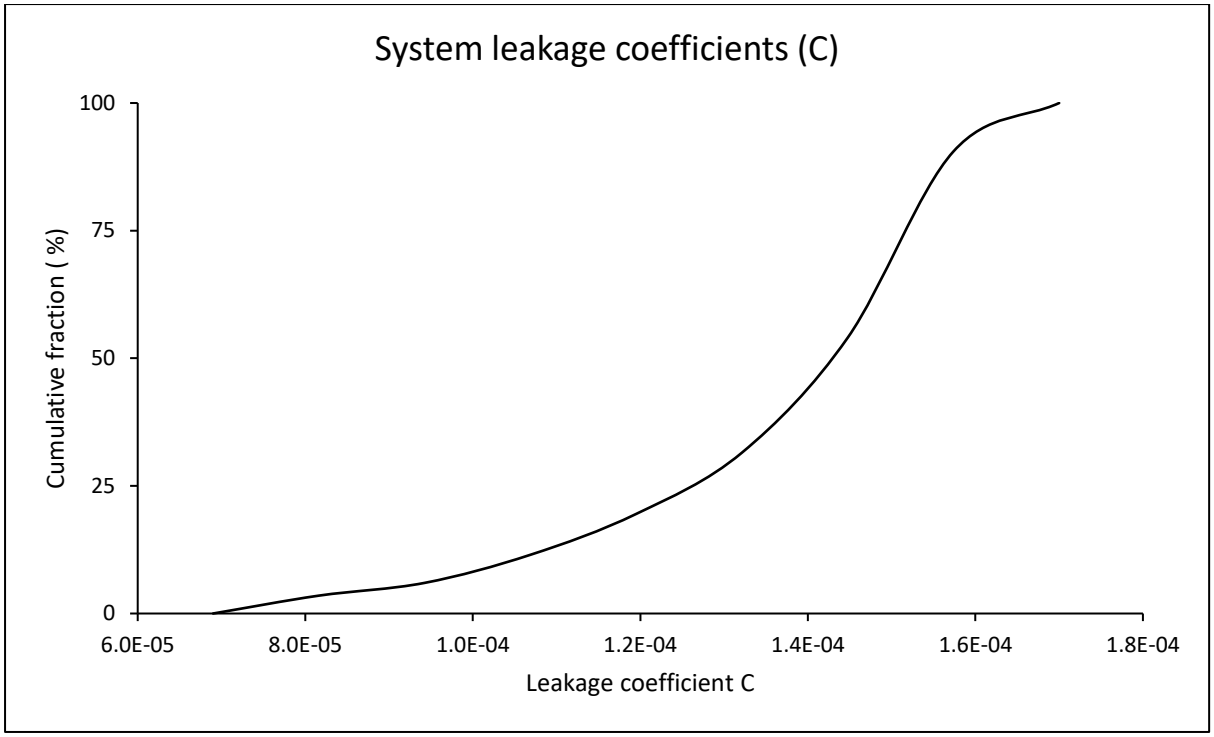
System leakage coefficients (C)
Cumulative fraction (%)
100
75
50
25
0
6.0E-05
8.0E-05
1.0E-04
1.2E-04
1.4E-04
1.6E-04
1.8E-04
Leakage coefficient C

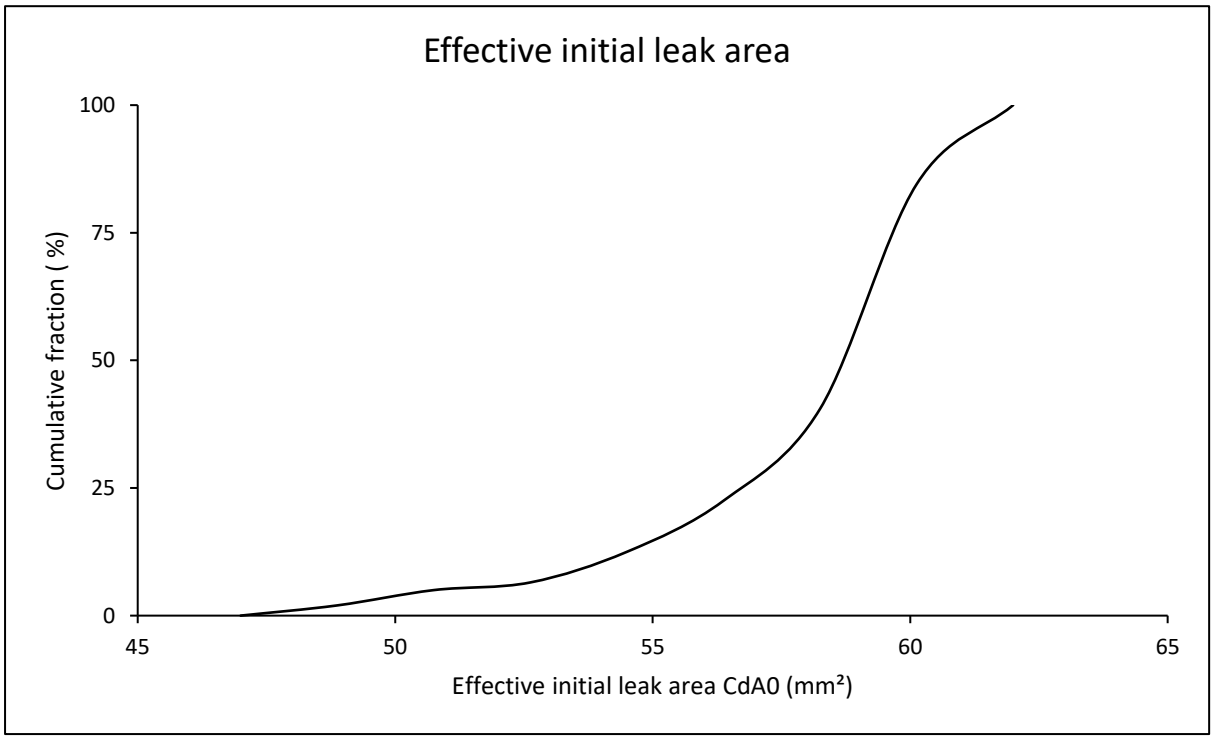
Effective initial leak area
Cumulative fraction (%)
100
75
50
25
0
45
50
55
60
65
Effective initial leak area CdA0 (mm²)

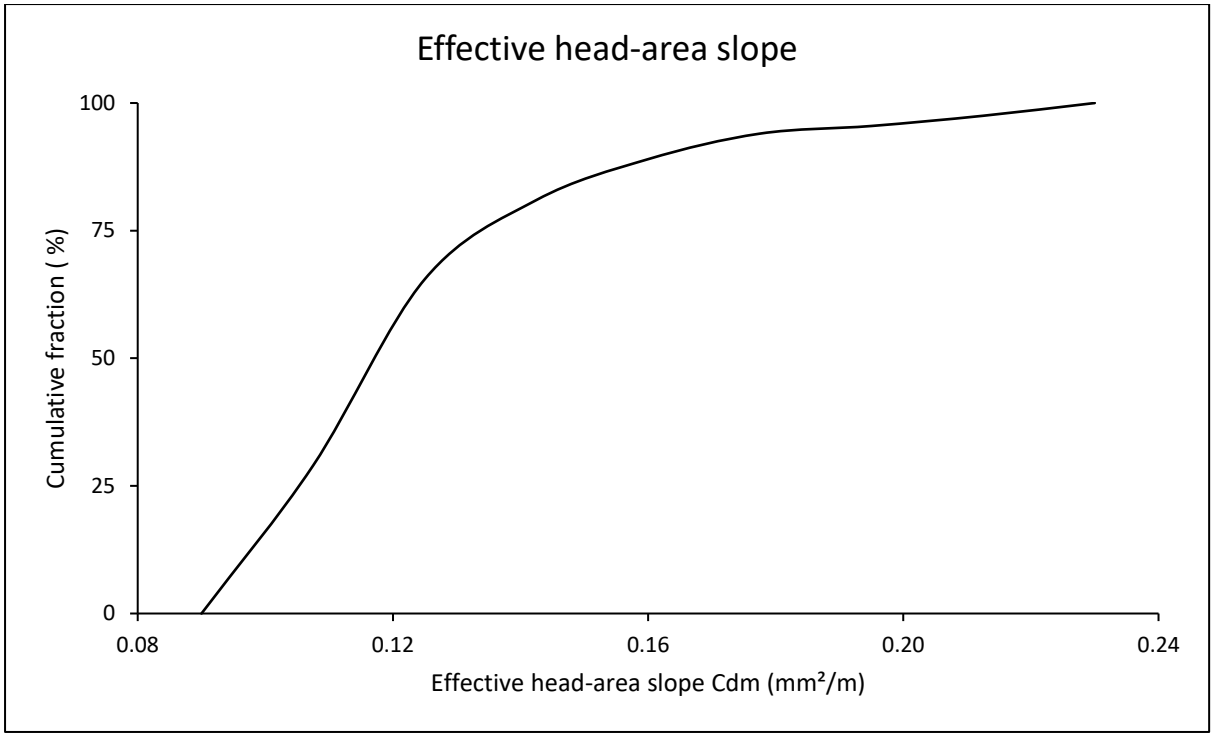
Effective head-area slope
100
75
50
25
0
Cumulative fraction (%)
0.08
0.12
0.16
0.20
0.24
Effective head-area slope Cdm (mm²/m)

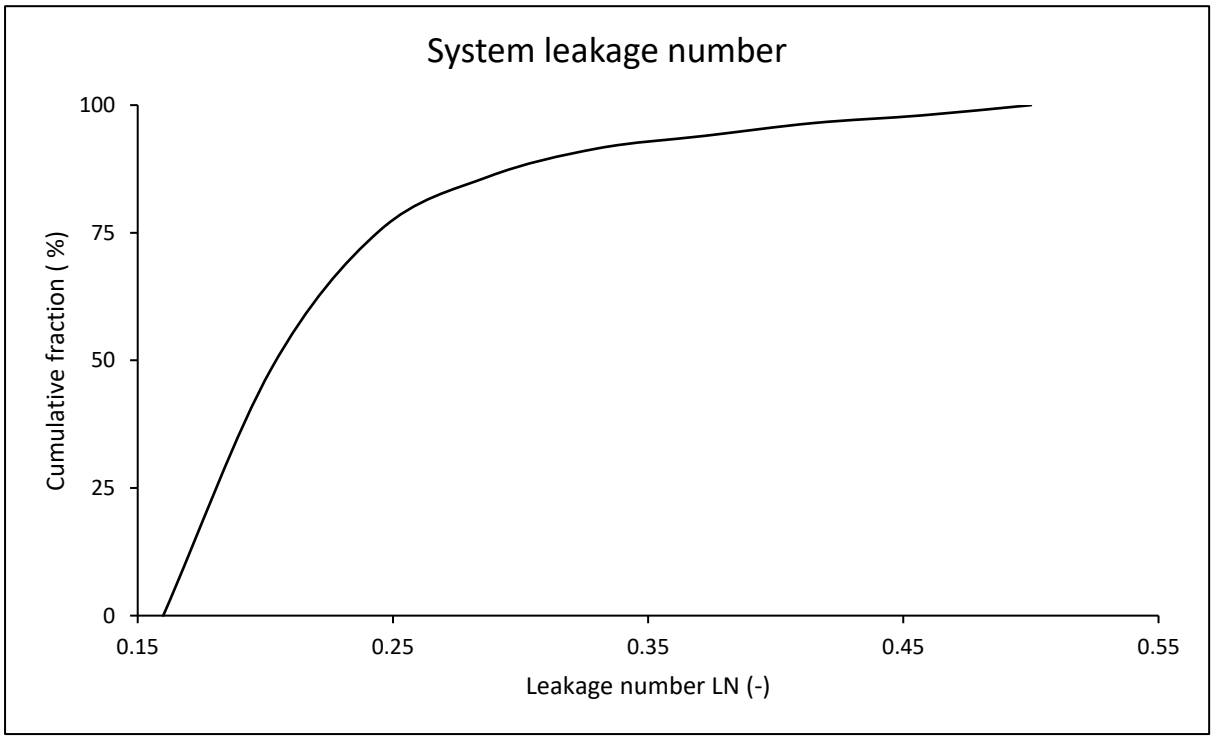
System leakage number
100
75
50
25
0
Cumulative fraction (%)
0.15
0.25
0.35
0.45
0.55
Leakage number LN (-)

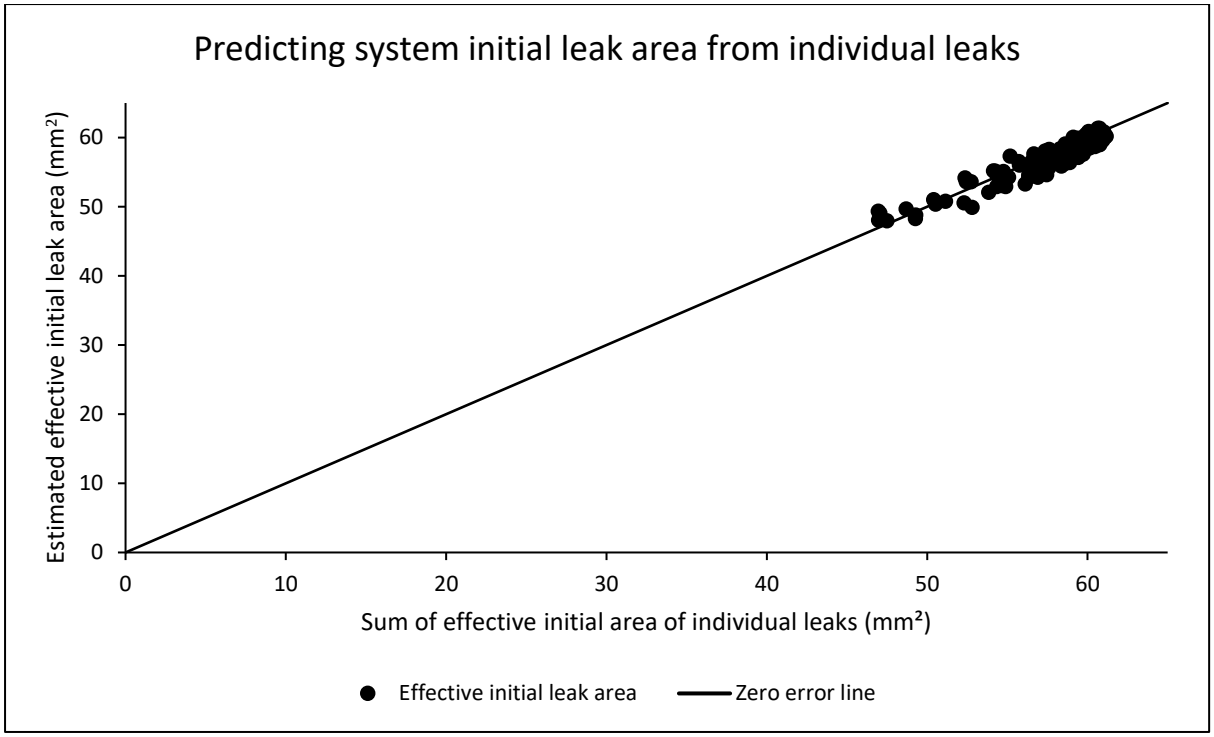
Predicting system initial leak area from individual leaks
Estimated effective initial leak area (mm²)
0
10
20
30
40
50
60
Sum of effective initial area of individual leaks (mm²)
Effective initial leak area
Zero error line

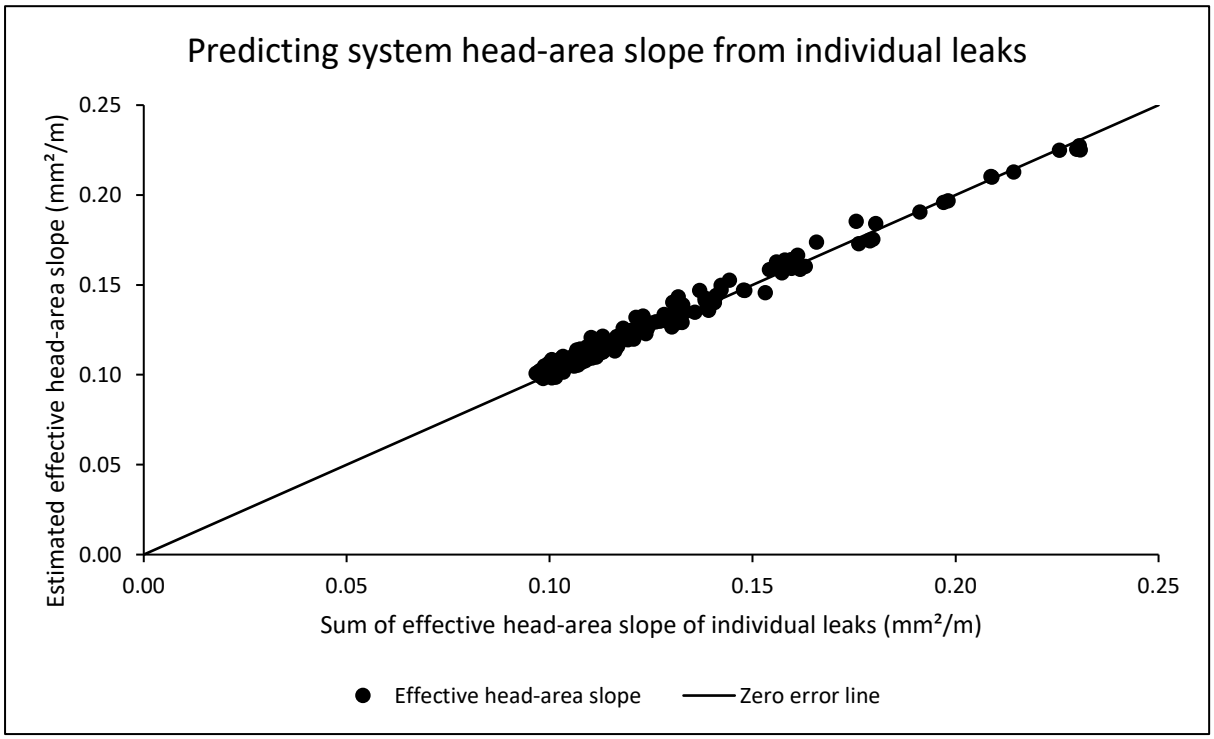
Predicting system head-area slope from individual leaks
Estimated effective head-area slope (mm²/m)
0.00
0.05
0.10
0.15
0.20
0.25
Sum of effective head-area slope of individual leaks (mm²/m)
Effective head-area slope
Zero error line

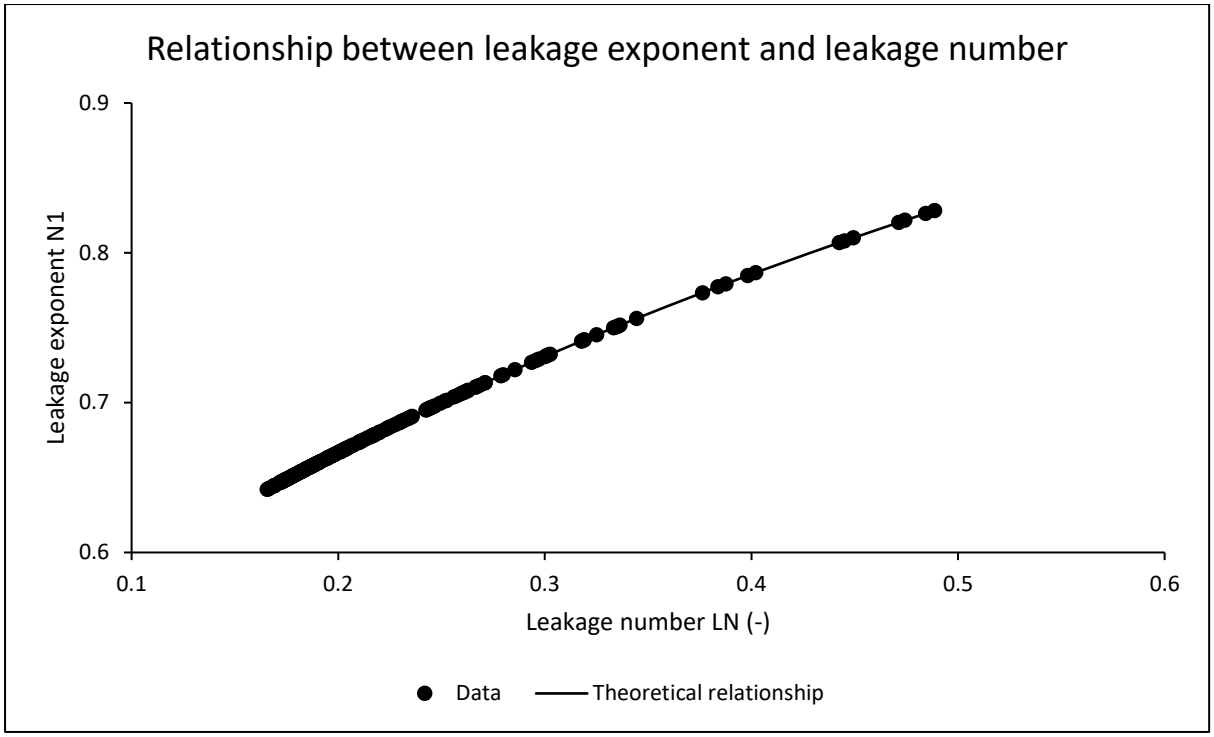
Relationship between leakage exponent and leakage number
Leakage exponent N1
0.9
0.8
0.7
0.6
0.1
0.2
0.3
0.4
0.5
0.6
Leakage number LN (-)
Data
Theoretical relationship

Average iterations required for a system to converge using both formulations

	Minimum	Arithmetic Mean	Median	Maximum
Modified orifice equation	5.12	5.16	5.16	5.20
Power equation	4.52	4.68	4.68	4.76

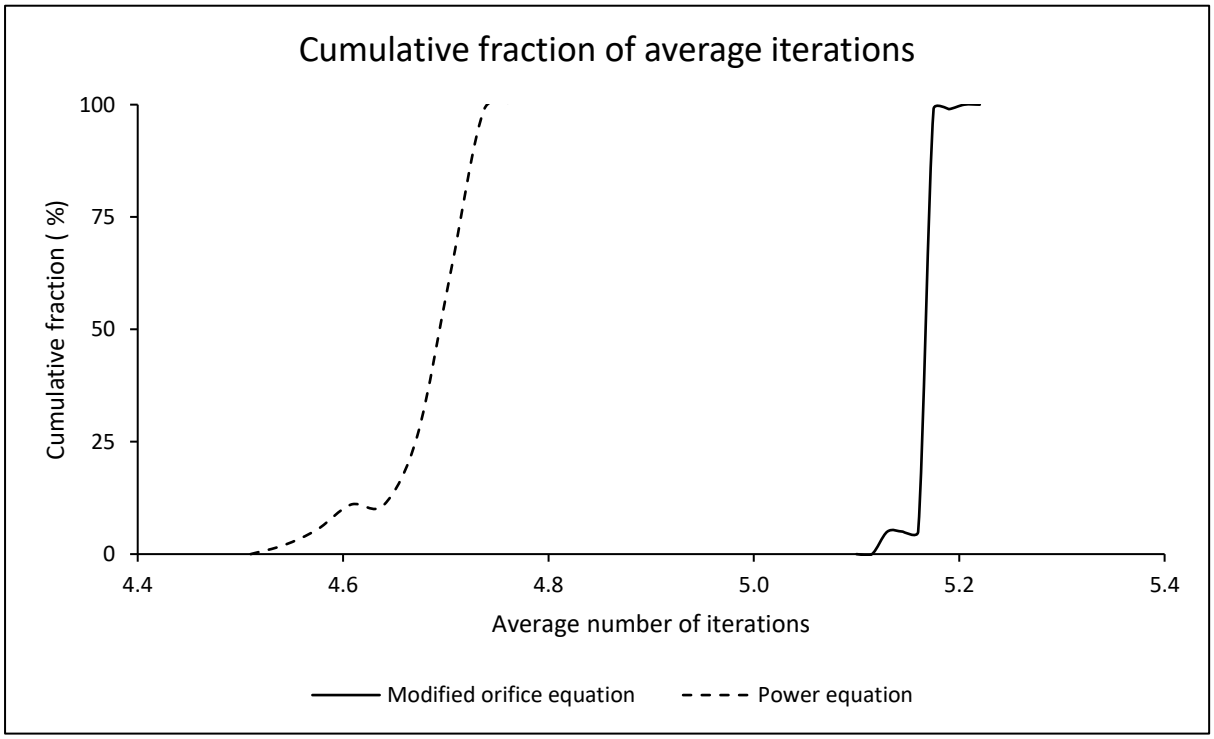

Effect of leakage on pressure at both average zone pressure (AZP) and critical nodes

AZP node								
	During MNF conditions				During peak demand conditions			
	Min (m)	Mean (m)	Median (m)	Max (m)	Min (m)	Mean (m)	Median (m)	Max (m)
Modified orifice equation	-0.22	-0.20	-0.20	-0.19	-0.28	-0.27	-0.27	-0.25
Power equation	-0.22	-0.20	-0.20	-0.19	-0.28	-0.27	-0.27	-0.25
Critical node								
Modified orifice equation	-0.20	-0.19	-0.19	-0.18	-0.27	-0.26	-0.26	-0.24
Power equation	-0.20	-0.19	-0.19	-0.18	-0.27	-0.25	-0.25	-0.23

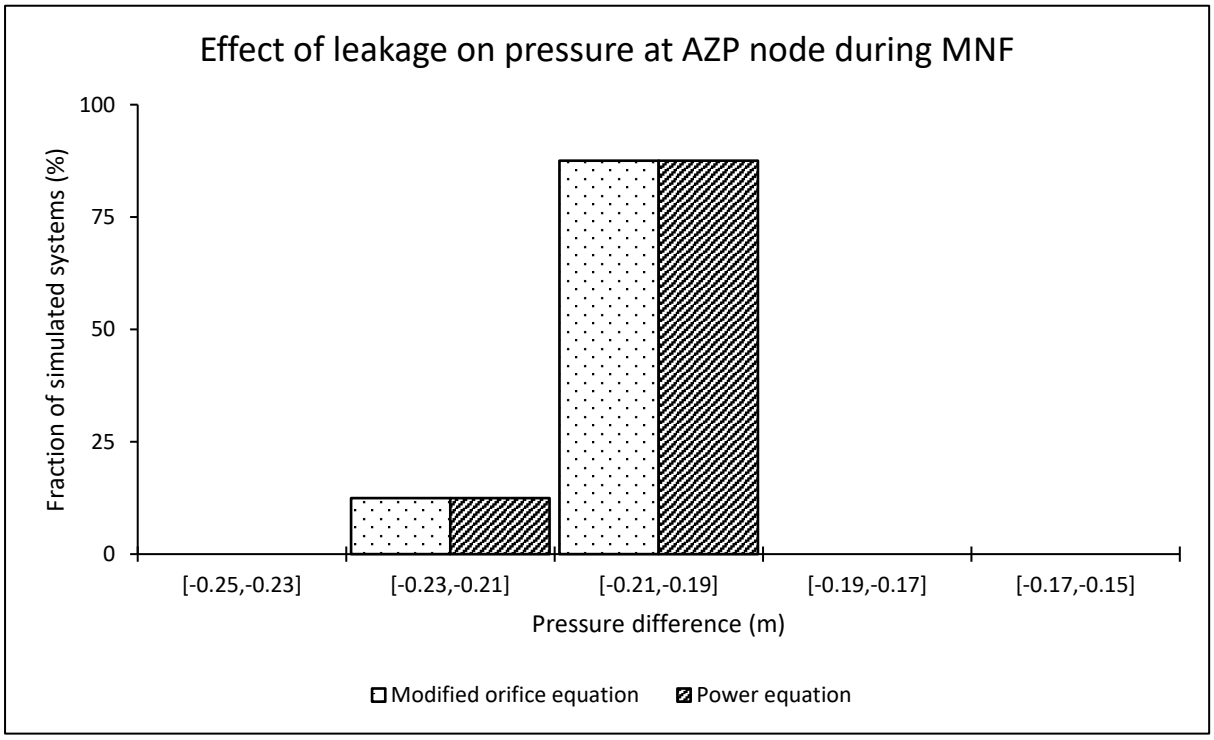

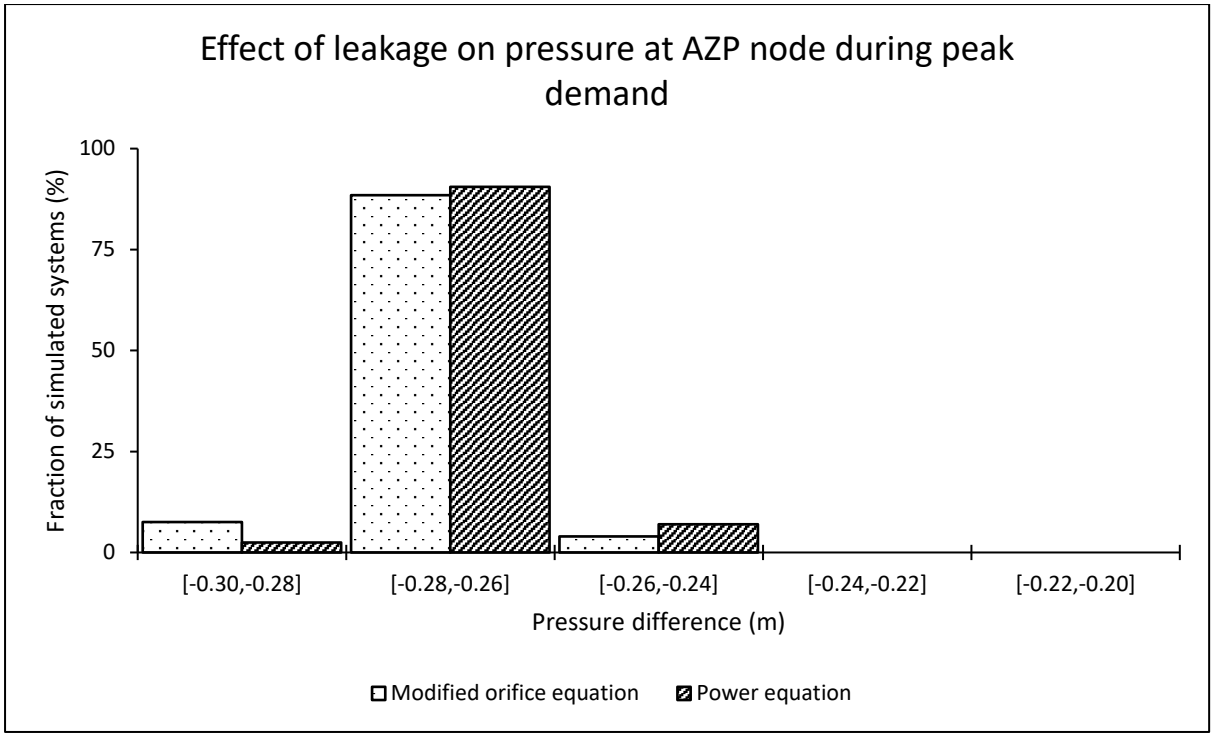
Effect of leakage on pressure at AZP node during peak demand
Fraction of simulated systems (%)
100
75
50
25
0
[-0.30,-0.28]
[-0.28,-0.26]
[-0.26,-0.24]
[-0.24,-0.22]
[-0.22,-0.20]
Pressure difference (m)
Modified orifice equation
Power equation

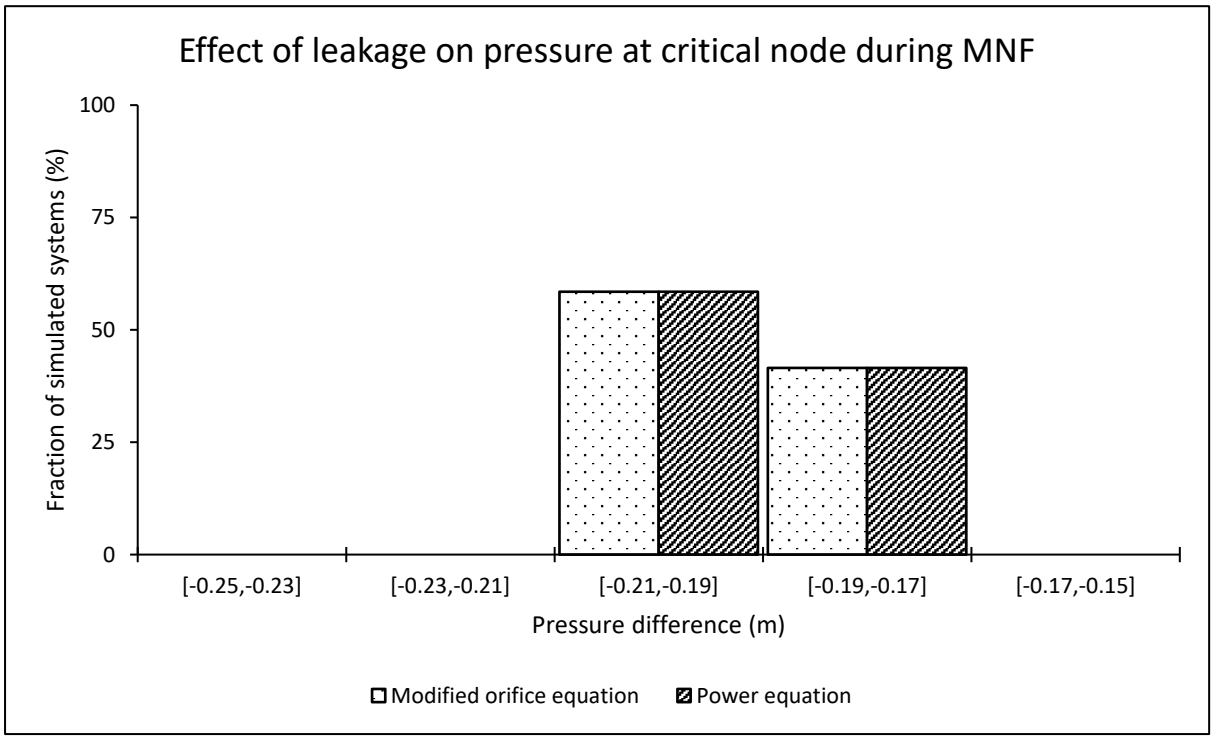
Effect of leakage on pressure at critical node during MNF
Fraction of simulated systems (%)
100
75
50
25
0
[-0.25,-0.23]
[-0.23,-0.21]
[-0.21,-0.19]
[-0.19,-0.17]
[-0.17,-0.15]
Pressure difference (m)
Modified orifice equation
Power equation

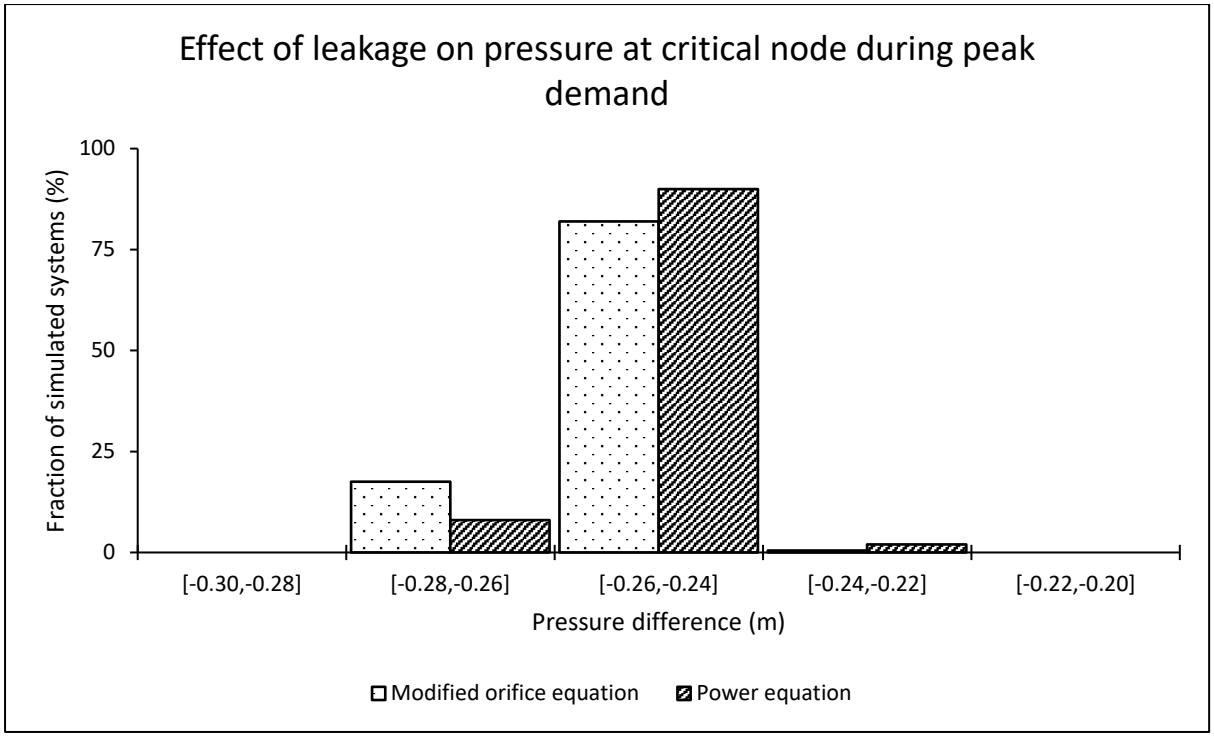
Effect of leakage on pressure at critical node during peak demand
Fraction of simulated systems (%)
100
75
50
25
0
[-0.30,-0.28]
[-0.28,-0.26]
[-0.26,-0.24]
[-0.24,-0.22]
[-0.22,-0.20]
Pressure difference (m)
Modified orifice equation
Power equation

Pressure estimation error when using the power equation at average zone pressure (AZP) and critical nodes

	During MNF conditions				During peak demand conditions			
	Min (%)	**Mean (%)**	**Median (%)**	**Max (%)**	**Min (%)**	**Mean (%)**	**Median (%)**	**Max (%)**
At the AZP node	0.00	0.00	0.00	0.00	0.00	0.00	0.00	0.01
At the critical node	0.00	0.00	0.00	0.00	0.00	0.00	0.00	0.01

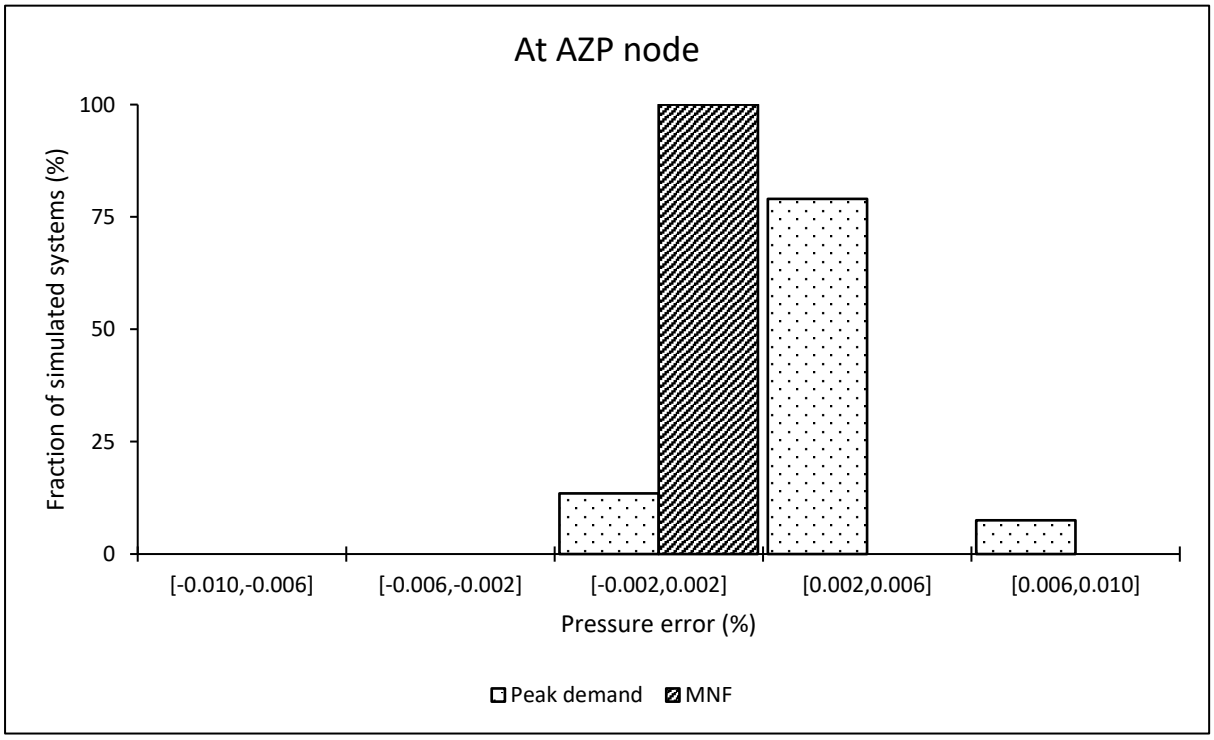

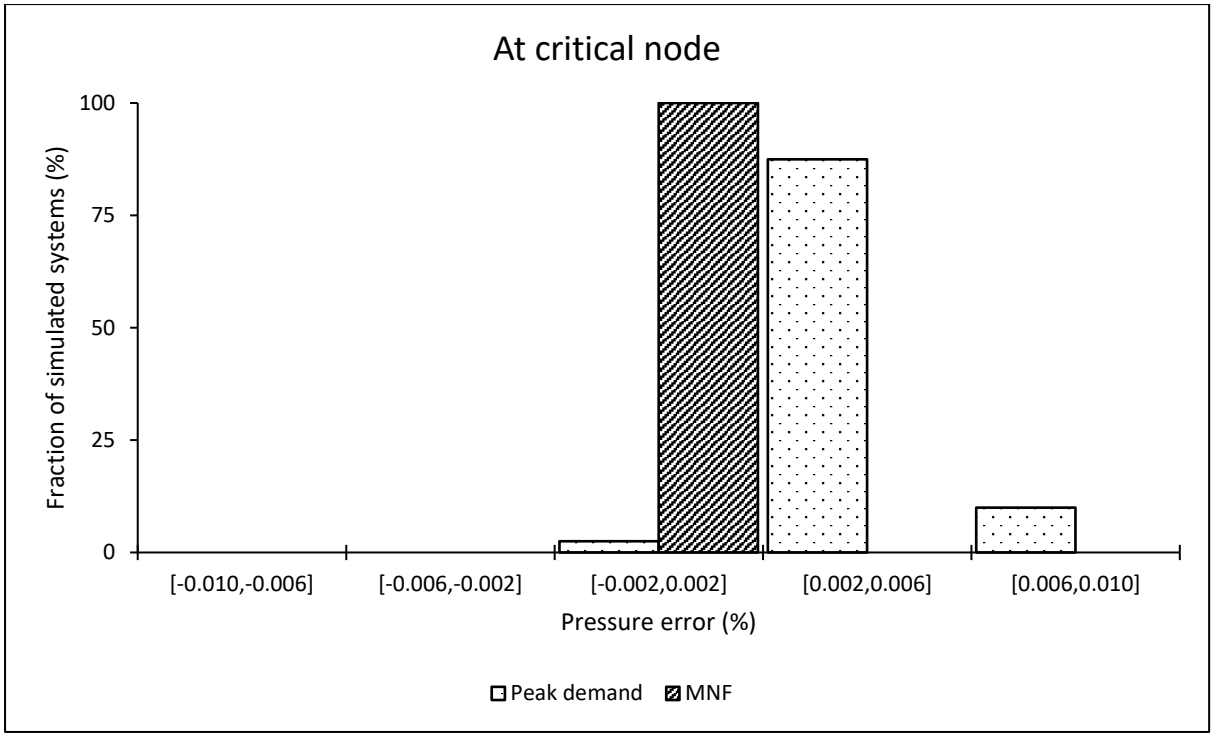
At critical node
Fraction of simulated systems (%)
100
75
50
25
0
[-0.010,-0.006]
[-0.006,-0.002]
[-0.002,0.002]
[0.002,0.006]
[0.006,0.010]
Pressure error (%)
Peak demand
MNF

System leakage estimation error when using the power equation

	Leakage estimation error (%)			
	Minimum	**Arithmetic Mean**	**Median**	**Maximum**
Before implementing pressure management	-0.80	-0.30	-0.29	0.11
After implementing pressure management	-10.46	-6.06	-5.84	-4.06

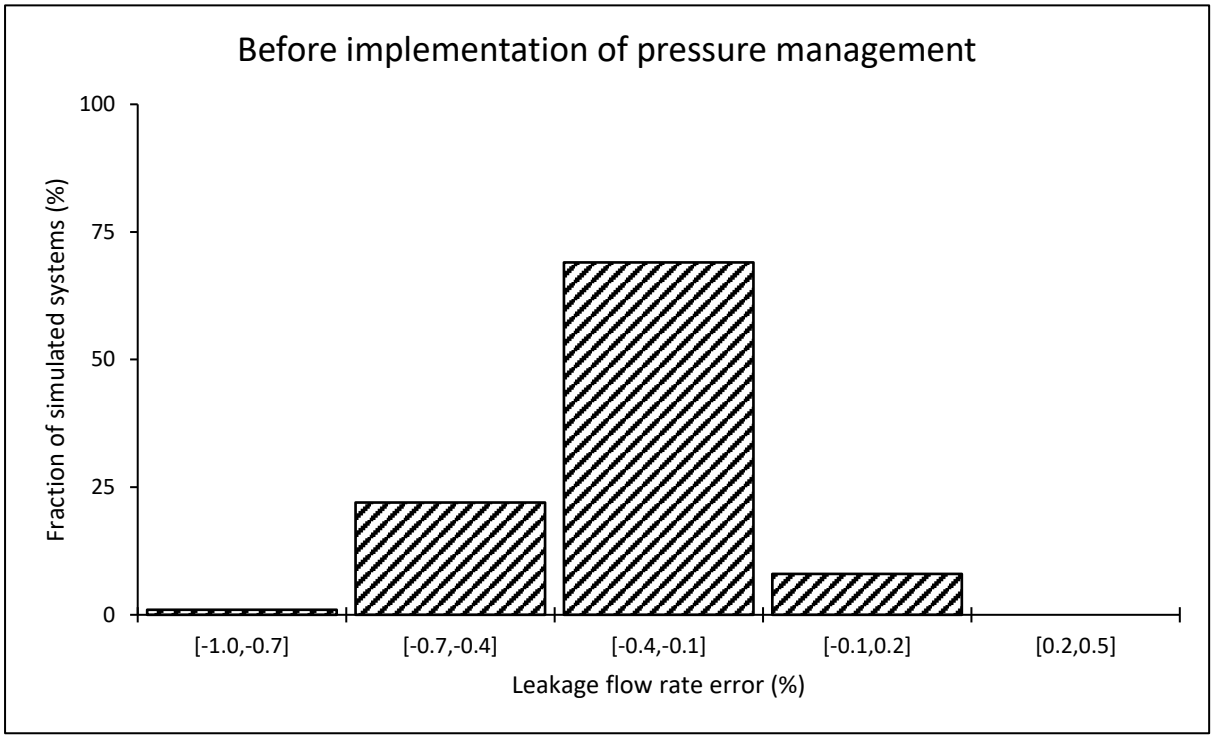

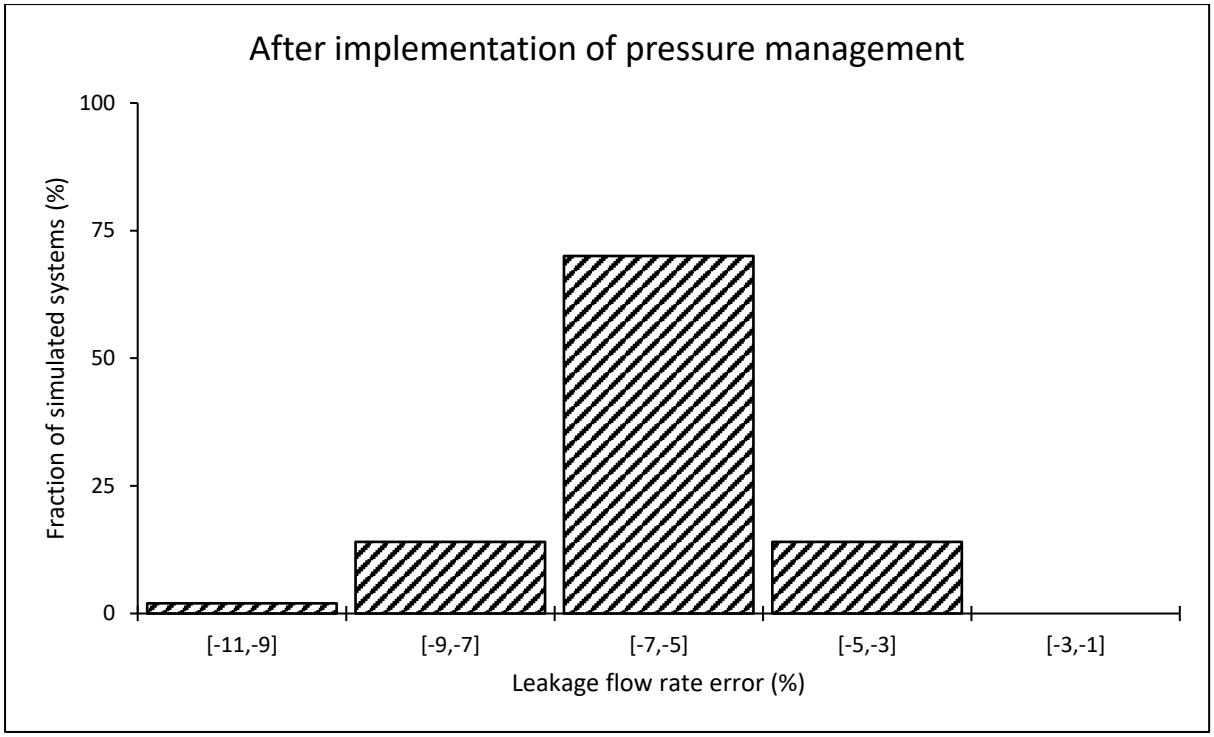
After implementation of pressure management
Fraction of simulated systems (%)
100
75
50
25
0
[-11,-9]
[-9,-7]
[-7,-5]
[-5,-3]
[-3,-1]
Leakage flow rate error (%)

Leakage estimation error when using the power equation at the critical node

	Leakage estimation error (%)			
	Minimum	**Arithmetic Mean**	**Median**	**Maximum**
Before implementing pressure management	-20.63	-0.73	-2.79	15.82
After implementing pressure management	-42.02	-3.52	-17.58	155.93

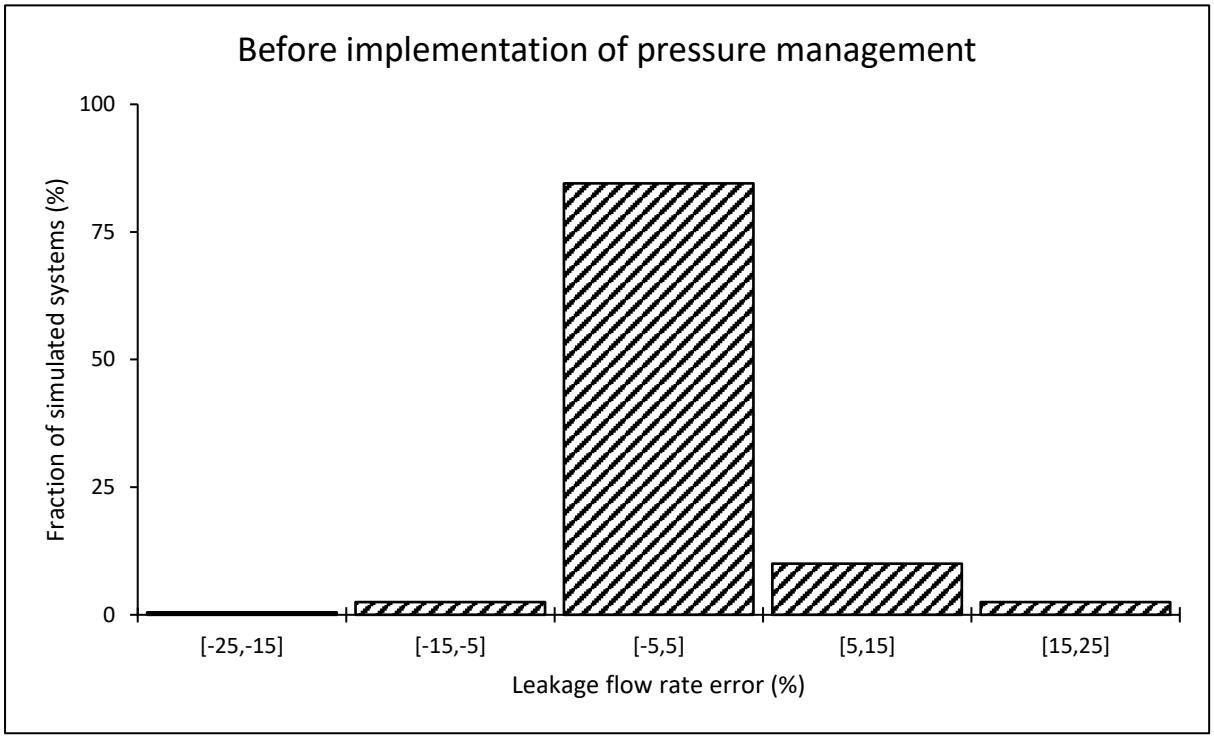

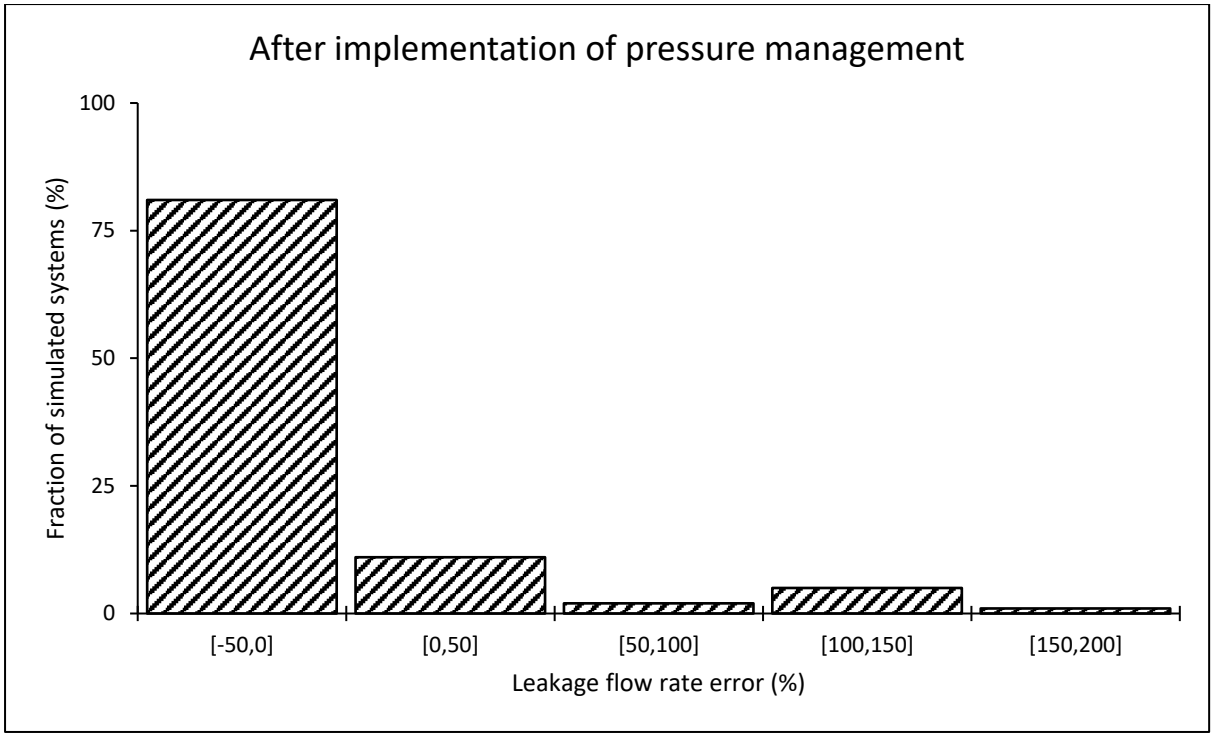
After implementation of pressure management
Fraction of simulated systems (%)
100
75
50
25
0
[-50,0]
[0,50]
[50,100]
[100,150]
[150,200]
Leakage flow rate error (%)

Appendix A-6: Medium-sized network with an ILI of 4

Results for an individual system

Pressure head at the average zone pressure (AZP) node

		Pressure head (m)			
		Minimum	**Arithmetic Mean**	**Median**	**Maximum**
Before pressure management	Without leaks	72.69	88.62	90.24	106.08
	Modified orifice equation	71.63	87.64	89.24	105.28
	Power equation	71.64	87.64	89.25	105.28
After pressure management	Modified orifice equation	22.17	38.05	39.65	55.57
	Power equation	22.23	38.09	39.69	55.58

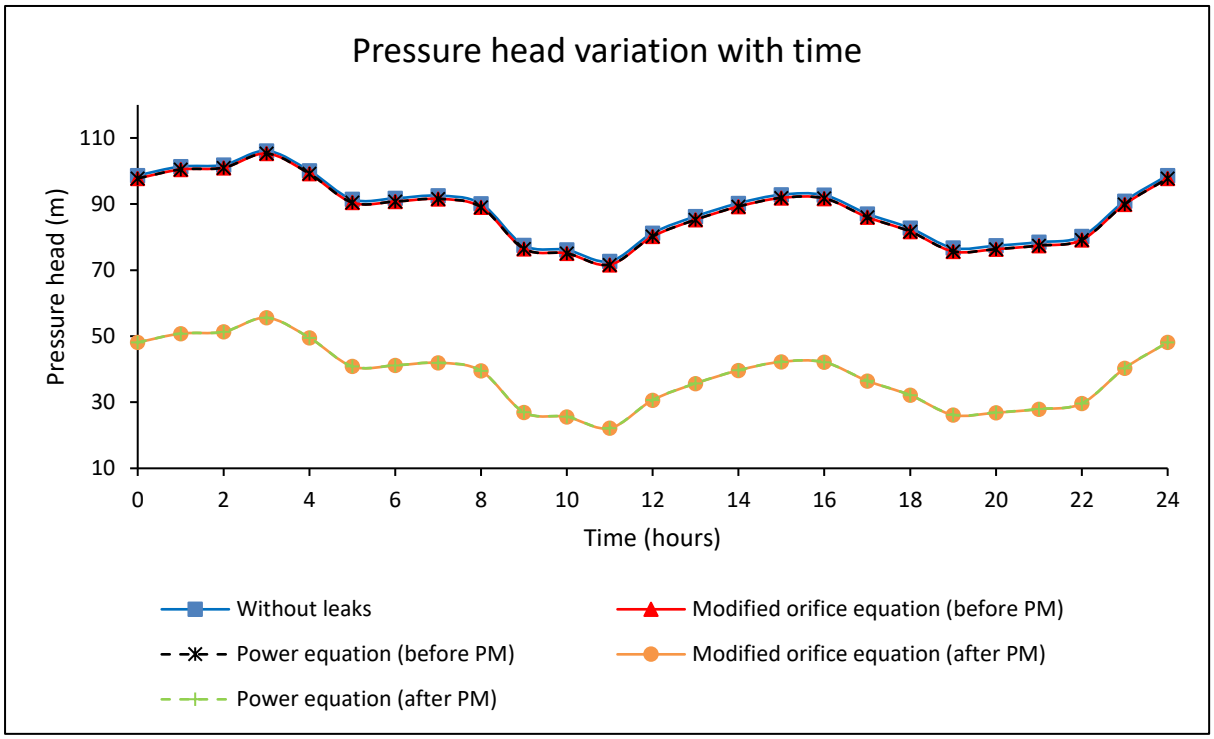

Pressure head at the critical node

		Pressure head (m)			
		Minimum	**Arithmetic Mean**	**Median**	**Maximum**
Before pressure management	Without leaks	60.21	75.09	76.77	90.93
	Modified orifice equation	59.20	74.15	75.82	90.17
	Power equation	59.21	74.15	75.83	90.17
After pressure management	Modified orifice equation	9.71	24.55	26.21	40.44
	Power equation	9.77	24.59	26.25	40.46

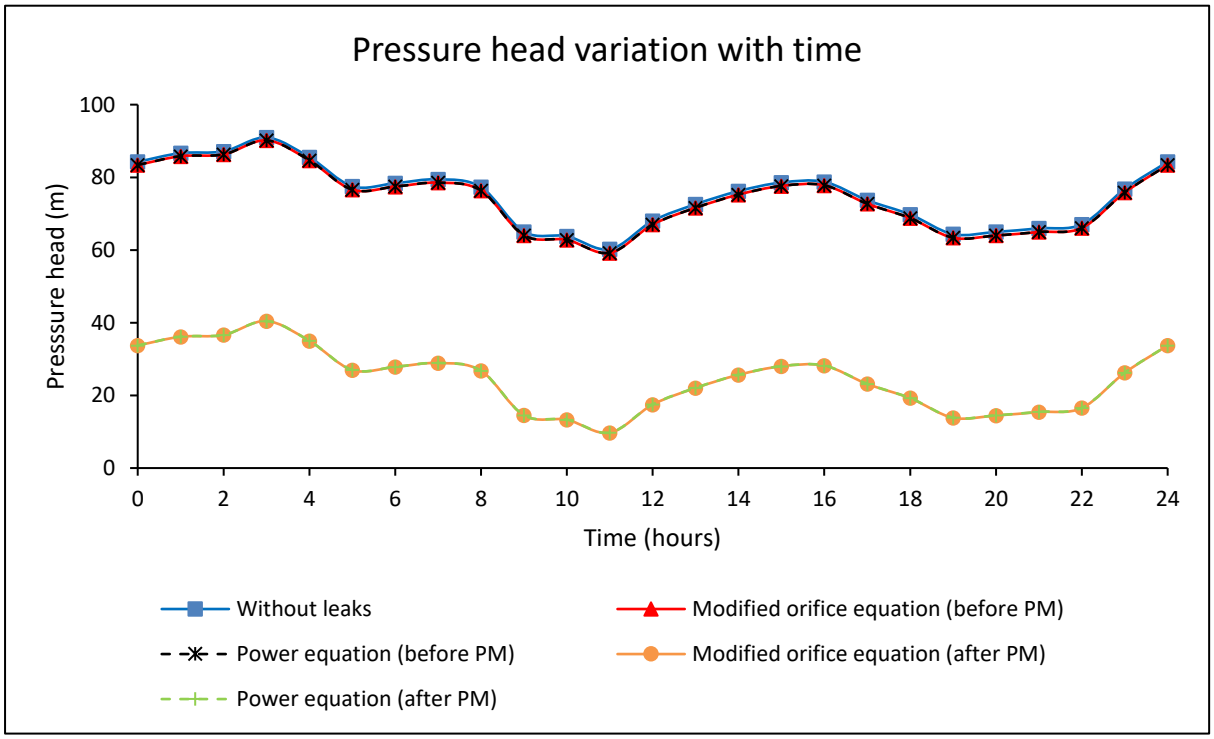

System leakage flow rate

		Leakage flow rate (m^3/h)			
		Minimum	**Arithmetic Mean**	**Median**	**Maximum**
Before pressure management	Modified orifice equation	36.53	41.74	42.38	47.35
	Power equation	36.20	41.63	42.29	47.35
After pressure management	Modified orifice equation	17.96	24.13	24.92	30.32
	Power equation	15.89	22.70	23.57	29.57

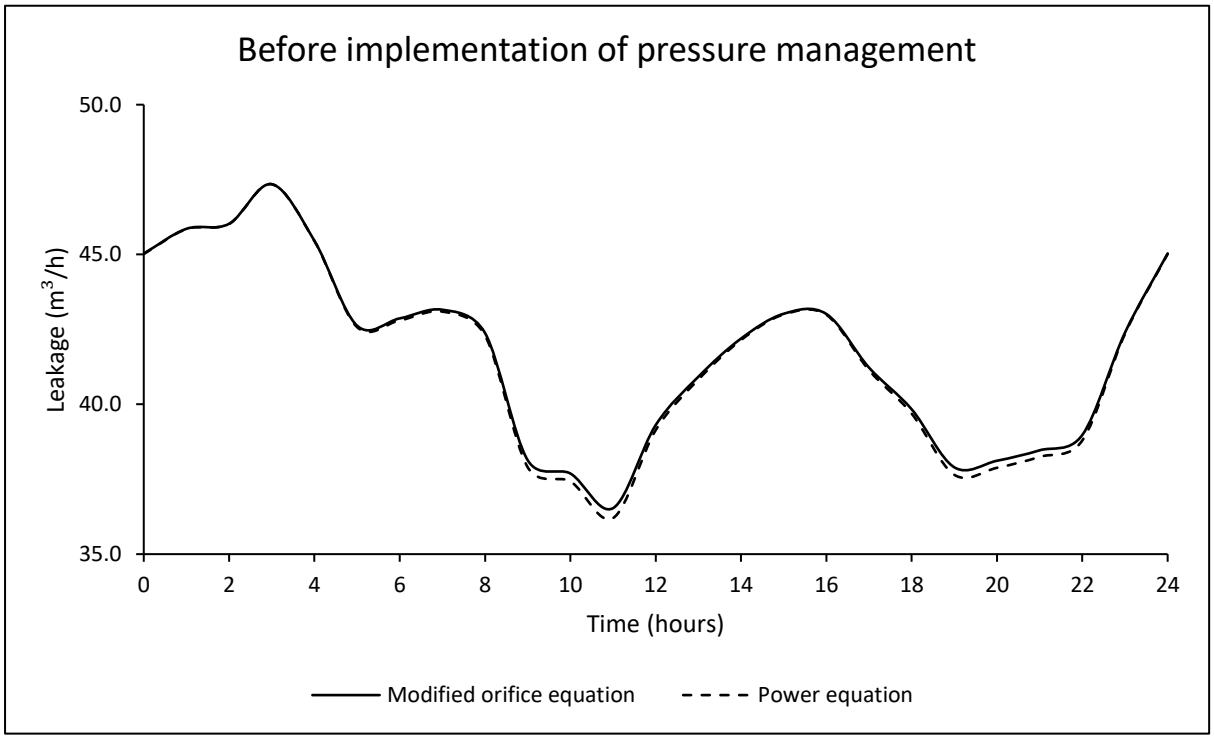

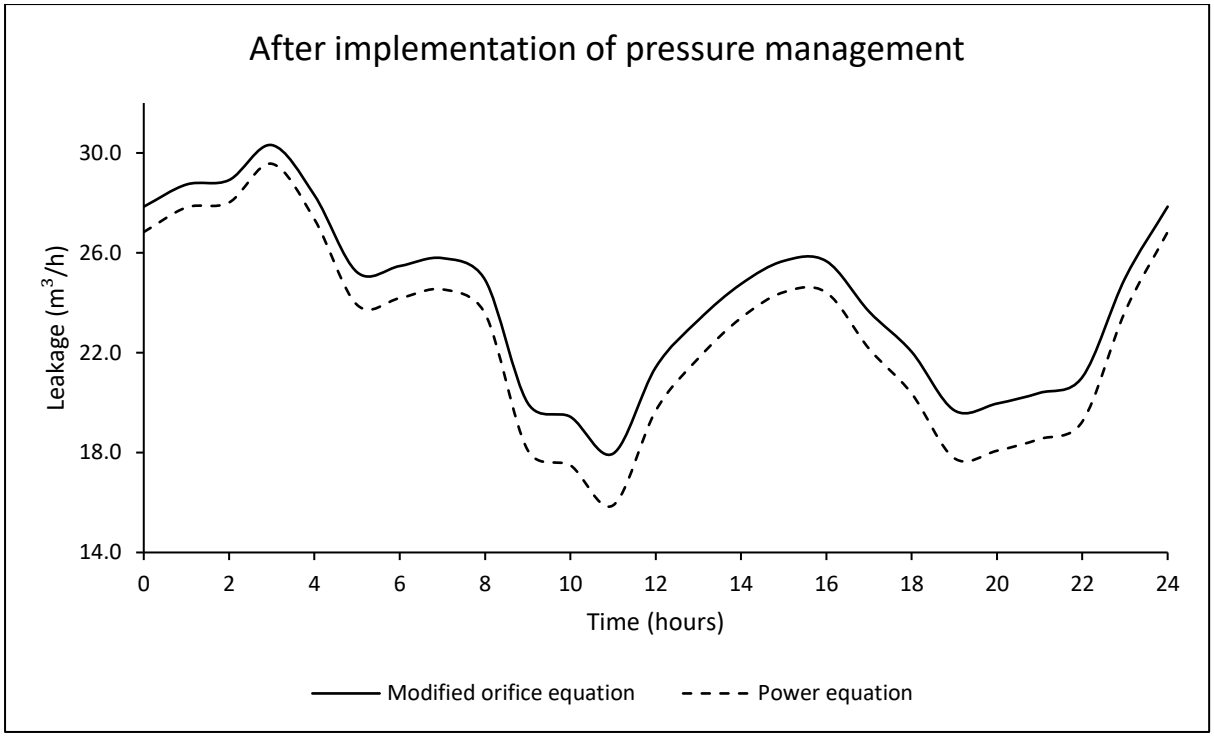
After implementation of pressure management
30.0
26.0
22.0
18.0
14.0
Leakage (m3/h)
0
2
4
6
8
10
12
14
16
18
20
22
24
Time (hours)
Modified orifice equation
Power equation

Leakage flow rate at the critical node

		Leakage flow rate (m^3/h)			
		Minimum	**Arithmetic Mean**	**Median**	**Maximum**
Before pressure management	Modified orifice equation	0.34	0.38	0.38	0.42
	Power equation	0.30	0.36	0.37	0.42
After pressure management	Modified orifice equation	0.14	0.21	0.22	0.28
	Power equation	0.08	0.16	0.17	0.23

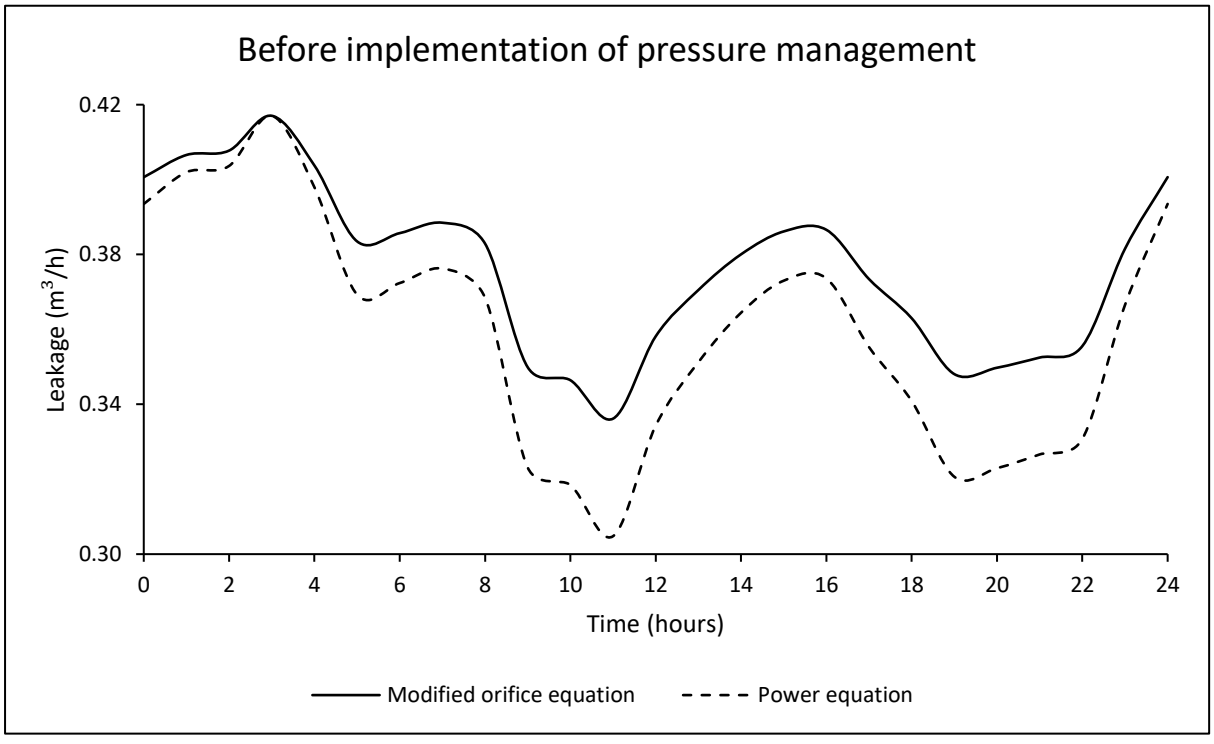

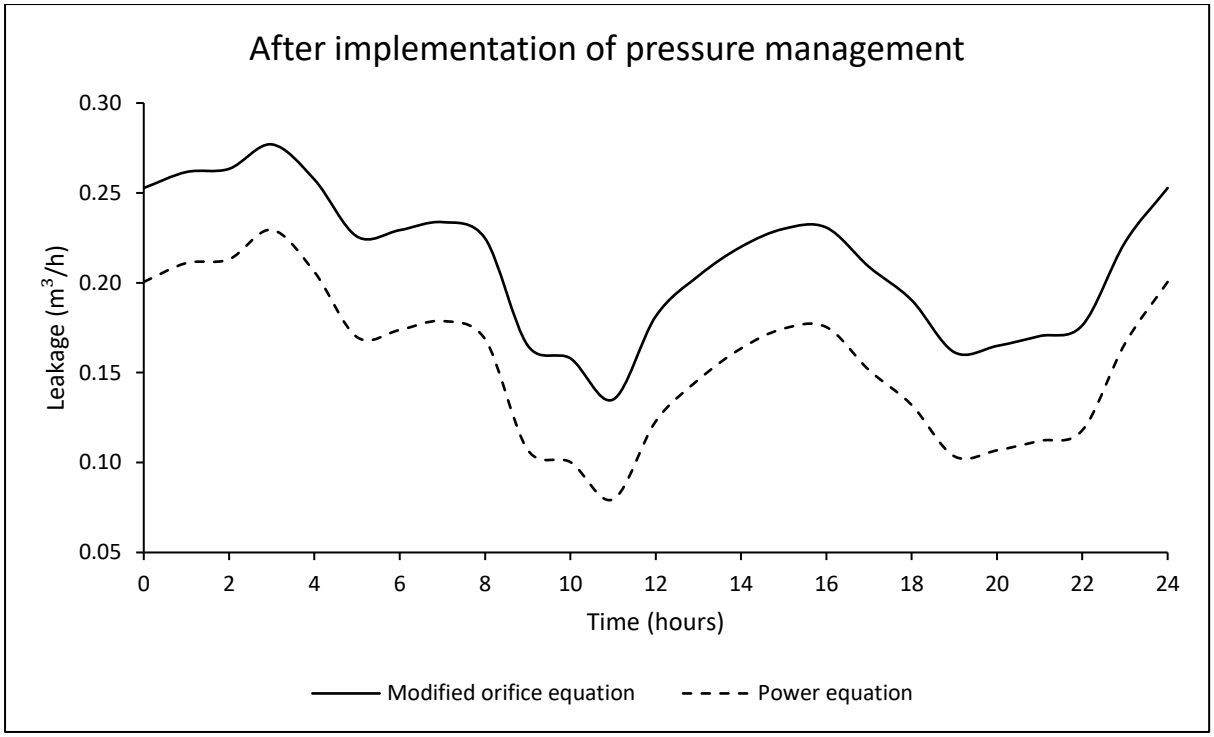
After implementation of pressure management
0.30
0.25
0.20
0.15
0.10
0.05
Leakage (m3/h)
0
2
4
6
8
10
12
14
16
18
20
22
24
Time (hours)
Modified orifice equation
Power equation

Number of iterations required for a system to converge to a hydraulic solution for both formulations

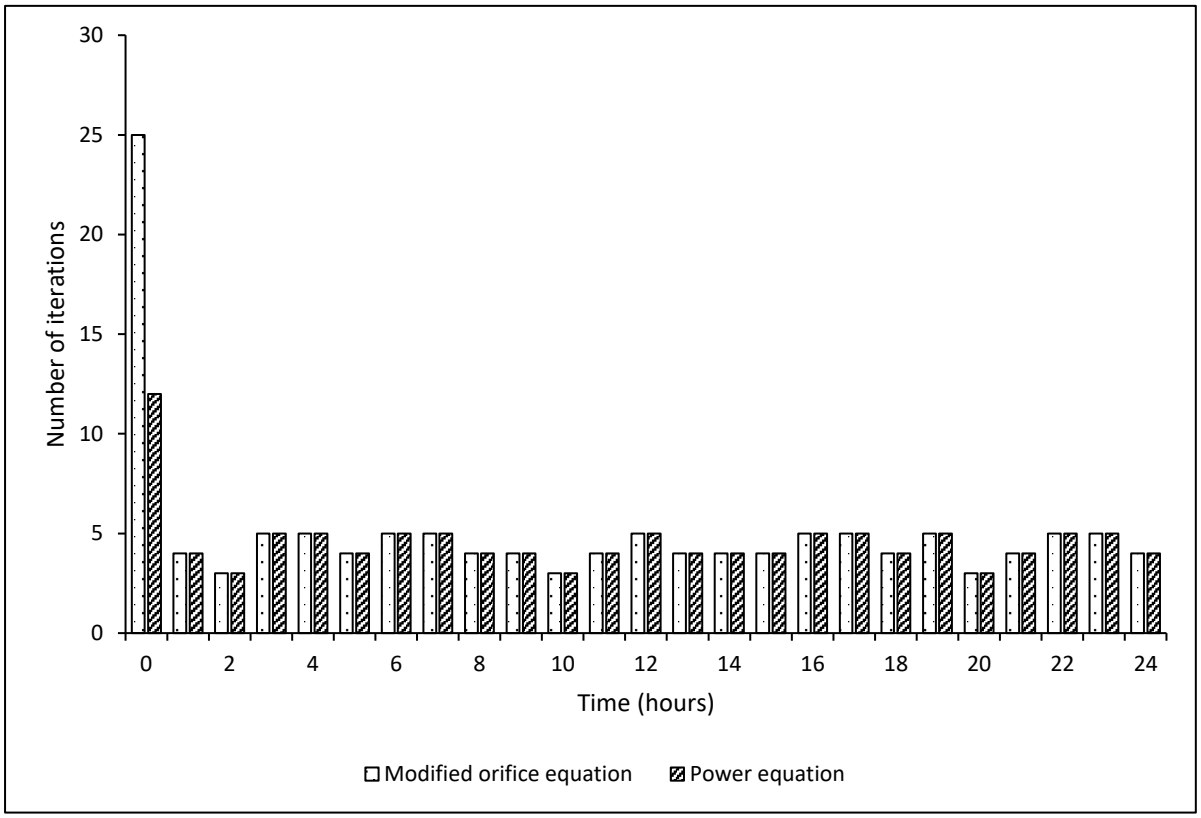

Results for combined systems

System parameters for both power and modified orifice formulations

	Minimum	Arithmetic Mean	Median	Maximum
Leakage exponent N1	0.57	0.83	0.84	1.10
Leakage coefficient C	7.4E-05	3.2E-04	2.6E-04	9.2E-04
Effective initial leak area C_dA0 (mm^2)	106.99	186.80	185.72	264.75
Effective head-area slope C_dm (mm^2/m)	0.18	0.91	0.93	1.60
Leakage number LN	0.07	0.56	0.52	1.52

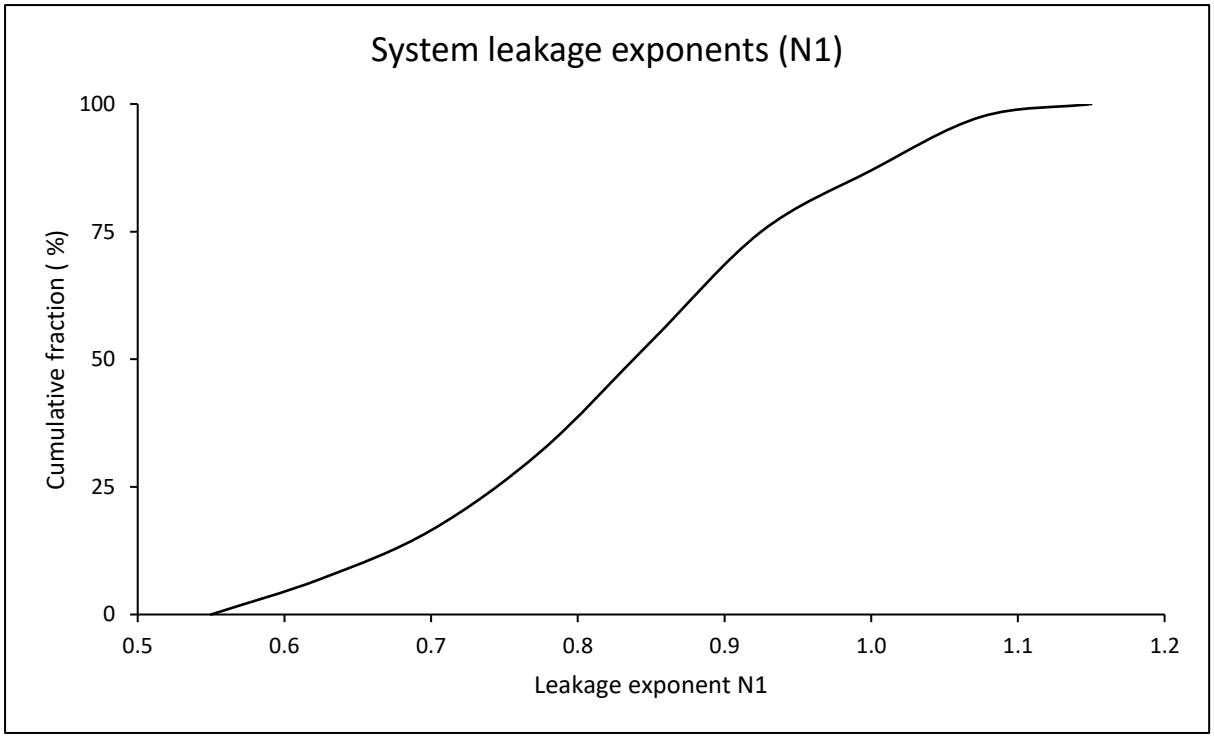

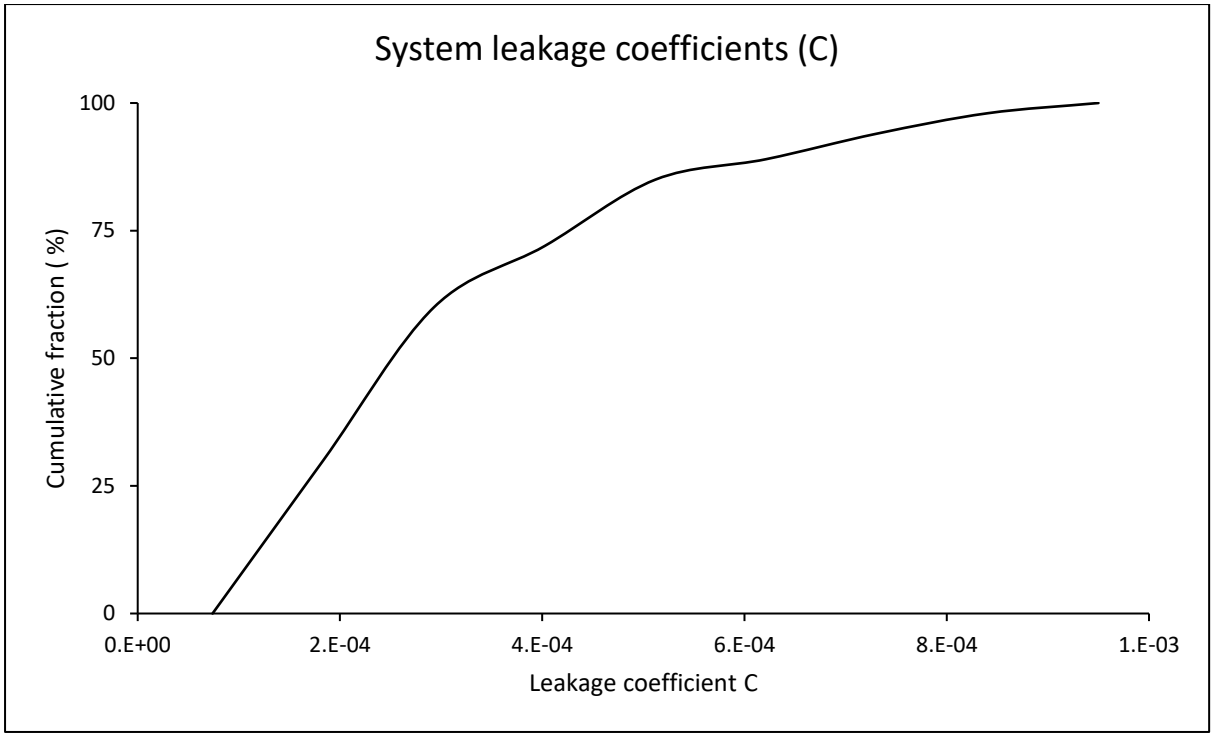
System leakage coefficients (C)
100
75
50
25
0
Cumulative fraction (%)
0.E+00
2.E-04
4.E-04
6.E-04
8.E-04
1.E-03
Leakage coefficient C

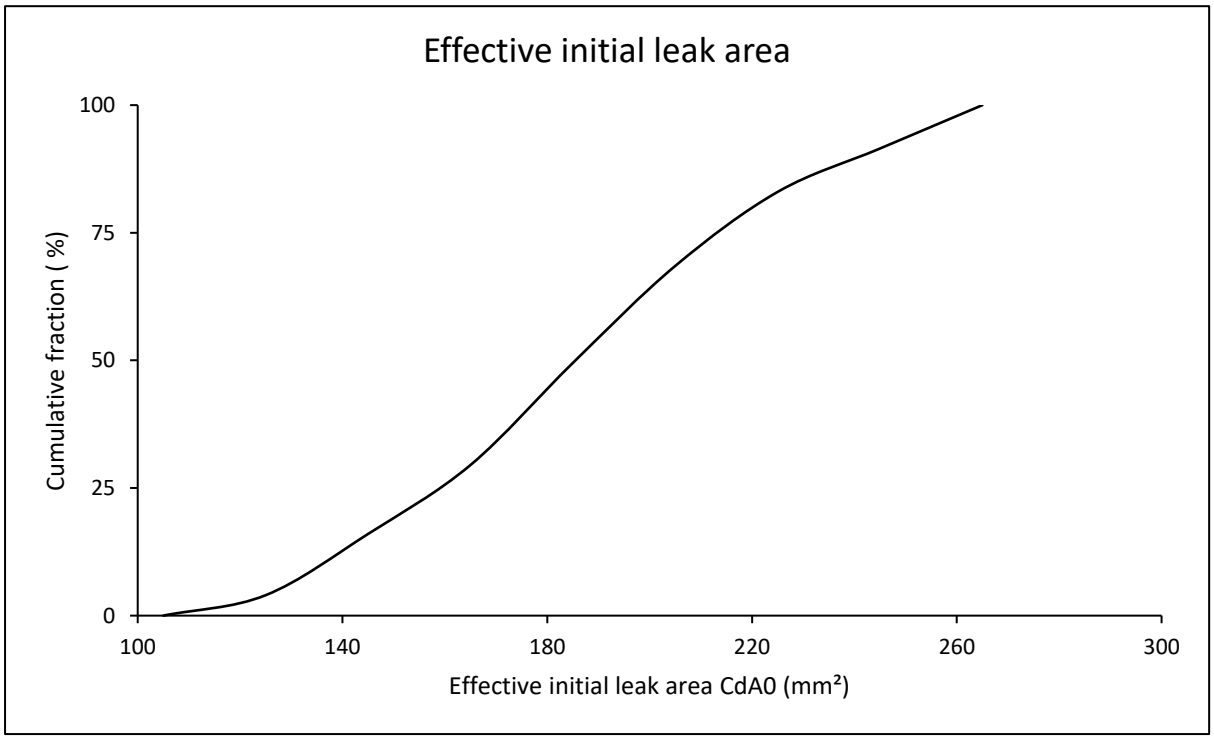
Effective initial leak area
100
75
50
25
0
Cumulative fraction (%)
100
140
180
220
260
300
Effective initial leak area CdA0 (mm²)

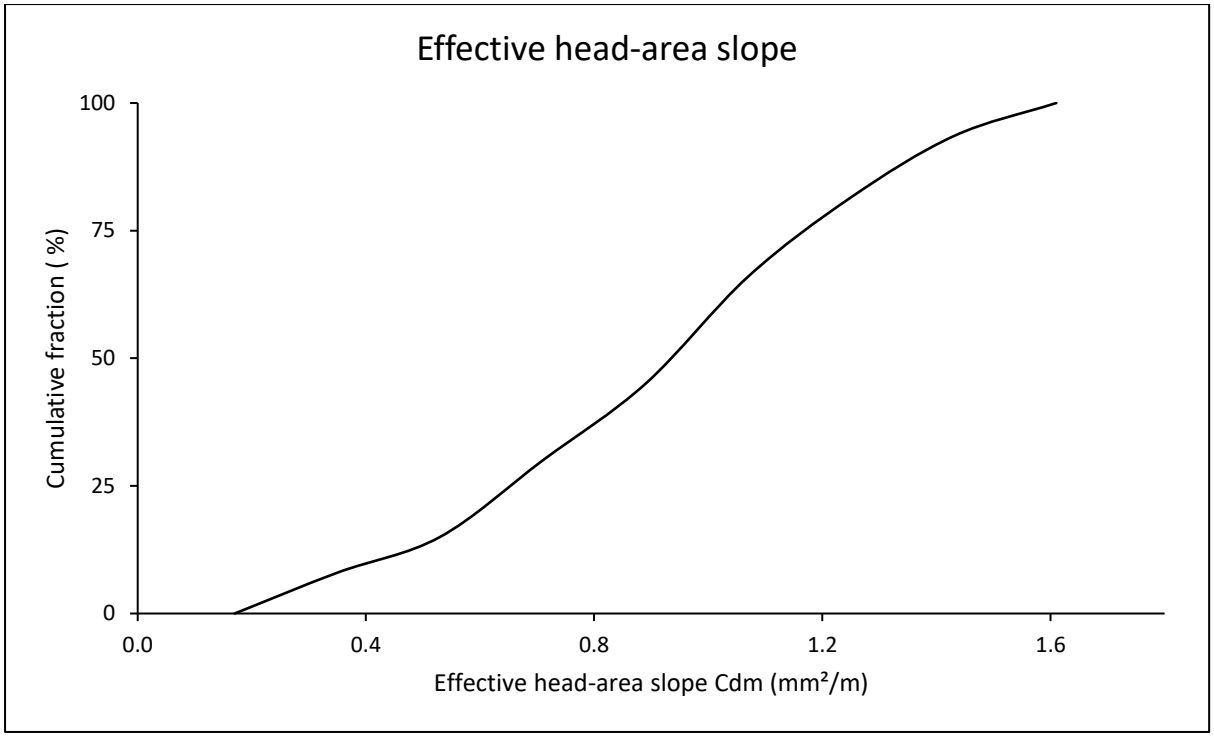
Effective head-area slope
100
75
50
25
0
Cumulative fraction (%)
0.0
0.4
0.8
1.2
1.6
Effective head-area slope Cdm (mm²/m)

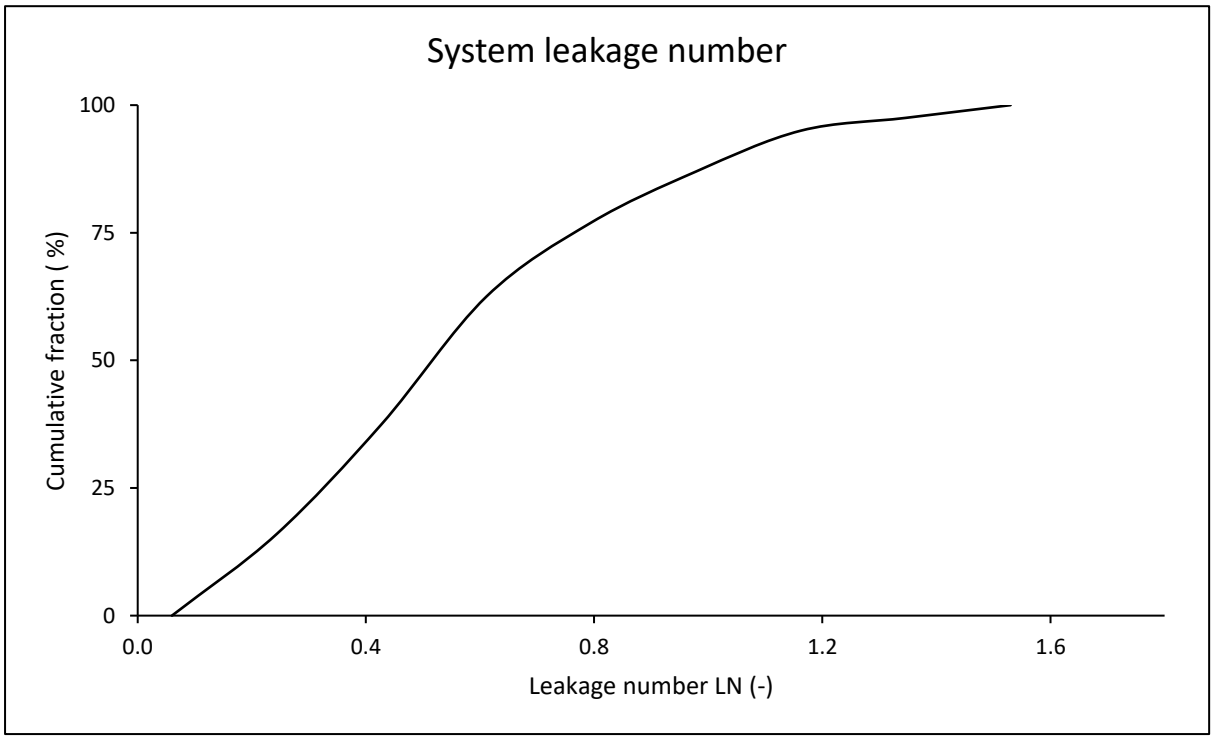
System leakage number
100
75
50
25
0
Cumulative fraction (%)
0.0
0.4
0.8
1.2
1.6
Leakage number LN (-)

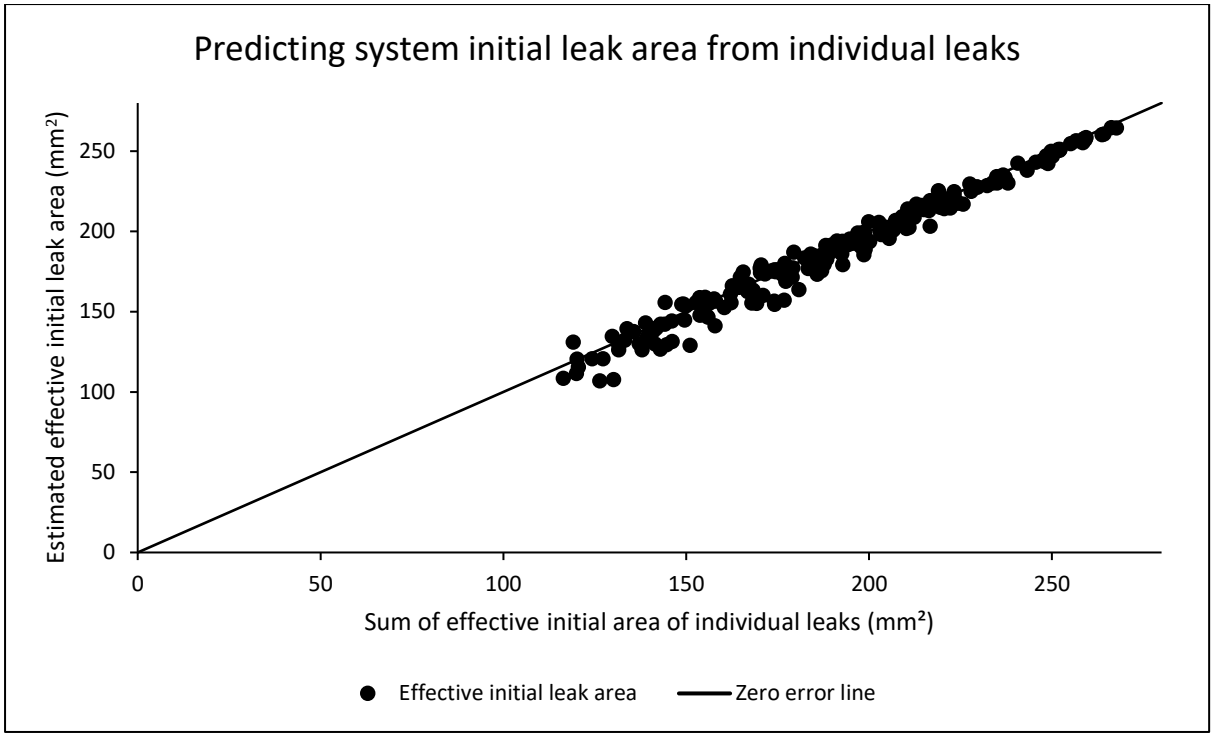
Predicting system initial leak area from individual leaks
Estimated effective initial leak area (mm²)
0
50
100
150
200
250
0
50
100
150
200
250
Sum of effective initial area of individual leaks (mm²)
Effective initial leak area
Zero error line

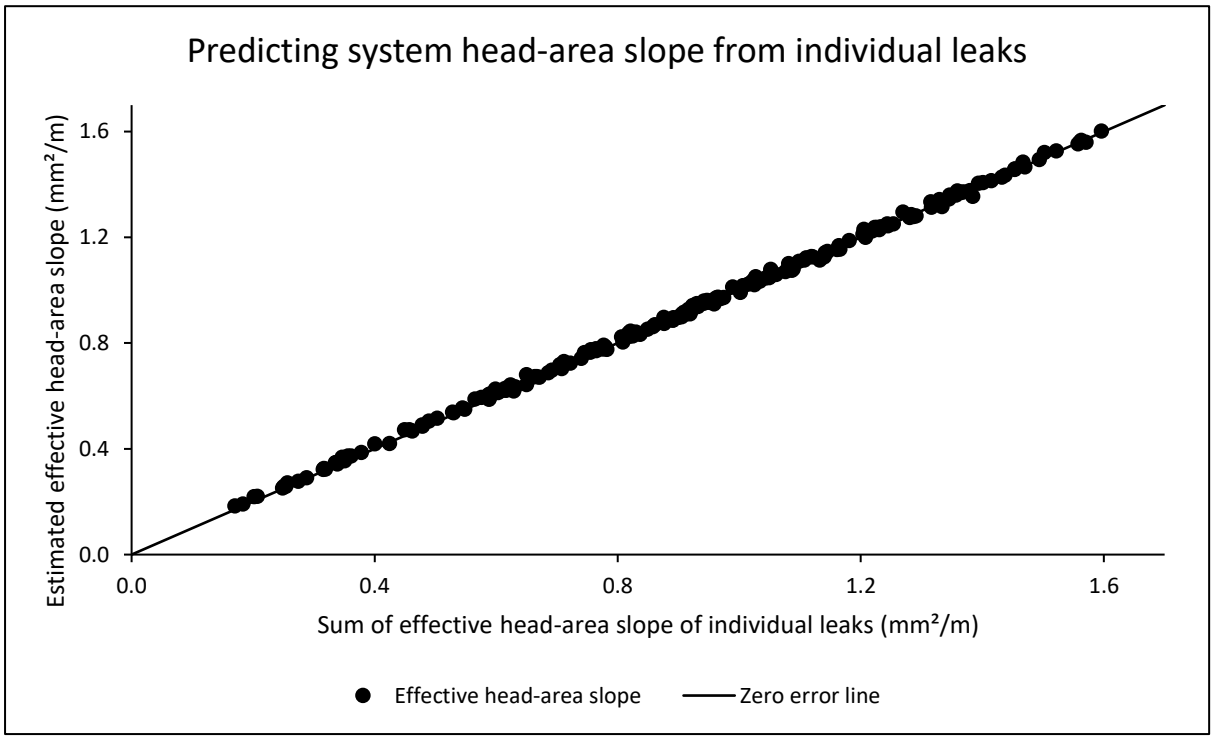
Predicting system head-area slope from individual leaks
Estimated effective head-area slope (mm²/m)
0.0
0.4
0.8
1.2
1.6
0.0
0.4
0.8
1.2
1.6
Sum of effective head-area slope of individual leaks (mm²/m)
Effective head-area slope
Zero error line

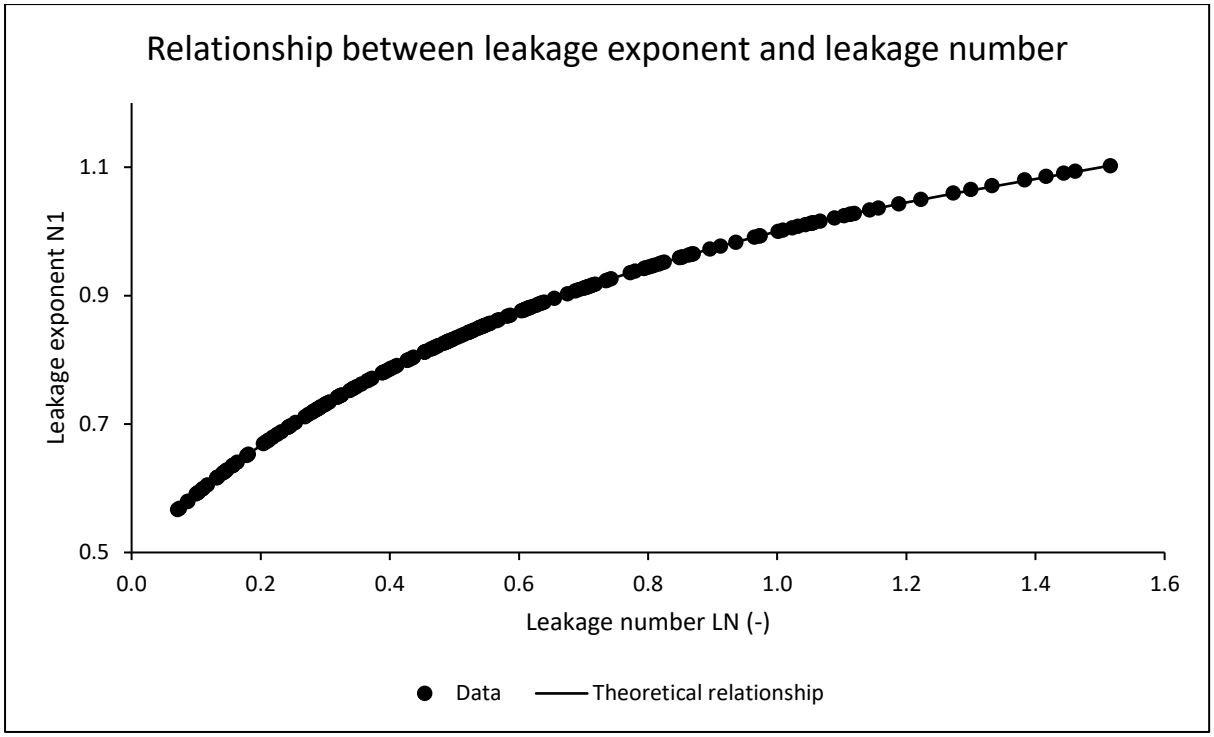
Relationship between leakage exponent and leakage number
Leakage exponent N1
1.1
0.9
0.7
0.5
0.0
0.2
0.4
0.6
0.8
1.0
1.2
1.4
1.6
Leakage number LN (-)
Data
Theoretical relationship

Average iterations required for a system to converge using both formulations

	Minimum	Arithmetic Mean	Median	Maximum
Modified orifice equation	5.08	5.15	5.16	5.24
Power equation	4.28	4.53	4.52	4.92

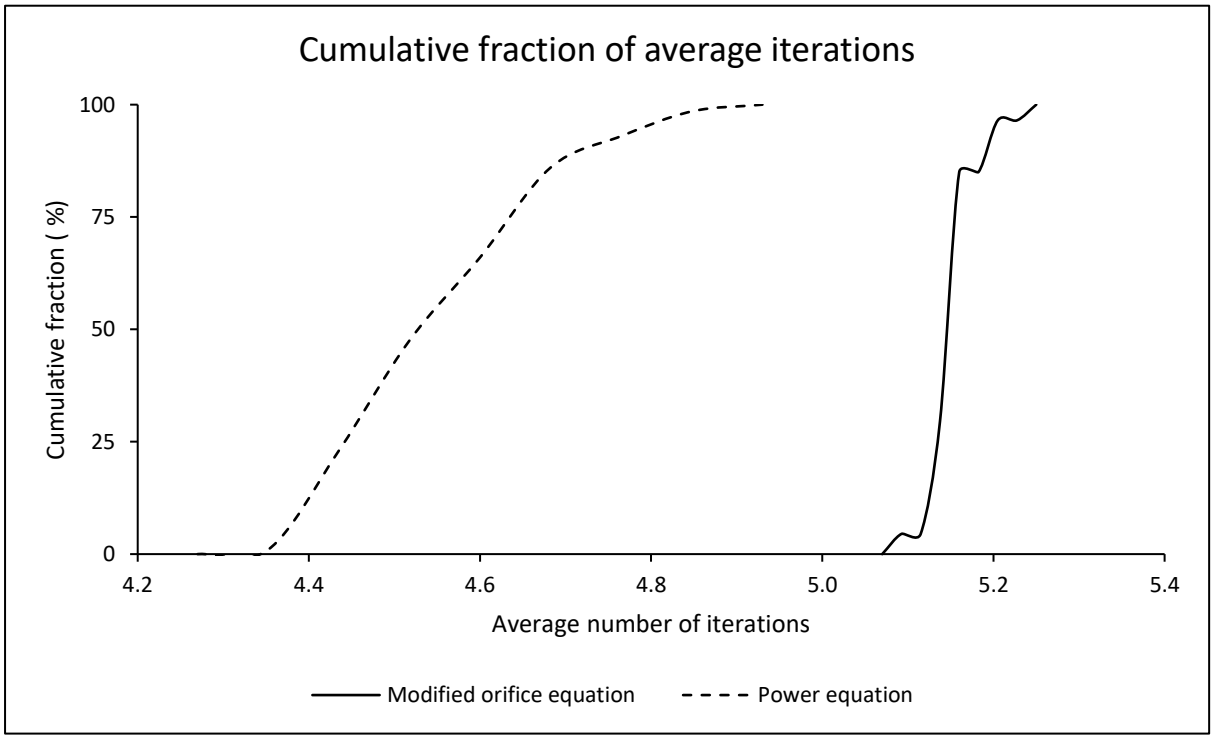

Effect of leakage on pressure at both average zone pressure (AZP) and critical nodes

AZP node								
	During MNF conditions				During peak demand conditions			
	Min (m)	Mean (m)	Median (m)	Max (m)	Min (m)	Mean (m)	Median (m)	Max (m)
Modified orifice equation	-0.95	-0.82	-0.82	-0.71	-1.15	-1.03	-1.03	-0.85
Power equation	-0.95	-0.82	-0.82	-0.71	-1.14	-1.01	-1.02	-0.81
Critical node								
Modified orifice equation	-0.87	-0.77	-0.76	-0.71	-1.07	-0.96	-0.96	-0.81
Power equation	-0.87	-0.77	-0.76	-0.71	-1.07	-0.95	-0.95	-0.77

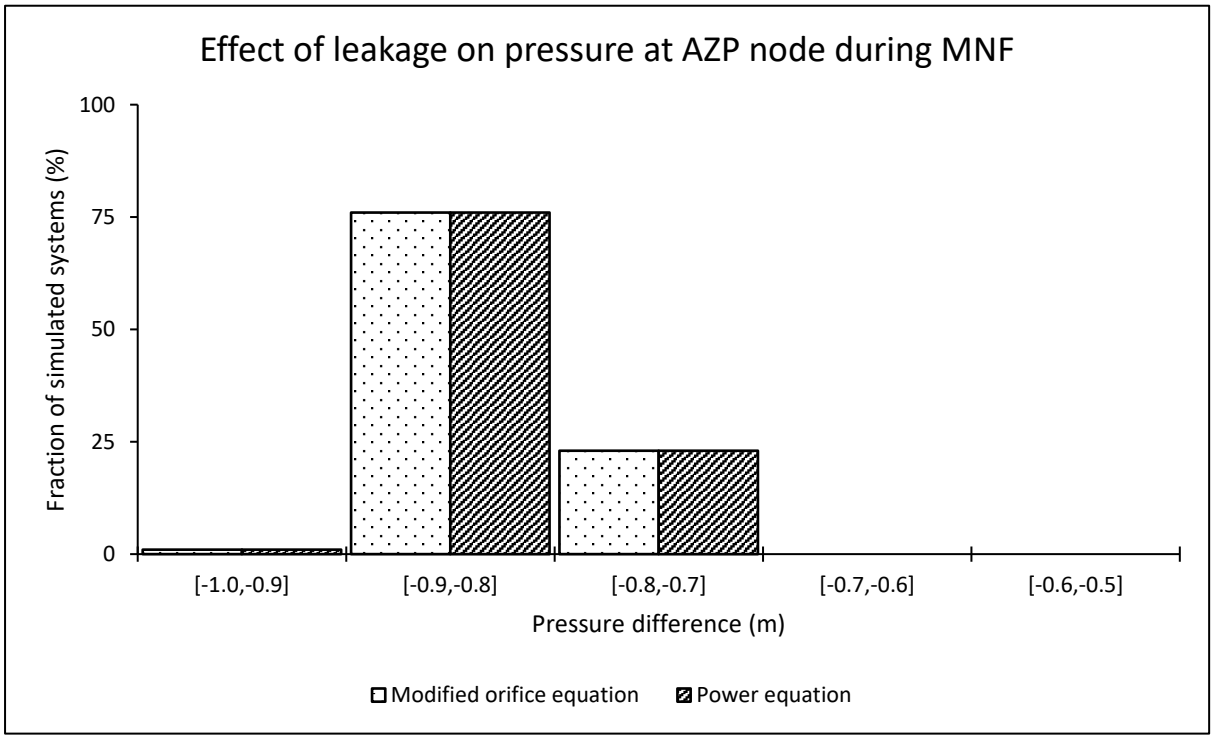

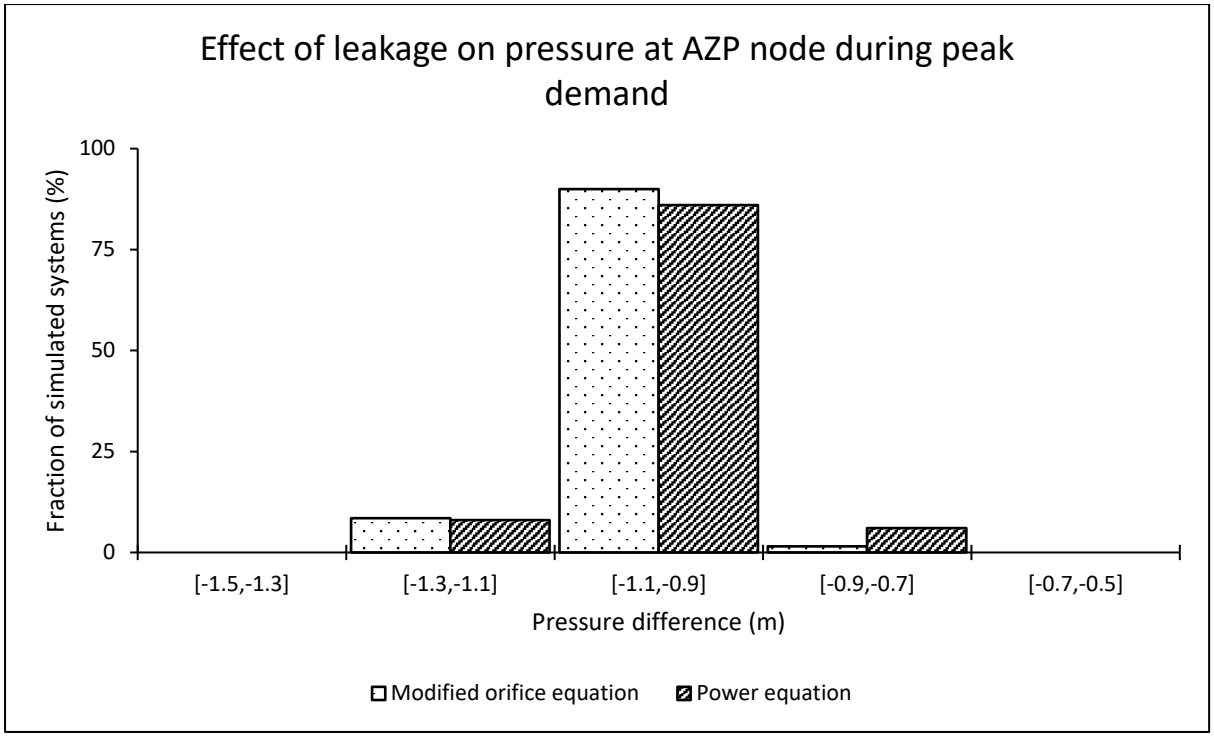
Effect of leakage on pressure at AZP node during peak demand
Fraction of simulated systems (%)
100
75
50
25
0
[-1.5,-1.3]
[-1.3,-1.1]
[-1.1,-0.9]
[-0.9,-0.7]
[-0.7,-0.5]
Pressure difference (m)
Modified orifice equation
Power equation

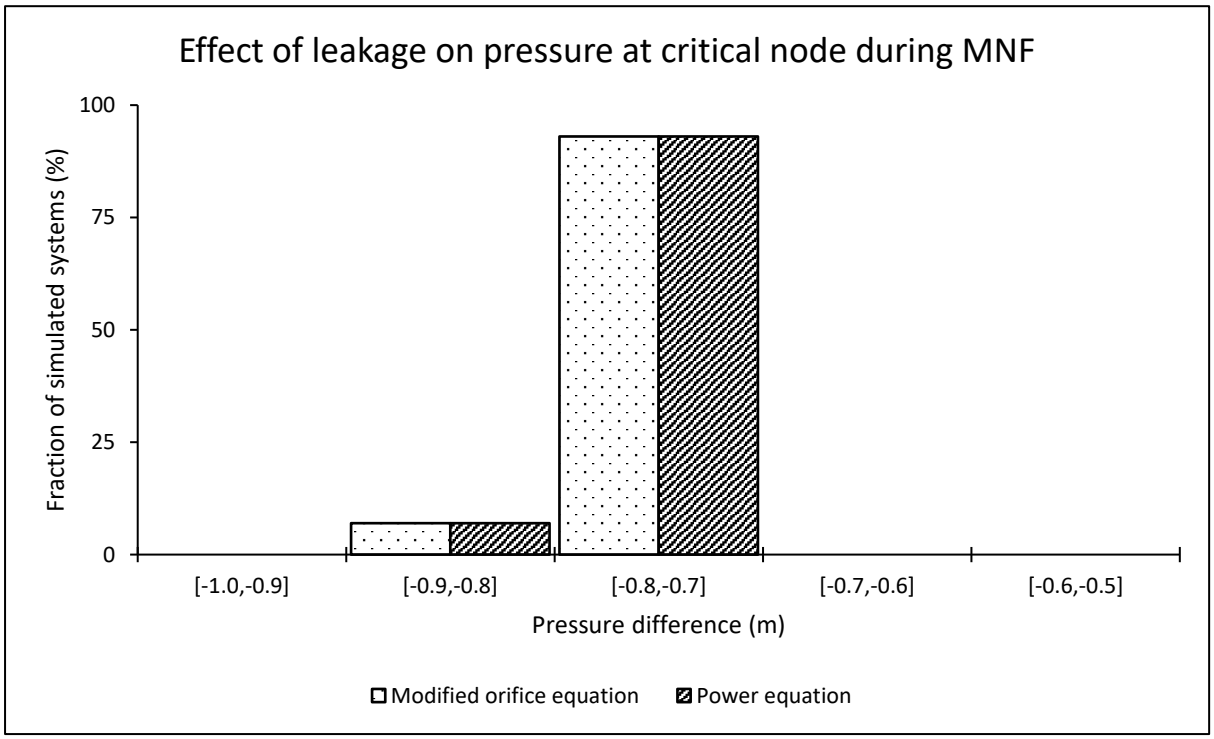
Effect of leakage on pressure at critical node during MNF
Fraction of simulated systems (%)
100
75
50
25
0
[-1.0,-0.9]
[-0.9,-0.8]
[-0.8,-0.7]
[-0.7,-0.6]
[-0.6,-0.5]
Pressure difference (m)
Modified orifice equation
Power equation

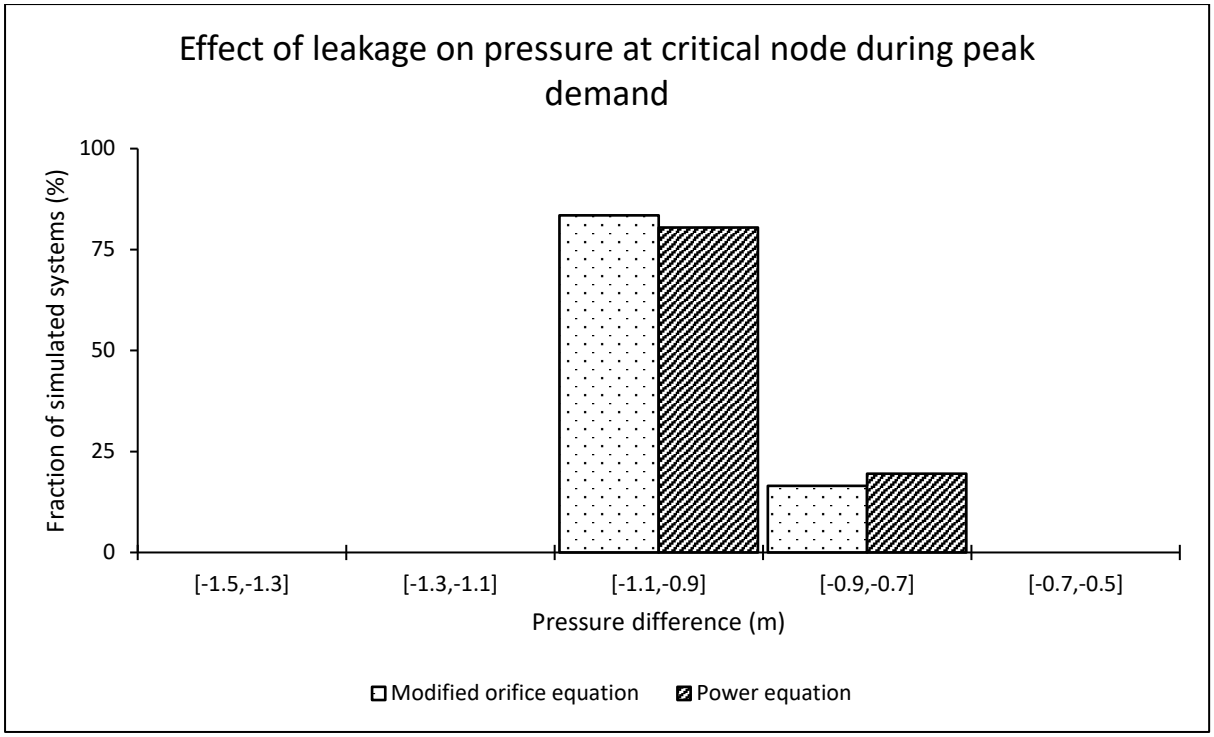
Effect of leakage on pressure at critical node during peak demand
Fraction of simulated systems (%)
100
75
50
25
0
[-1.5,-1.3]
[-1.3,-1.1]
[-1.1,-0.9]
[-0.9,-0.7]
[-0.7,-0.5]
Pressure difference (m)
Modified orifice equation
Power equation

Pressure estimation error when using the power equation at average zone pressure (AZP) and critical nodes

	During MNF conditions				During peak demand conditions			
	Min (%)	**Mean (%)**	**Median (%)**	**Max (%)**	**Min (%)**	**Mean (%)**	**Median (%)**	**Max (%)**
At the AZP node	0.00	0.00	0.00	0.00	0.00	0.02	0.02	0.06
At the critical node	0.00	0.00	0.00	0.00	0.00	0.02	0.02	0.06

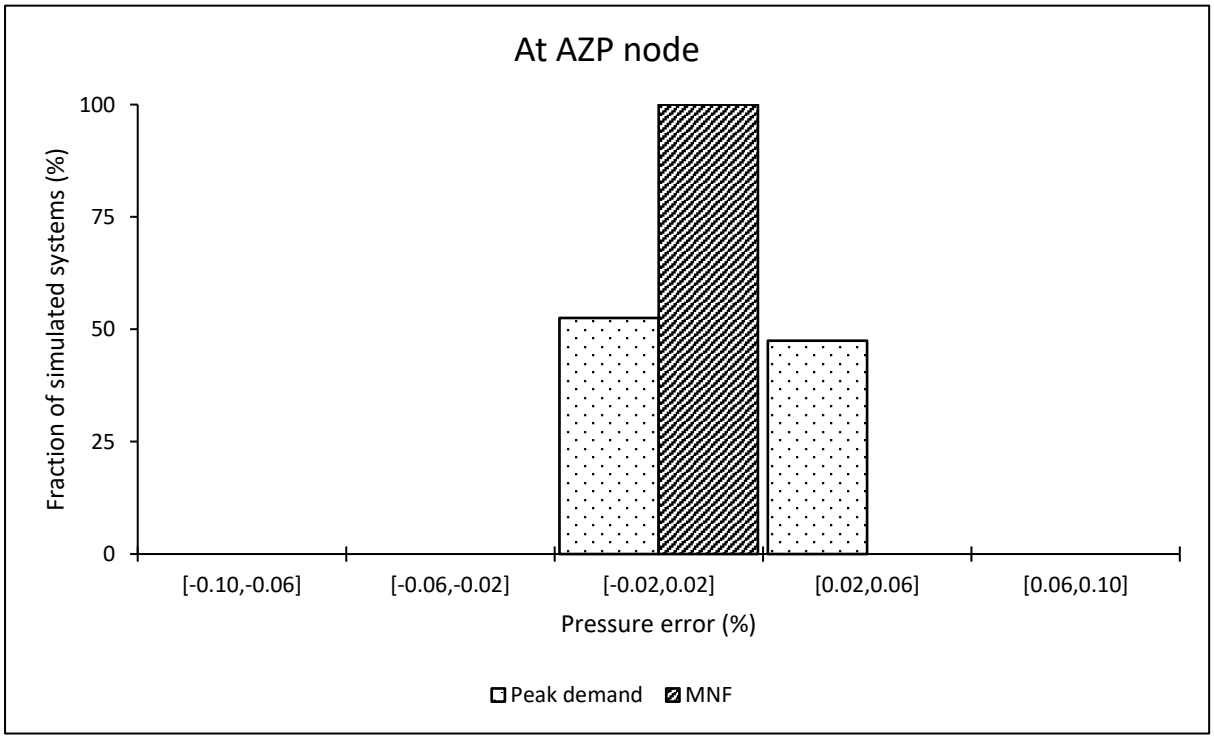

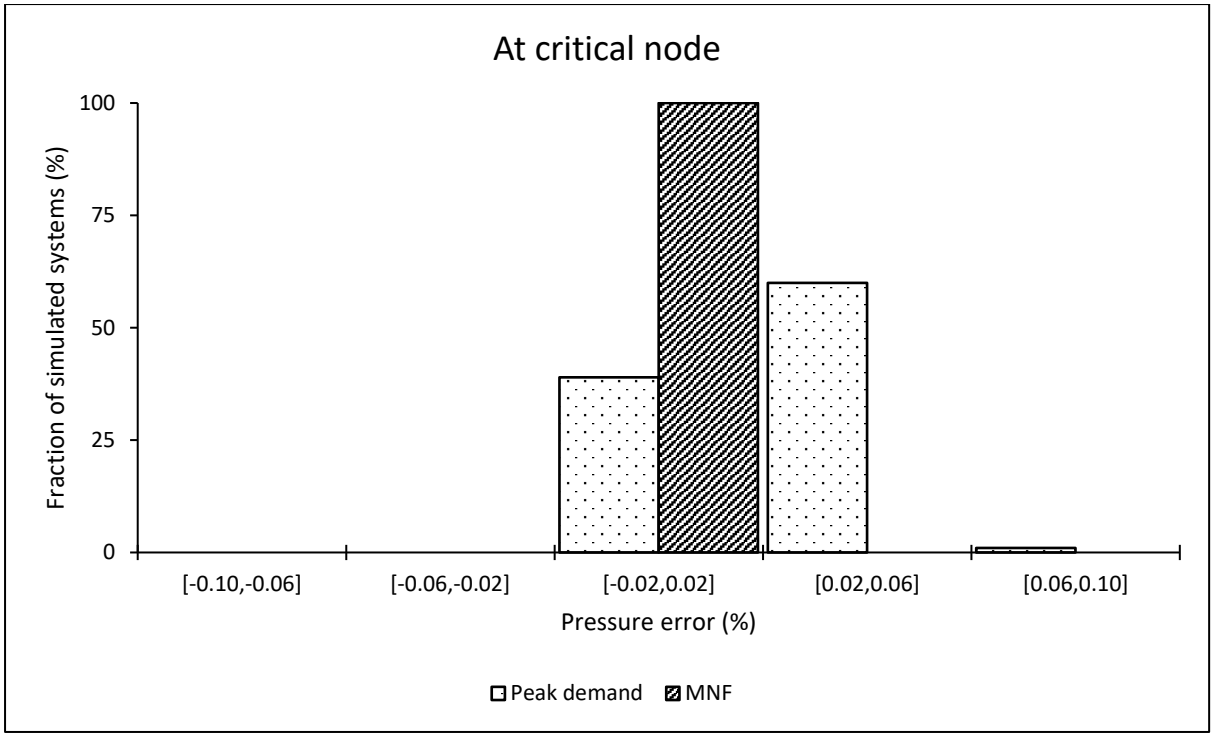
At critical node
Fraction of simulated systems (%)
100
75
50
25
0
[-0.10,-0.06]
[-0.06,-0.02]
[-0.02,0.02]
[0.02,0.06]
[0.06,0.10]
Pressure error (%)
Peak demand
MNF

System leakage estimation error when using the power equation

	Leakage estimation error (%)			
	Minimum	**Arithmetic Mean**	**Median**	**Maximum**
Before implementing pressure management	-1.57	-0.46	-0.38	0.15
After implementing pressure management	-20.18	-9.21	-8.97	-2.57

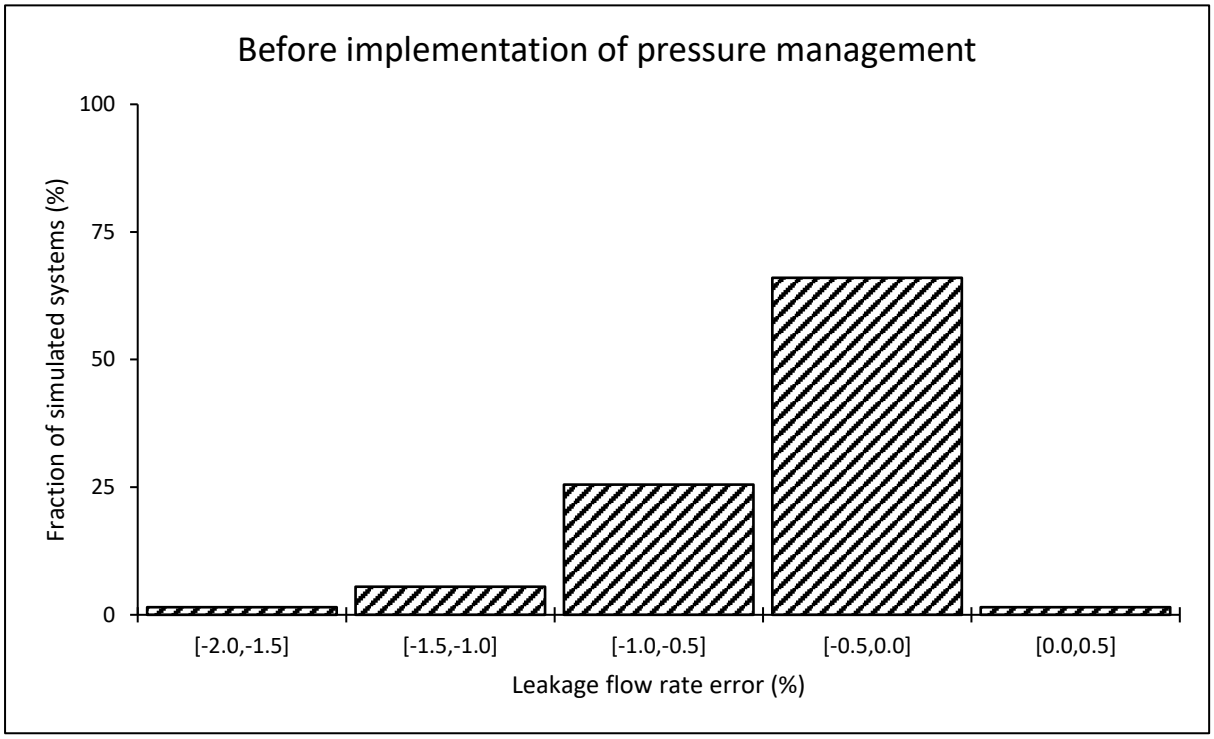

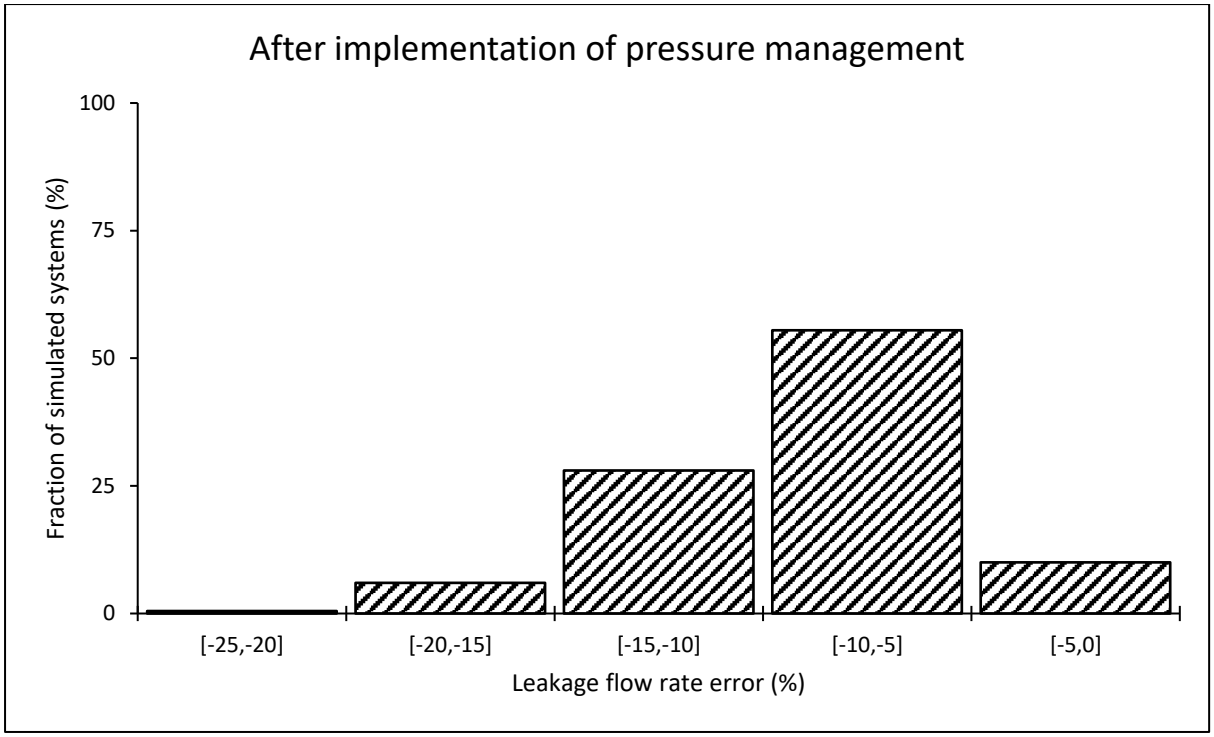
After implementation of pressure management
Fraction of simulated systems (%)
100
75
50
25
0
[-25,-20]
[-20,-15]
[-15,-10]
[-10,-5]
[-5,0]
Leakage flow rate error (%)

Leakage estimation error when using the power equation at the critical node

	Leakage estimation error (%)			
	Minimum	**Arithmetic Mean**	**Median**	**Maximum**
Before implementing pressure management	-10.36	-4.50	-5.08	10.91
After implementing pressure management	-51.74	-27.00	-30.31	72.68

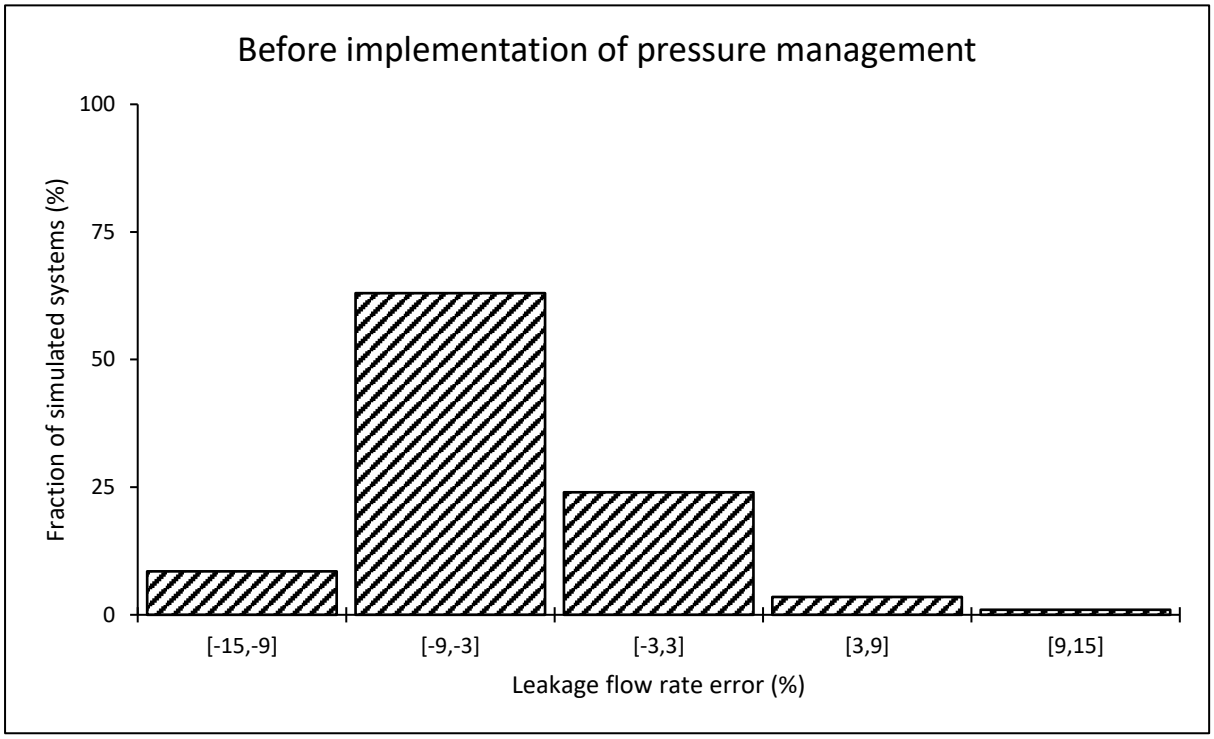

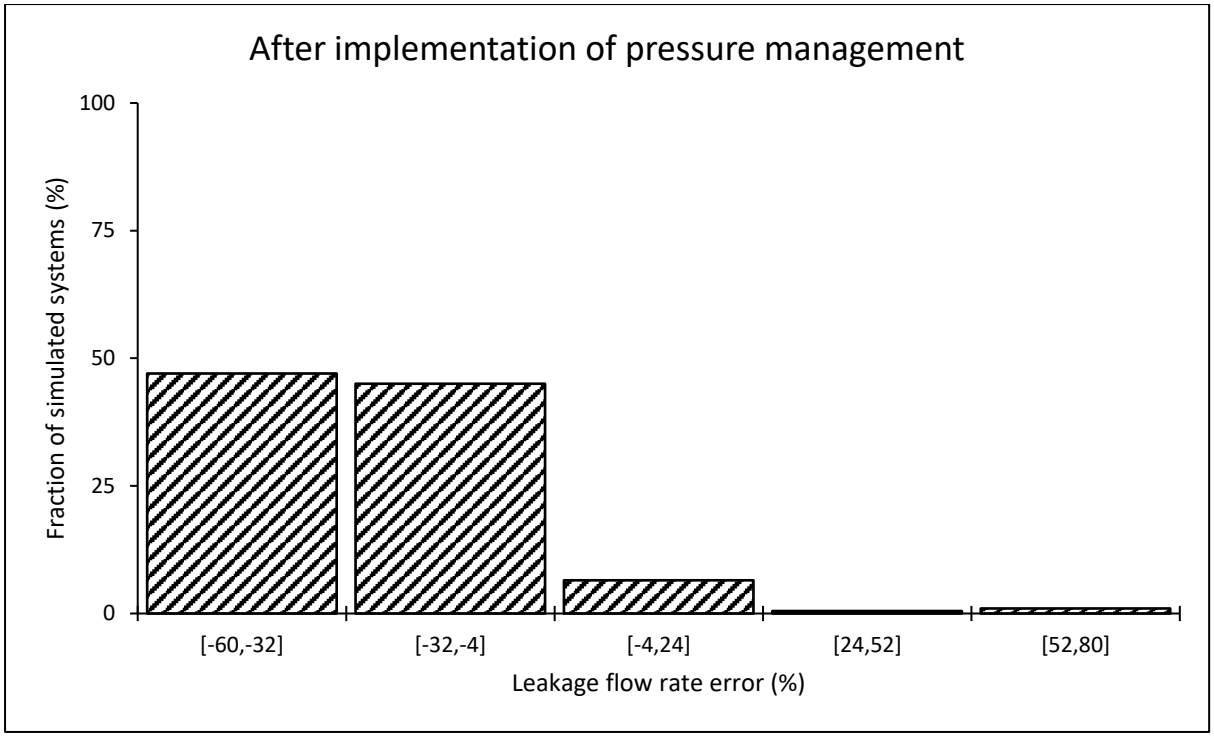
After implementation of pressure management
Fraction of simulated systems (%)
100
75
50
25
0
[-60,-32]
[-32,-4]
[-4,24]
[24,52]
[52,80]
Leakage flow rate error (%)

Appendix A-7: Medium-sized network with an ILI of 16

Results for an individual system

Pressure head at the average zone pressure (AZP) node

		Pressure head (m)			
		Minimum	**Arithmetic Mean**	**Median**	**Maximum**
Before pressure management	Without leaks	72.69	88.62	90.24	106.08
	Modified orifice equation	69.16	84.99	86.53	102.78
	Power equation	69.21	85.01	86.54	102.78
After pressure management	Modified orifice equation	21.52	37.11	38.65	54.48
	Power equation	21.80	37.29	38.81	54.55

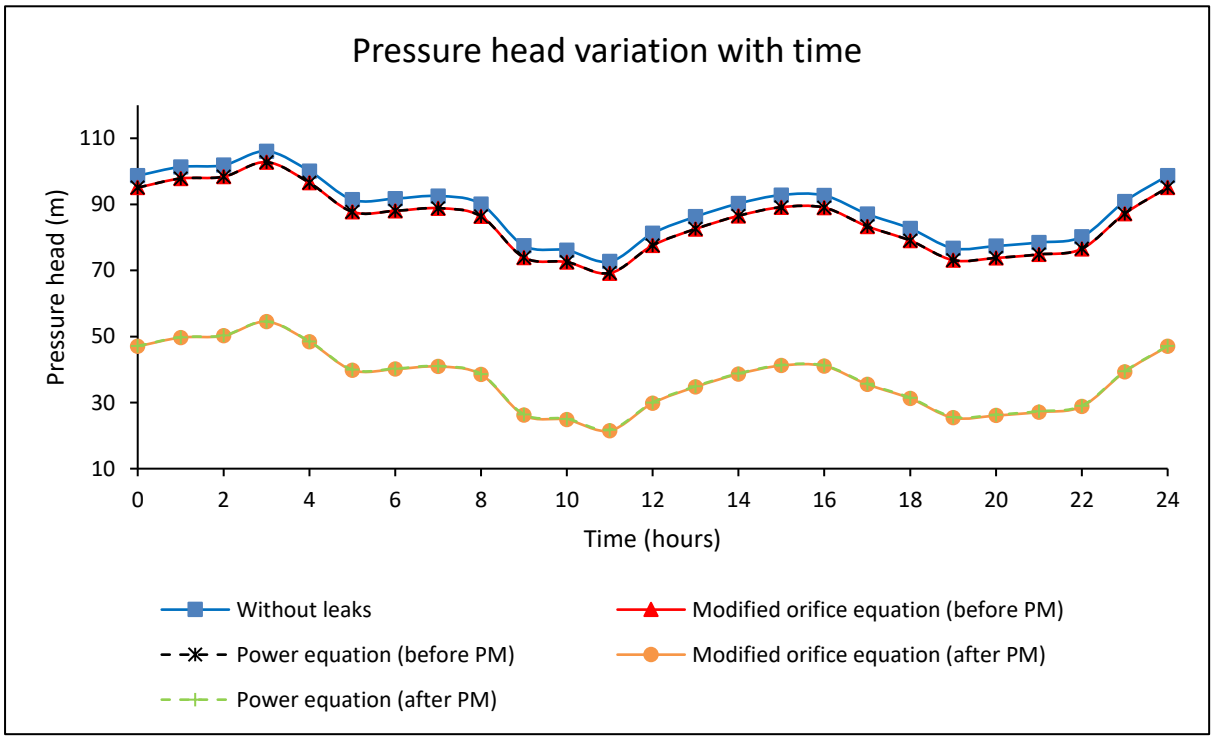

Pressure head at the critical node

		Pressure head (m)			
		Minimum	**Arithmetic Mean**	**Median**	**Maximum**
Before pressure management	Without leaks	60.21	75.09	76.77	90.93
	Modified orifice equation	56.97	71.77	73.36	87.90
	Power equation	57.02	71.78	73.37	87.90
After pressure management	Modified orifice equation	9.13	23.71	25.30	39.46
	Power equation	9.39	23.87	25.45	39.53

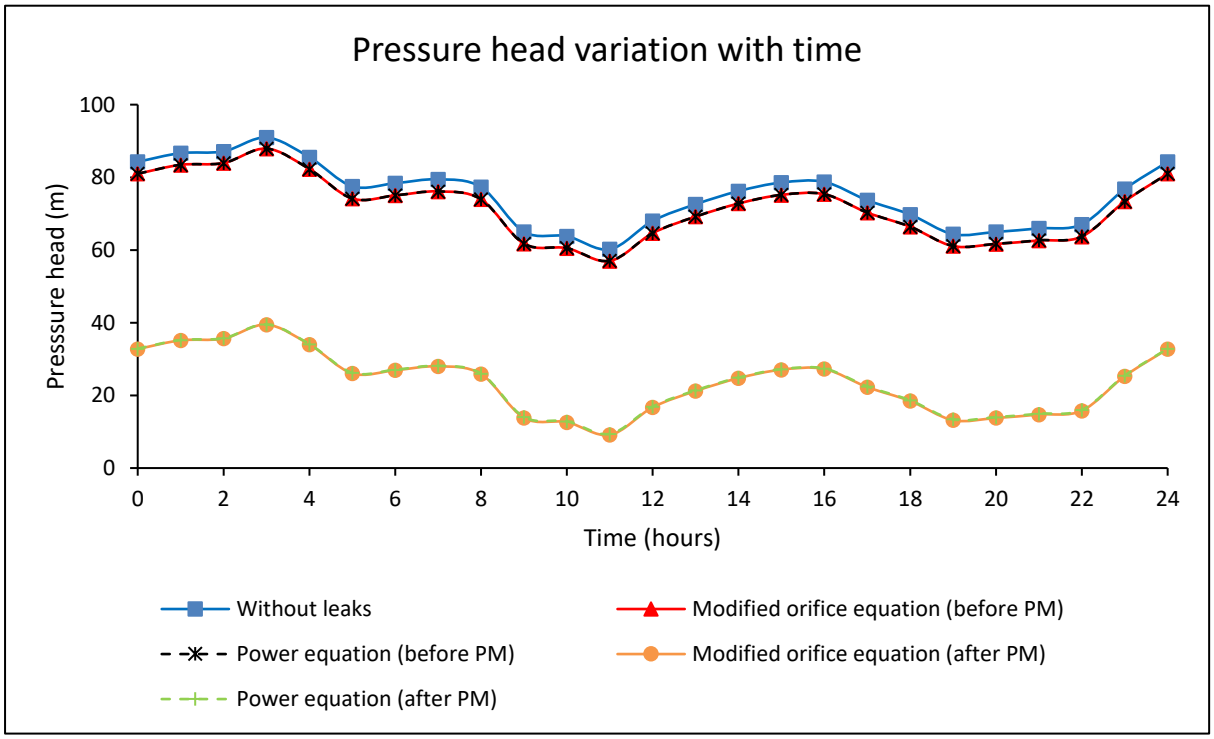

System leakage flow rate

		Leakage flow rate (m^3/h)			
		Minimum	**Arithmetic Mean**	**Median**	**Maximum**
Before pressure management	Modified orifice equation	115.15	144.78	147.42	179.23
	Power equation	113.44	144.22	147.06	179.23
After pressure management	Modified orifice equation	38.76	61.98	64.00	89.07
	Power equation	29.43	55.22	57.50	85.15

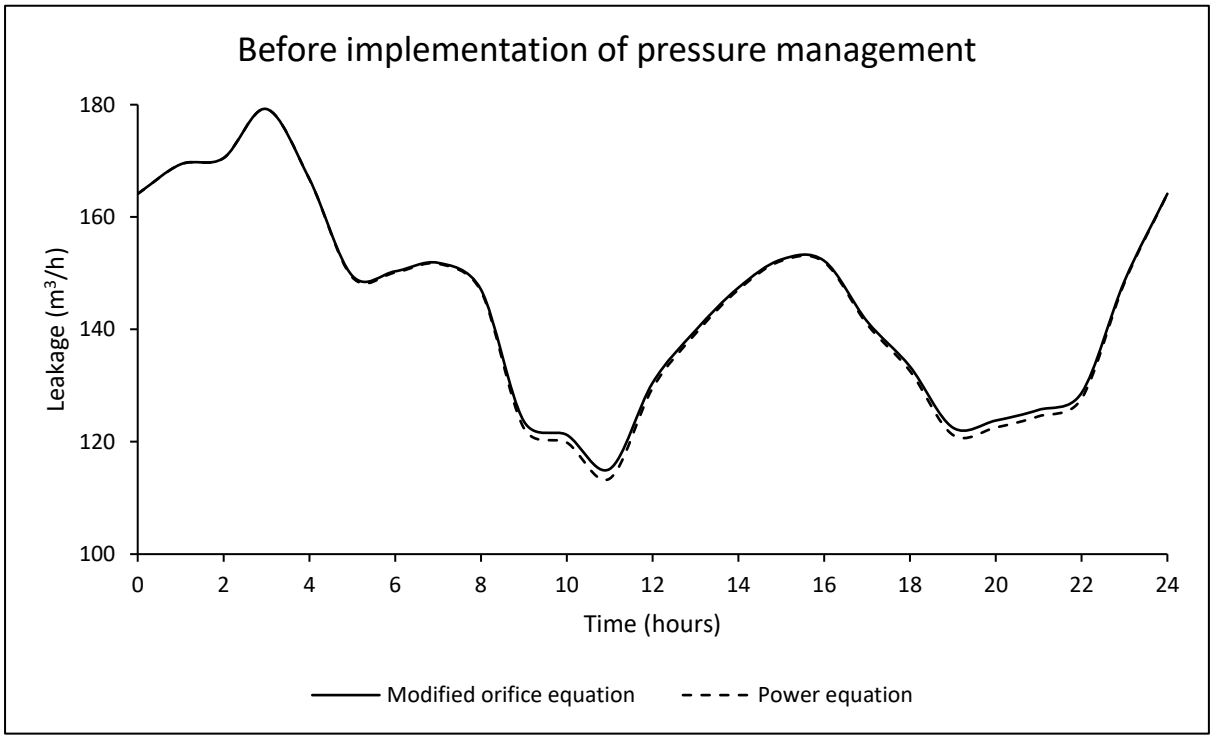

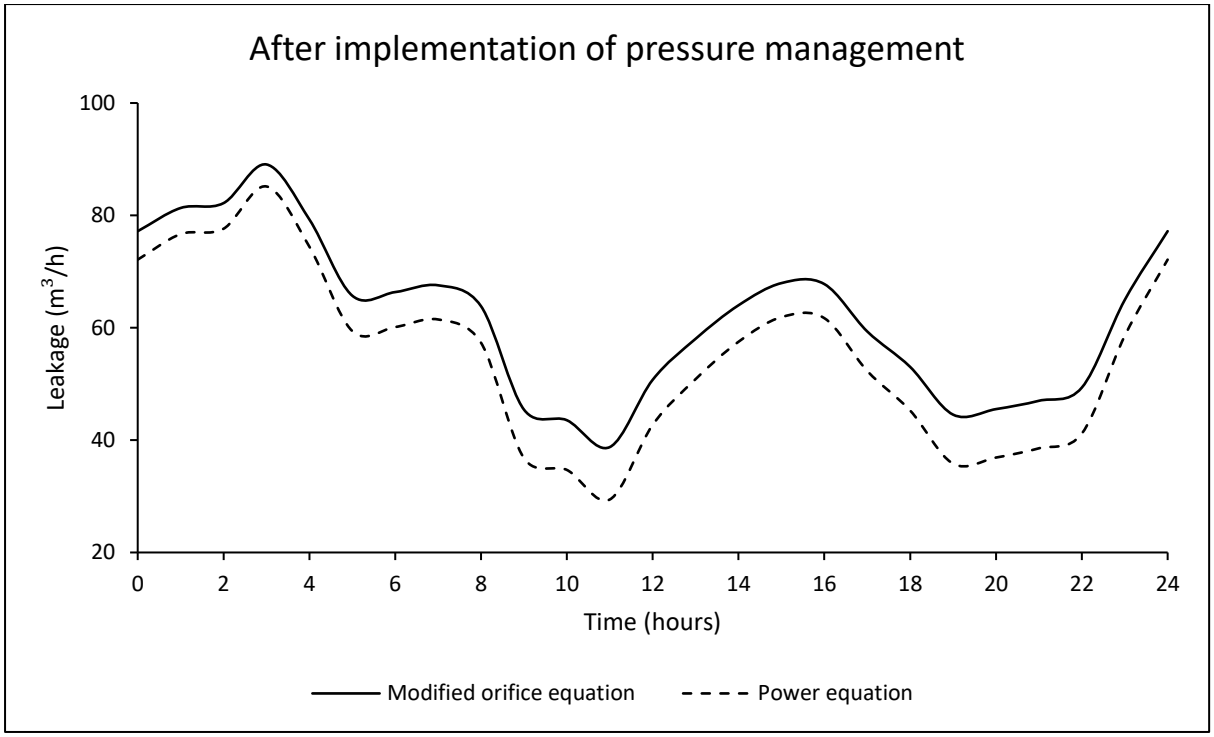
After implementation of pressure management
100
80
60
40
20
Leakage (m3/h)
0
2
4
6
8
10
12
14
16
18
20
22
24
Time (hours)
Modified orifice equation
Power equation

Leakage flow rate at the critical node

		Leakage flow rate (m^3/h)			
		Minimum	**Arithmetic Mean**	**Median**	**Maximum**
Before pressure management	Modified orifice equation	0.13	0.15	0.15	0.16
	Power equation	0.10	0.13	0.13	0.16
After pressure management	Modified orifice equation	0.05	0.08	0.09	0.11
	Power equation	0.01	0.04	0.04	0.06

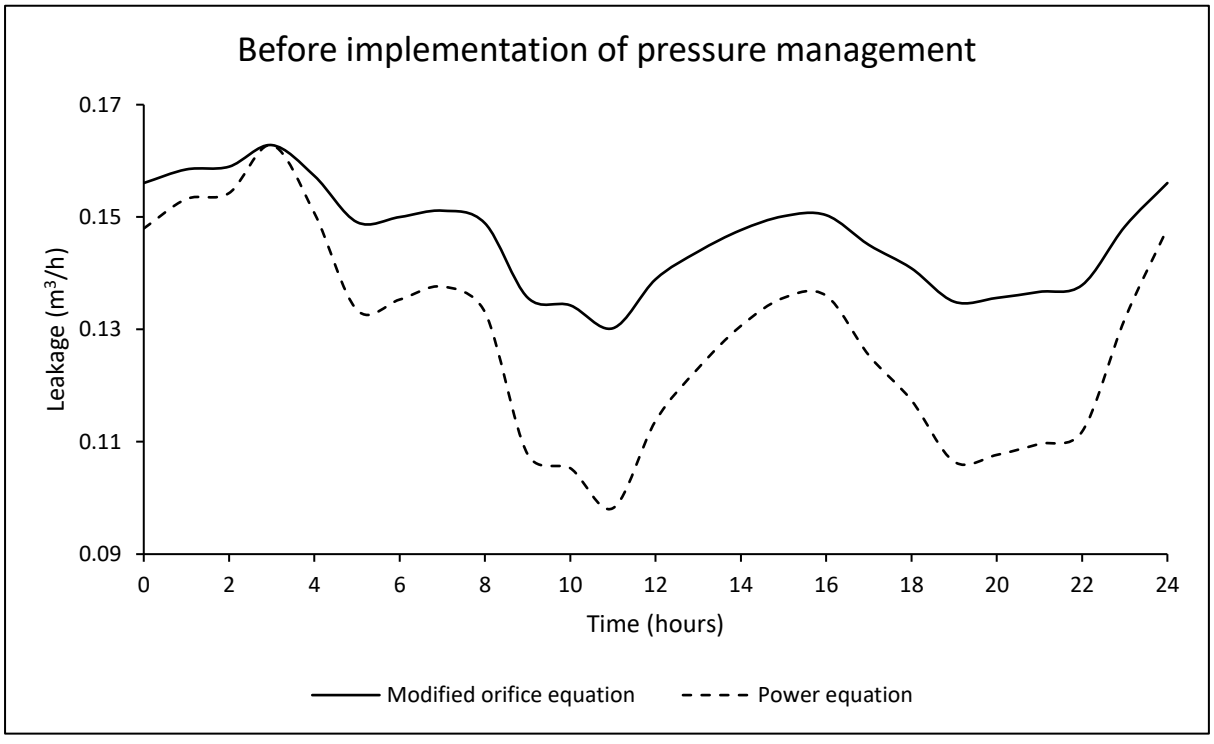

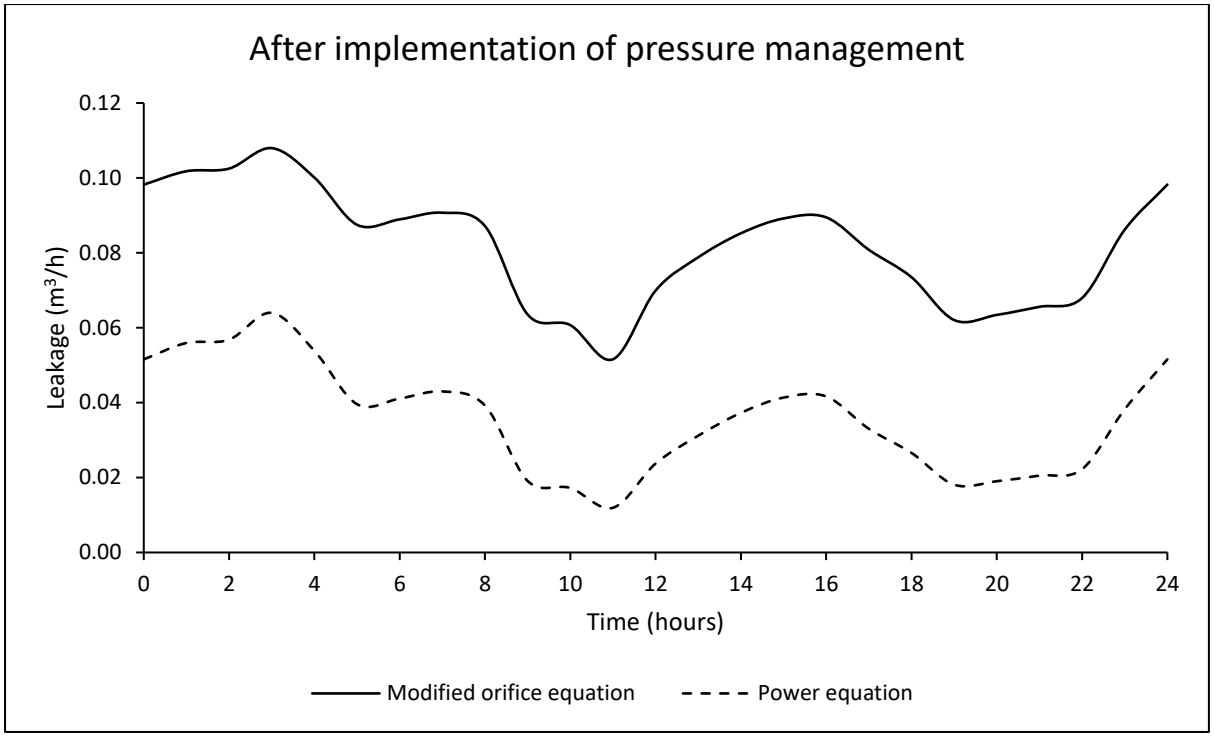
After implementation of pressure management
0.12
0.10
0.08
0.06
0.04
0.02
0.00
Leakage (m3/h)
0
2
4
6
8
10
12
14
16
18
20
22
24
Time (hours)
Modified orifice equation
Power equation

Number of iterations required for a system to converge to a hydraulic solution for both formulations

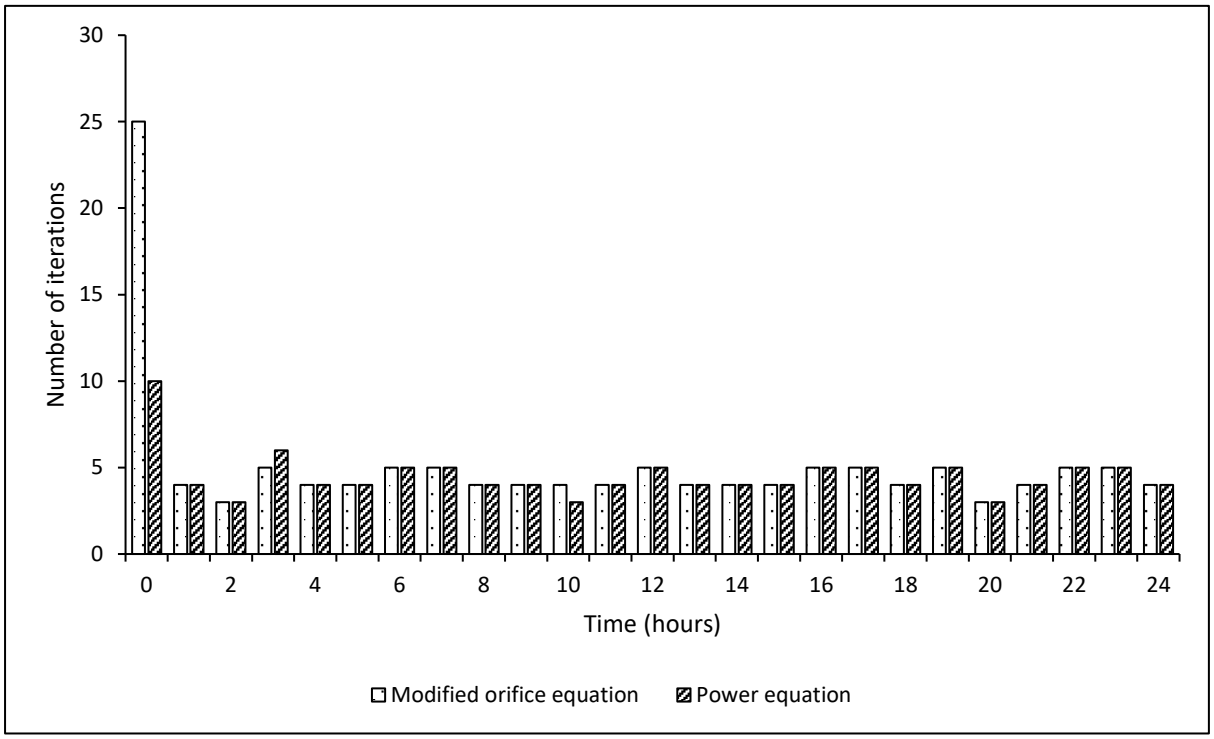

Results for combined systems

System parameters for both power and modified orifice formulations

	Minimum	Arithmetic Mean	Median	Maximum
Leakage exponent N1	0.81	1.07	1.07	1.35
Leakage coefficient C	9.2E-05	3.9E-04	3.6E-04	1.2E-03
Effective initial leak area C_dA0 (mm^2)	158.20	472.64	475.04	781.98
Effective head-area slope C_dm (mm^2/m)	3.52	6.20	6.20	9.17
Leakage number LN	0.45	1.49	1.32	5.54

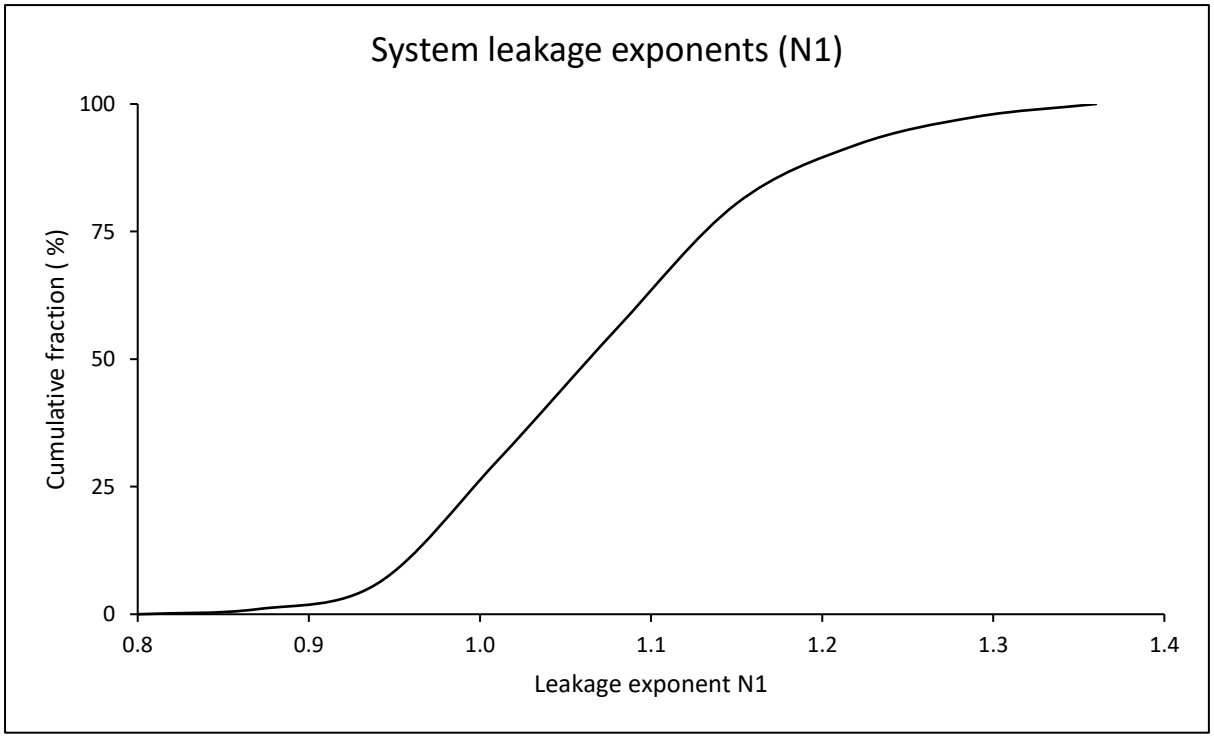

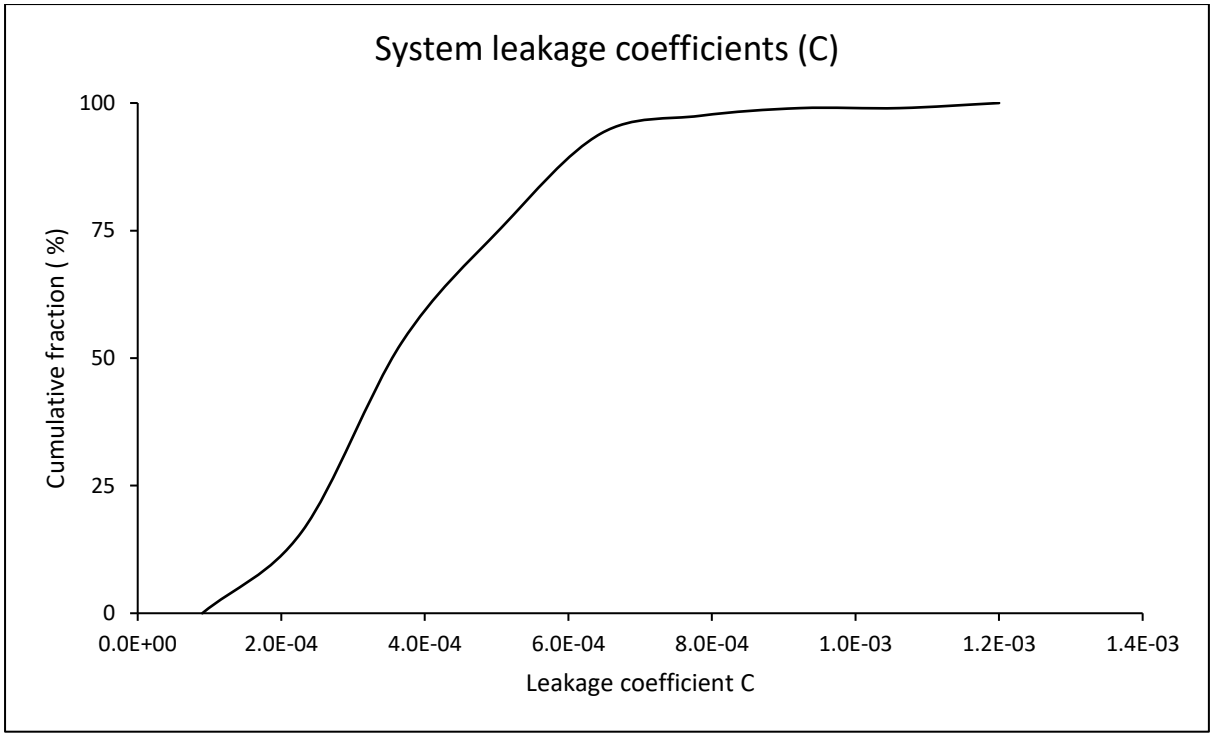
System leakage coefficients (C)
Cumulative fraction (%)
100
75
50
25
0
0.0E+00
2.0E-04
4.0E-04
6.0E-04
8.0E-04
1.0E-03
1.2E-03
1.4E-03
Leakage coefficient C

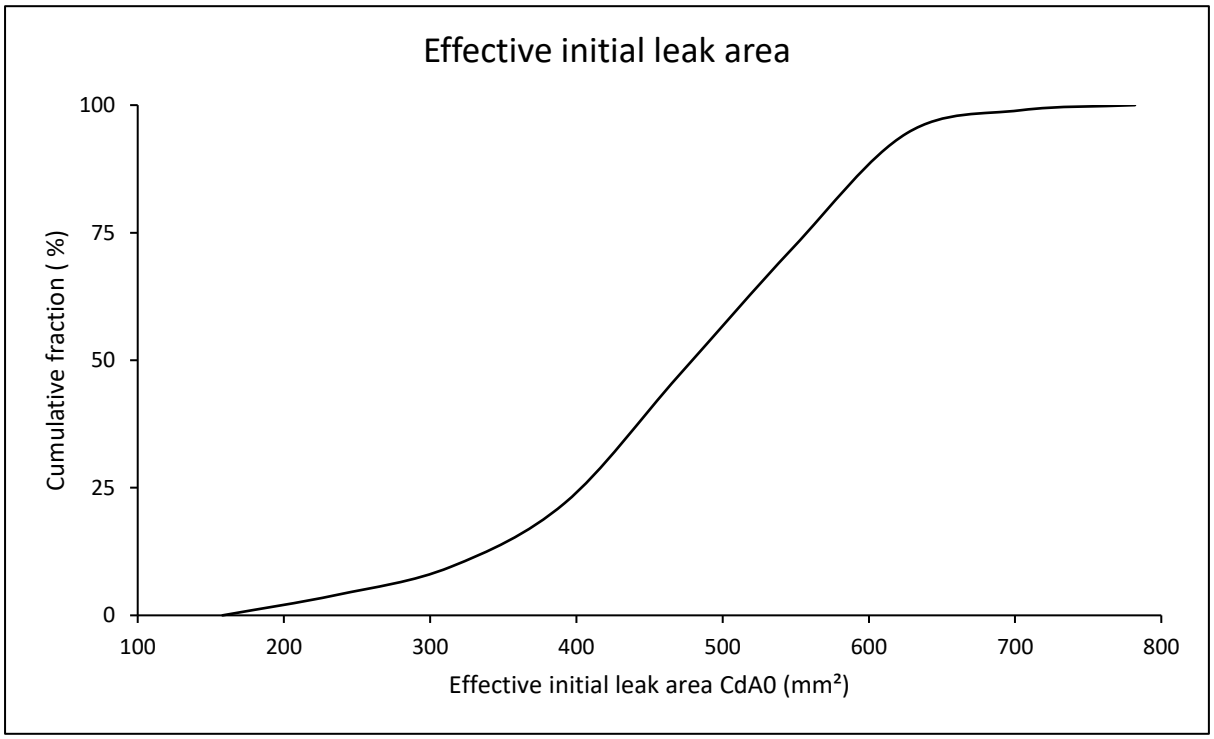
Effective initial leak area
Cumulative fraction (%)
100
75
50
25
0
100
200
300
400
500
600
700
800
Effective initial leak area CdA0 (mm²)

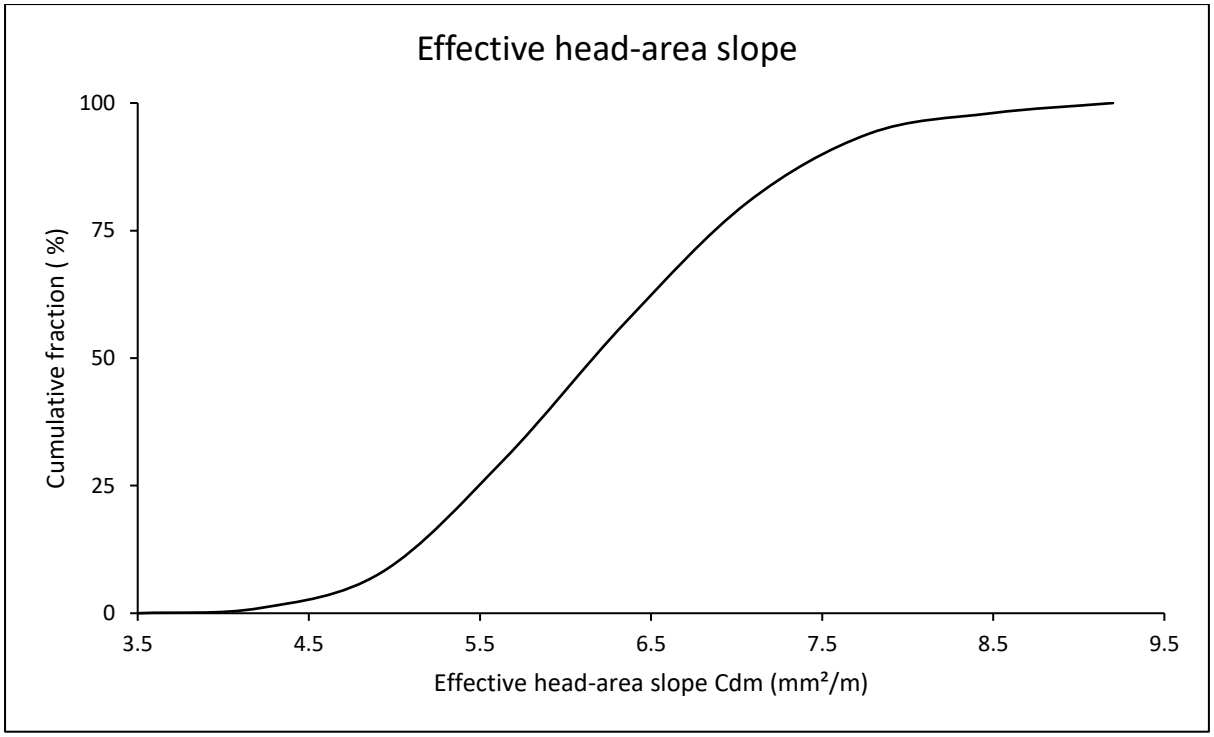
Effective head-area slope
Cumulative fraction (%)
100
75
50
25
0
3.5
4.5
5.5
6.5
7.5
8.5
9.5
Effective head-area slope Cdm (mm²/m)

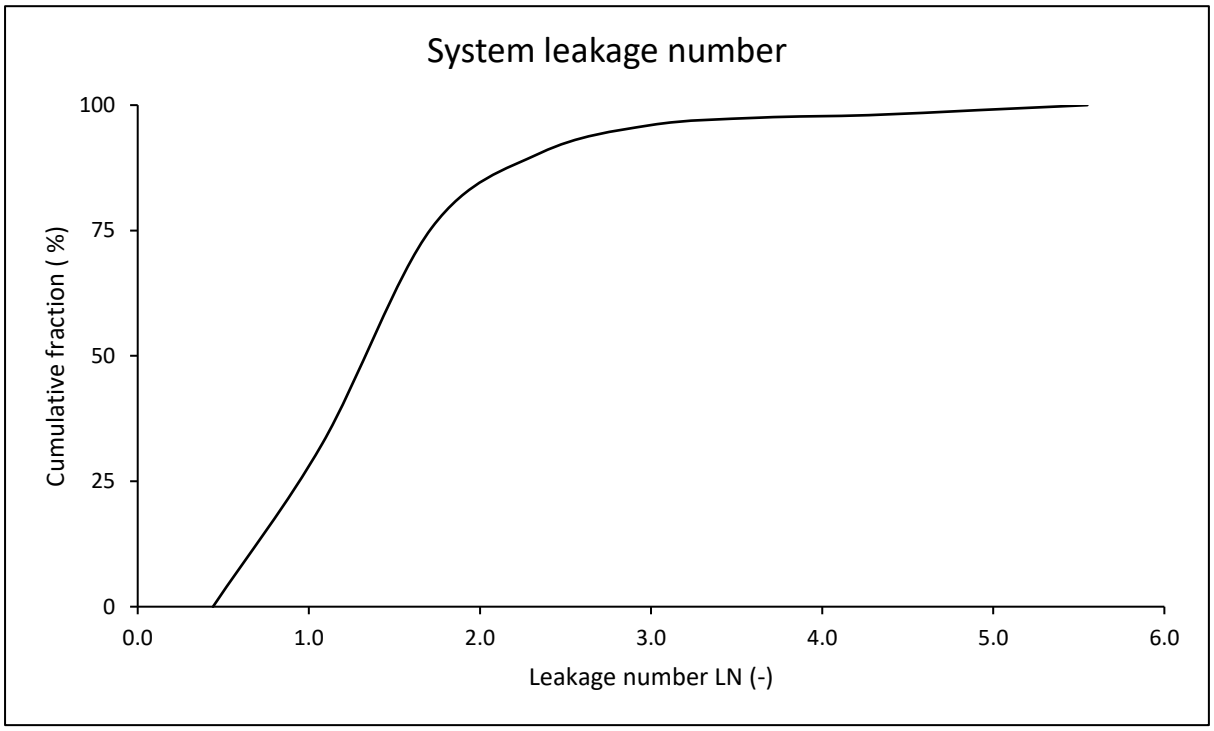
System leakage number
Cumulative fraction (%)
100
75
50
25
0
0.0
1.0
2.0
3.0
4.0
5.0
6.0
Leakage number LN (-)

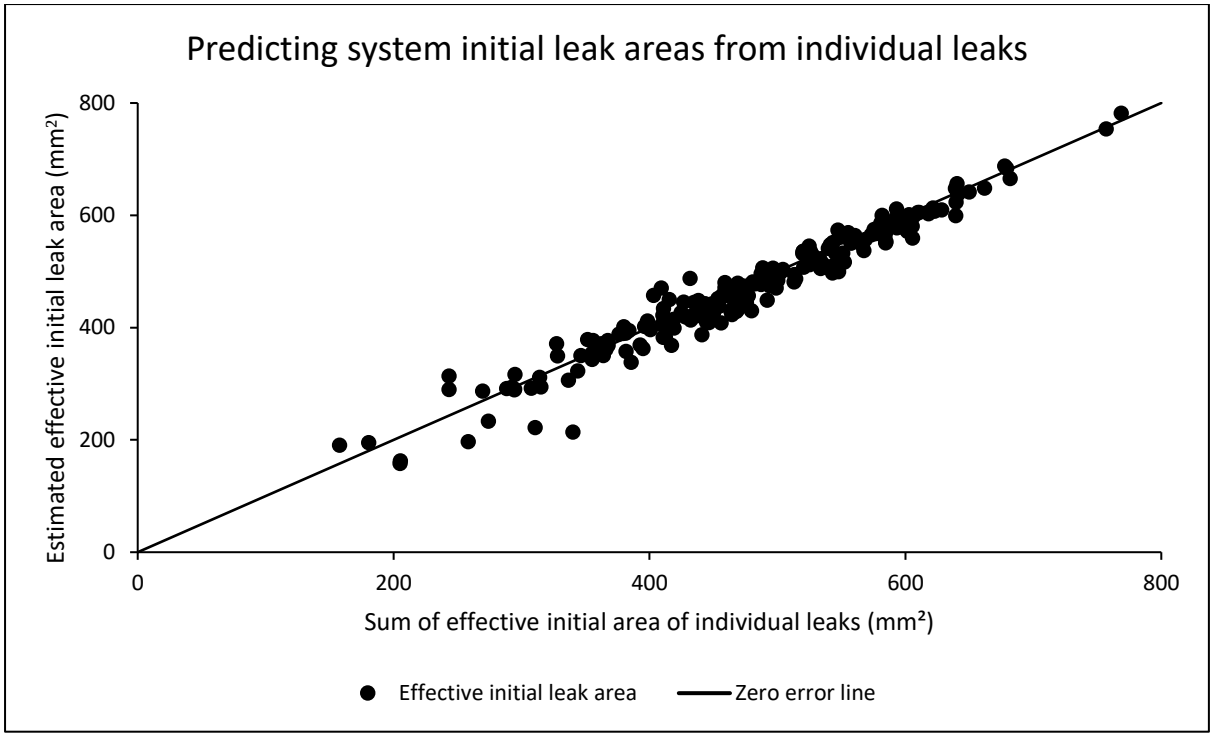
Predicting system initial leak areas from individual leaks
Estimated effective initial leak area (mm²)
0
200
400
600
800
Sum of effective initial area of individual leaks (mm²)
Effective initial leak area
Zero error line

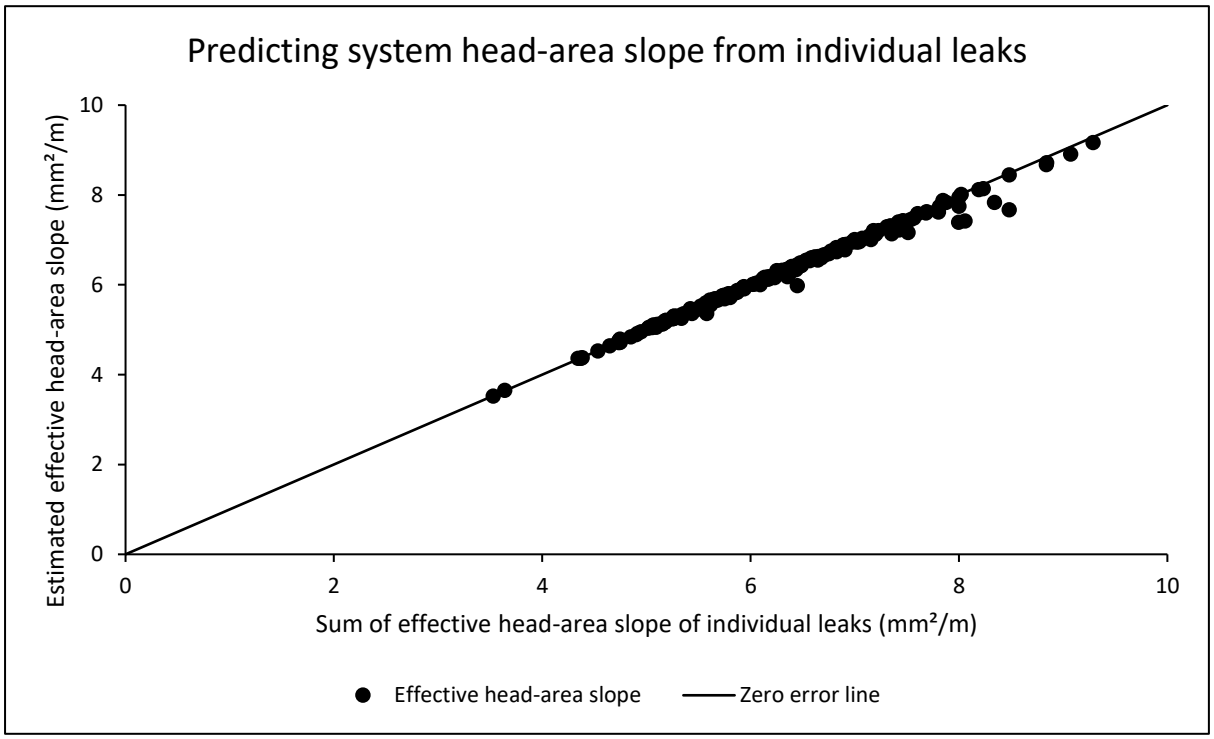
Predicting system head-area slope from individual leaks
Estimated effective head-area slope (mm²/m)
0
2
4
6
8
10
Sum of effective head-area slope of individual leaks (mm²/m)
Effective head-area slope
Zero error line

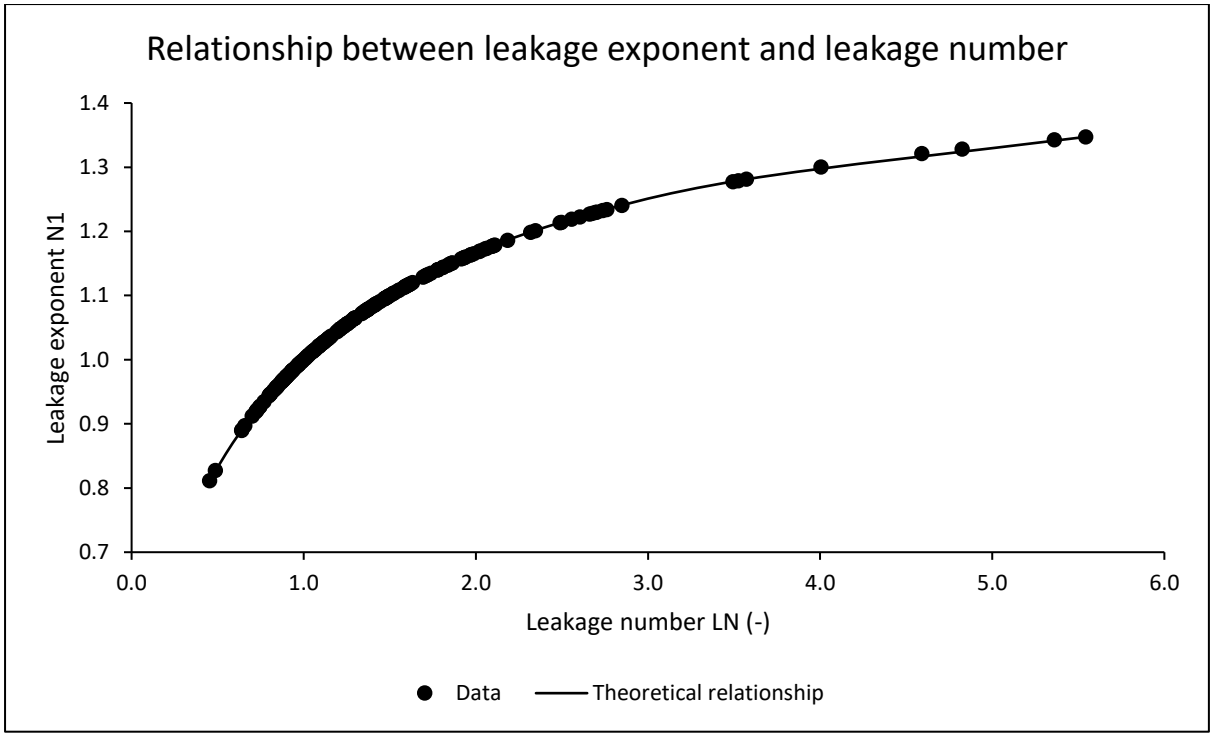
Relationship between leakage exponent and leakage number
Leakage exponent N1
1.4
1.3
1.2
1.1
1.0
0.9
0.8
0.7
0.0
1.0
2.0
3.0
4.0
5.0
6.0
Leakage number LN (-)
Data
Theoretical relationship

Average iterations required for a system to converge using both formulations

	Minimum	Arithmetic Mean	Median	Maximum
Modified orifice equation	4.92	5.12	5.12	5.24
Power equation	4.20	4.43	4.40	4.72

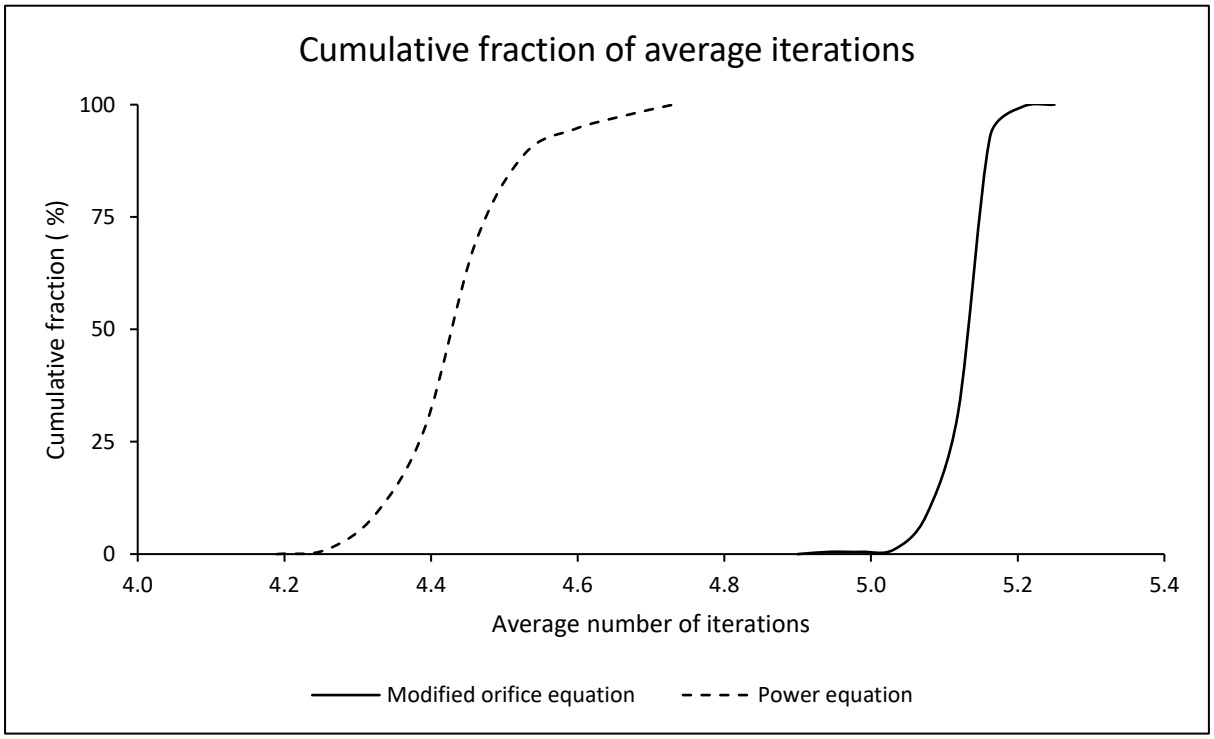

Effect of leakage on pressure at both average zone pressure (AZP) and critical nodes

AZP node								
	During MNF conditions				During peak demand conditions			
	Min (m)	Mean (m)	Median (m)	Max (m)	Min (m)	Mean (m)	Median (m)	Max (m)
Modified orifice equation	-3.86	-3.31	-3.30	-2.73	-4.13	-3.66	-3.68	-2.85
Power equation	-3.86	-3.31	-3.30	-2.73	-4.07	-3.60	-3.61	-2.73
Critical node								
Modified orifice equation	-3.82	-3.10	-3.08	-2.72	-3.91	-3.44	-3.48	-2.61
Power equation	-3.82	-3.10	-3.08	-2.72	-3.86	-3.38	-3.41	-2.51

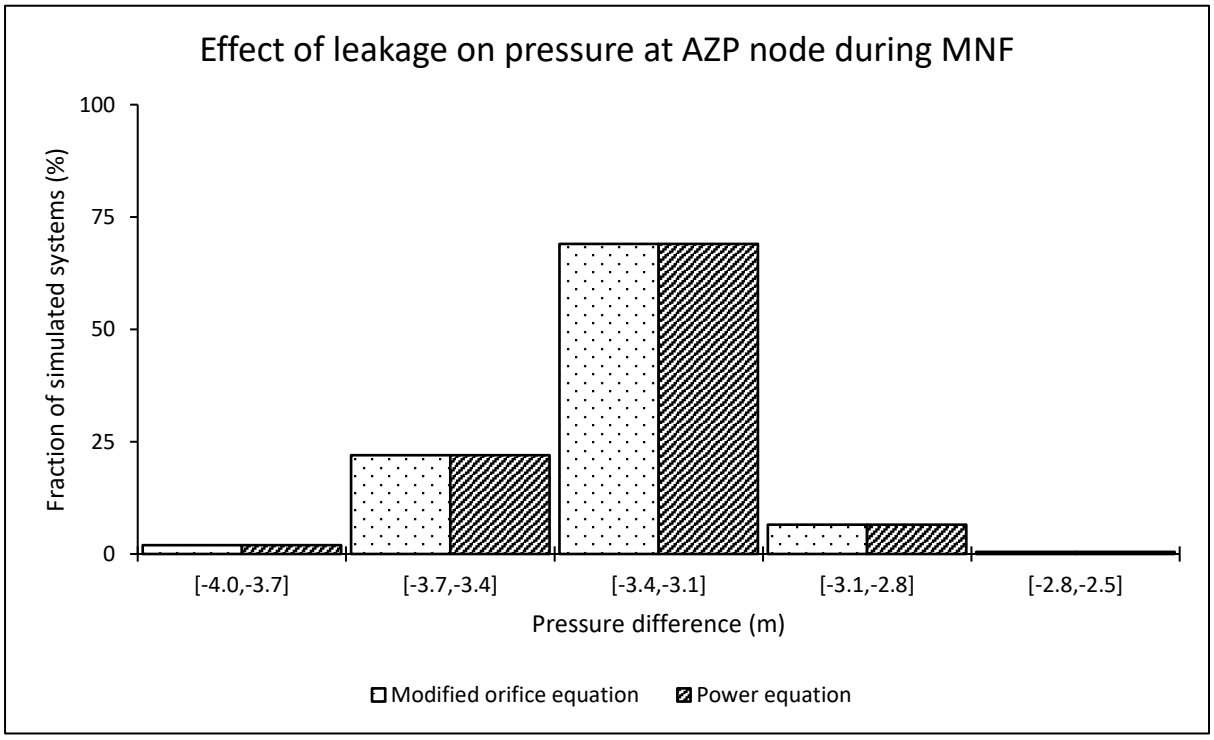

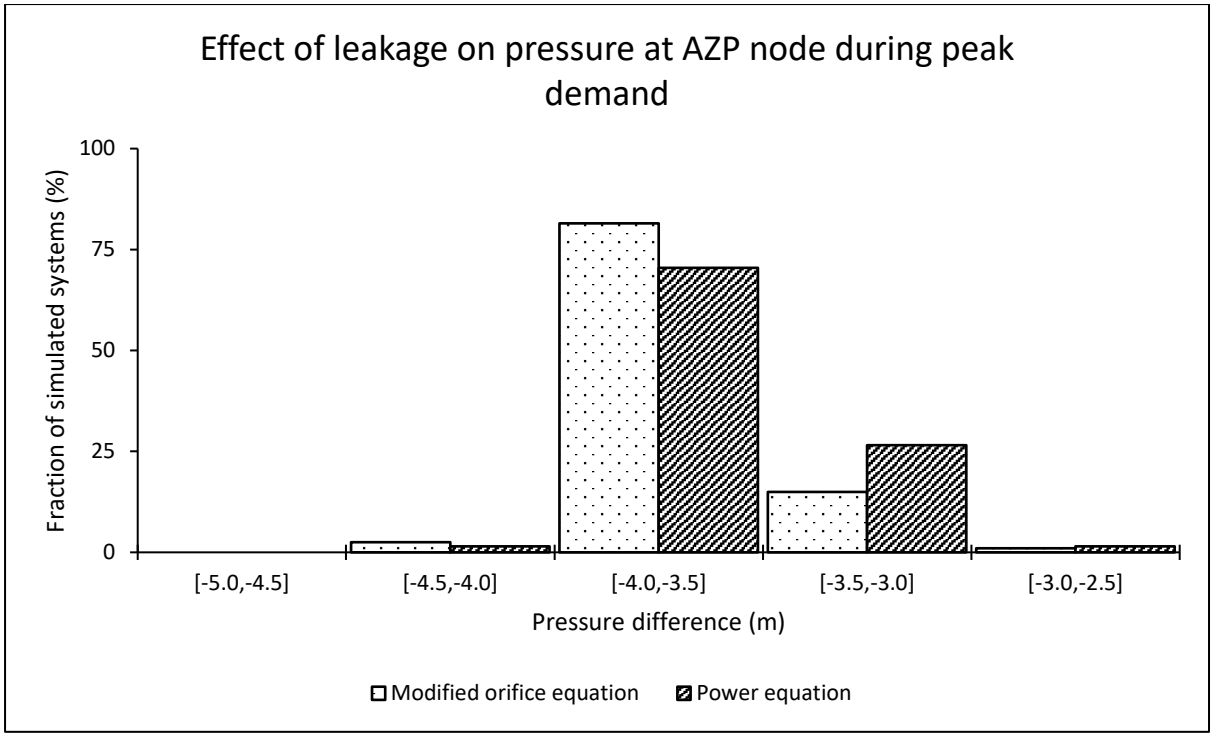
Effect of leakage on pressure at AZP node during peak demand
Fraction of simulated systems (%)
100
75
50
25
0
[-5.0,-4.5]
[-4.5,-4.0]
[-4.0,-3.5]
[-3.5,-3.0]
[-3.0,-2.5]
Pressure difference (m)
Modified orifice equation
Power equation

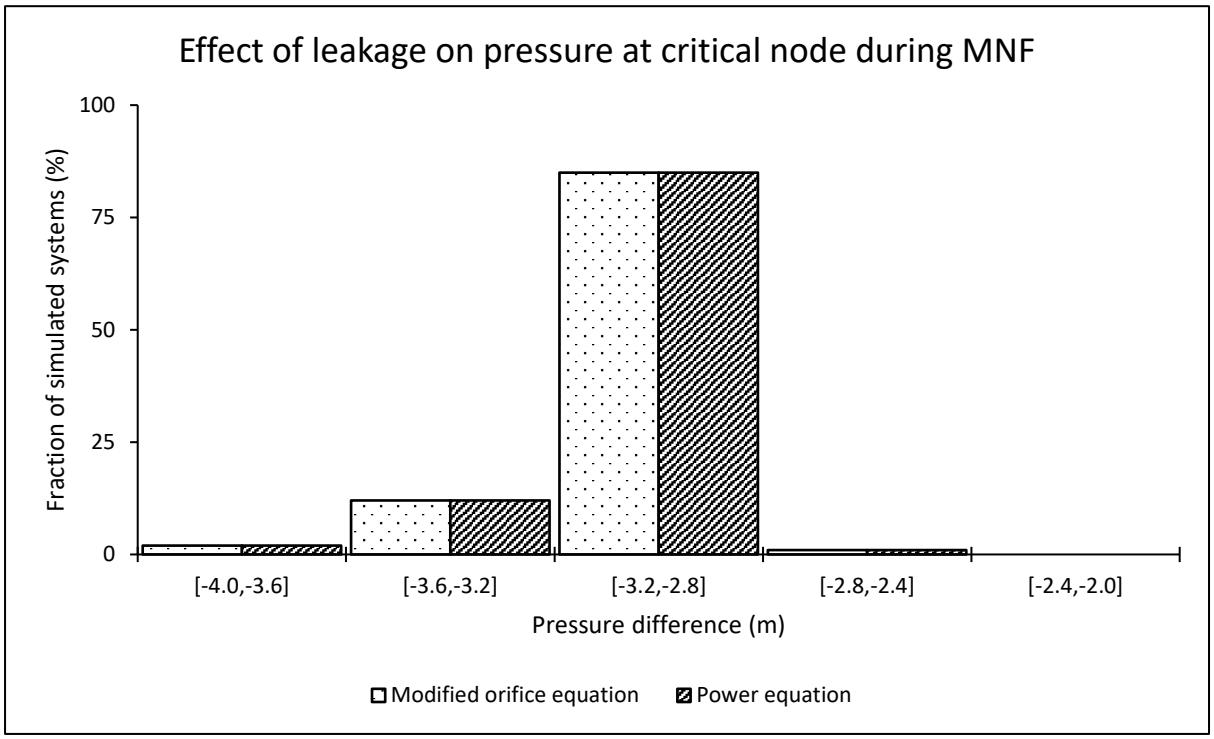
Effect of leakage on pressure at critical node during MNF
Fraction of simulated systems (%)
100
75
50
25
0
[-4.0,-3.6]
[-3.6,-3.2]
[-3.2,-2.8]
[-2.8,-2.4]
[-2.4,-2.0]
Pressure difference (m)
Modified orifice equation
Power equation

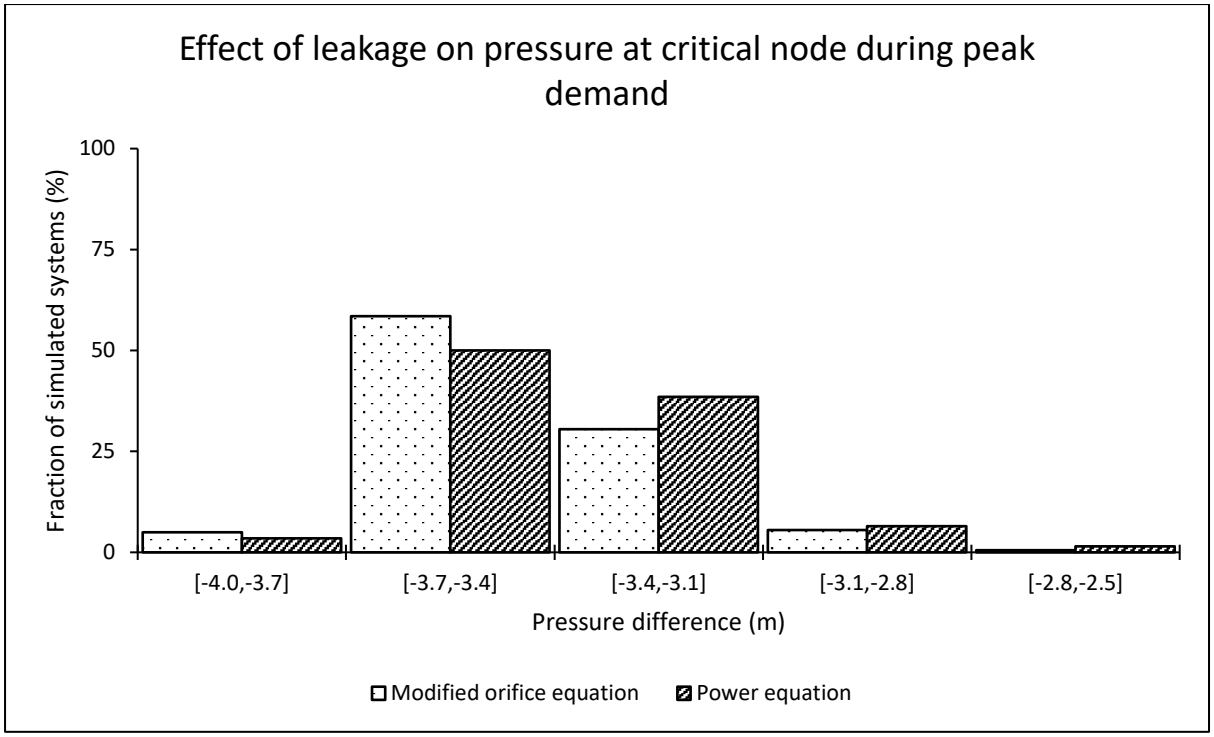
Effect of leakage on pressure at critical node during peak demand
Fraction of simulated systems (%)
100
75
50
25
0
[-4.0,-3.7]
[-3.7,-3.4]
[-3.4,-3.1]
[-3.1,-2.8]
[-2.8,-2.5]
Pressure difference (m)
Modified orifice equation
Power equation

Pressure estimation error when using the power equation at average zone pressure (AZP) and critical nodes

	During MNF conditions				During peak demand conditions			
	Min (%)	**Mean (%)**	**Median (%)**	**Max (%)**	**Min (%)**	**Mean (%)**	**Median (%)**	**Max (%)**
At the AZP node	0.00	0.00	0.00	0.00	-0.03	0.09	0.09	0.26
At the critical node	0.00	0.00	0.00	0.00	-0.06	0.11	0.11	0.27

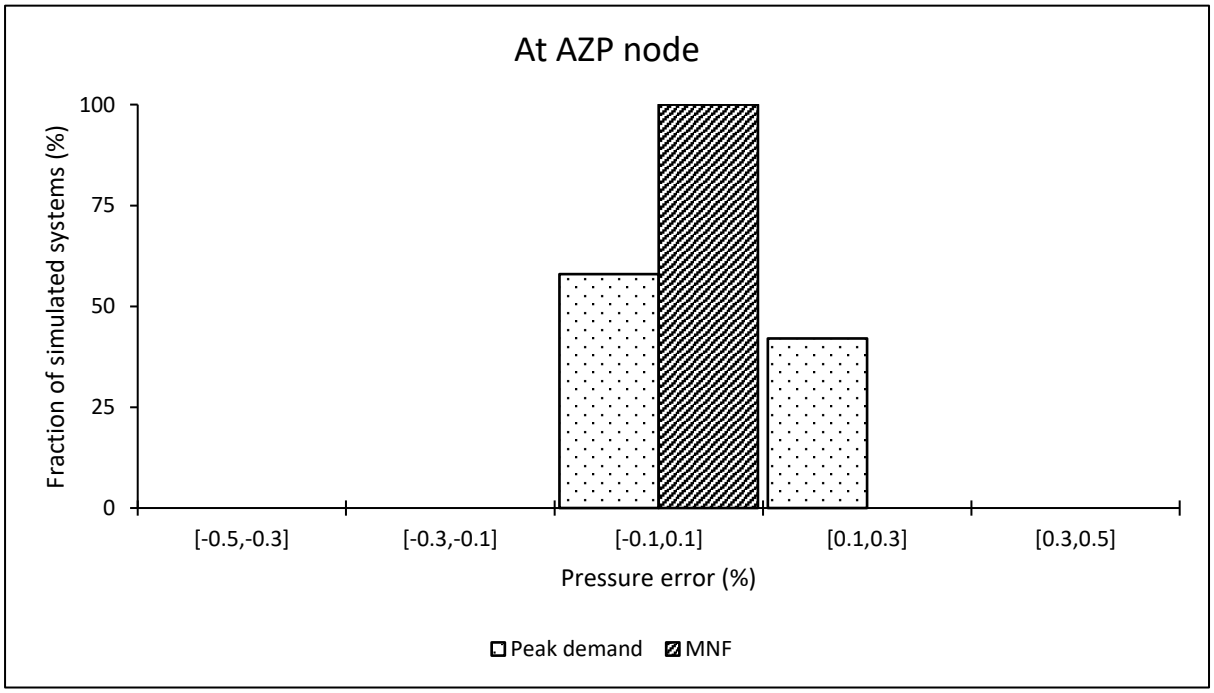

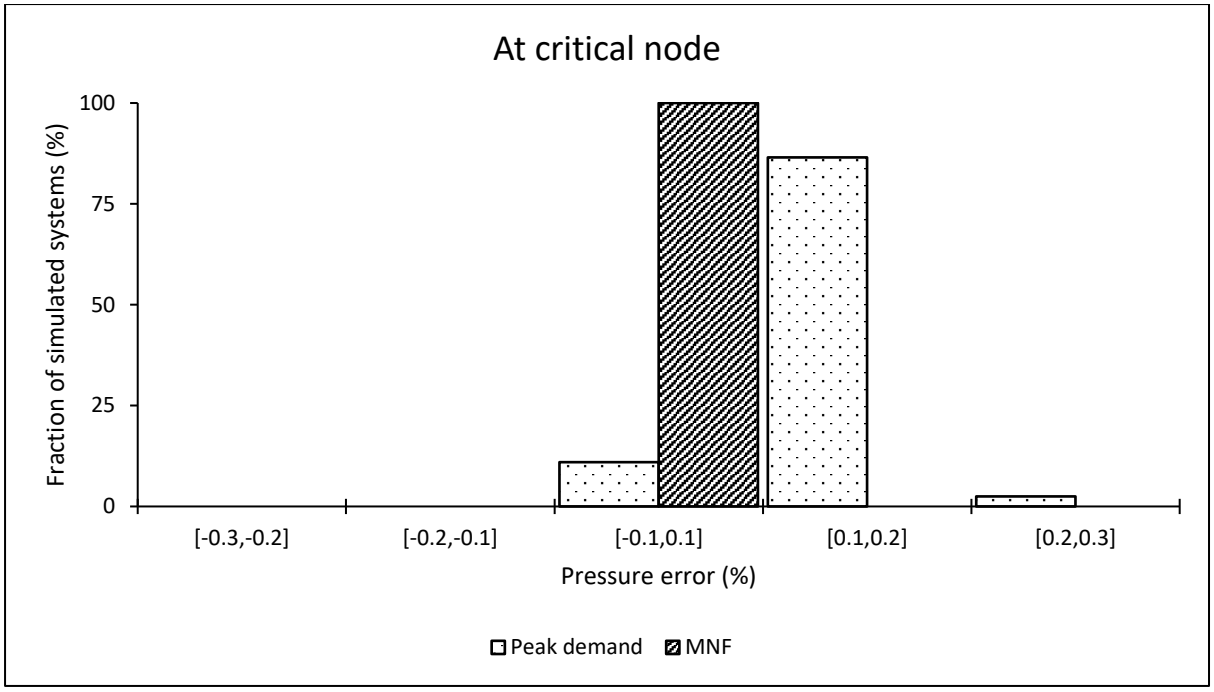
At critical node
Fraction of simulated systems (%)
100
75
50
25
0
[-0.3,-0.2]
[-0.2,-0.1]
[-0.1,0.1]
[0.1,0.2]
[0.2,0.3]
Pressure error (%)
Peak demand
MNF

System leakage estimation error when using the power equation

	Leakage estimation error (%)			
	Minimum	**Arithmetic Mean**	**Median**	**Maximum**
Before implementing pressure management	-2.32	-0.51	-0.48	0.50
After implementing pressure management	-23.60	-11.04	-10.91	-2.40

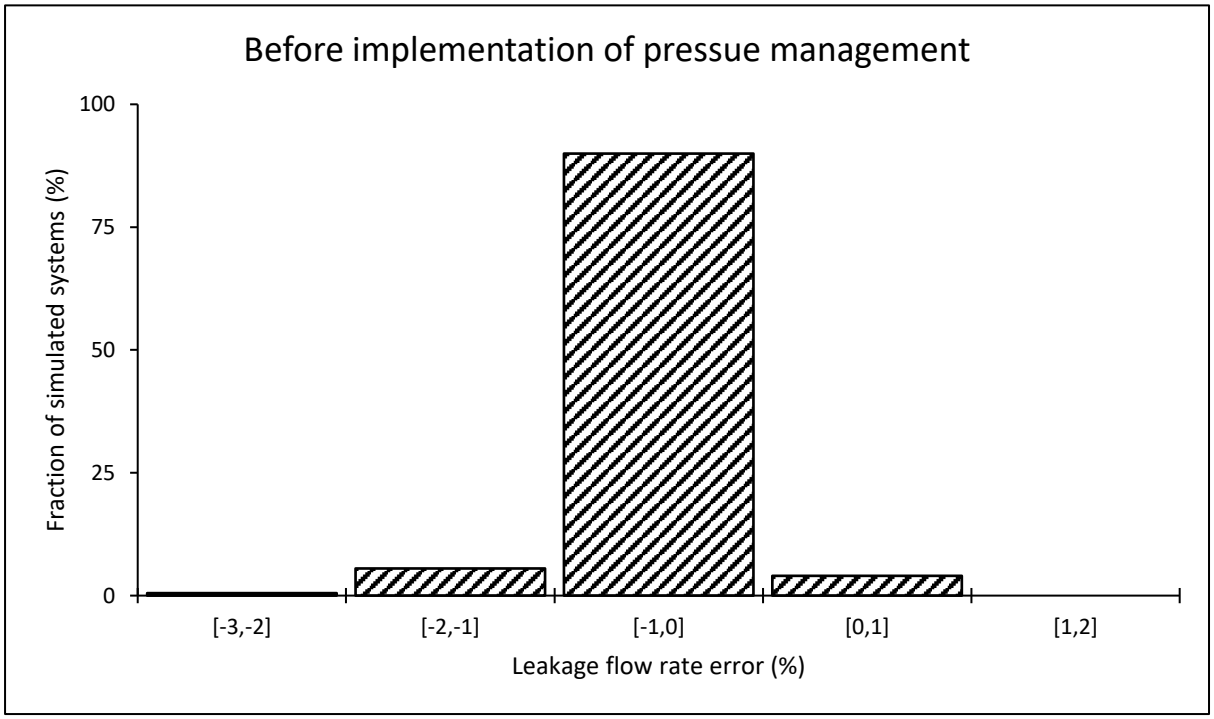

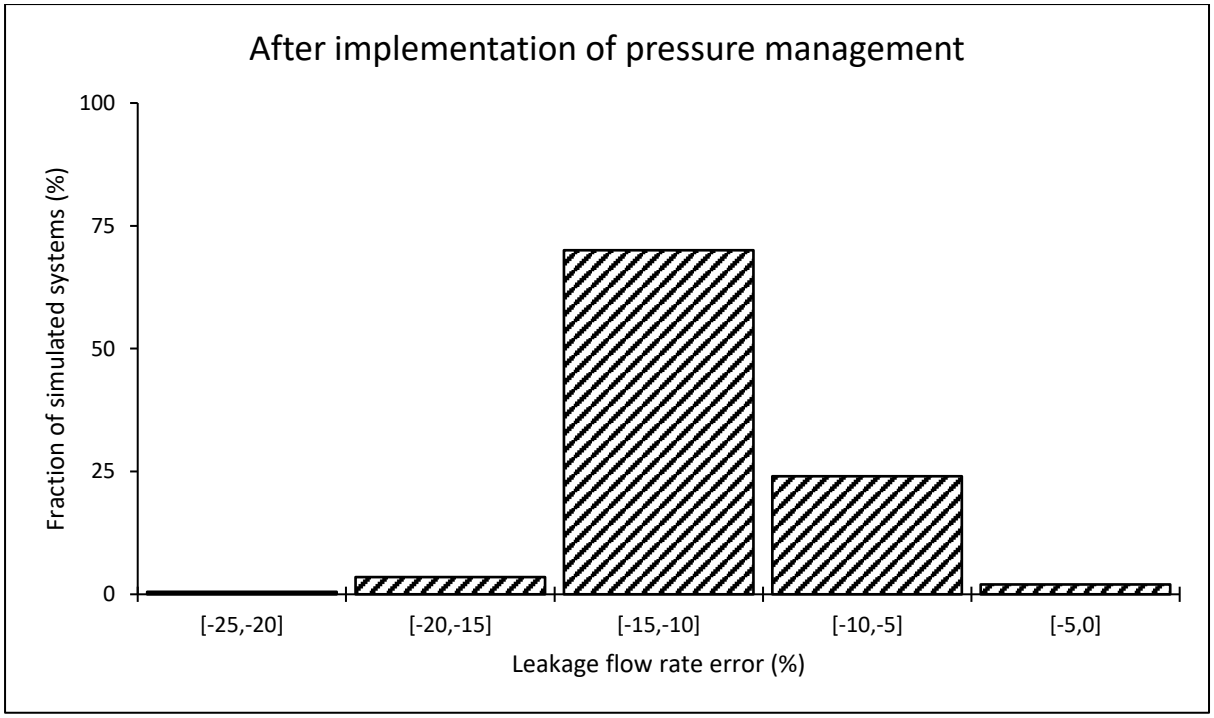
After implementation of pressure management
Fraction of simulated systems (%)
100
75
50
25
0
[-25,-20]
[-20,-15]
[-15,-10]
[-10,-5]
[-5,0]
Leakage flow rate error (%)

Leakage estimation error when using the power equation at the critical node

	Leakage estimation error (%)			
	Minimum	**Arithmetic Mean**	**Median**	**Maximum**
Before implementing pressure management	-14.95	-7.74	-9.04	5.29
After implementing pressure management	-64.43	-41.27	-46.11	26.00

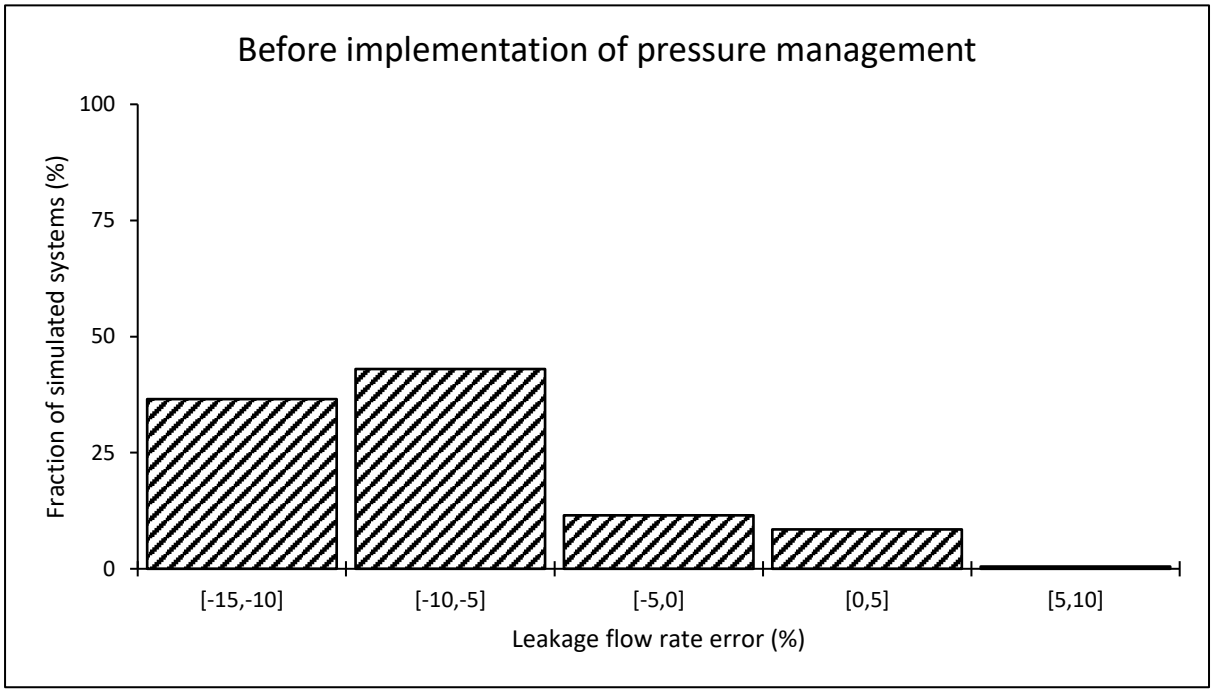

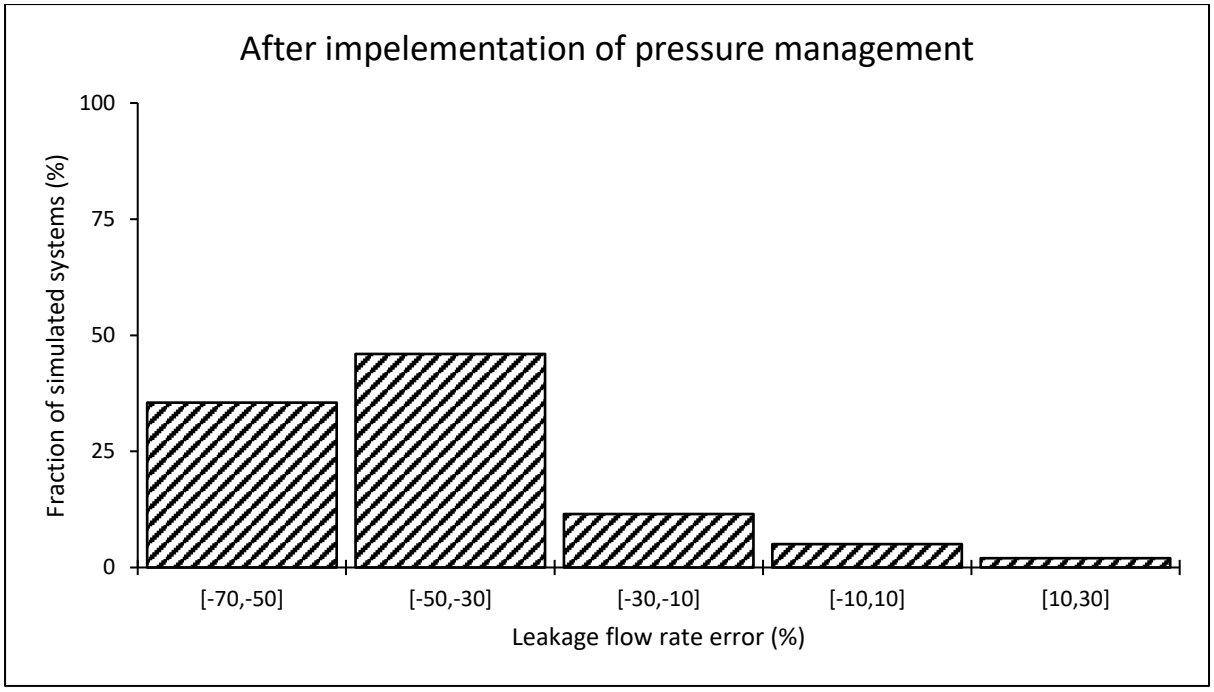
After impelementation of pressure management
Fraction of simulated systems (%)
100
75
50
25
0
[-70,-50]
[-50,-30]
[-30,-10]
[-10,10]
[10,30]
Leakage flow rate error (%)

Appendix A-8: Medium-sized network with an ILI of 64

Results for an individual system

Pressure head at the average zone pressure (AZP) node

		Pressure head (m)			
		Minimum	**Arithmetic Mean**	**Median**	**Maximum**
Before pressure management	Without leaks	72.69	88.62	90.24	106.08
	Modified orifice equation	60.79	75.87	77.16	93.58
	Power equation	61.02	75.94	77.21	93.58
After pressure management	Modified orifice equation	18.75	33.31	34.64	50.10
	Power equation	19.75	33.95	35.24	50.38

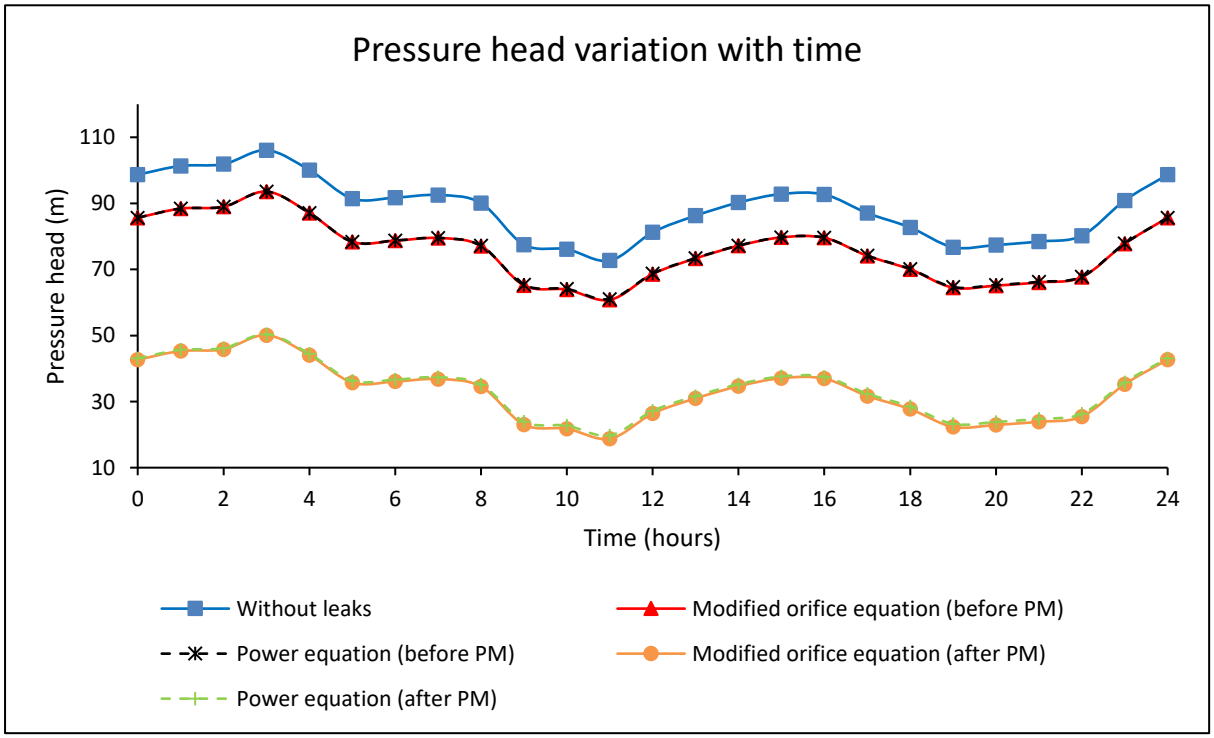

Pressure head at the critical node

		Pressure head (m)			
		Minimum	**Arithmetic Mean**	**Median**	**Maximum**
Before pressure management	Without leaks	60.21	75.09	76.77	90.93
	Modified orifice equation	49.20	63.36	64.66	79.39
	Power equation	49.42	63.43	64.70	79.39
After pressure management	Modified orifice equation	6.57	20.21	21.56	35.42
	Power equation	7.50	20.80	22.10	35.67

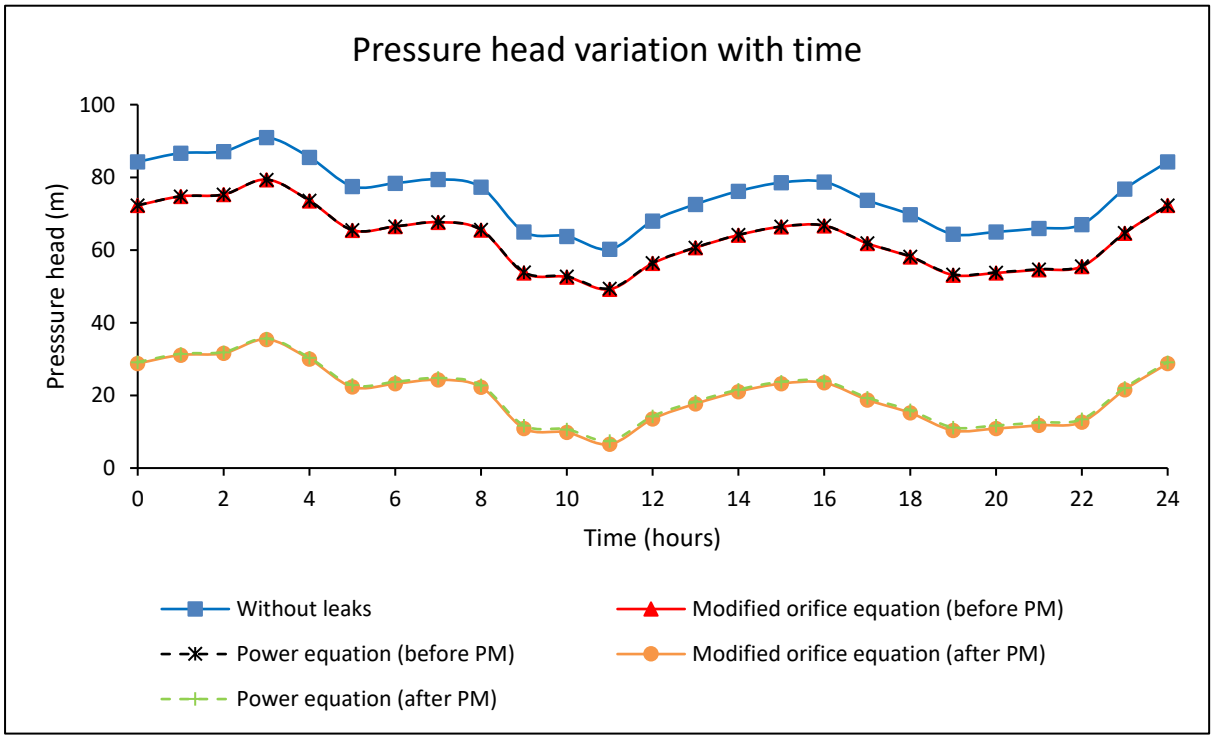

System leakage flow rate

		Leakage flow rate (m^3/h)			
		Minimum	**Arithmetic Mean**	**Median**	**Maximum**
Before pressure management	Modified orifice equation	377.57	483.09	492.53	613.61
	Power equation	370.59	480.66	490.87	613.61
After pressure management	Modified orifice equation	129.37	213.28	220.57	314.71
	Power equation	97.23	189.93	198.16	301.59

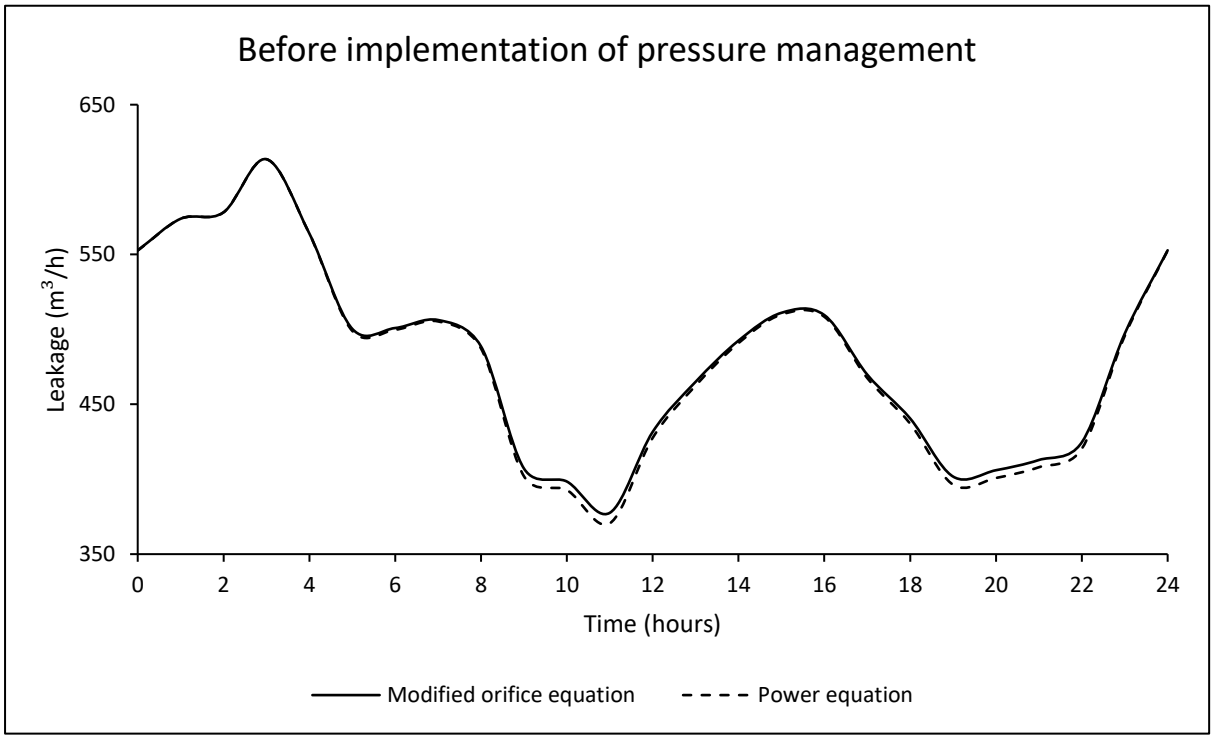

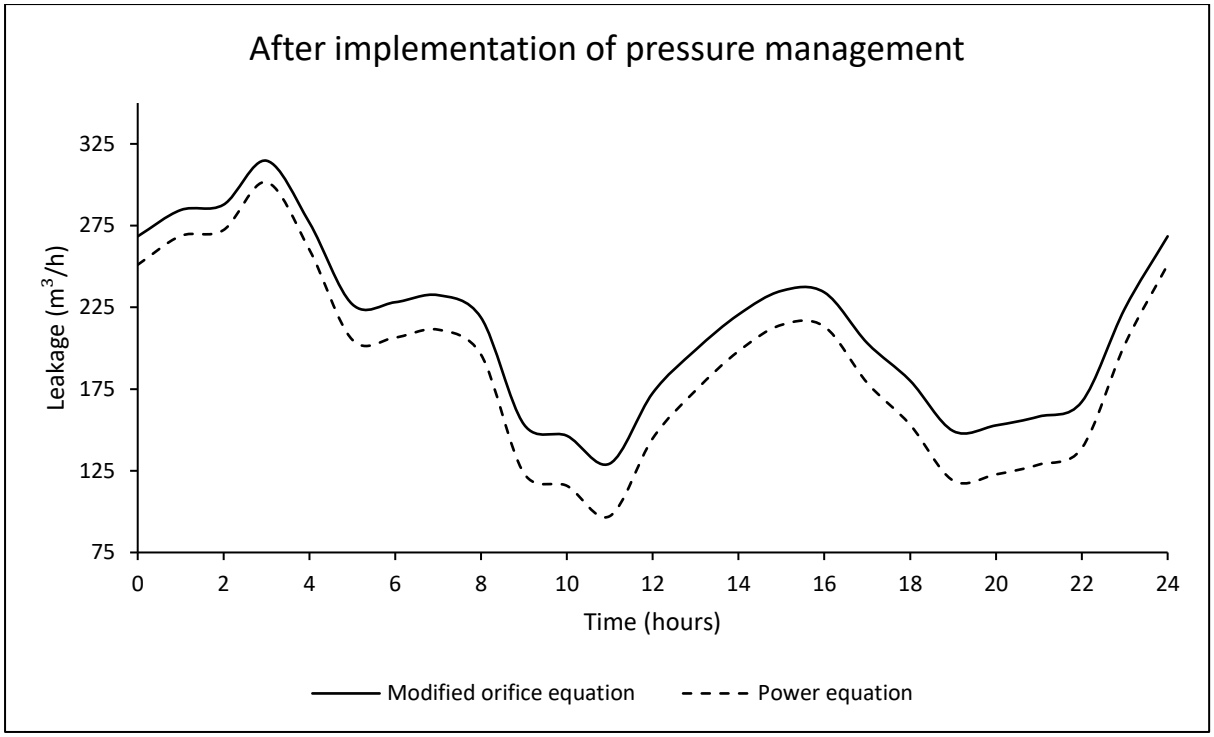
After implementation of pressure management
325
275
225
175
125
75
Leakage (m3/h)
0
2
4
6
8
10
12
14
16
18
20
22
24
Time (hours)
Modified orifice equation
Power equation

Leakage flow rate at the critical node

		Leakage flow rate (m^3/h)			
		Minimum	**Arithmetic Mean**	**Median**	**Maximum**
Before pressure management	Modified orifice equation	13.41	17.89	18.26	23.28
	Power equation	13.64	18.09	18.48	23.28
After pressure management	Modified orifice equation	2.36	5.62	5.90	9.47
	Power equation	1.63	5.19	5.50	9.44

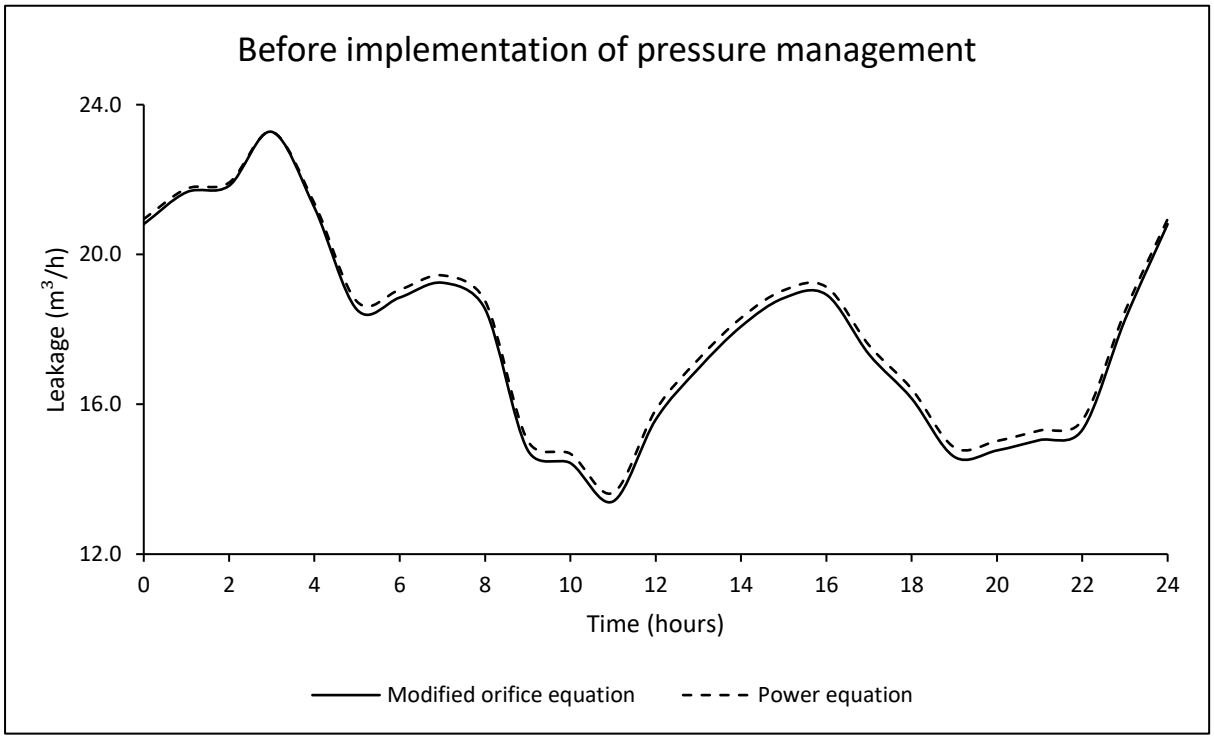

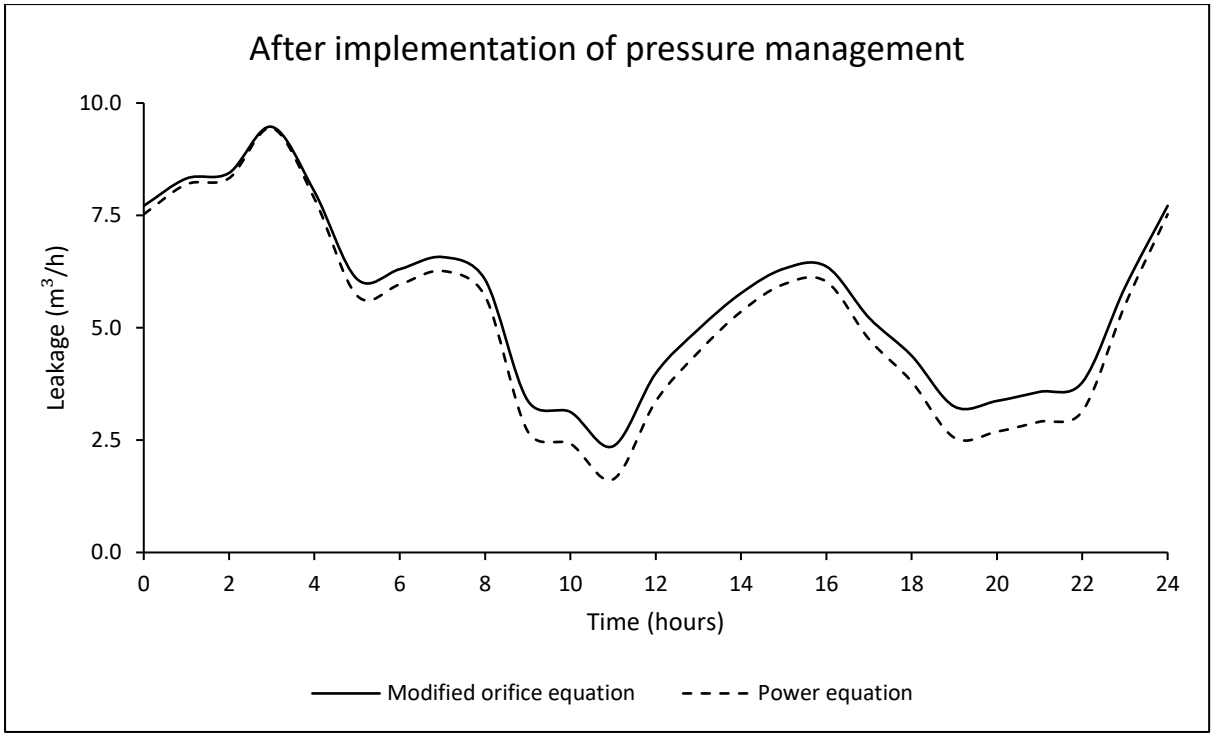
After implementation of pressure management
10.0
7.5
5.0
2.5
0.0
Leakage (m3/h)
0
2
4
6
8
10
12
14
16
18
20
22
24
Time (hours)
Modified orifice equation
Power equation

Number of iterations required for a system to converge to a hydraulic solution for both formulations

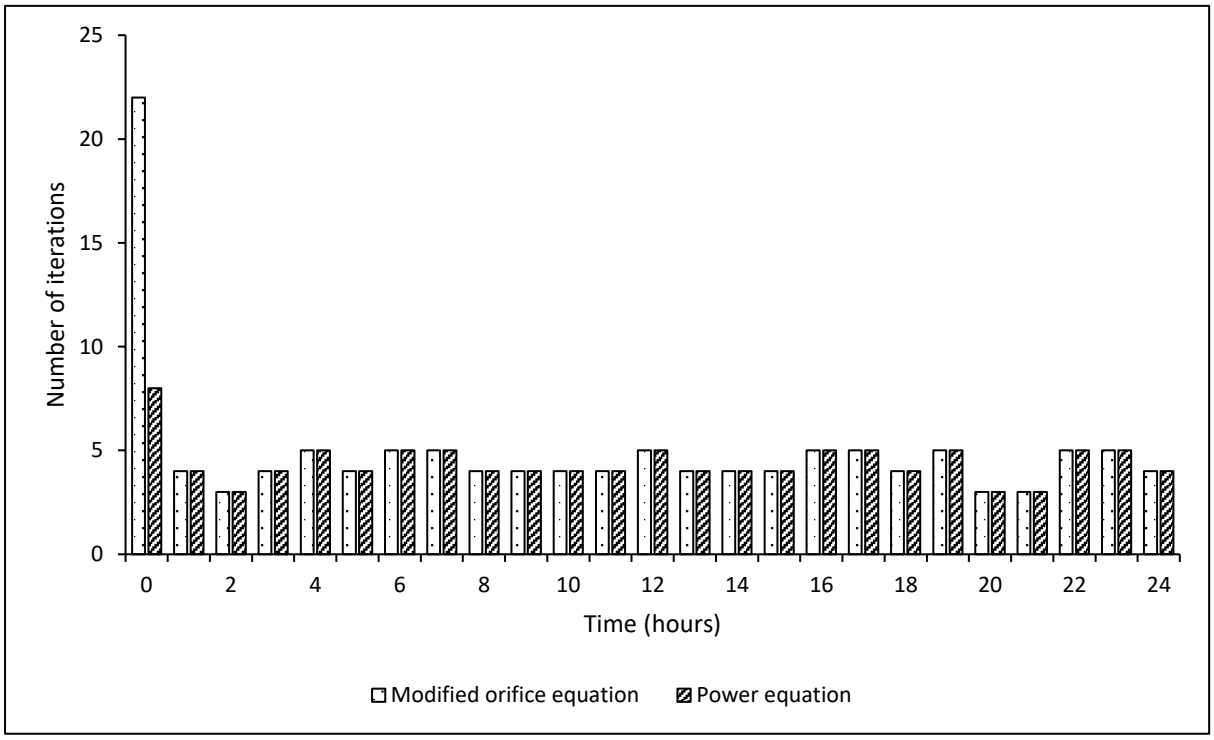

Results for combined systems

System parameters for both power and modified orifice formulations

	Minimum	Arithmetic Mean	Median	Maximum
Leakage exponent N1	1.06	1.18	1.18	1.40
Leakage coefficient C	2.6E-04	8.6E-04	8.1E-04	1.5E-03
Effective initial leak area C_dA0 (mm^2)	341.31	1282.37	1266.55	1808.13
Effective head-area slope C_dm (mm^2/m)	24.27	29.96	29.94	37.18
Leakage number LN	1.27	2.32	2.14	9.18

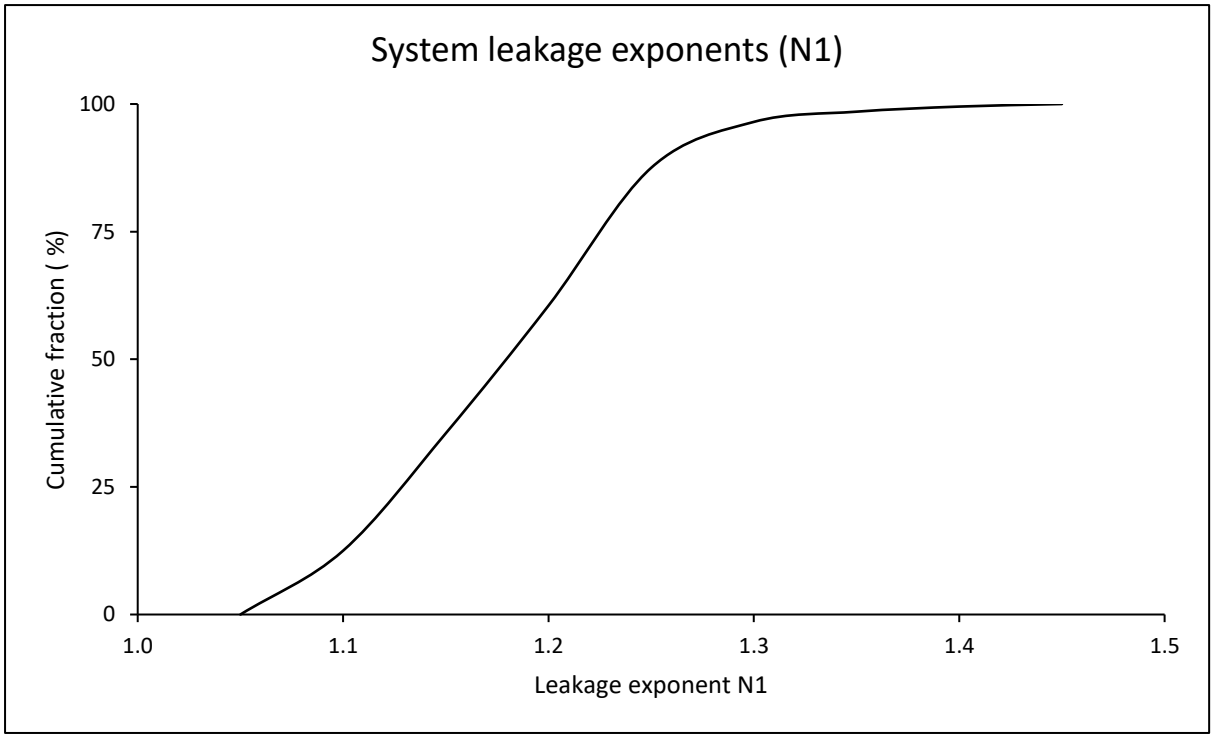

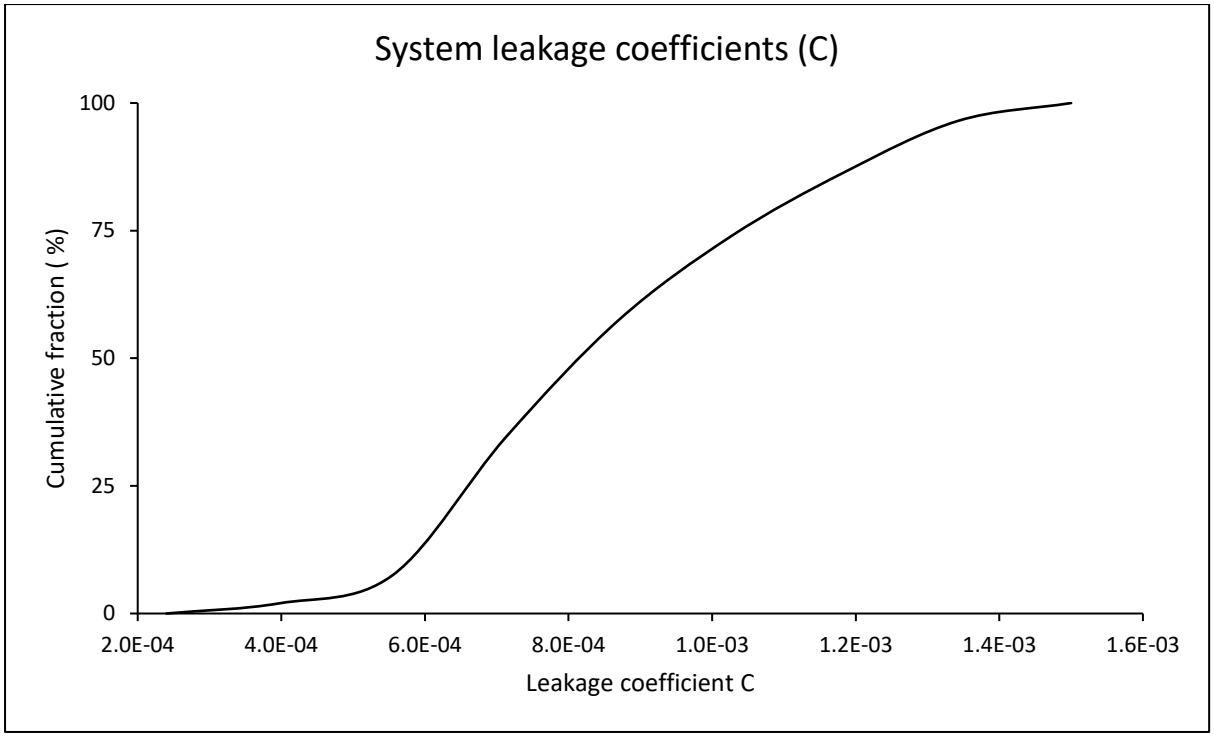
System leakage coefficients (C)
Cumulative fraction (%)
100
75
50
25
0
2.0E-04
4.0E-04
6.0E-04
8.0E-04
1.0E-03
1.2E-03
1.4E-03
1.6E-03
Leakage coefficient C

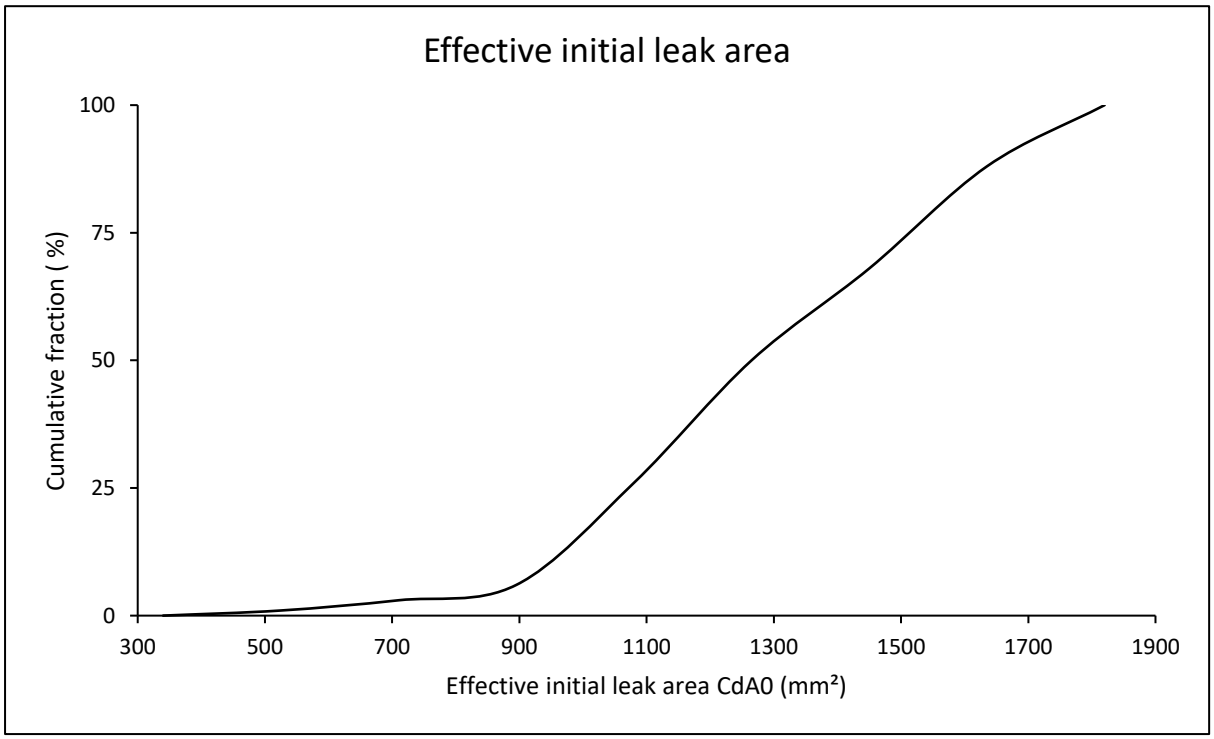
Effective initial leak area
Cumulative fraction (%)
100
75
50
25
0
300
500
700
900
1100
1300
1500
1700
1900
Effective initial leak area CdA0 (mm²)

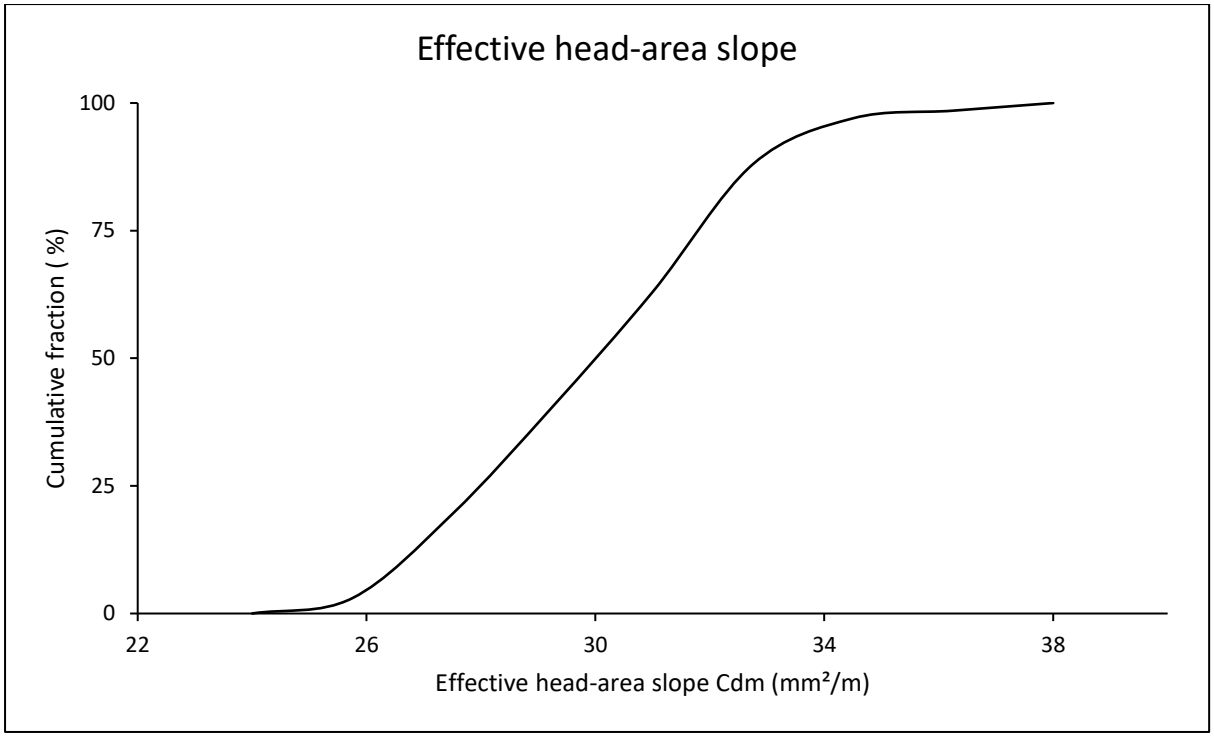
Effective head-area slope
100
75
50
25
0
Cumulative fraction (%)
22
26
30
34
38
Effective head-area slope Cdm (mm²/m)

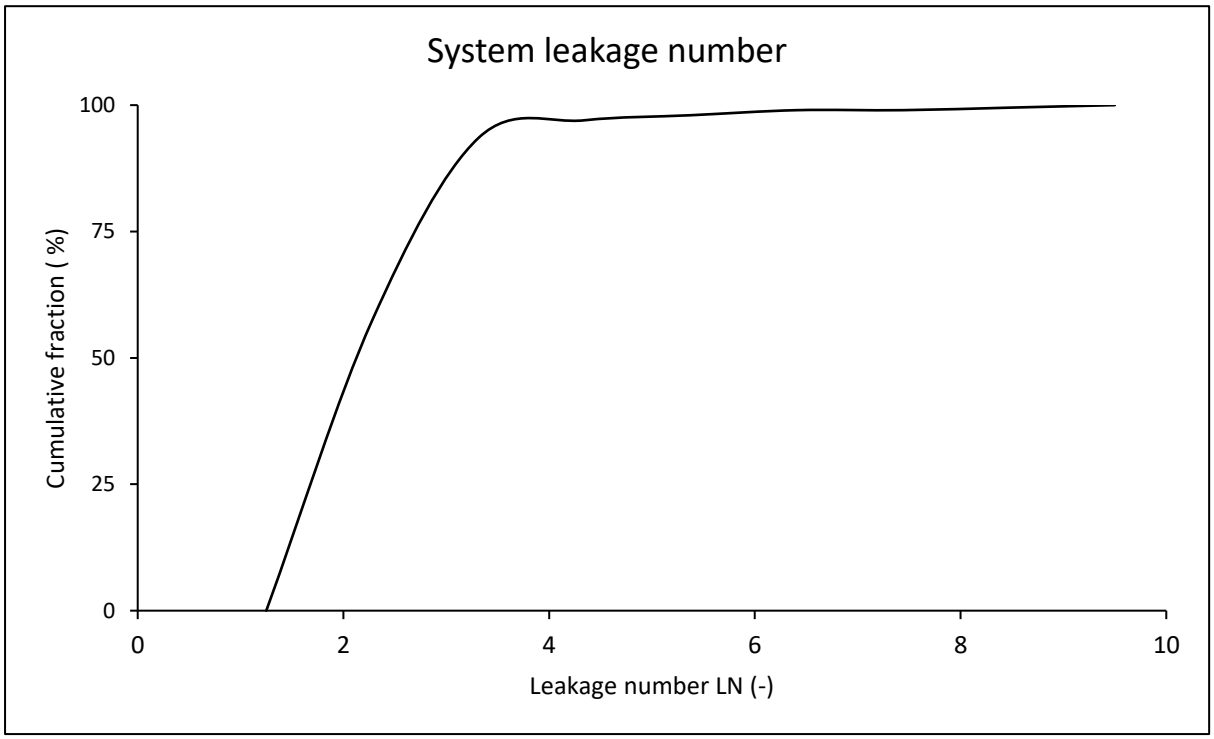
System leakage number
100
75
50
25
0
Cumulative fraction (%)
0
2
4
6
8
10
Leakage number LN (-)

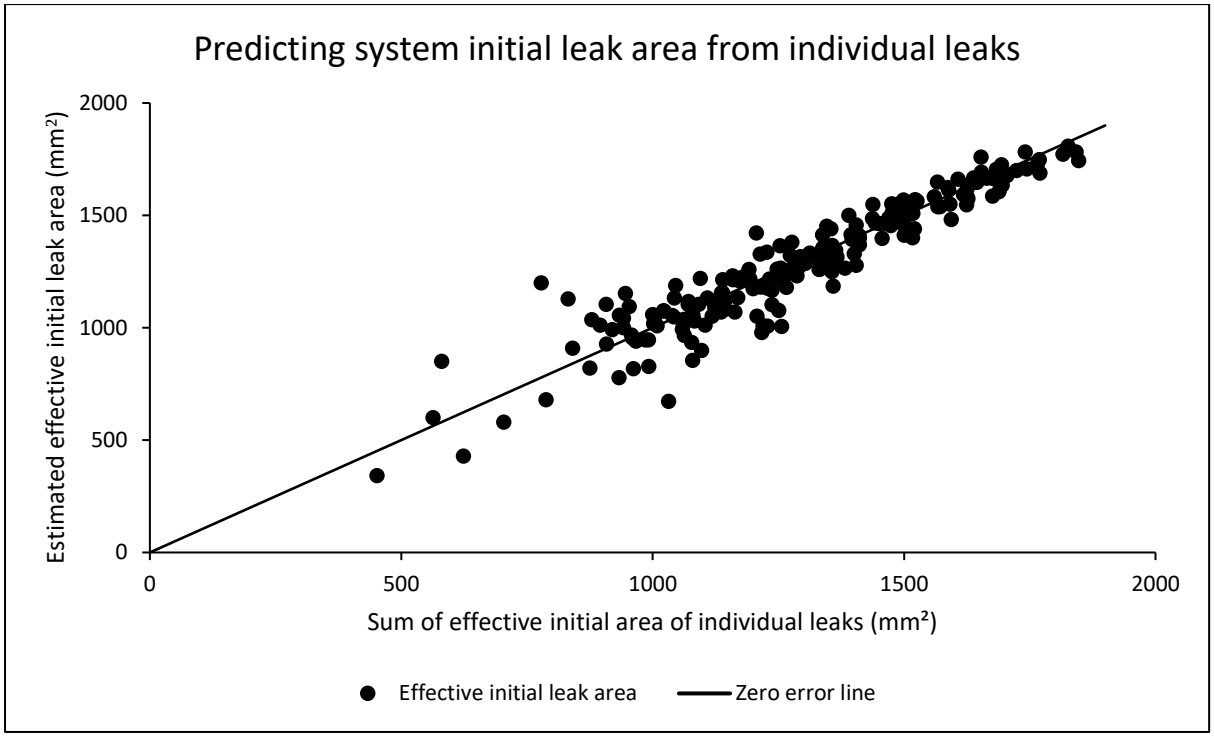
Predicting system initial leak area from individual leaks
Estimated effective initial leak area (mm²)
2000
1500
1000
500
0
0
500
1000
1500
2000
Sum of effective initial area of individual leaks (mm²)
Effective initial leak area
Zero error line

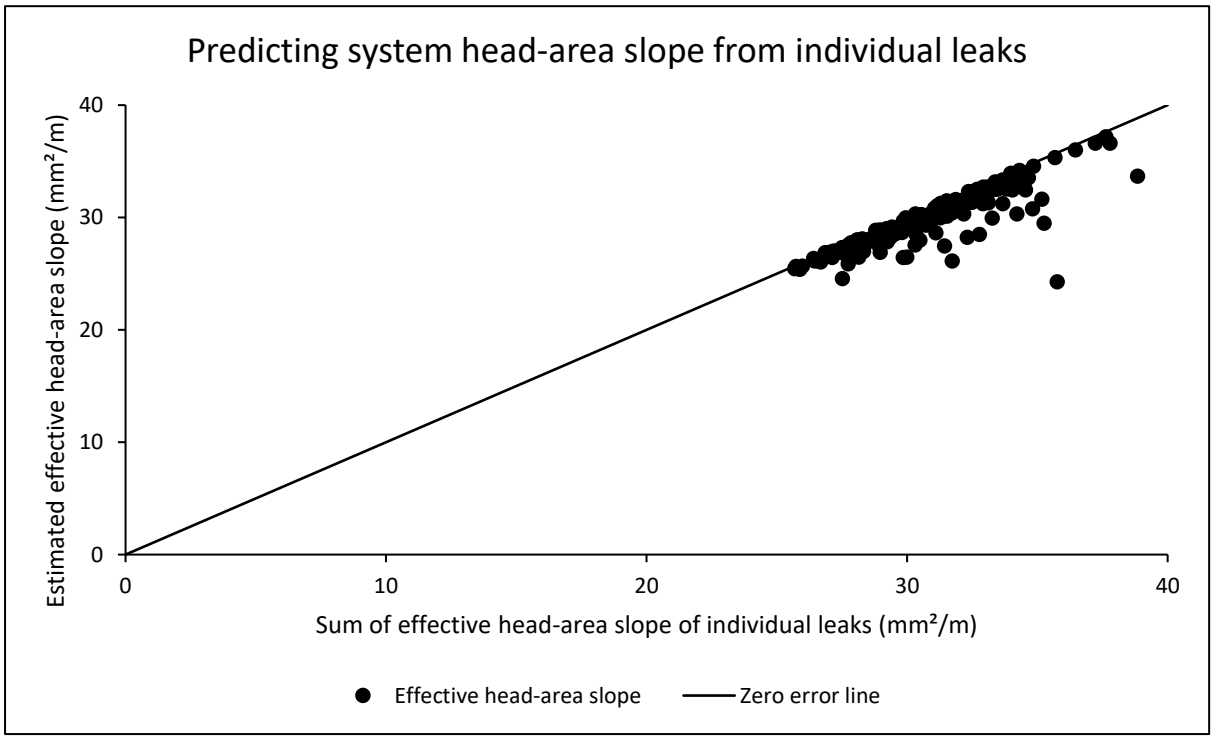
Predicting system head-area slope from individual leaks
Estimated effective head-area slope (mm²/m)
40
30
20
10
0
0
10
20
30
40
Sum of effective head-area slope of individual leaks (mm²/m)
Effective head-area slope
Zero error line

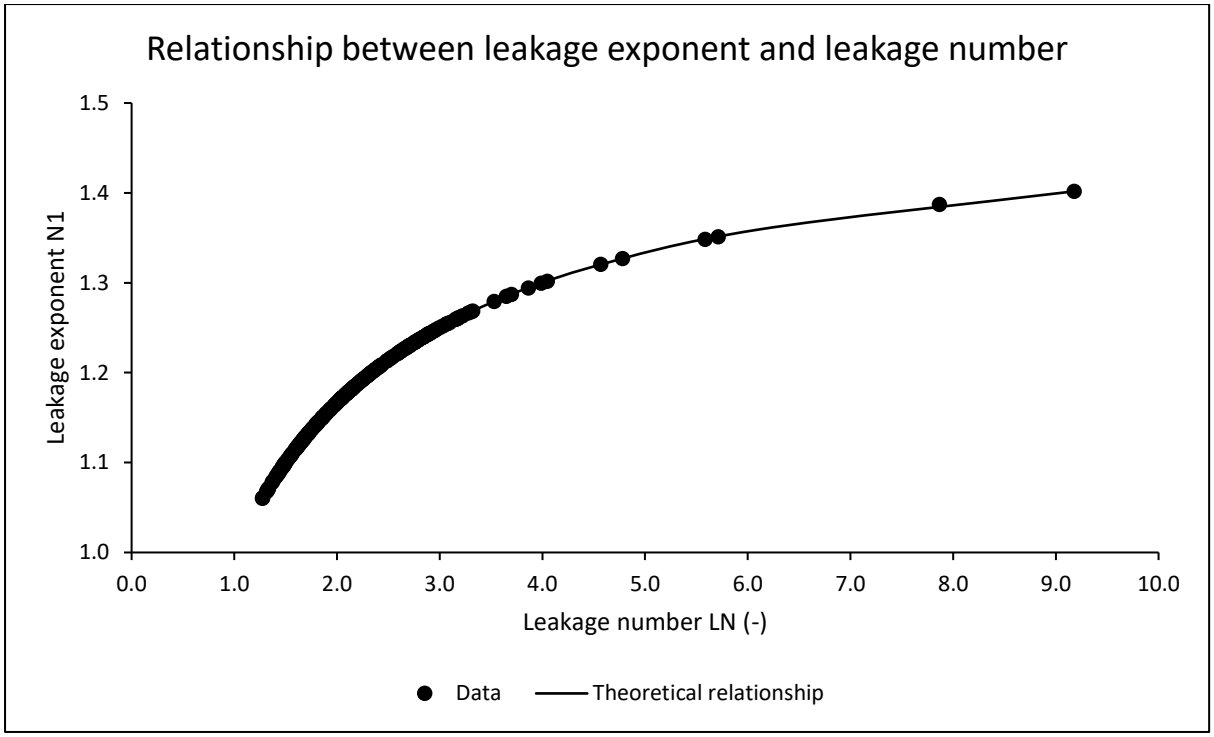
Relationship between leakage exponent and leakage number
Leakage exponent N1
1.5
1.4
1.3
1.2
1.1
1.0
0.0
1.0
2.0
3.0
4.0
5.0
6.0
7.0
8.0
9.0
10.0
Leakage number LN (-)
Data
Theoretical relationship

Average iterations required for a system to converge using both formulations

	Minimum	Arithmetic Mean	Median	Maximum
Modified orifice equation	4.76	4.97	4.96	5.20
Power equation	4.16	4.42	4.40	4.84

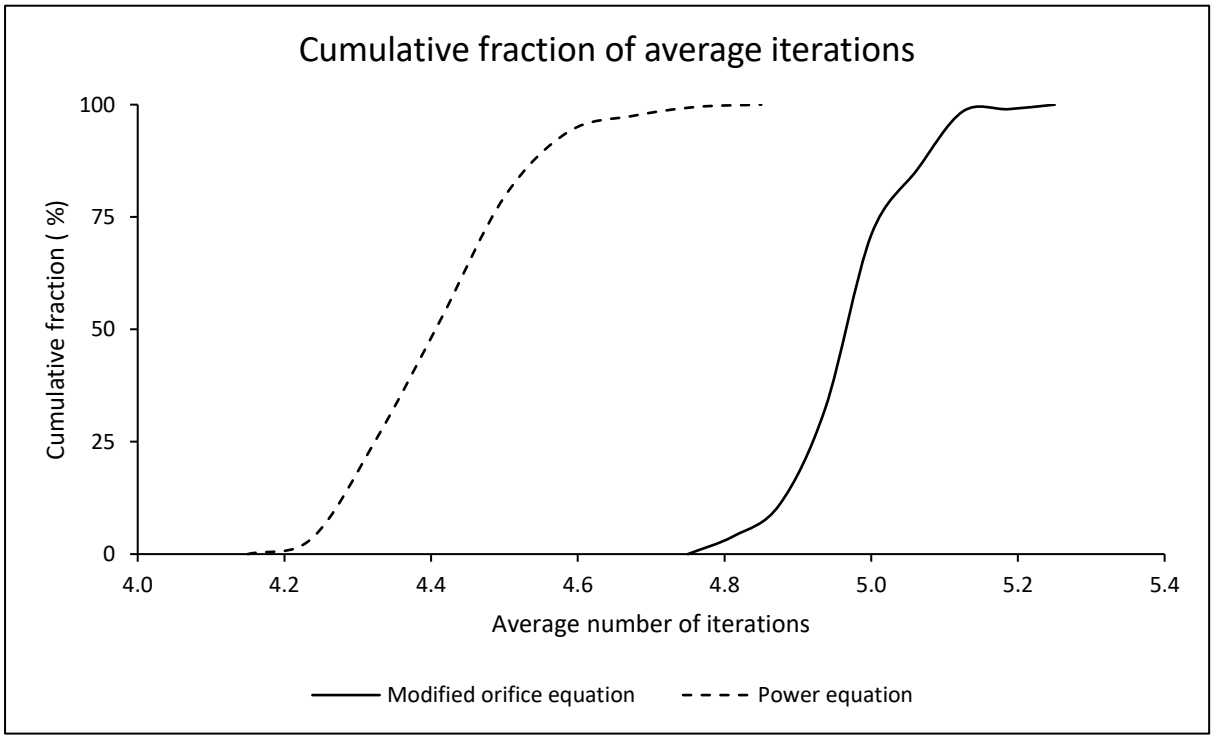

Effect of leakage on pressure at both average zone pressure (AZP) and critical nodes

AZP node								
	During MNF conditions				During peak demand conditions			
	Min (m)	Mean (m)	Median (m)	Max (m)	Min (m)	Mean (m)	Median (m)	Max (m)
Modified orifice equation	-14.16	-12.87	-12.91	-10.76	-13.36	-12.24	-12.33	-9.72
Power equation	-14.16	-12.87	-12.91	-10.76	-13.14	-12.05	-12.15	-9.97
Critical node								
Modified orifice equation	-13.91	-12.12	-12.11	-9.87	-13.01	-11.52	-11.54	-8.57
Power equation	-13.91	-12.12	-12.11	-9.87	-12.96	-11.34	-11.36	-8.41

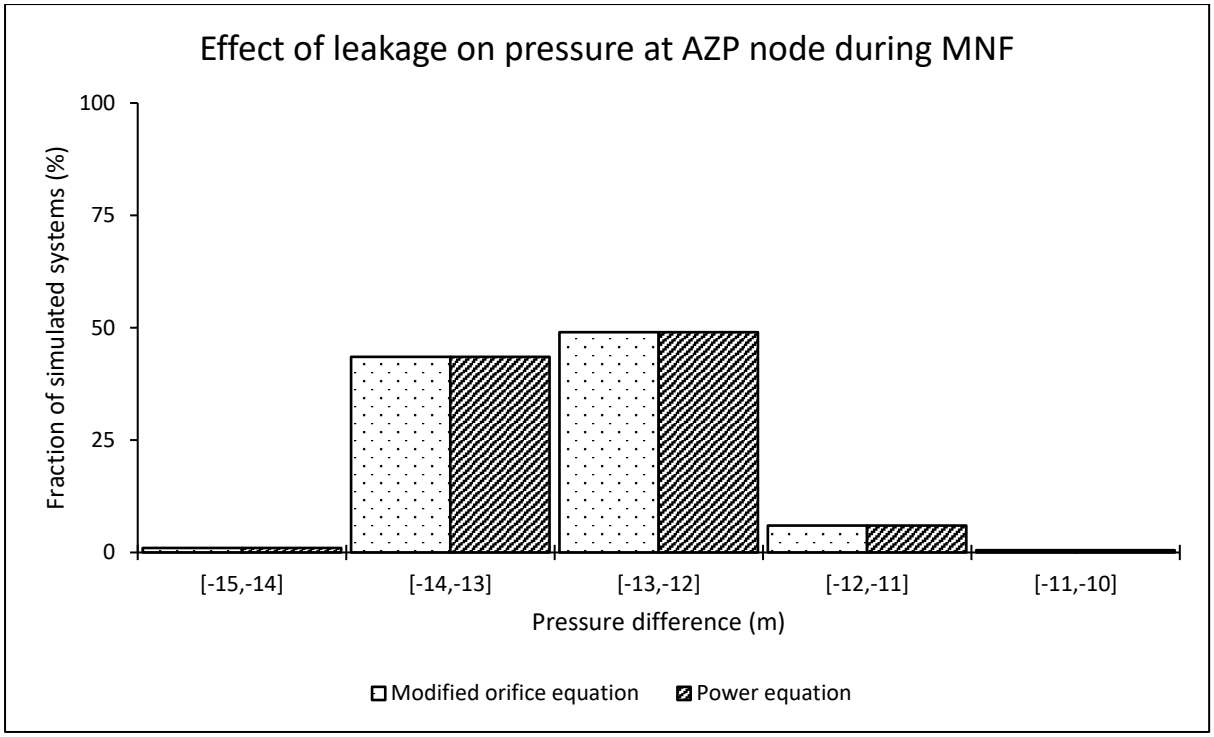
Effect of leakage on pressure at AZP node during MNF
Fraction of simulated systems (%)
100
75
50
25
0
[-15,-14]
[-14,-13]
[-13,-12]
[-12,-11]
[-11,-10]
Pressure difference (m)
Modified orifice equation
Power equation

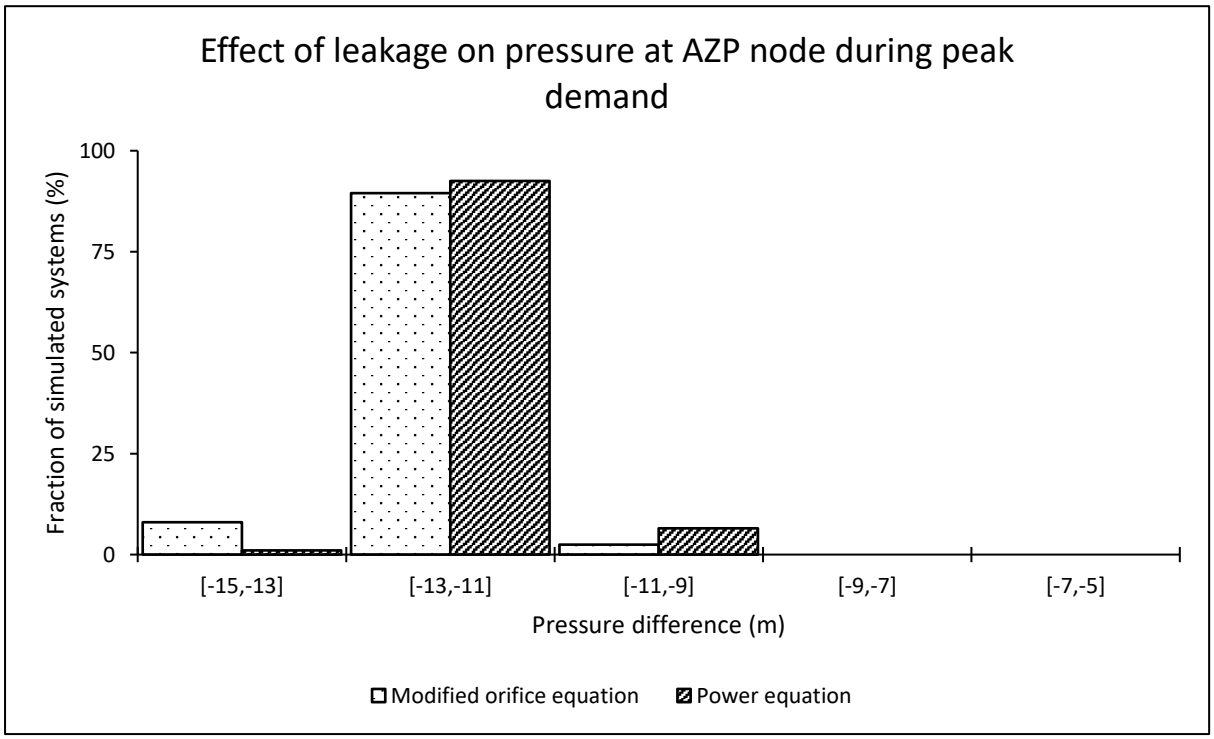
Effect of leakage on pressure at AZP node during peak demand
Fraction of simulated systems (%)
100
75
50
25
0
[-15,-13]
[-13,-11]
[-11,-9]
[-9,-7]
[-7,-5]
Pressure difference (m)
Modified orifice equation
Power equation

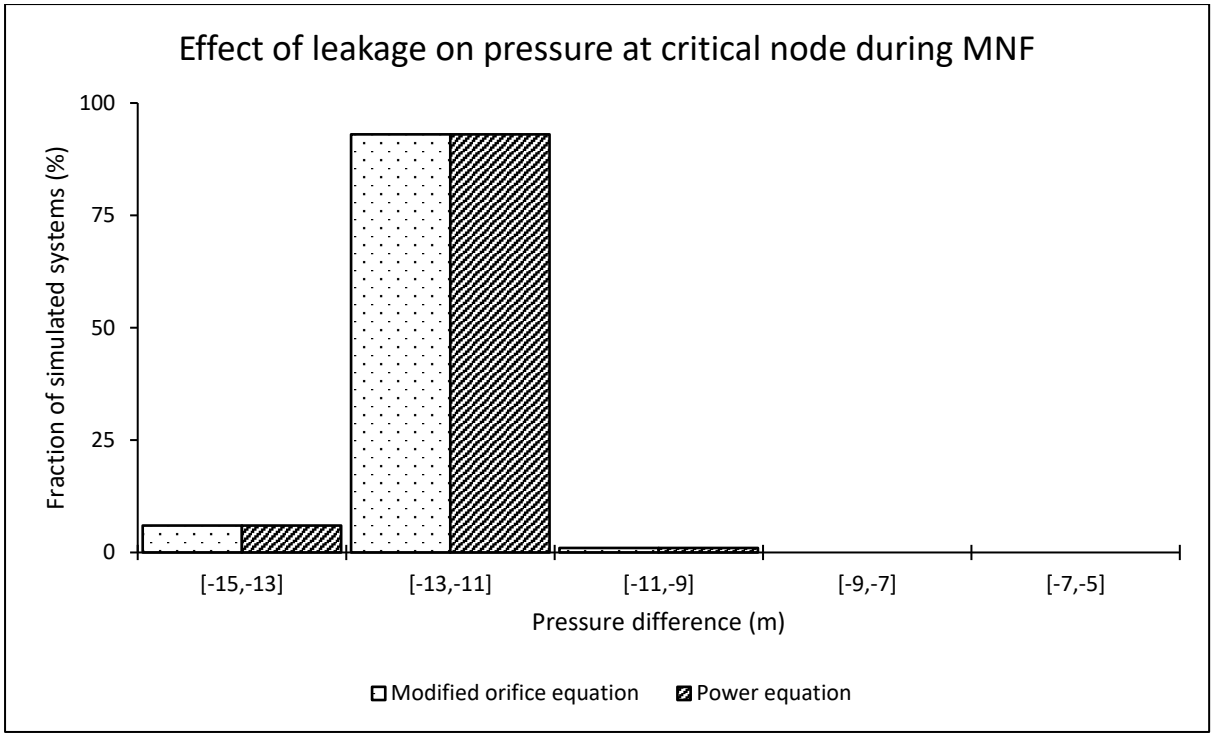
Effect of leakage on pressure at critical node during MNF
Fraction of simulated systems (%)
100
75
50
25
0
[-15,-13]
[-13,-11]
[-11,-9]
[-9,-7]
[-7,-5]
Pressure difference (m)
Modified orifice equation
Power equation

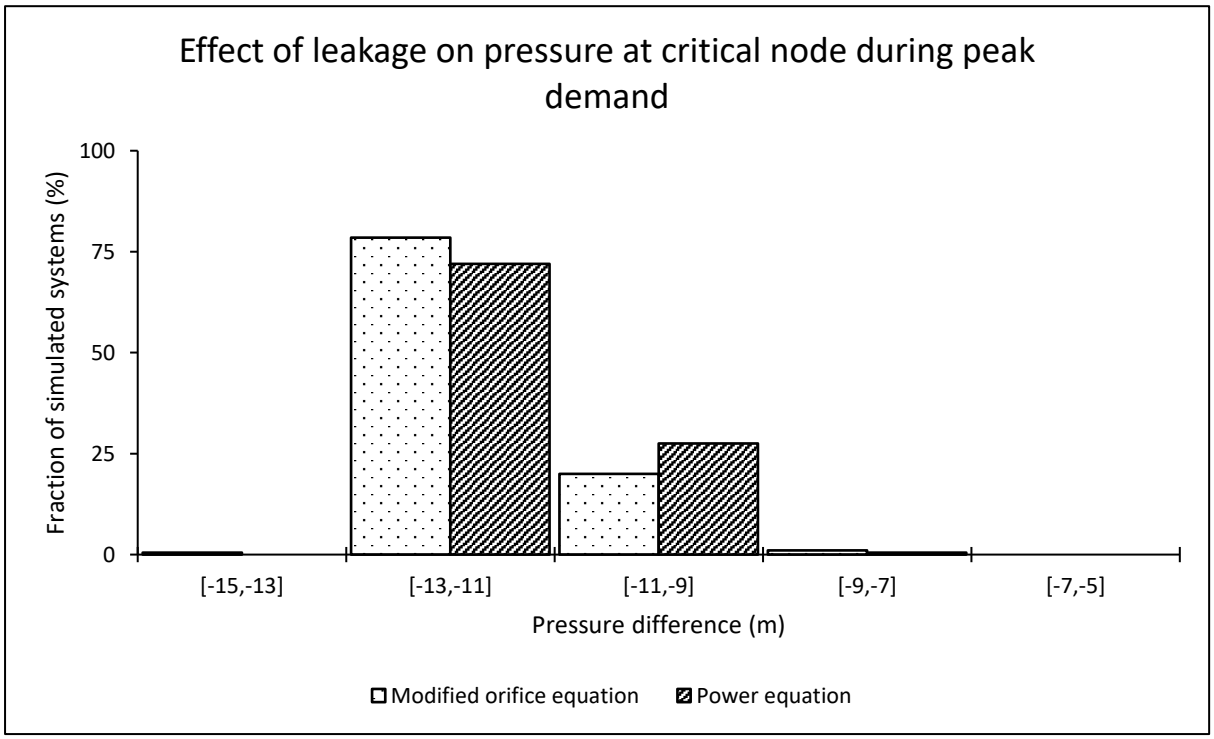
Effect of leakage on pressure at critical node during peak demand
Fraction of simulated systems (%)
100
75
50
25
0
[-15,-13]
[-13,-11]
[-11,-9]
[-9,-7]
[-7,-5]
Pressure difference (m)
Modified orifice equation
Power equation

Pressure estimation error when using the power equation at average zone pressure (AZP) and critical nodes

	During MNF conditions				During peak demand conditions			
	Min (%)	**Mean (%)**	**Median (%)**	**Max (%)**	**Min (%)**	**Mean (%)**	**Median (%)**	**Max (%)**
At the AZP node	0.00	0.00	0.00	0.00	-0.41	0.32	0.32	0.84
At the critical node	0.00	0.00	0.00	0.00	-0.45	0.36	0.37	0.93

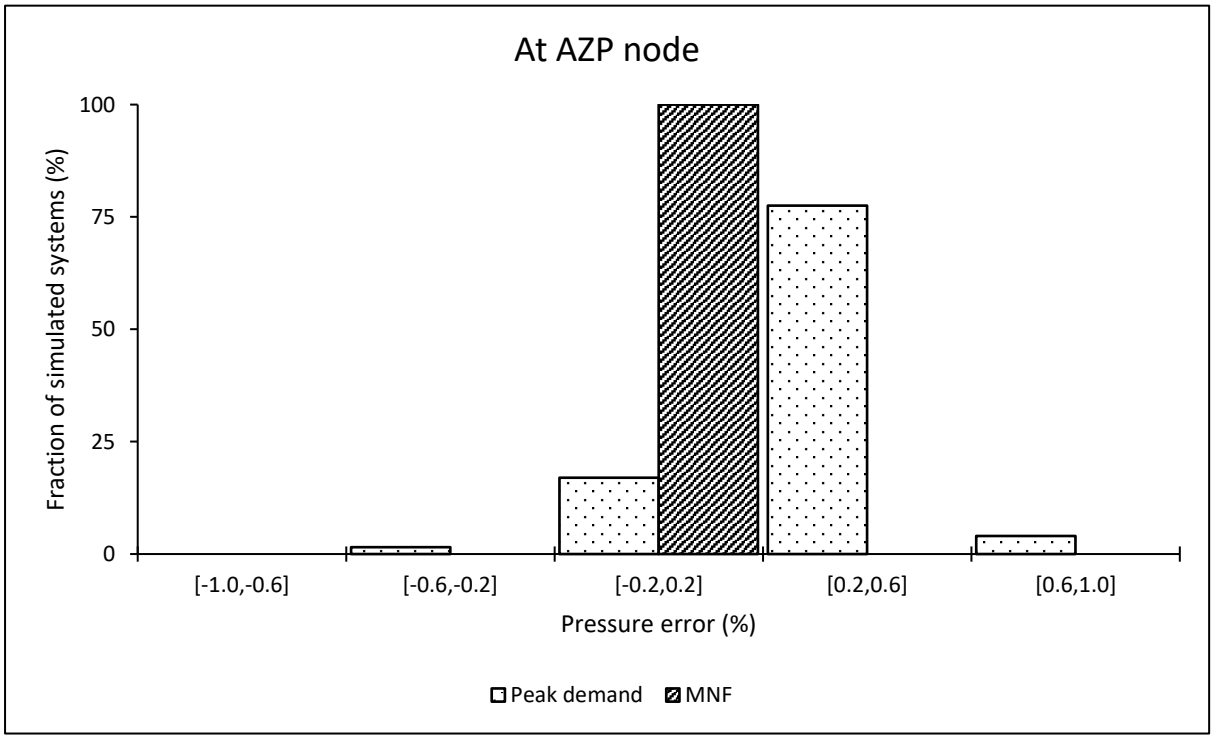

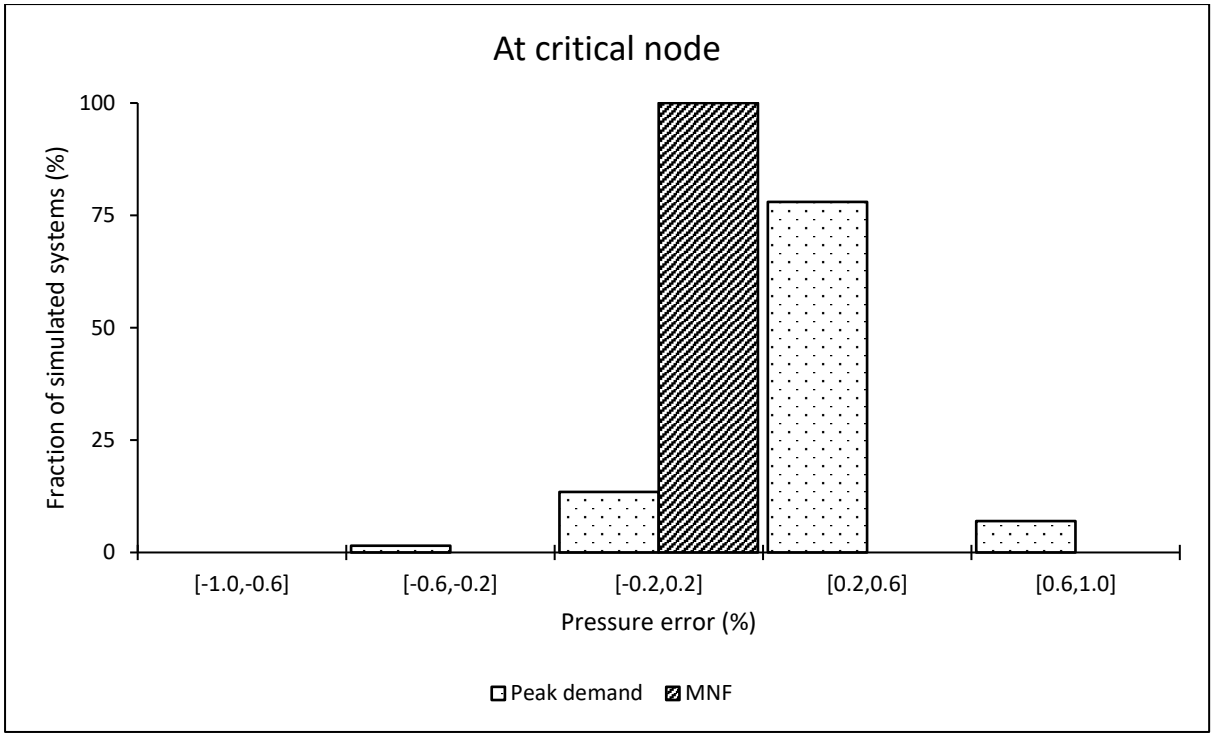
At critical node
Fraction of simulated systems (%)
100
75
50
25
0
[-1.0,-0.6]
[-0.6,-0.2]
[-0.2,0.2]
[0.2,0.6]
[0.6,1.0]
Pressure error (%)
Peak demand
MNF

System leakage estimation error when using the power equation

	Leakage estimation error (%)			
	Minimum	**Arithmetic Mean**	**Median**	**Maximum**
Before implementing pressure management	-1.74	-0.41	-0.42	1.41
After implementing pressure management	-17.13	-9.18	-9.38	1.28

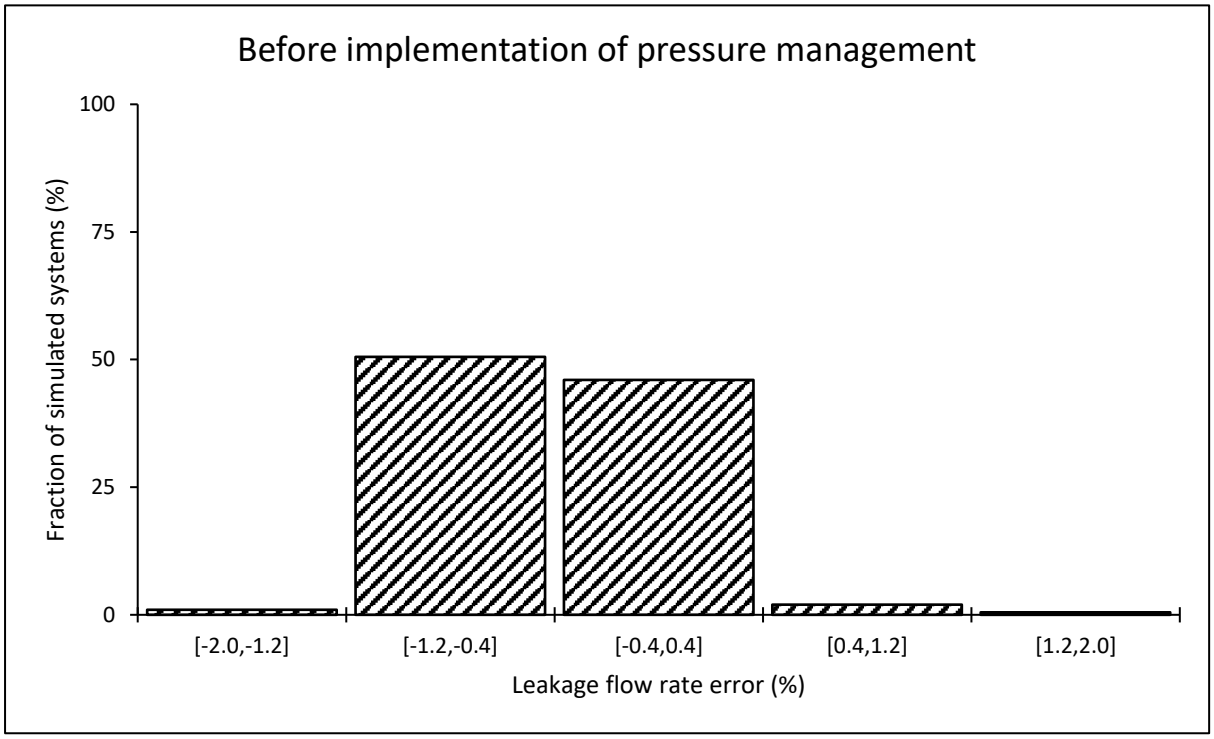

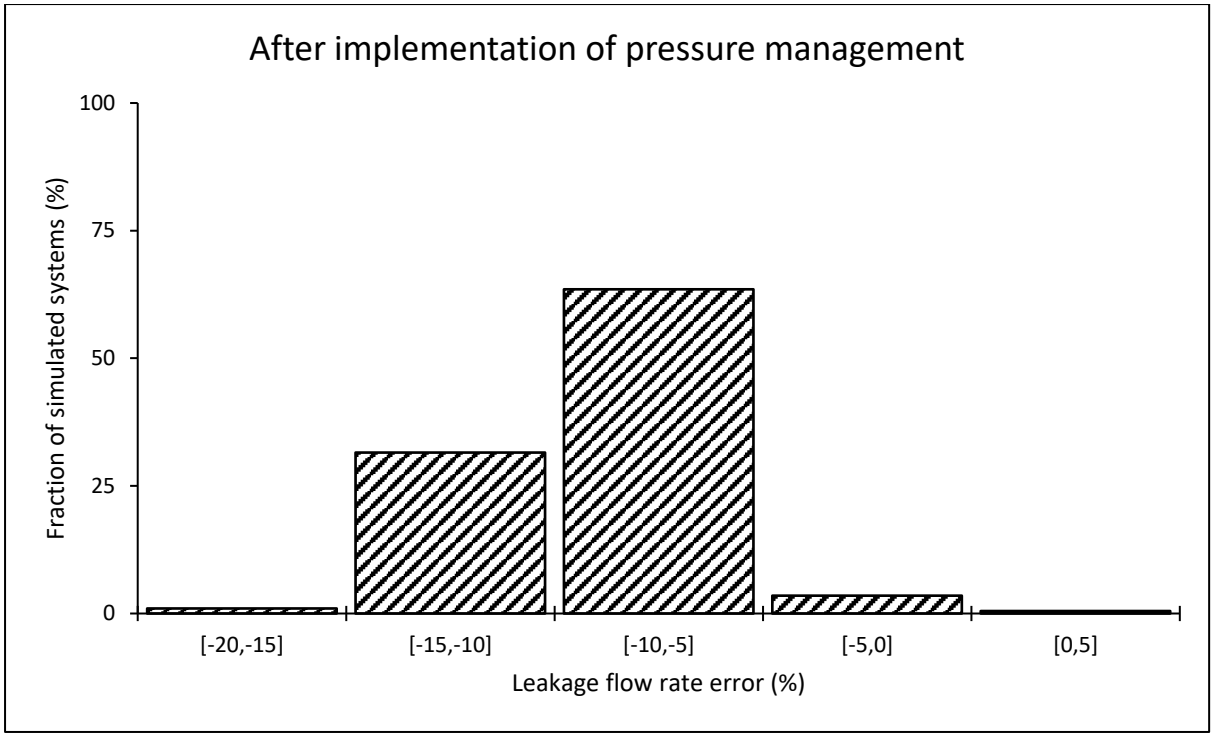
After implementation of pressure management
Fraction of simulated systems (%)
100
75
50
25
0
[-20,-15]
[-15,-10]
[-10,-5]
[-5,0]
[0,5]
Leakage flow rate error (%)

Leakage estimation error when using the power equation at the critical node

	Leakage estimation error (%)			
	Minimum	**Arithmetic Mean**	**Median**	**Maximum**
Before implementing pressure management	-16.85	-8.51	-11.28	4.10
After implementing pressure management	-66.10	-42.08	-51.98	13.73

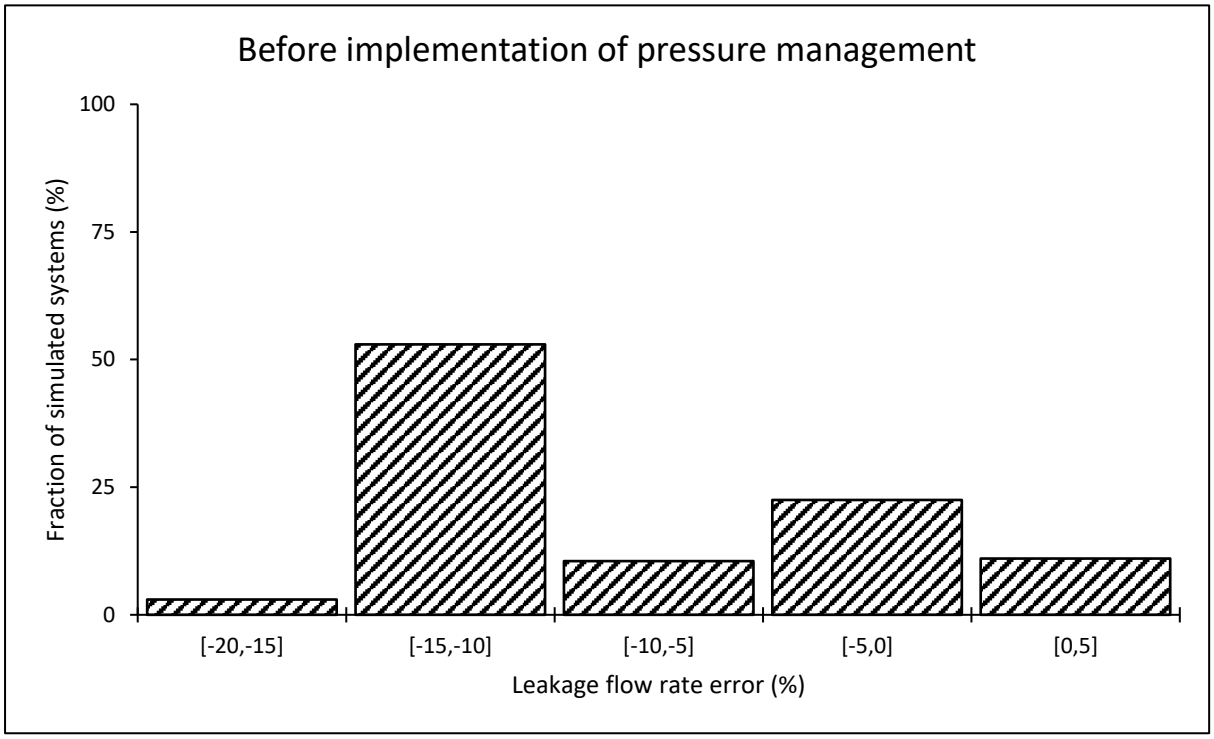

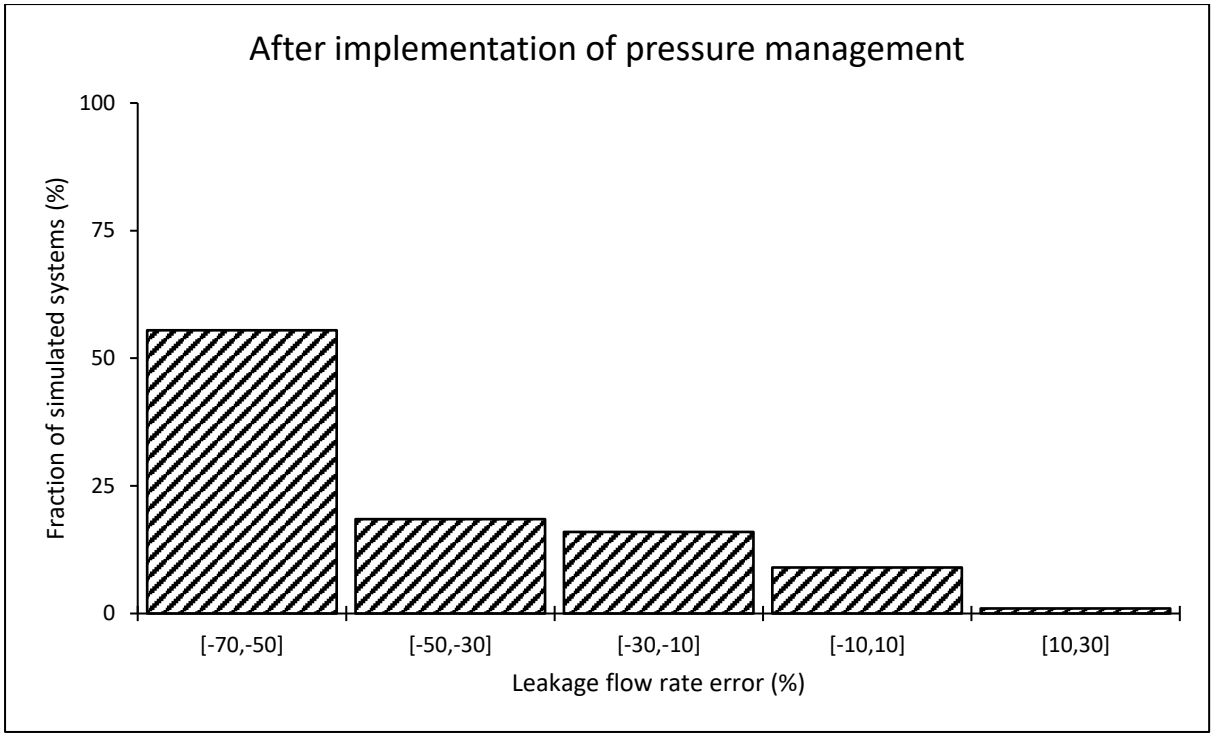
After implementation of pressure management
Fraction of simulated systems (%)
100
75
50
25
0
[-70,-50]
[-50,-30]
[-30,-10]
[-10,10]
[10,30]
Leakage flow rate error (%)

Appendix A-9: Large-sized network with an ILI of 1

Results for an individual system

Pressure head at the average zone pressure (AZP) node

		Pressure head (m)			
		Minimum	**Arithmetic Mean**	**Median**	**Maximum**
Before pressure management	Without leaks	99.13	108.33	106.63	113.44
	Modified orifice equation	99.01	108.26	106.54	113.42
	Power equation	99.01	108.26	106.54	113.42
After pressure management	Modified orifice equation	19.24	28.46	26.75	33.59
	Power equation	19.25	28.47	26.76	33.59

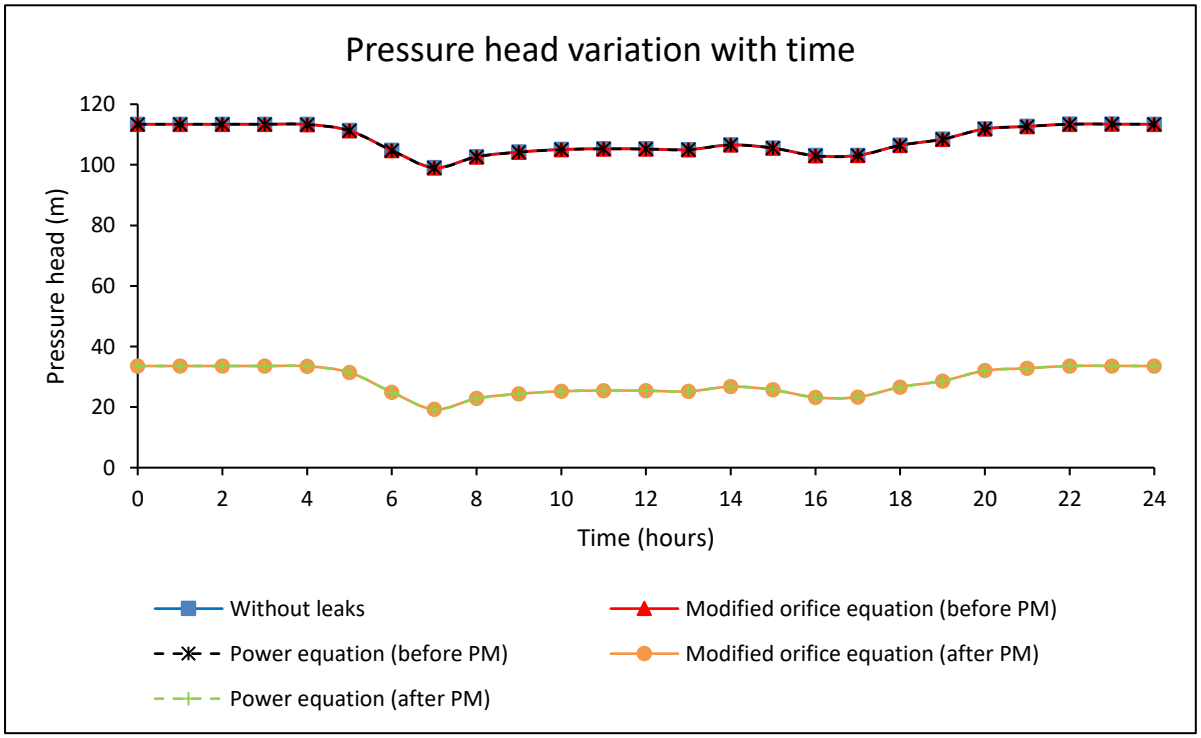

Pressure head at the critical node

		Pressure head (m)			
		Minimum	**Arithmetic Mean**	**Median**	**Maximum**
Before pressure management	Without leaks	89.91	100.55	98.69	106.46
	Modified orifice equation	89.76	100.46	98.58	106.43
	Power equation	89.76	100.46	98.58	106.43
After pressure management	Modified orifice equation	10.02	20.67	18.80	26.60
	Power equation	10.02	20.68	18.81	26.60

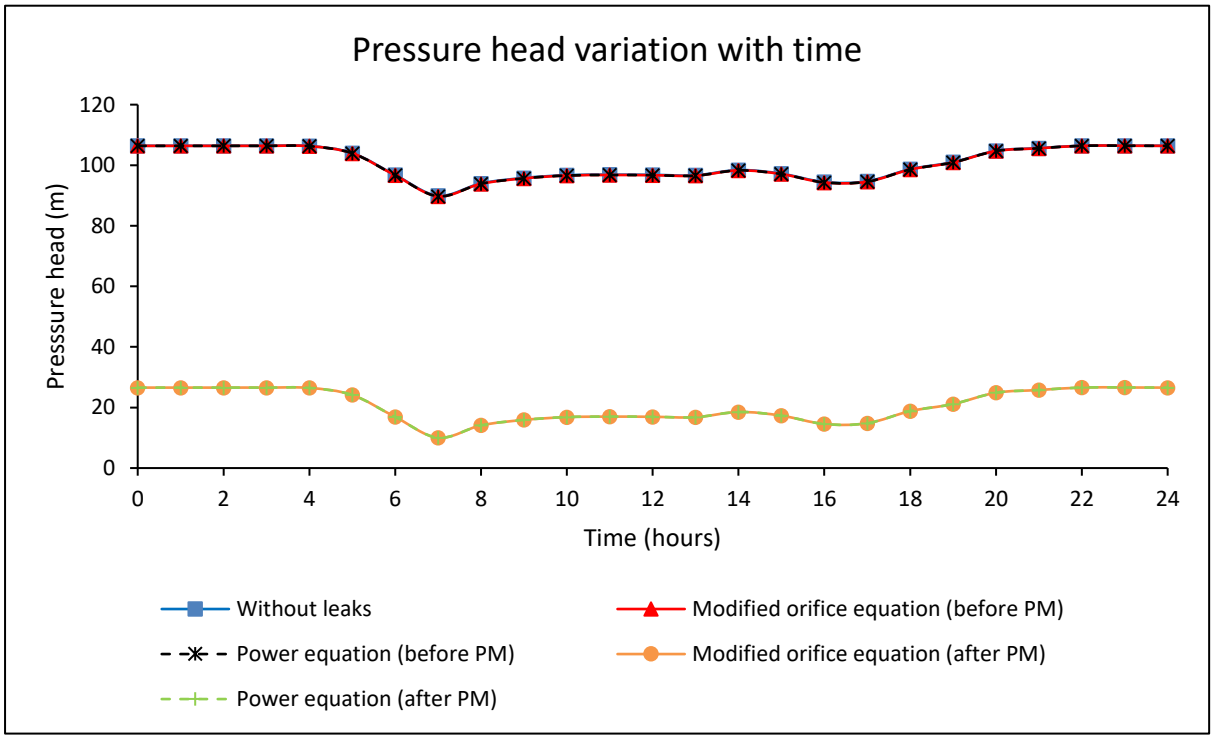

System leakage flow rate

		Leakage flow rate (m^3/h)			
		Minimum	**Arithmetic Mean**	**Median**	**Maximum**
Before pressure management	Modified orifice equation	28.74	30.69	30.34	31.78
	Power equation	28.74	30.70	30.35	31.78
After pressure management	Modified orifice equation	10.56	13.28	12.85	14.69
	Power equation	8.84	11.85	11.36	13.44

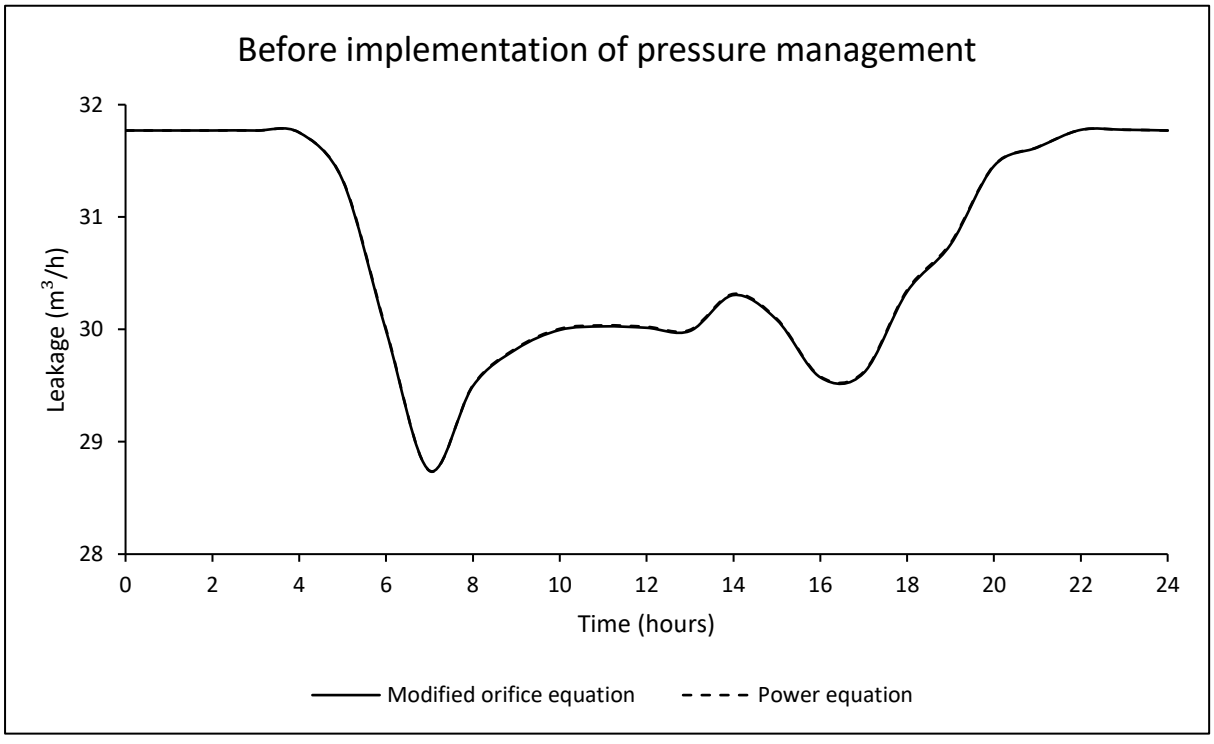

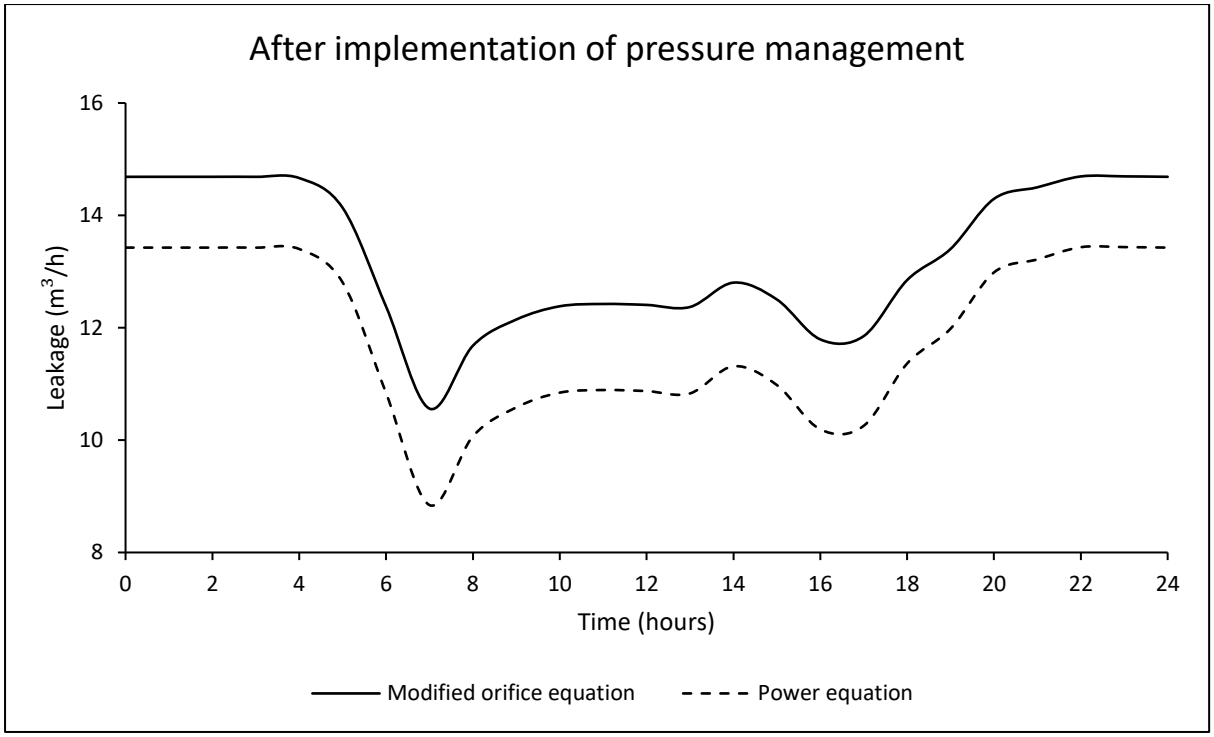
After implementation of pressure management
16
14
12
10
8
Leakage (m3/h)
0
2
4
6
8
10
12
14
16
18
20
22
24
Time (hours)
Modified orifice equation
Power equation

Leakage flow rate at the critical node

		Leakage flow rate (m^3/h)			
		Minimum	**Arithmetic Mean**	**Median**	**Maximum**
Before pressure management	Modified orifice equation	0.83	0.90	0.88	0.93
	Power equation	0.83	0.90	0.89	0.93
After pressure management	Modified orifice equation	0.23	0.34	0.32	0.39
	Power equation	0.18	0.29	0.27	0.35

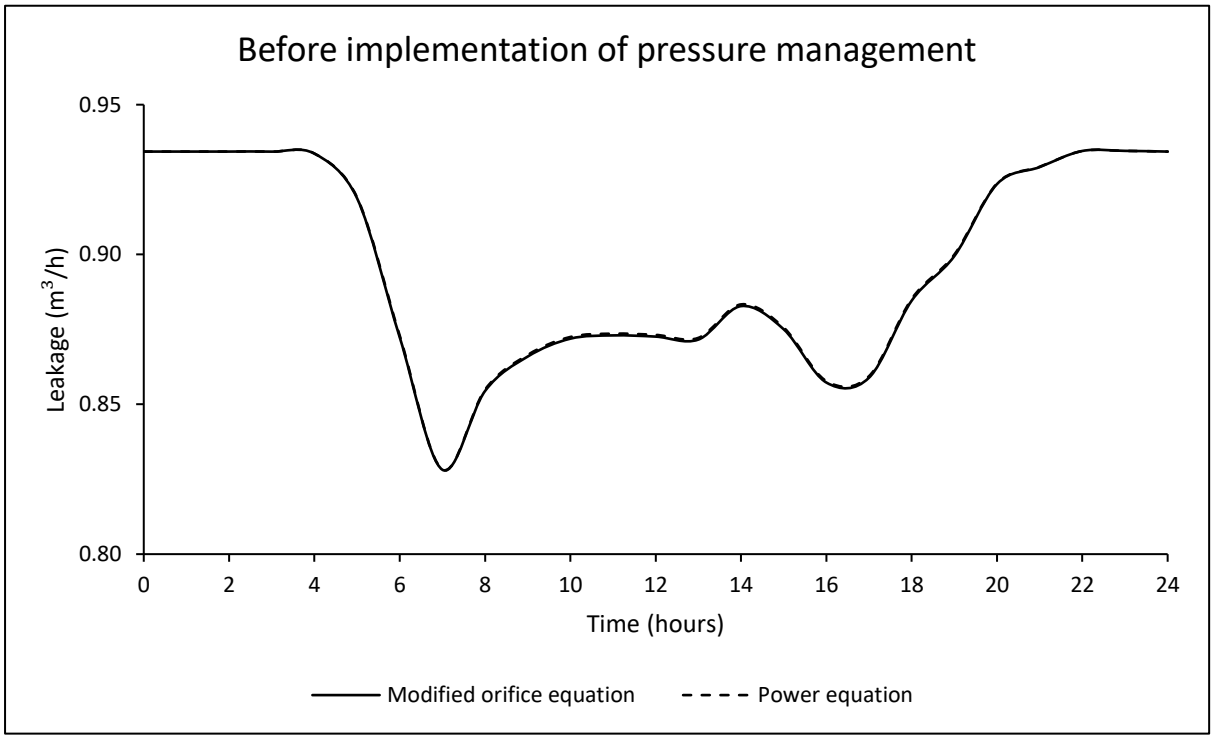

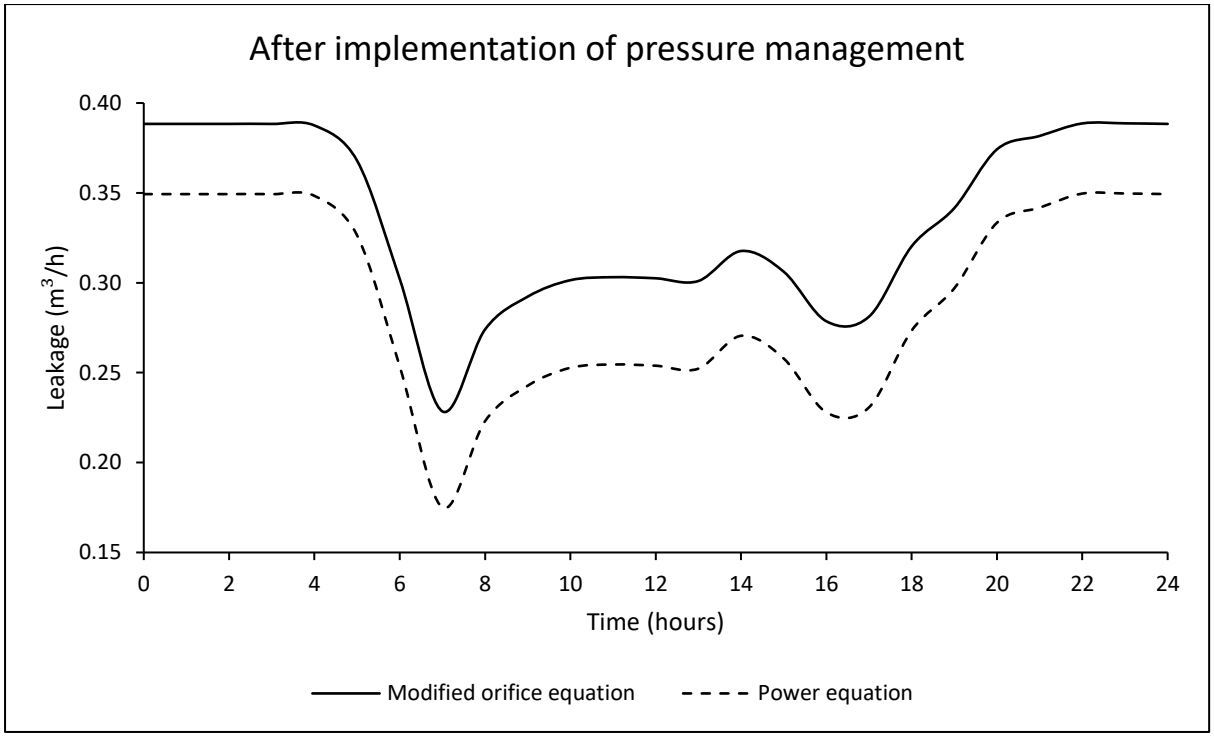
After implementation of pressure management
0.40
0.35
0.30
0.25
0.20
0.15
Leakage (m3/h)
0
2
4
6
8
10
12
14
16
18
20
22
24
Time (hours)
Modified orifice equation
Power equation

Number of iterations required for a system to converge to a hydraulic solution for both formulations

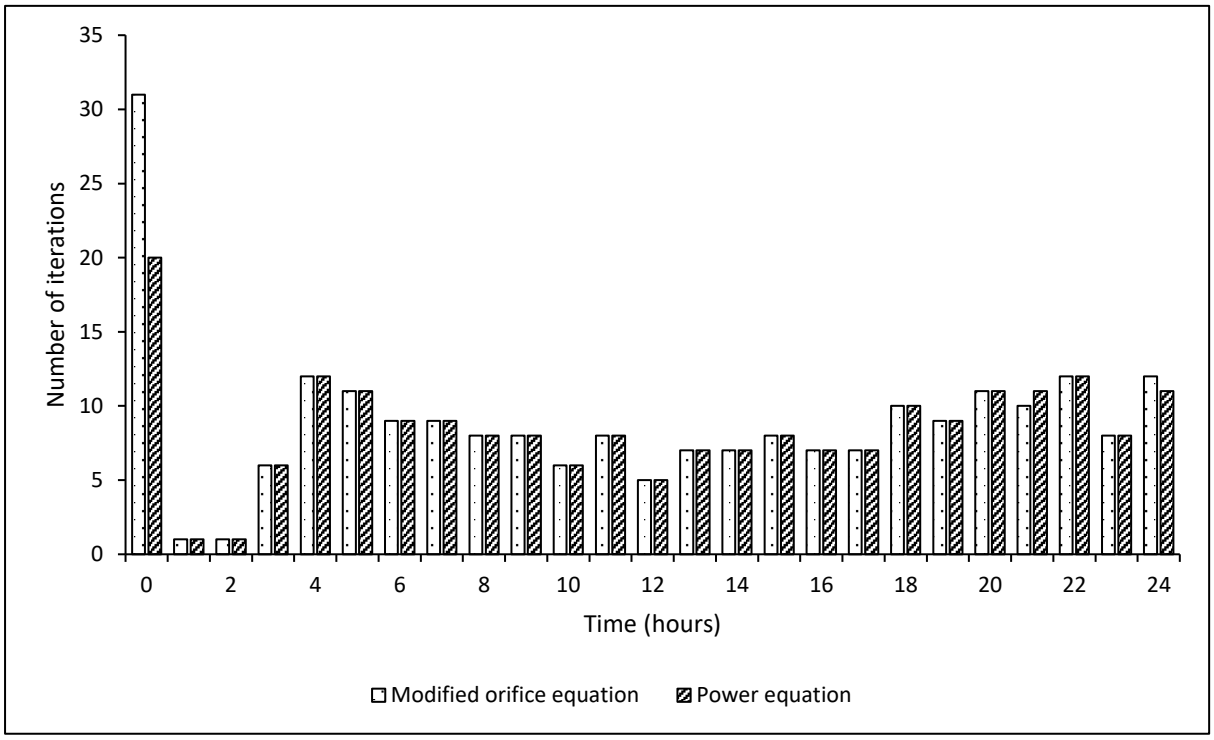

Results for combined systems

System parameters for both power and modified orifice formulations

	Minimum	Arithmetic Mean	Median	Maximum
Leakage exponent N1	0.65	0.72	0.70	0.97
Leakage coefficient C	8.7E-05	3.0E-04	3.2E-04	4.0E-04
Effective initial leak area C_dA0 (mm^2)	95.83	144.46	147.90	157.95
Effective head-area slope C_dm (mm^2/m)	0.26	0.37	0.34	0.78
Leakage number LN	0.18	0.29	0.26	0.90

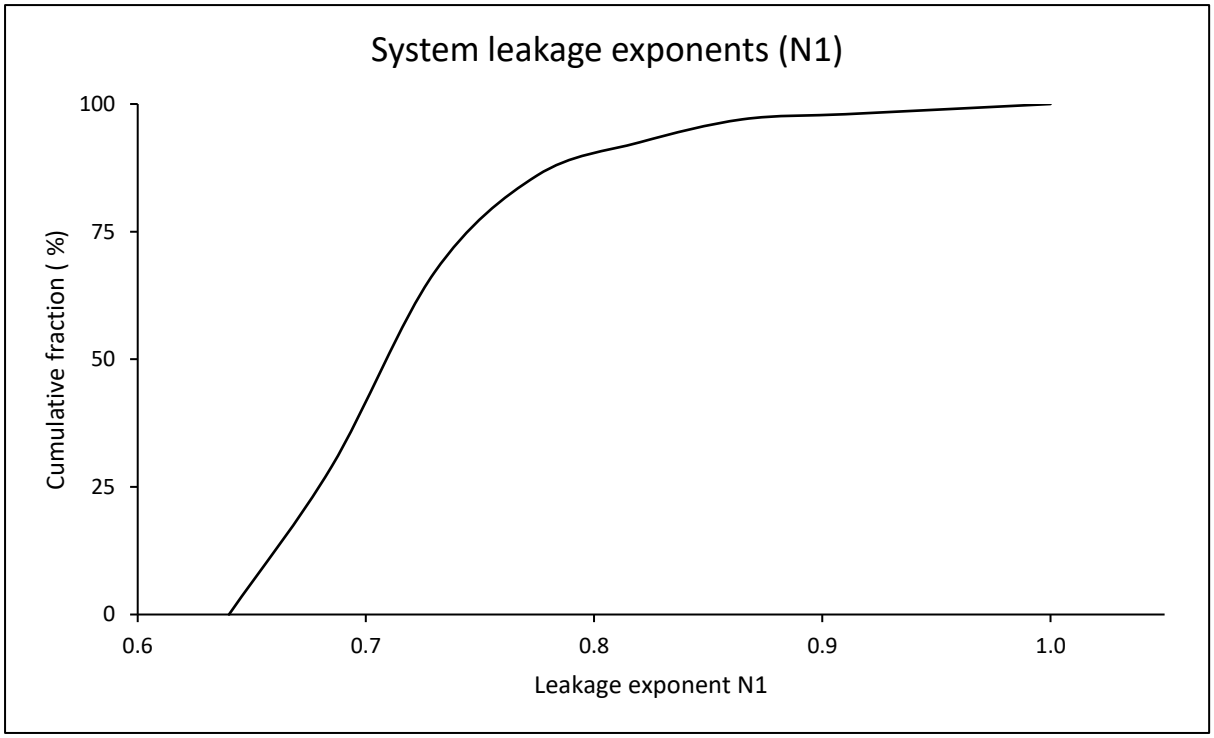

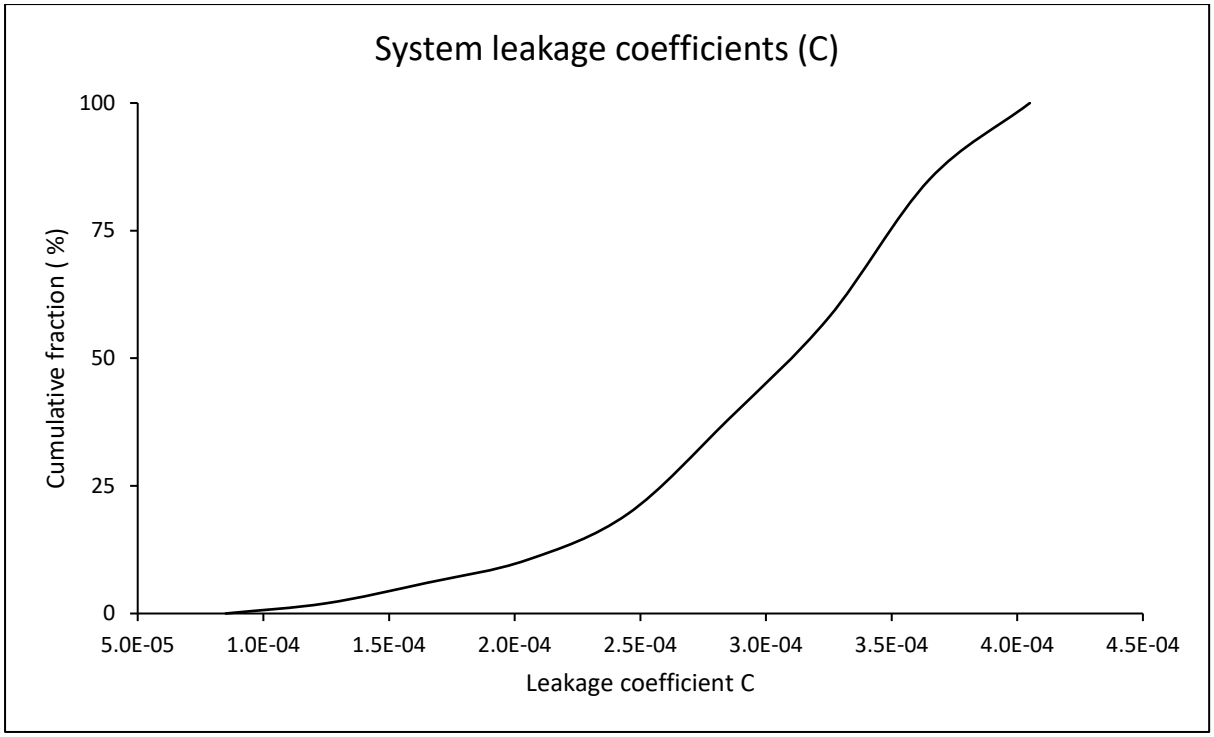
System leakage coefficients (C)
Cumulative fraction (%)
100
75
50
25
0
5.0E-05
1.0E-04
1.5E-04
2.0E-04
2.5E-04
3.0E-04
3.5E-04
4.0E-04
4.5E-04
Leakage coefficient C

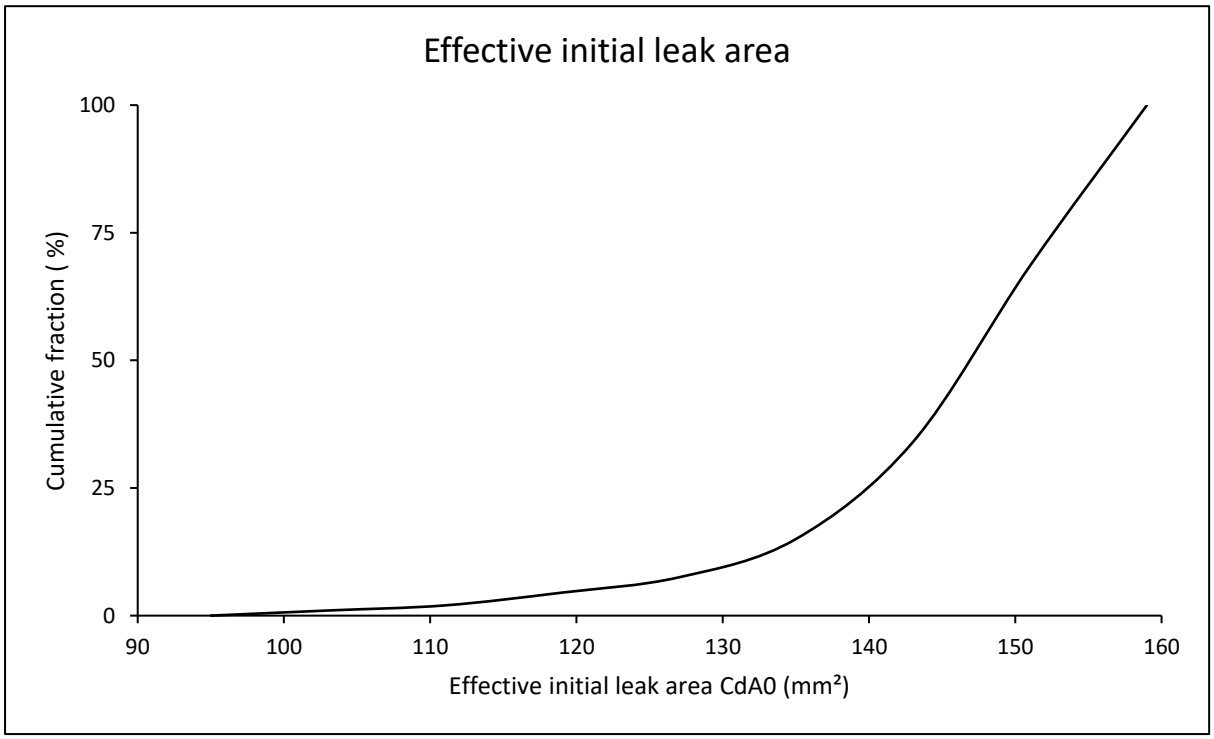
Effective initial leak area
Cumulative fraction (%)
100
75
50
25
0
90
100
110
120
130
140
150
160
Effective initial leak area CdA0 (mm²)

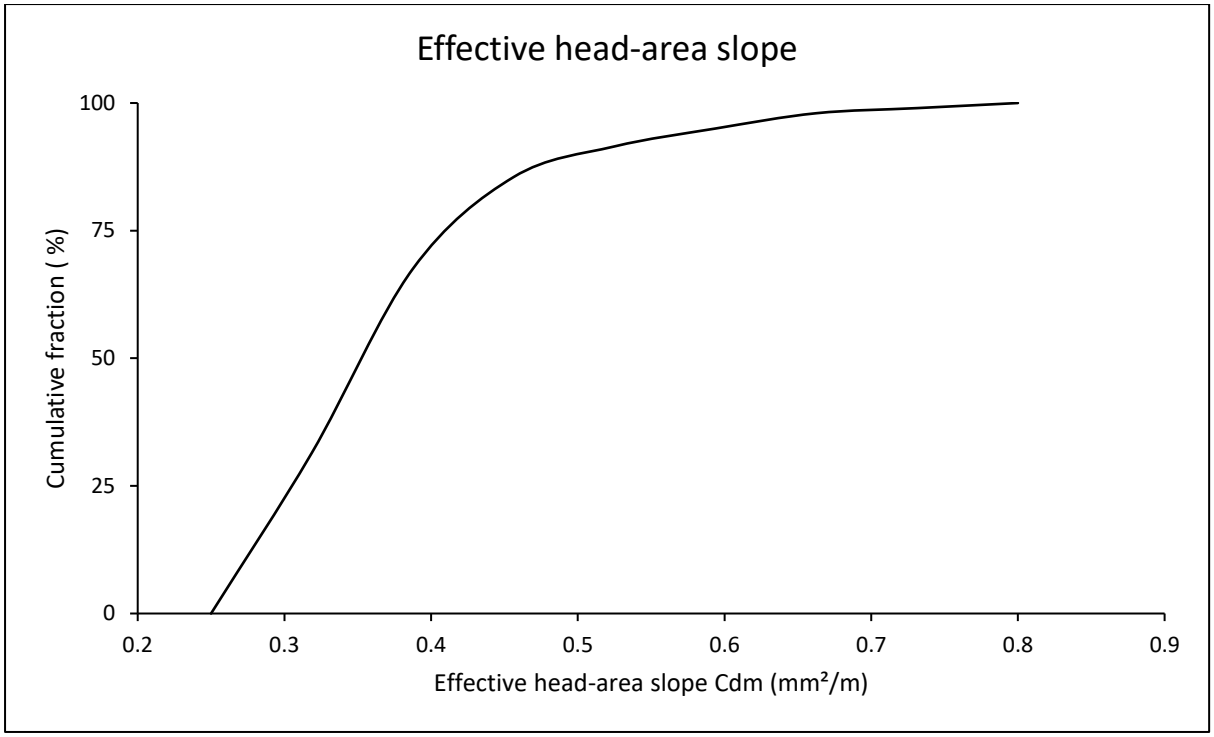
Effective head-area slope
100
75
50
25
0
Cumulative fraction (%)
0.2
0.3
0.4
0.5
0.6
0.7
0.8
0.9
Effective head-area slope Cdm (mm²/m)

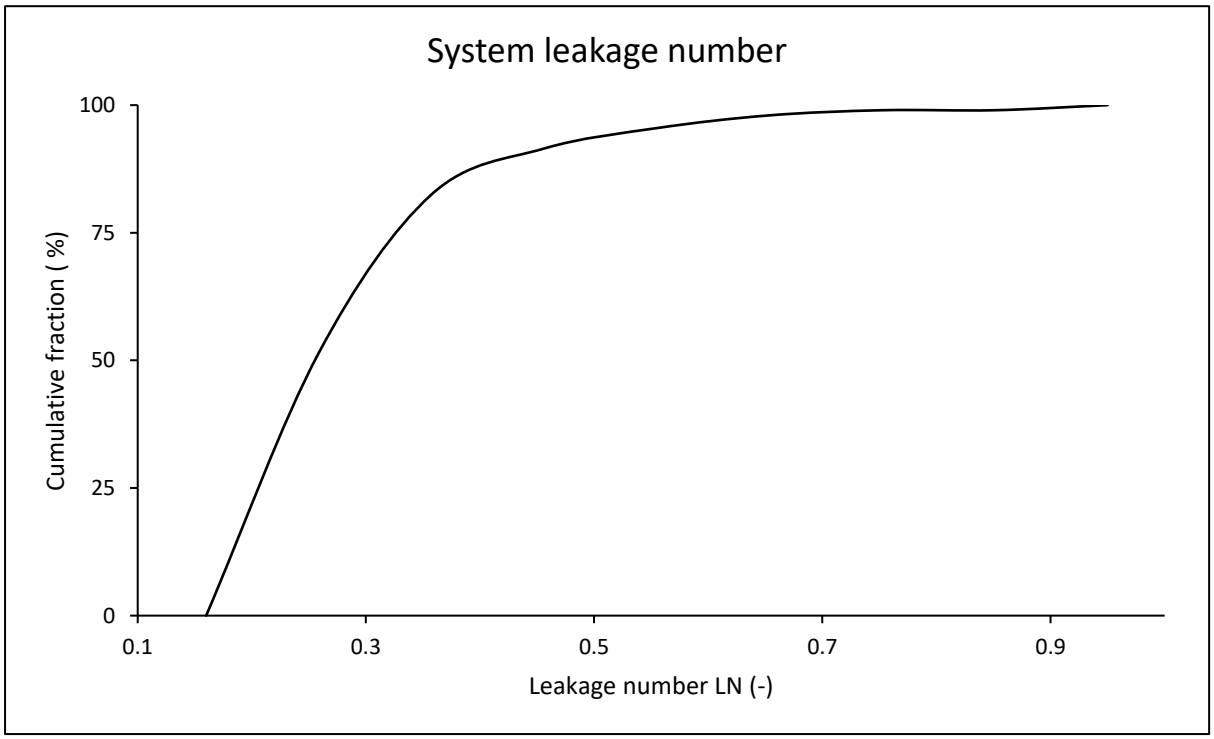
System leakage number
100
75
50
25
0
Cumulative fraction (%)
0.1
0.3
0.5
0.7
0.9
Leakage number LN (-)

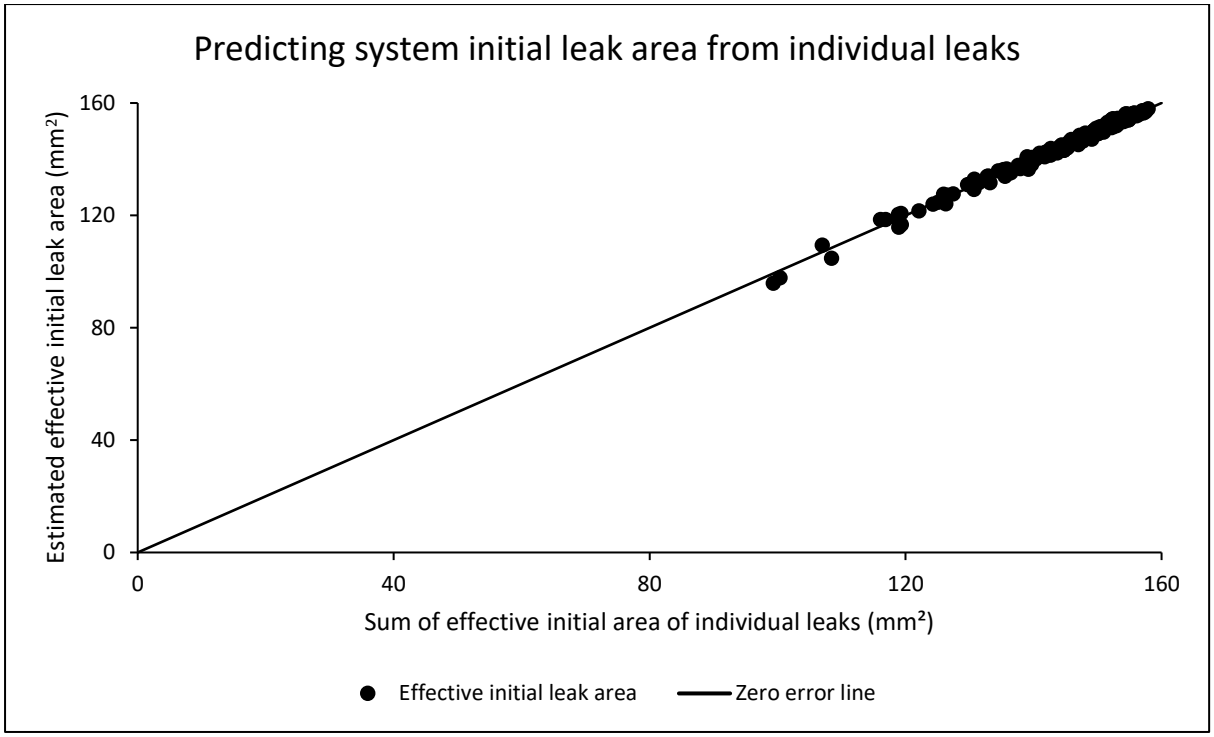
Predicting system initial leak area from individual leaks
Estimated effective initial leak area (mm²)
160
120
80
40
0
0
40
80
120
160
Sum of effective initial area of individual leaks (mm²)
Effective initial leak area
Zero error line

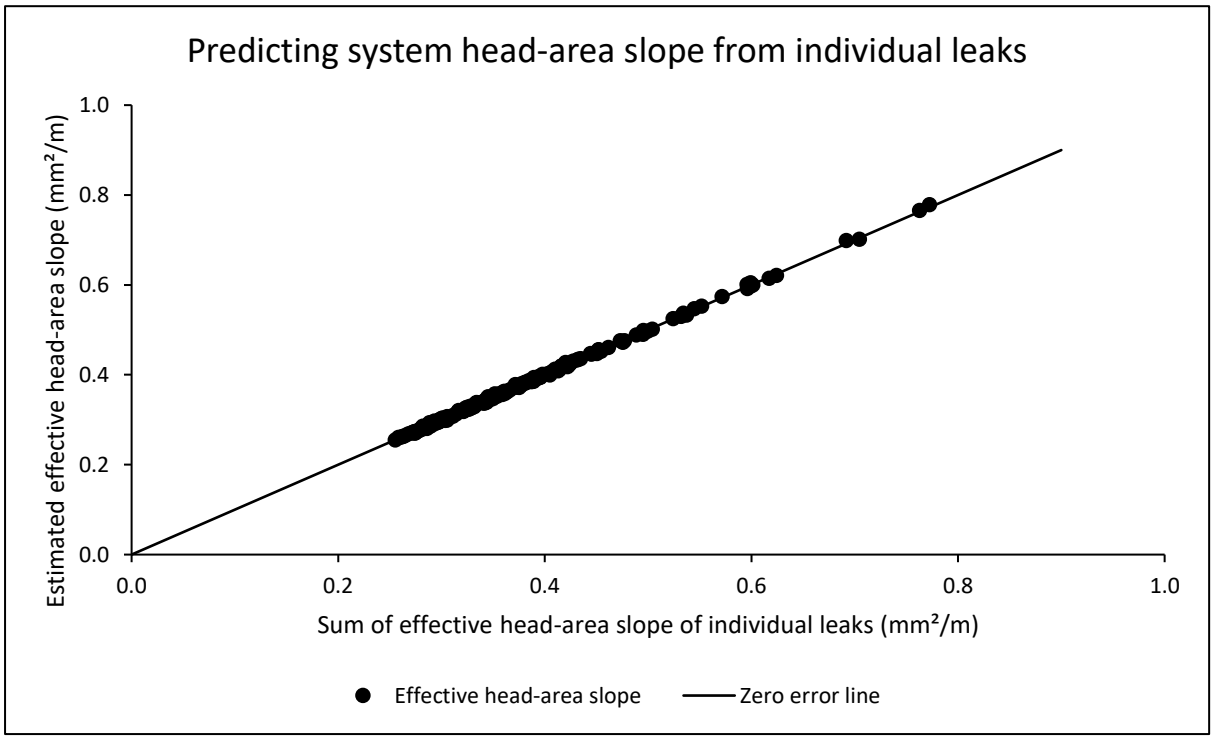
Predicting system head-area slope from individual leaks
Estimated effective head-area slope (mm²/m)
1.0
0.8
0.6
0.4
0.2
0.0
0.0
0.2
0.4
0.6
0.8
1.0
Sum of effective head-area slope of individual leaks (mm²/m)
Effective head-area slope
Zero error line

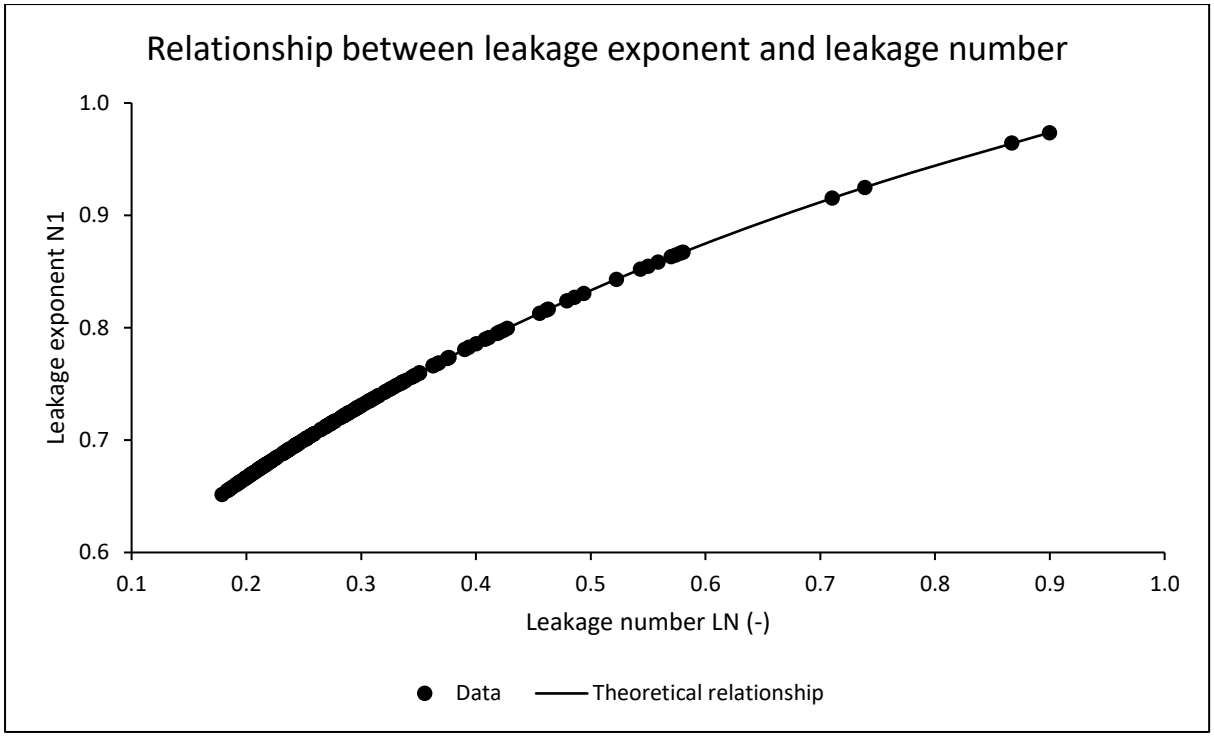
Relationship between leakage exponent and leakage number
Leakage exponent N1
1.0
0.9
0.8
0.7
0.6
0.1
0.2
0.3
0.4
0.5
0.6
0.7
0.8
0.9
1.0
Leakage number LN (-)
Data
Theoretical relationship

Average iterations required for a system to converge using both formulations

	Minimum	Arithmetic Mean	Median	Maximum
Modified orifice equation	8.72	9.00	9.00	9.36
Power equation	8.32	8.60	8.60	8.92

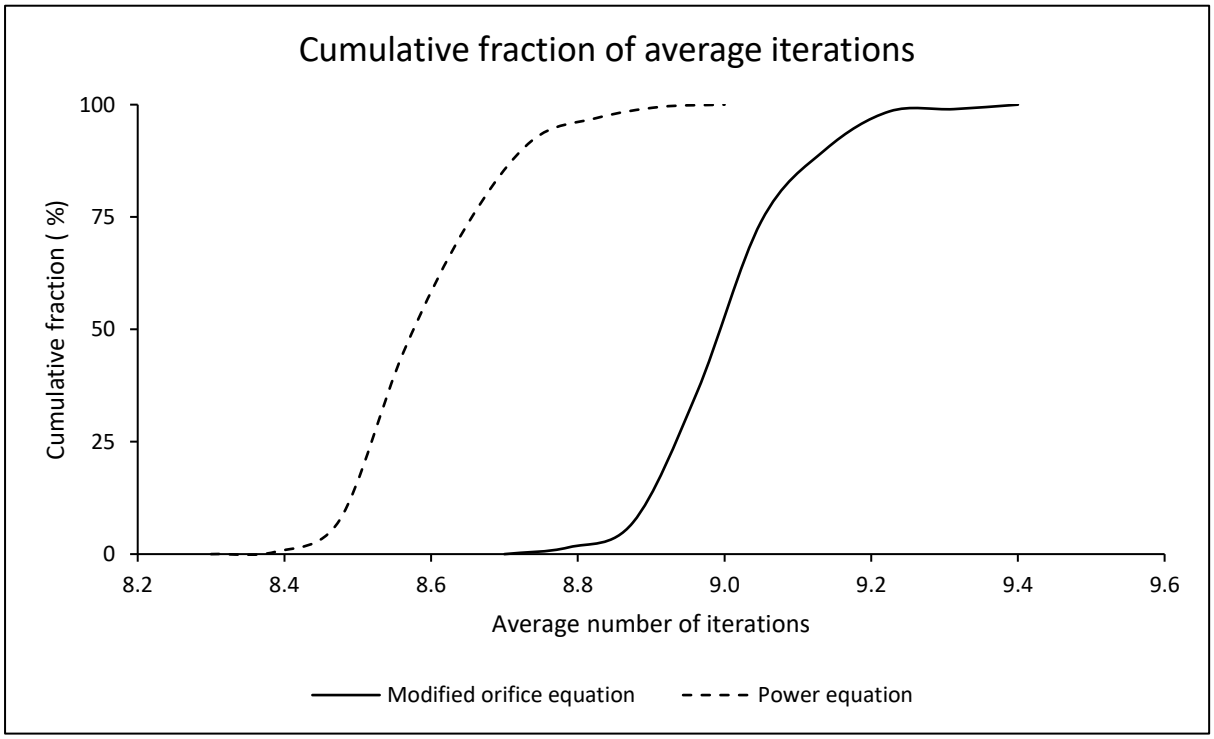

Effect of leakage on pressure at both average zone pressure (AZP) and critical nodes

AZP node								
	During MNF conditions				During peak demand conditions			
	Min (m)	Mean (m)	Median (m)	Max (m)	Min (m)	Mean (m)	Median (m)	Max (m)
Modified orifice equation	-0.03	-0.02	-0.02	-0.02	-0.13	-0.12	-0.12	-0.09
Power equation	-0.03	-0.02	-0.02	-0.02	-0.13	-0.12	-0.12	-0.09
Critical node								
Modified orifice equation	-0.05	-0.03	-0.03	-0.02	-0.20	-0.15	-0.14	-0.10
Power equation	-0.05	-0.03	-0.03	-0.02	-0.20	-0.14	-0.14	-0.10

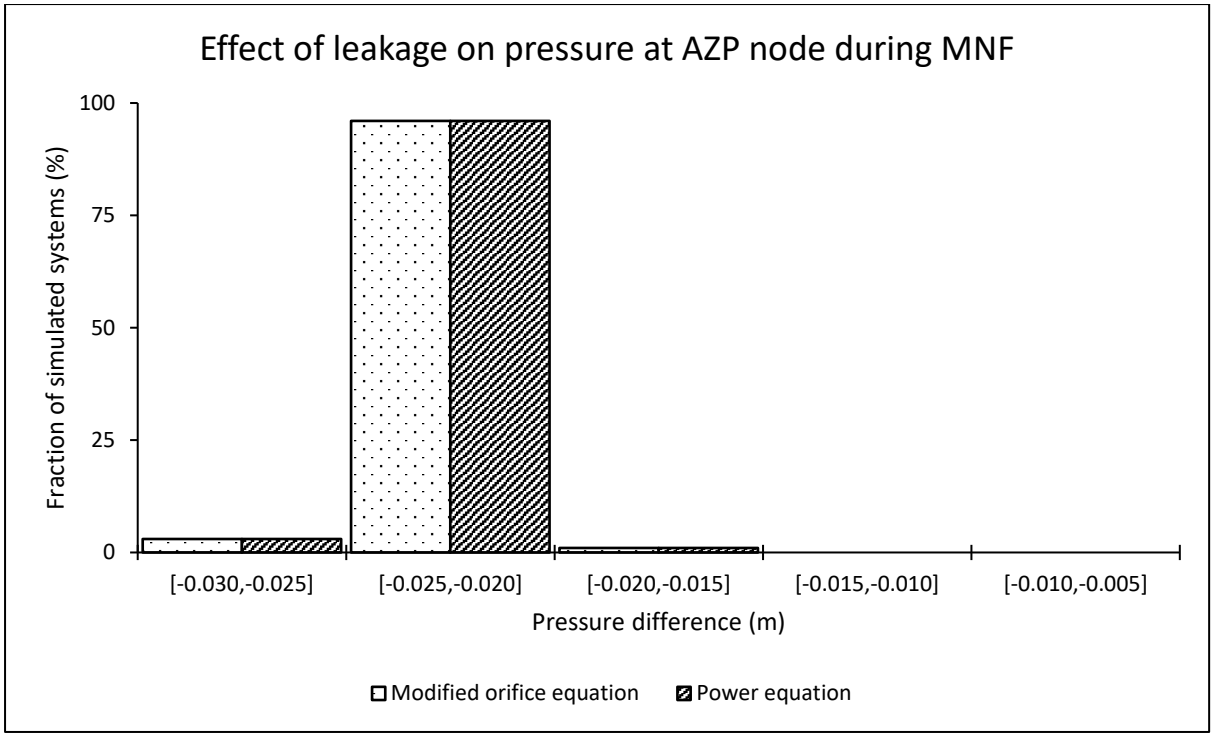
Effect of leakage on pressure at AZP node during MNF
Fraction of simulated systems (%)
100
75
50
25
0
[-0.030,-0.025]
[-0.025,-0.020]
[-0.020,-0.015]
[-0.015,-0.010]
[-0.010,-0.005]
Pressure difference (m)
Modified orifice equation
Power equation

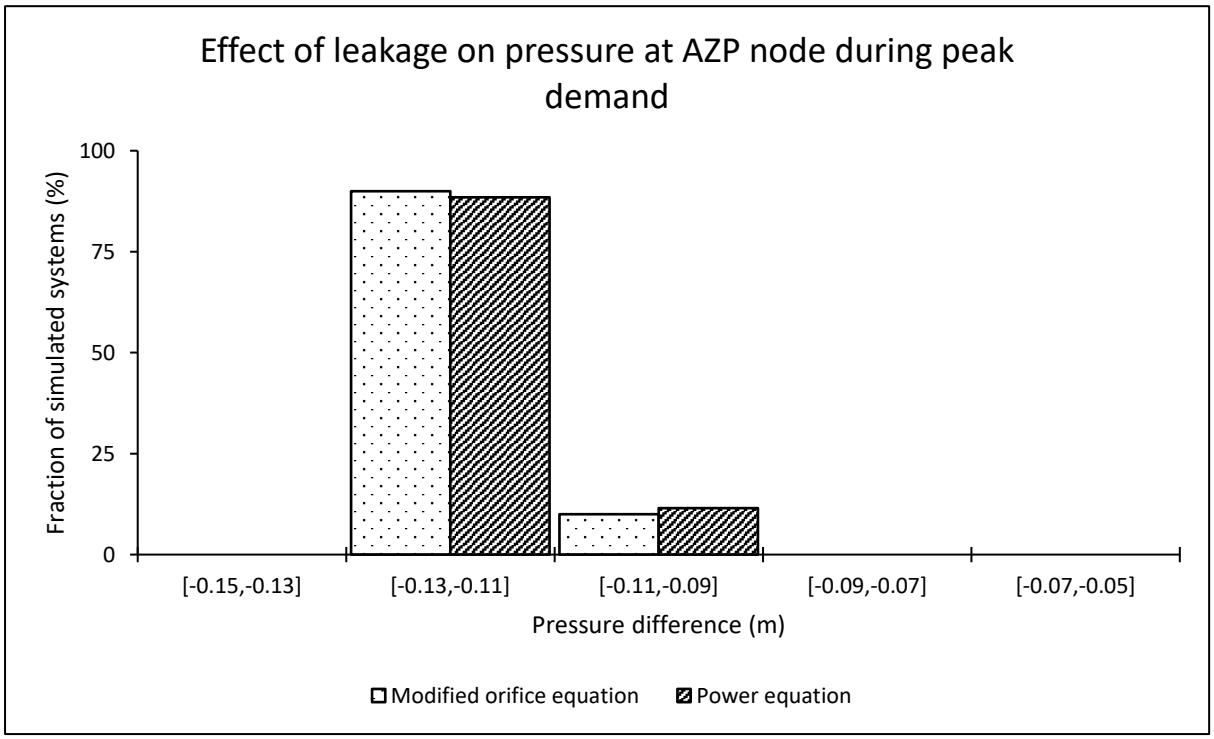
Effect of leakage on pressure at AZP node during peak demand
Fraction of simulated systems (%)
100
75
50
25
0
[-0.15,-0.13]
[-0.13,-0.11]
[-0.11,-0.09]
[-0.09,-0.07]
[-0.07,-0.05]
Pressure difference (m)
Modified orifice equation
Power equation

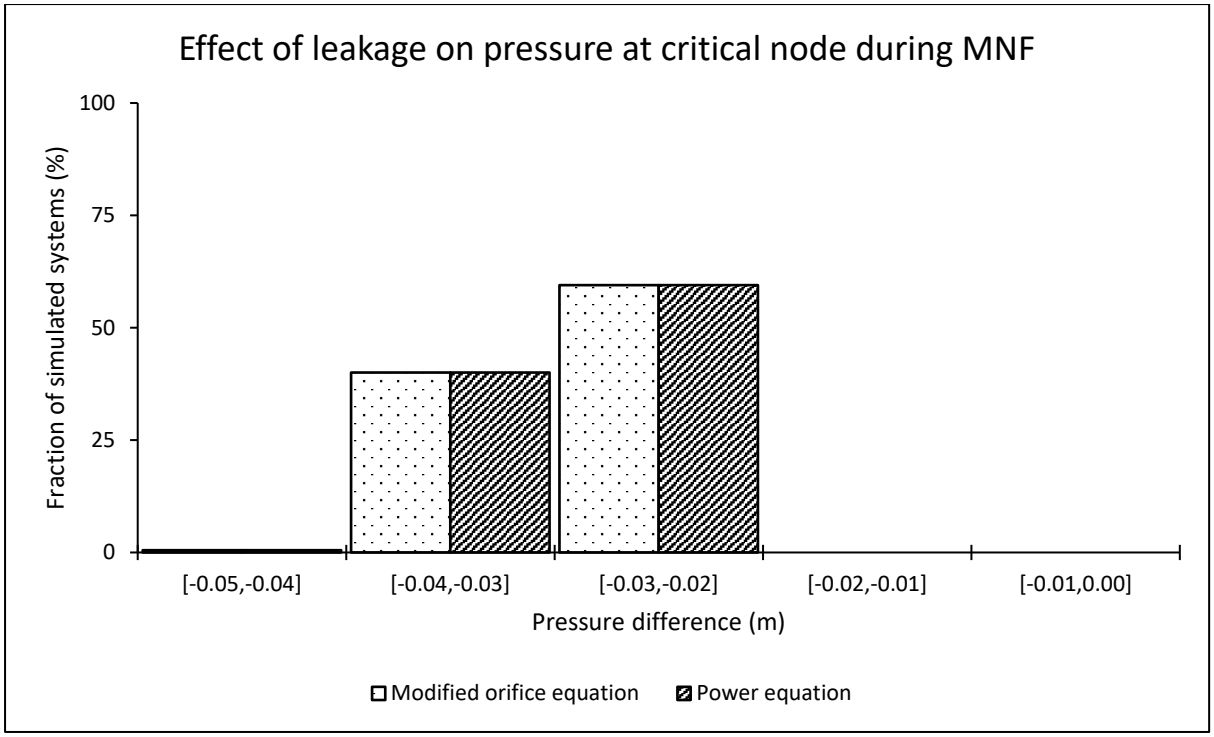
Effect of leakage on pressure at critical node during MNF
Fraction of simulated systems (%)
100
75
50
25
0
[-0.05,-0.04]
[-0.04,-0.03]
[-0.03,-0.02]
[-0.02,-0.01]
[-0.01,0.00]
Pressure difference (m)
Modified orifice equation
Power equation

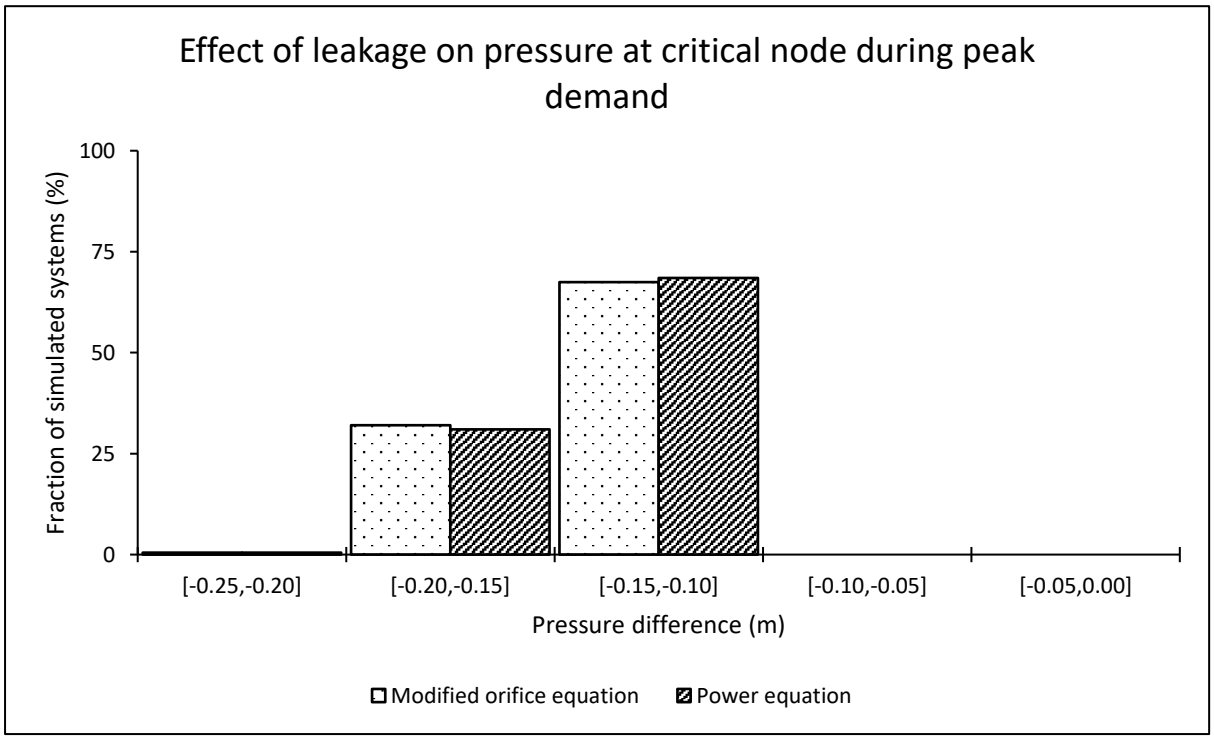
Effect of leakage on pressure at critical node during peak demand
Fraction of simulated systems (%)
100
75
50
25
0
[-0.25,-0.20]
[-0.20,-0.15]
[-0.15,-0.10]
[-0.10,-0.05]
[-0.05,0.00]
Pressure difference (m)
Modified orifice equation
Power equation

Pressure estimation error when using the power equation at average zone pressure (AZP) and critical nodes

	During MNF conditions				During peak demand conditions			
	Min (%)	**Mean (%)**	**Median (%)**	**Max (%)**	**Min (%)**	**Mean (%)**	**Median (%)**	**Max (%)**
At the AZP node	0.00	0.00	0.00	0.00	0.00	0.00	0.00	0.00
At the critical node	0.00	0.00	0.00	0.00	0.00	0.00	0.00	0.00

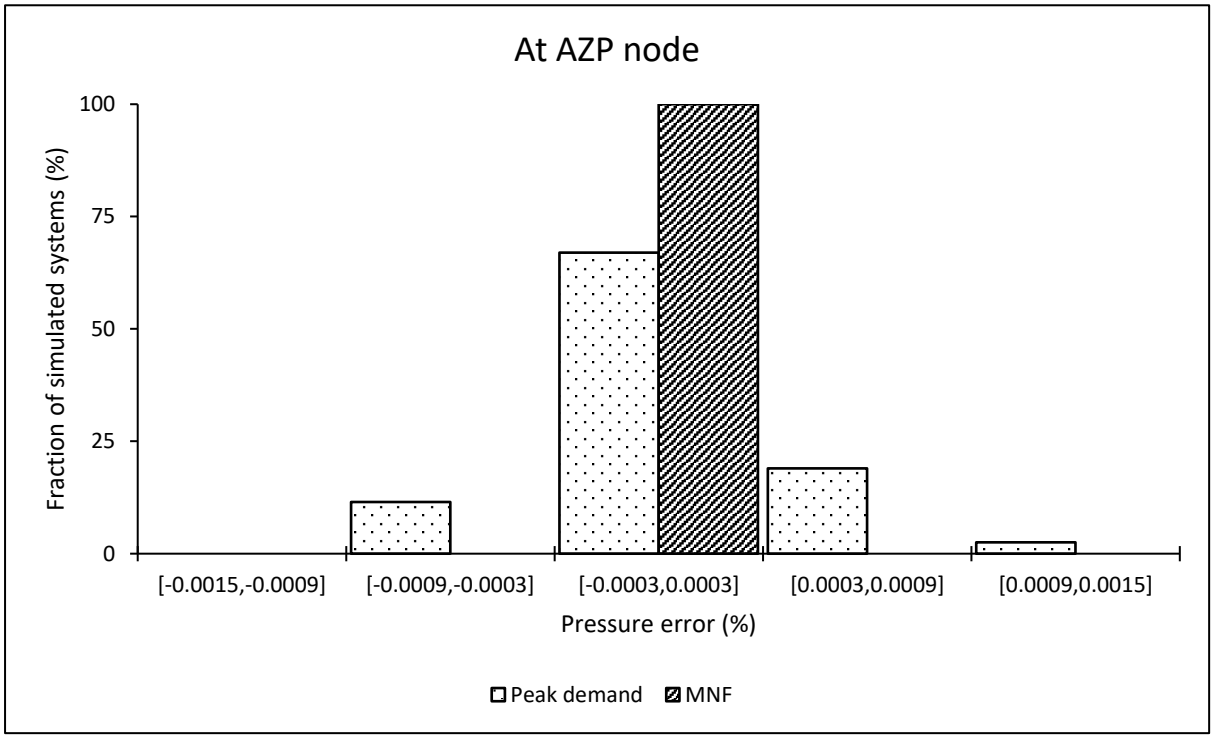

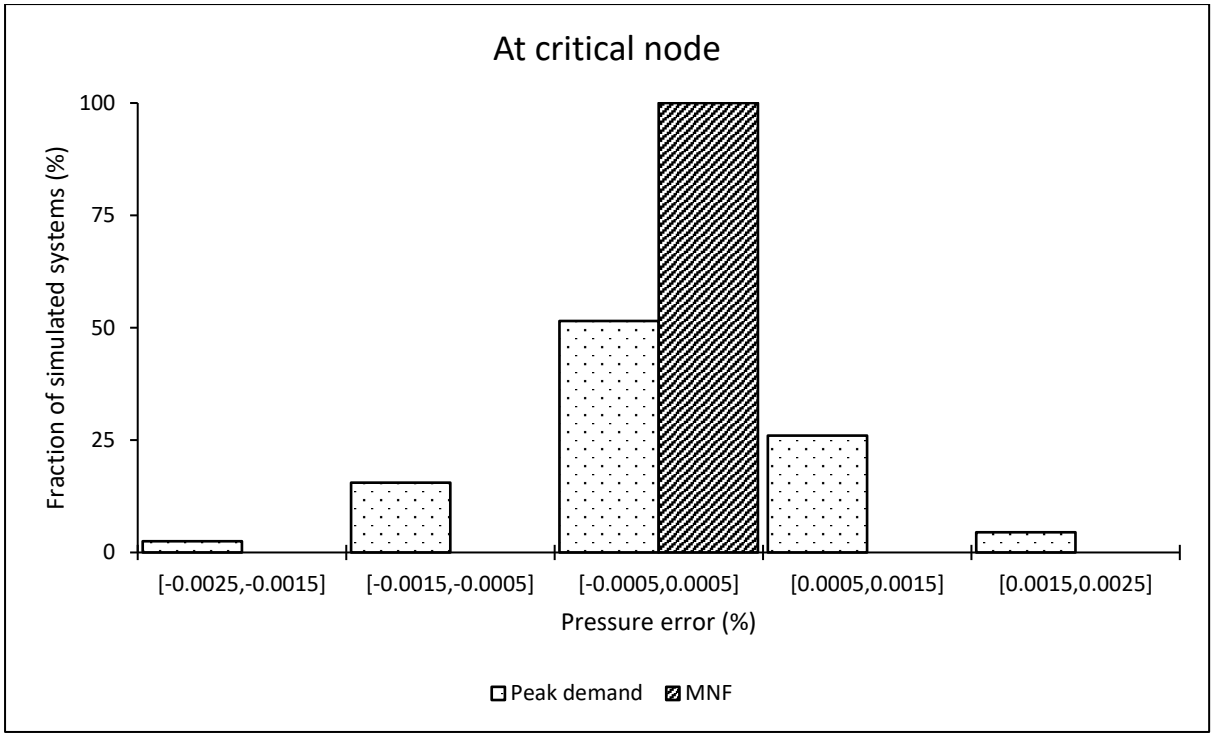
At critical node
Fraction of simulated systems (%)
100
75
50
25
0
[-0.0025,-0.0015]
[-0.0015,-0.0005]
[-0.0005,0.0005]
[0.0005,0.0015]
[0.0015,0.0025]
Pressure error (%)
Peak demand
MNF

System leakage estimation error when using the power equation

	Leakage estimation error (%)			
	Minimum	**Arithmetic Mean**	**Median**	**Maximum**
Before implementing pressure management	-0.21	-0.01	-0.01	0.16
After implementing pressure management	-21.51	-11.44	-10.93	-8.25

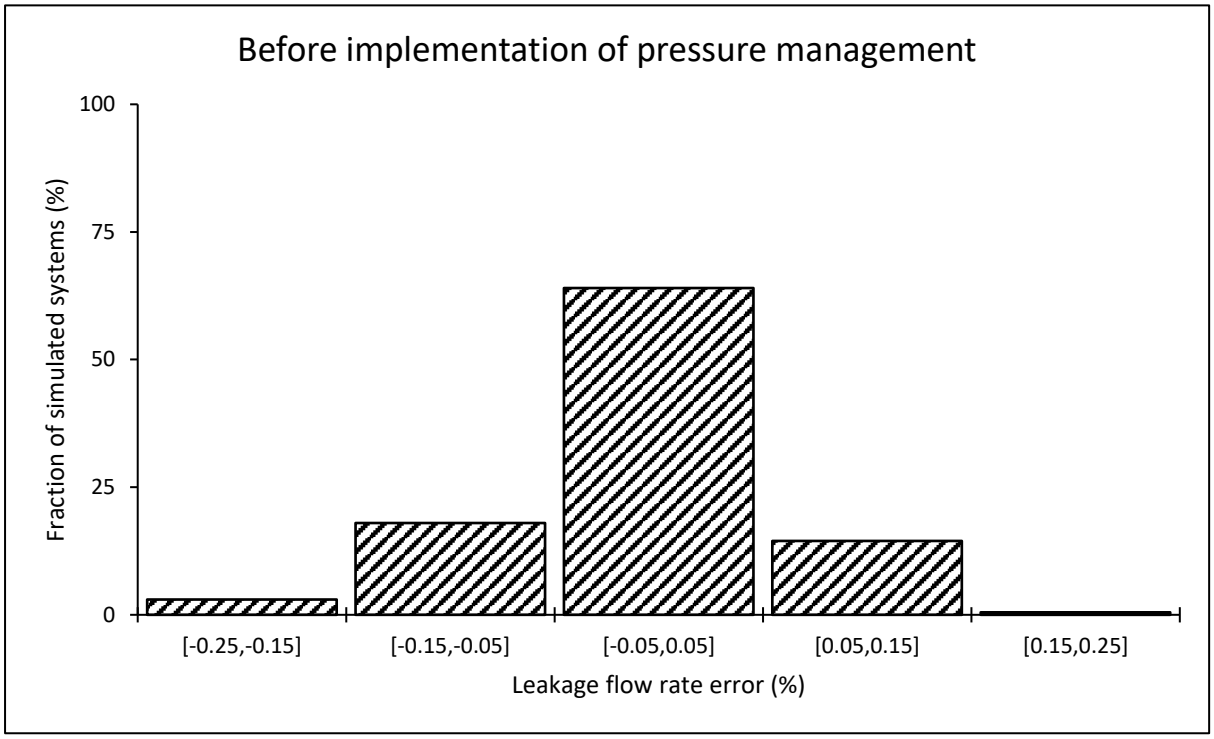

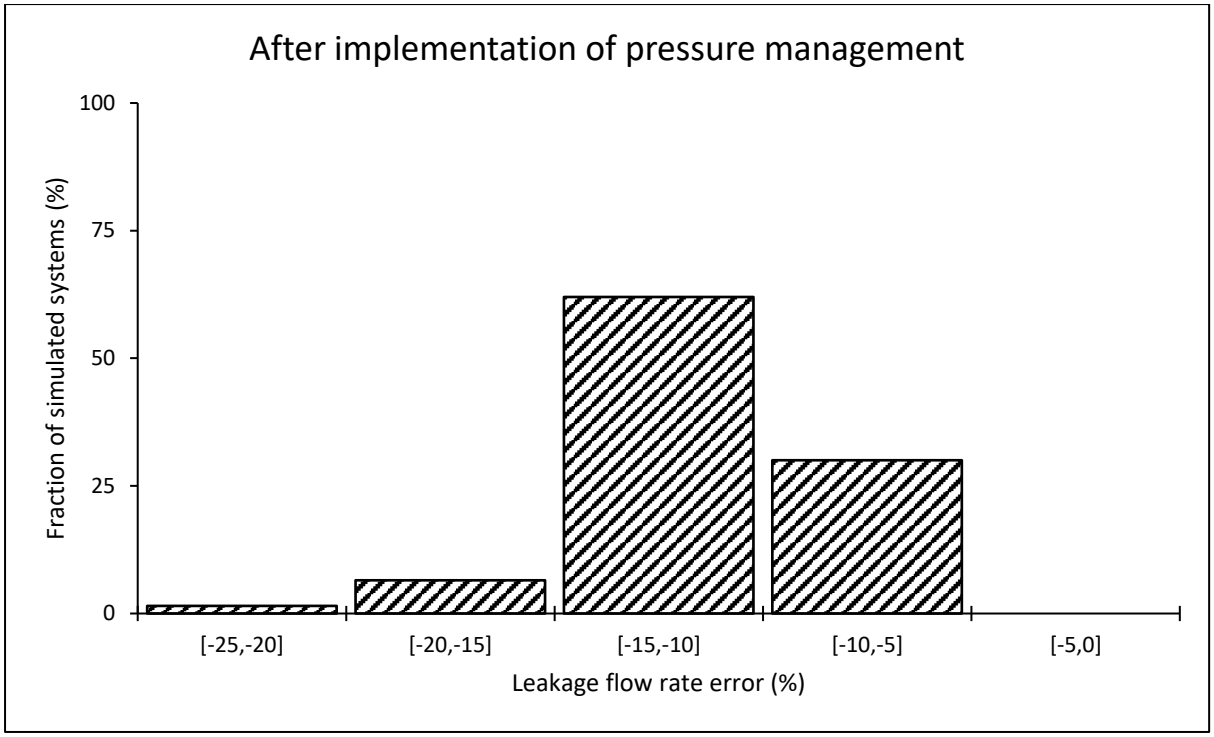
After implementation of pressure management
Fraction of simulated systems (%)
100
75
50
25
0
[-25,-20]
[-20,-15]
[-15,-10]
[-10,-5]
[-5,0]
Leakage flow rate error (%)

Leakage estimation error when using the power equation at the critical node

	Leakage estimation error (%)			
	Minimum	**Arithmetic Mean**	**Median**	**Maximum**
Before implementing pressure management	-2.76	-0.71	-1.11	4.56
After implementing pressure management	-53.60	-12.47	-27.27	252.13

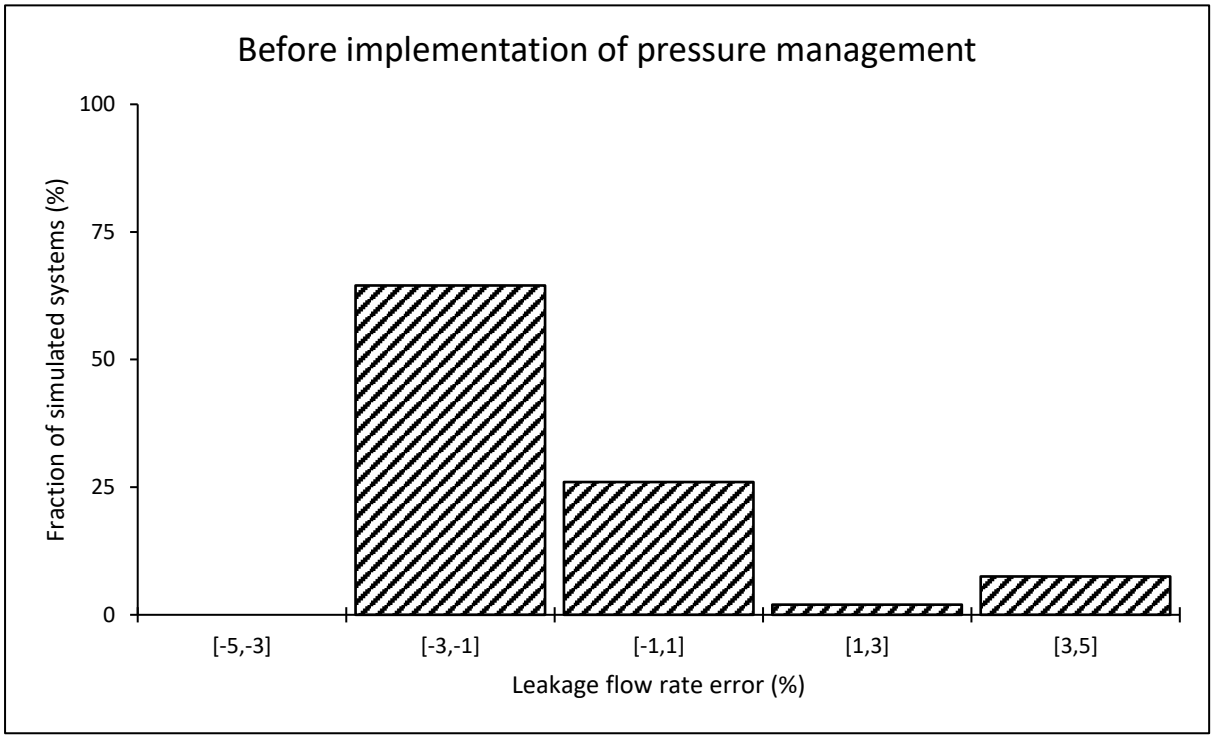

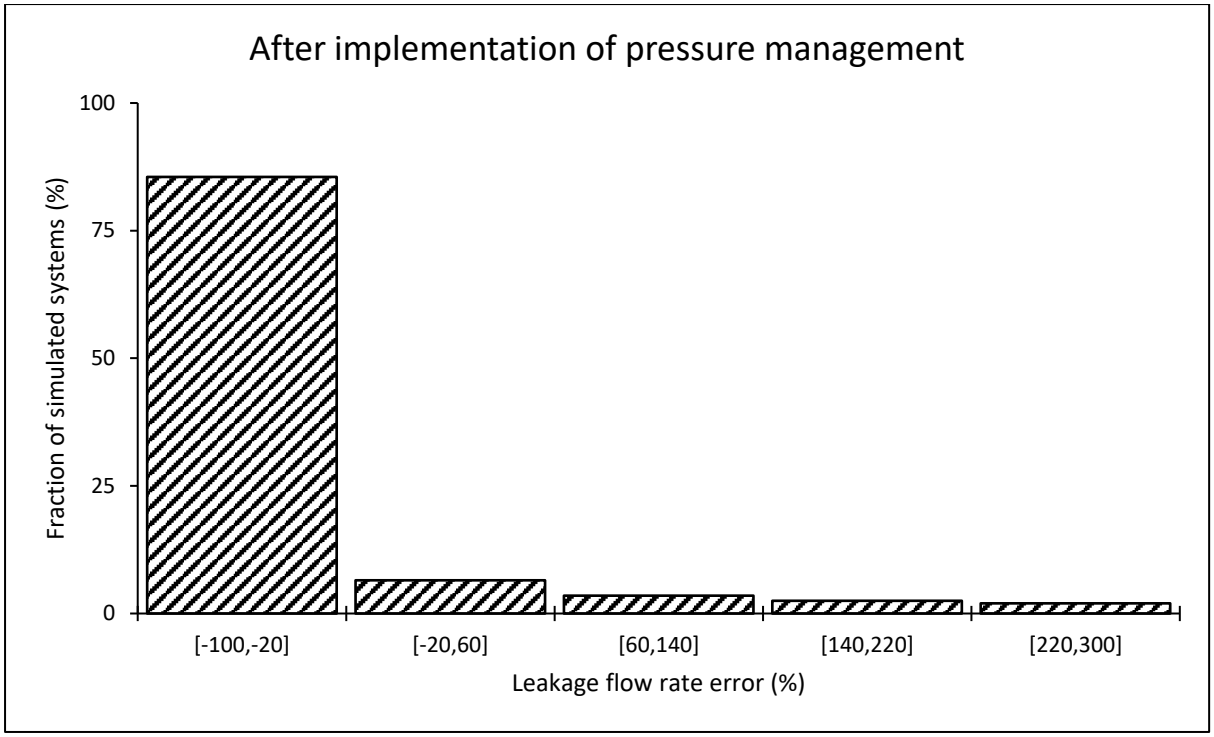
After implementation of pressure management
Fraction of simulated systems (%)
100
75
50
25
0
[-100,-20]
[-20,60]
[60,140]
[140,220]
[220,300]
Leakage flow rate error (%)

Appendix A-10: Large-sized network with an ILI of 4

Results for an individual system

Pressure head at the average zone pressure (AZP) node

		Pressure head (m)			
		Minimum	**Arithmetic Mean**	**Median**	**Maximum**
Before pressure management	Without leaks	99.13	108.33	106.63	113.44
	Modified orifice equation	98.69	108.07	106.29	113.35
	Power equation	98.69	108.07	106.29	113.35
After pressure management	Modified orifice equation	19.16	28.41	26.68	33.57
	Power equation	19.20	28.43	26.70	33.57

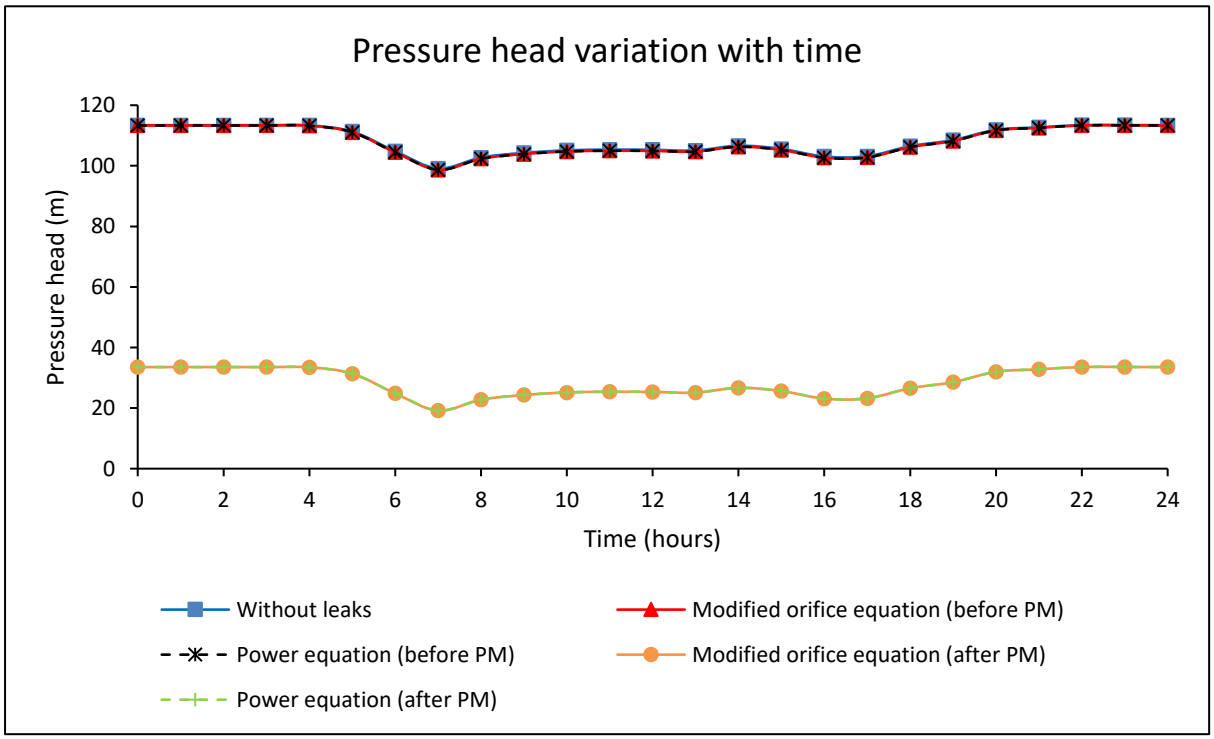

Pressure head at the critical node

		Pressure head (m)			
		Minimum	**Arithmetic Mean**	**Median**	**Maximum**
Before pressure management	Without leaks	89.91	100.55	98.69	106.46
	Modified orifice equation	89.41	100.25	98.30	106.35
	Power equation	89.41	100.25	98.31	106.35
After pressure management	Modified orifice equation	9.93	20.61	18.72	26.58
	Power equation	9.97	20.63	18.75	26.59

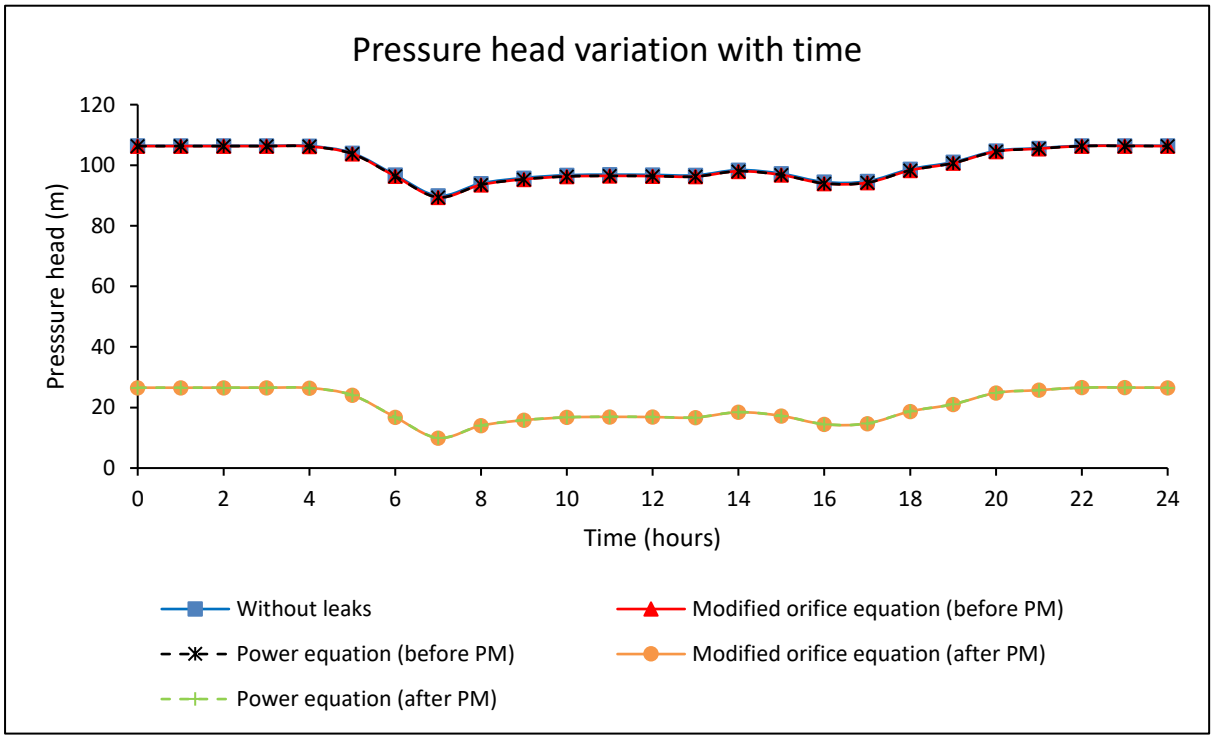

System leakage flow rate

		Leakage flow rate (m^3/h)			
		Minimum	**Arithmetic Mean**	**Median**	**Maximum**
Before pressure management	Modified orifice equation	111.80	121.65	119.79	127.25
	Power equation	111.38	121.53	119.64	127.25
After pressure management	Modified orifice equation	30.71	39.96	38.35	44.99
	Power equation	22.49	32.63	30.78	38.29

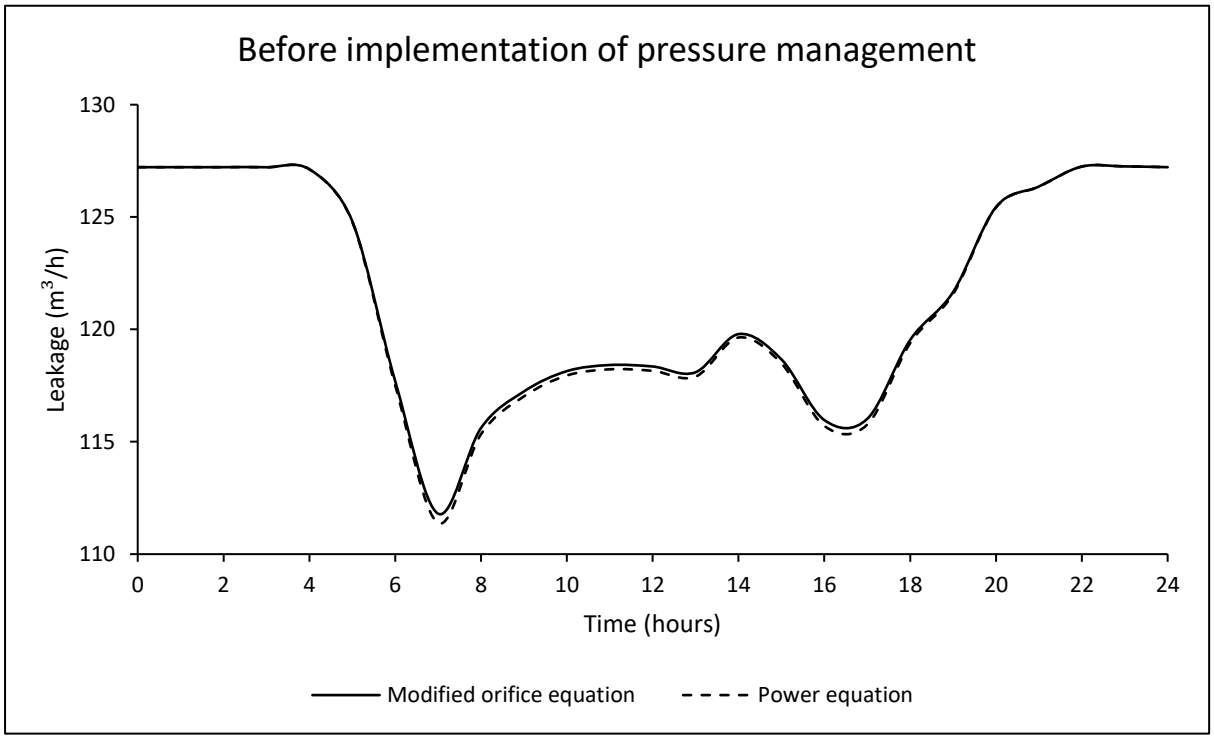

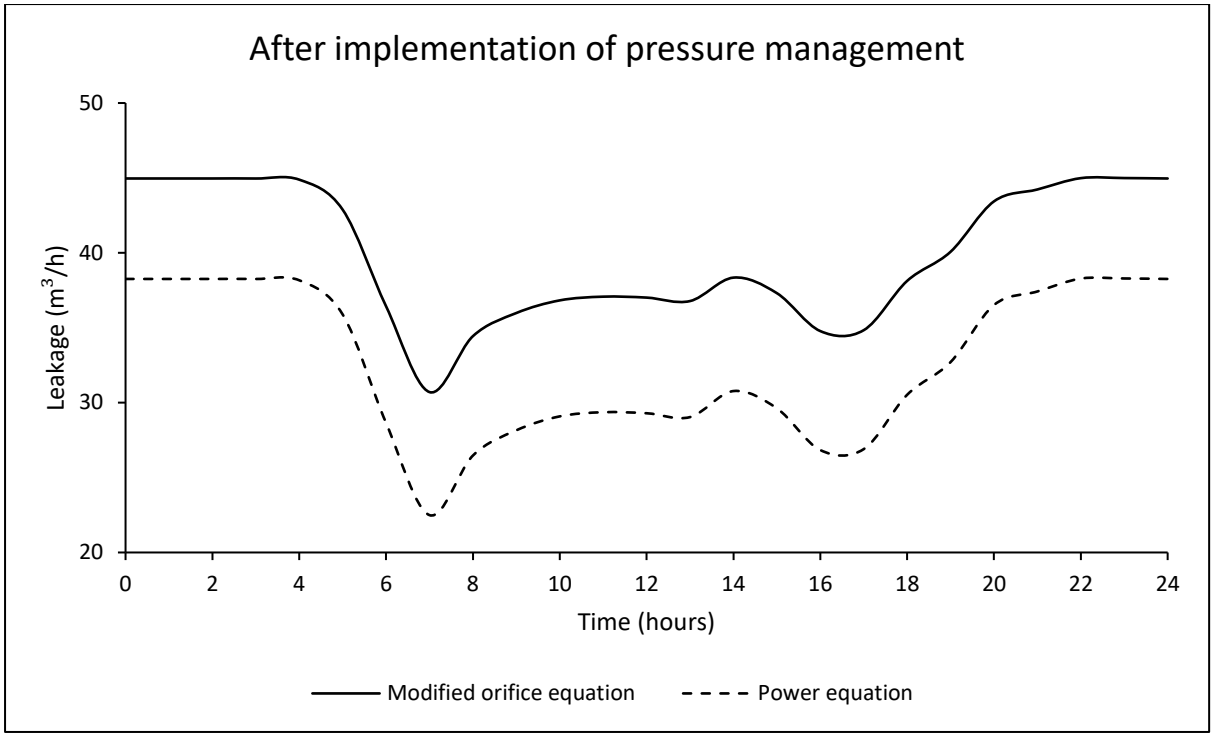
After implementation of pressure management
50
40
30
20
Leakage (m3/h)
0
2
4
6
8
10
12
14
16
18
20
22
24
Time (hours)
Modified orifice equation
Power equation

Leakage flow rate at the critical node

		Leakage flow rate (m^3/h)			
		Minimum	**Arithmetic Mean**	**Median**	**Maximum**
Before pressure management	Modified orifice equation	0.0091	0.0096	0.0095	0.0099
	Power equation	0.0083	0.0093	0.0092	0.0099
After pressure management	Modified orifice equation	0.0030	0.0043	0.0041	0.0049
	Power equation	0.0010	0.0020	0.0018	0.0025

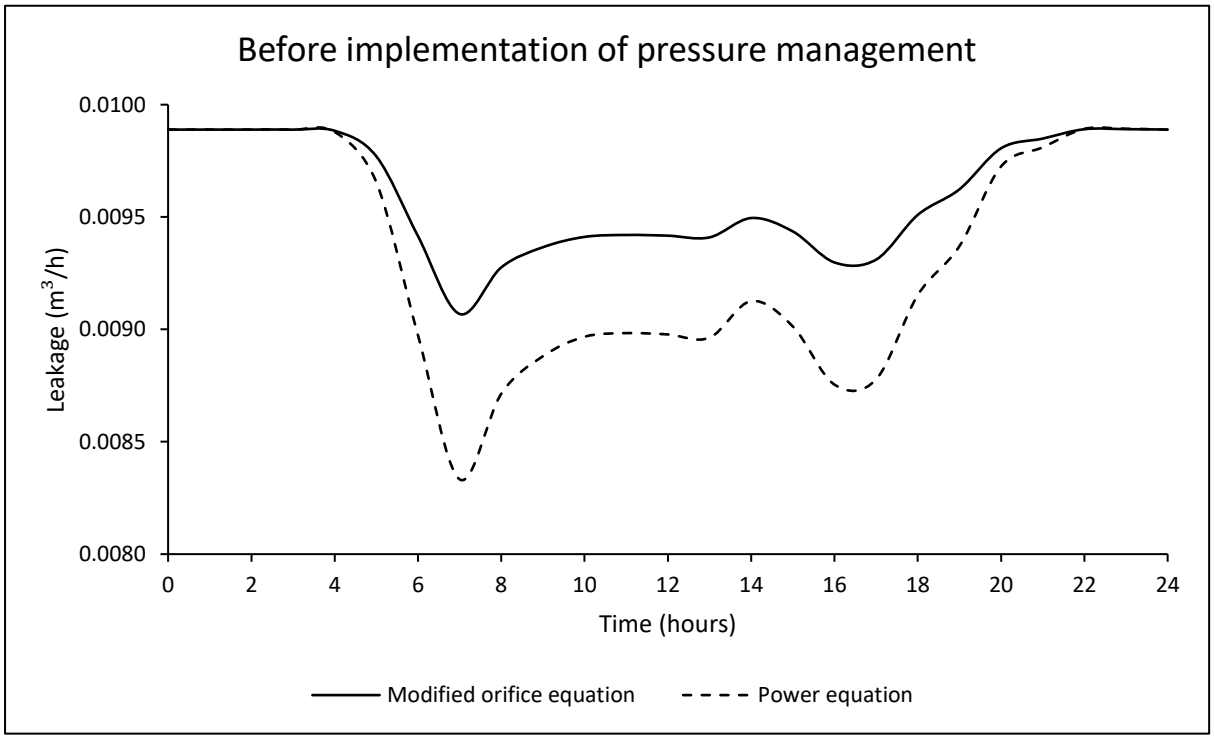

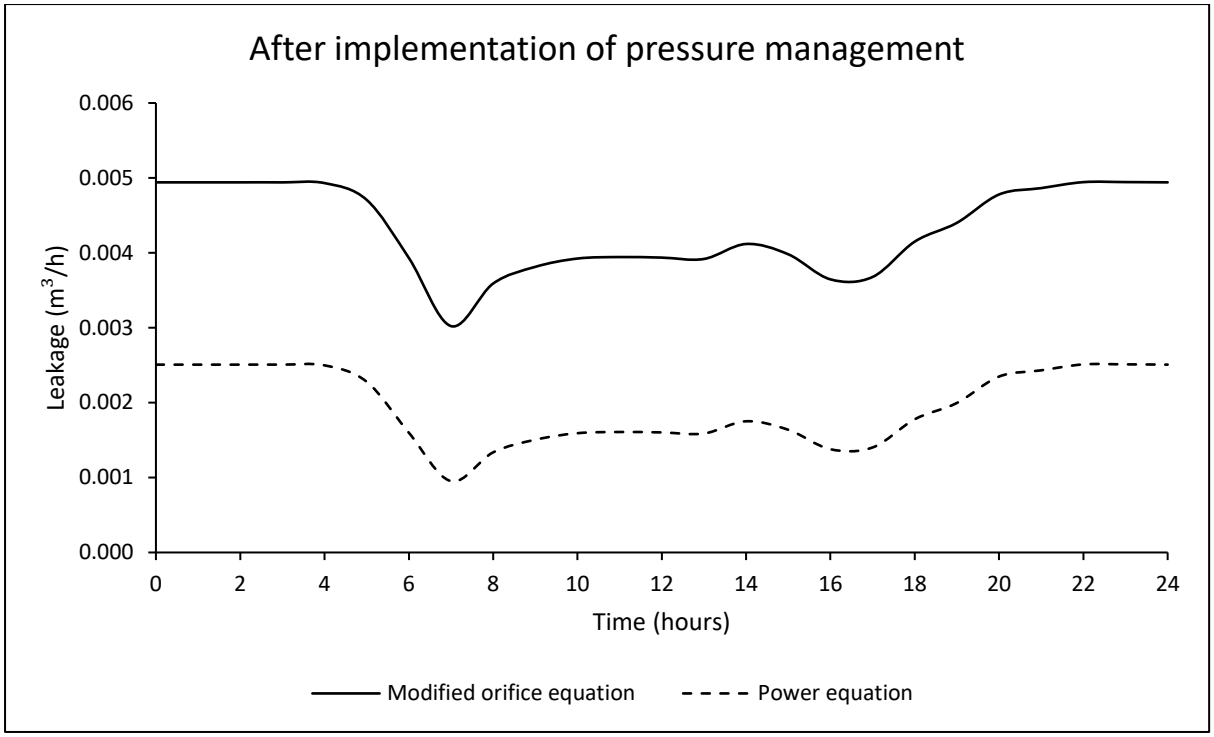
After implementation of pressure management
0.006
0.005
0.004
0.003
0.002
0.001
0.000
Leakage (m3/h)
0
2
4
6
8
10
12
14
16
18
20
22
24
Time (hours)
Modified orifice equation
Power equation

Number of iterations required for a system to converge to a hydraulic solution for both formulations

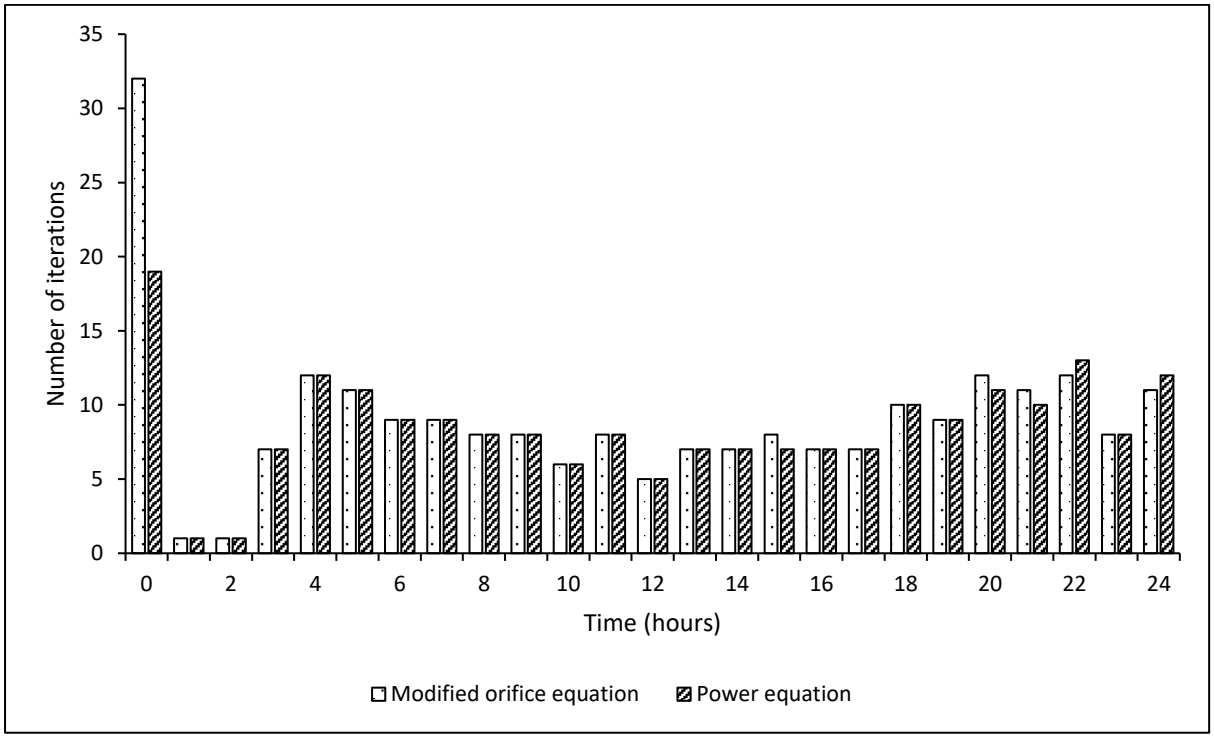

Results for combined systems

System parameters for both power and modified orifice formulations

	Minimum	Arithmetic Mean	Median	Maximum
Leakage exponent N1	0.76	0.98	0.98	1.26
Leakage coefficient C	8.6E-05	3.8E-04	3.5E-04	9.6E-04
Effective initial leak area C_dA0 (mm^2)	167.30	386.85	388.44	547.86
Effective head-area slope C_dm (mm^2/m)	1.75	3.18	3.18	4.88
Leakage number LN	0.35	0.98	0.91	3.23

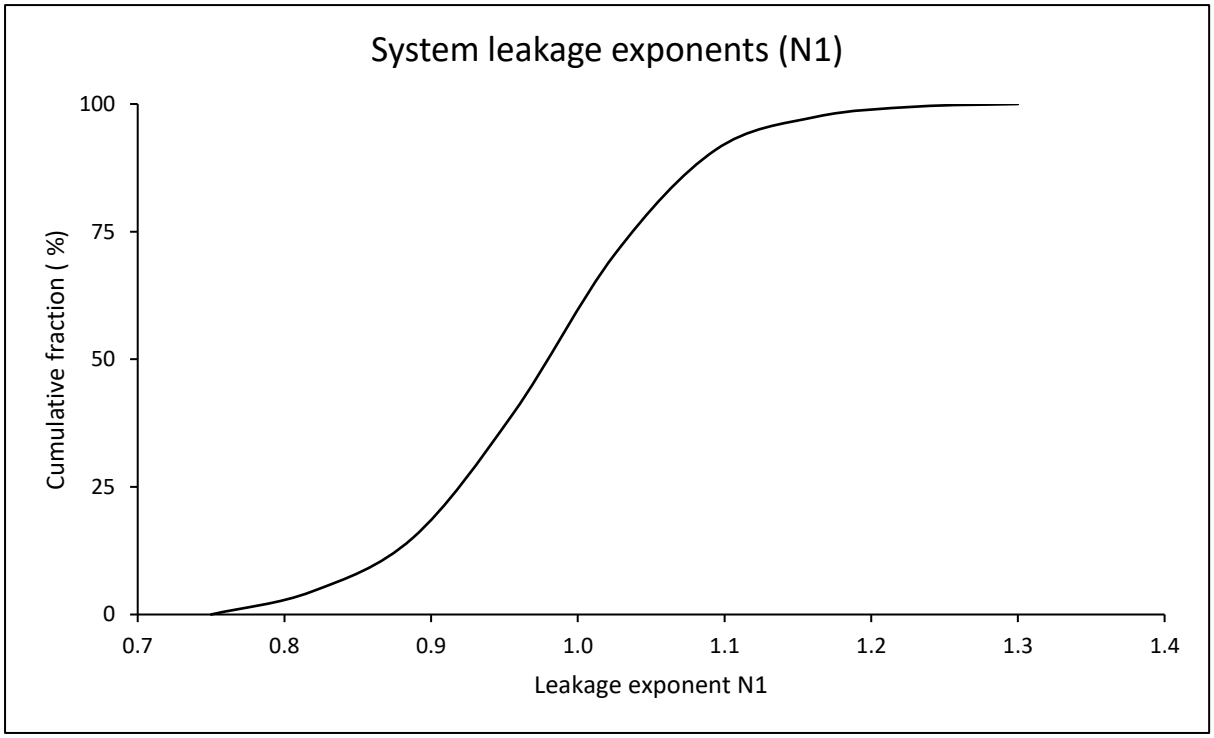

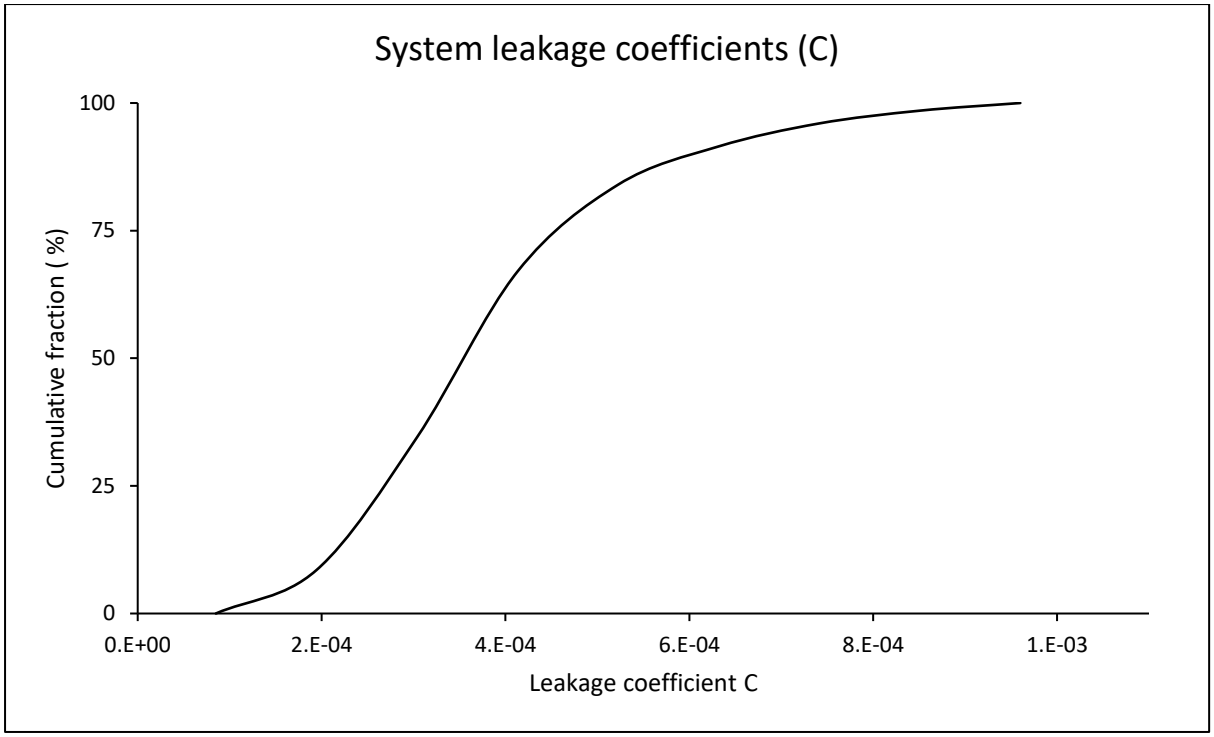
System leakage coefficients (C)
Cumulative fraction (%)
100
75
50
25
0
0.E+00
2.E-04
4.E-04
6.E-04
8.E-04
1.E-03
Leakage coefficient C

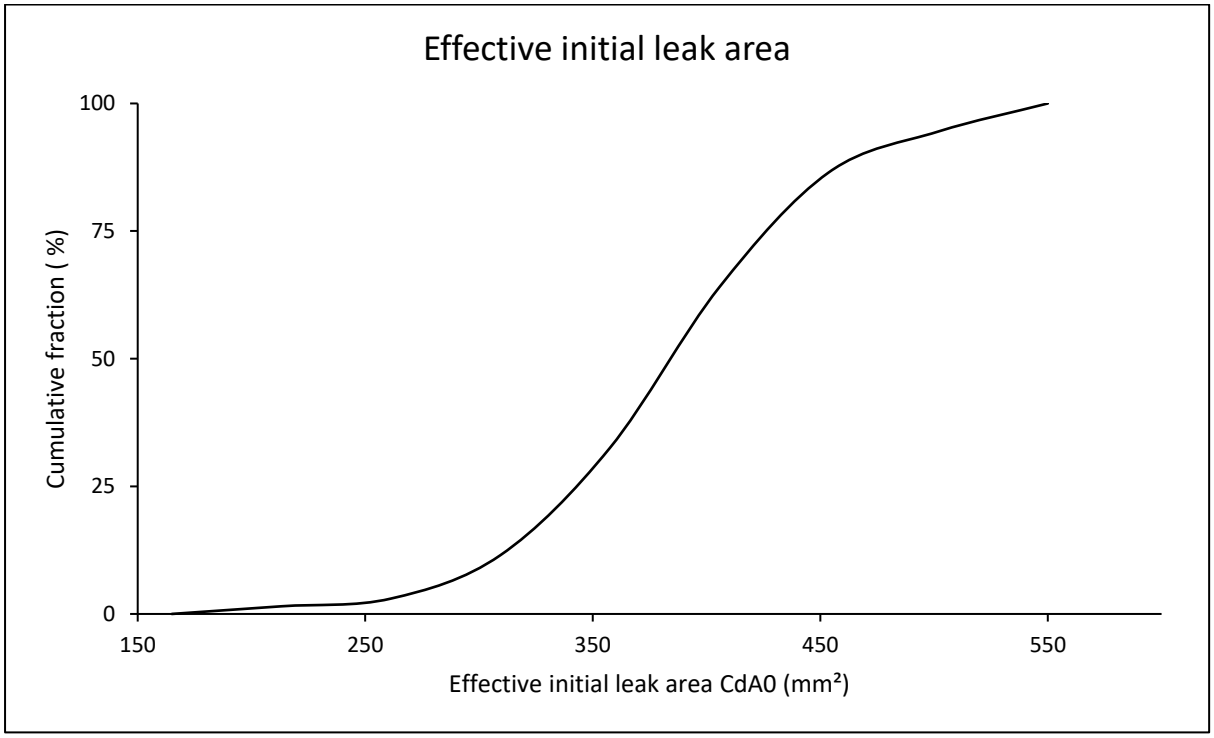
Effective initial leak area
Cumulative fraction (%)
100
75
50
25
0
150
250
350
450
550
Effective initial leak area CdA0 (mm²)

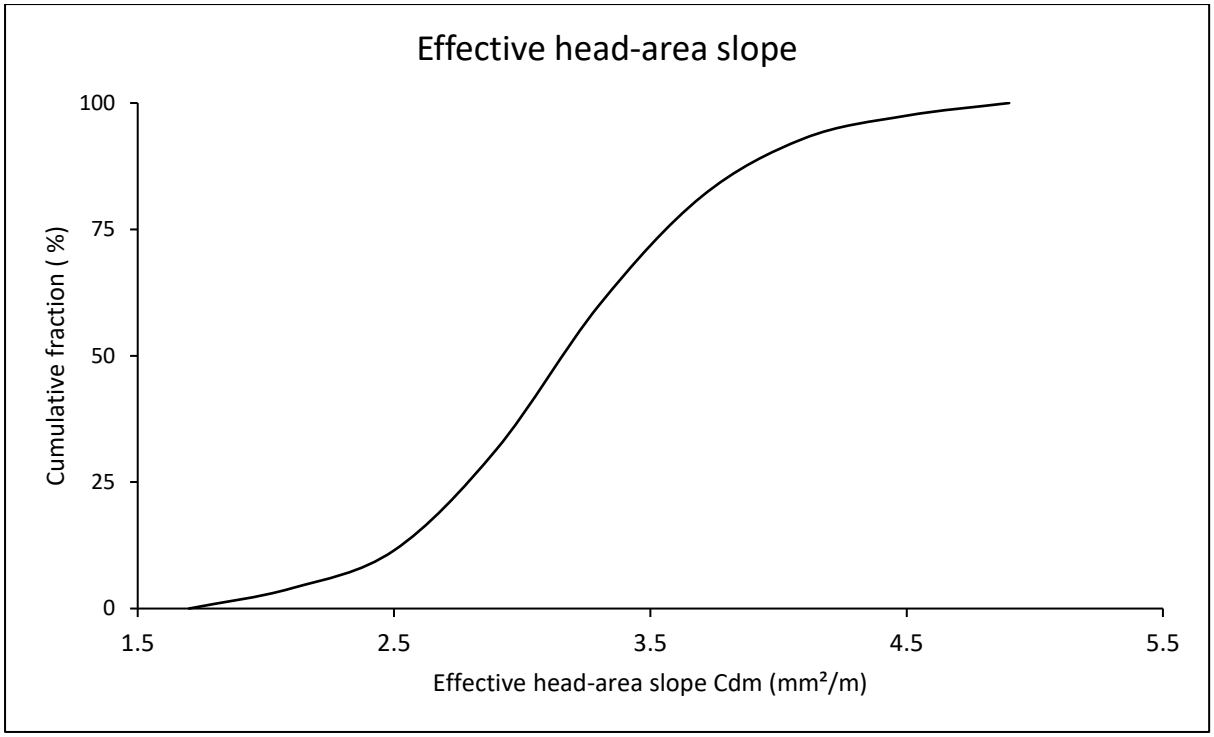
Effective head-area slope
Cumulative fraction (%)
100
75
50
25
0
1.5
2.5
3.5
4.5
5.5
Effective head-area slope Cdm (mm²/m)

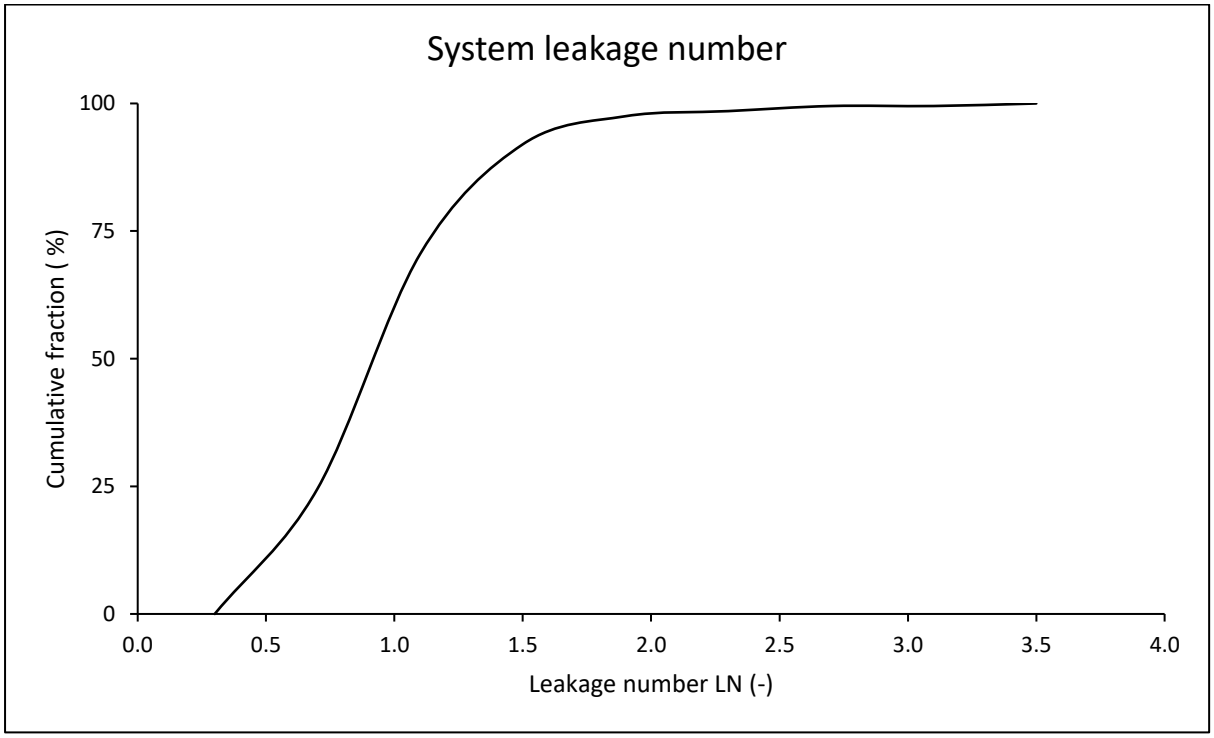
System leakage number
Cumulative fraction (%)
100
75
50
25
0
0.0
0.5
1.0
1.5
2.0
2.5
3.0
3.5
4.0
Leakage number LN (-)

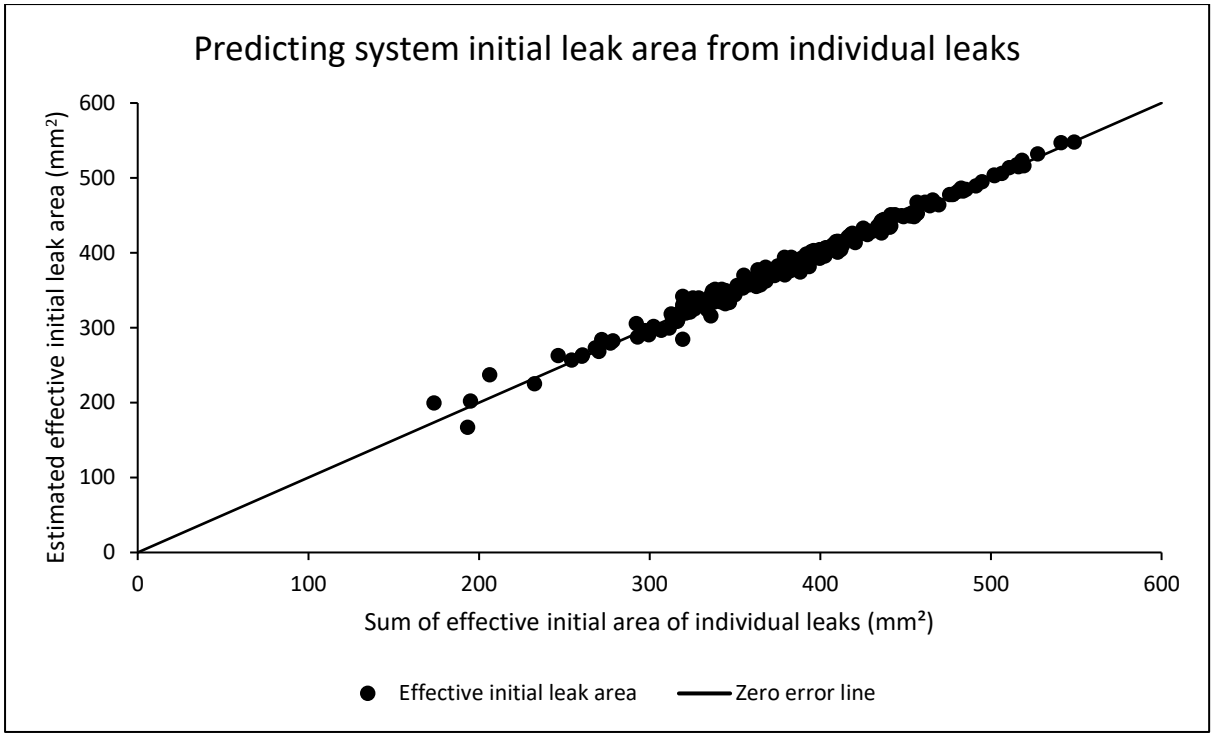
Predicting system initial leak area from individual leaks
Estimated effective initial leak area (mm²)
0
100
200
300
400
500
600
Sum of effective initial area of individual leaks (mm²)
Effective initial leak area
Zero error line

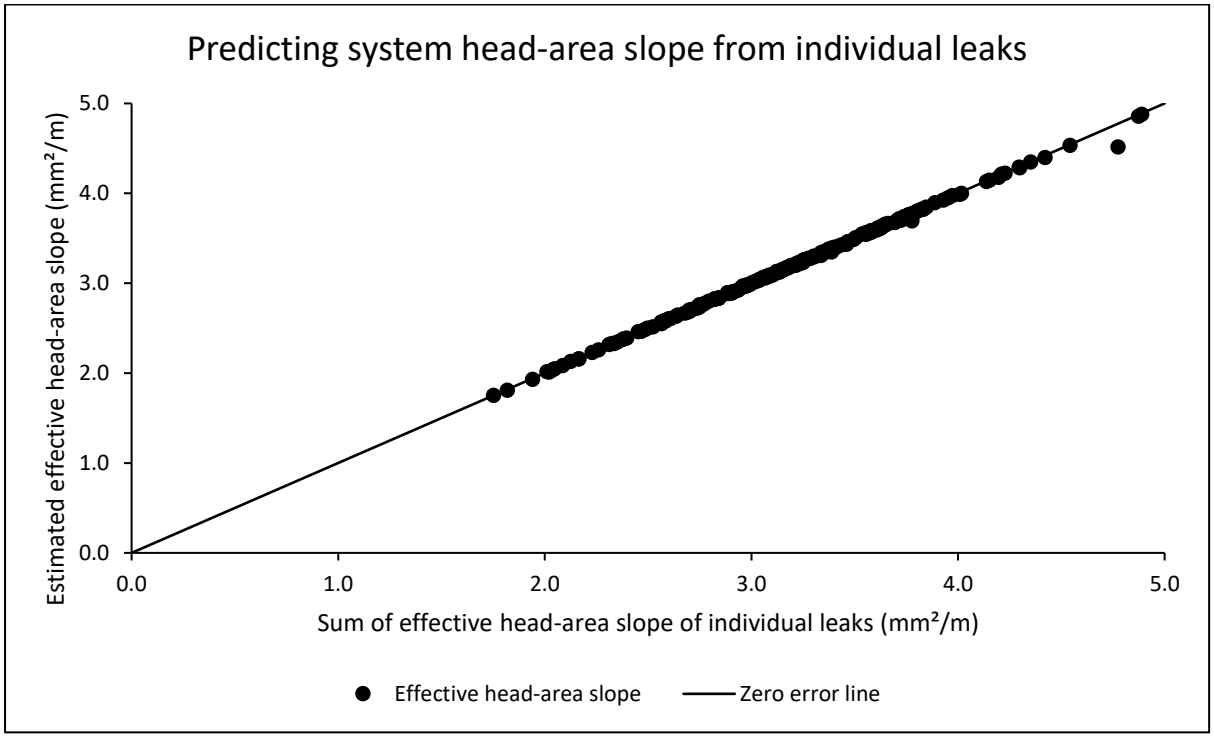
Predicting system head-area slope from individual leaks
Estimated effective head-area slope (mm²/m)
0.0
1.0
2.0
3.0
4.0
5.0
Sum of effective head-area slope of individual leaks (mm²/m)
Effective head-area slope
Zero error line

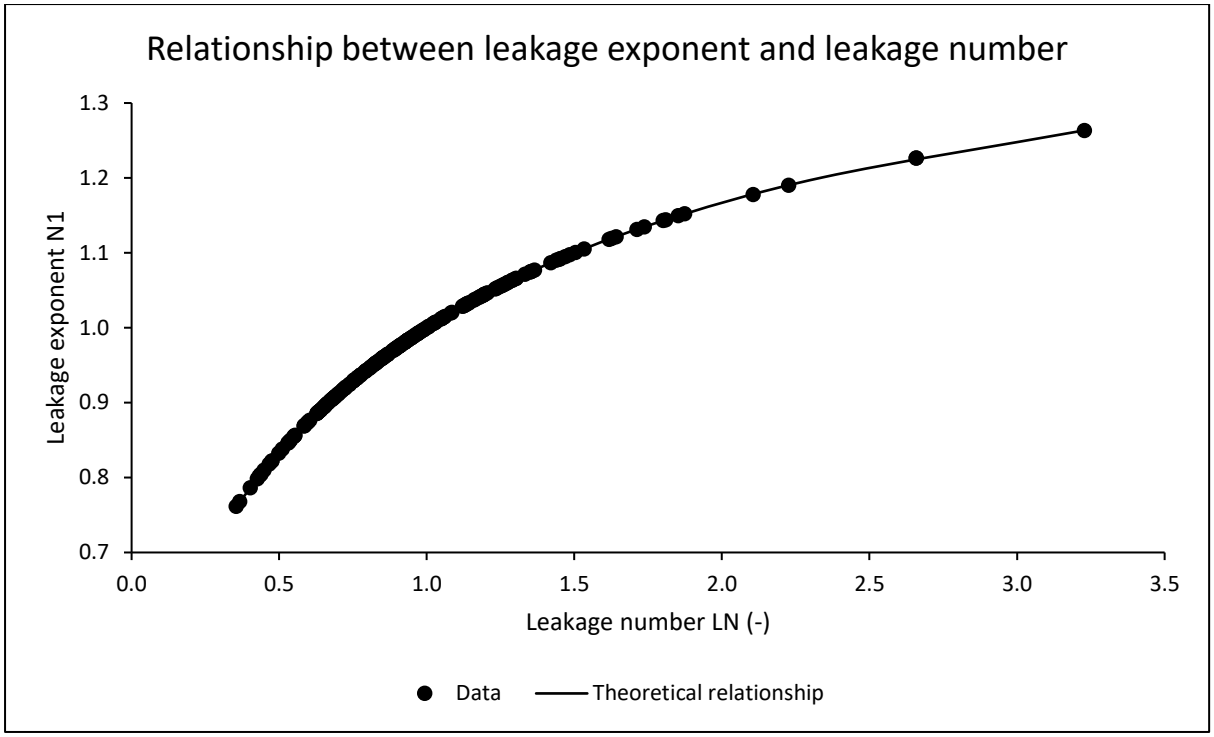
Relationship between leakage exponent and leakage number
Leakage exponent N1
1.3
1.2
1.1
1.0
0.9
0.8
0.7
0.0
0.5
1.0
1.5
2.0
2.5
3.0
3.5
Leakage number LN (-)
Data
Theoretical relationship

Average iterations required for a system to converge using both formulations

	Minimum	Arithmetic Mean	Median	Maximum
Modified orifice equation	8.64	8.95	8.96	9.32
Power equation	8.28	8.54	8.52	8.84

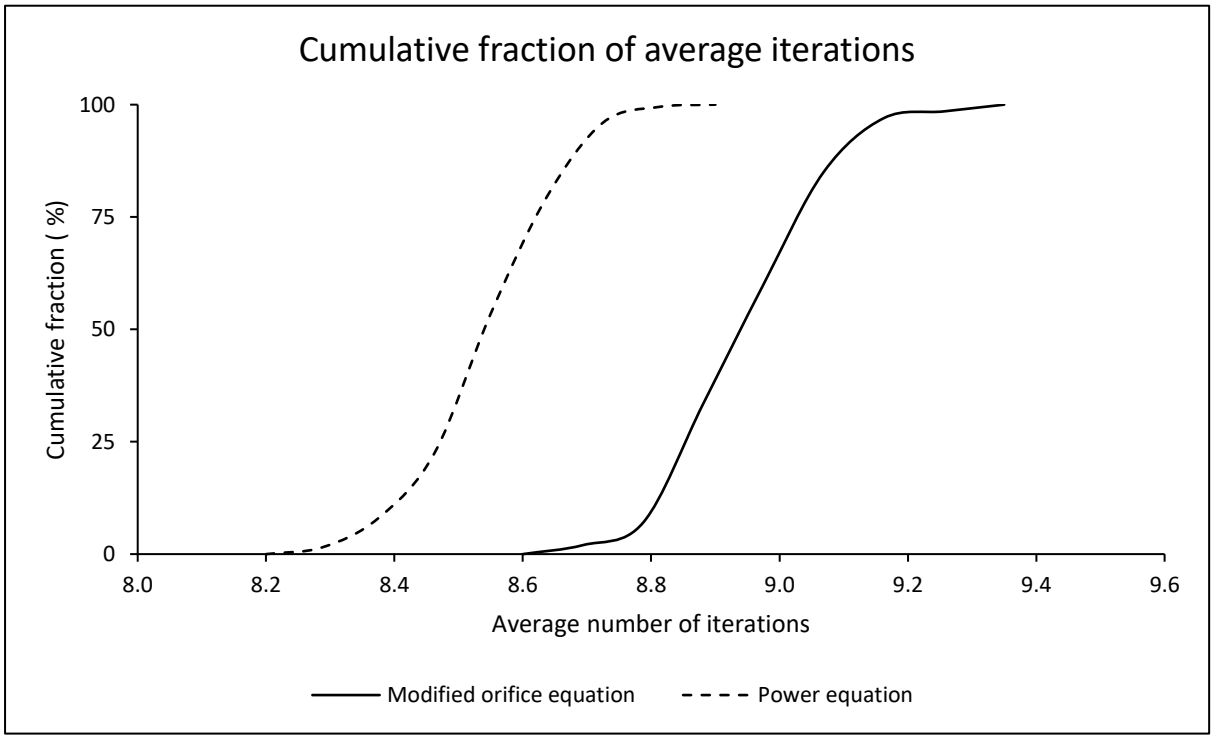

Effect of leakage on pressure at both average zone pressure (AZP) and critical nodes

AZP node								
	During MNF conditions				During peak demand conditions			
	Min (m)	Mean (m)	Median (m)	Max (m)	Min (m)	Mean (m)	Median (m)	Max (m)
Modified orifice equation	-0.11	-0.10	-0.10	-0.07	-0.50	-0.45	-0.46	-0.35
Power equation	-0.11	-0.10	-0.10	-0.07	-0.50	-0.45	-0.46	-0.34
Critical node								
Modified orifice equation	-0.41	-0.13	-0.12	-0.08	-1.07	-0.56	-0.54	-0.40
Power equation	-0.41	-0.13	-0.12	-0.08	-1.09	-0.56	-0.53	-0.39

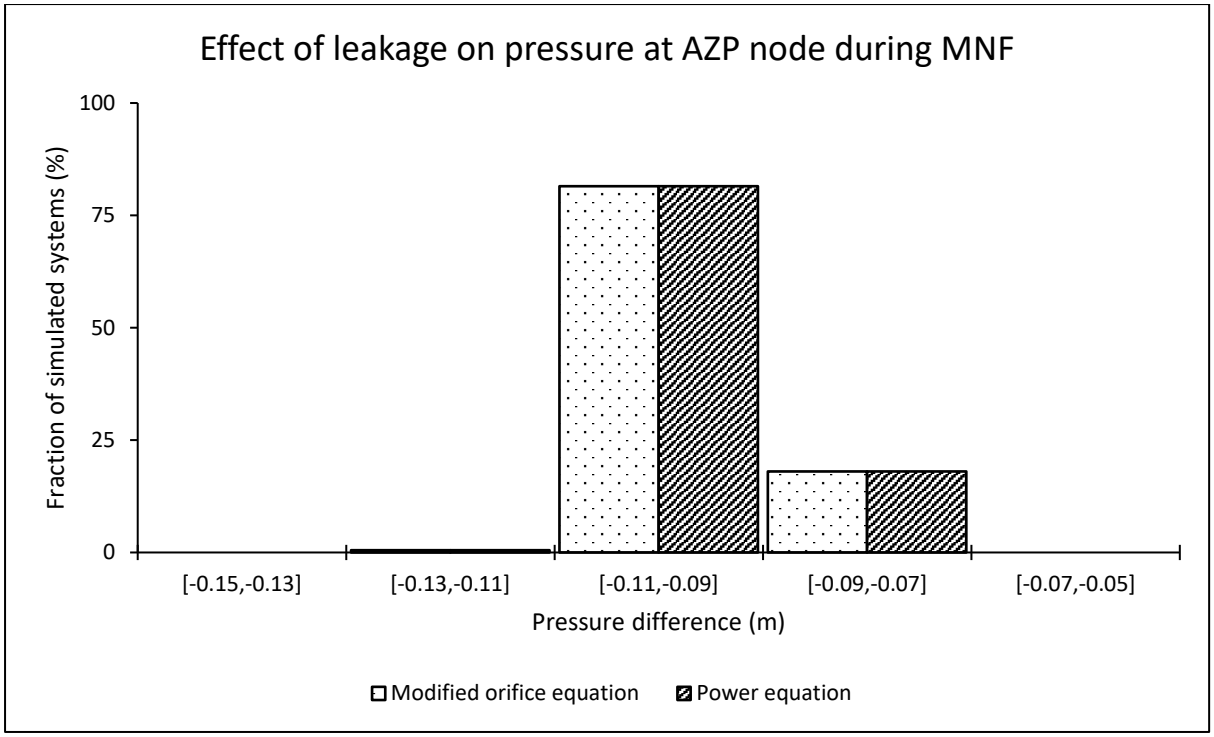
Effect of leakage on pressure at AZP node during MNF
Fraction of simulated systems (%)
100
75
50
25
0
[-0.15,-0.13]
[-0.13,-0.11]
[-0.11,-0.09]
[-0.09,-0.07]
[-0.07,-0.05]
Pressure difference (m)
Modified orifice equation
Power equation

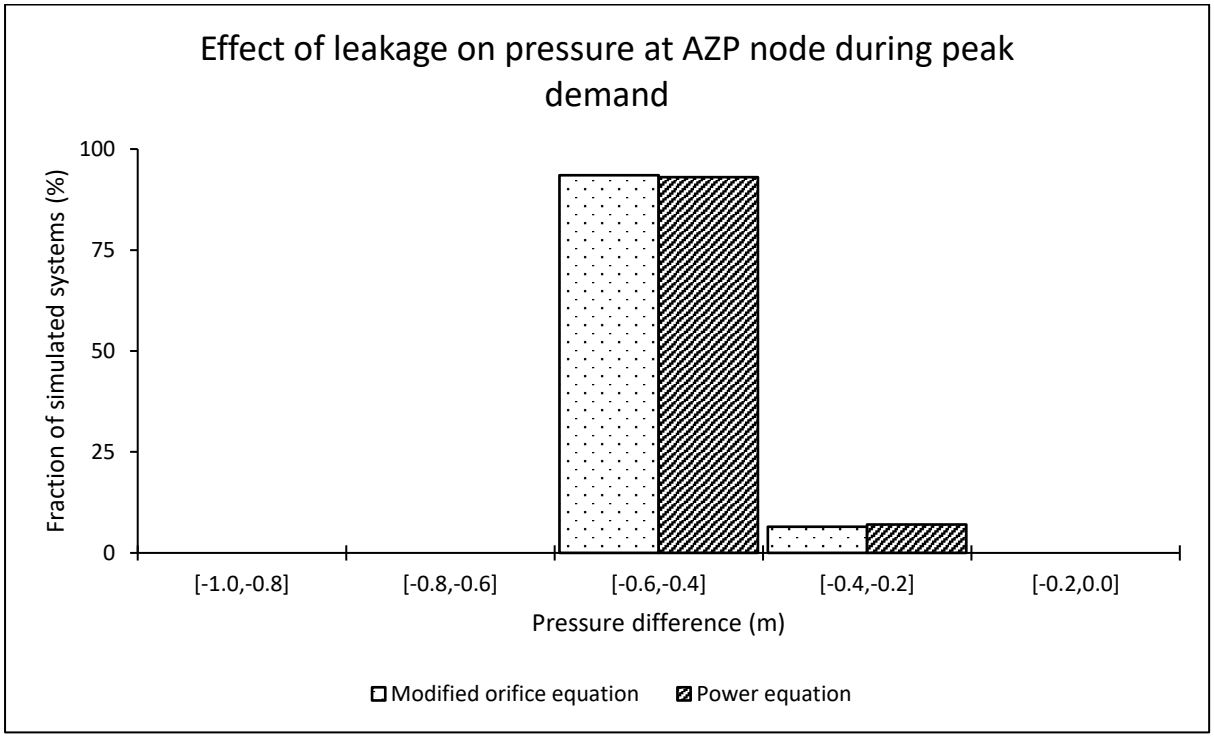
Effect of leakage on pressure at AZP node during peak demand
Fraction of simulated systems (%)
100
75
50
25
0
[-1.0,-0.8]
[-0.8,-0.6]
[-0.6,-0.4]
[-0.4,-0.2]
[-0.2,0.0]
Pressure difference (m)
Modified orifice equation
Power equation

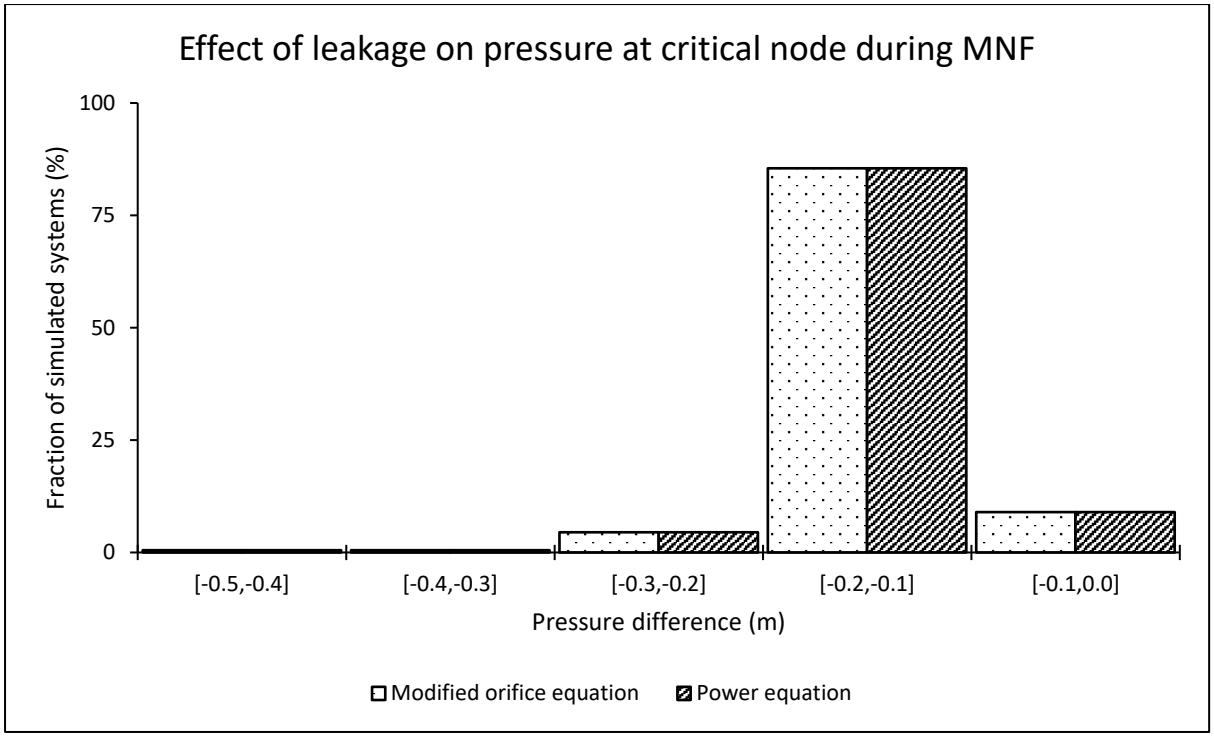
Effect of leakage on pressure at critical node during MNF
Fraction of simulated systems (%)
100
75
50
25
0
[-0.5,-0.4]
[-0.4,-0.3]
[-0.3,-0.2]
[-0.2,-0.1]
[-0.1,0.0]
Pressure difference (m)
Modified orifice equation
Power equation

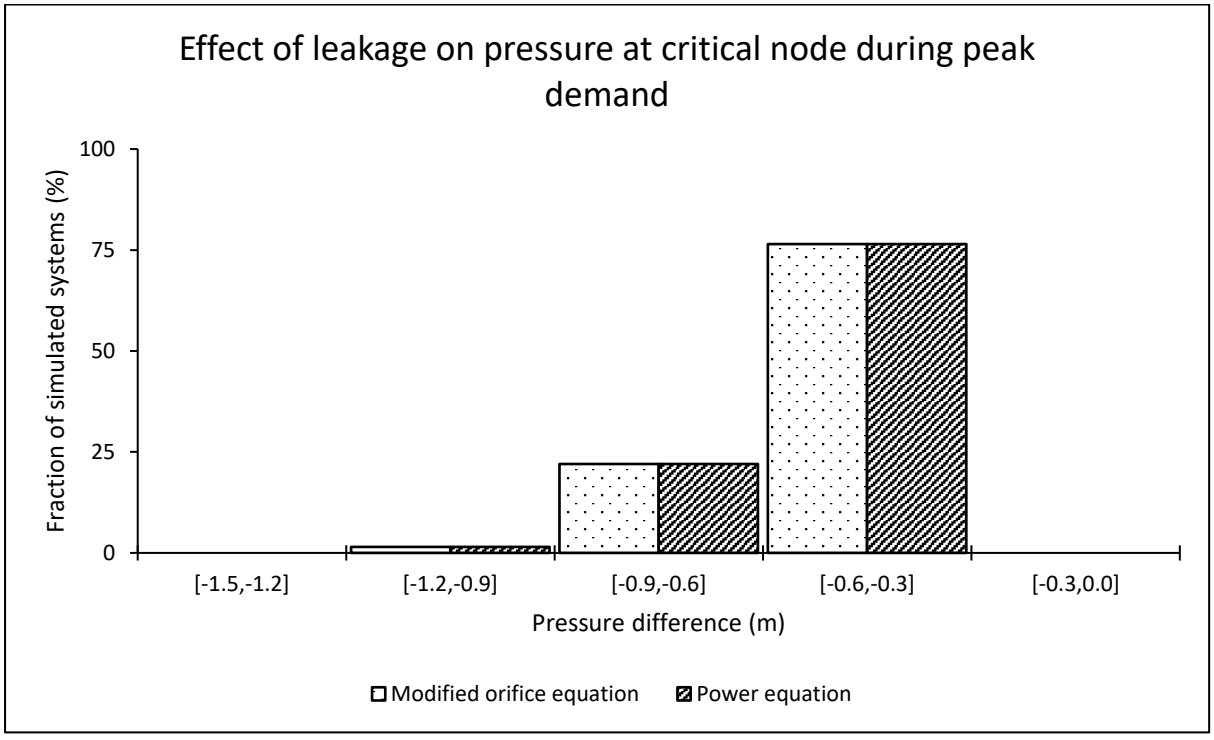
Effect of leakage on pressure at critical node during peak demand
Fraction of simulated systems (%)
100
75
50
25
0
[-1.5,-1.2]
[-1.2,-0.9]
[-0.9,-0.6]
[-0.6,-0.3]
[-0.3,0.0]
Pressure difference (m)
Modified orifice equation
Power equation

Pressure estimation error when using the power equation at average zone pressure (AZP) and critical nodes

	During MNF conditions				During peak demand conditions			
	Min (%)	**Mean (%)**	**Median (%)**	**Max (%)**	**Min (%)**	**Mean (%)**	**Median (%)**	**Max (%)**
At the AZP node	0.00	0.00	0.00	0.00	0.00	0.00	0.00	0.01
At the critical node	0.00	0.00	0.00	0.00	-0.02	0.00	0.00	0.01

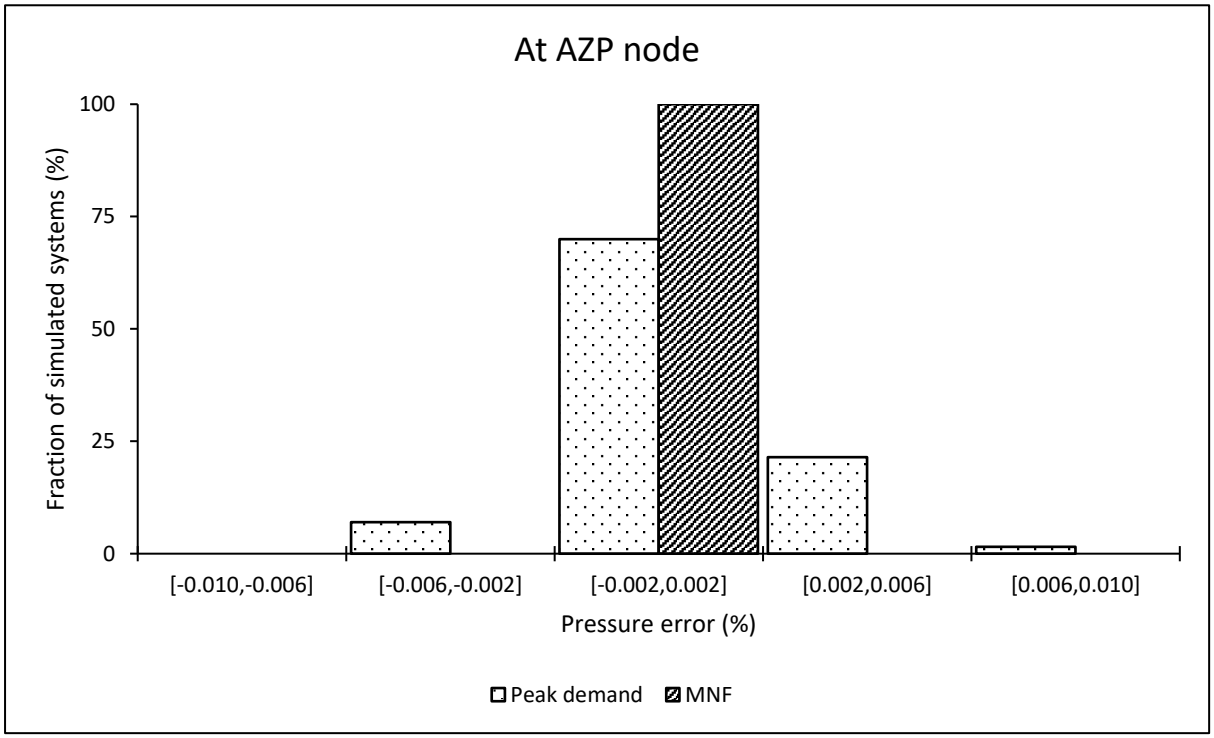

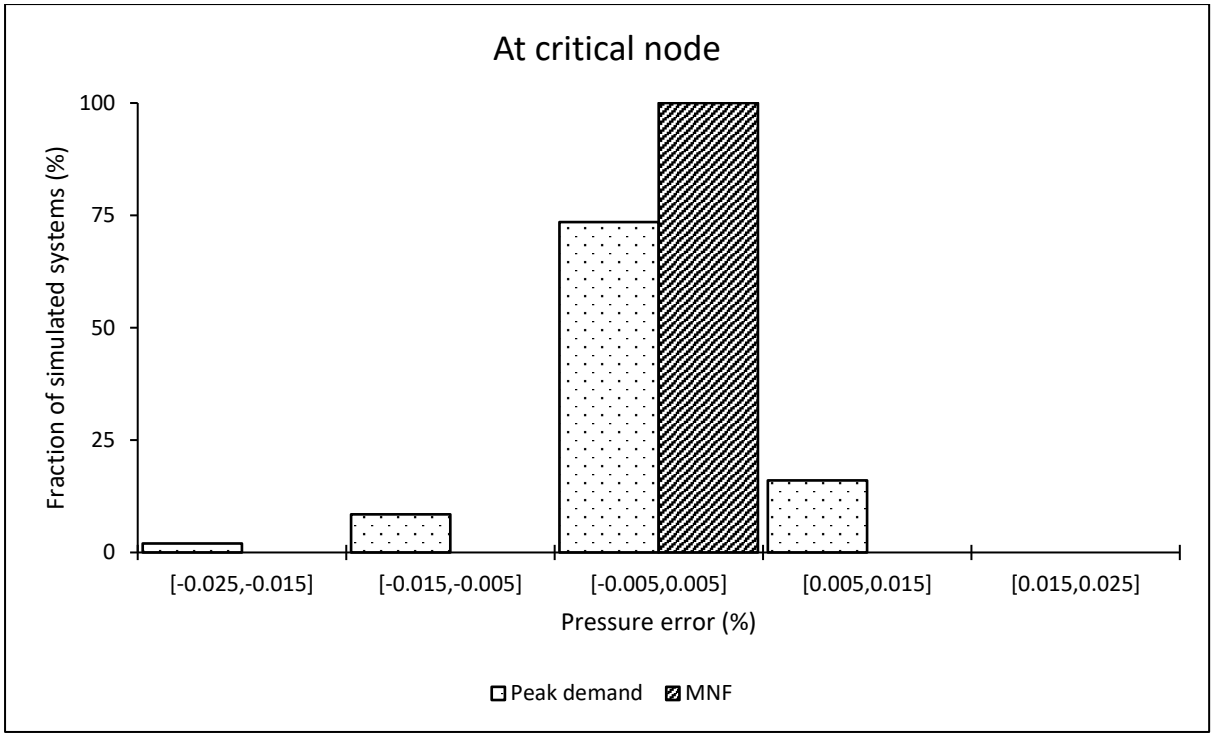
At critical node
Fraction of simulated systems (%)
100
75
50
25
0
[-0.025,-0.015]
[-0.015,-0.005]
[-0.005,0.005]
[0.005,0.015]
[0.015,0.025]
Pressure error (%)
Peak demand
MNF

System leakage estimation error when using the power equation

	Leakage estimation error (%)			
	Minimum	**Arithmetic Mean**	**Median**	**Maximum**
Before implementing pressure management	-0.33	-0.01	0.00	0.30
After implementing pressure management	-28.93	-18.40	-18.36	-12.39

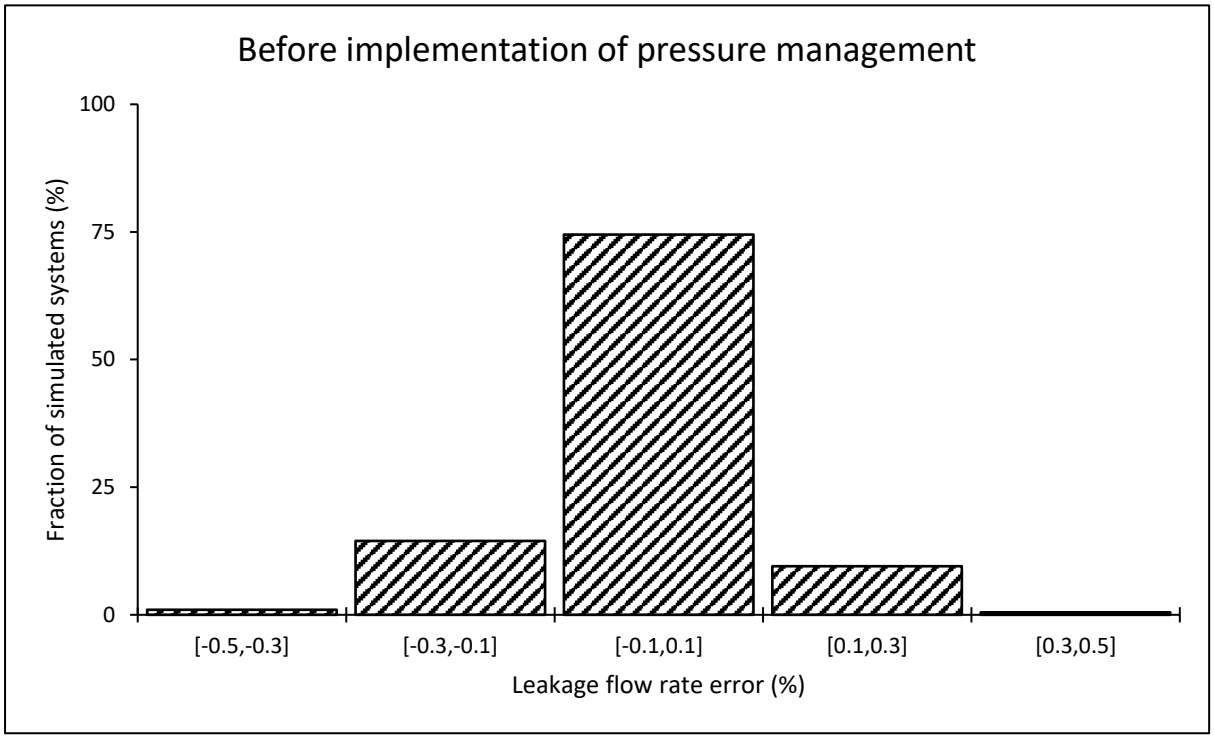

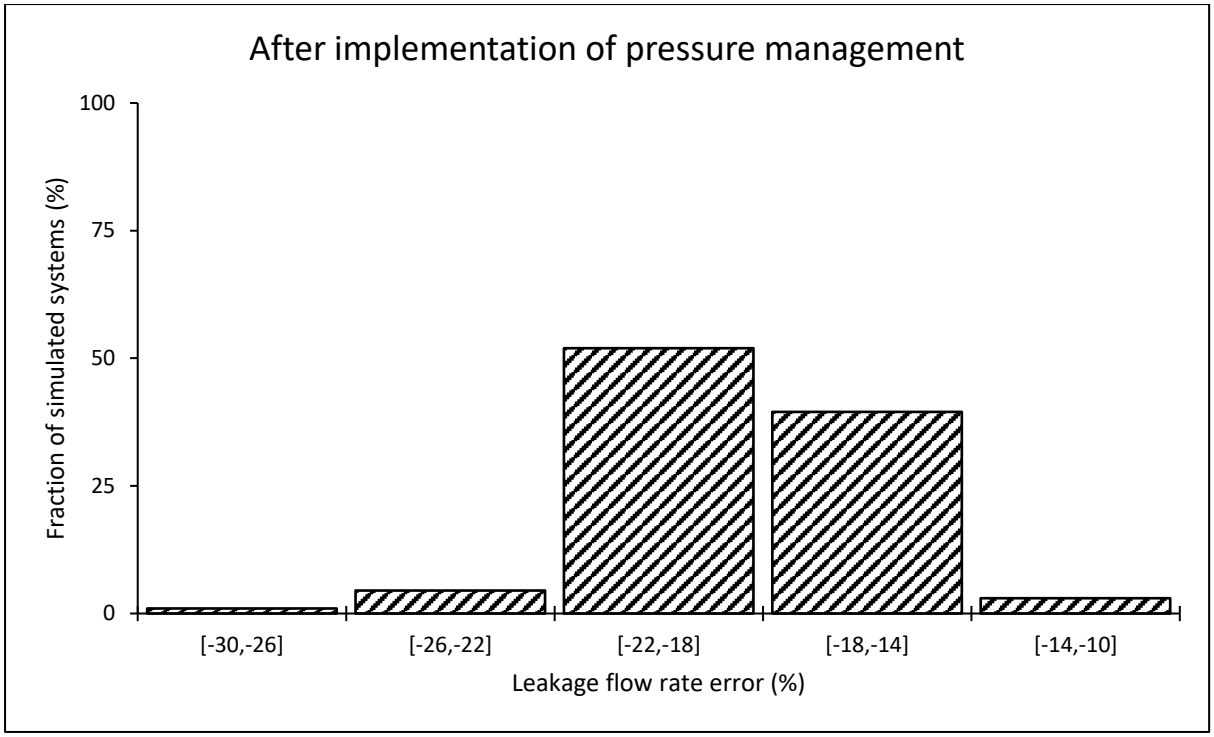
After implementation of pressure management
Fraction of simulated systems (%)
100
75
50
25
0
[-30,-26]
[-26,-22]
[-22,-18]
[-18,-14]
[-14,-10]
Leakage flow rate error (%)

Leakage estimation error when using the power equation at the critical node

	Leakage estimation error (%)			
	Minimum	**Arithmetic Mean**	**Median**	**Maximum**
Before implementing pressure management	-28.30	-2.22	-2.59	3.37
After implementing pressure management	-70.19	-38.52	-52.14	148.21

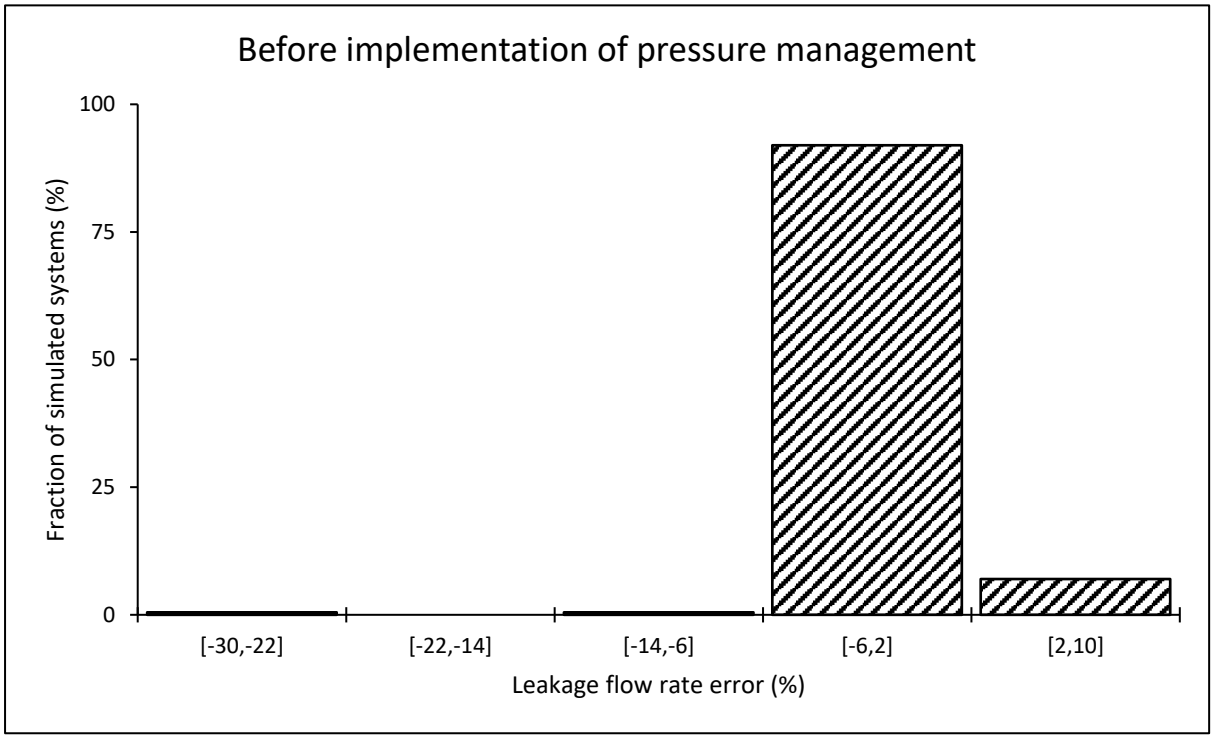

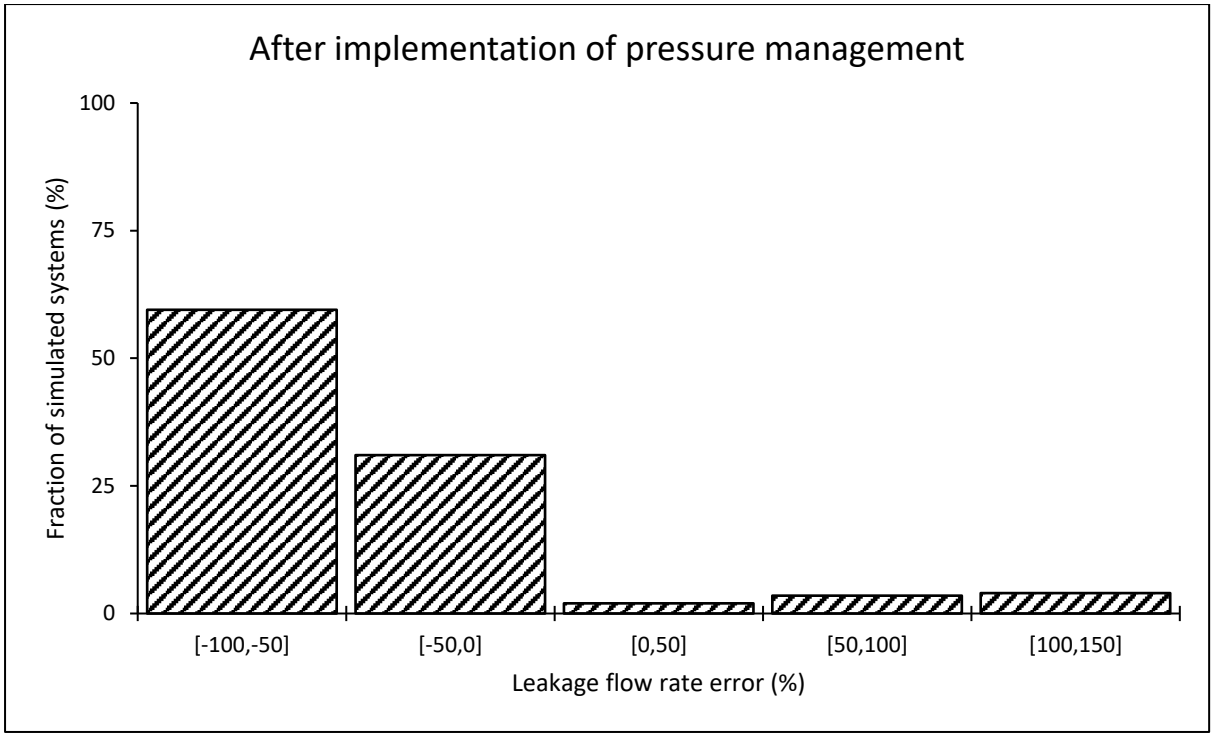
After implementation of pressure management
Fraction of simulated systems (%)
100
75
50
25
0
[-100,-50]
[-50,0]
[0,50]
[50,100]
[100,150]
Leakage flow rate error (%)

Appendix A-11: Large-sized network with an ILI of 16

Results for an individual system

Pressure head at the average zone pressure (AZP) node

		Pressure head (m)			
		Minimum	**Arithmetic Mean**	**Median**	**Maximum**
Before pressure management	Without leaks	99.13	108.33	106.63	113.44
	Modified orifice equation	97.28	107.17	105.14	112.96
	Power equation	97.27	107.17	105.14	112.96
After pressure management	Modified orifice equation	18.90	28.21	26.42	33.48
	Power equation	19.02	28.27	26.49	33.50

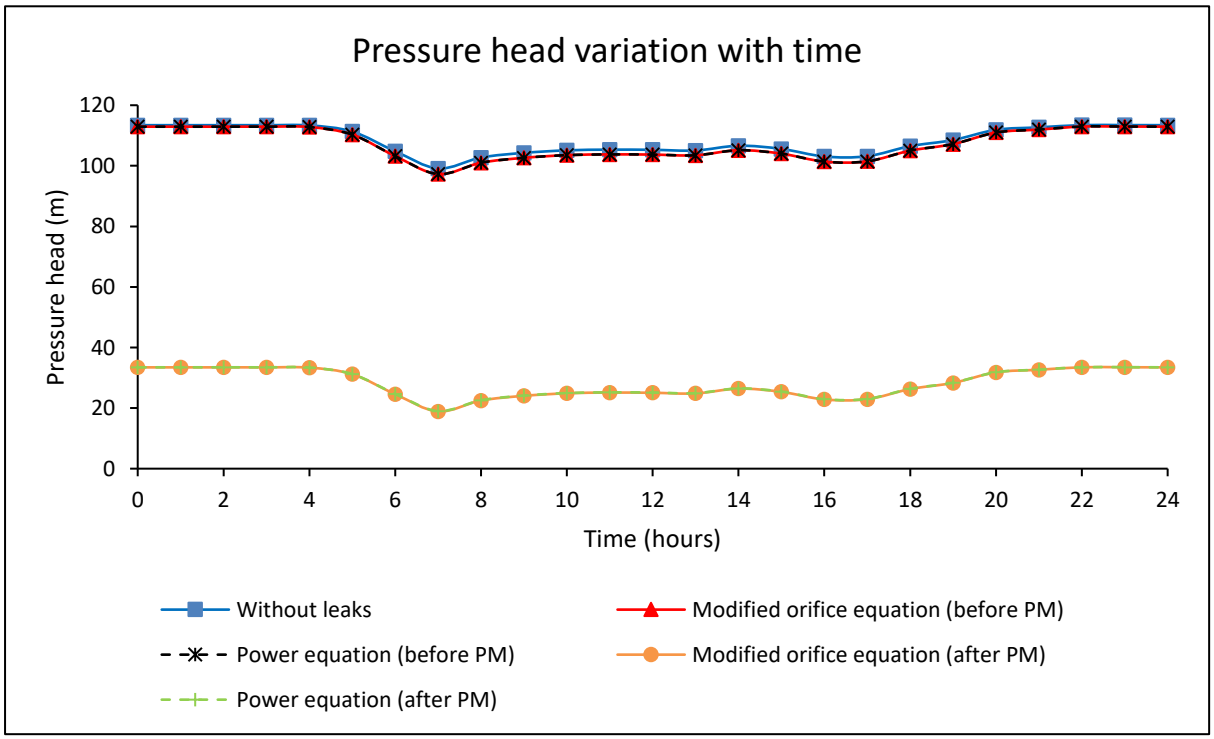

Pressure head at the critical node

		Pressure head (m)			
		Minimum	**Arithmetic Mean**	**Median**	**Maximum**
Before pressure management	Without leaks	89.91	100.55	98.69	106.46
	Modified orifice equation	87.54	99.05	96.82	105.82
	Power equation	87.54	99.05	96.82	105.82
After pressure management	Modified orifice equation	9.57	20.34	18.38	26.46
	Power equation	9.73	20.42	18.48	26.48

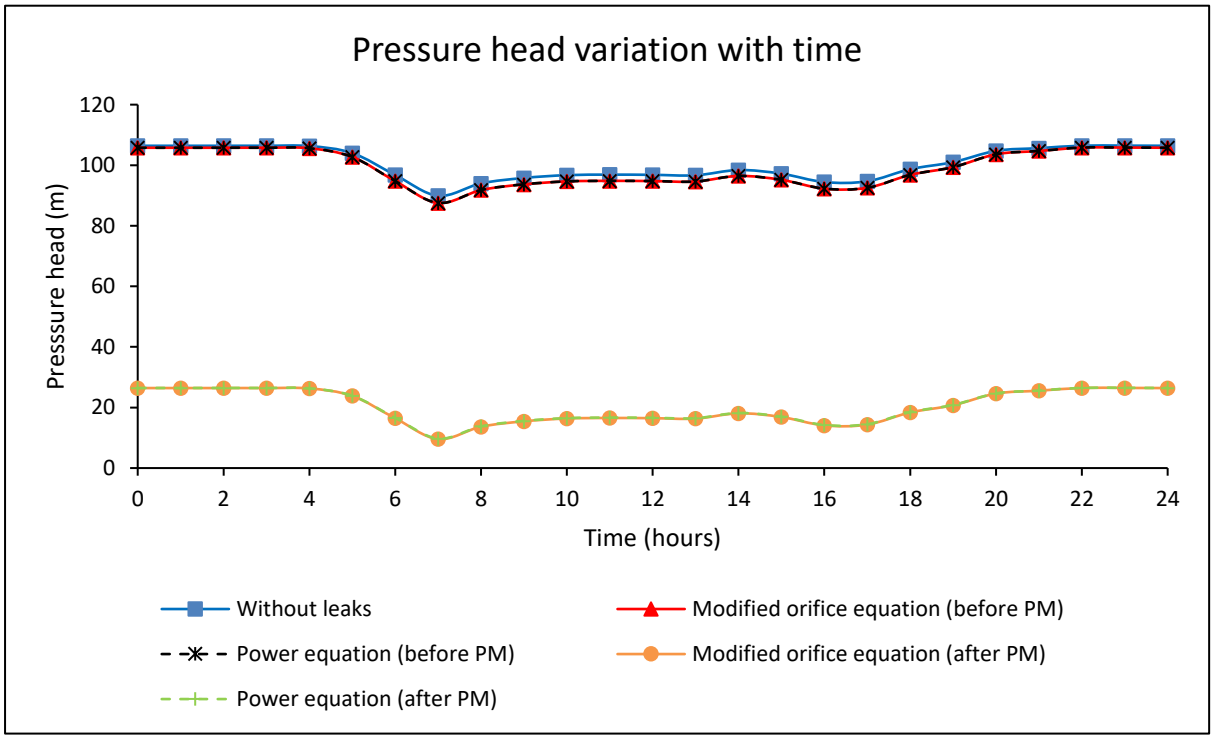

System leakage flow rate

		Leakage flow rate (m^3/h)			
		Minimum	**Arithmetic Mean**	**Median**	**Maximum**
Before pressure management	Modified orifice equation	419.74	475.57	463.91	509.14
	Power equation	420.51	476.10	464.67	509.13
After pressure management	Modified orifice equation	90.86	129.01	121.50	151.07
	Power equation	62.80	104.90	96.49	129.52

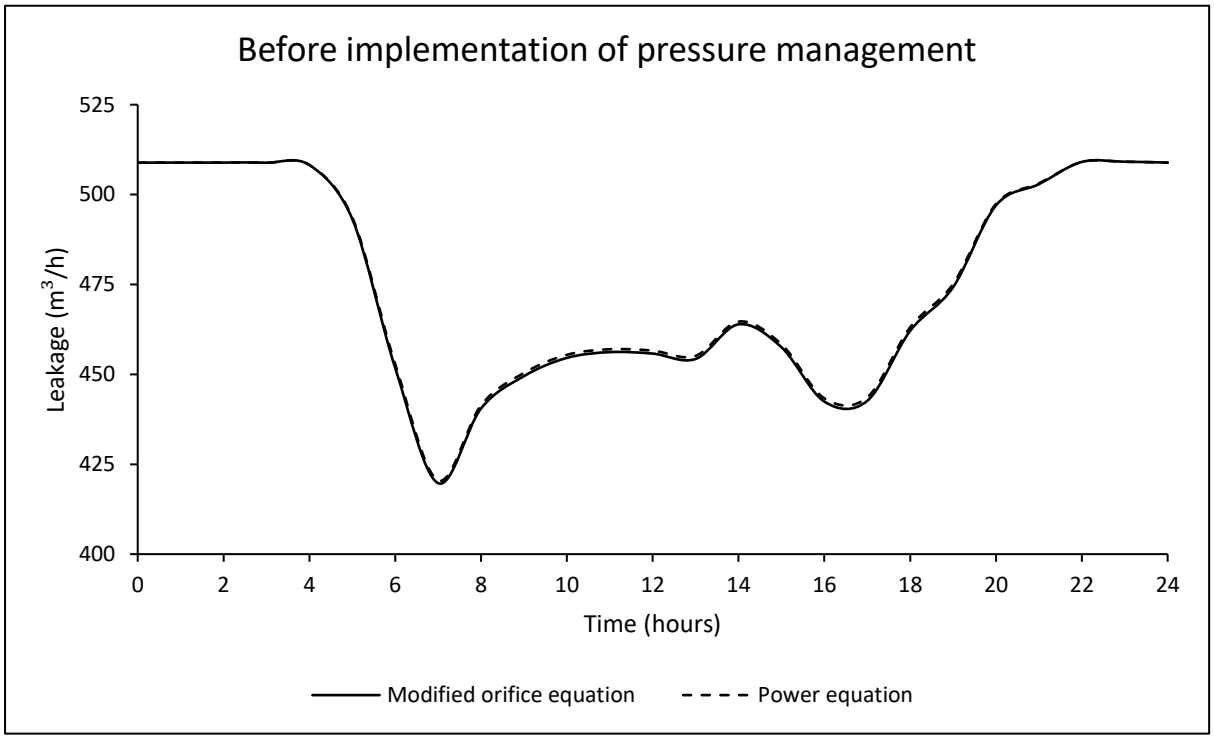

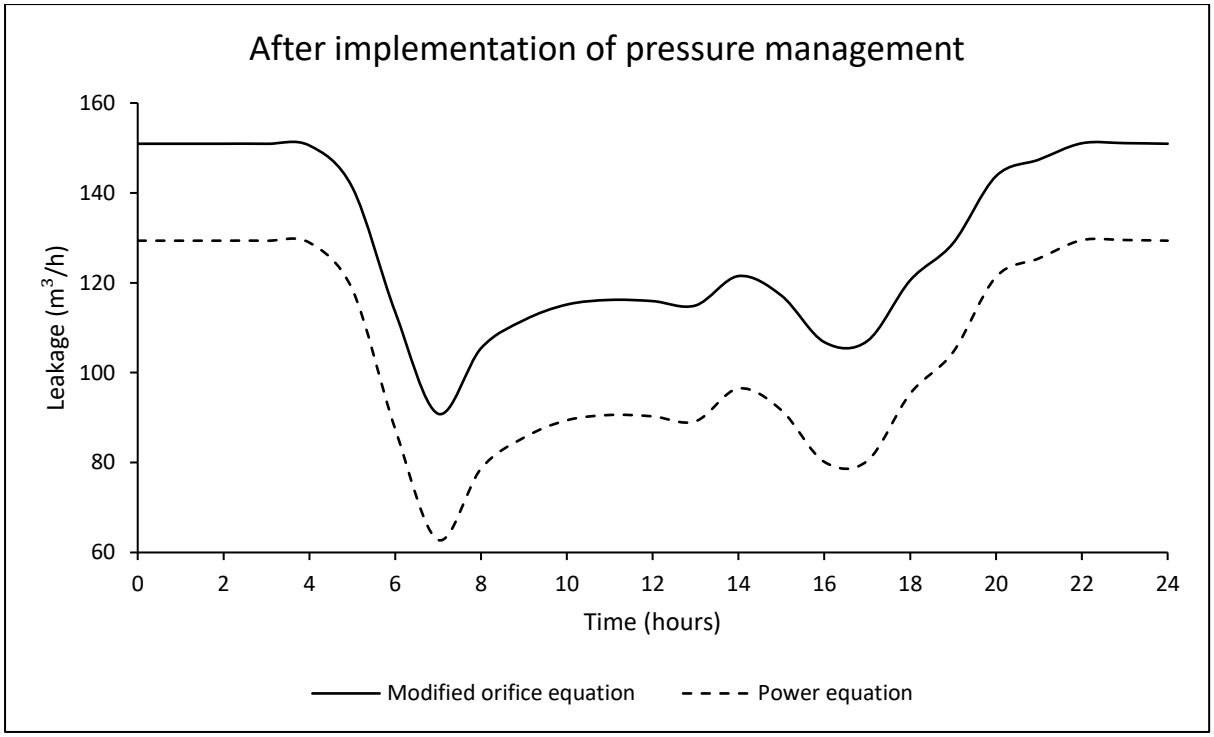
After implementation of pressure management
160
140
120
100
80
60
Leakage (m3/h)
0
2
4
6
8
10
12
14
16
18
20
22
24
Time (hours)
Modified orifice equation
Power equation

Leakage flow rate at the critical node

		Leakage flow rate (m^3/h)			
		Minimum	**Arithmetic Mean**	**Median**	**Maximum**
Before pressure management	Modified orifice equation	0.30	0.32	0.31	0.33
	Power equation	0.26	0.30	0.29	0.33
After pressure management	Modified orifice equation	0.10	0.14	0.14	0.16
	Power equation	0.02	0.05	0.04	0.07

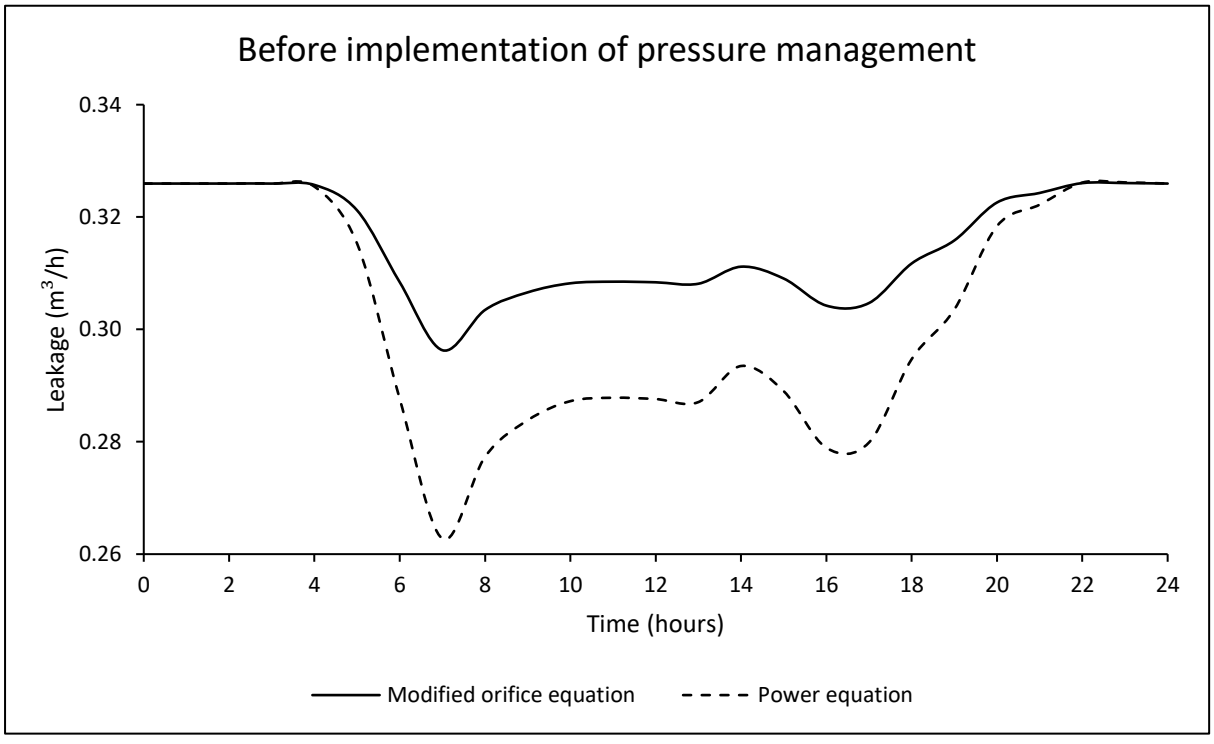

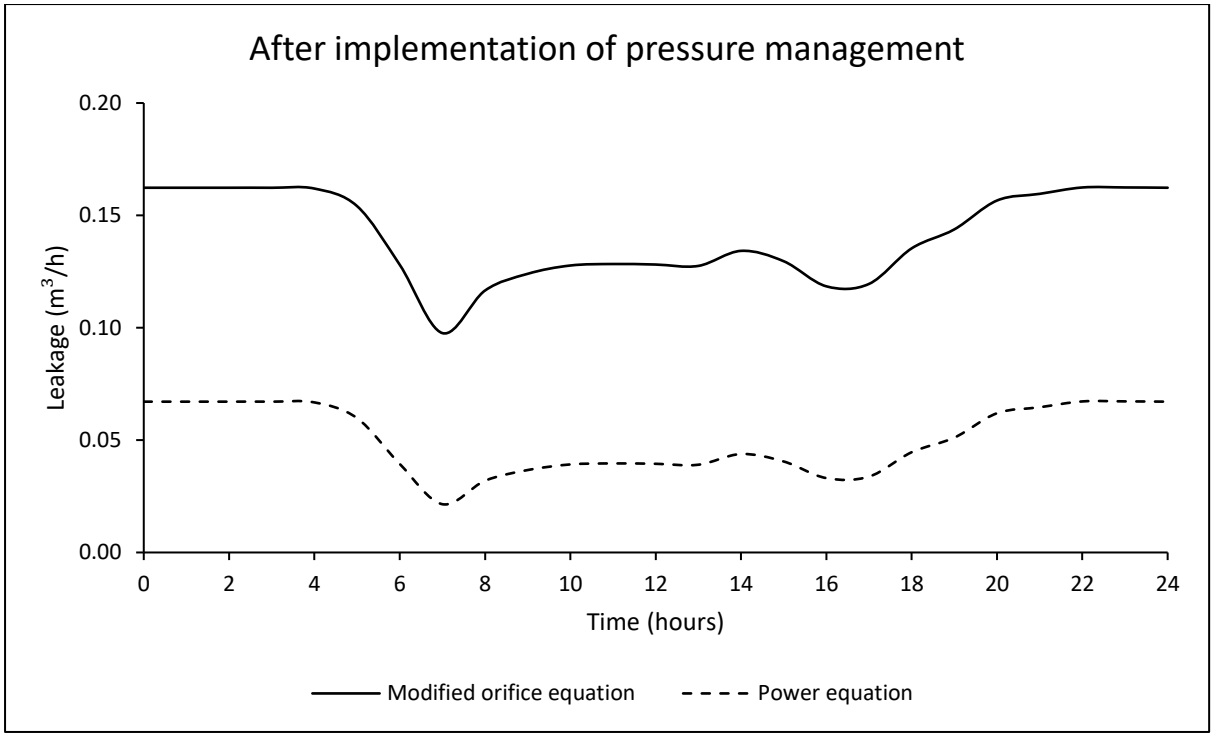
After implementation of pressure management
0.20
0.15
0.10
0.05
0.00
Leakage (m3/h)
0
2
4
6
8
10
12
14
16
18
20
22
24
Time (hours)
Modified orifice equation
Power equation

Number of iterations required for a system to converge to a hydraulic solution for both formulations

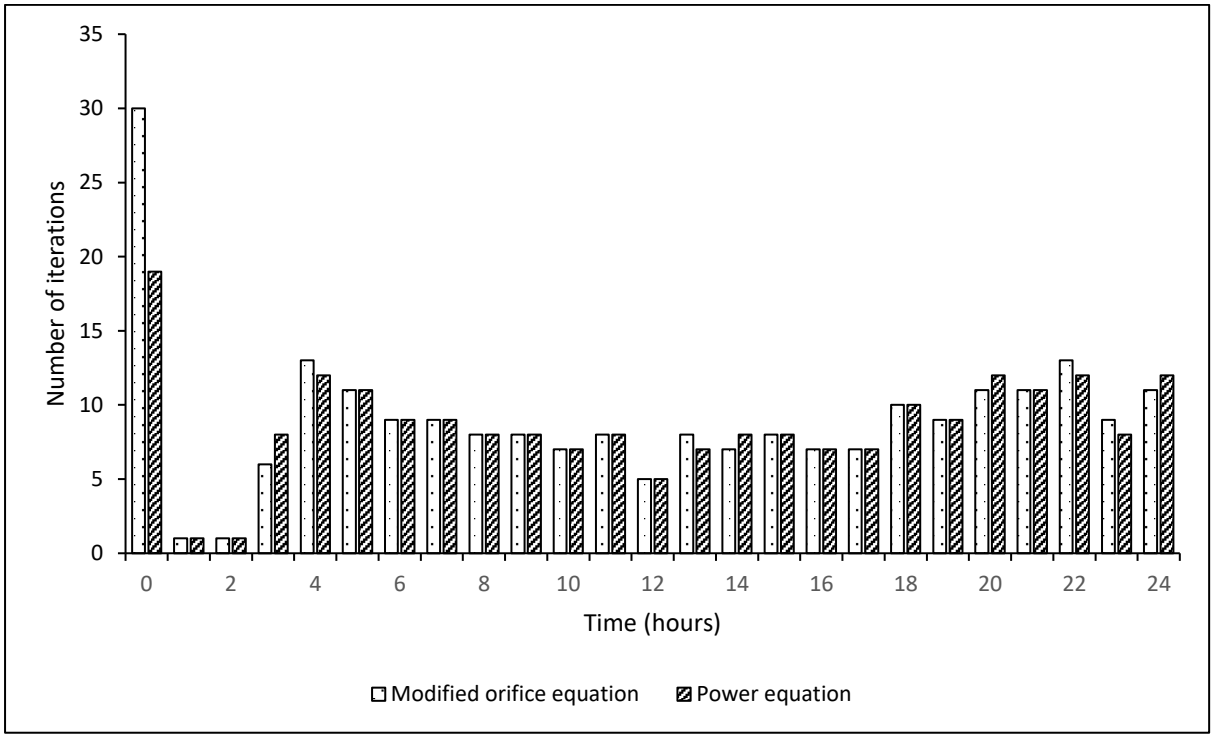

Results for combined systems

System parameters for both power and modified orifice formulations

	Minimum	Arithmetic Mean	Median	Maximum
Leakage exponent N1	0.99	1.16	1.16	1.37
Leakage coefficient C	2.1E-04	6.0E-04	5.7E-04	1.3E-03
Effective initial leak area C_dA0 (mm^2)	361.60	984.52	974.18	1520.65
Effective head-area slope C_dm (mm^2/m)	13.06	17.59	17.68	22.47
Leakage number LN	0.95	2.12	1.98	6.81

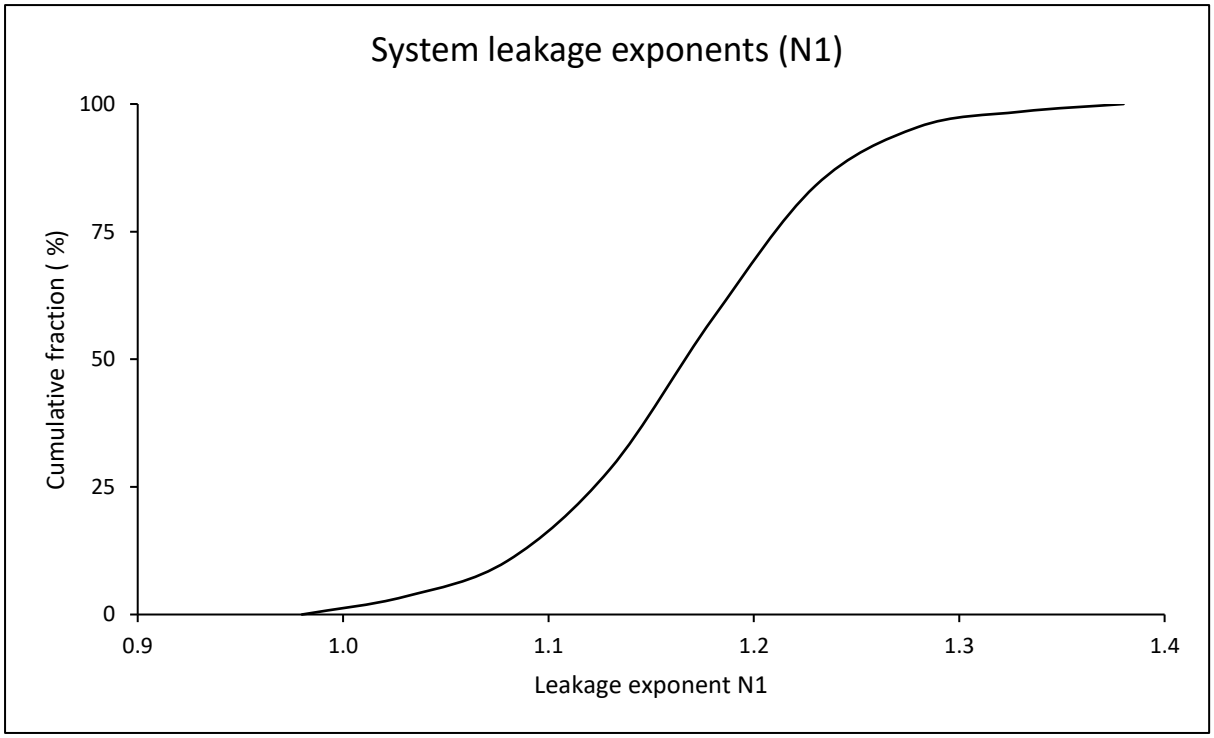

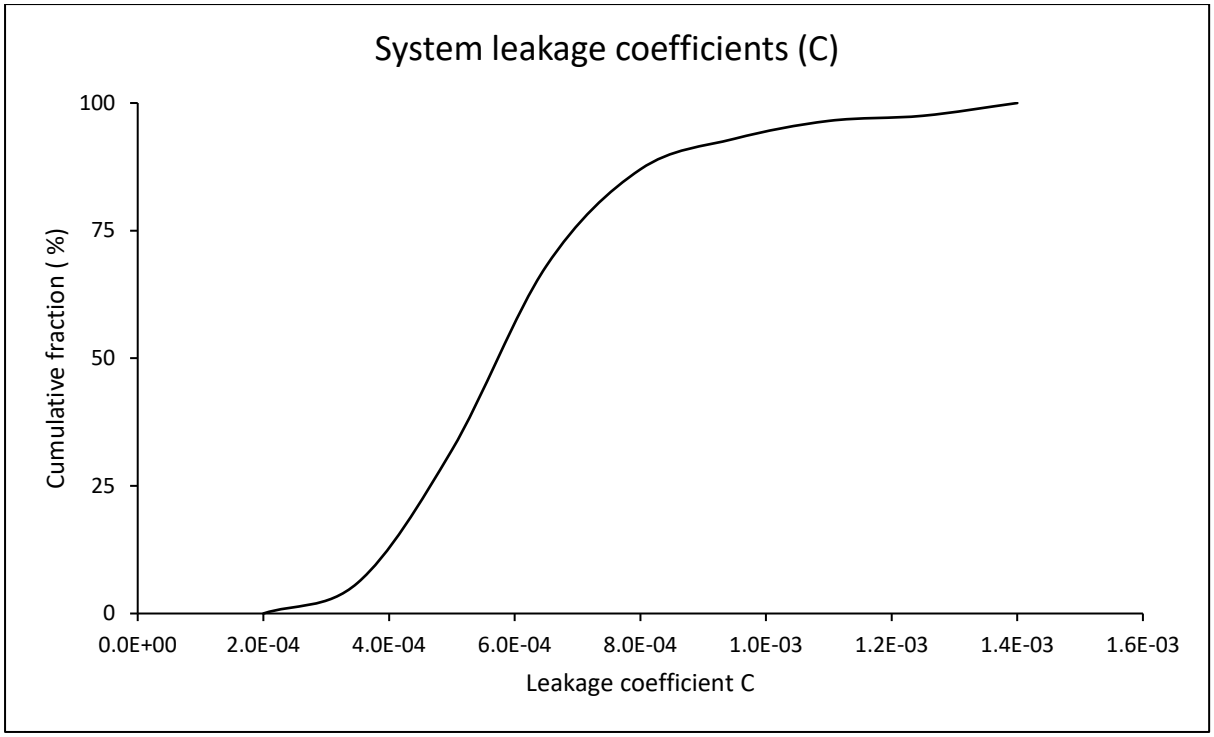
System leakage coefficients (C)
Cumulative fraction (%)
100
75
50
25
0
0.0E+00
2.0E-04
4.0E-04
6.0E-04
8.0E-04
1.0E-03
1.2E-03
1.4E-03
1.6E-03
Leakage coefficient C

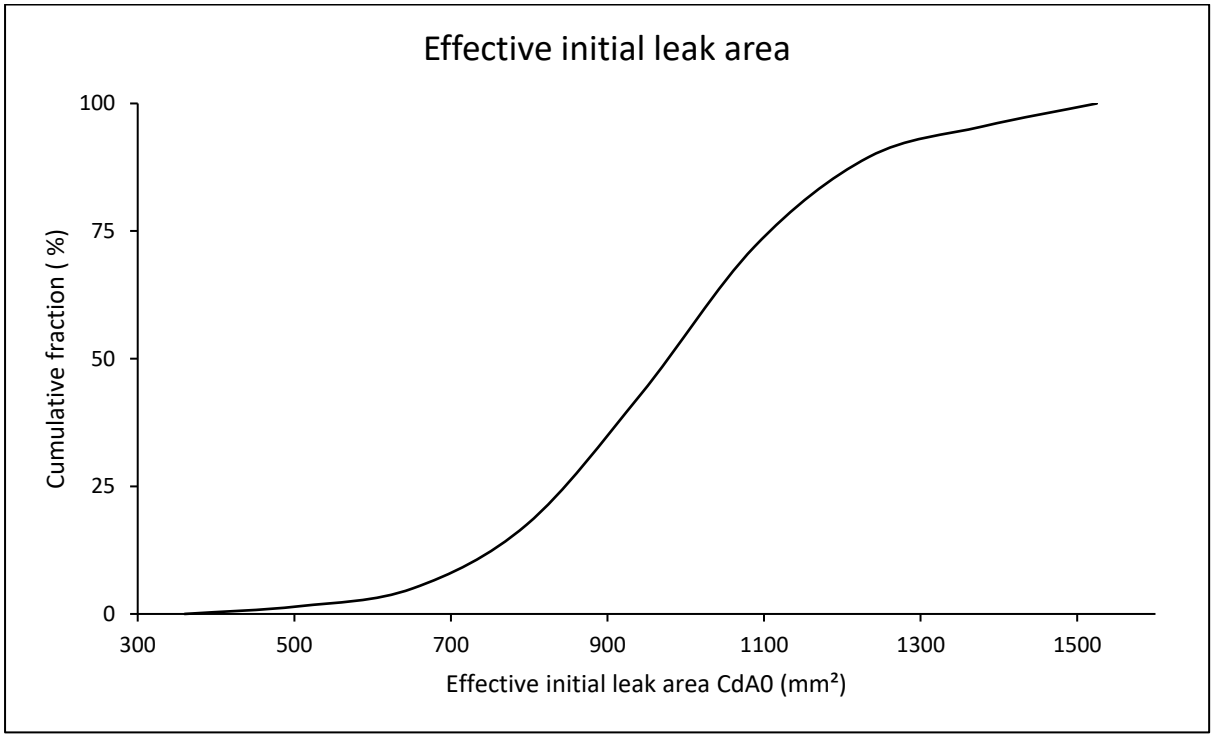
Effective initial leak area
Cumulative fraction (%)
100
75
50
25
0
300
500
700
900
1100
1300
1500
Effective initial leak area CdA0 (mm²)

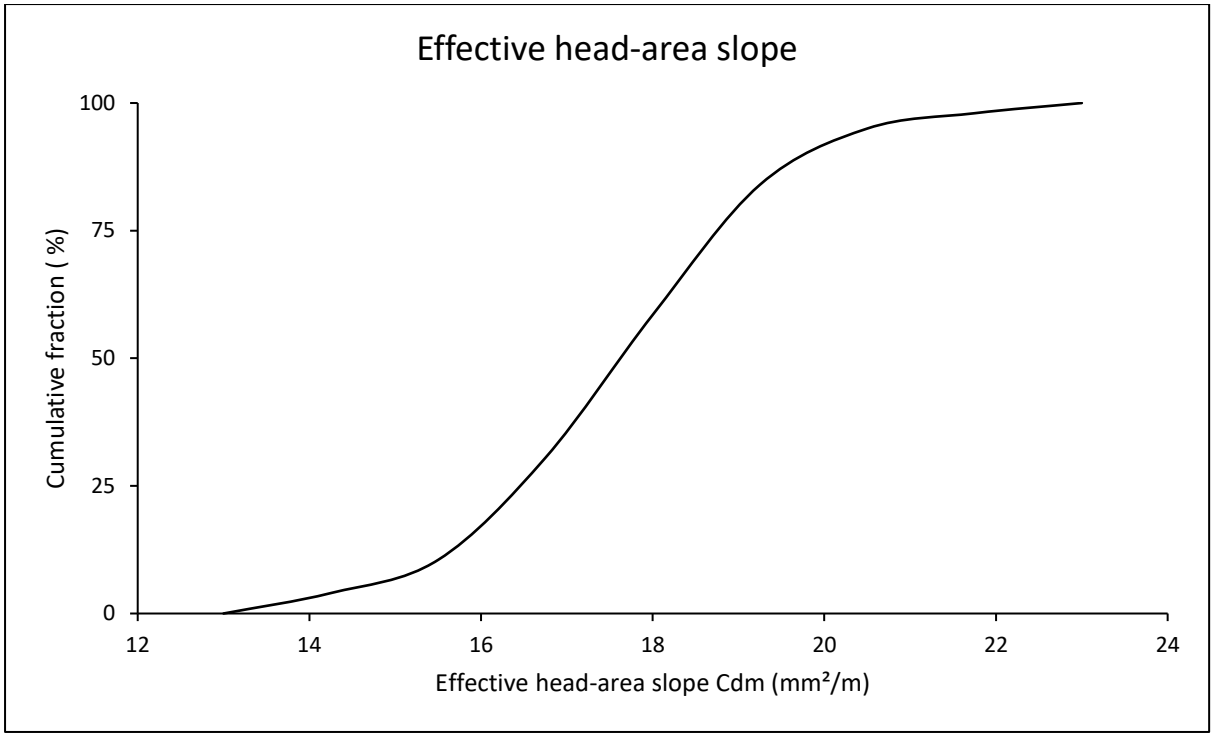
Effective head-area slope
Cumulative fraction (%)
100
75
50
25
0
12
14
16
18
20
22
24
Effective head-area slope Cdm (mm²/m)

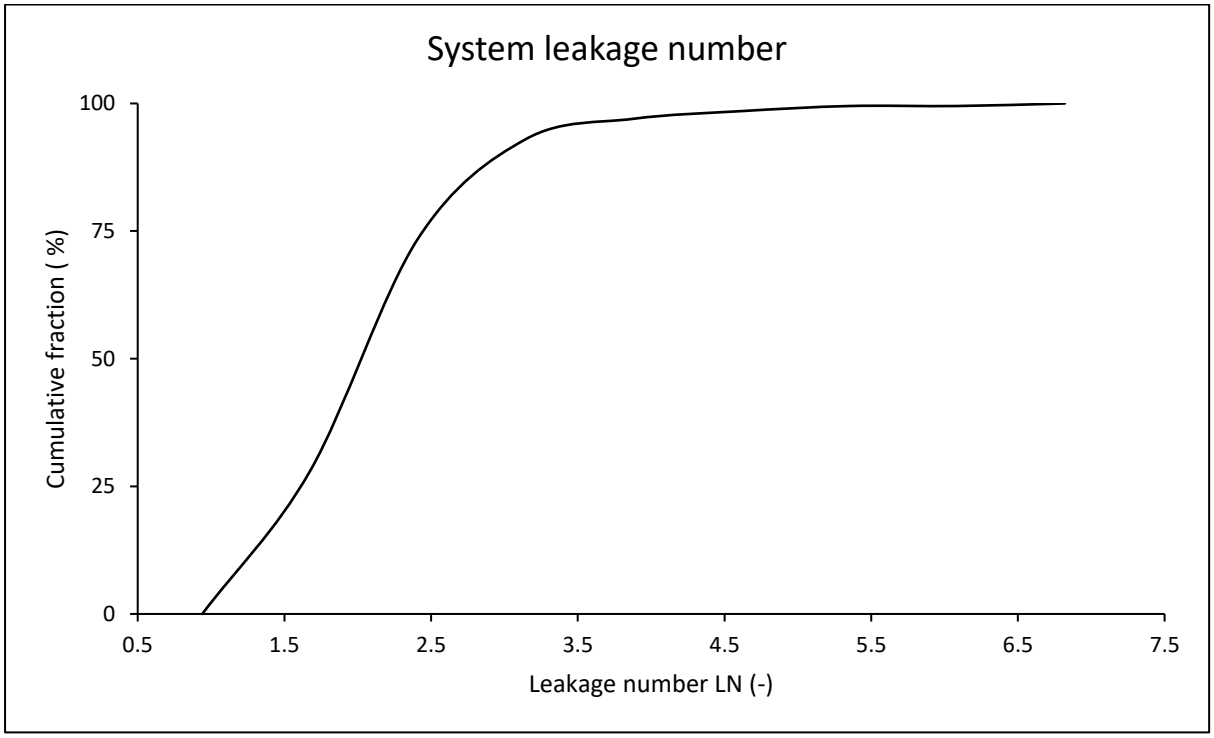
System leakage number
Cumulative fraction (%)
100
75
50
25
0
0.5
1.5
2.5
3.5
4.5
5.5
6.5
7.5
Leakage number LN (-)

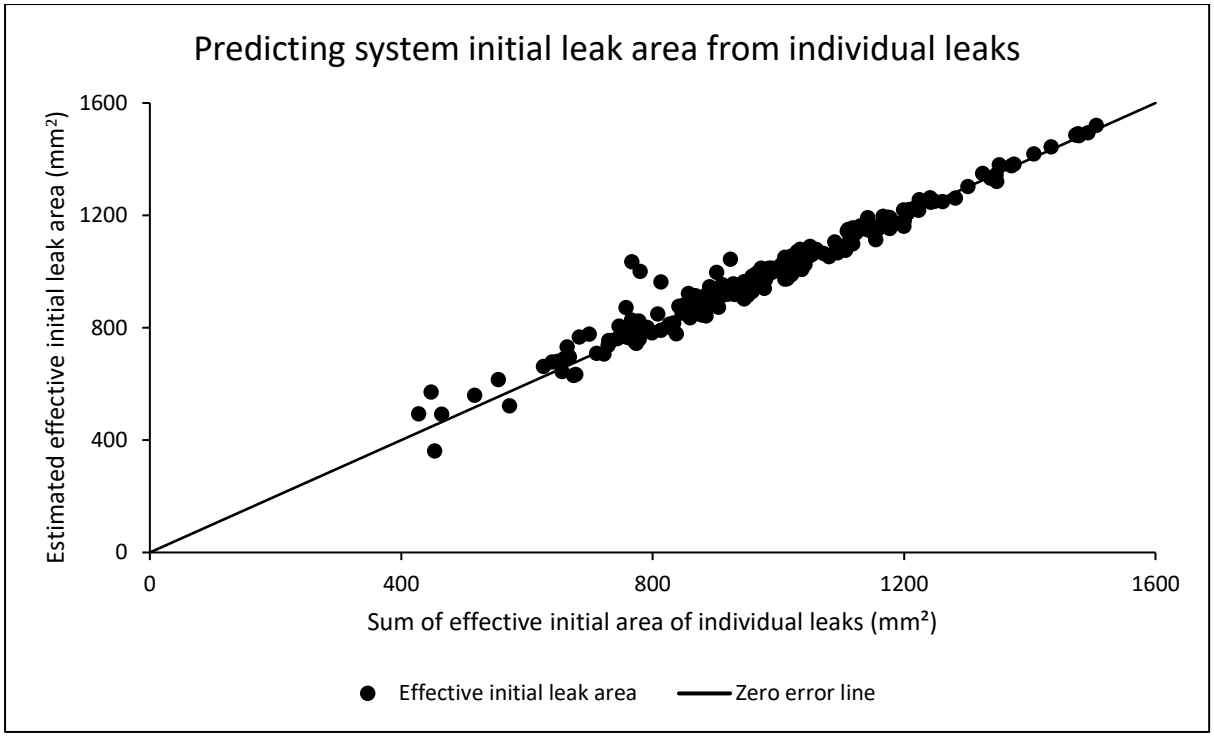
Predicting system initial leak area from individual leaks
Estimated effective initial leak area (mm²)
1600
1200
800
400
0
0
400
800
1200
1600
Sum of effective initial area of individual leaks (mm²)
Effective initial leak area
Zero error line

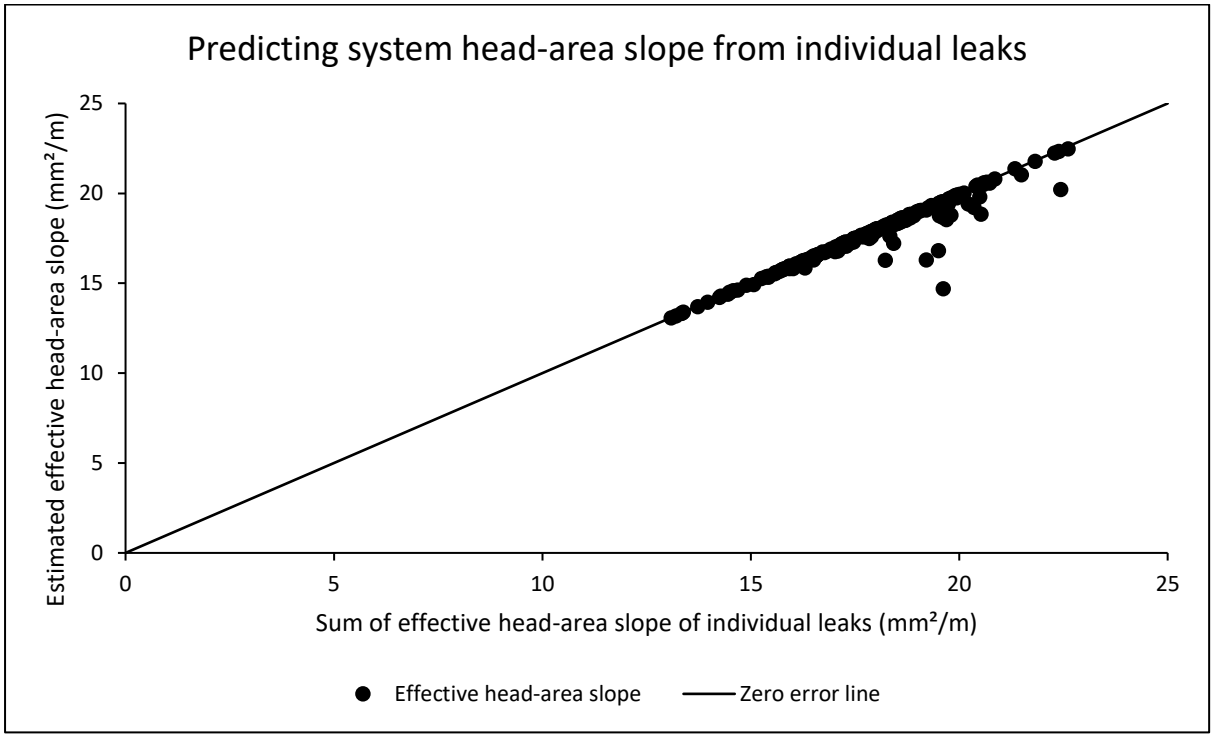
Predicting system head-area slope from individual leaks
Estimated effective head-area slope (mm²/m)
25
20
15
10
5
0
0
5
10
15
20
25
Sum of effective head-area slope of individual leaks (mm²/m)
Effective head-area slope
Zero error line

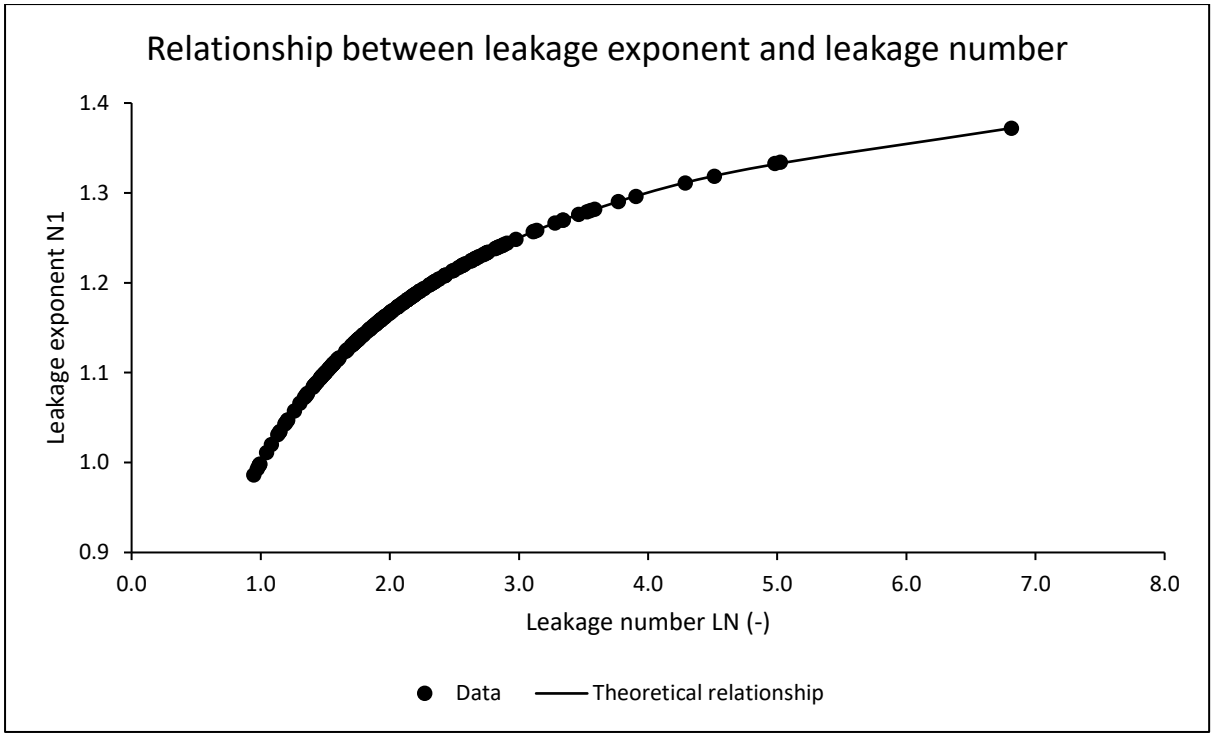
Relationship between leakage exponent and leakage number
Leakage exponent N1
1.4
1.3
1.2
1.1
1.0
0.9
0.0
1.0
2.0
3.0
4.0
5.0
6.0
7.0
8.0
Leakage number LN (-)
Data
Theoretical relationship

Average iterations required for a system to converge using both formulations

	Minimum	Arithmetic Mean	Median	Maximum
Modified orifice equation	8.40	8.83	8.84	9.16
Power equation	8.08	8.45	8.46	8.72

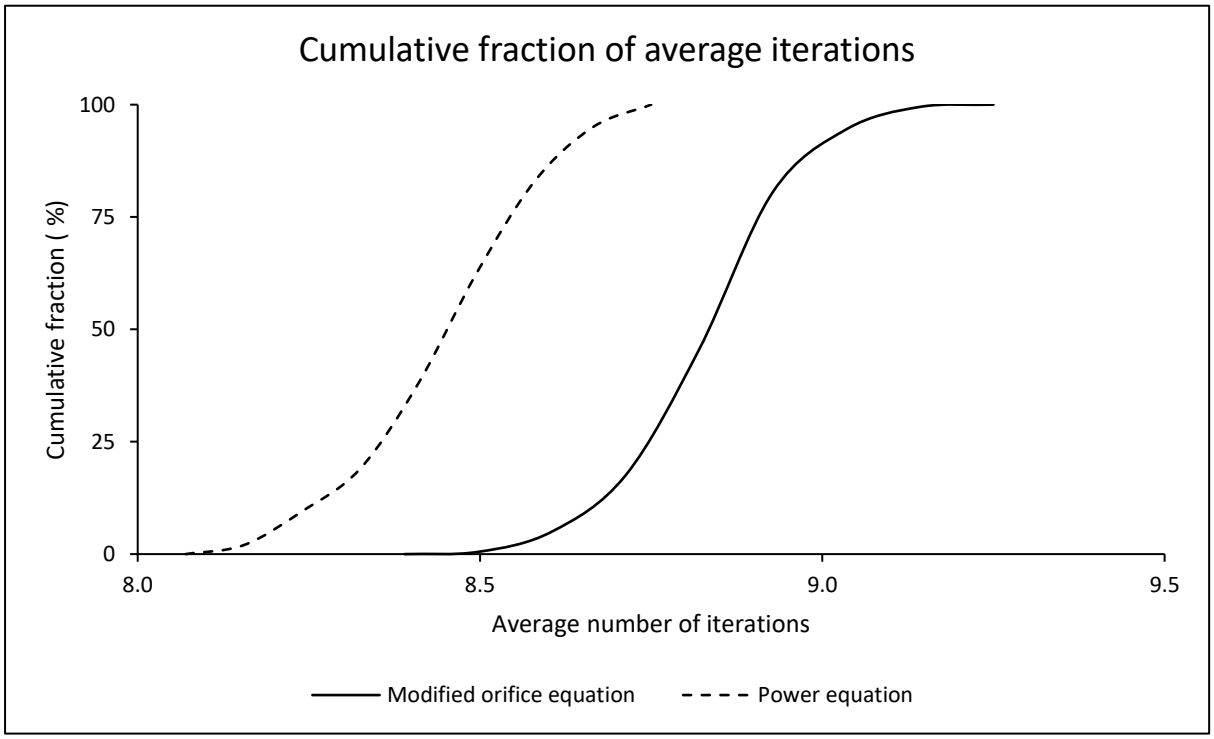

Effect of leakage on pressure at both average zone pressure (AZP) and critical nodes

AZP node								
	During MNF conditions				During peak demand conditions			
	Min (m)	Mean (m)	Median (m)	Max (m)	Min (m)	Mean (m)	Median (m)	Max (m)
Modified orifice equation	-0.52	-0.45	-0.46	-0.27	-1.94	-1.74	-1.77	-1.17
Power equation	-0.52	-0.45	-0.46	-0.27	-1.95	-1.74	-1.77	-1.15
Critical node								
Modified orifice equation	-1.82	-0.63	-0.57	-0.29	-3.68	-2.21	-2.14	-1.25
Power equation	-1.82	-0.63	-0.57	-0.29	-3.78	-2.21	-2.14	-1.21

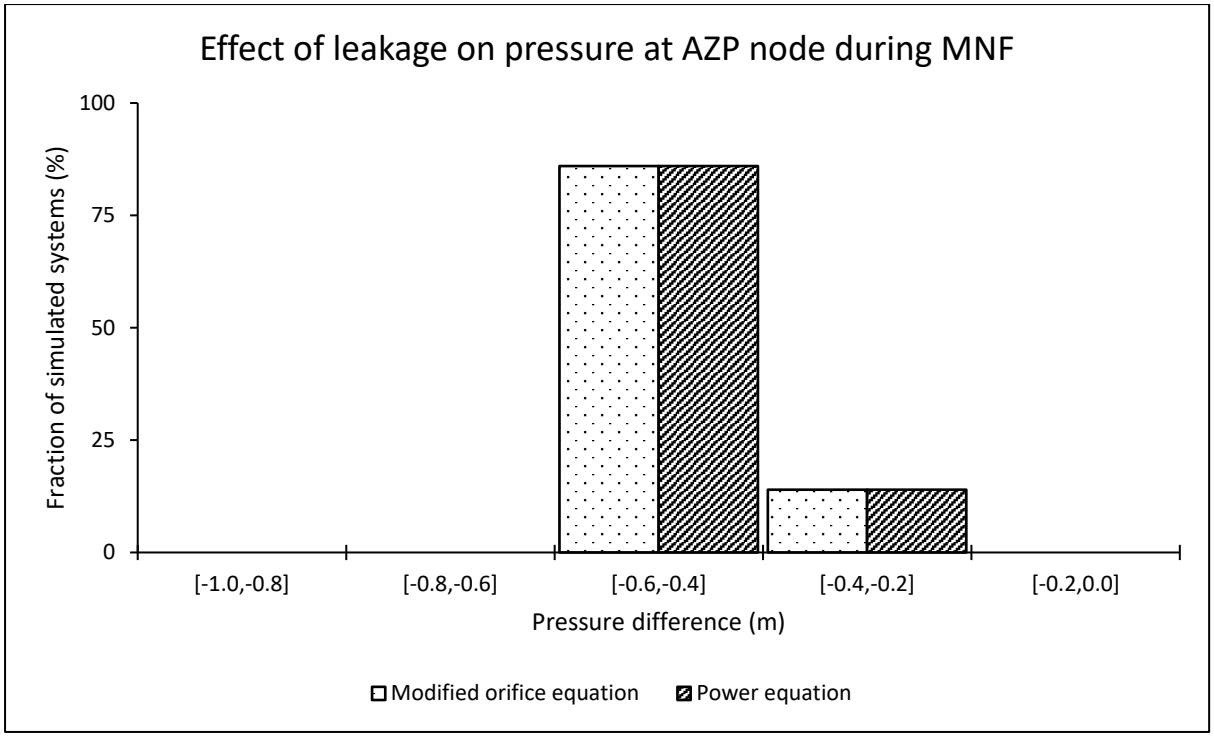
Effect of leakage on pressure at AZP node during MNF
Fraction of simulated systems (%)
100
75
50
25
0
[-1.0,-0.8]
[-0.8,-0.6]
[-0.6,-0.4]
[-0.4,-0.2]
[-0.2,0.0]
Pressure difference (m)
Modified orifice equation
Power equation

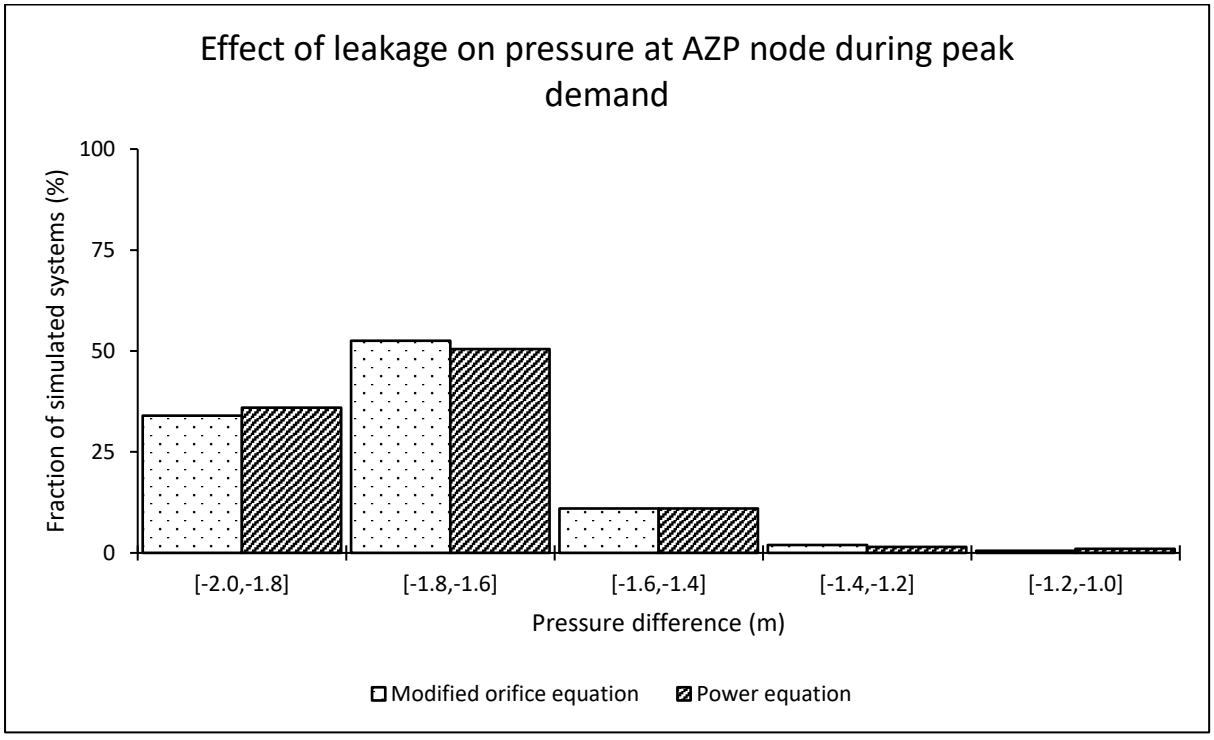
Effect of leakage on pressure at AZP node during peak demand
Fraction of simulated systems (%)
100
75
50
25
0
[-2.0,-1.8]
[-1.8,-1.6]
[-1.6,-1.4]
[-1.4,-1.2]
[-1.2,-1.0]
Pressure difference (m)
Modified orifice equation
Power equation

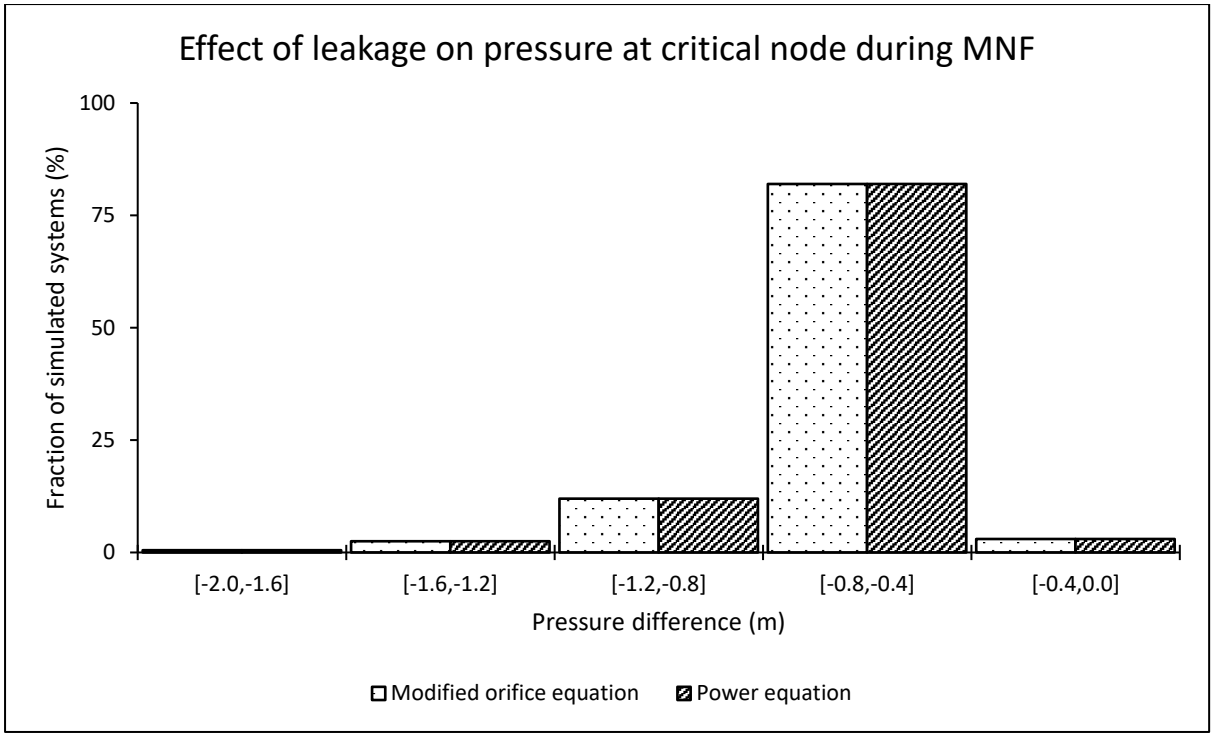
Effect of leakage on pressure at critical node during MNF
Fraction of simulated systems (%)
100
75
50
25
0
[-2.0,-1.6]
[-1.6,-1.2]
[-1.2,-0.8]
[-0.8,-0.4]
[-0.4,0.0]
Pressure difference (m)
Modified orifice equation
Power equation

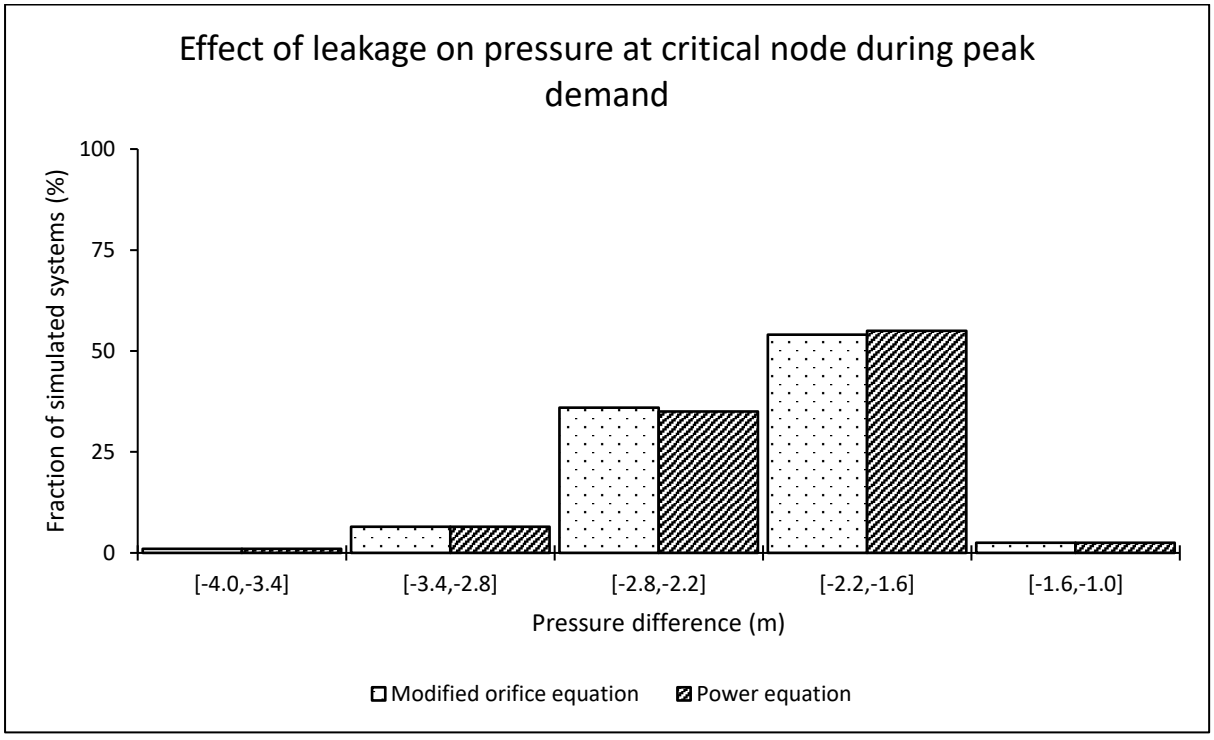
Effect of leakage on pressure at critical node during peak demand
Fraction of simulated systems (%)
100
75
50
25
0
[-4.0,-3.4]
[-3.4,-2.8]
[-2.8,-2.2]
[-2.2,-1.6]
[-1.6,-1.0]
Pressure difference (m)
Modified orifice equation
Power equation

Pressure estimation error when using the power equation at average zone pressure (AZP) and critical nodes

	During MNF conditions				During peak demand conditions			
	Min (%)	**Mean (%)**	**Median (%)**	**Max (%)**	**Min (%)**	**Mean (%)**	**Median (%)**	**Max (%)**
At the AZP node	0.00	0.00	0.00	0.00	-0.02	0.00	0.00	0.03
At the critical node	0.00	0.00	0.00	0.00	-0.11	0.00	0.00	0.04

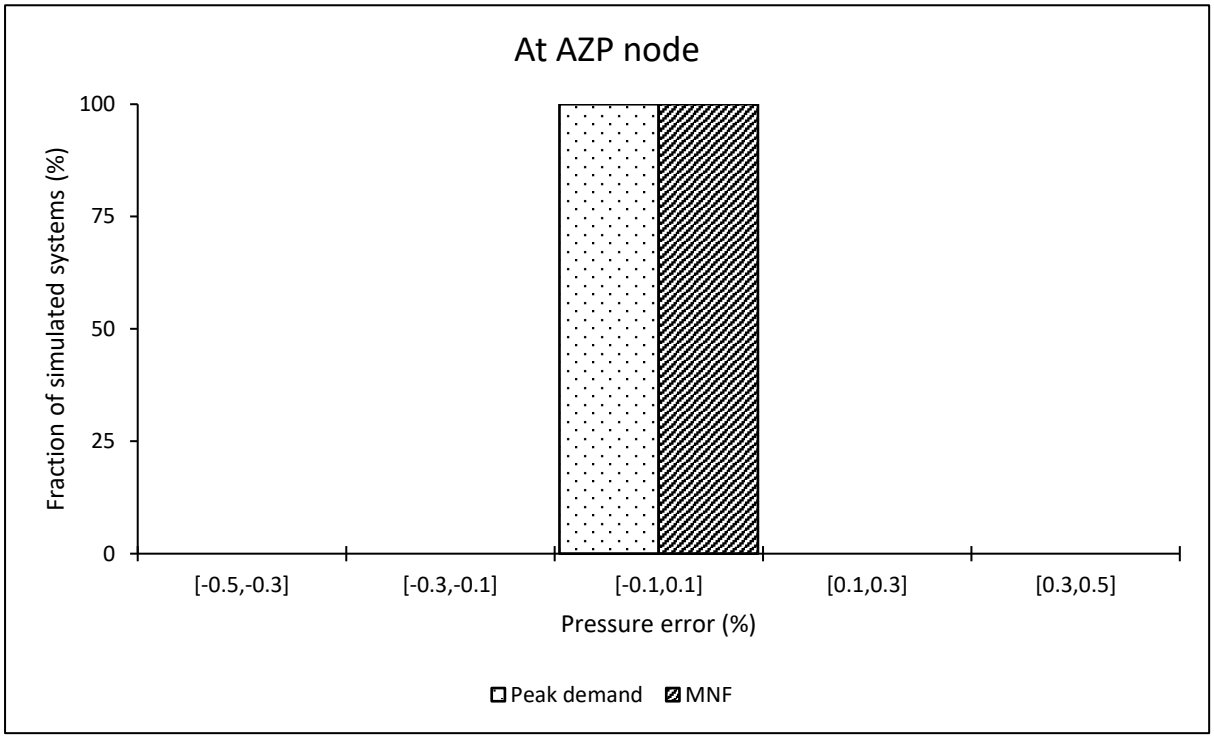

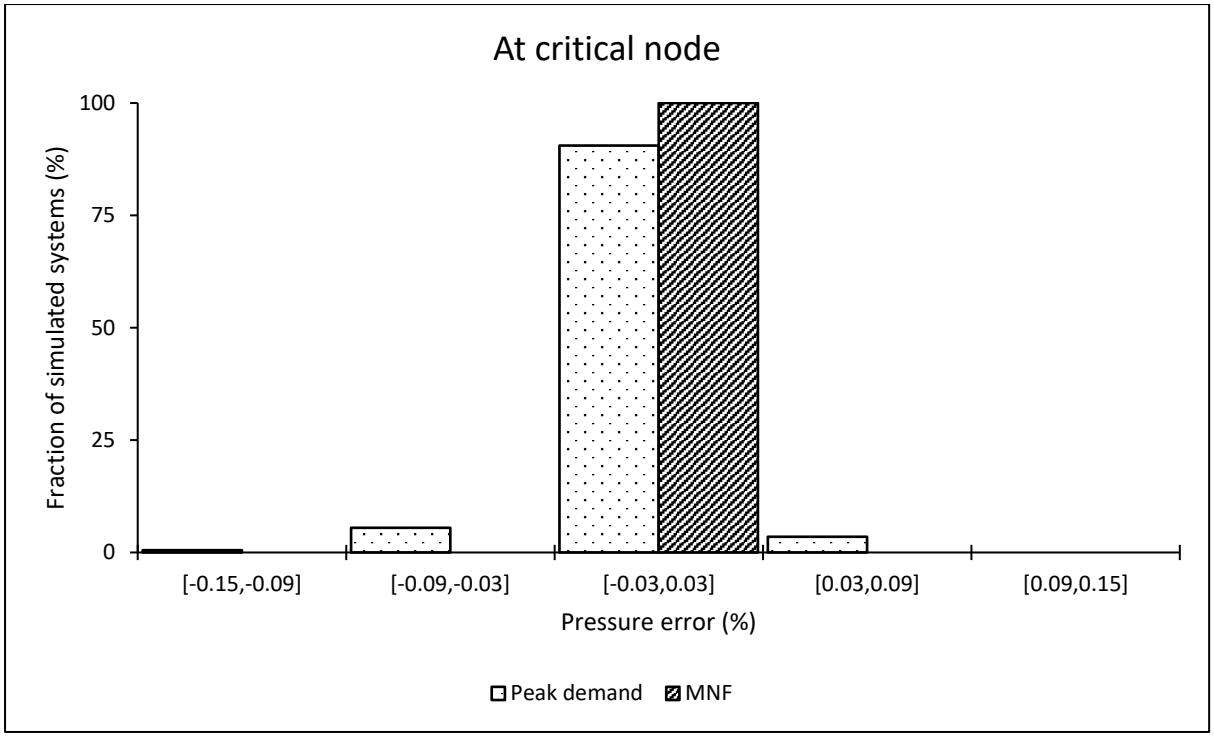
At critical node
Fraction of simulated systems (%)
100
75
50
25
0
[-0.15,-0.09]
[-0.09,-0.03]
[-0.03,0.03]
[0.03,0.09]
[0.09,0.15]
Pressure error (%)
Peak demand
MNF

System leakage estimation error when using the power equation

	Leakage estimation error (%)			
	Minimum	**Arithmetic Mean**	**Median**	**Maximum**
Before implementing pressure management	-0.32	0.00	0.00	0.51
After implementing pressure management	-23.07	-18.91	-19.33	-7.39

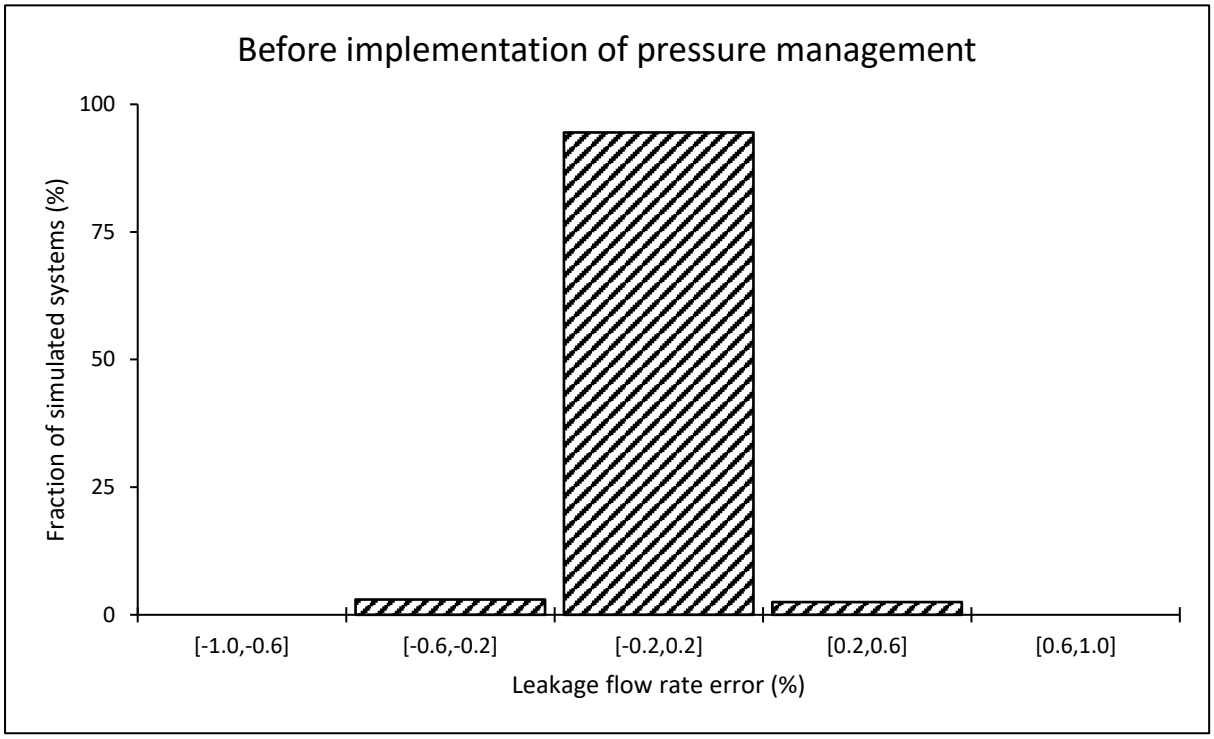

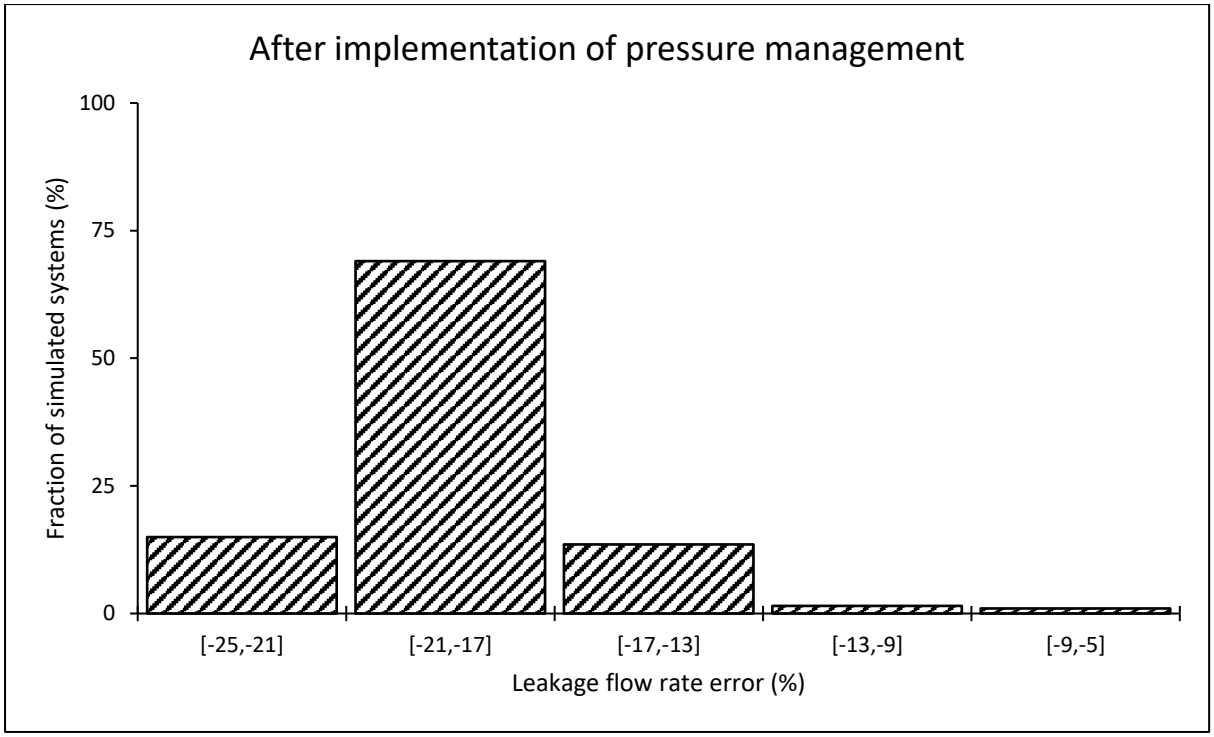
After implementation of pressure management
Fraction of simulated systems (%)
100
75
50
25
0
[-25,-21]
[-21,-17]
[-17,-13]
[-13,-9]
[-9,-5]
Leakage flow rate error (%)

Leakage estimation error when using the power equation at the critical node

	Leakage estimation error (%)			
	Minimum	**Arithmetic Mean**	**Median**	**Maximum**
Before implementing pressure management	-8.35	-3.57	-3.97	1.83
After implementing pressure management	-75.53	-59.02	-64.29	54.50

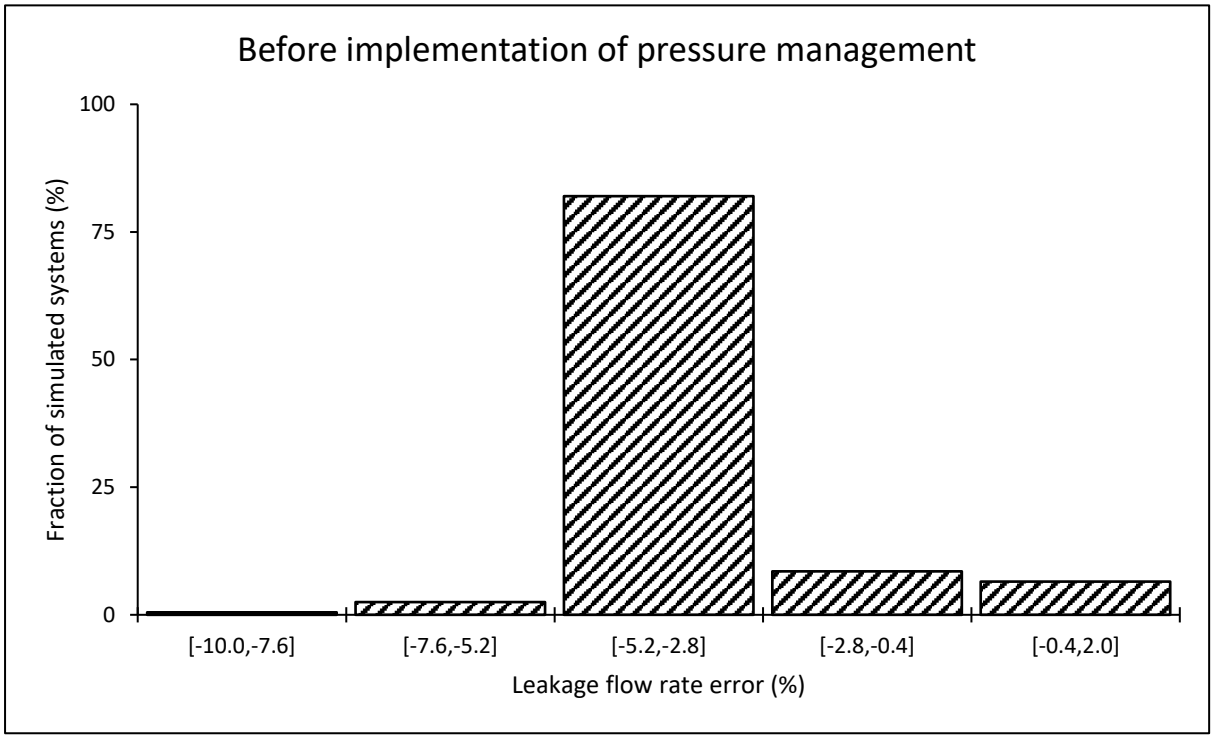

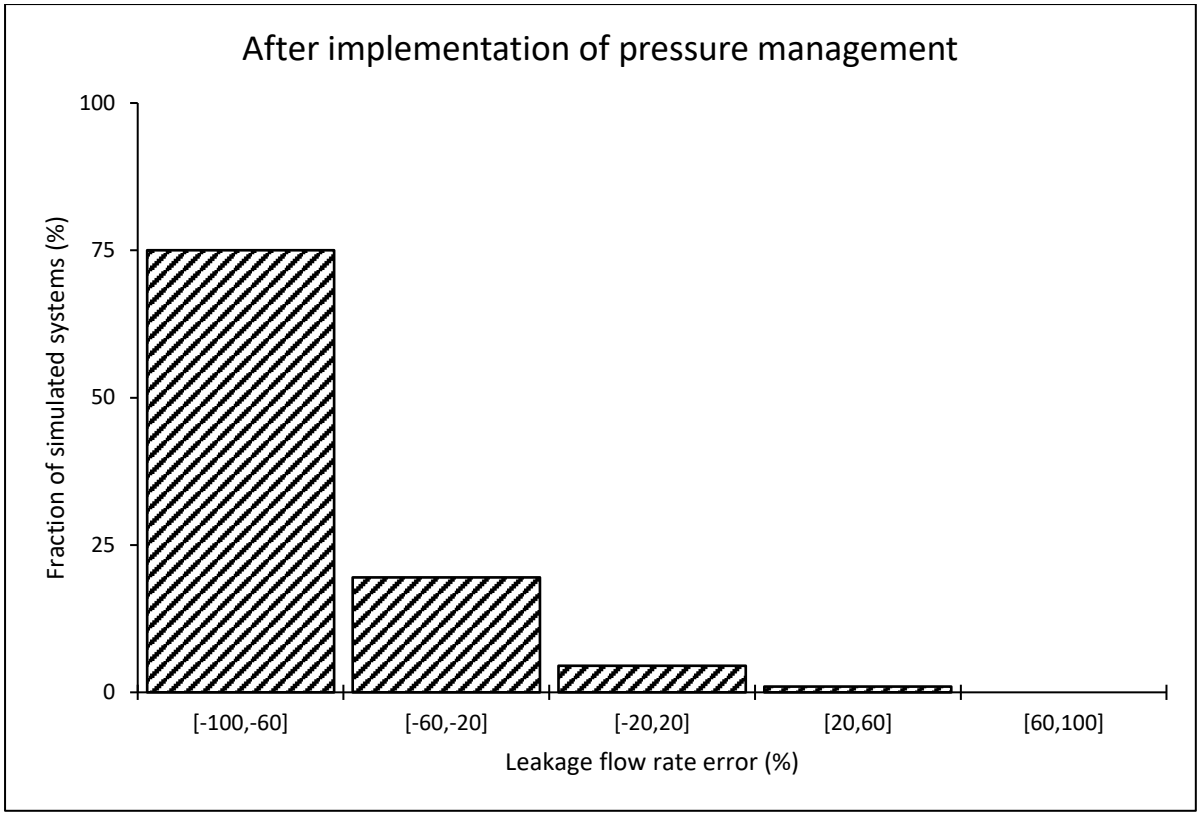
After implementation of pressure management
100
75
50
25
0
Fraction of simulated systems (%)
[-100,-60]
[-60,-20]
[-20,20]
[20,60]
[60,100]
Leakage flow rate error (%)

Appendix A-12: Large-sized network with an ILI of 64

Results for an individual system

Pressure head at the average zone pressure (AZP) node

		Pressure head (m)			
		Minimum	**Arithmetic Mean**	**Median**	**Maximum**
Before pressure management	Without leaks	99.13	108.33	106.63	113.44
	Modified orifice equation	92.01	103.44	100.66	110.79
	Power equation	92.04	103.45	100.66	110.79
After pressure management	Modified orifice equation	17.99	27.50	25.51	33.12
	Power equation	18.37	27.71	25.78	33.20

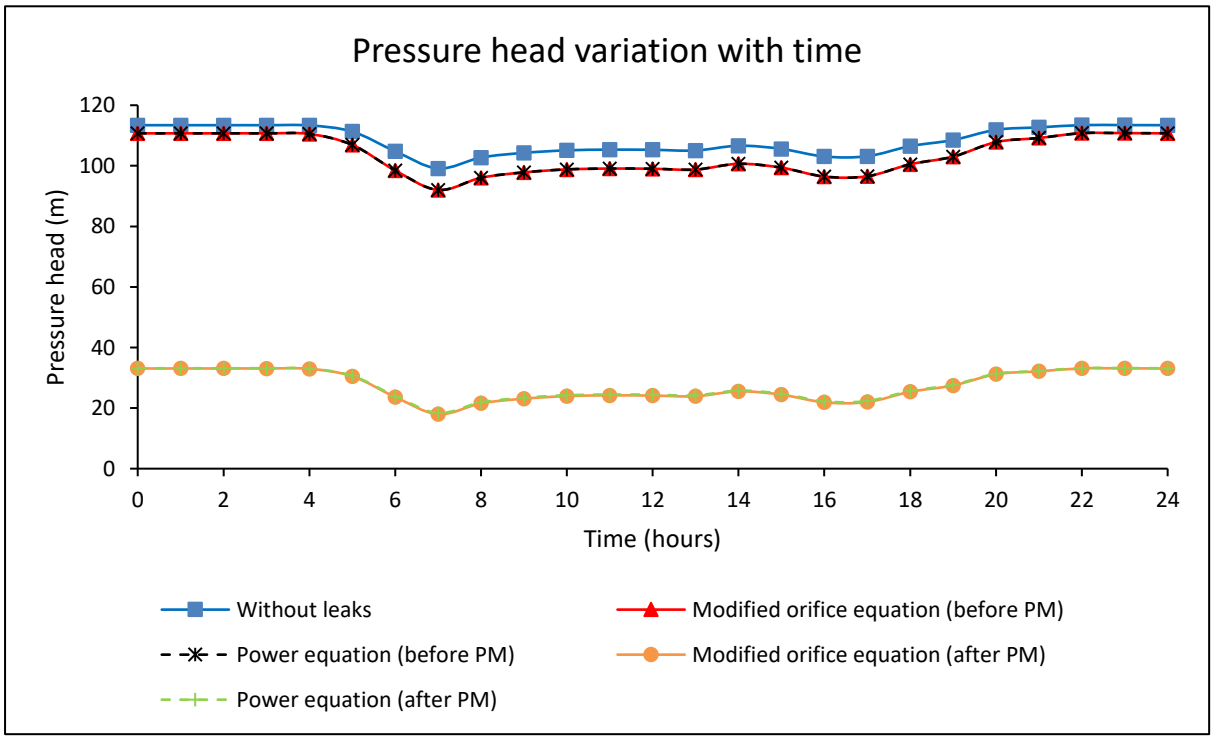

Pressure head at the critical node

		Pressure head (m)			
		Minimum	**Arithmetic Mean**	**Median**	**Maximum**
Before pressure management	Without leaks	89.91	100.55	98.69	106.46
	Modified orifice equation	81.31	94.55	91.51	103.09
	Power equation	81.36	94.57	91.52	103.09
After pressure management	Modified orifice equation	8.50	19.49	17.31	26.01
	Power equation	9.00	19.78	17.66	26.13

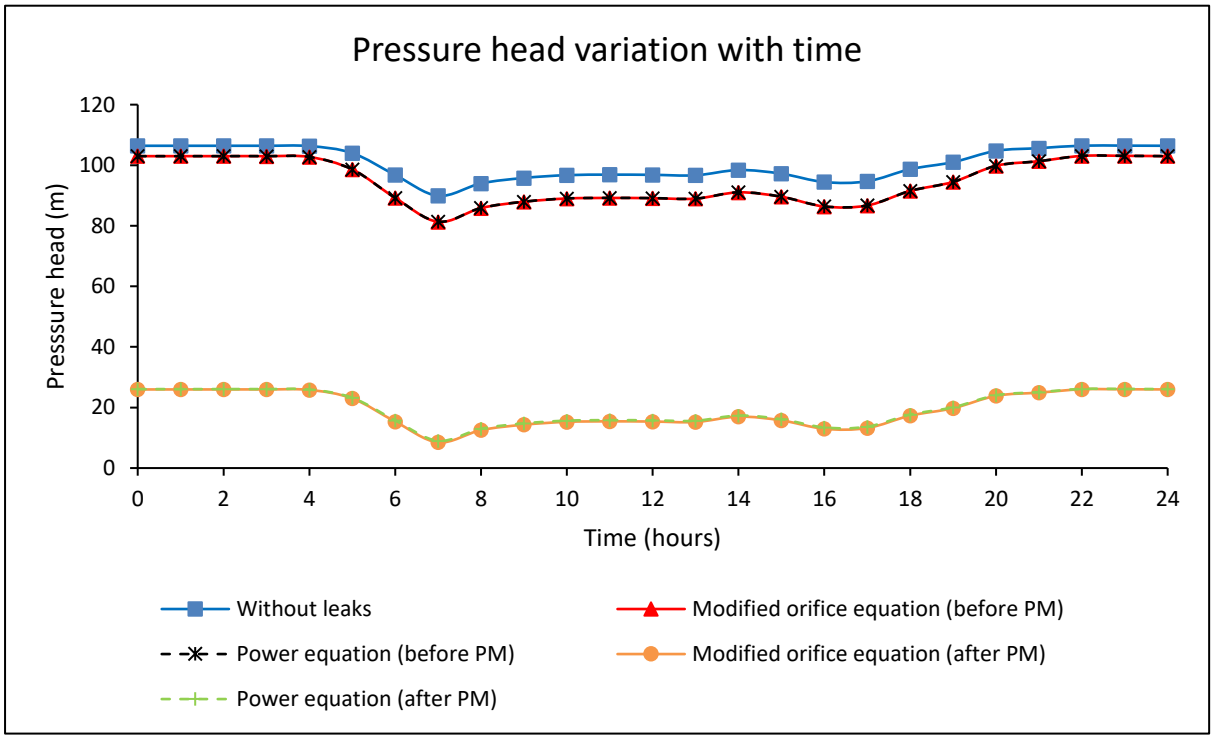

System leakage flow rate

		Leakage flow rate (m^3/h)			
		Minimum	**Arithmetic Mean**	**Median**	**Maximum**
Before pressure management	Modified orifice equation	1584.57	1819.05	1758.90	1972.66
	Power equation	1580.29	1818.03	1757.81	1972.61
After pressure management	Modified orifice equation	318.31	454.56	424.49	536.65
	Power equation	226.26	370.53	337.99	458.57

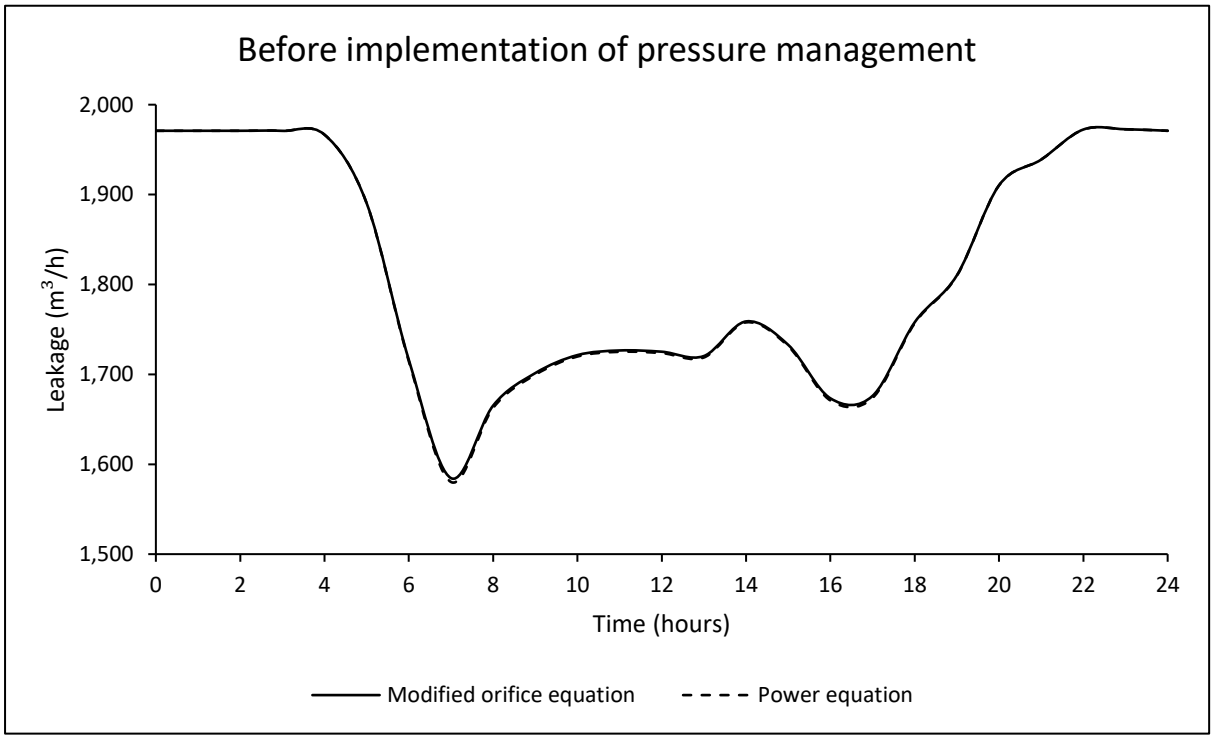

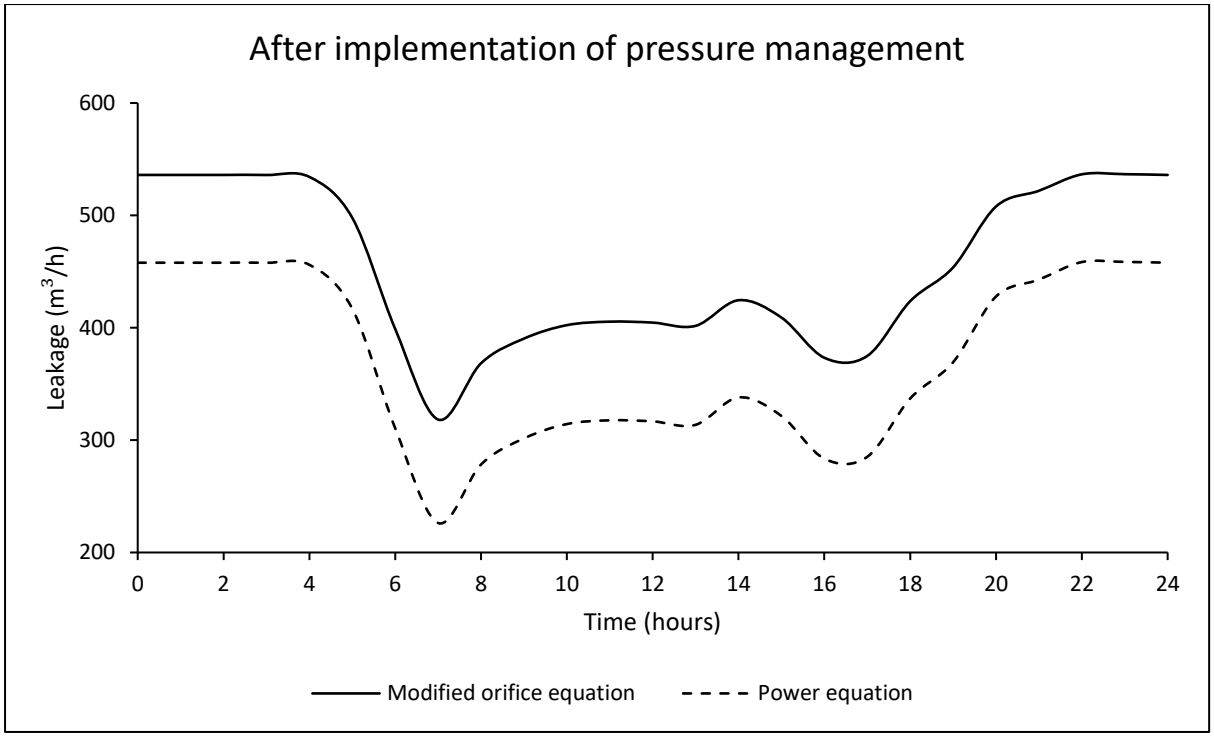
After implementation of pressure management
600
500
400
300
200
Leakage (m3/h)
0
2
4
6
8
10
12
14
16
18
20
22
24
Time (hours)
Modified orifice equation
Power equation

Leakage flow rate at the critical node

		Leakage flow rate (m^3/h)			
		Minimum	**Arithmetic Mean**	**Median**	**Maximum**
Before pressure management	Modified orifice equation	0.11	0.12	0.12	0.13
	Power equation	0.10	0.11	0.11	0.13
After pressure management	Modified orifice equation	0.04	0.05	0.05	0.06
	Power equation	0.01	0.02	0.02	0.02

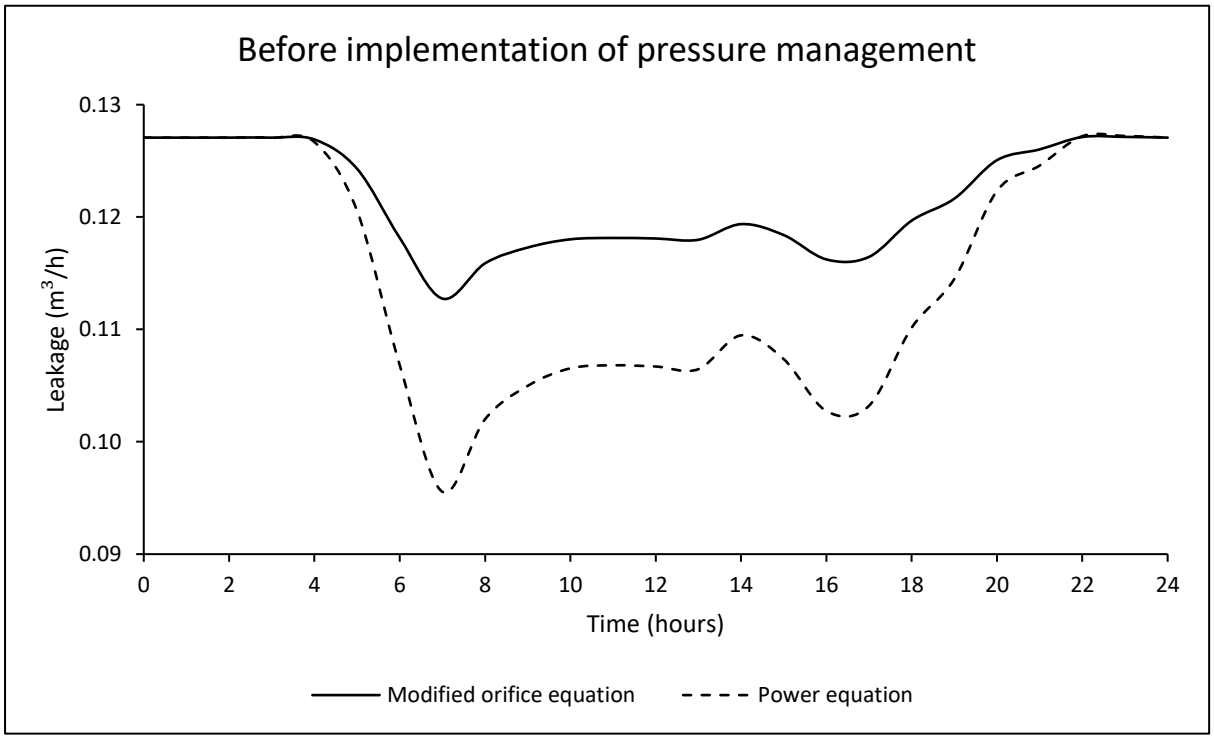

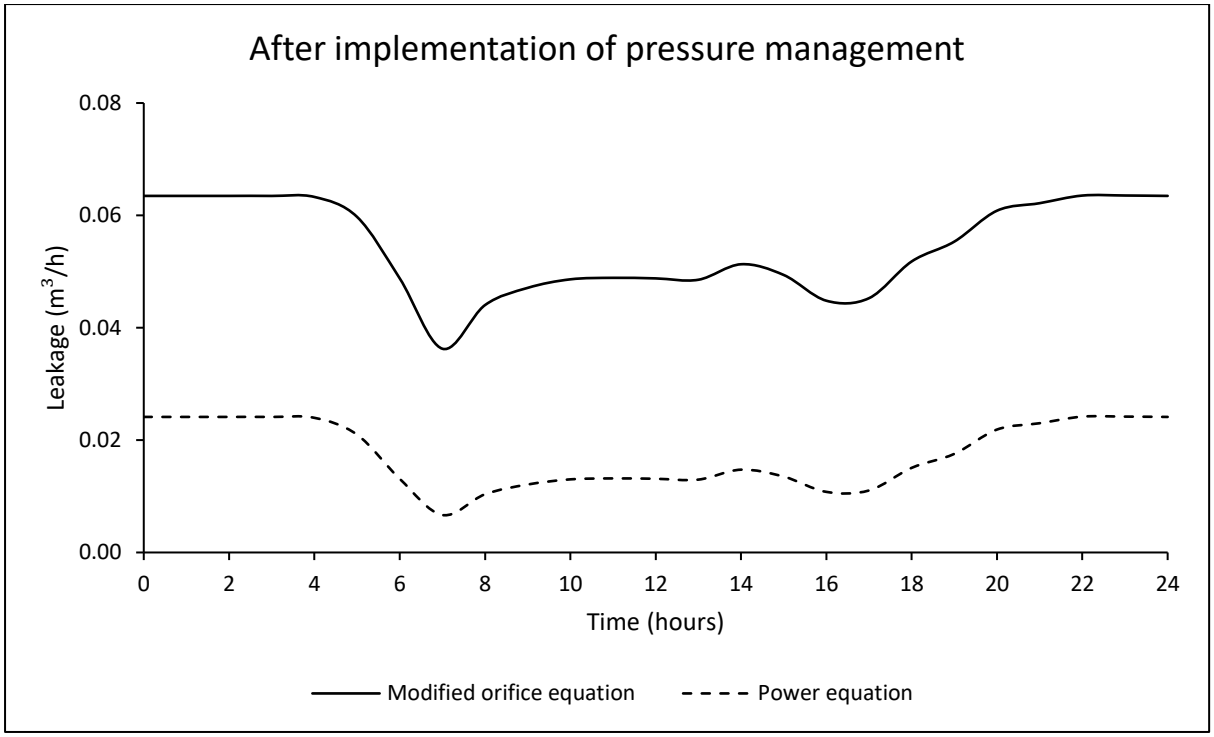
After implementation of pressure management
0.08
0.06
0.04
0.02
0.00
Leakage (m3/h)
0
2
4
6
8
10
12
14
16
18
20
22
24
Time (hours)
Modified orifice equation
Power equation

Number of iterations required for a system to converge to a hydraulic solution for both formulations

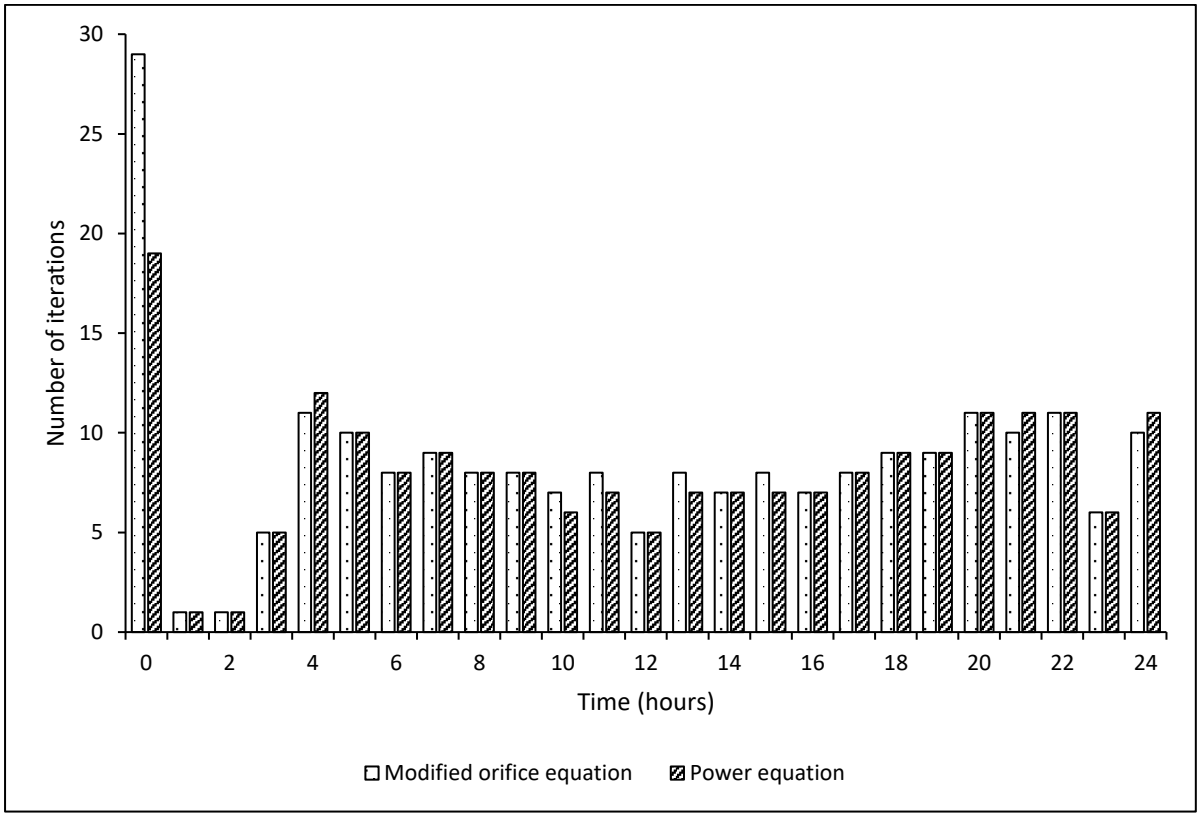

Results for combined systems

System parameters for both power and modified orifice formulations

	Minimum	Arithmetic Mean	Median	Maximum
Leakage exponent N1	1.08	1.21	1.21	1.31
Leakage coefficient C	1.1E-03	1.8E-03	1.8E-03	3.1E-03
Effective initial leak area C_dA0 (mm^2)	2120.22	3309.51	3305.48	4464.77
Effective head-area slope C_dm (mm^2/m)	56.10	75.65	75.91	85.85
Leakage number LN	1.36	2.53	2.46	4.34

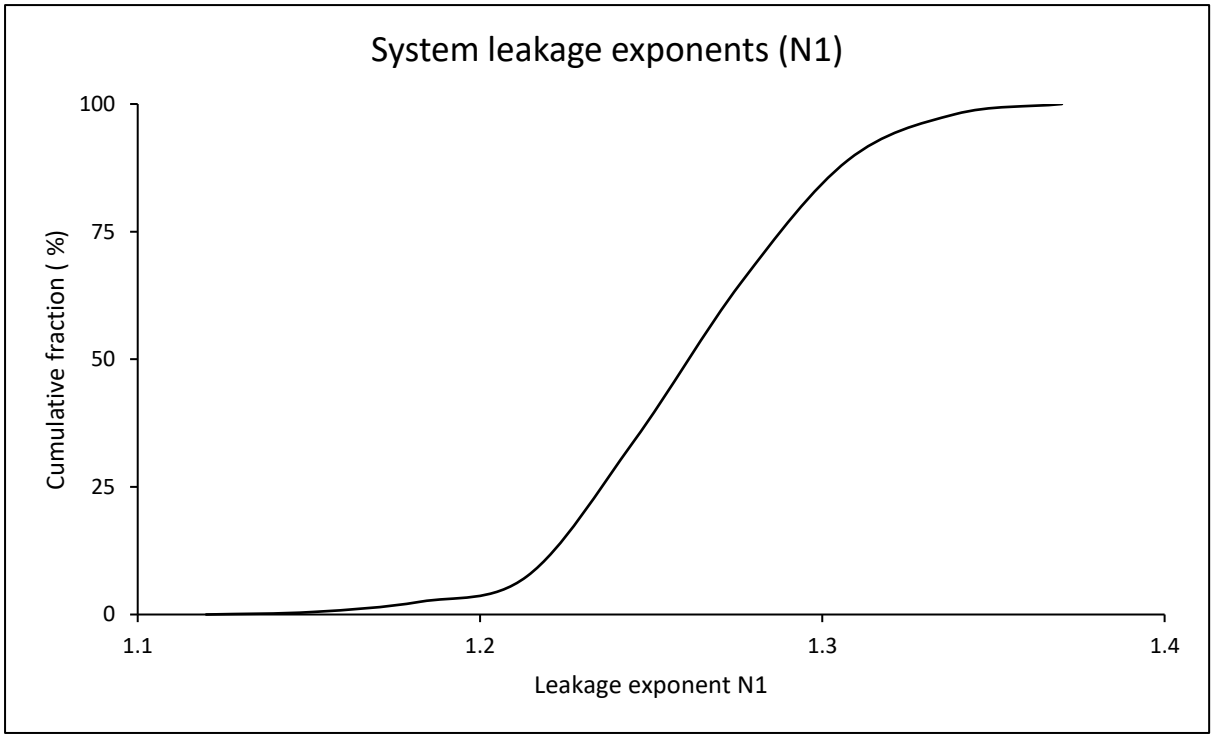

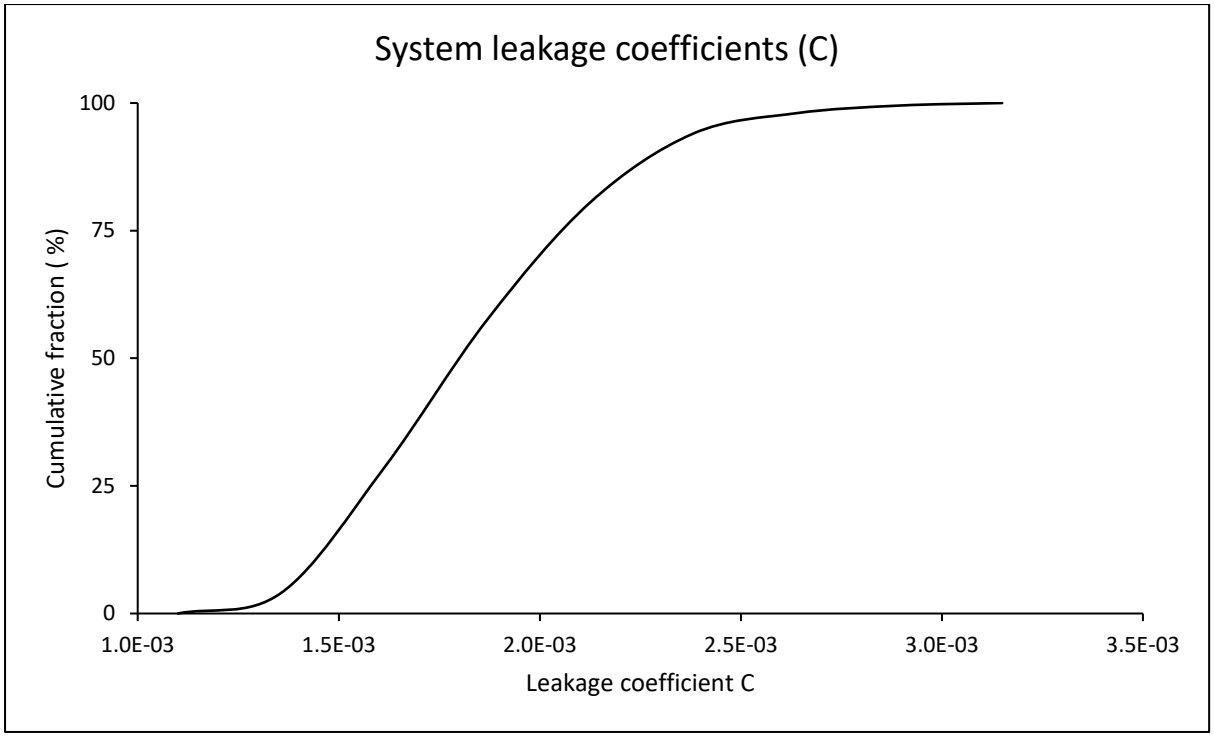
System leakage coefficients (C)
100
75
50
25
0
Cumulative fraction (%)
1.0E-03
1.5E-03
2.0E-03
2.5E-03
3.0E-03
3.5E-03
Leakage coefficient C

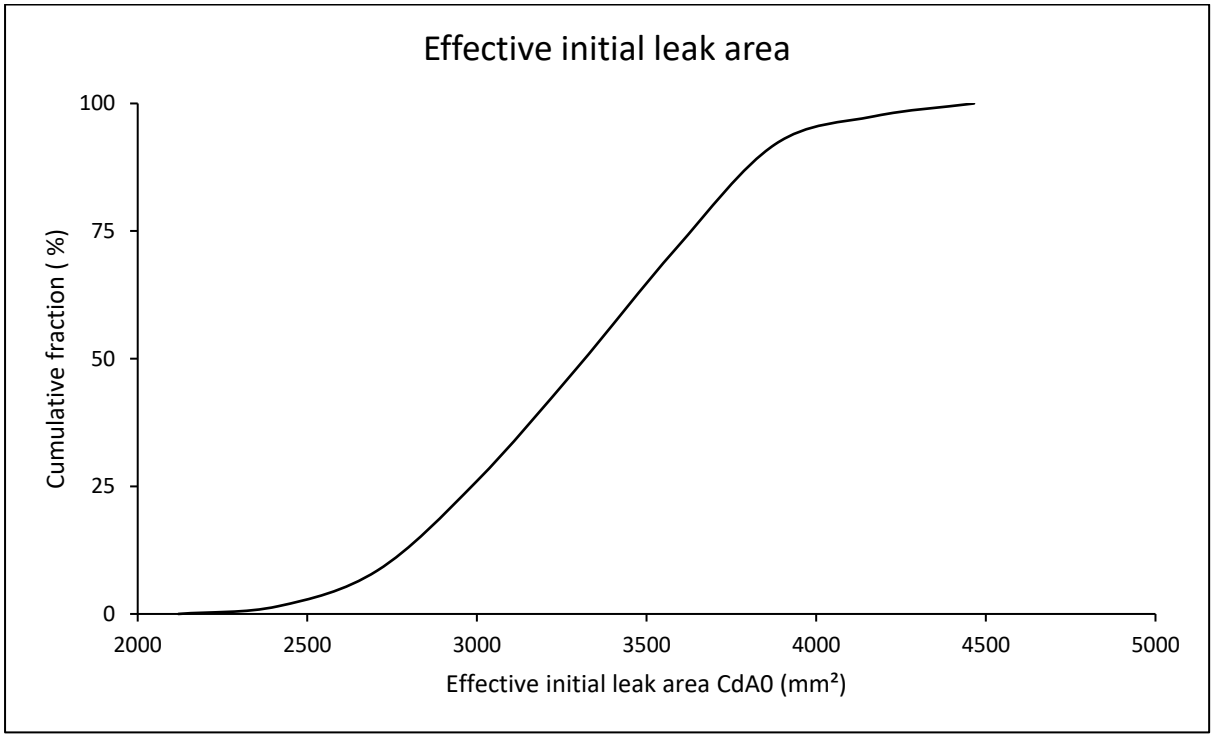
Effective initial leak area
100
75
50
25
0
Cumulative fraction (%)
2000
2500
3000
3500
4000
4500
5000
Effective initial leak area CdA0 (mm²)

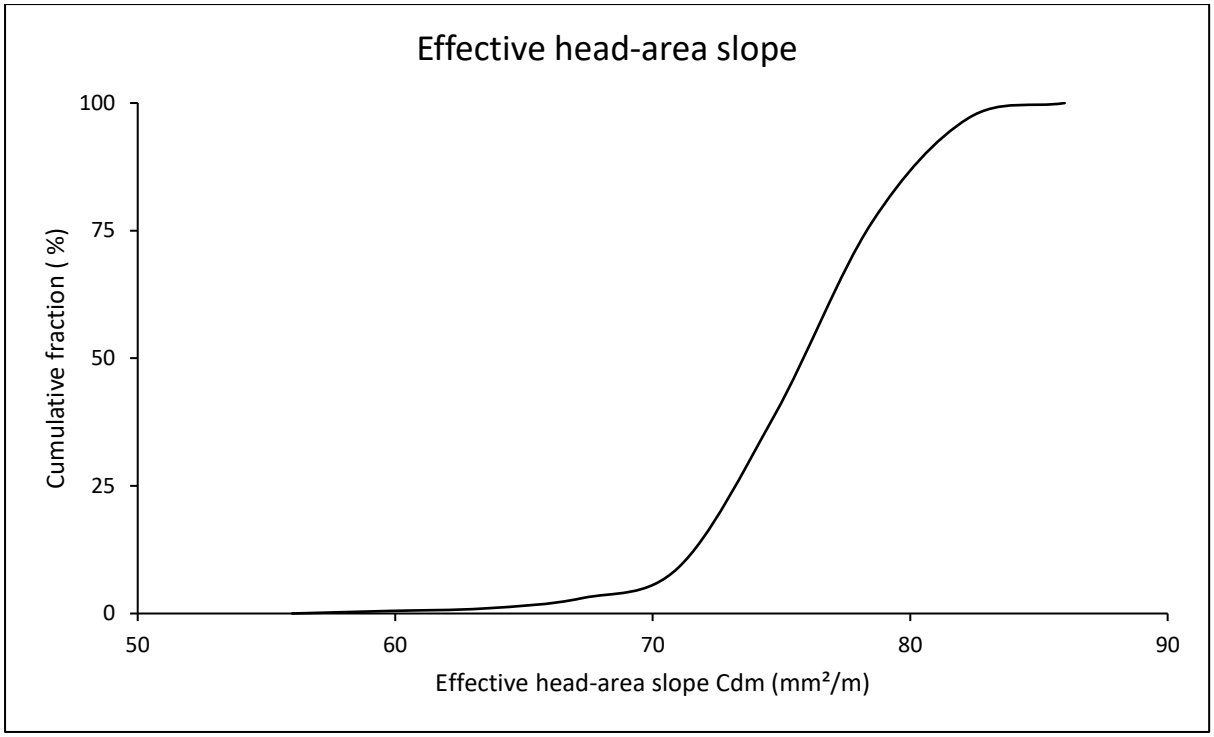
Effective head-area slope
100
75
50
25
0
Cumulative fraction (%)
50
60
70
80
90
Effective head-area slope Cdm (mm²/m)

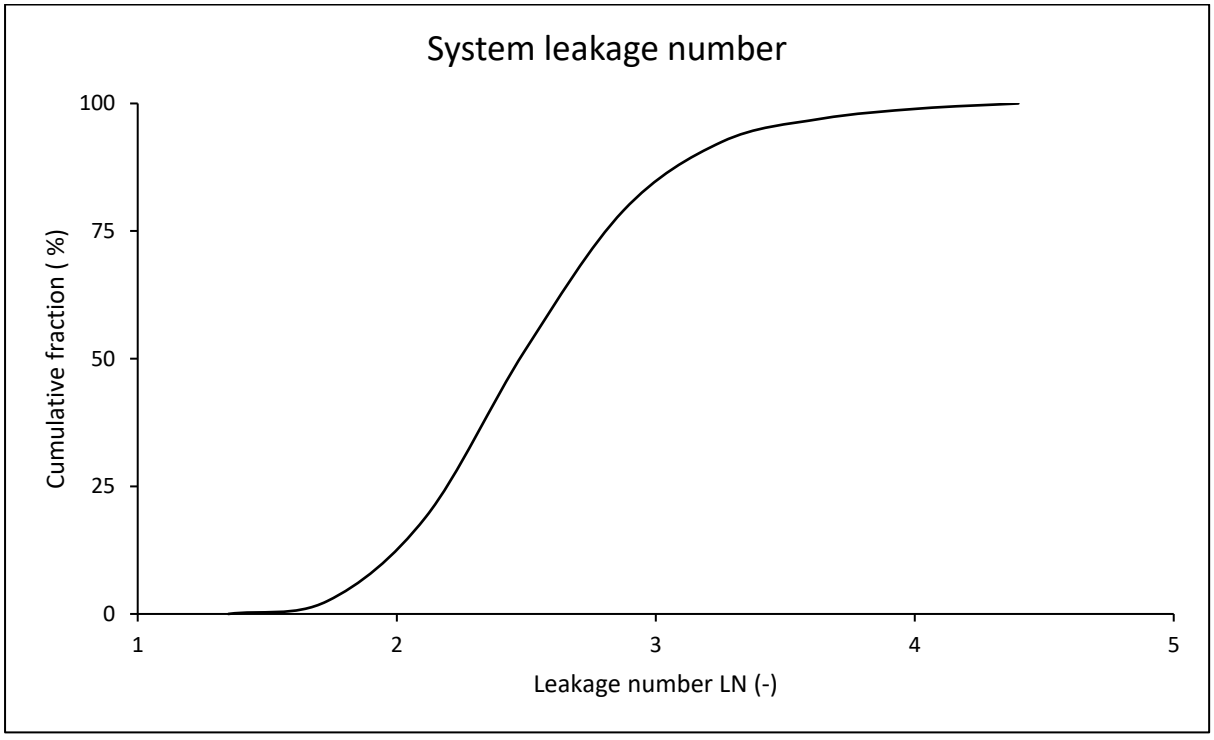
System leakage number
100
75
50
25
0
Cumulative fraction (%)
1
2
3
4
5
Leakage number LN (-)

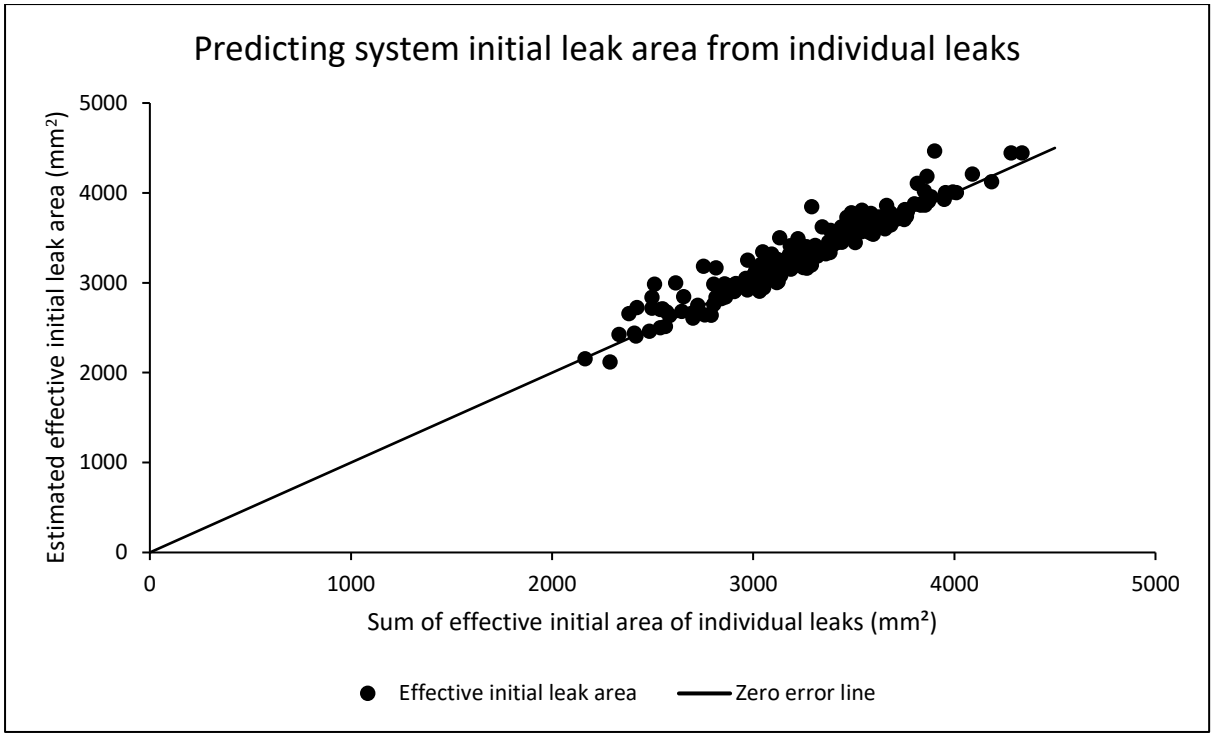
Predicting system initial leak area from individual leaks
Estimated effective initial leak area (mm²)
5000
4000
3000
2000
1000
0
0
1000
2000
3000
4000
5000
Sum of effective initial area of individual leaks (mm²)
Effective initial leak area
Zero error line

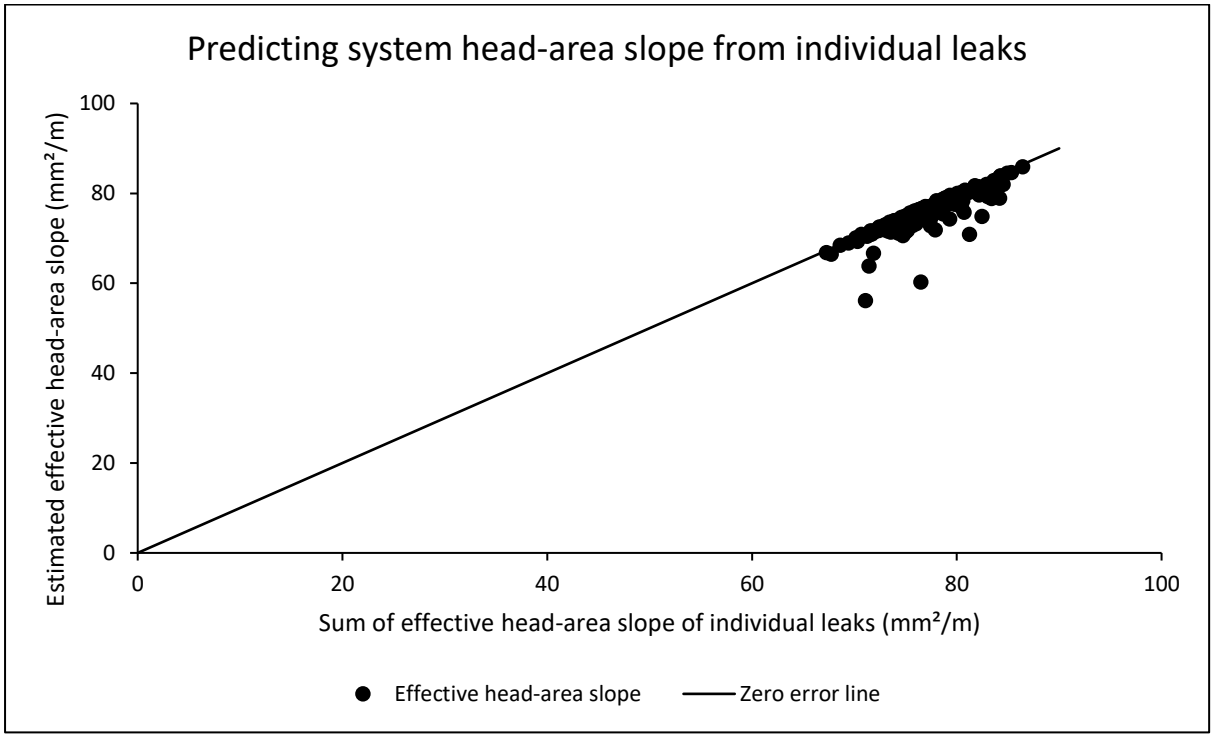
Predicting system head-area slope from individual leaks
Estimated effective head-area slope (mm²/m)
100
80
60
40
20
0
0
20
40
60
80
100
Sum of effective head-area slope of individual leaks (mm²/m)
Effective head-area slope
Zero error line

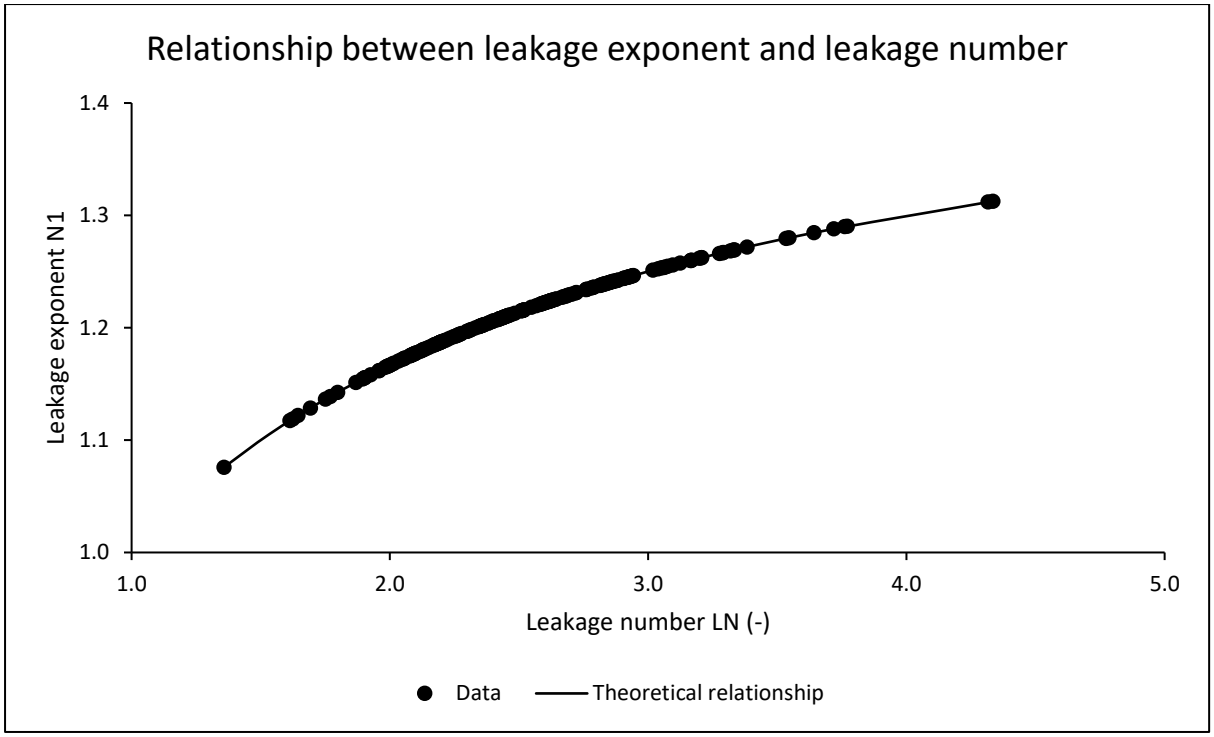
Relationship between leakage exponent and leakage number
Leakage exponent N1
1.4
1.3
1.2
1.1
1.0
1.0
2.0
3.0
4.0
5.0
Leakage number LN (-)
Data
Theoretical relationship

Average iterations required for a system to converge using both formulations

	Minimum	Arithmetic Mean	Median	Maximum
Modified orifice equation	7.80	8.30	8.32	8.80
Power equation	7.52	8.05	8.04	8.60

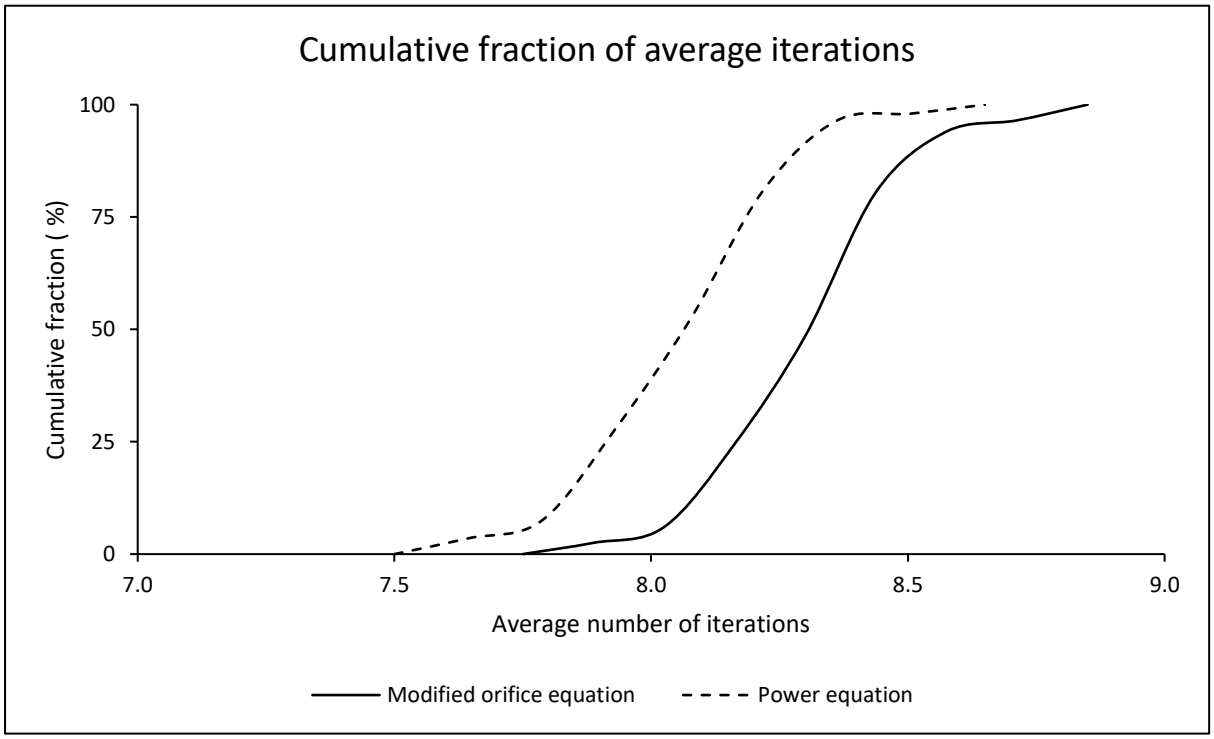

Effect of leakage on pressure at both average zone pressure (AZP) and critical nodes

AZP node								
	During MNF conditions				During peak demand conditions			
	Min (m)	Mean (m)	Median (m)	Max (m)	Min (m)	Mean (m)	Median (m)	Max (m)
Modified orifice equation	-2.94	-2.59	-2.61	-2.12	-7.40	-6.86	-6.89	-6.05
Power equation	-2.94	-2.59	-2.61	-2.12	-7.41	-6.84	-6.87	-5.98
Critical node								
Modified orifice equation	-7.00	-3.69	-3.58	-2.46	-11.54	-8.71	-8.64	-6.86
Power equation	-7.00	-3.69	-3.58	-2.46	-11.69	-8.69	-8.62	-6.78

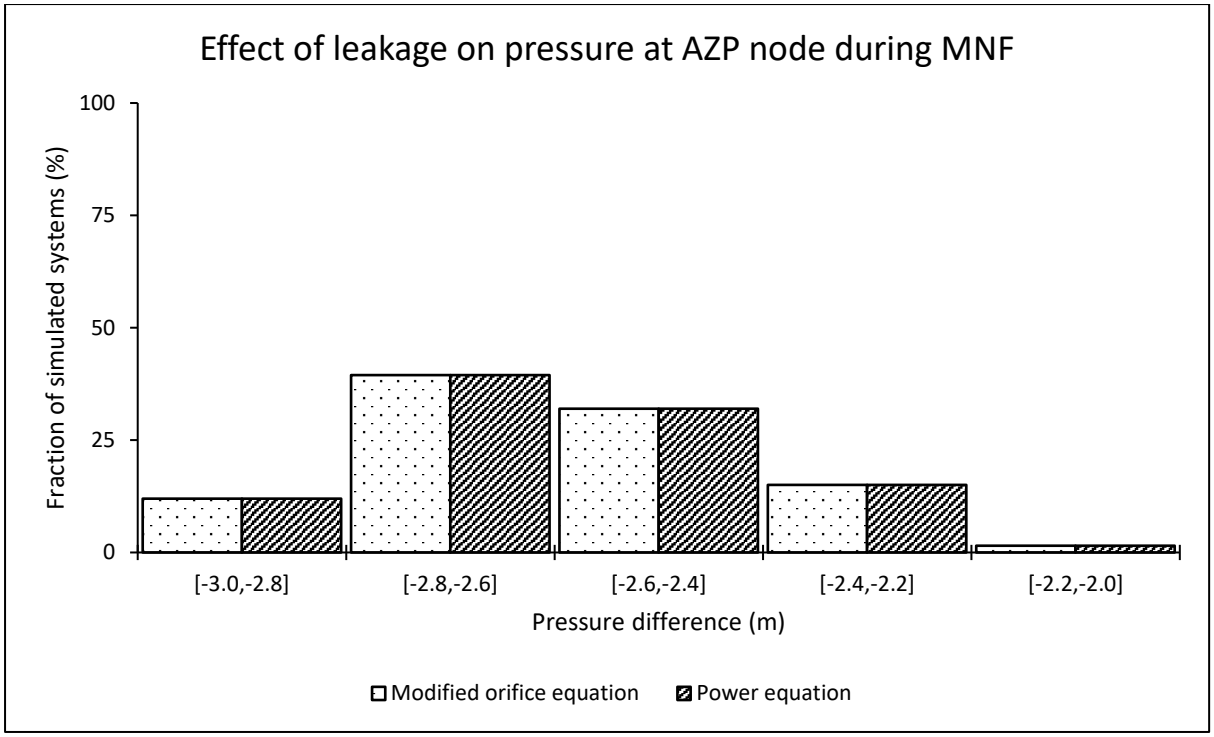
Effect of leakage on pressure at AZP node during MNF
Fraction of simulated systems (%)
100
75
50
25
0
[-3.0,-2.8]
[-2.8,-2.6]
[-2.6,-2.4]
[-2.4,-2.2]
[-2.2,-2.0]
Pressure difference (m)
Modified orifice equation
Power equation

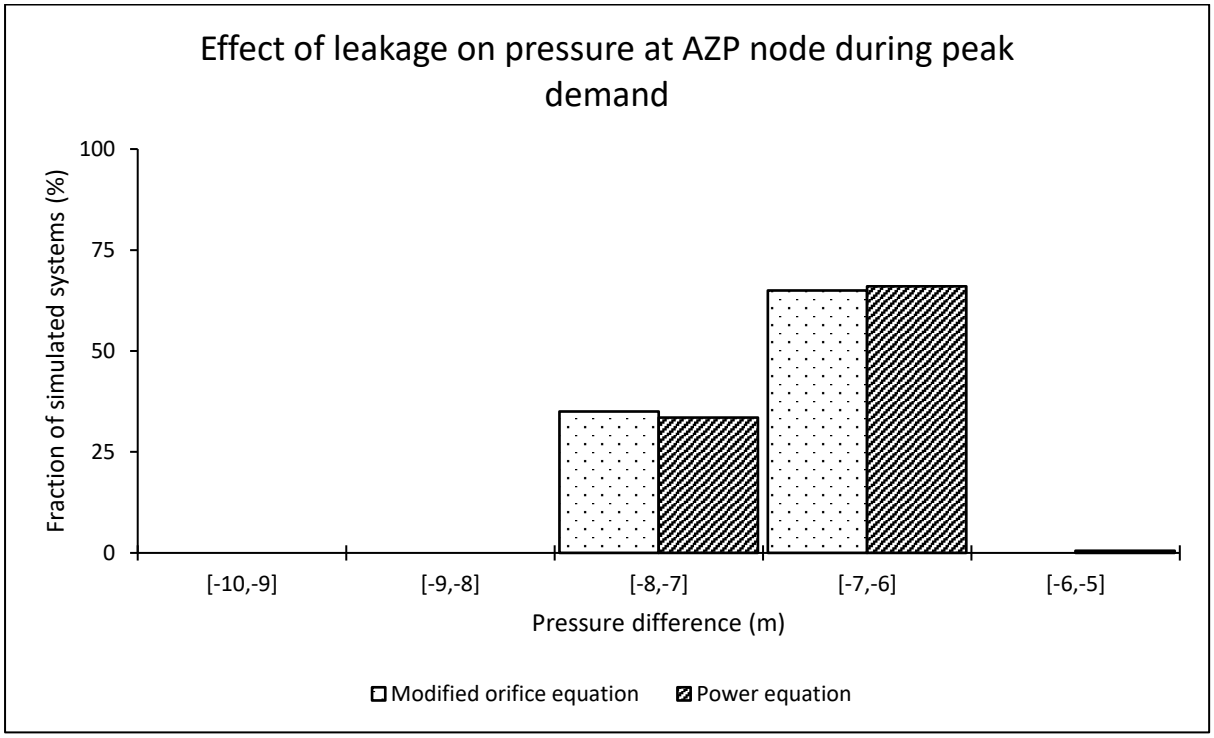
Effect of leakage on pressure at AZP node during peak demand
Fraction of simulated systems (%)
100
75
50
25
0
[-10,-9]
[-9,-8]
[-8,-7]
[-7,-6]
[-6,-5]
Pressure difference (m)
Modified orifice equation
Power equation

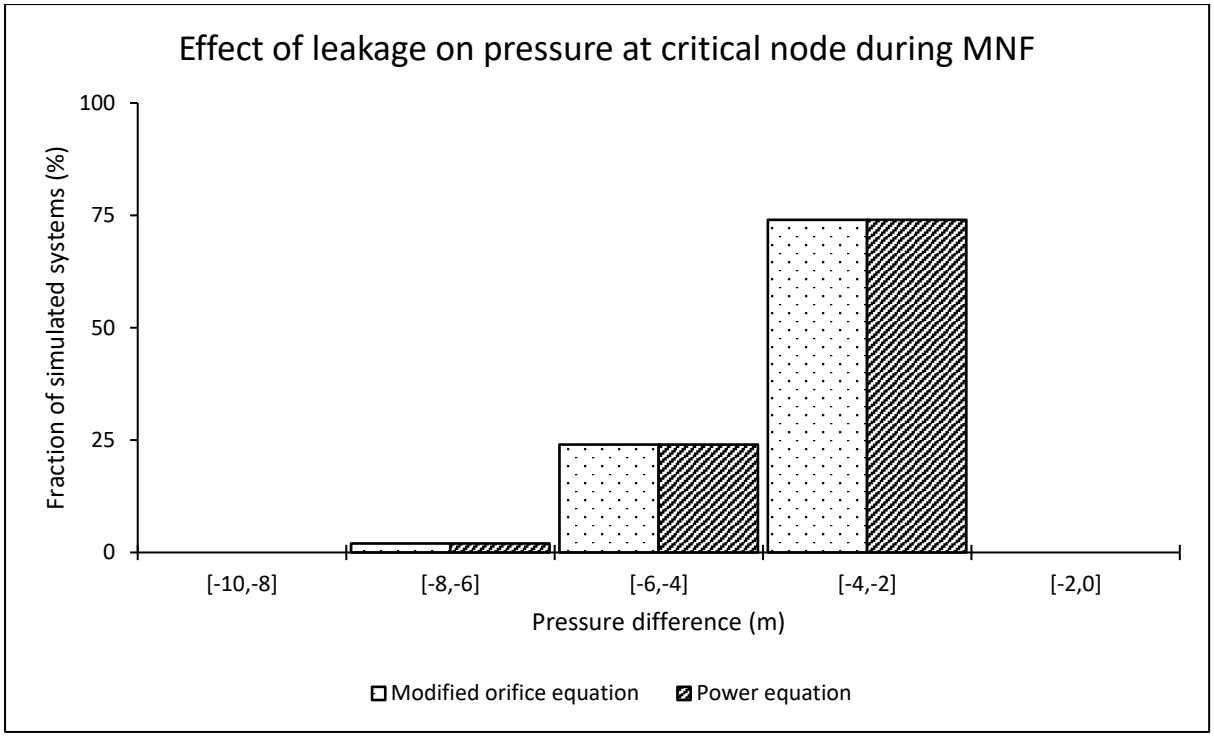
Effect of leakage on pressure at critical node during MNF
Fraction of simulated systems (%)
100
75
50
25
0
[-10,-8]
[-8,-6]
[-6,-4]
[-4,-2]
[-2,0]
Pressure difference (m)
Modified orifice equation
Power equation

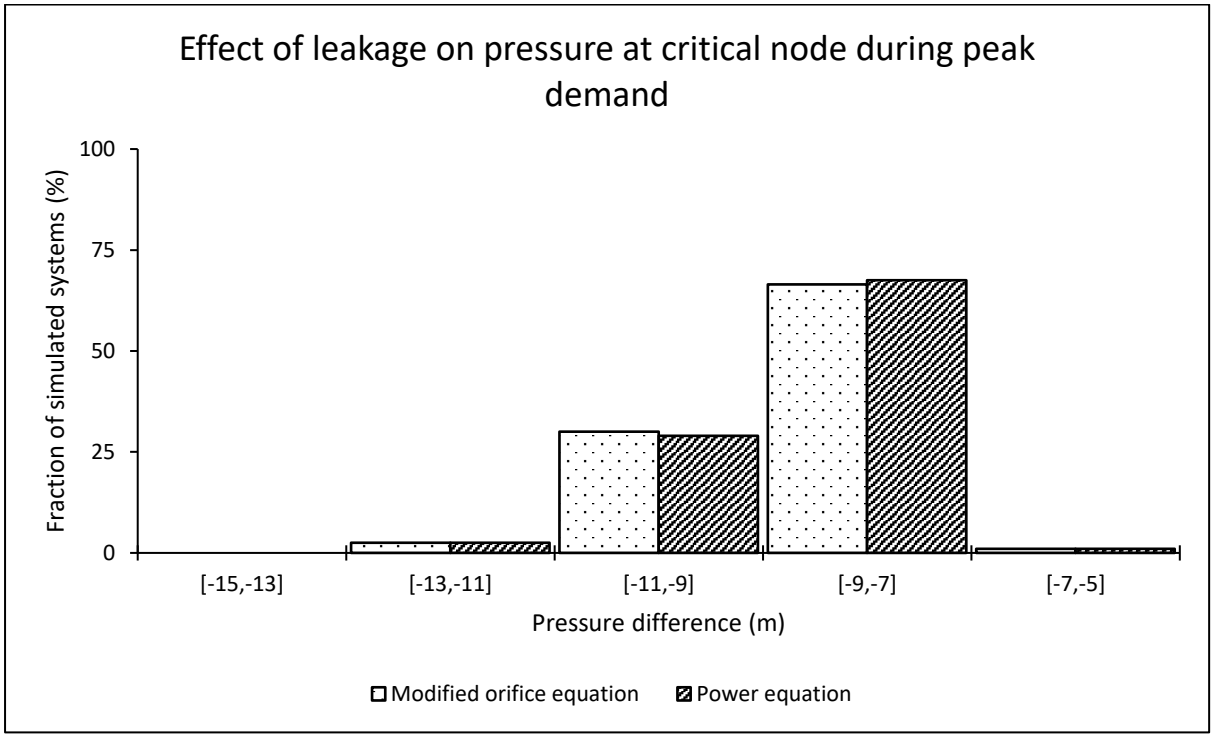
Effect of leakage on pressure at critical node during peak demand
Fraction of simulated systems (%)
100
75
50
25
0
[-15,-13]
[-13,-11]
[-11,-9]
[-9,-7]
[-7,-5]
Pressure difference (m)
Modified orifice equation
Power equation

Pressure estimation error when using the power equation at average zone pressure (AZP) and critical nodes

	During MNF conditions				During peak demand conditions			
	Min (%)	**Mean (%)**	**Median (%)**	**Max (%)**	**Min (%)**	**Mean (%)**	**Median (%)**	**Max (%)**
At the AZP node	0.00	0.00	0.00	0.00	-0.05	0.02	0.02	0.07
At the critical node	0.00	0.00	0.00	0.00	-0.20	0.03	0.03	0.14

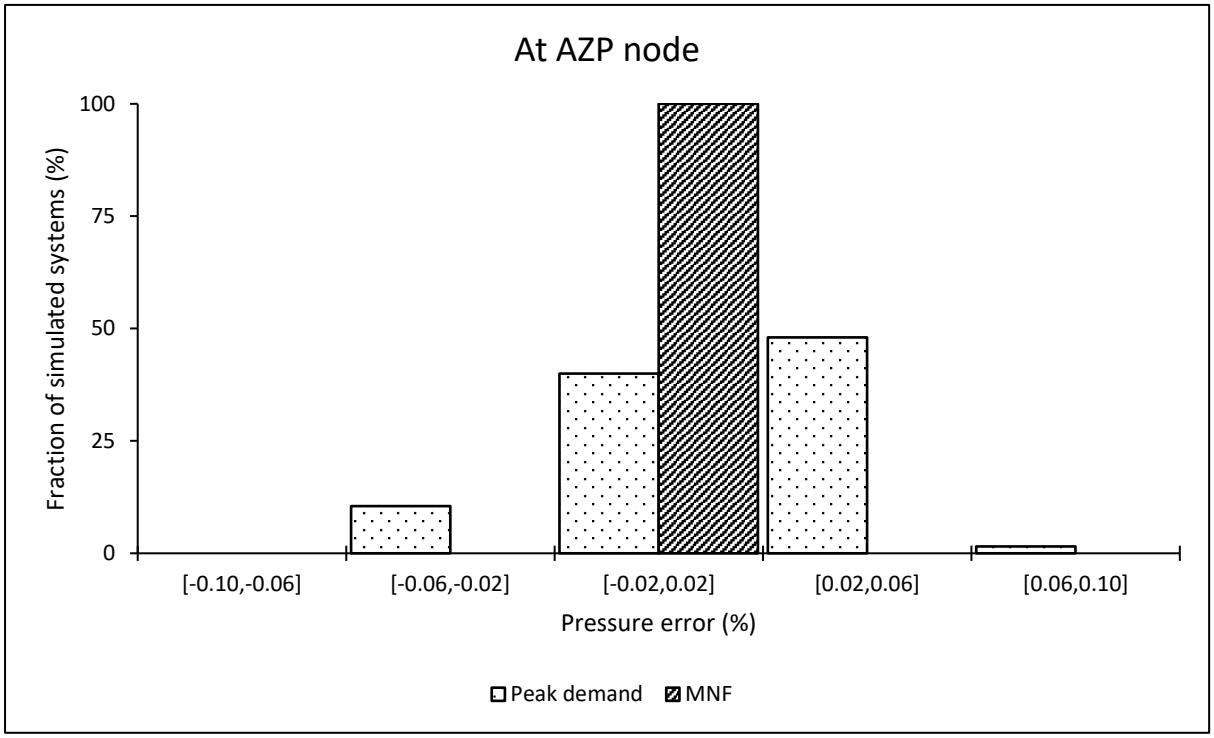

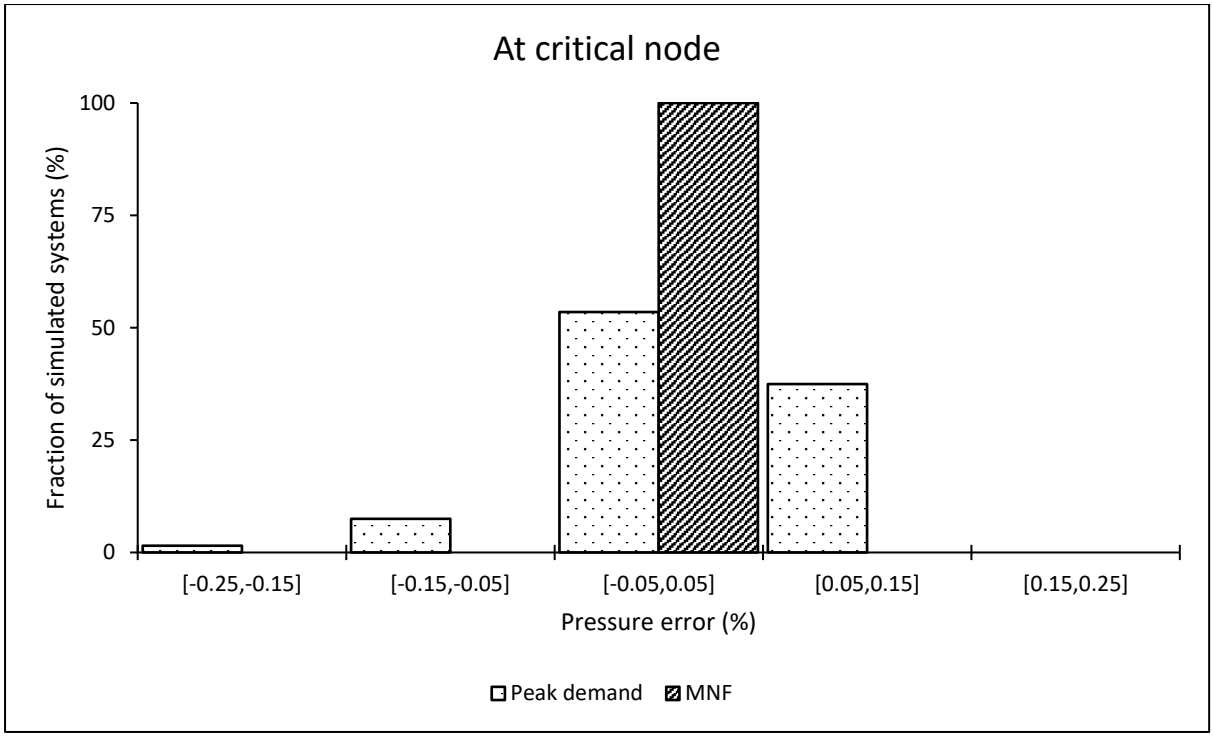
At critical node
Fraction of simulated systems (%)
100
75
50
25
0
[-0.25,-0.15]
[-0.15,-0.05]
[-0.05,0.05]
[0.05,0.15]
[0.15,0.25]
Pressure error (%)
Peak demand
MNF

System leakage estimation error when using the power equation

	Leakage estimation error (%)			
	Minimum	**Arithmetic Mean**	**Median**	**Maximum**
Before implementing pressure management	-0.21	-0.02	-0.03	0.22
After implementing pressure management	-20.55	-17.74	-17.95	-11.71

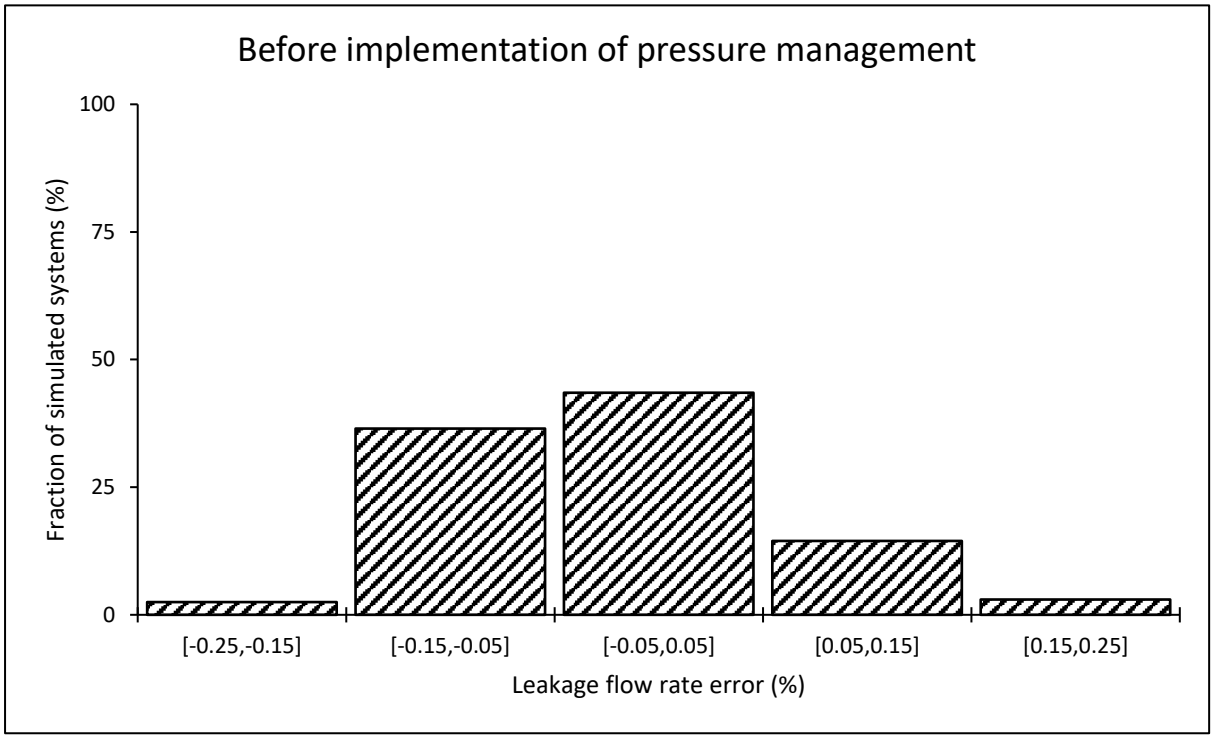

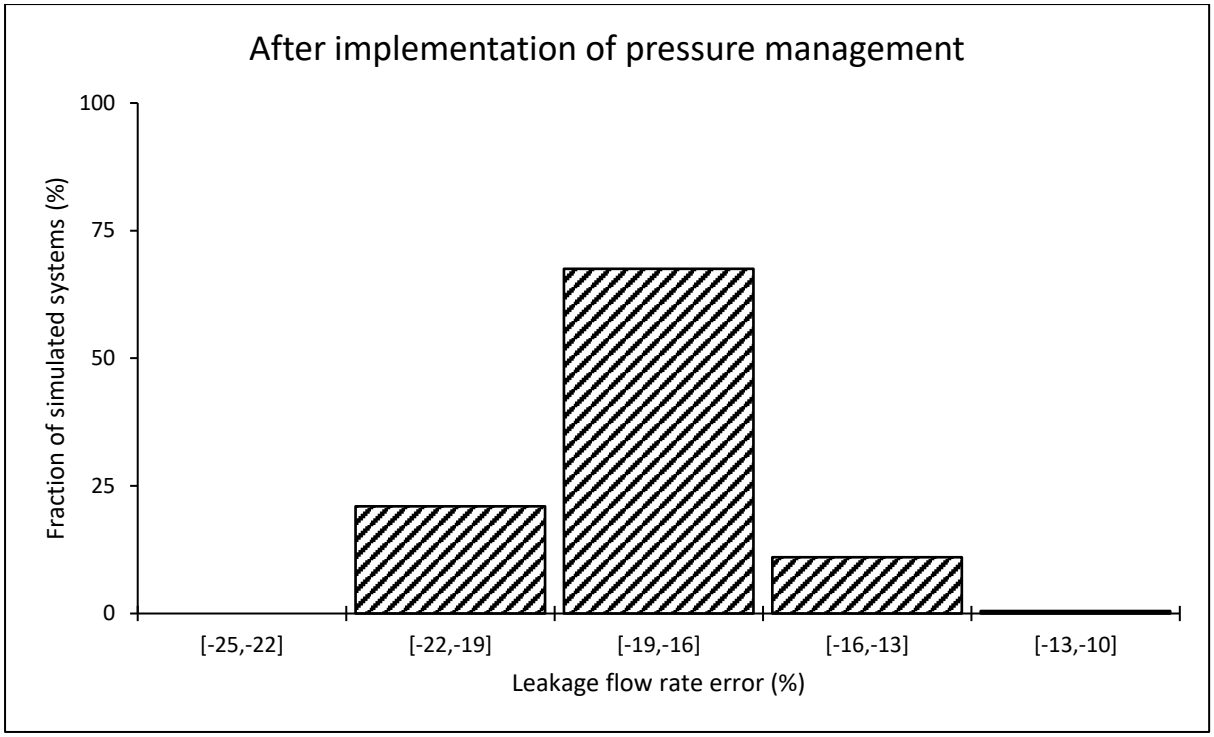
After implementation of pressure management
Fraction of simulated systems (%)
100
75
50
25
0
[-25,-22]
[-22,-19]
[-19,-16]
[-16,-13]
[-13,-10]
Leakage flow rate error (%)

Leakage estimation error when using the power equation at the critical node

	Leakage estimation error (%)			
	Minimum	**Arithmetic Mean**	**Median**	**Maximum**
Before implementing pressure management	-34.79	-4.64	-5.45	1.66
After implementing pressure management	-75.84	-58.64	-66.65	31.34

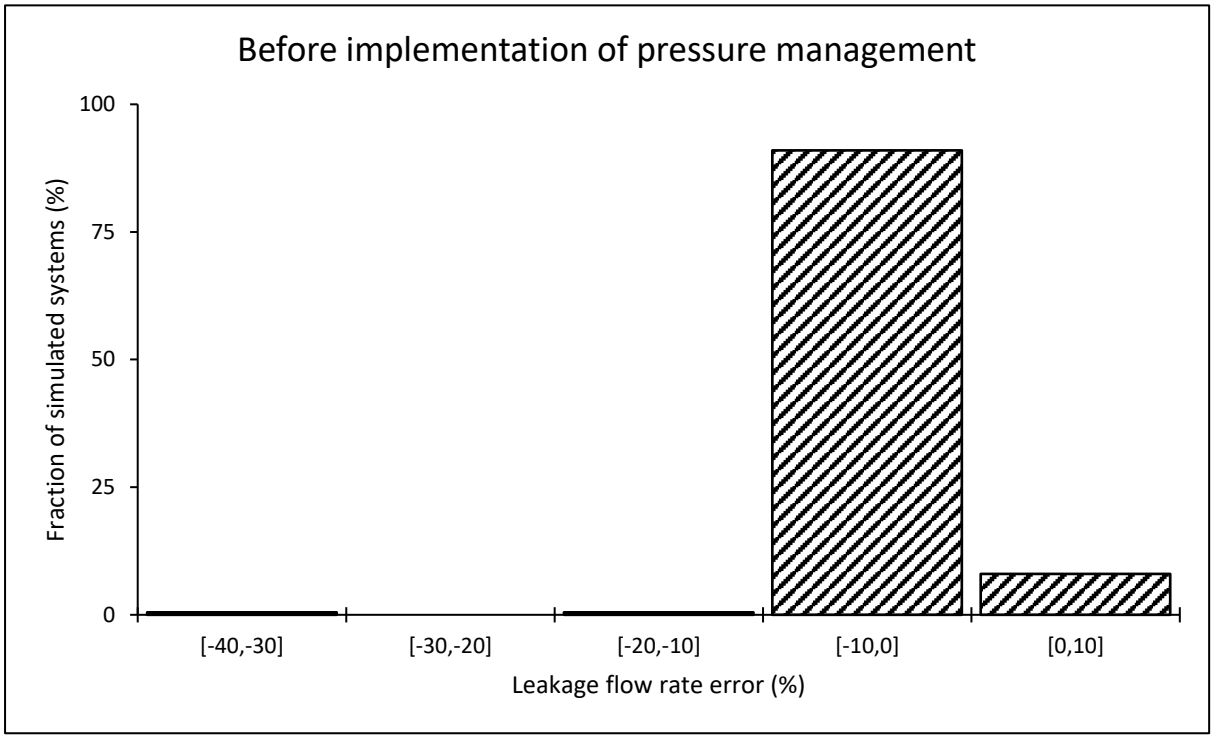

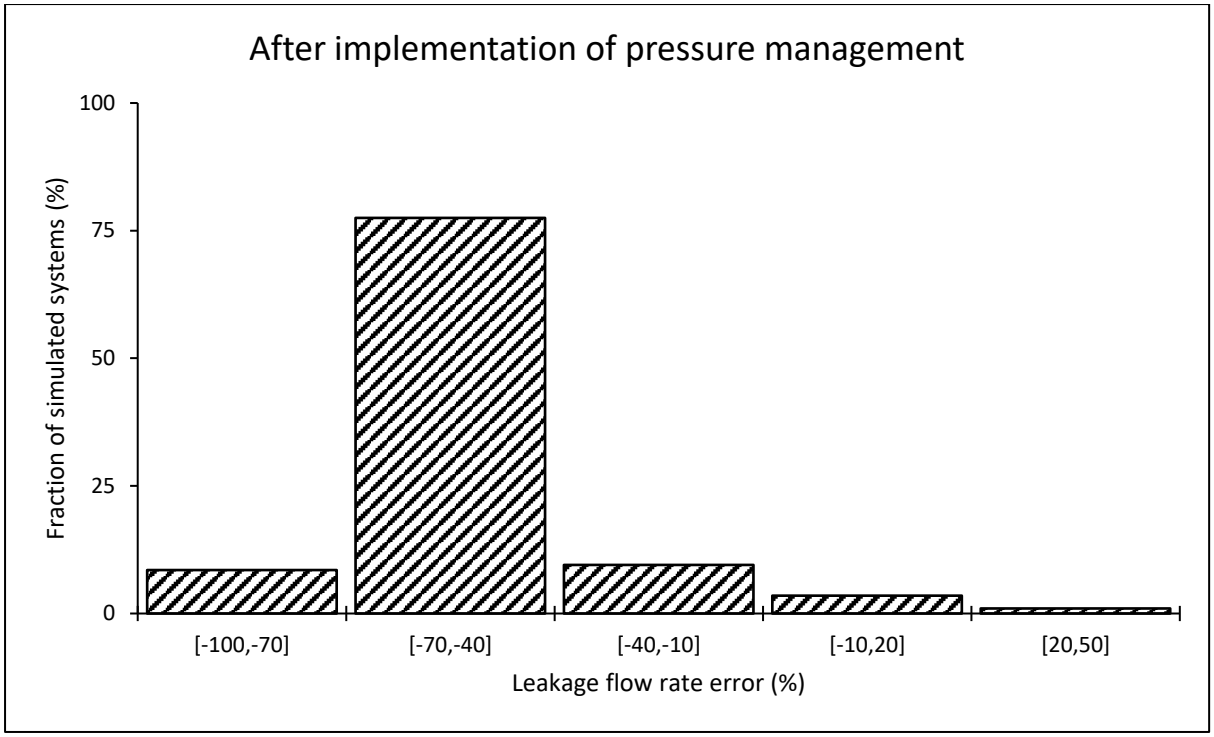
After implementation of pressure management
Fraction of simulated systems (%)
100
75
50
25
0
[-100,-70]
[-70,-40]
[-40,-10]
[-10,20]
[20,50]
Leakage flow rate error (%)

Appendix B-1: Impact of the leakage level (ILIs of 1, 4, 16 and 64) on simulation results for small systems

System leakage exponents of the power equation

Infrastructure Leakage Index (ILI)	System leakage exponents (N1)			
	Minimum	Arithmetic Mean	Median	Maximum
1	0.63	0.65	0.64	0.72
4	0.54	0.62	0.58	0.96
16	0.65	0.92	0.91	1.25
64	0.89	1.08	1.07	1.37

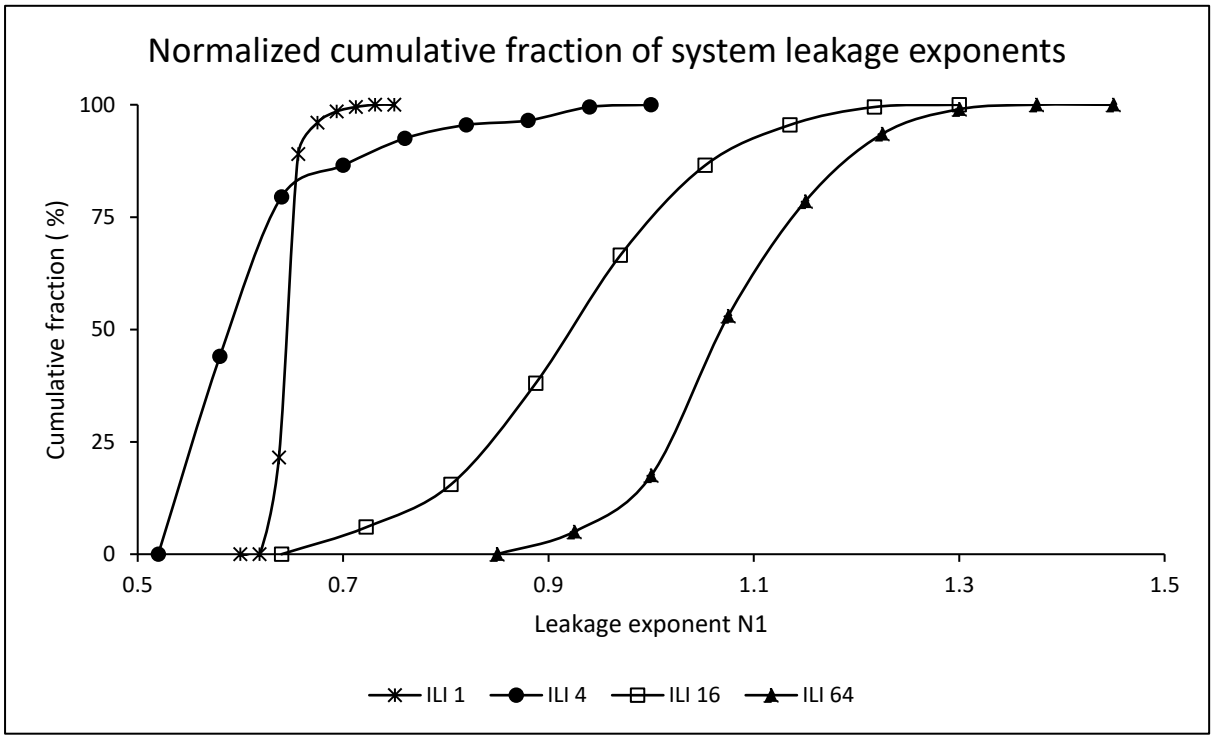

Predicting the system parameters for the modified orifice equation

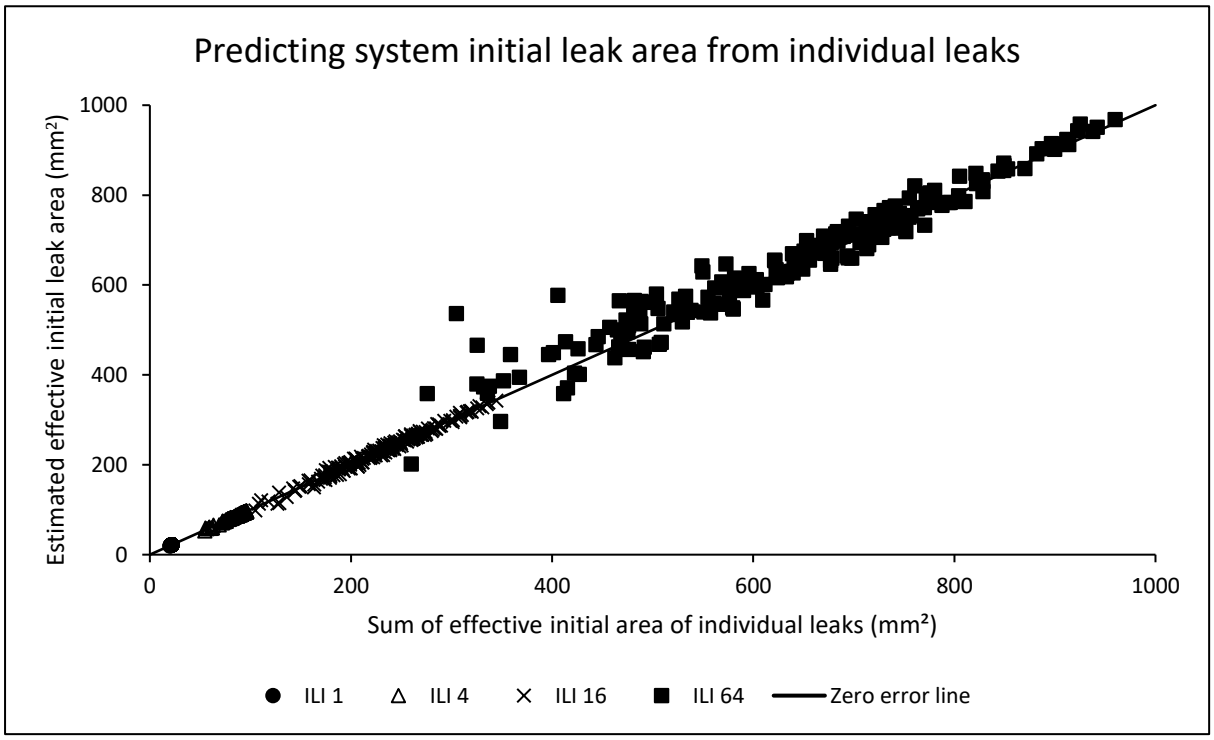

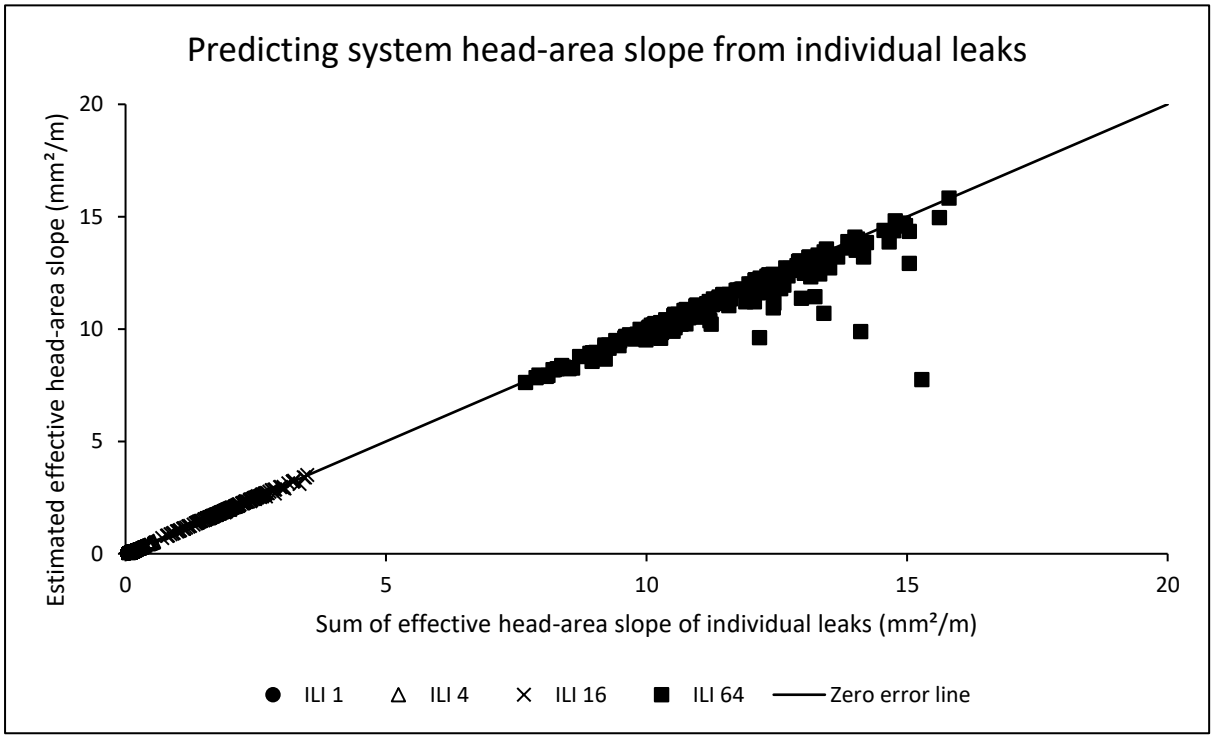

Pressure estimation error when using the power equation at the AZP node

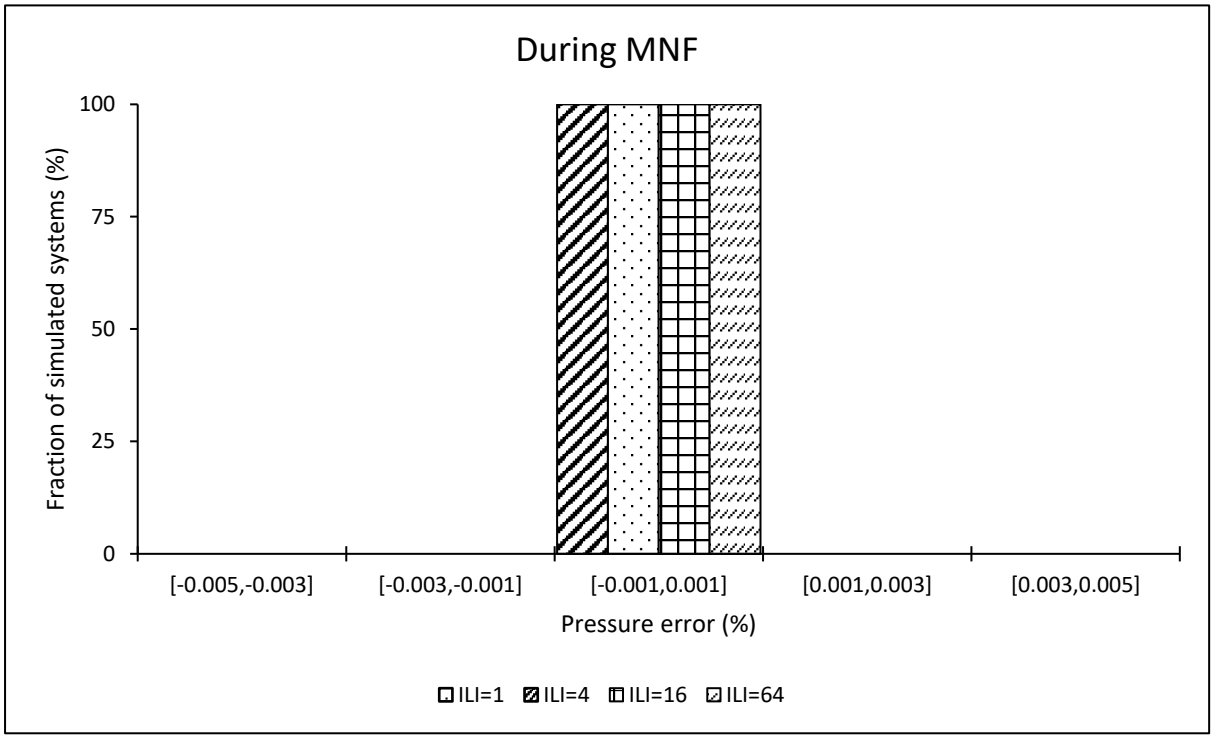

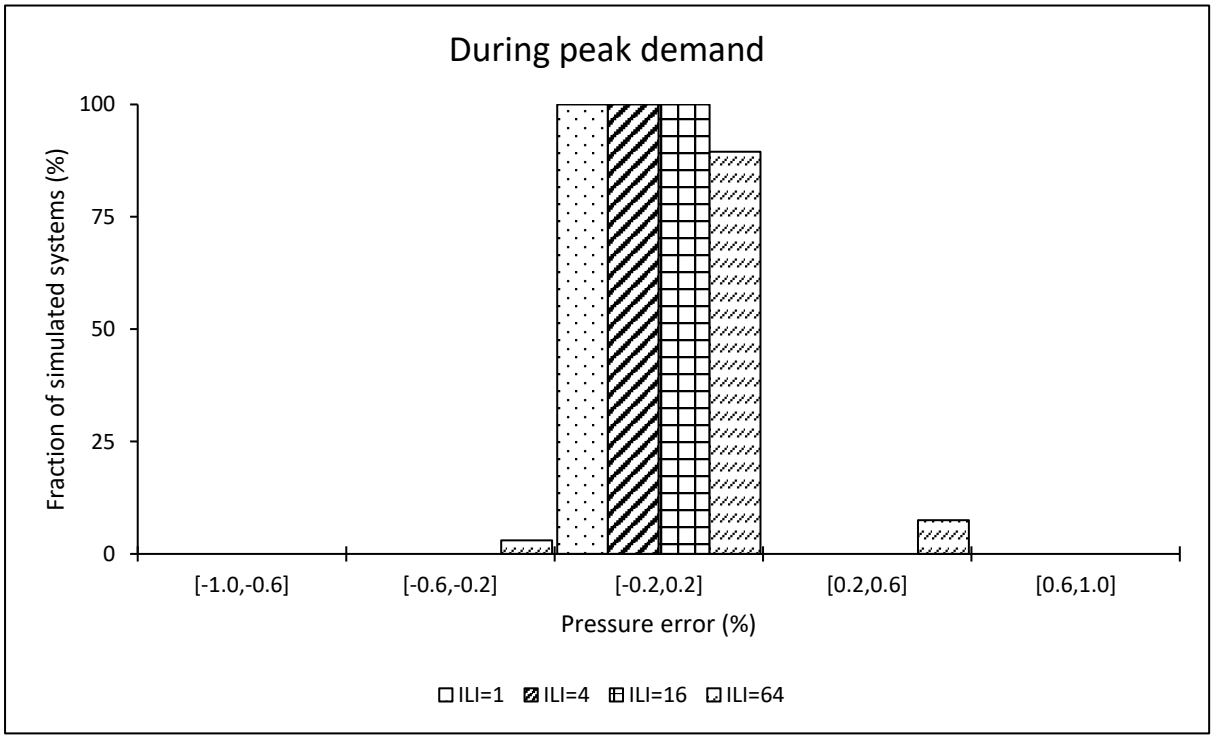

System leakage estimation error when using the power equation

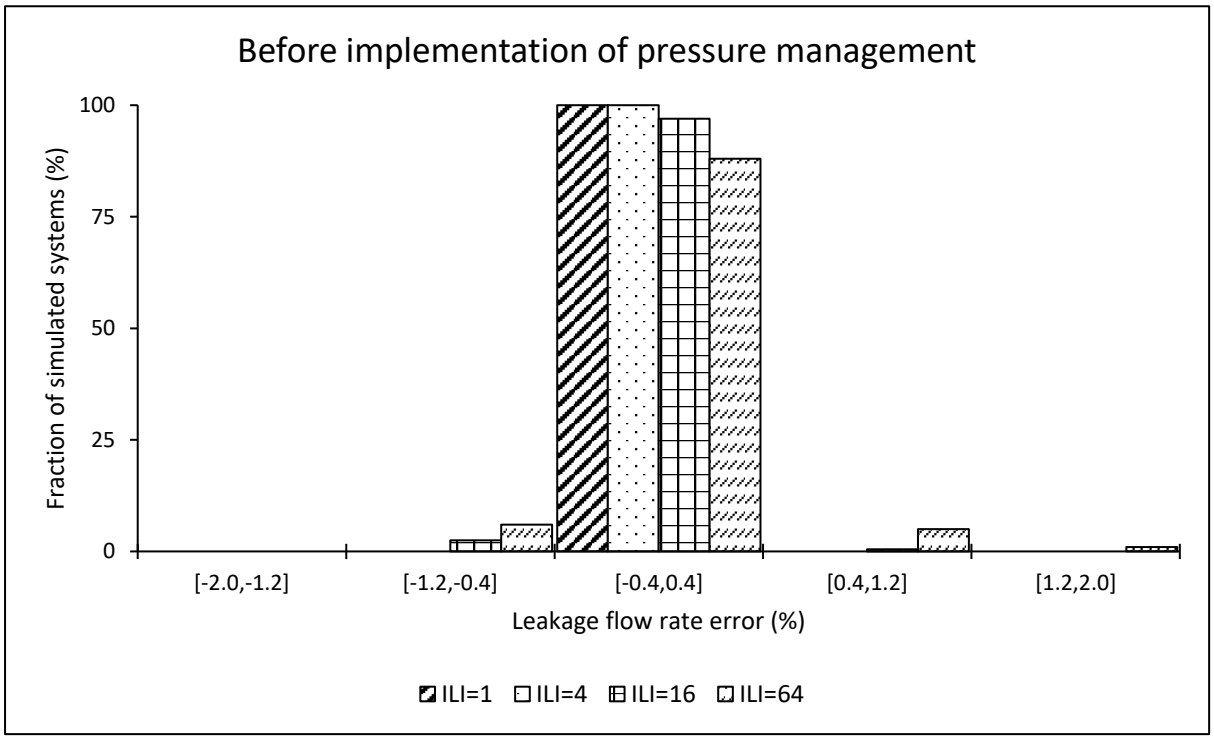

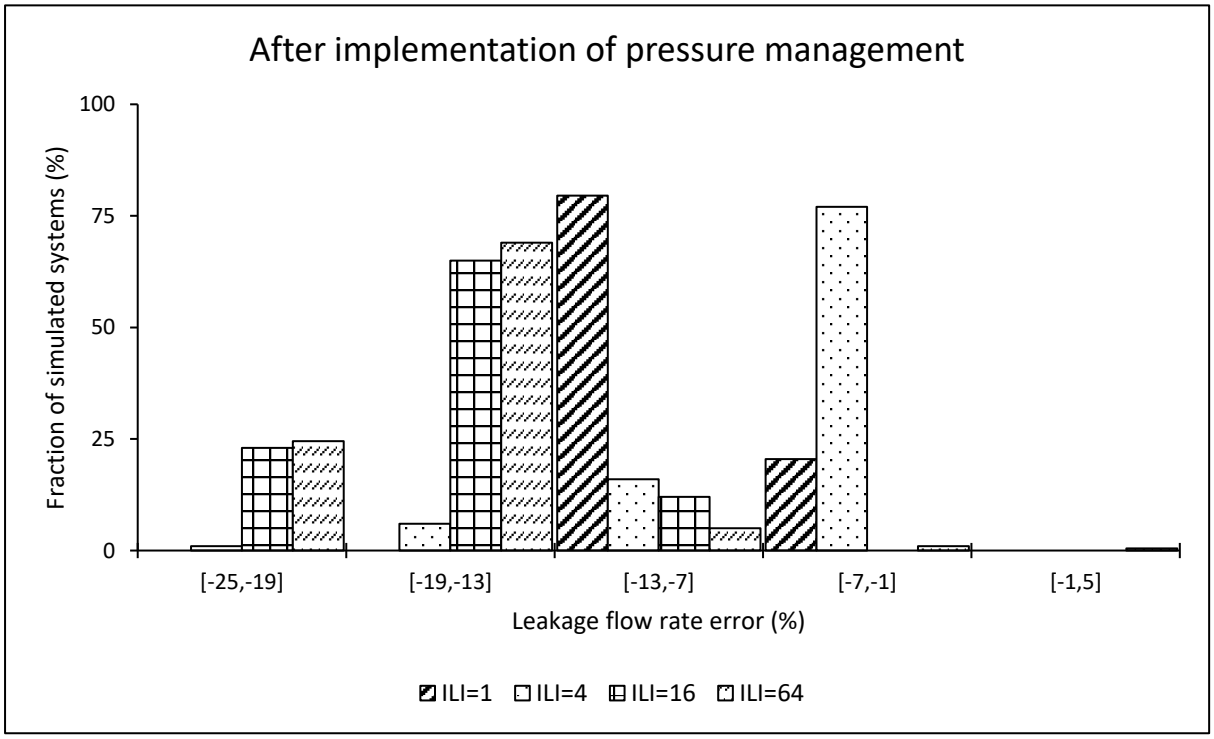

Leakage estimation error when using the power equation at the critical node

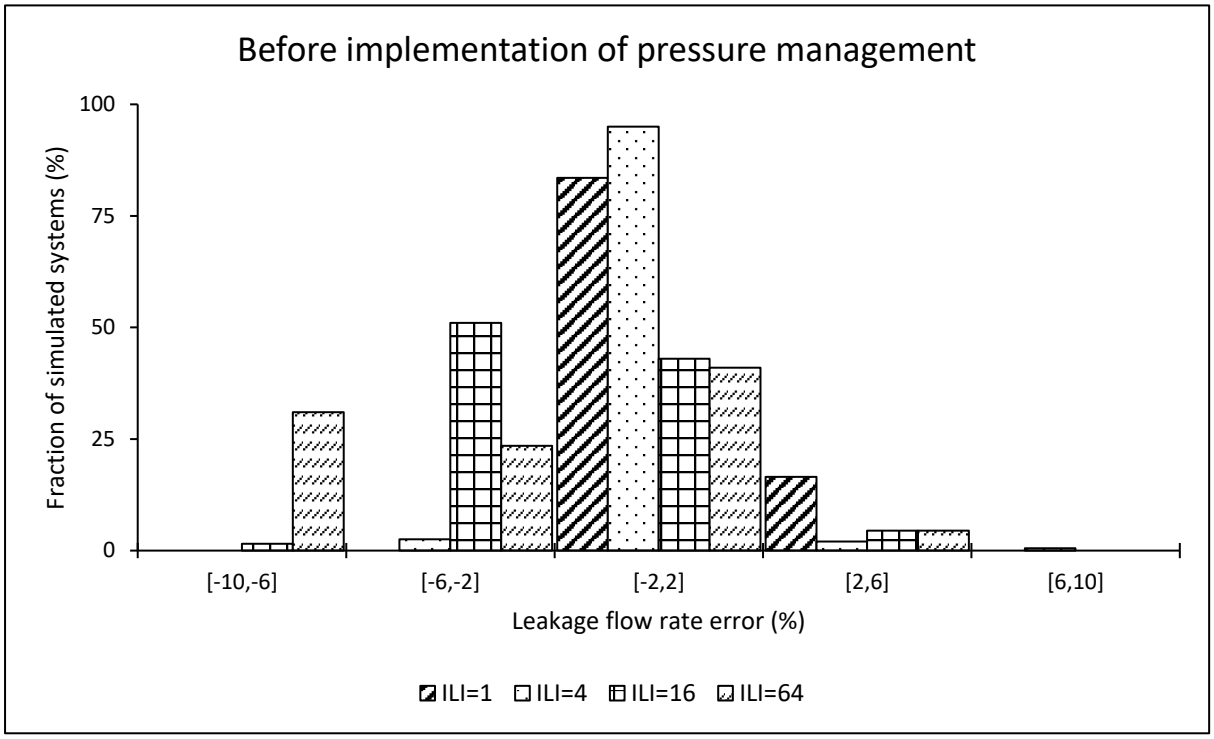

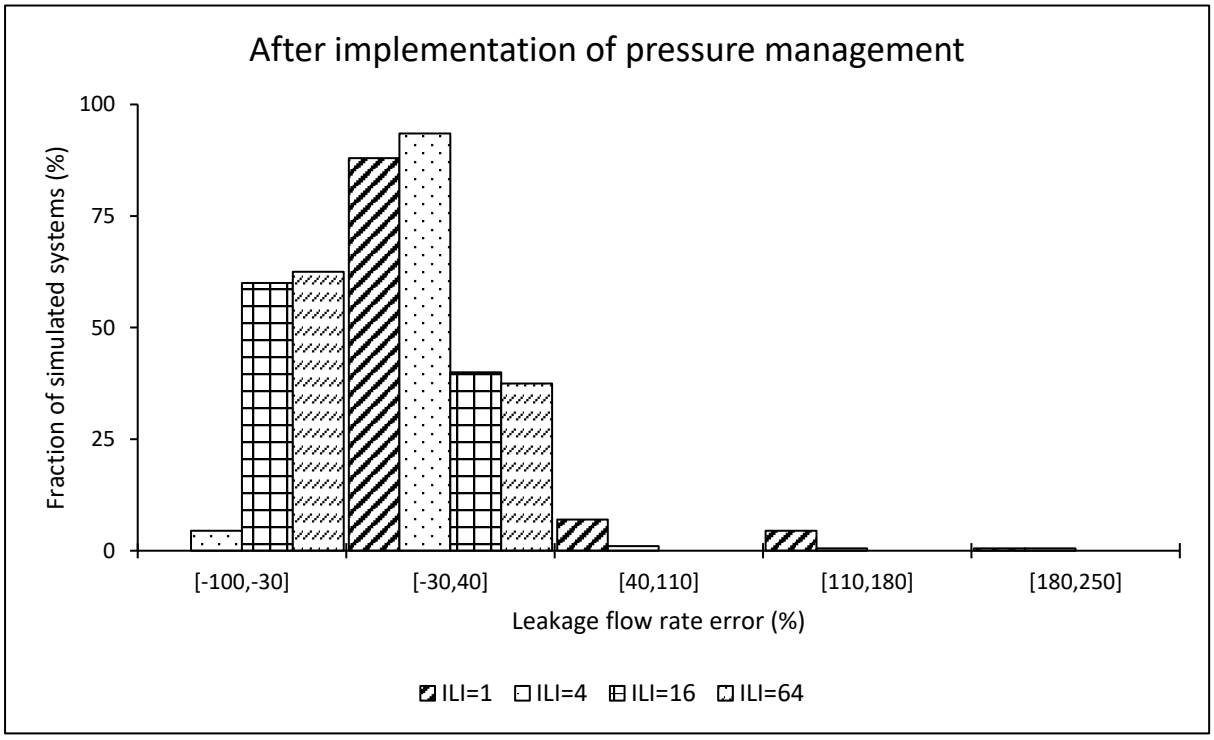

Appendix B-2: Impact of the leakage level (ILIs of 1, 4, 16 and 64) on simulation results for medium systems

System leakage exponents of the power equation

Infrastructure Leakage Index (ILI)	System leakage exponents (N1)			
	Minimum	Arithmetic Mean	Median	Maximum
1	0.64	0.68	0.67	0.83
4	0.57	0.83	0.84	1.10
16	0.81	1.07	1.07	1.35
64	1.06	1.18	1.18	1.40

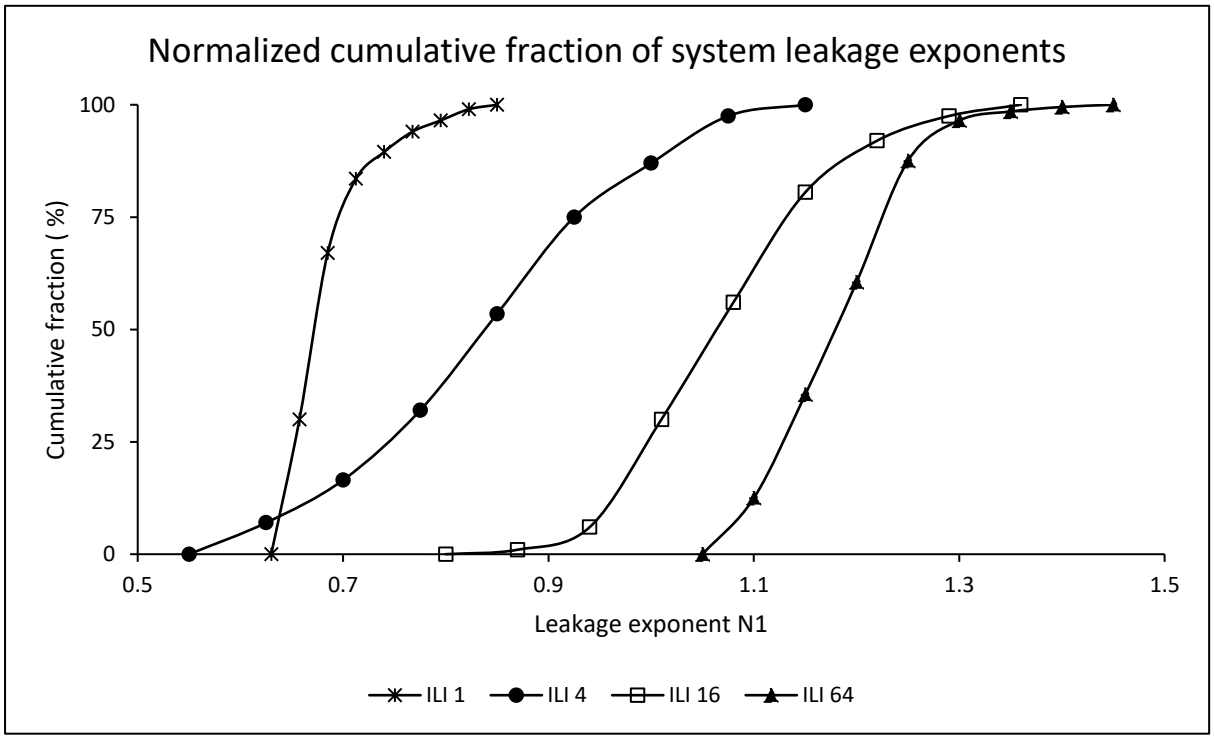

Predicting the system parameters for the modified orifice equation

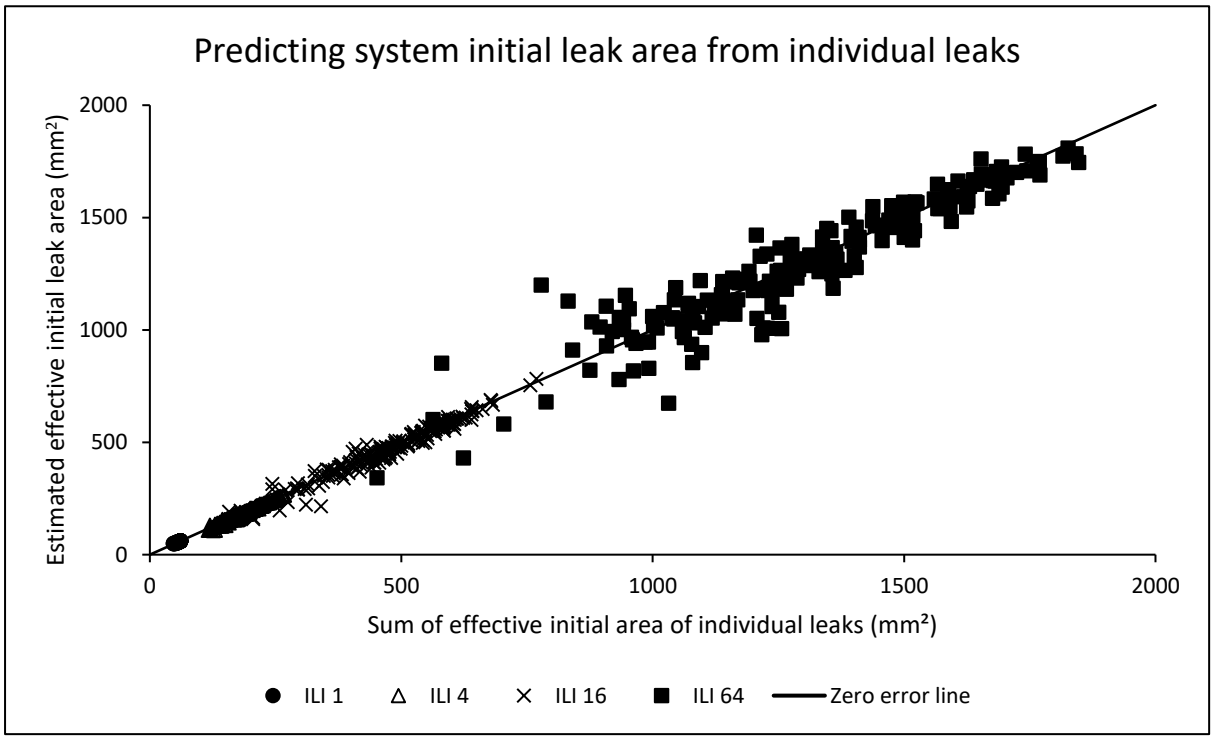

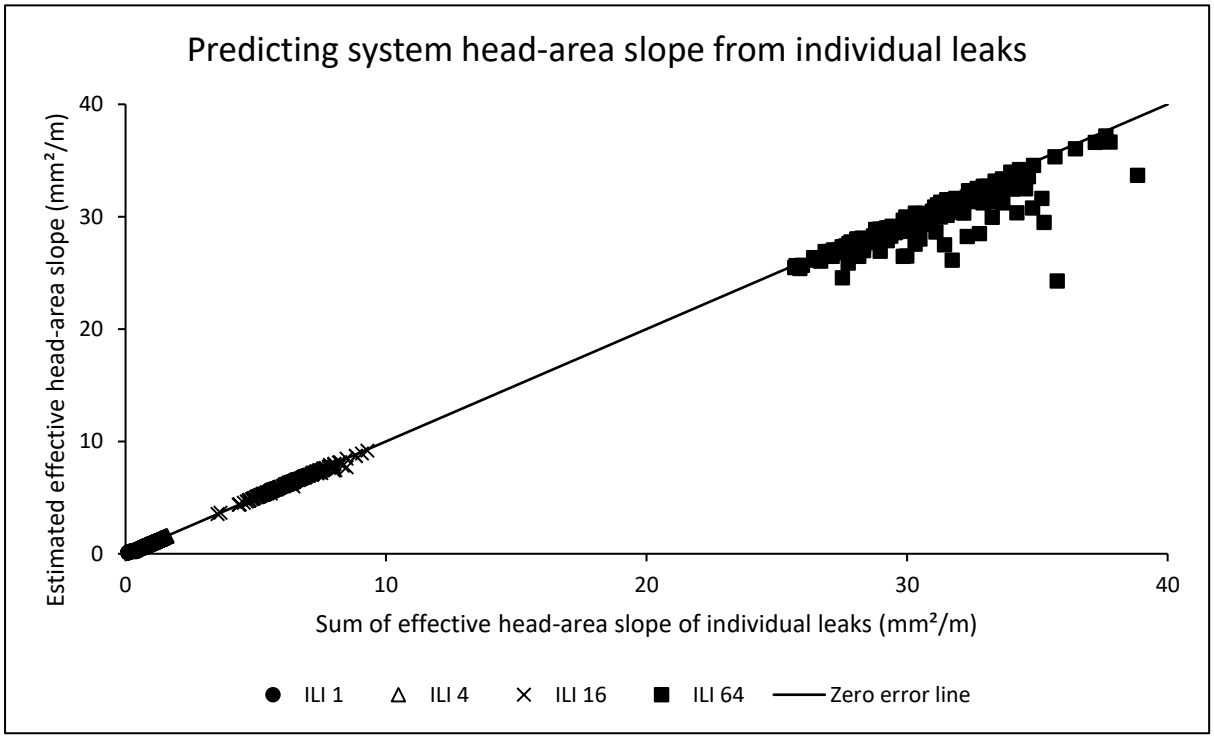

Pressure estimation error when using the power equation at the AZP node

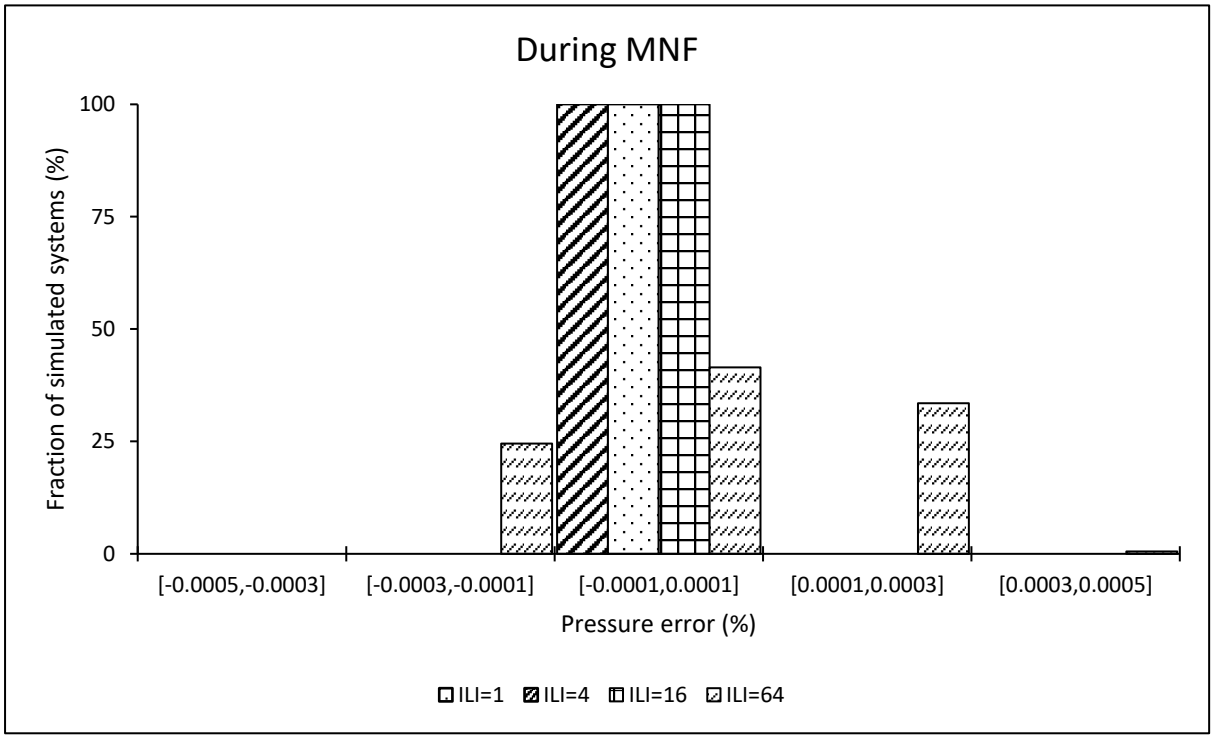

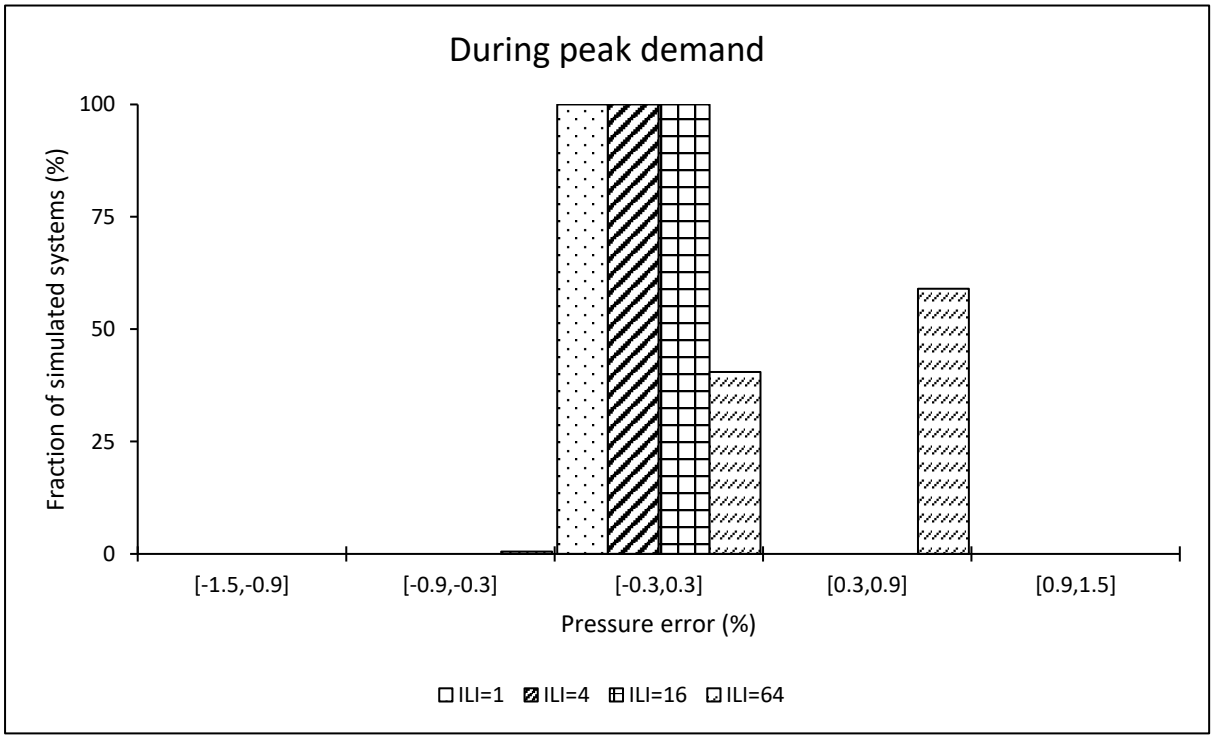

System leakage estimation error when using the power equation

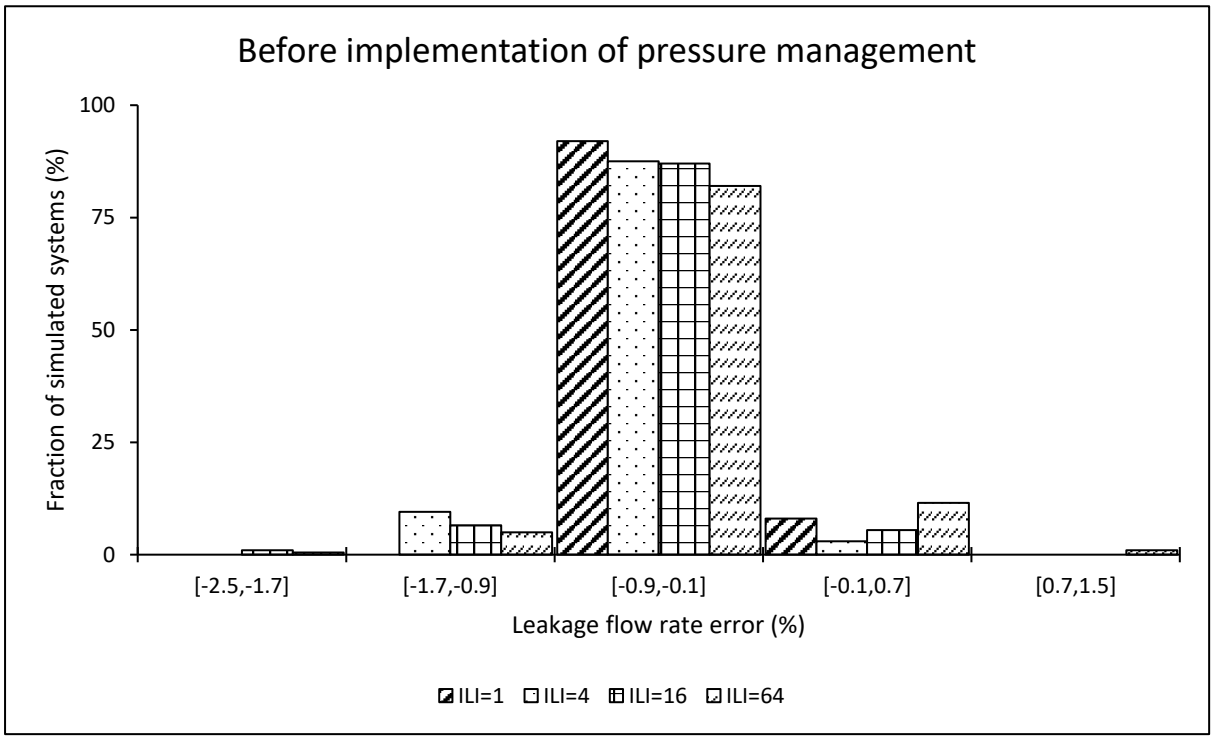

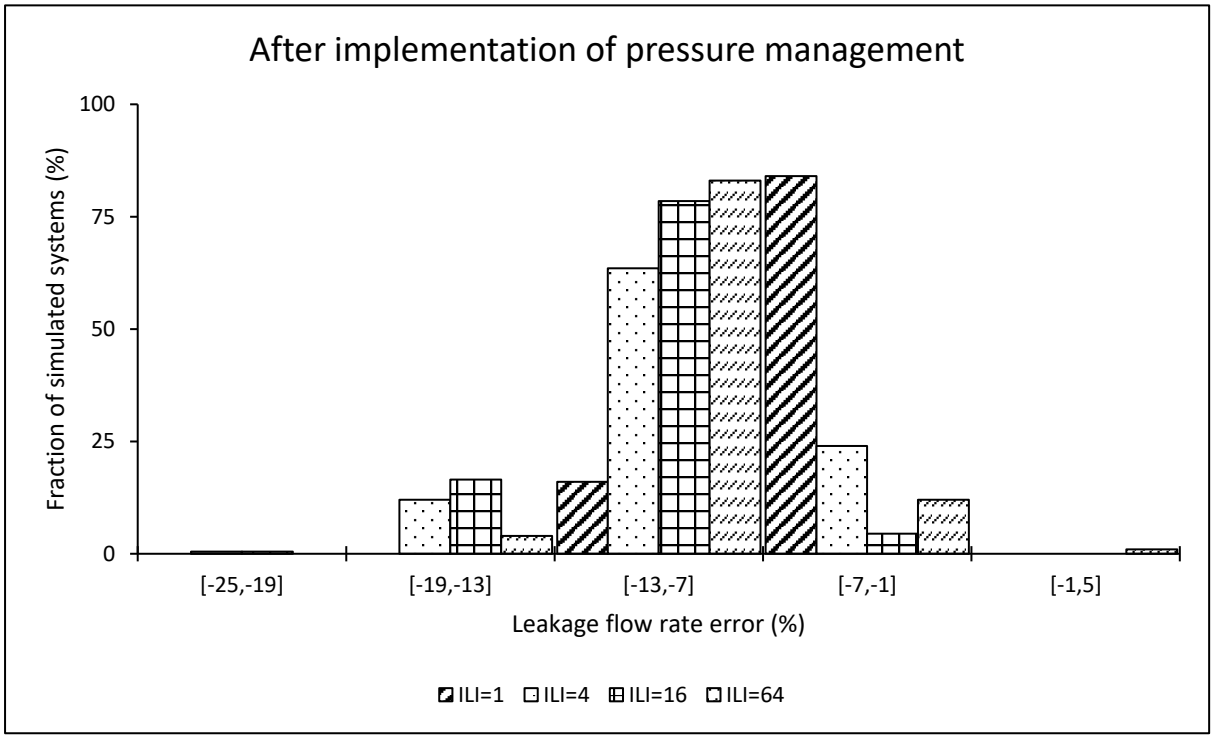

Leakage estimation error when using the power equation at the critical node

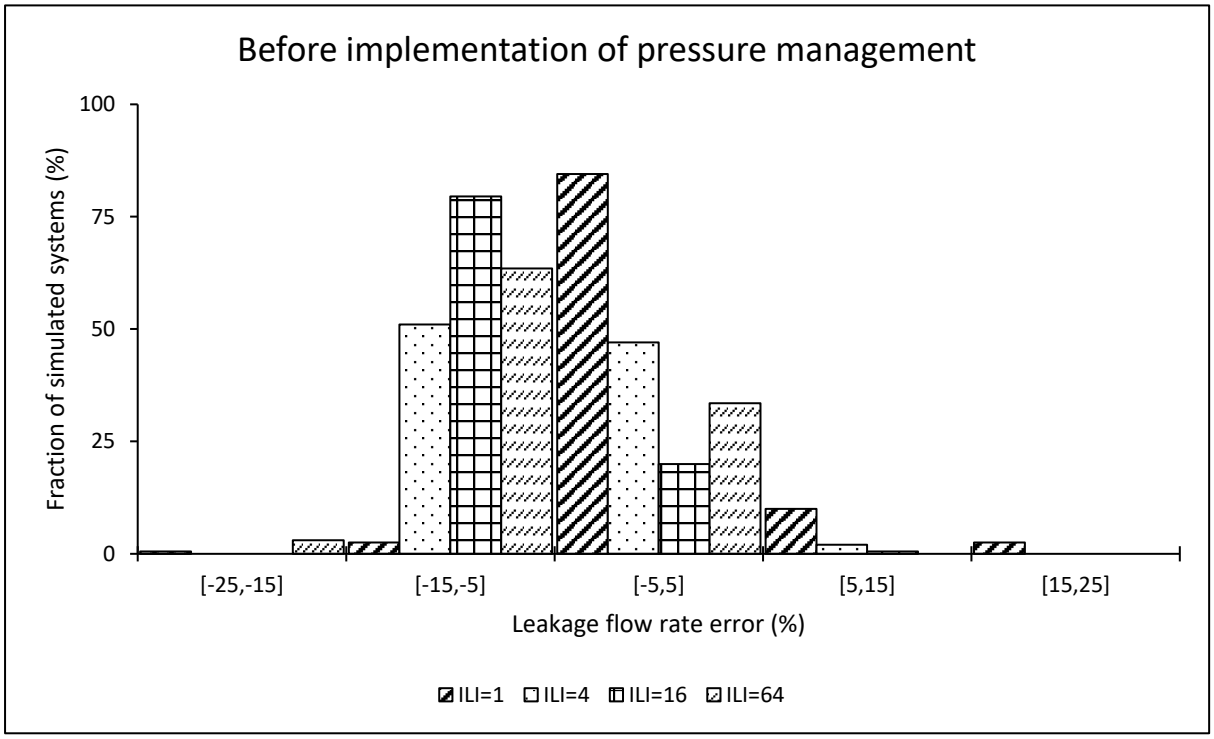

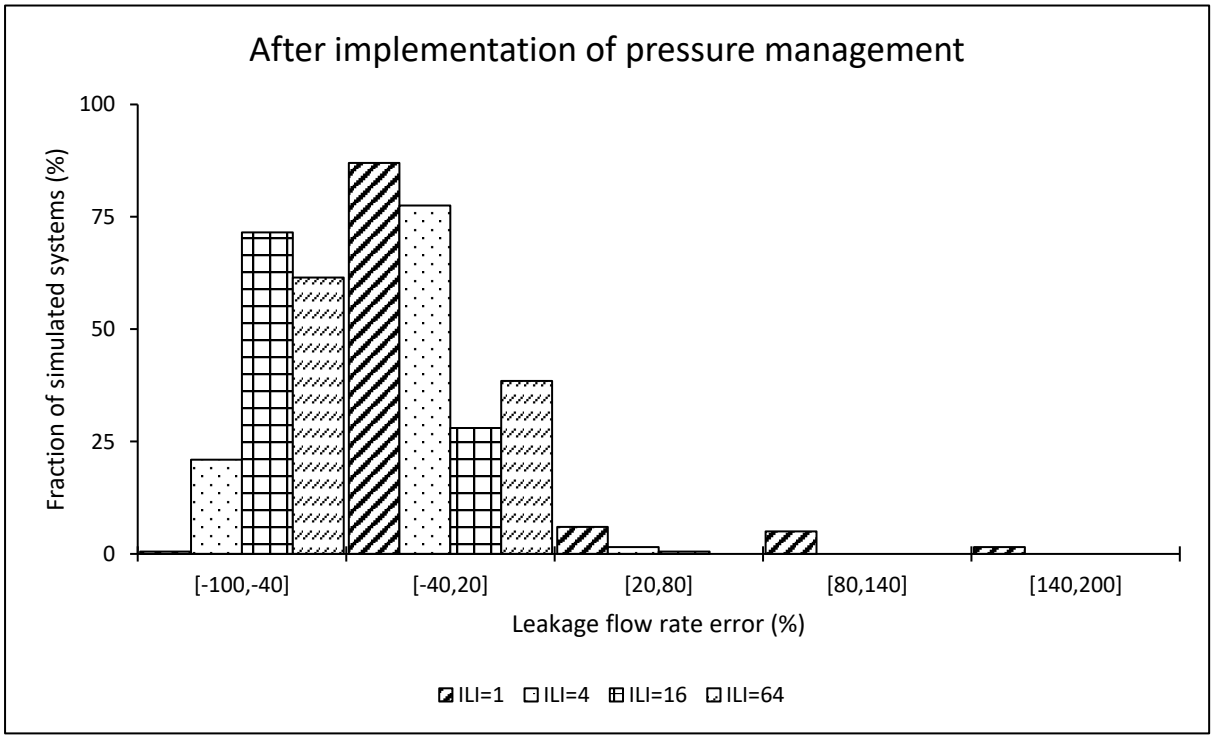

Appendix B-3: Impact of the leakage level (ILIs of 1, 4, 16 and 64) on simulation results for large systems

System leakage exponents of the power equation

Infrastructure Leakage Index (ILI)	System leakage exponents (N1)			
	Minimum	Arithmetic Mean	Median	Maximum
1	0.65	0.72	0.70	0.97
4	0.76	0.98	0.98	1.26
16	0.99	1.16	1.16	1.37
64	1.08	1.21	1.21	1.31

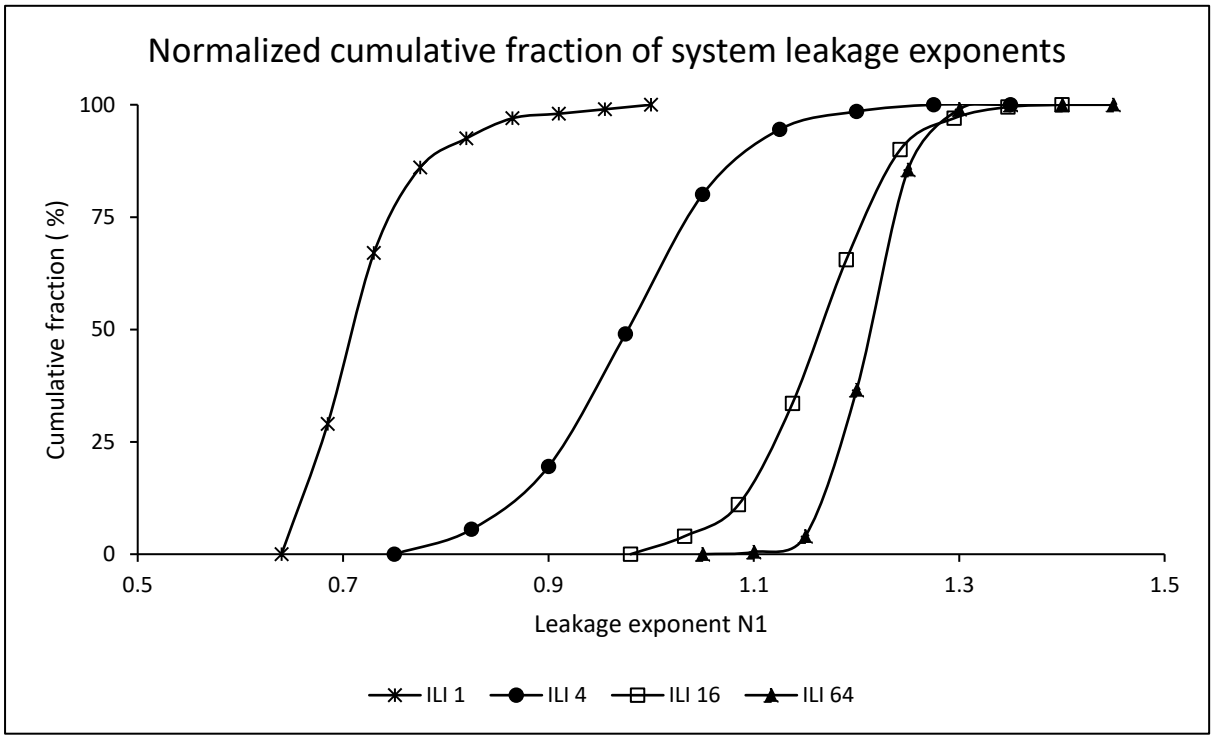

Predicting the system parameters for the modified orifice equation

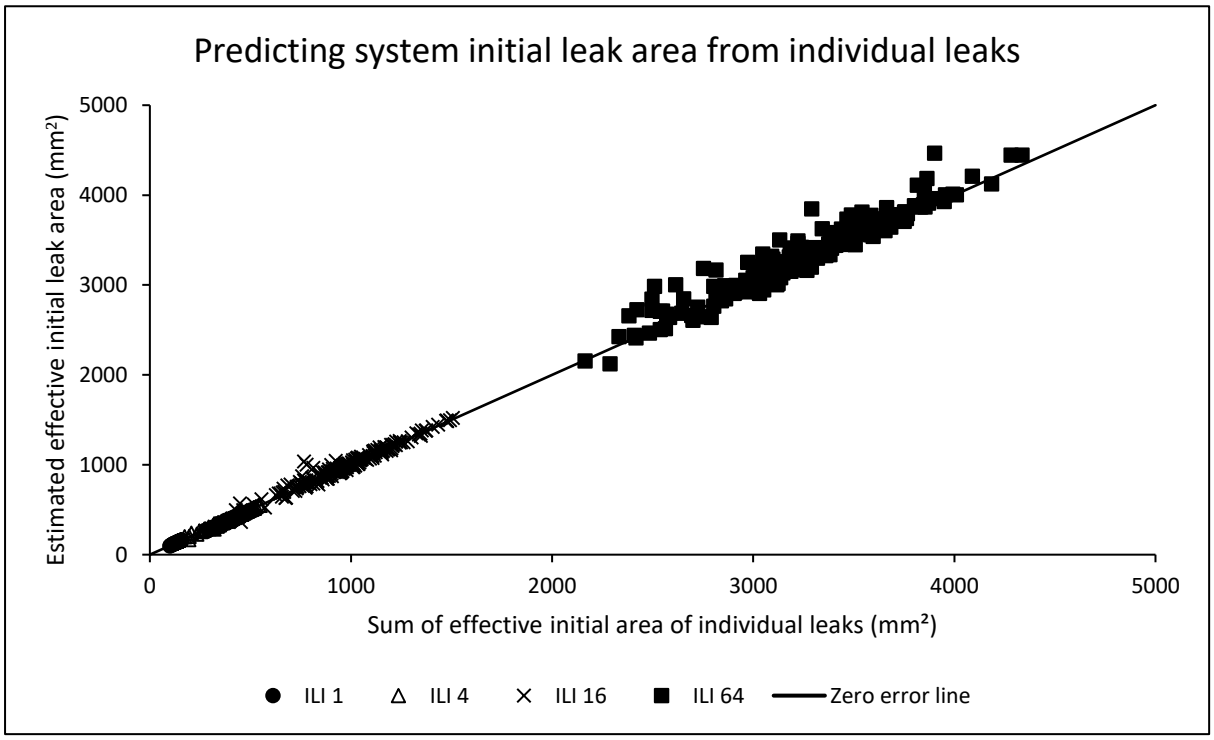

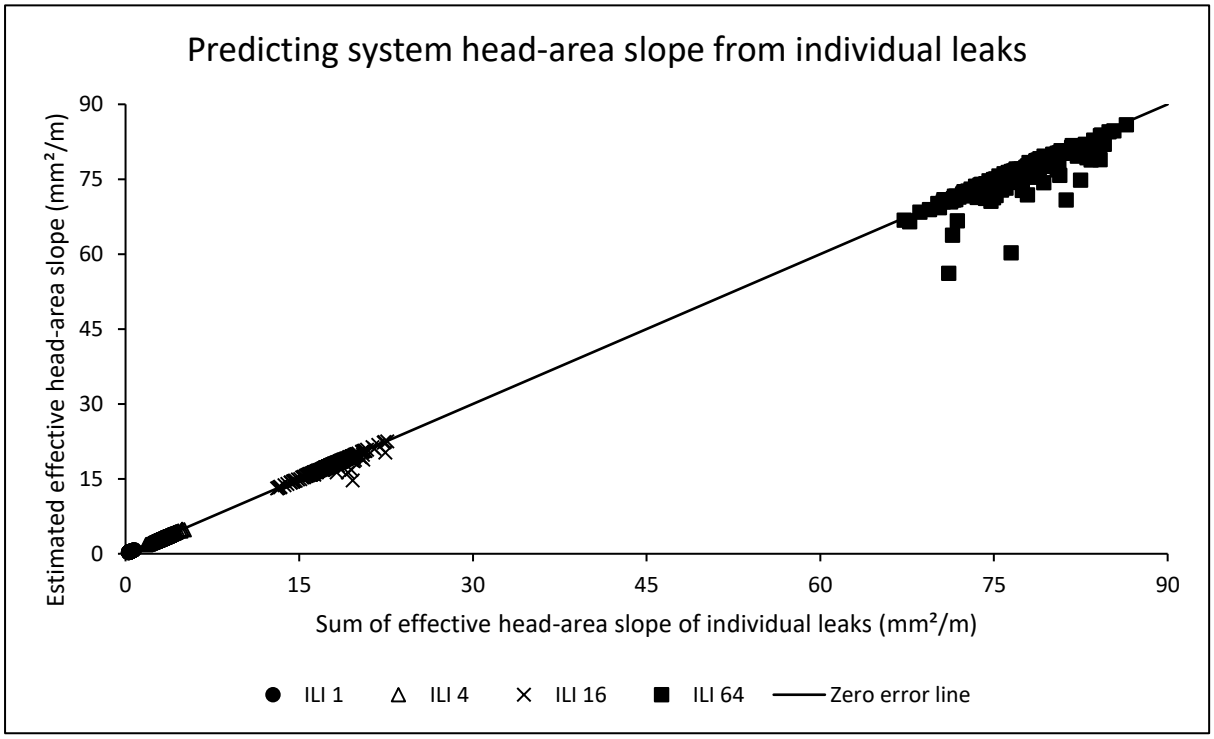

Pressure estimation error when using the power equation at the AZP node

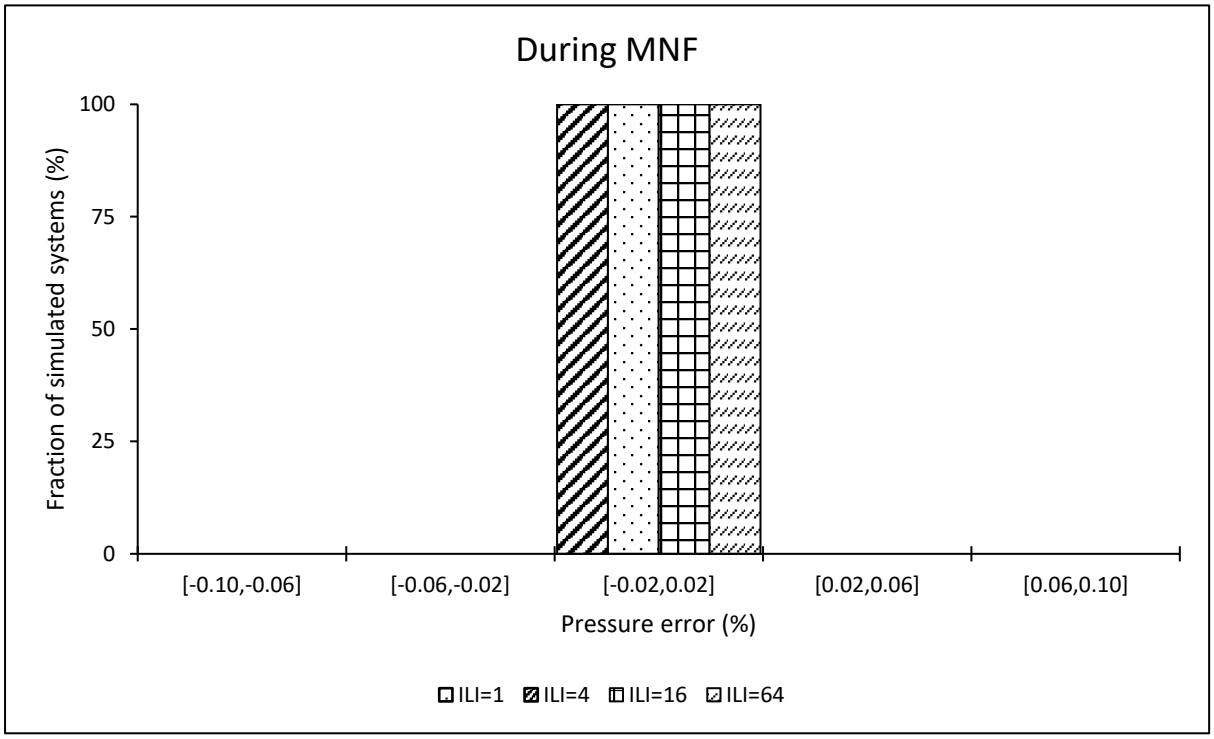

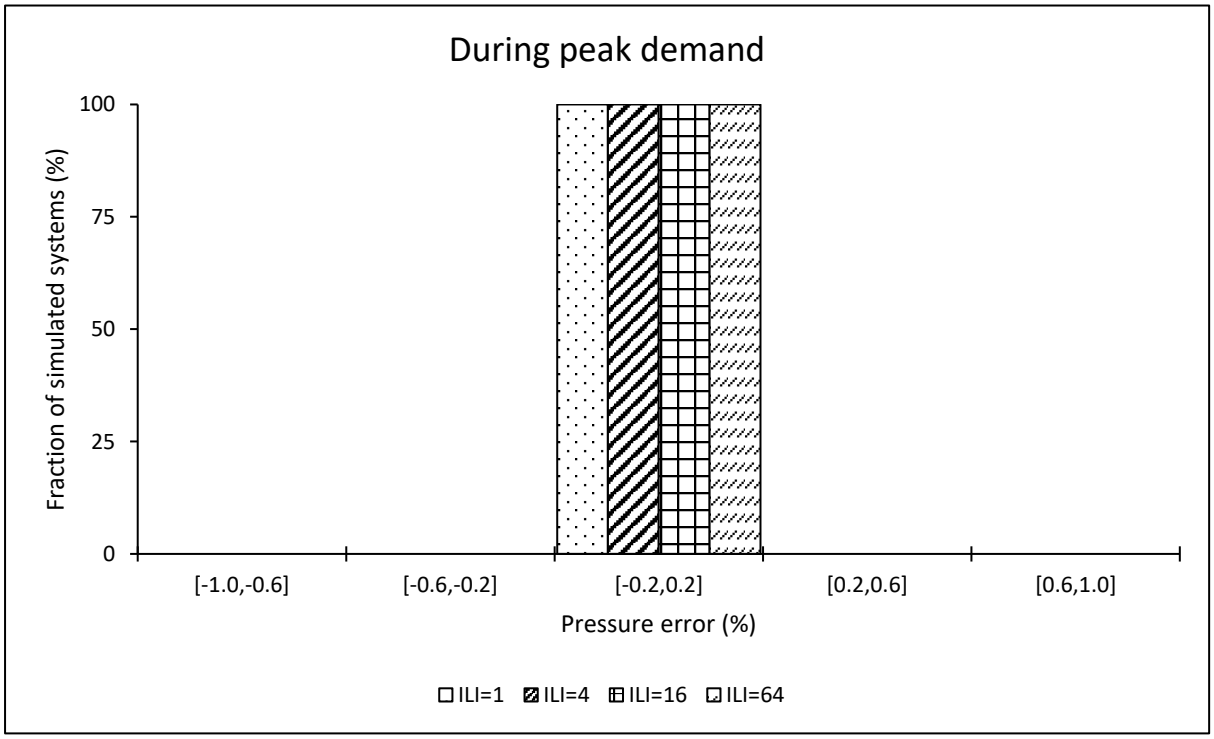

System leakage estimation error when using the power equation

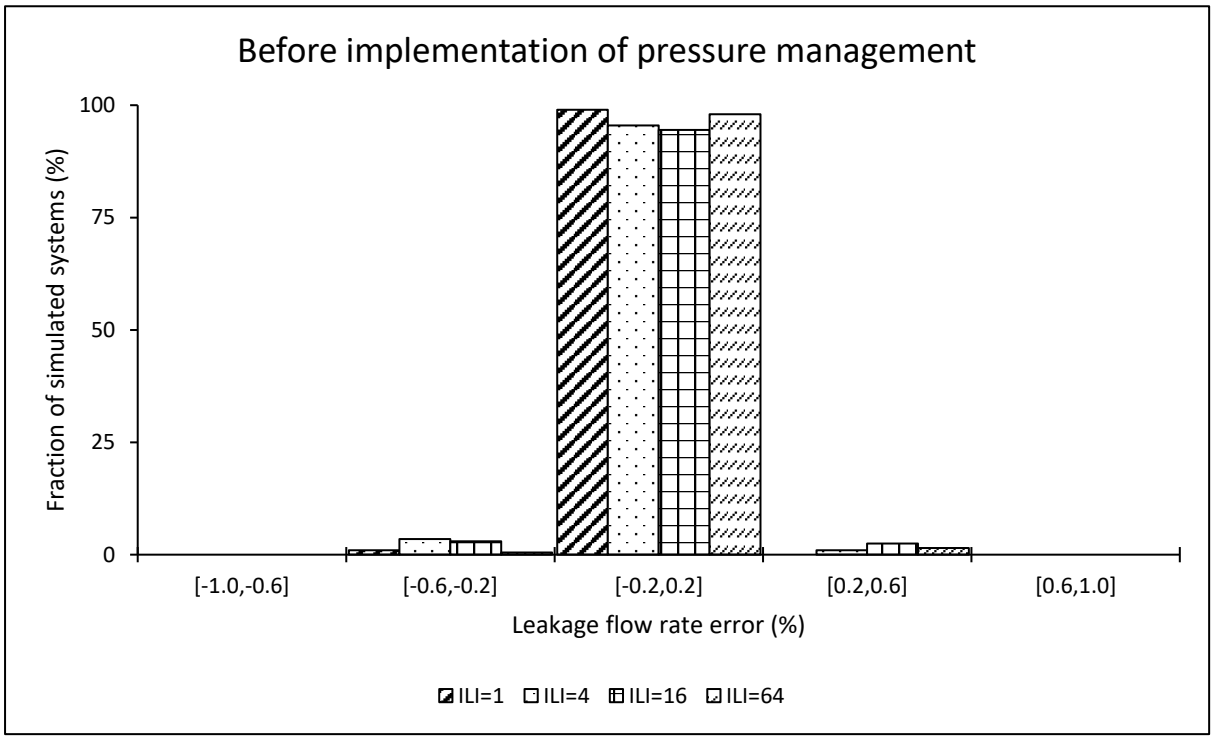

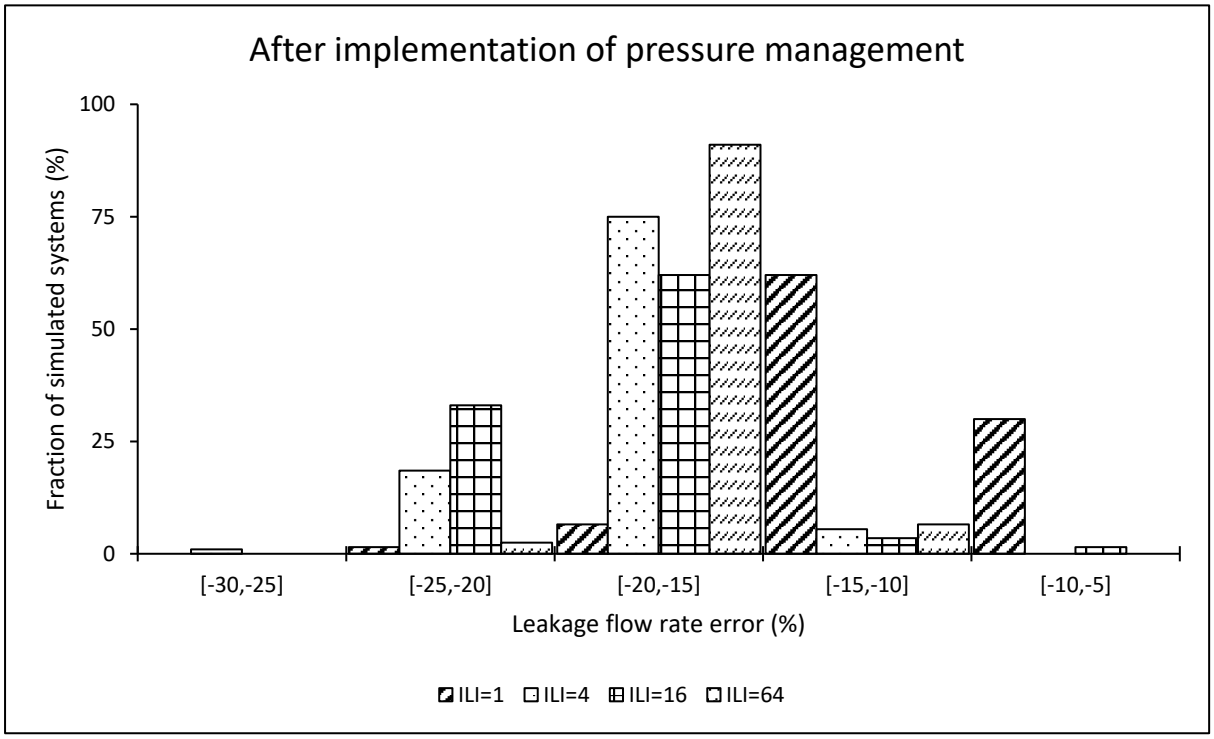

Leakage estimation error when using the power equation at the critical node

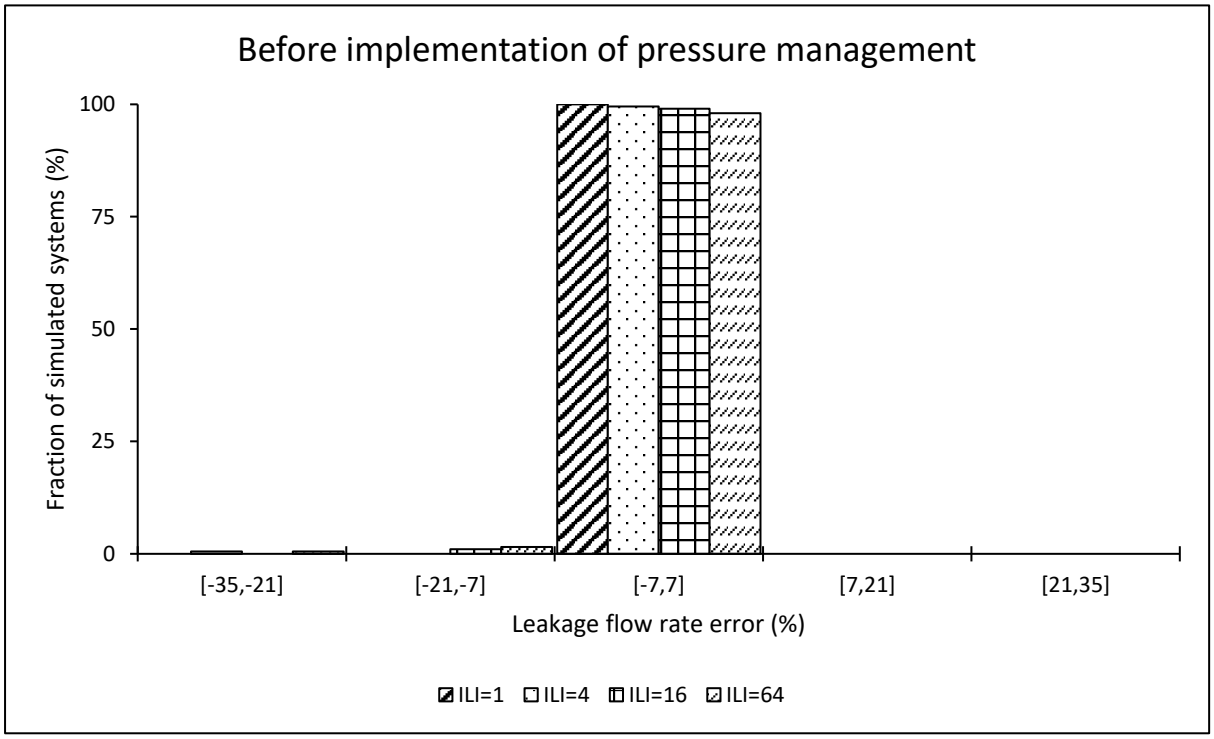

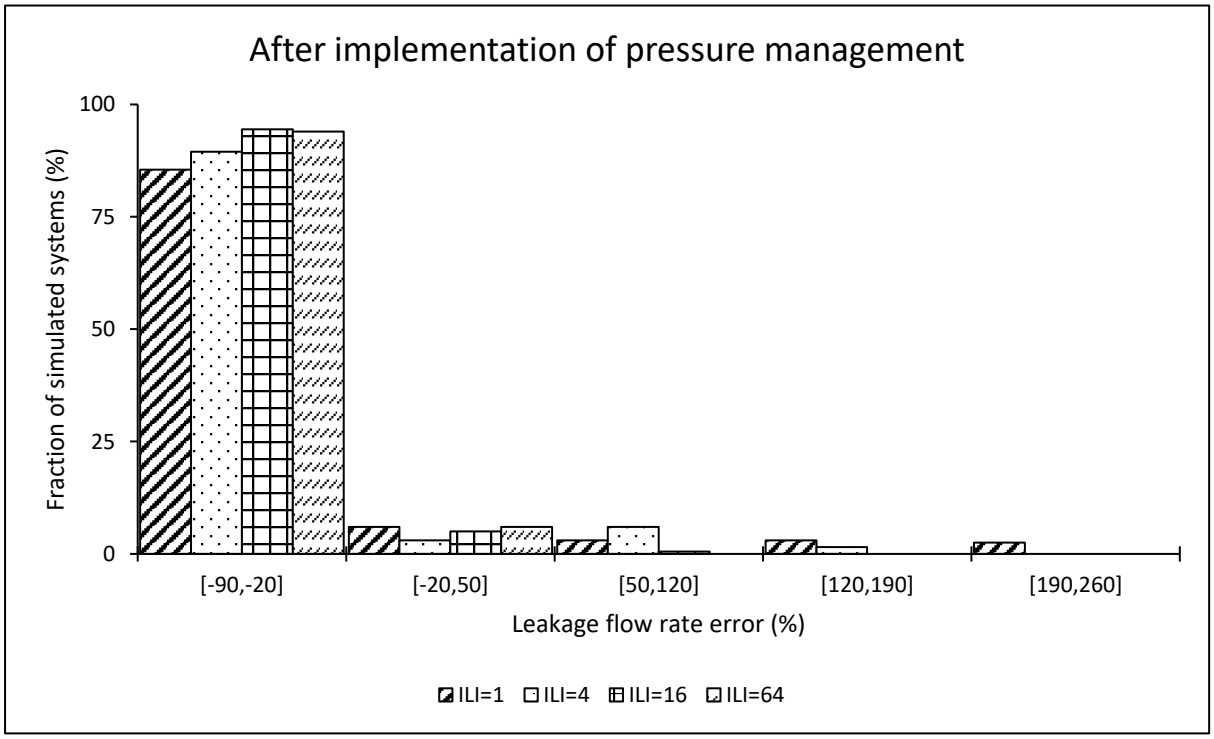

Appendix C-1: Impact of network size on simulation results for systems with leakage equivalent to ILI of 1

Impact on the system leakage exponents of the power equation

	System leakage exponents (N1)			
	Minimum	**Arithmetic Mean**	**Median**	**Maximum**
Small	0.63	0.64	0.64	0.72
Medium	0.64	0.68	0.67	0.83
Large	0.65	0.72	0.70	0.97

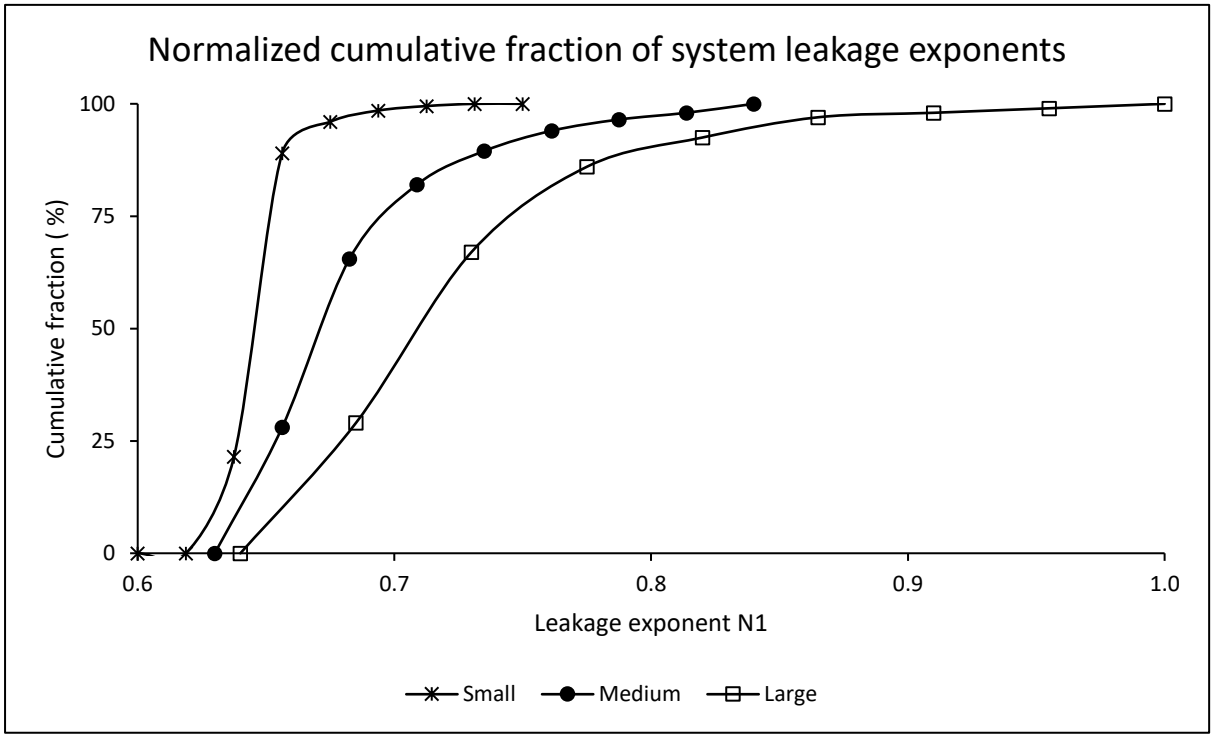

Impact on predicting the system parameters for the modified orifice equation

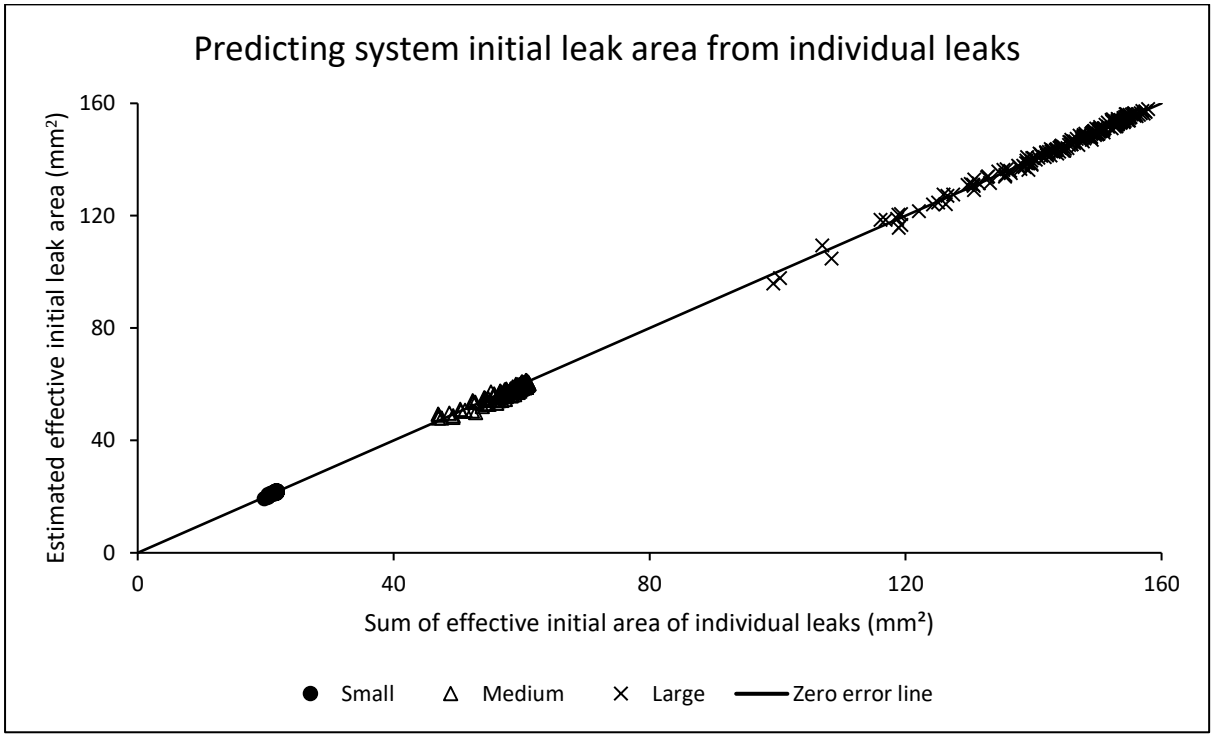

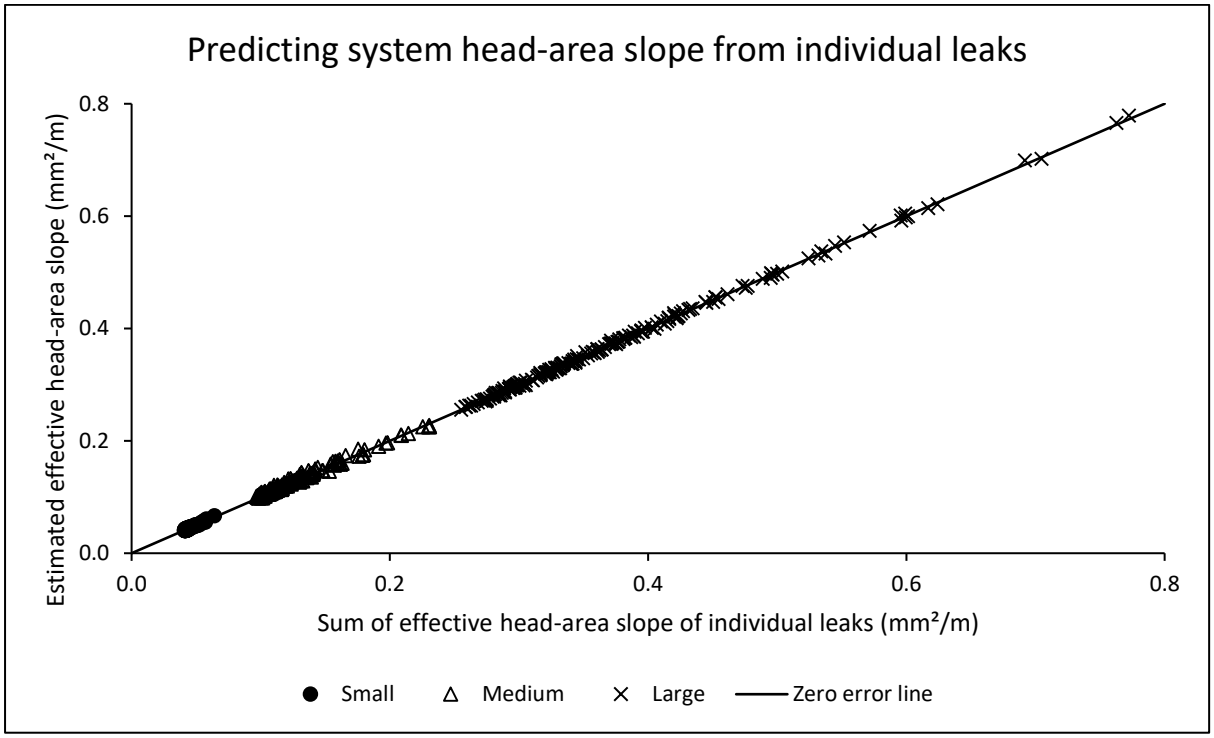

Impact on the pressure estimation error when using the power equation at the AZP node

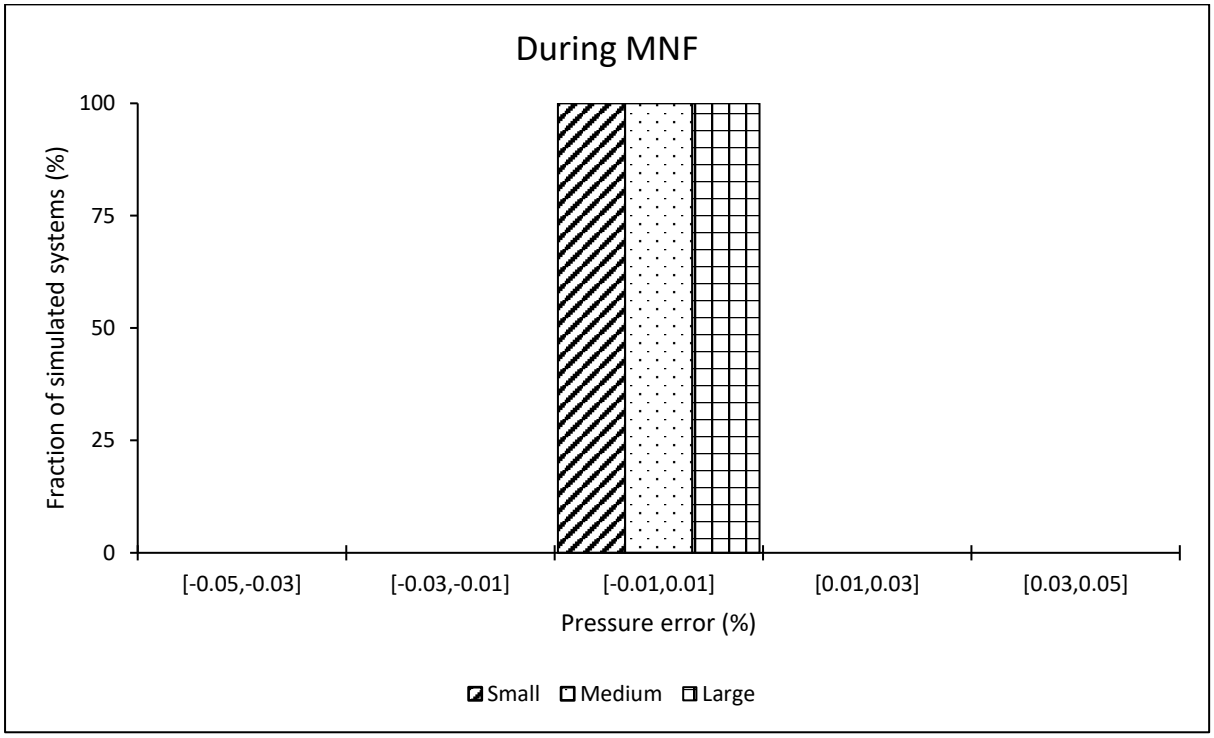

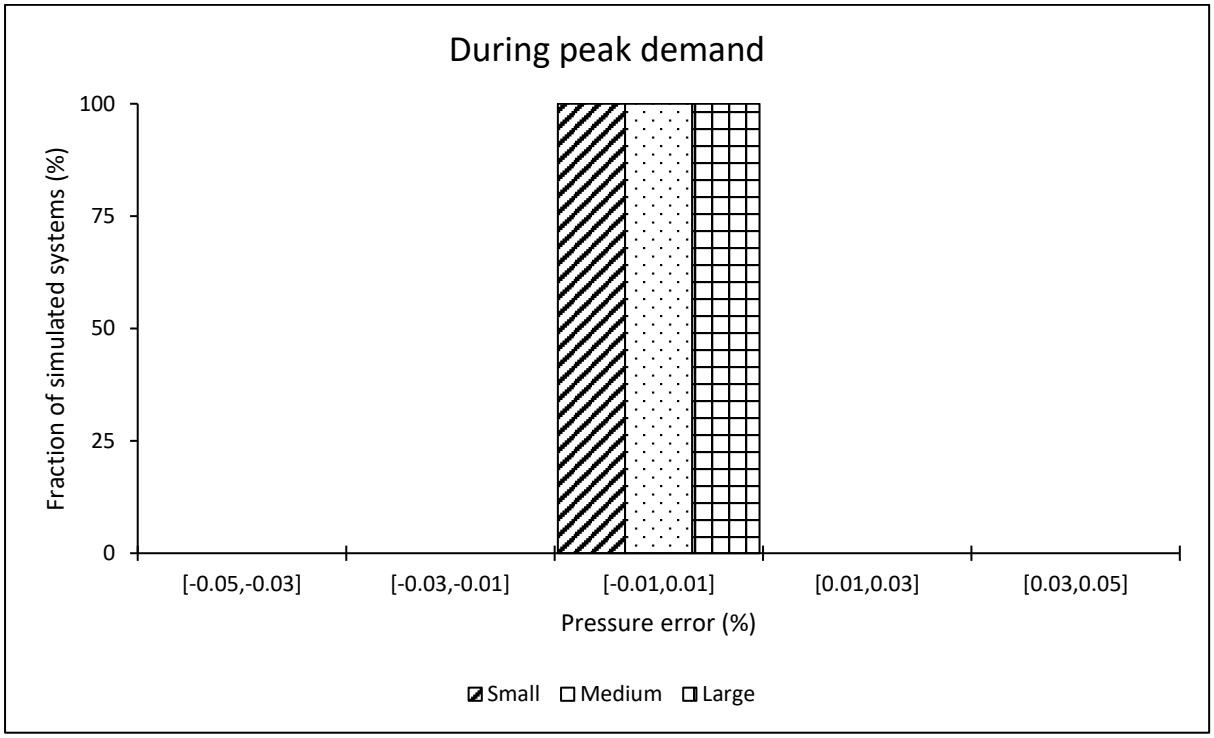

Impact on the system leakage estimation error when using the power equation

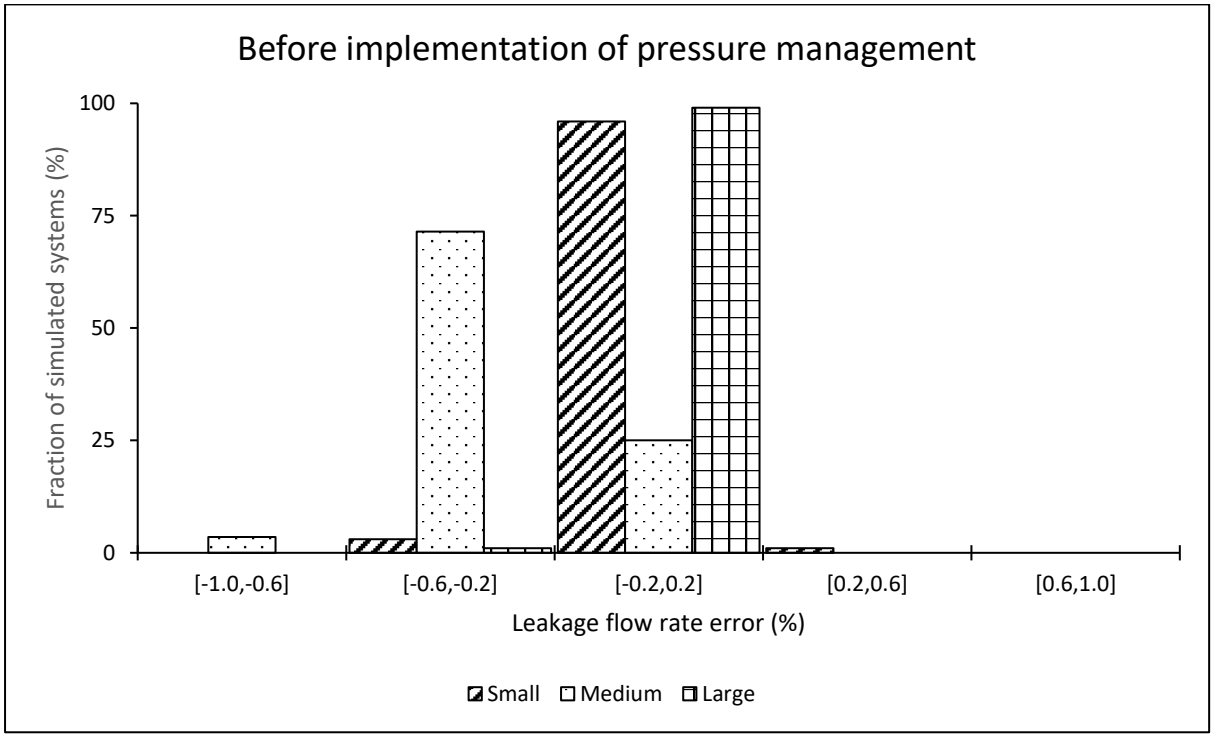

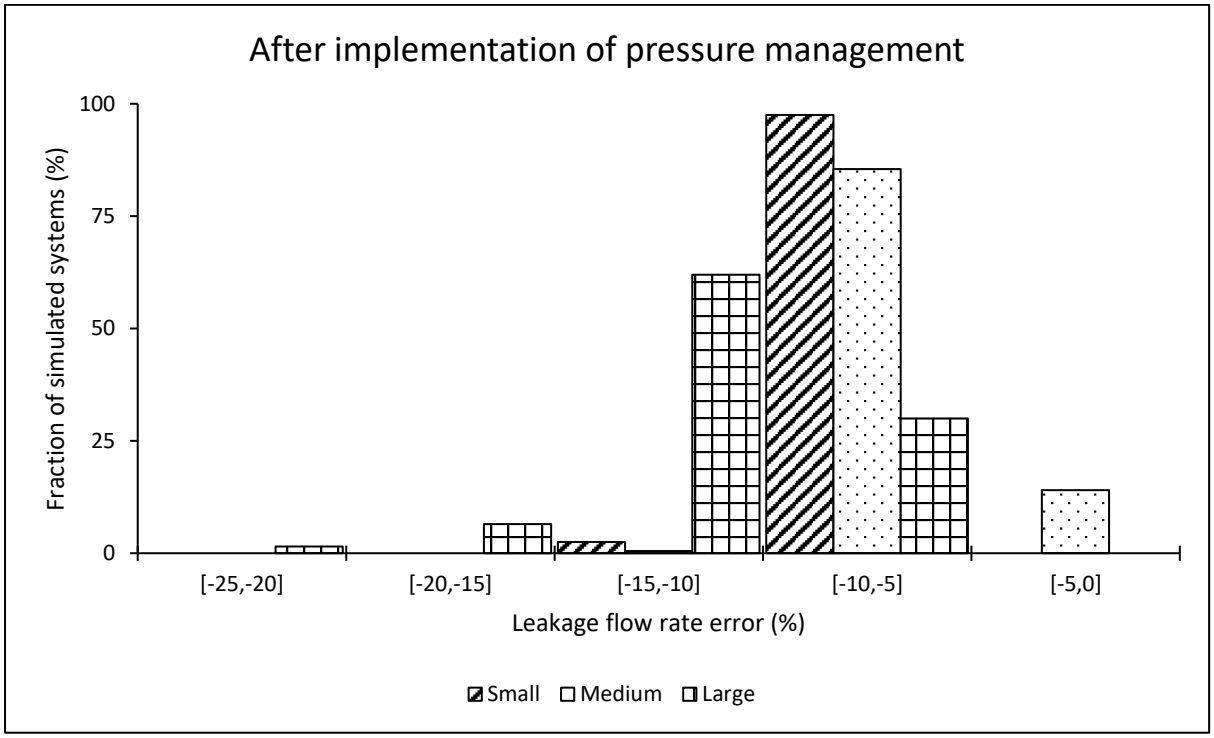

Impact on the leakage estimation error when using the power equation at the critical node

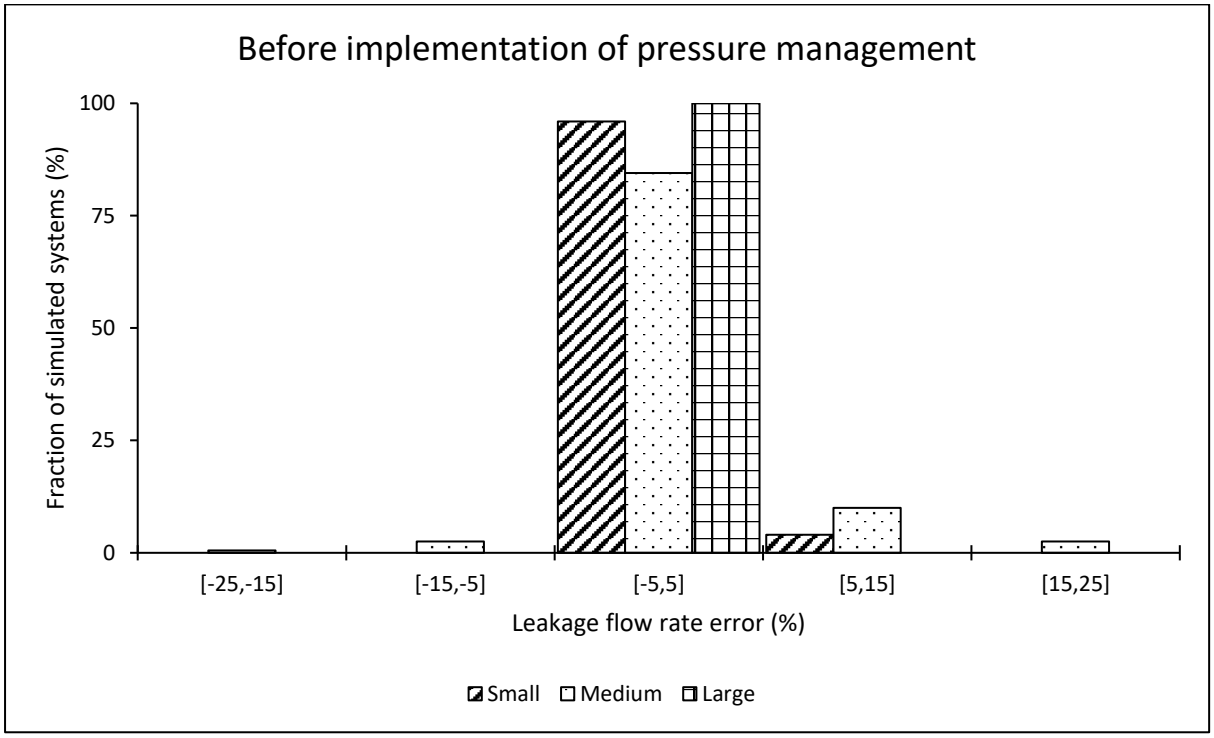

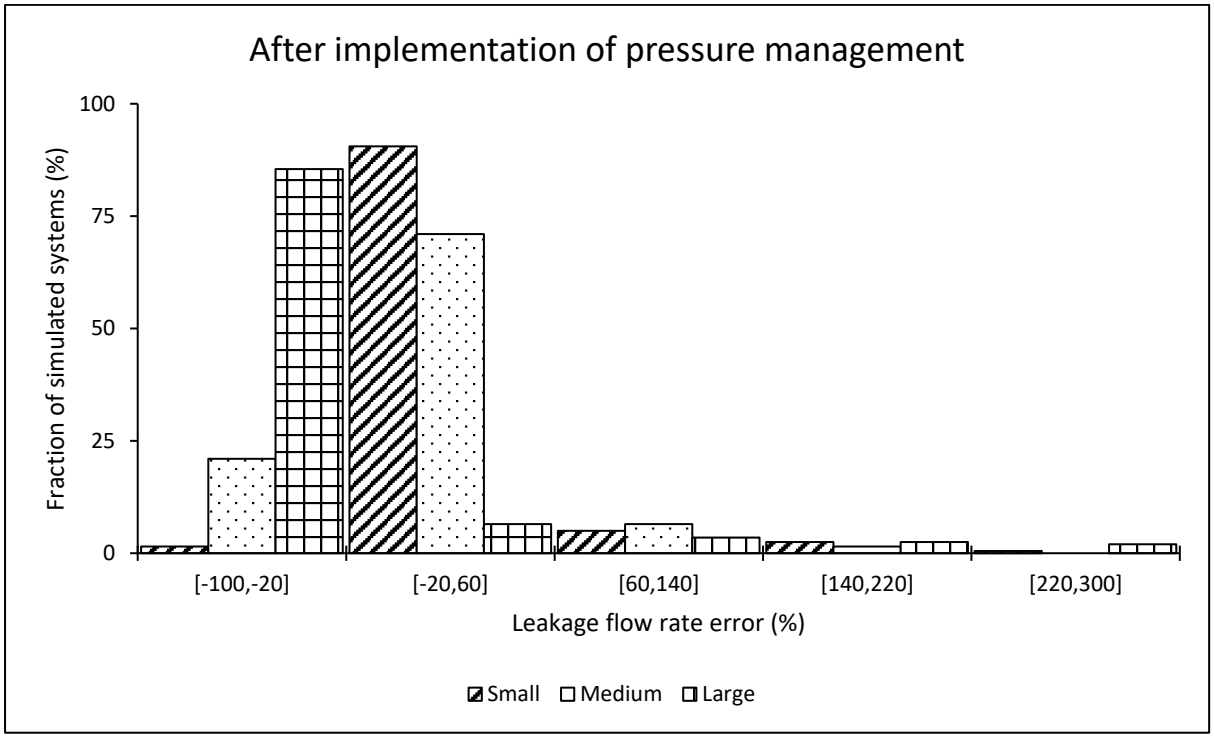

Impact on system convergence to a hydraulic solution

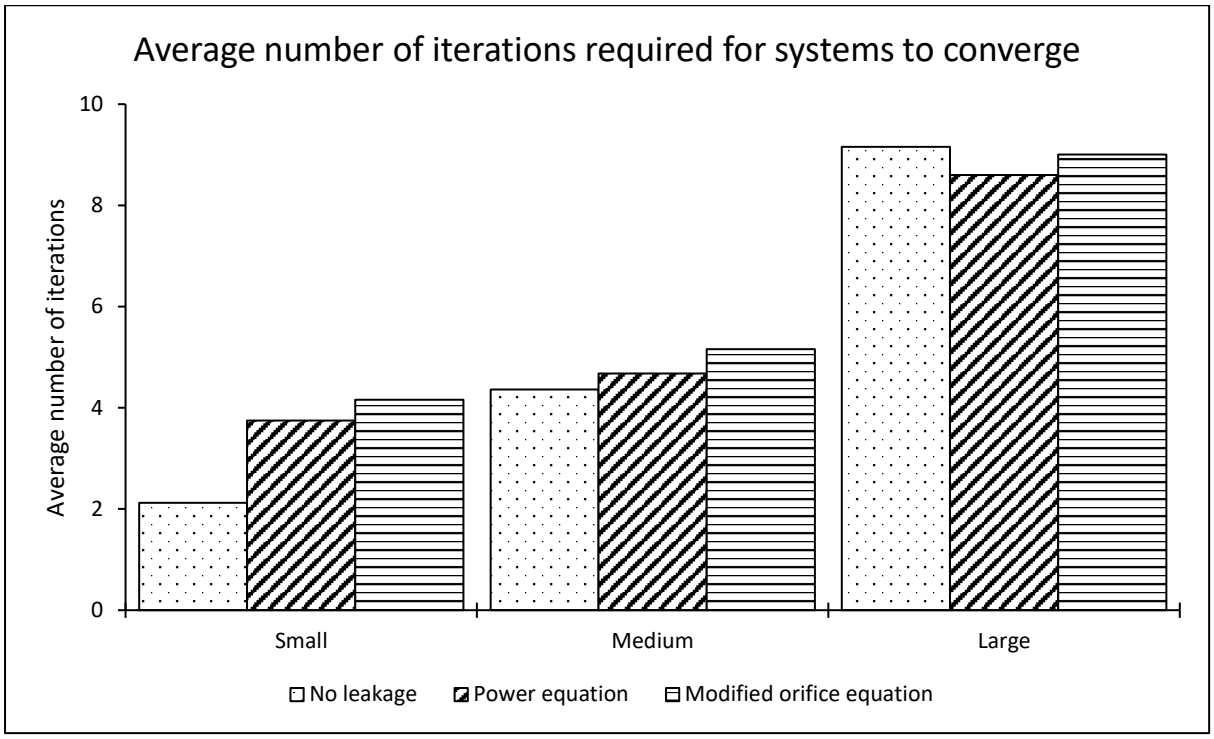

Appendix C-2: Impact of network size on simulation results for systems with leakage equivalent to ILI of 4

Impact on the system leakage exponents of the power equation

	System leakage exponents (N1)			
	Minimum	**Arithmetic Mean**	**Median**	**Maximum**
Small	0.54	0.62	0.58	0.96
Medium	0.57	0.83	0.84	1.10
Large	0.76	0.98	0.98	1.26

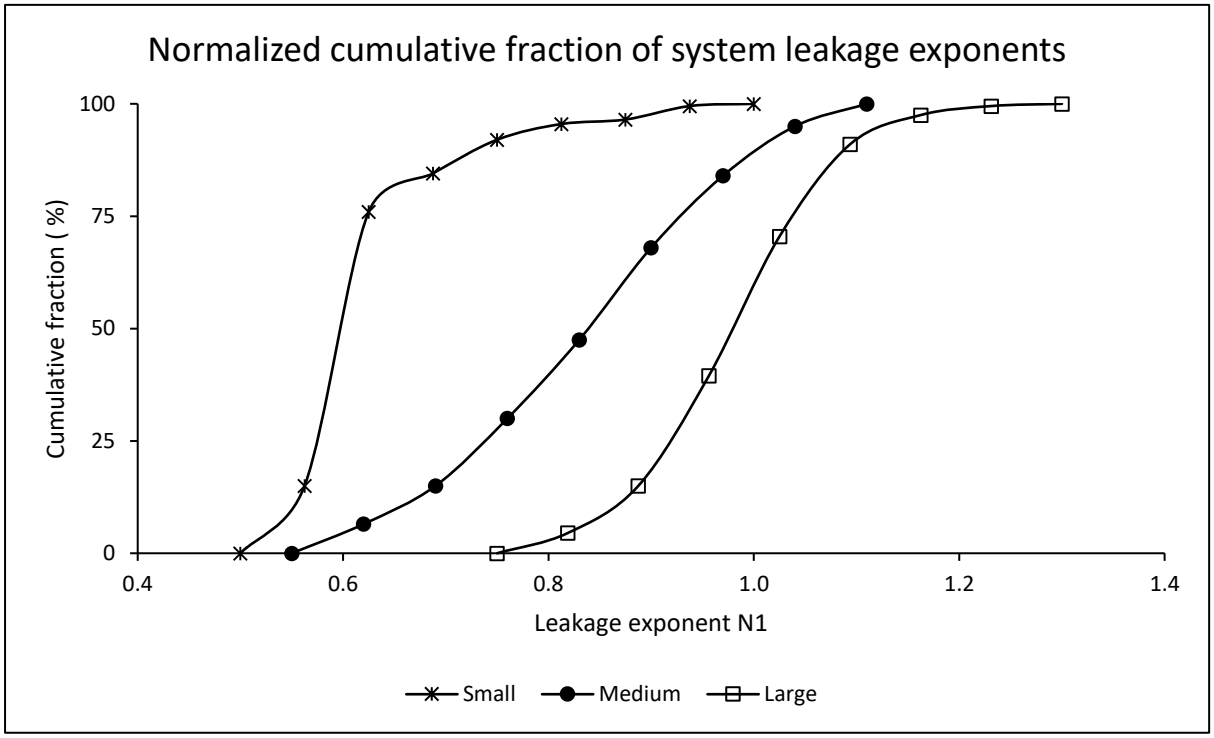

Impact on predicting system parameters for the modified orifice equation

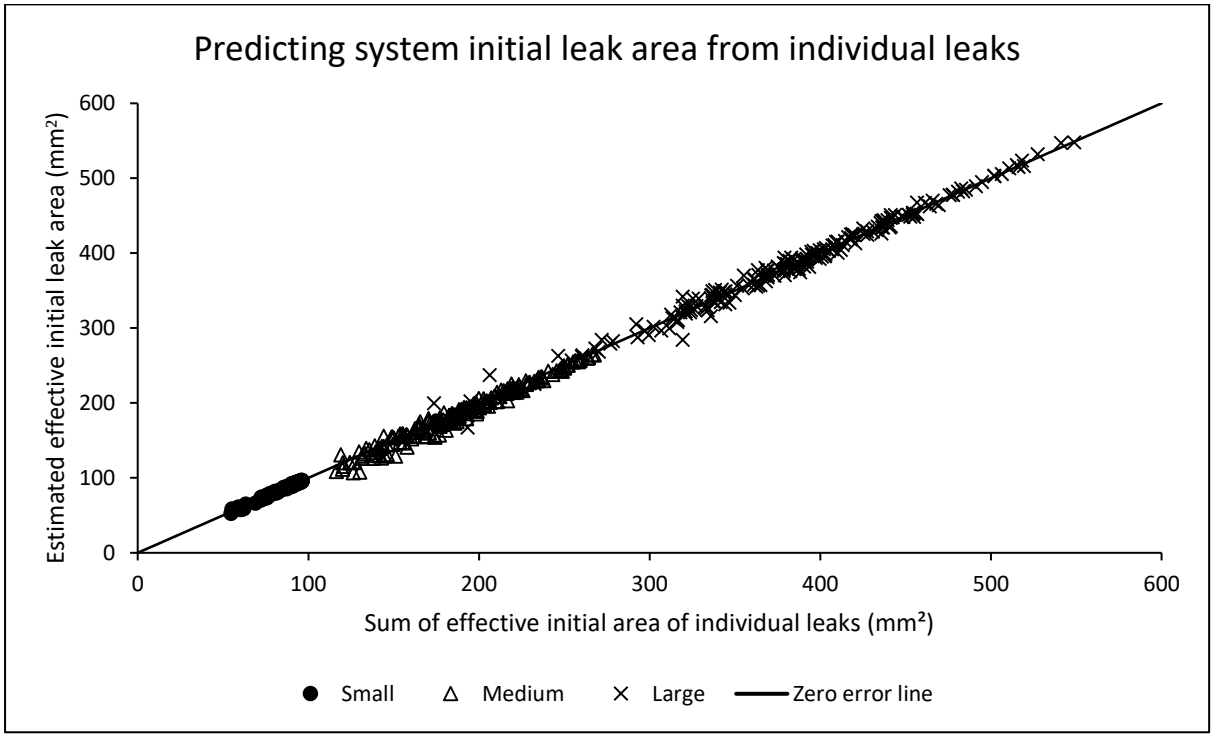

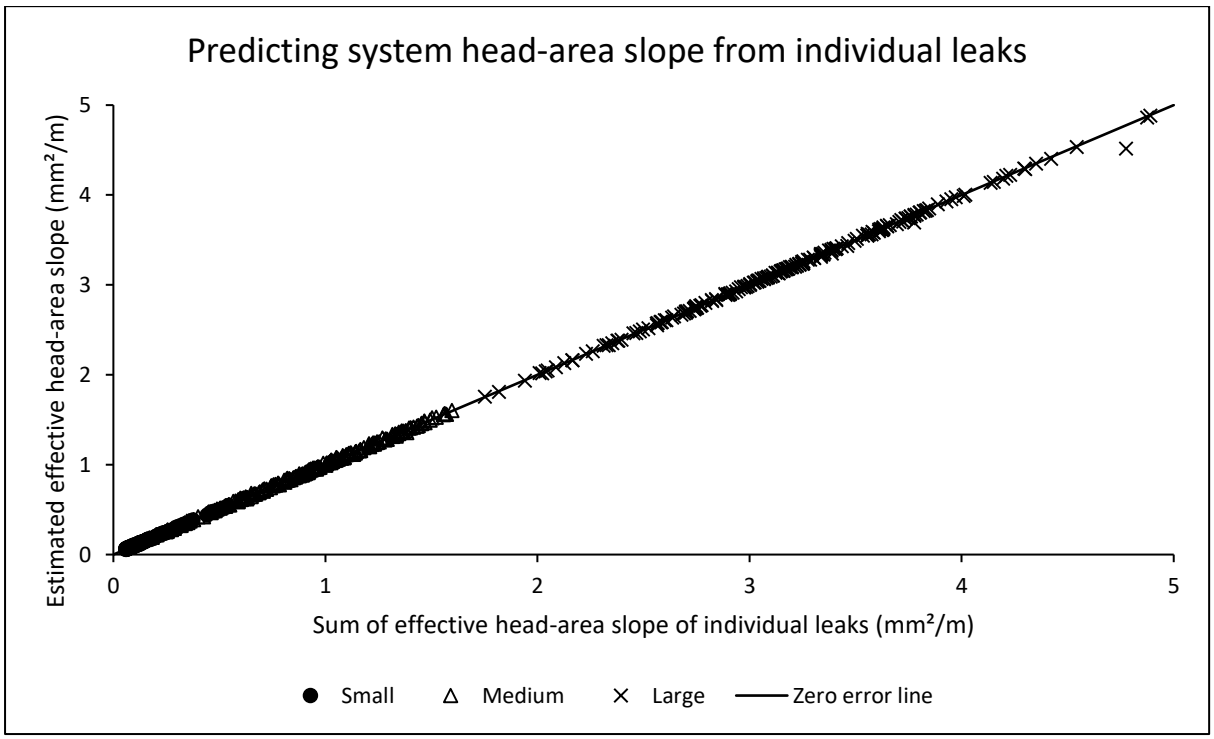

Impact on the pressure estimation error when using the power equation at the AZP node

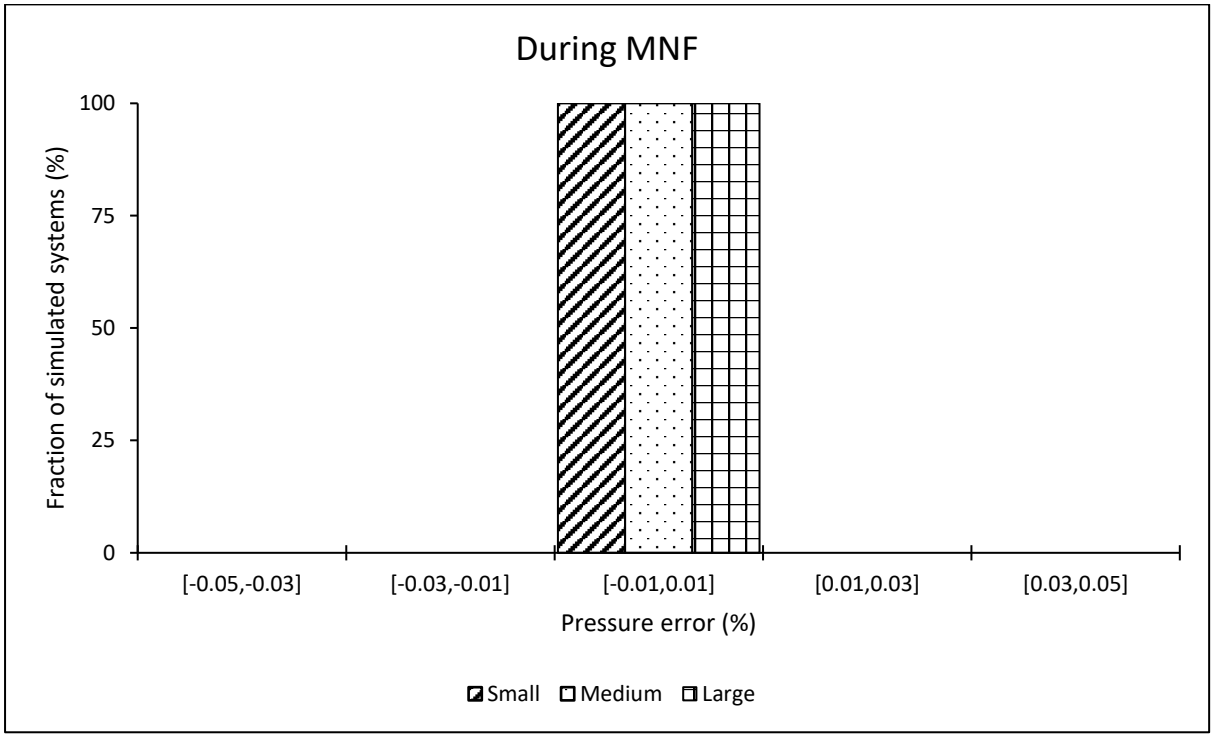

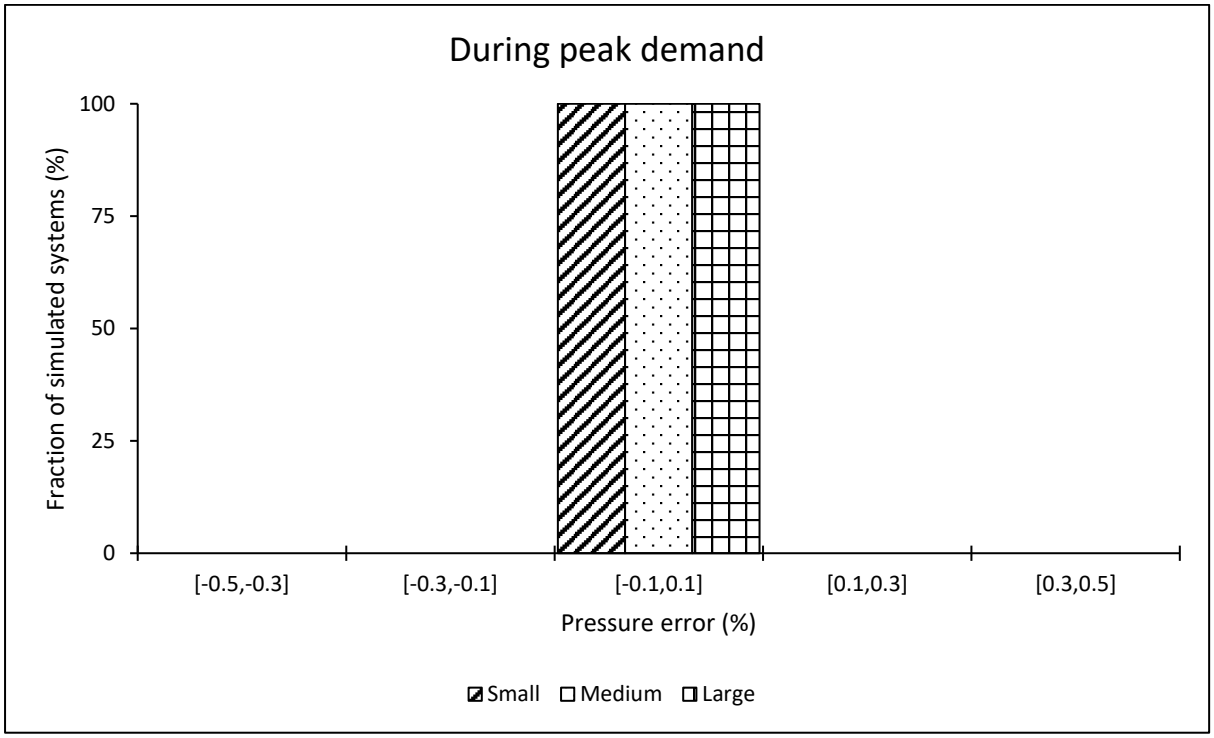

Impact on the system leakage estimation error when using the power equation

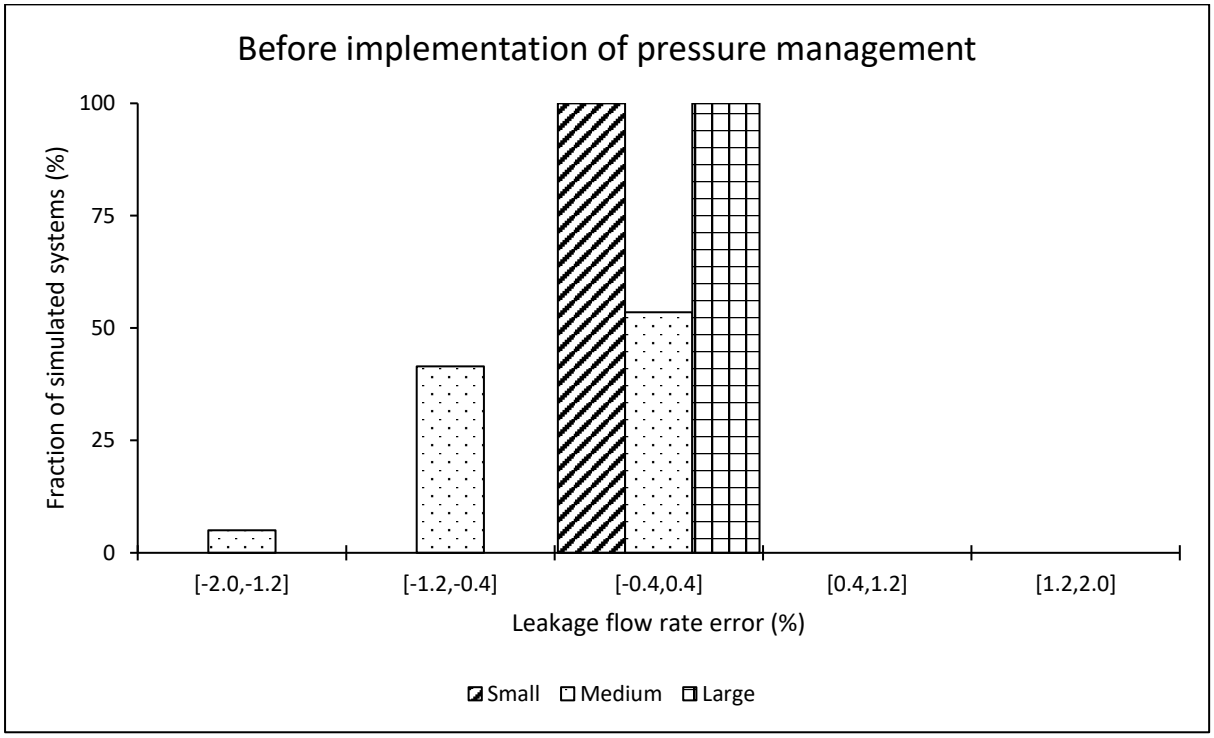

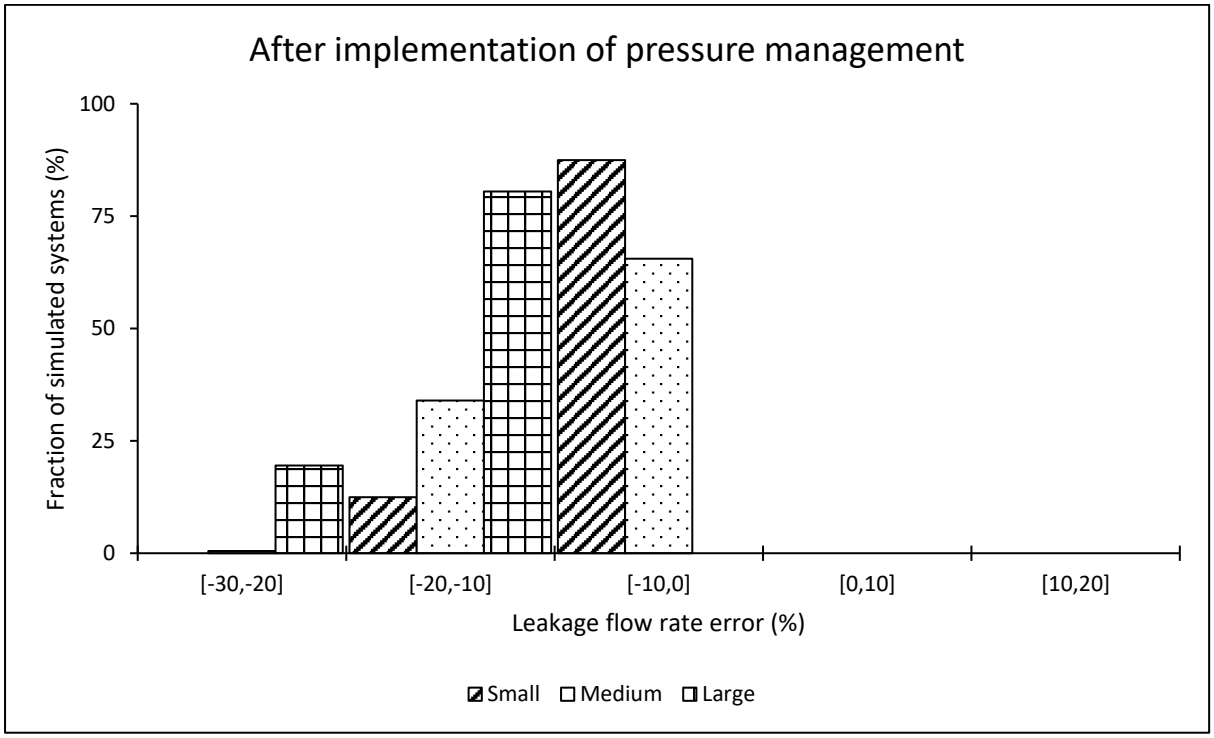

Impact on the leakage estimation error when using the power equation at the critical node

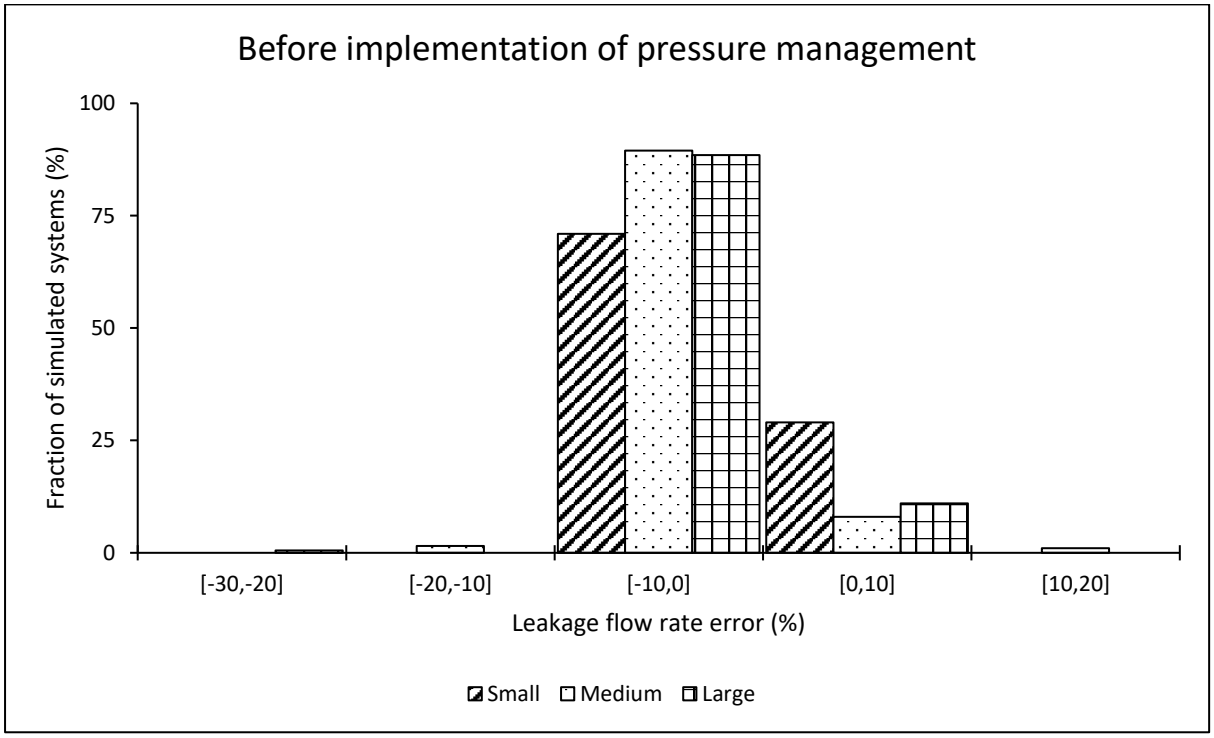

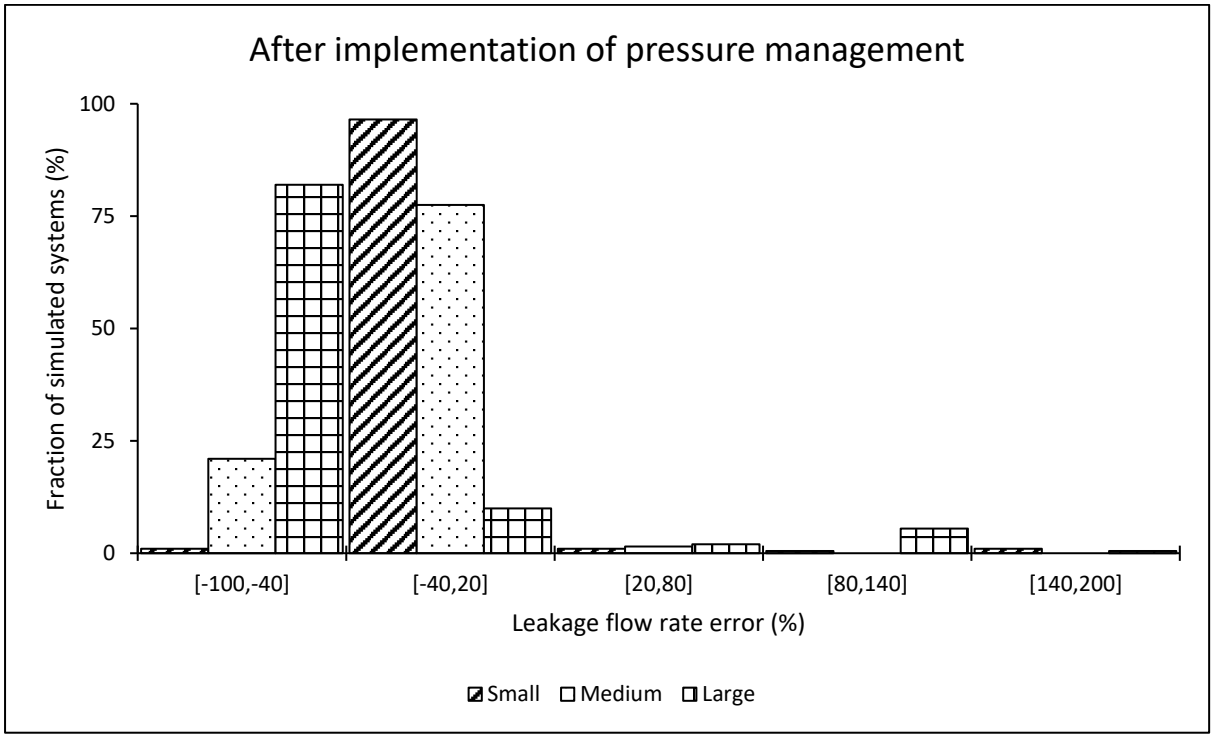

Impact on system convergence to a hydraulic solution

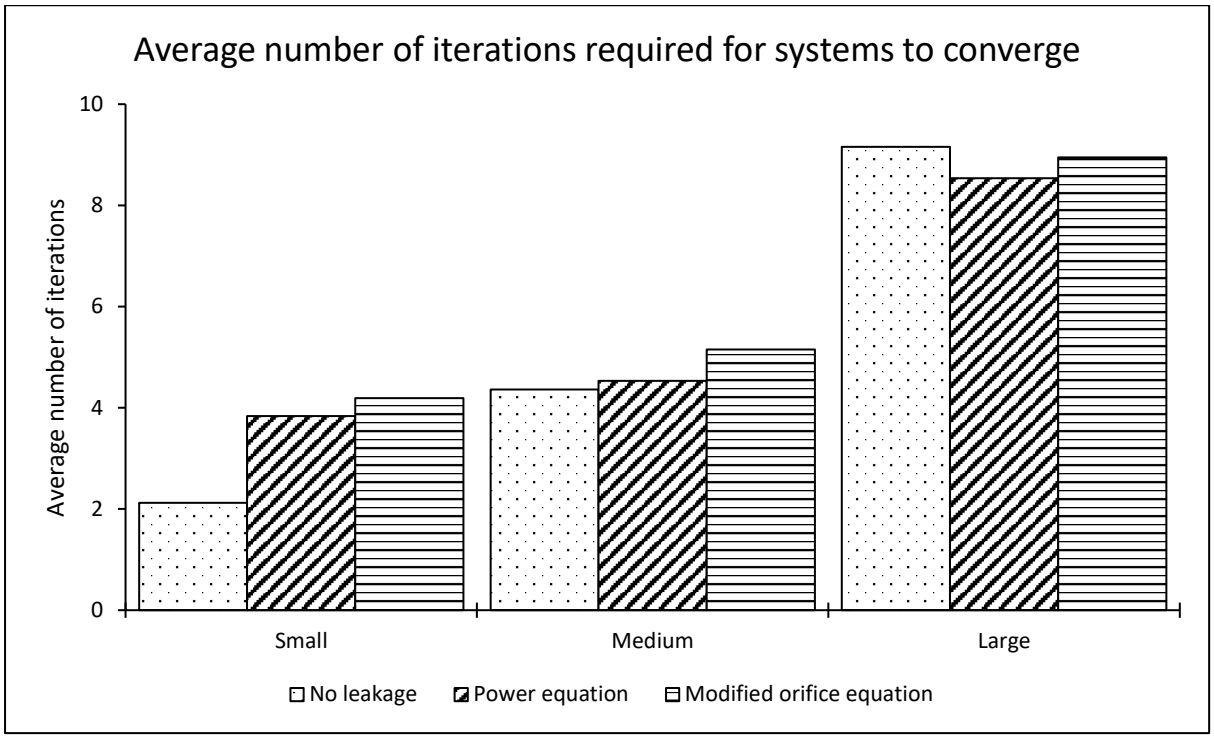

Appendix C-3: Impact of network size on simulation results for systems with leakage equivalent to ILI of 16

Impact on the system leakage exponents of the power equation

	System leakage exponents (N1)			
	Minimum	**Arithmetic Mean**	**Median**	**Maximum**
Small	0.65	0.92	0.91	1.25
Medium	0.81	1.07	1.07	1.35
Large	0.99	1.16	1.16	1.37

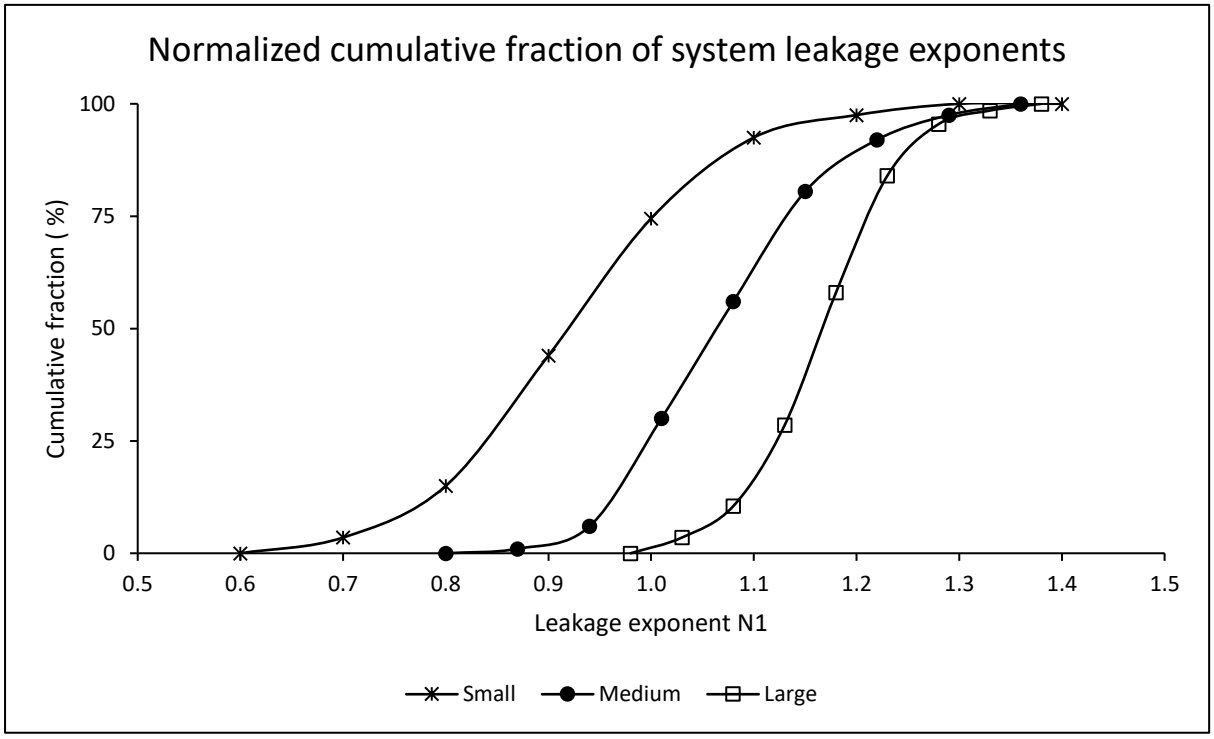

Impact on predicting system parameters for the modified orifice equation

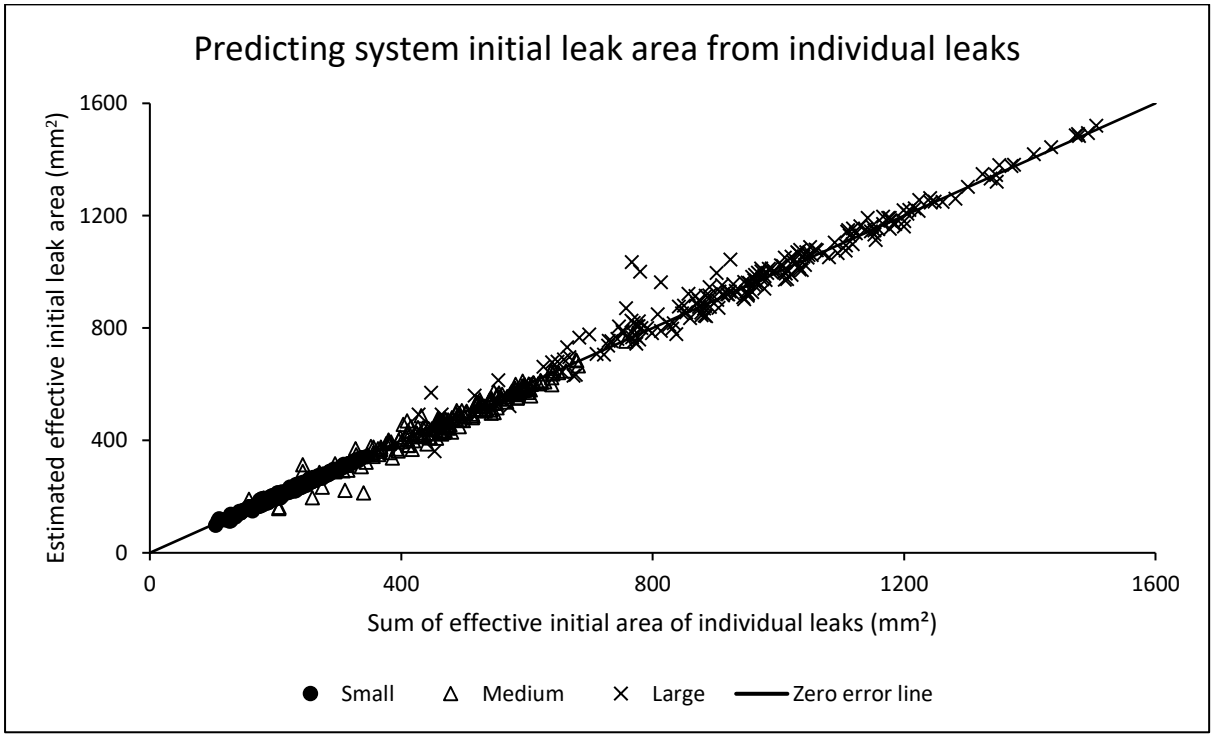

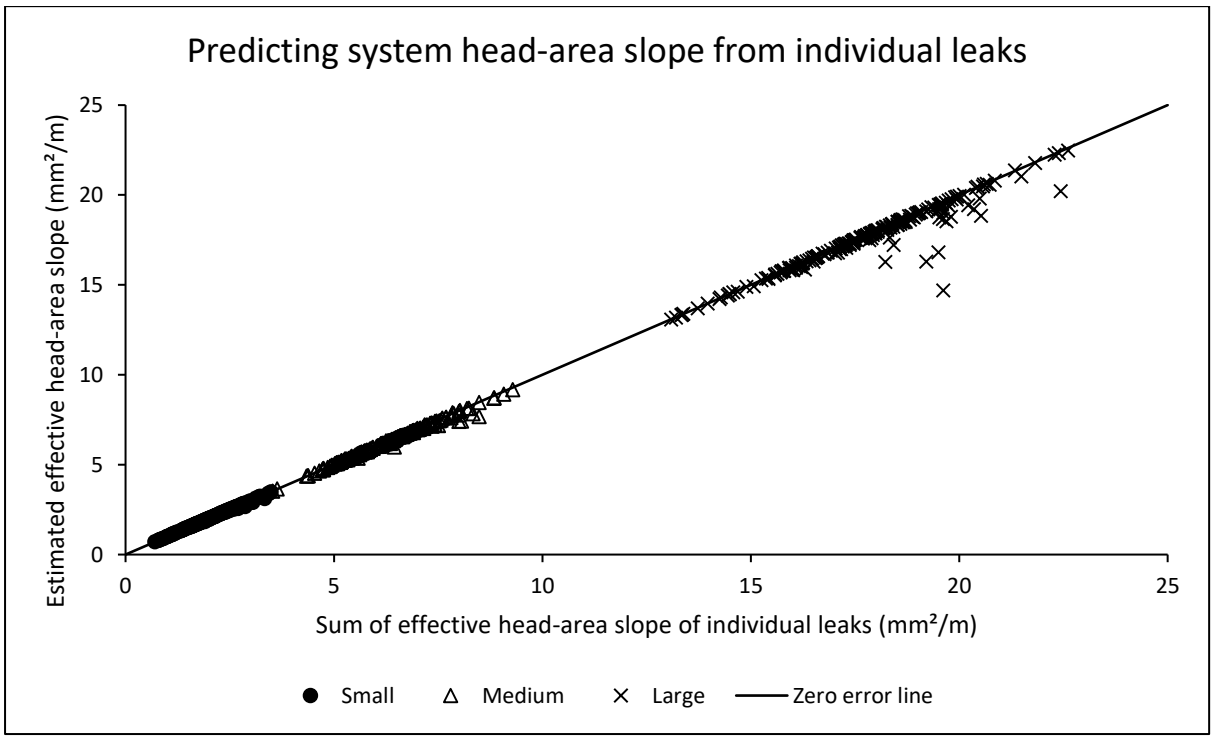

Impact on the pressure estimation error when using the power equation at the AZP node

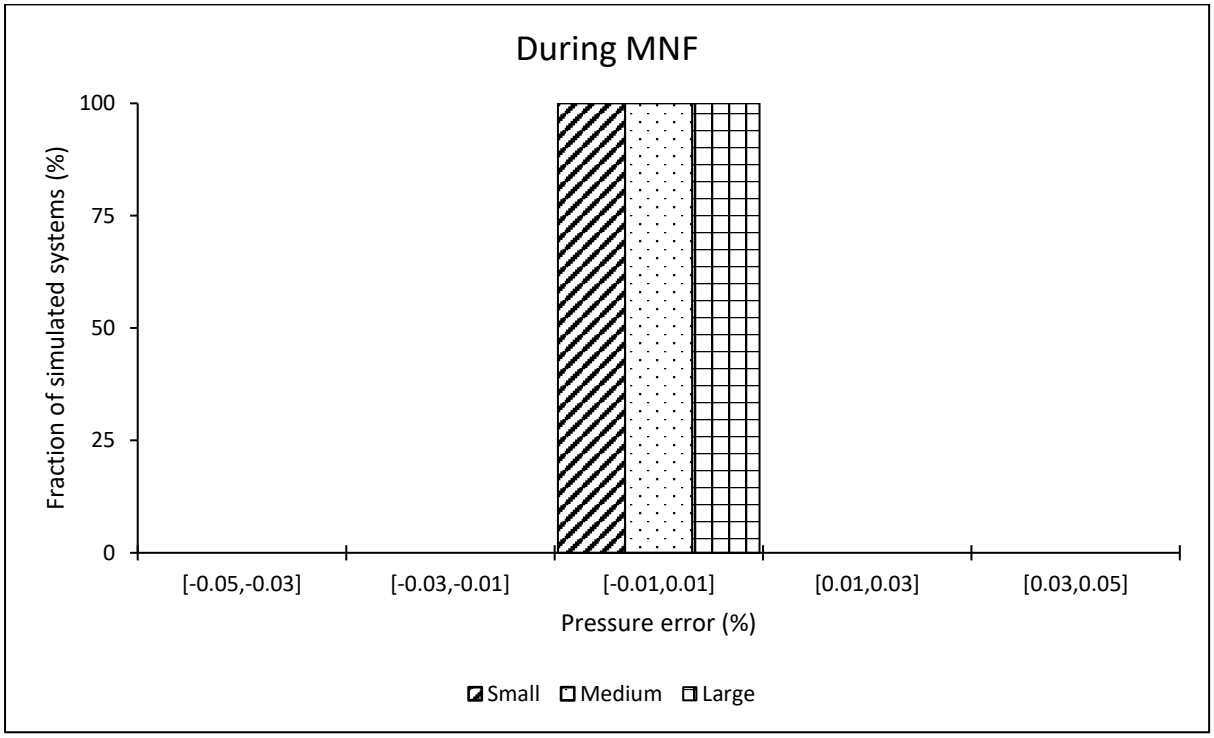

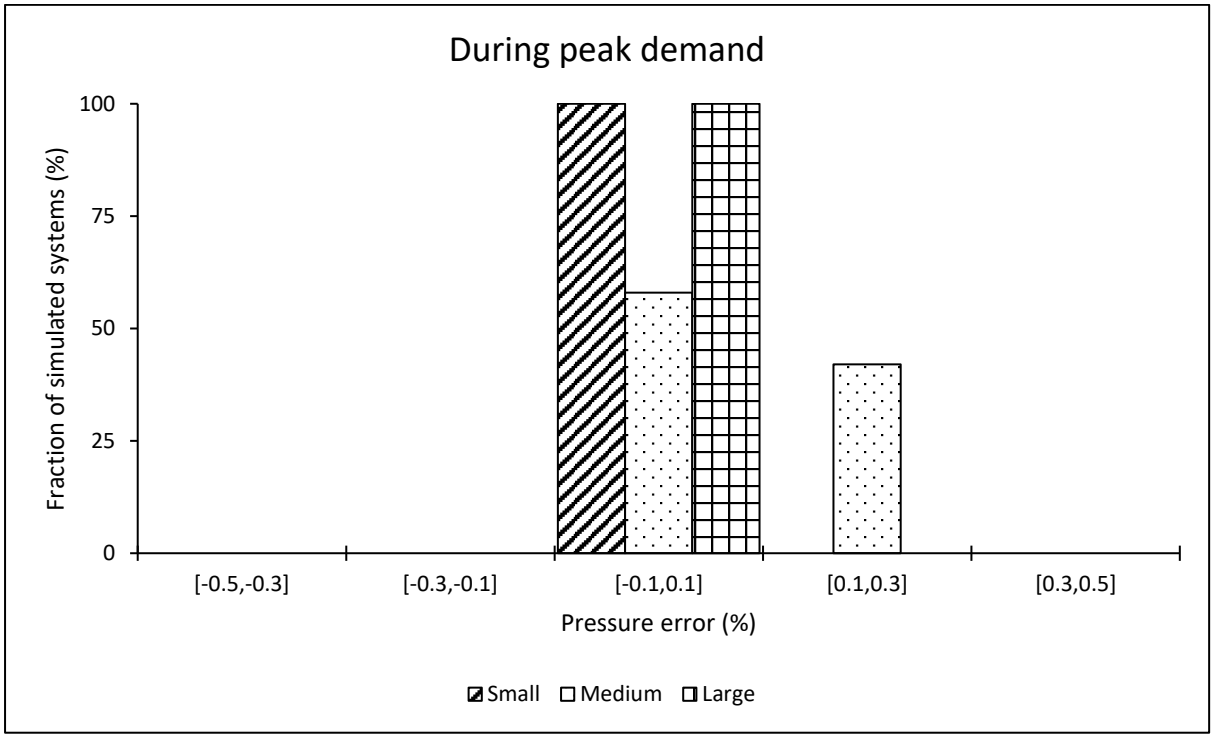

Impact on the system leakage estimation error when using the power equation

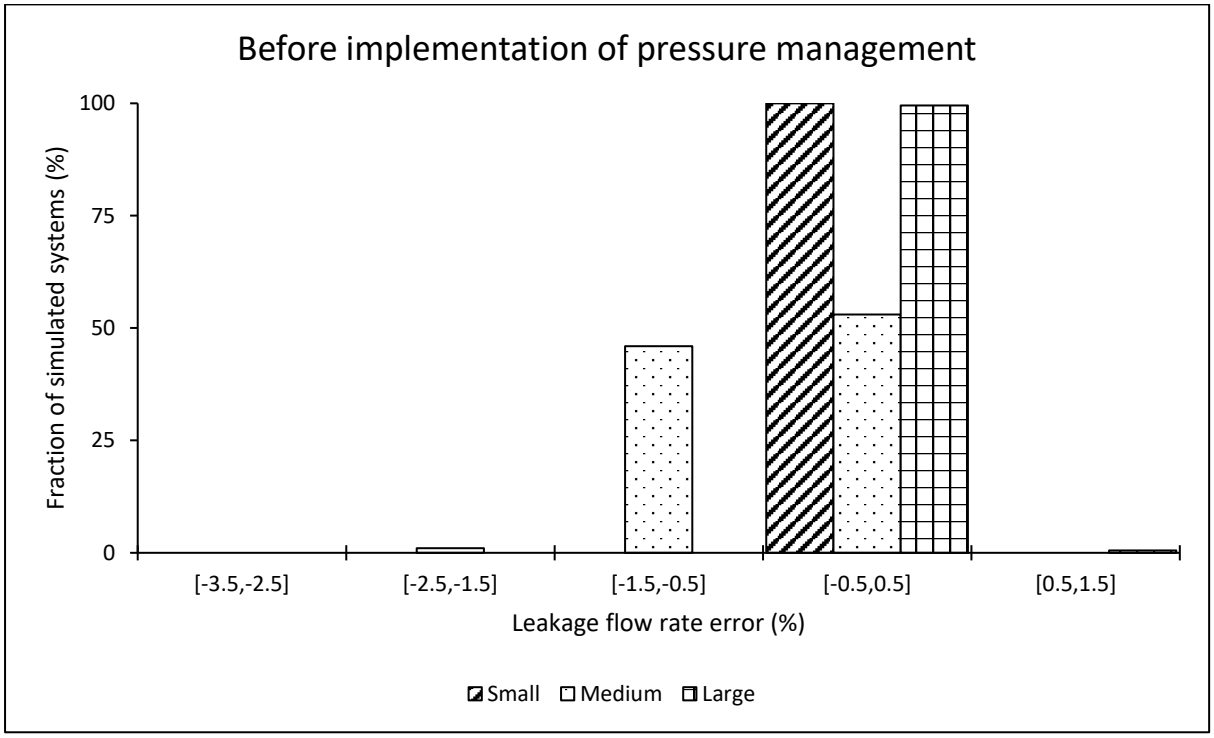

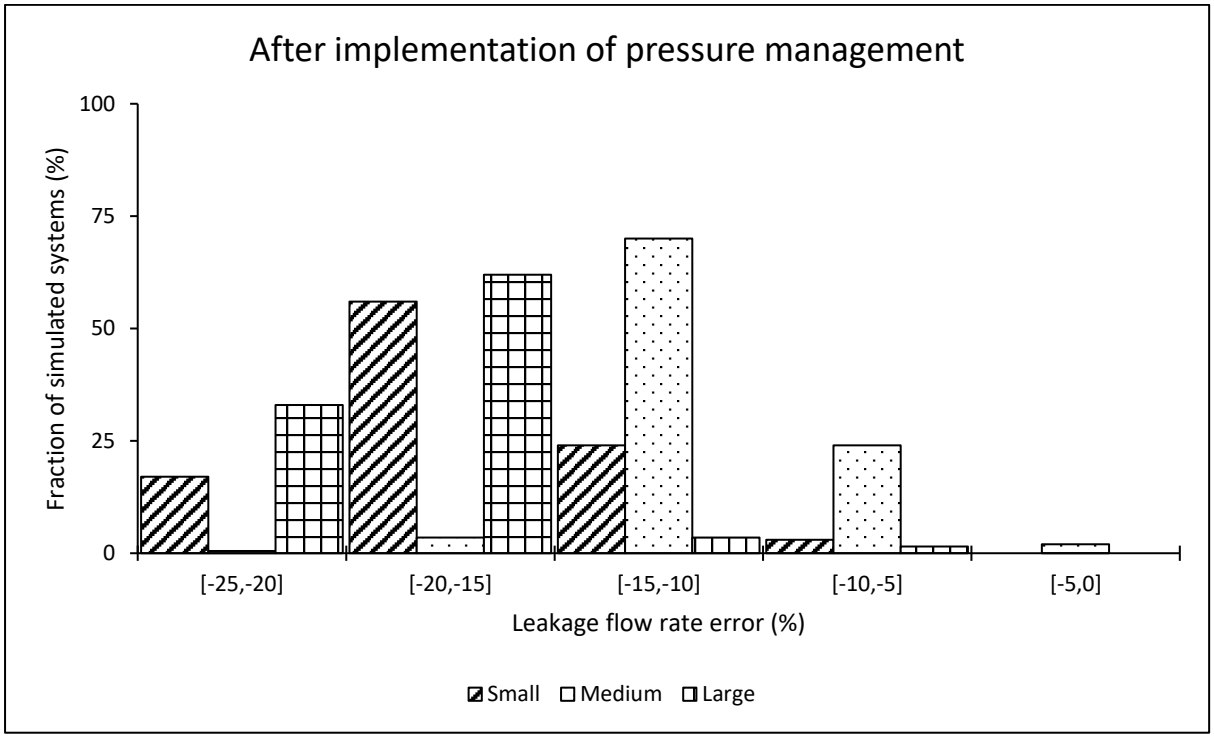

Impact on the leakage estimation error when using the power equation at the critical node

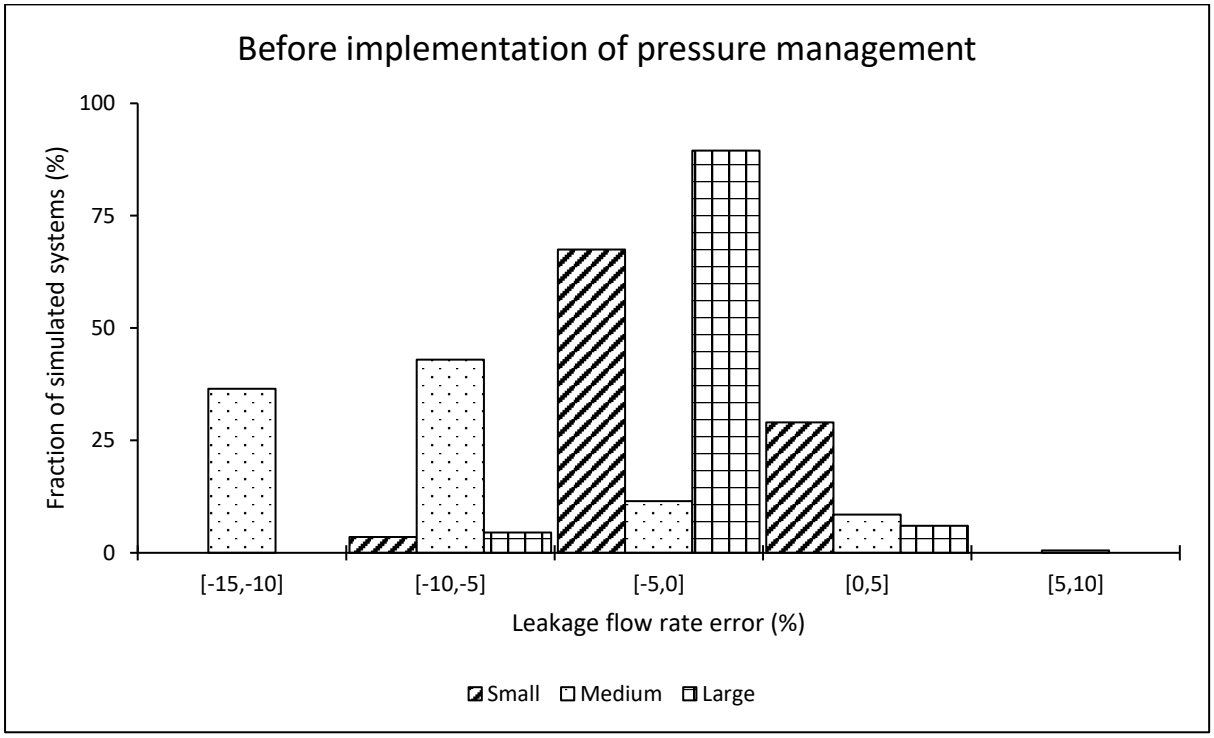

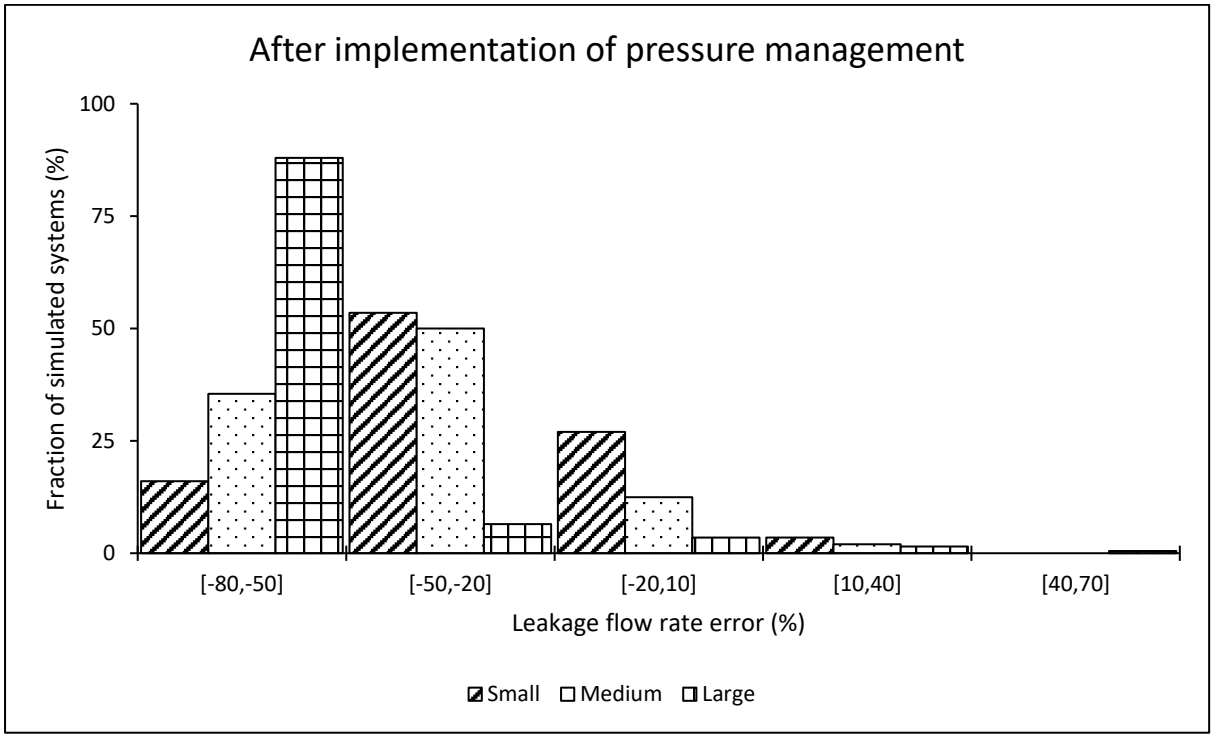

Impact on system convergence to a hydraulic solution

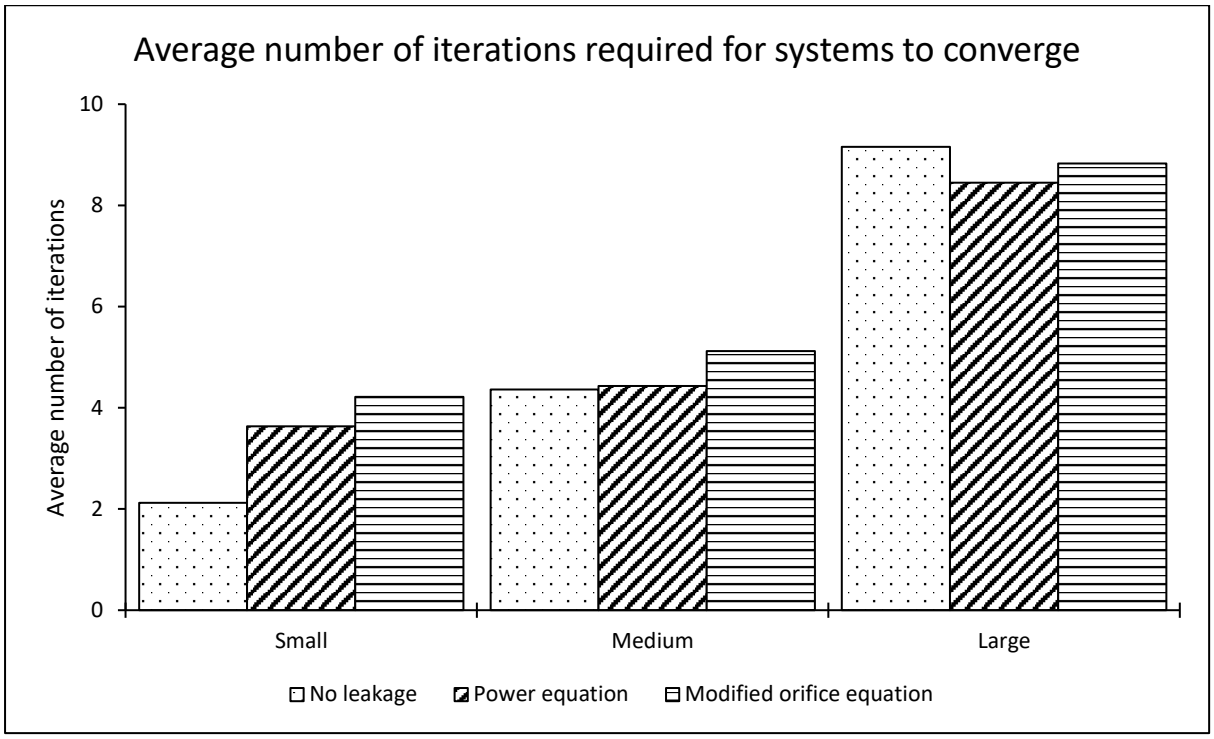

Appendix C-4: Impact of network size on simulation results for systems with leakage equivalent to ILI of 64

Impact on the system leakage exponents of the power equation

	System leakage exponents (N1)			
	Minimum	**Arithmetic Mean**	**Median**	**Maximum**
Small	0.89	1.08	1.07	1.37
Medium	1.06	1.18	1.18	1.40
Large	1.08	1.21	1.21	1.31

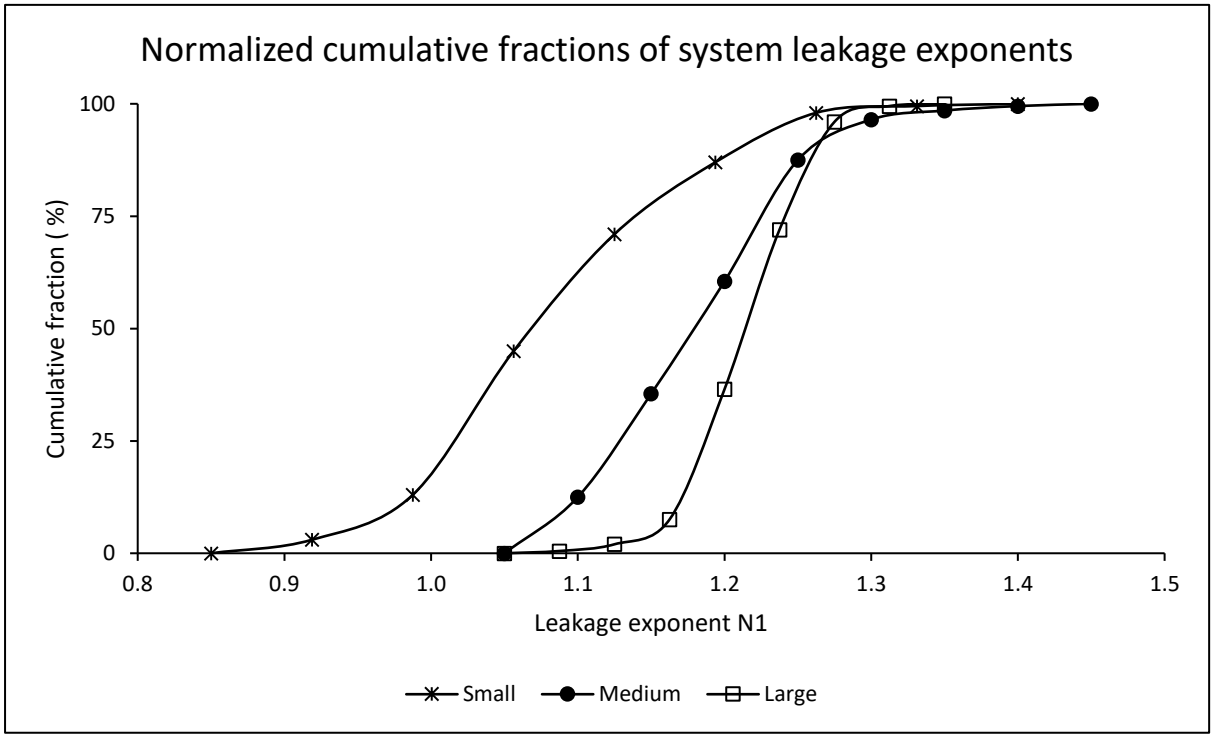

Impact on predicting the system parameters for the modified orifice equation

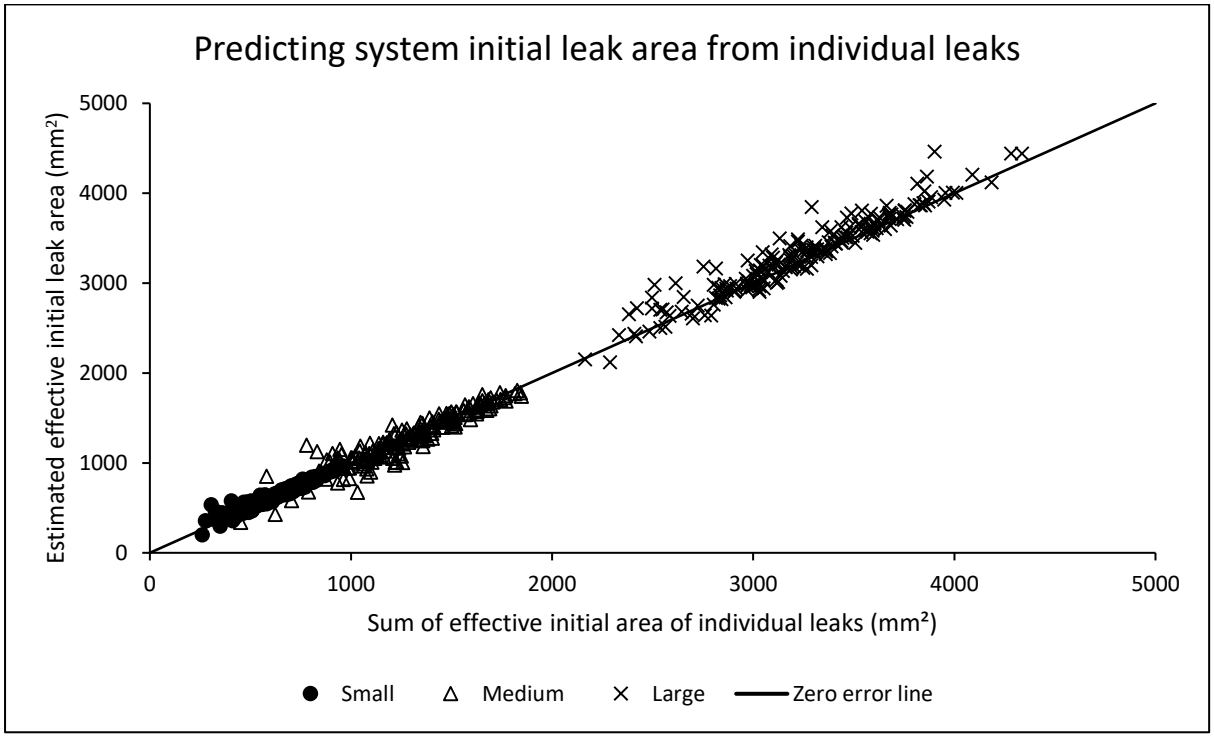

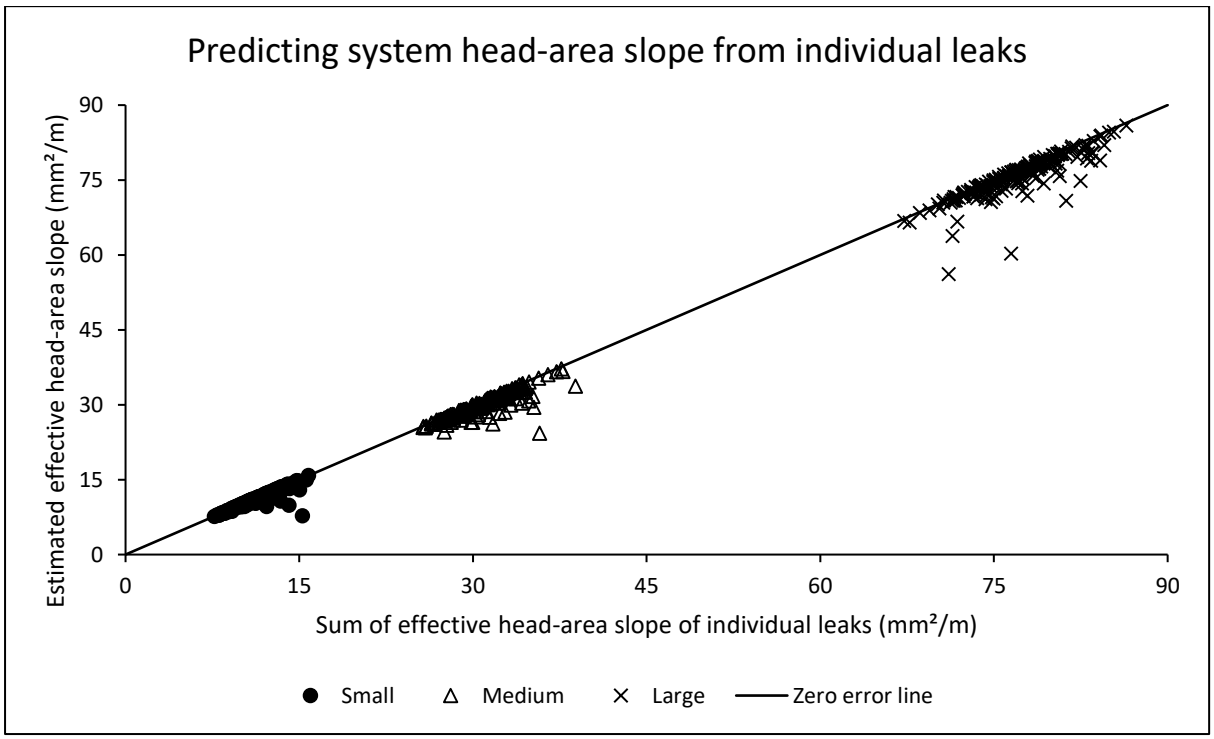

Impact on the pressure estimation error when using the power equation at the AZP node

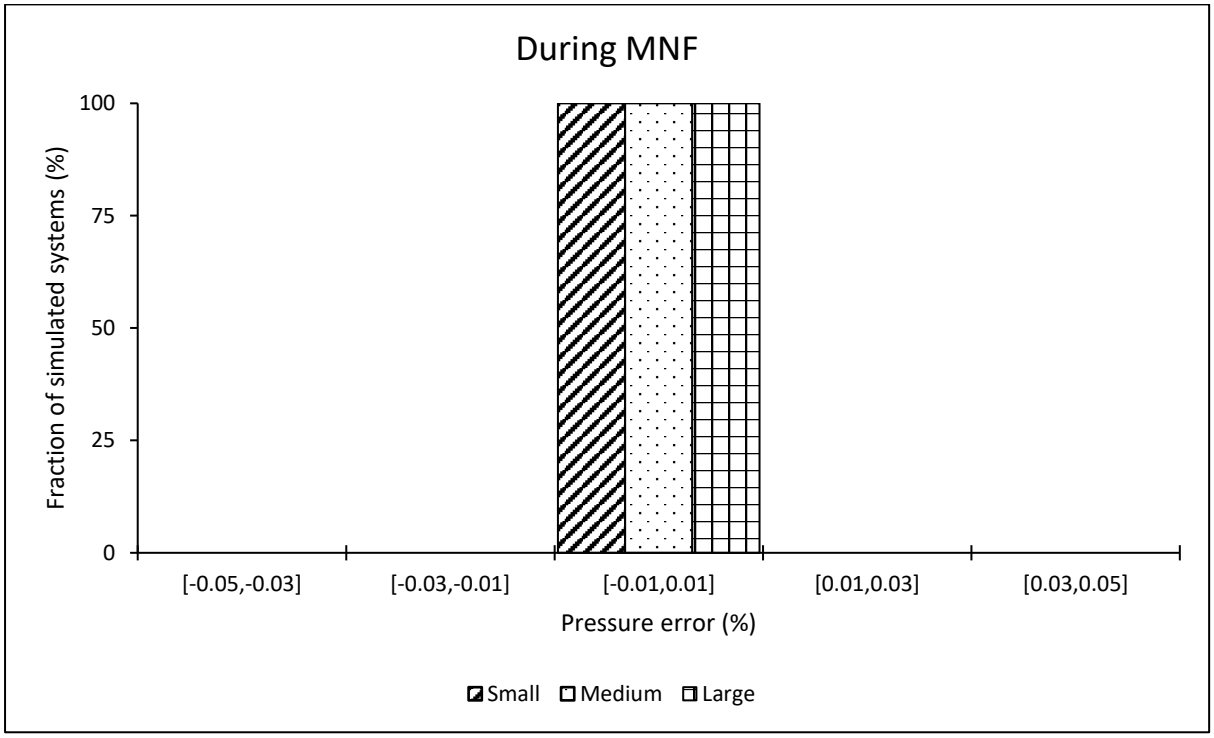

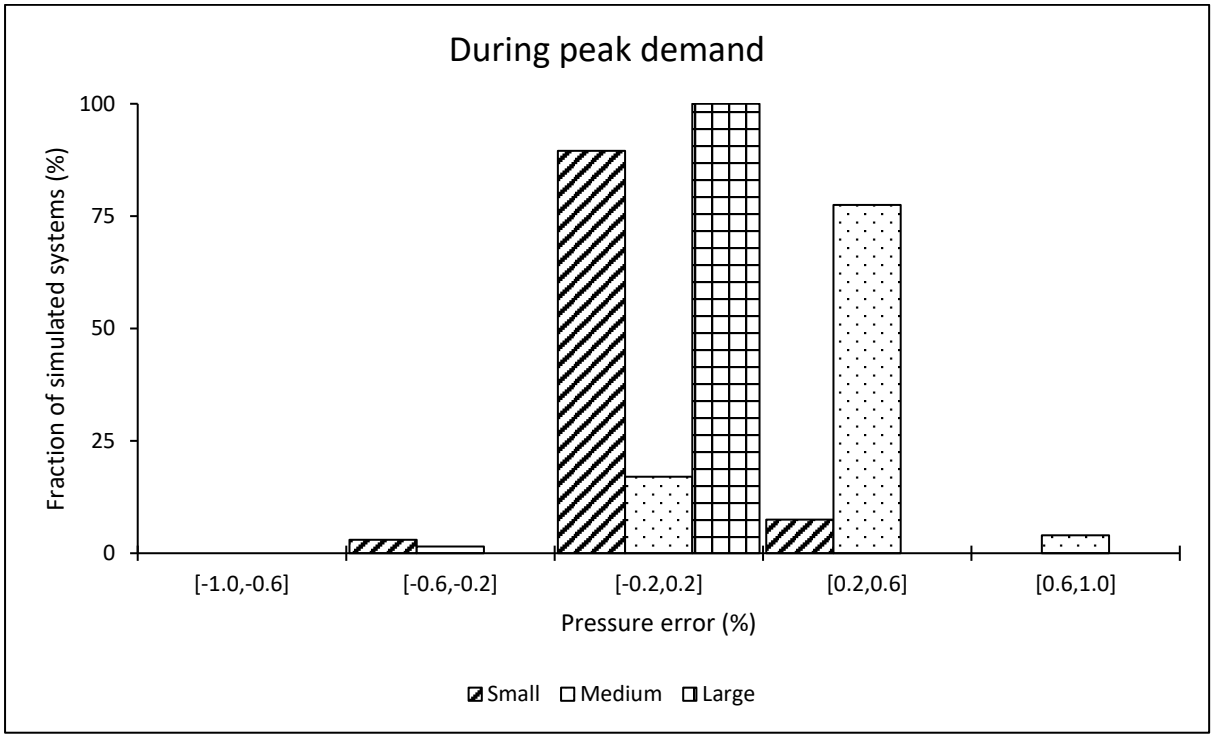

Impact on the system leakage estimation error when using the power equation

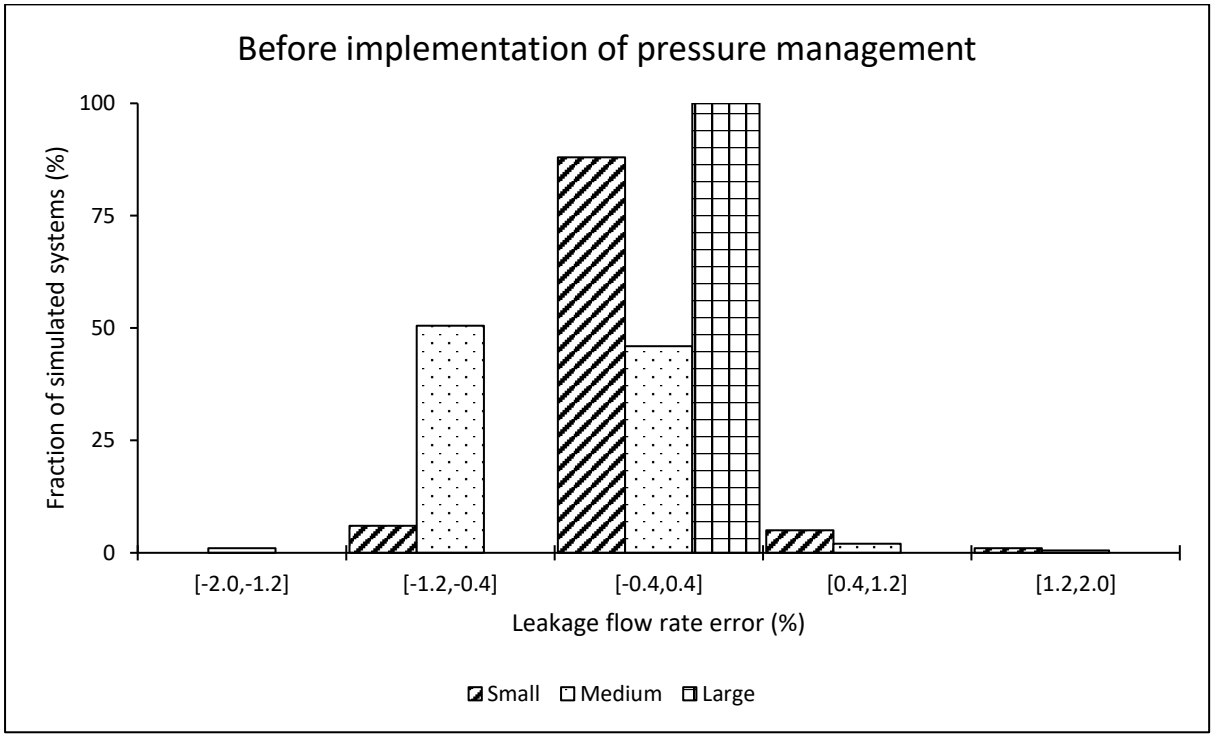

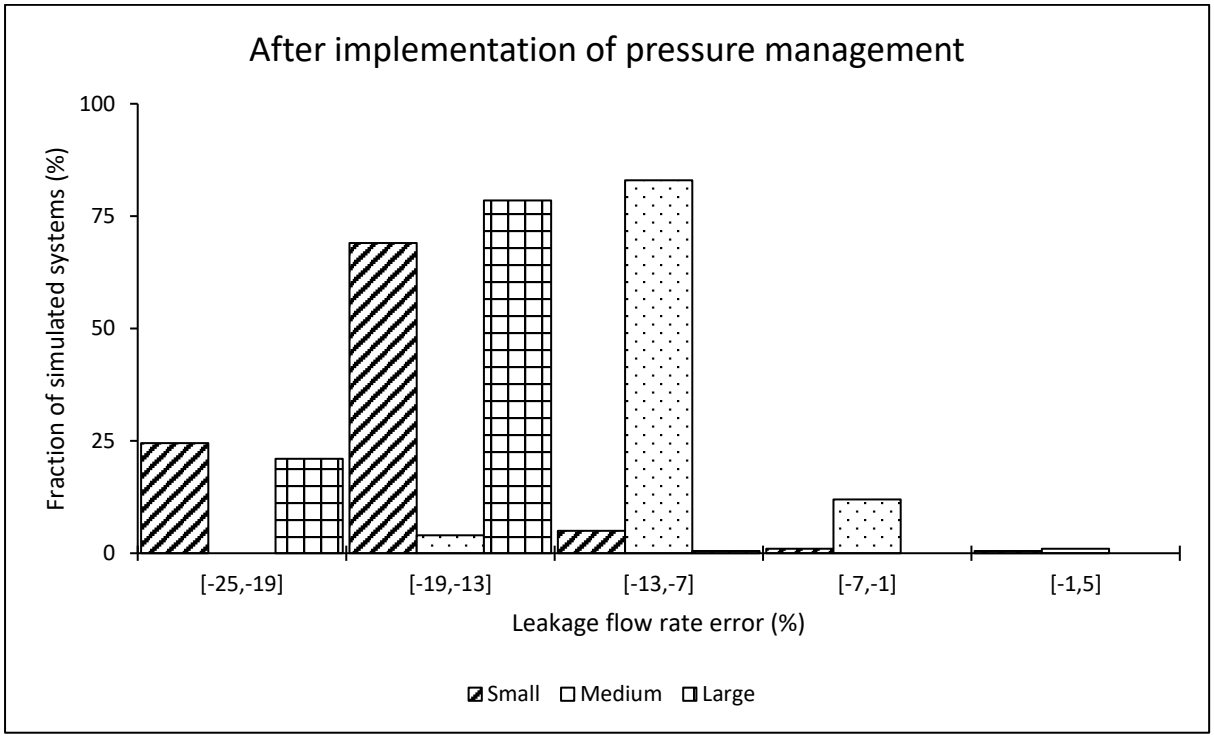

Impact on the leakage estimation error when using the power equation at the critical node

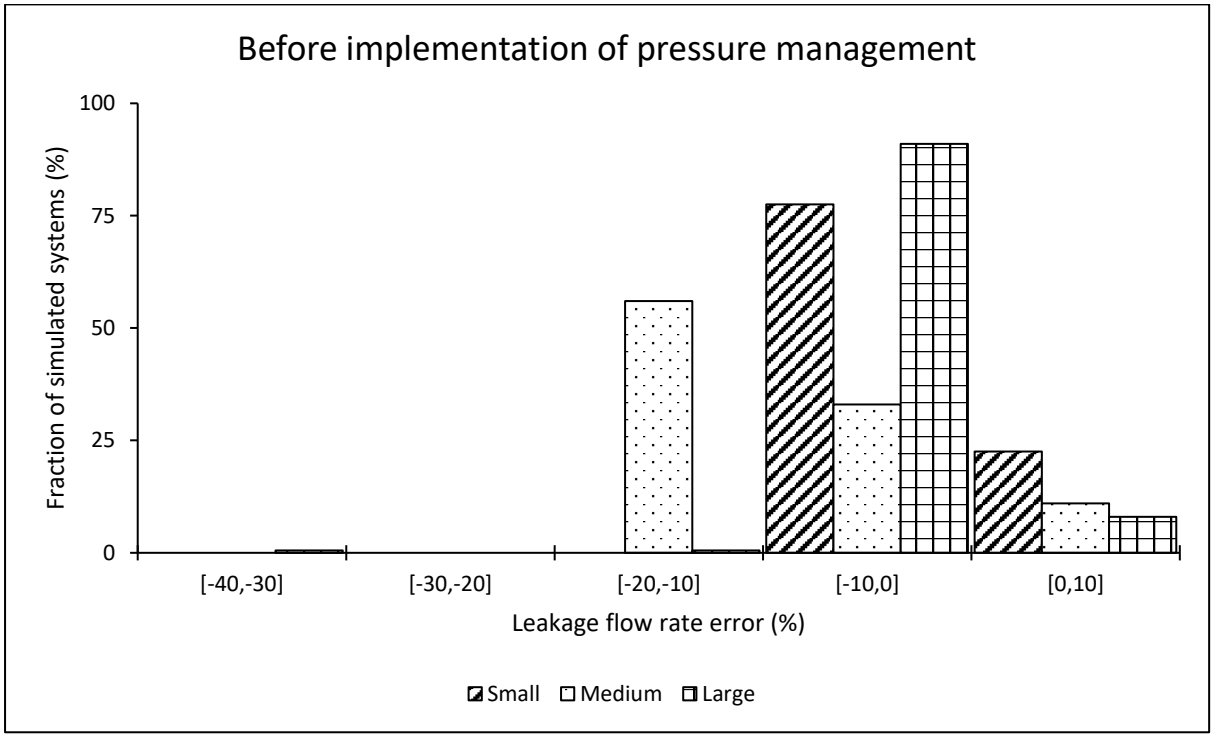

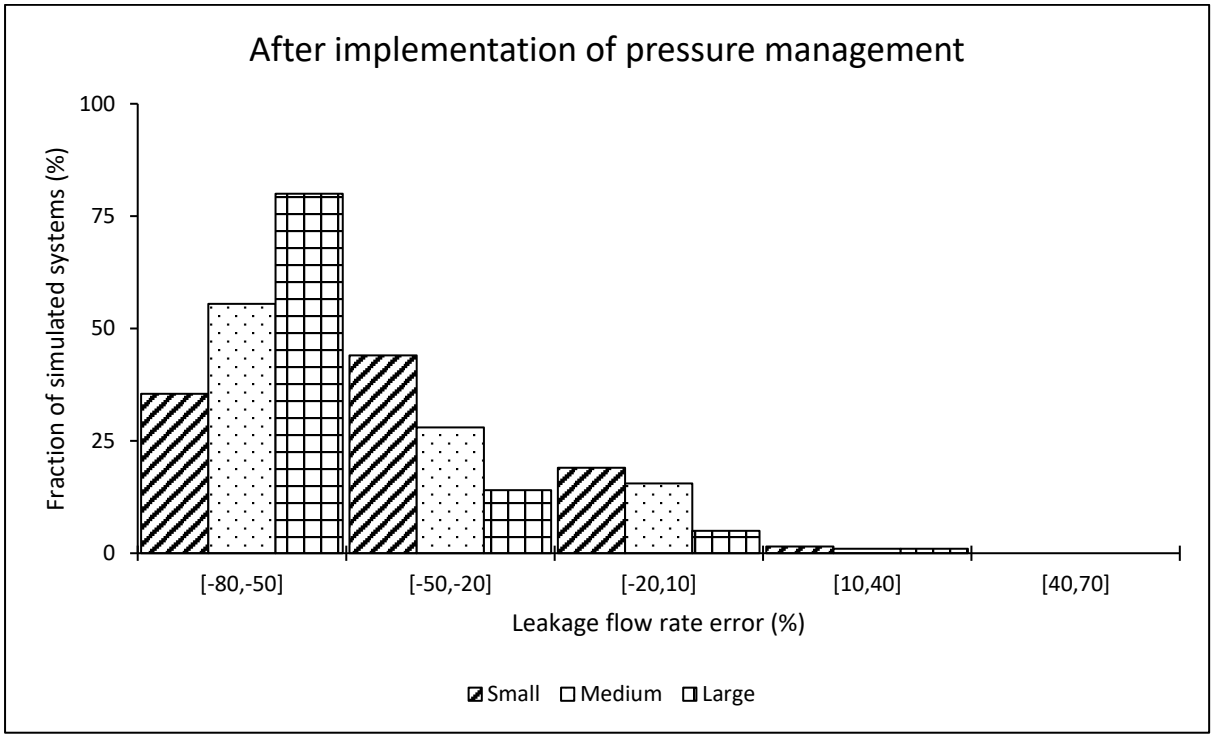

Impact on system convergence to a hydraulic solution

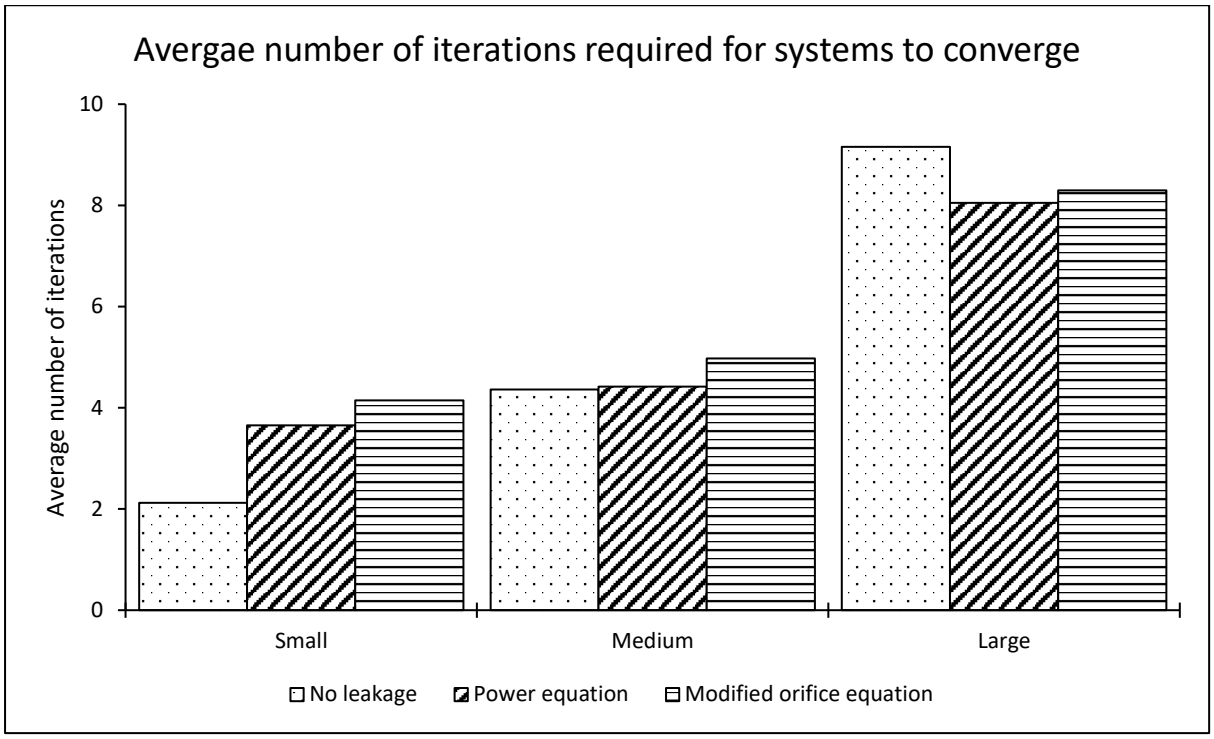

Appendix D: Results of the LP-MILP iterative approach for leak detection before and after adjustment of input parameters

Large system with an ILI of 8

A. During MNF conditions

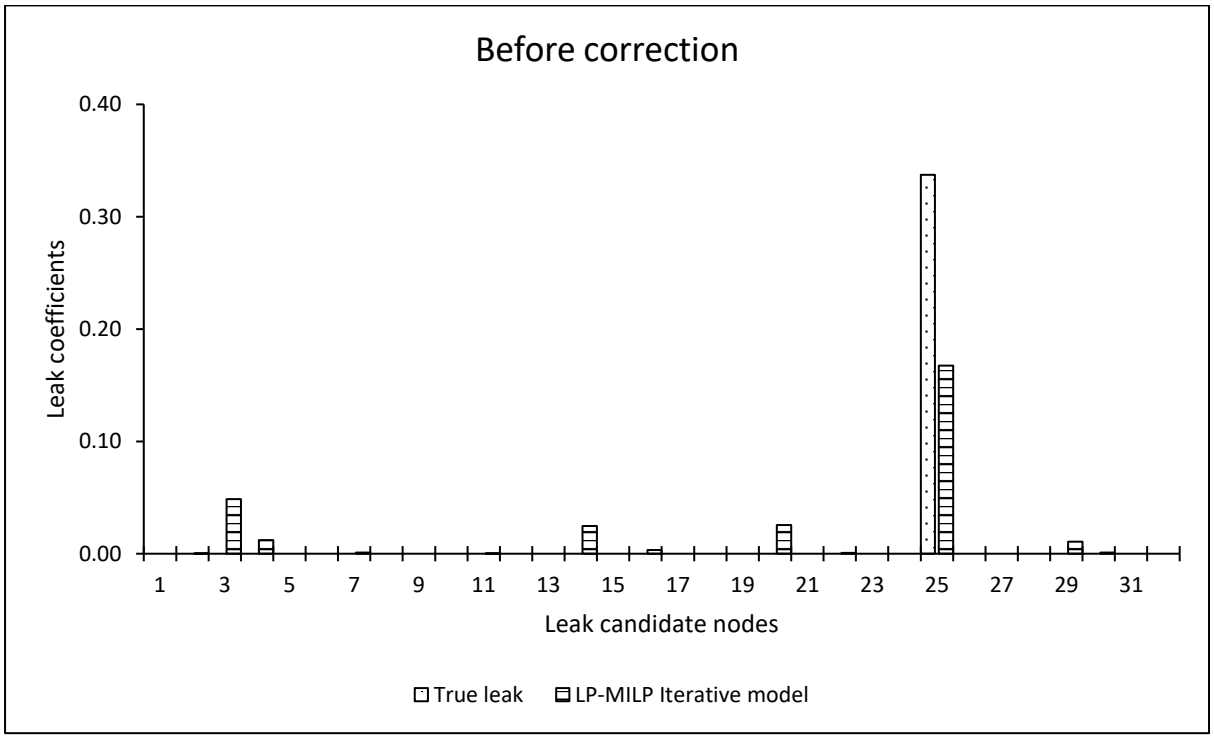

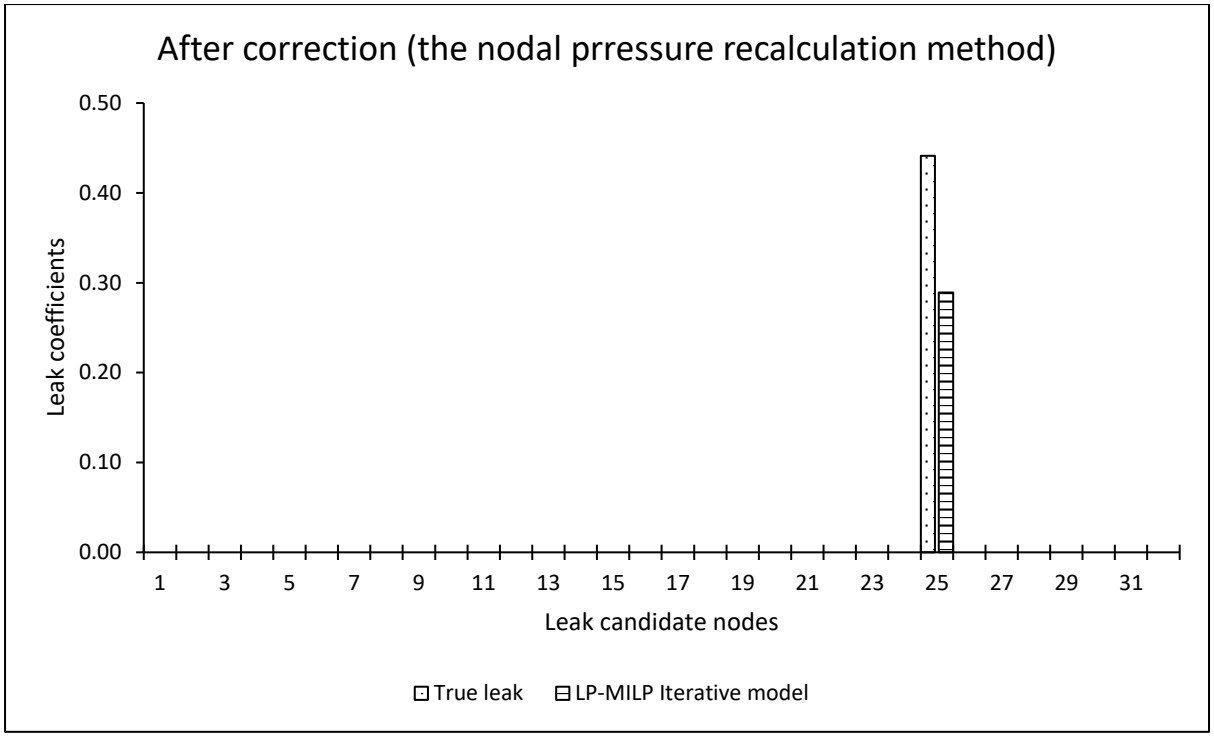
After correction (the nodal prressure recalculation method)
Leak coefficients
0.50
0.40
0.30
0.20
0.10
0.00
1 3 5 7 9 11 13 15 17 19 21 23 25 27 29 31
Leak candidate nodes
True leak
LP-MILP Iterative model

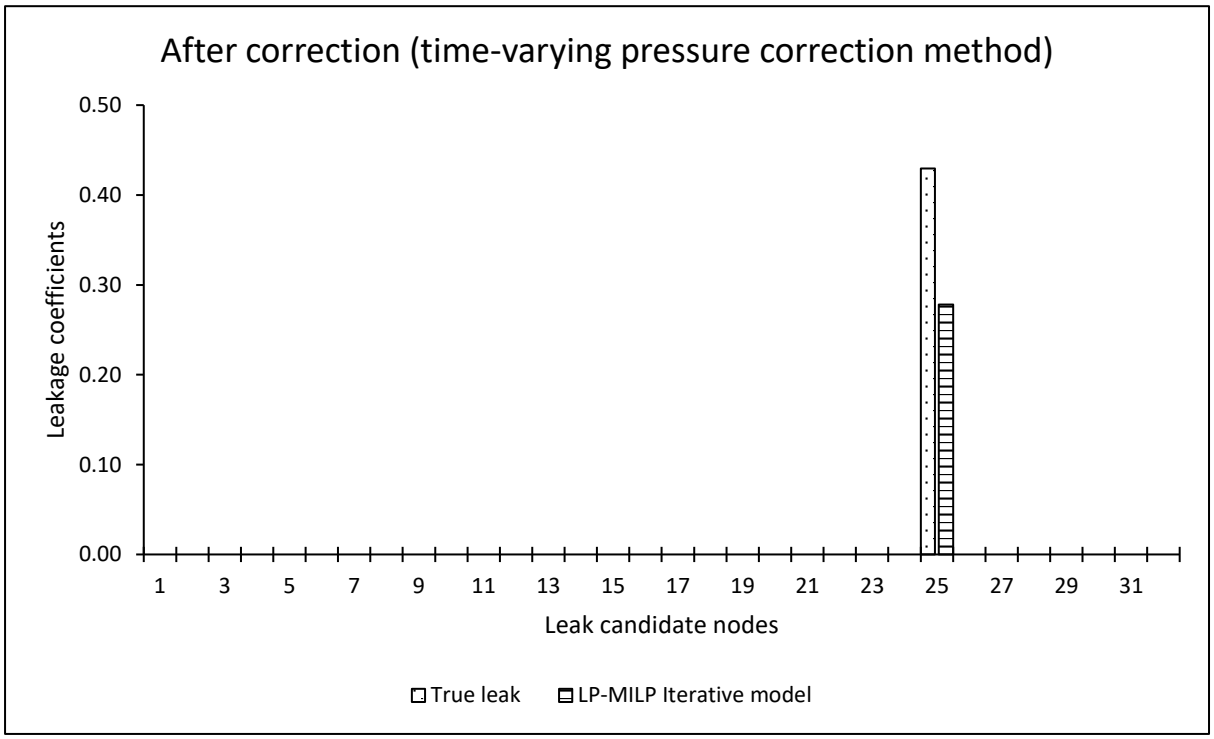
After correction (time-varying pressure correction method)
Leakage coefficients
0.50
0.40
0.30
0.20
0.10
0.00
1 3 5 7 9 11 13 15 17 19 21 23 25 27 29 31
Leak candidate nodes
True leak
LP-MILP Iterative model

B. During peak demand conditions

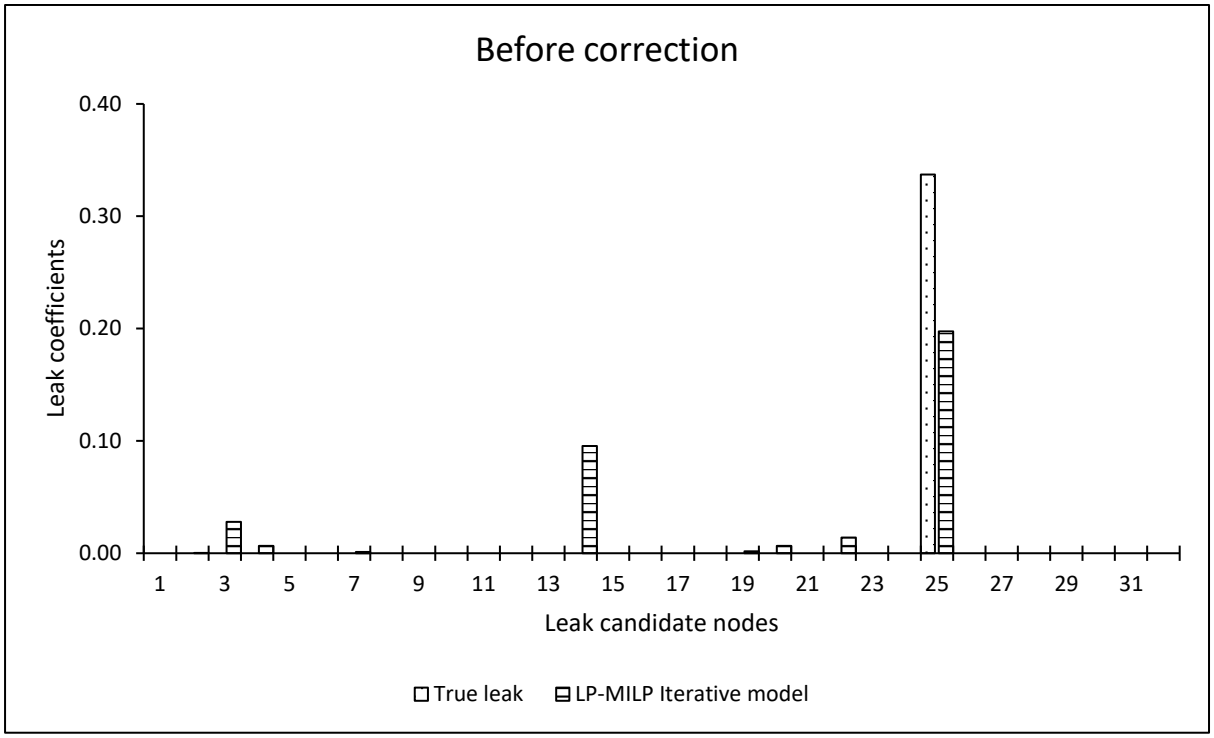

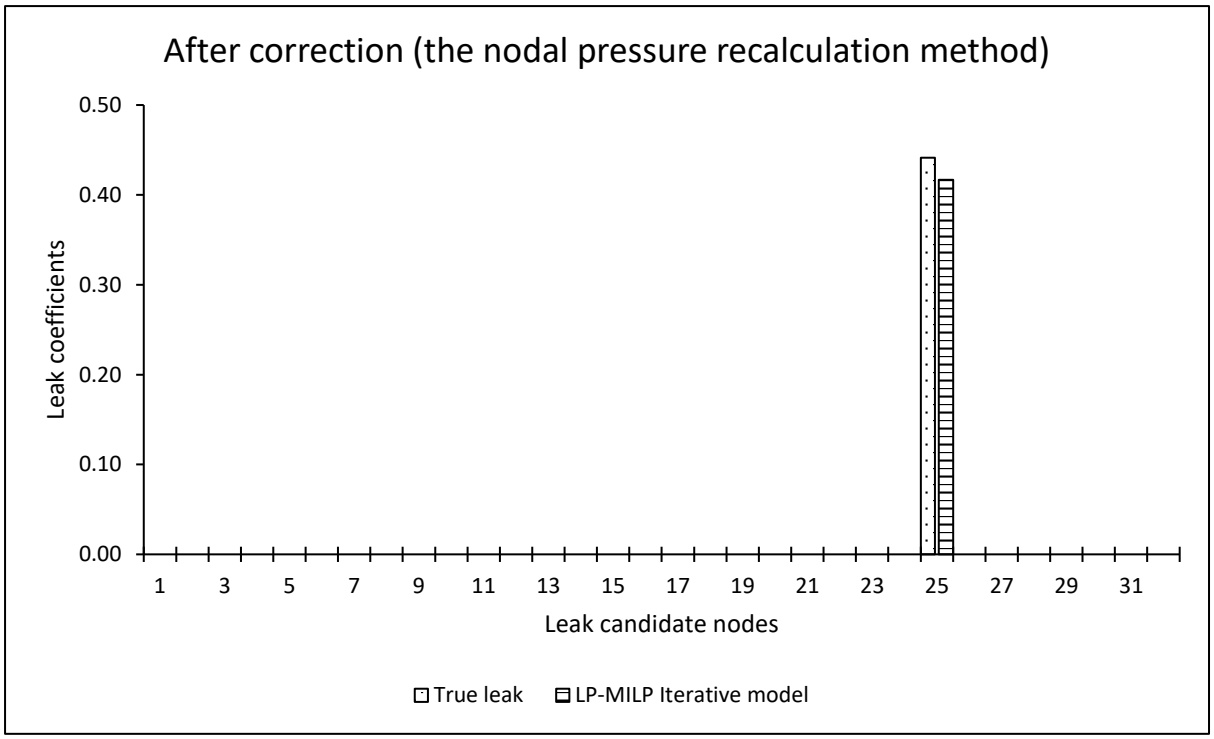

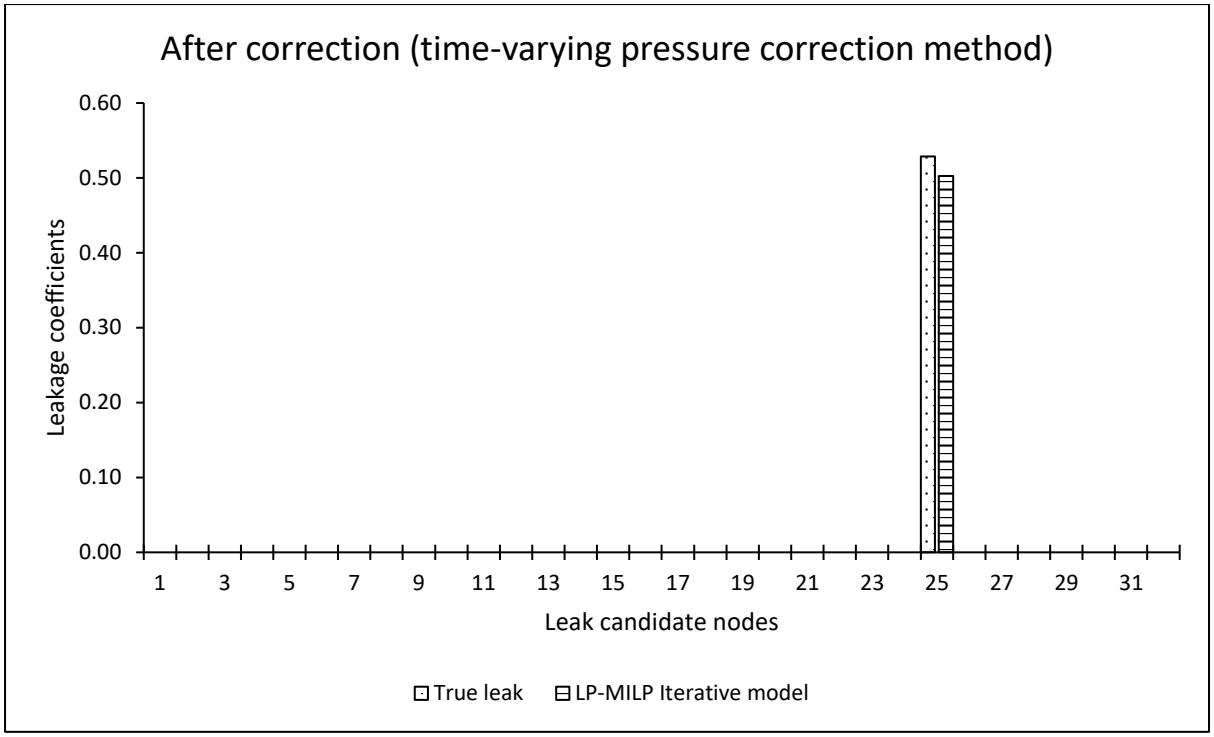
After correction (time-varying pressure correction method)
Leakage coefficients
0.60
0.50
0.40
0.30
0.20
0.10
0.00
1 3 5 7 9 11 13 15 17 19 21 23 25 27 29 31
Leak candidate nodes
True leak
LP-MILP Iterative model

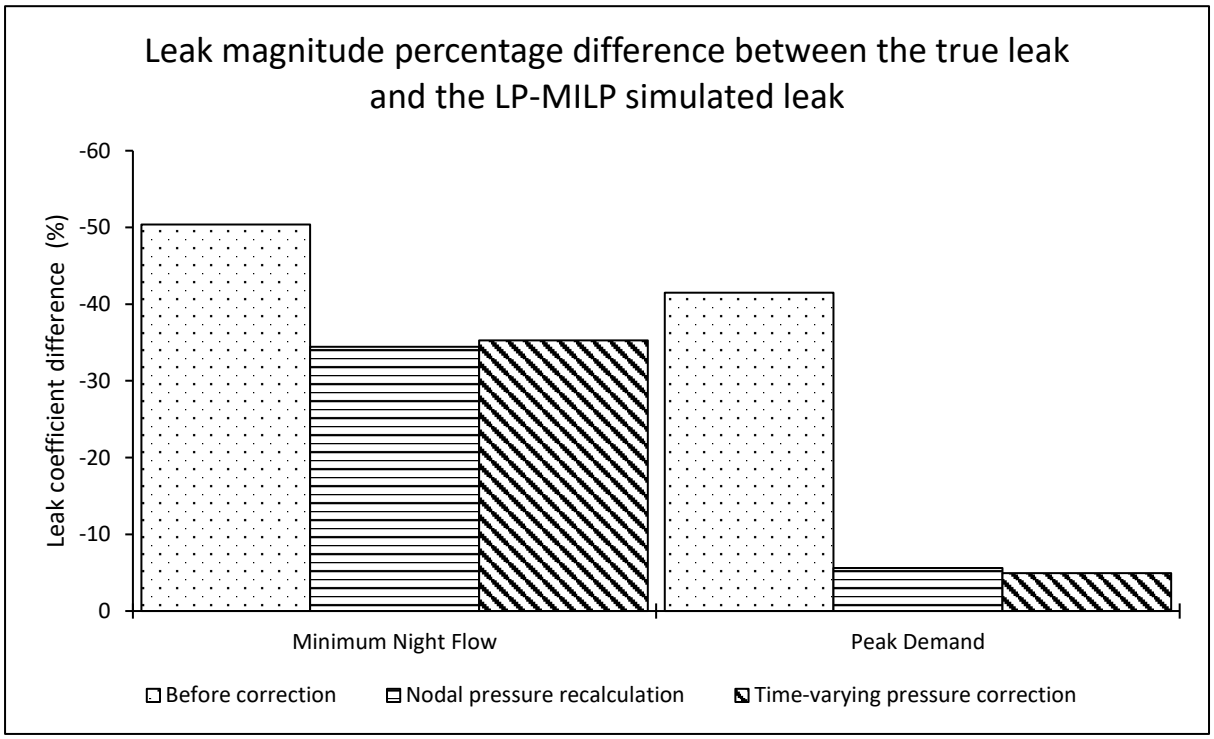
Leak magnitude percentage difference between the true leak and the LP-MILP simulated leak
Leak coefficient difference (%)
-60
-50
-40
-30
-20
-10
0
Minimum Night Flow
Peak Demand
Before correction
Nodal pressure recalculation
Time-varying pressure correction

Large system with an ILI of 4

A. During MNF conditions

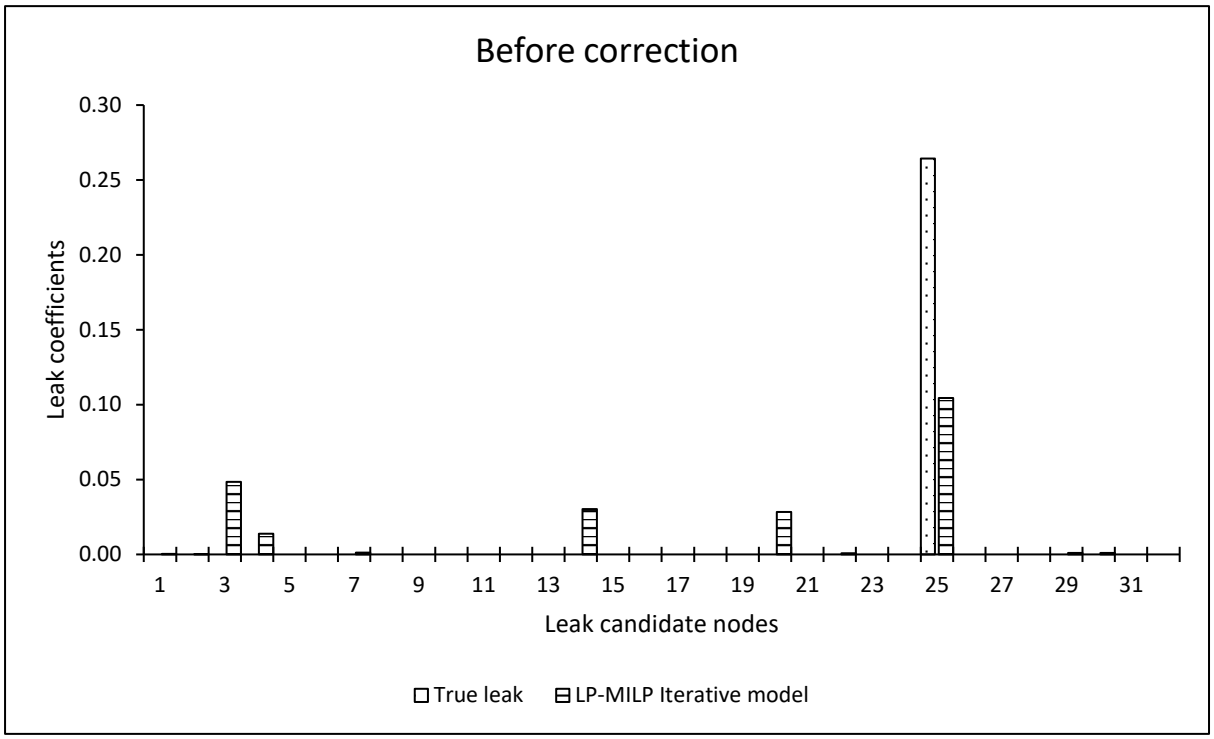

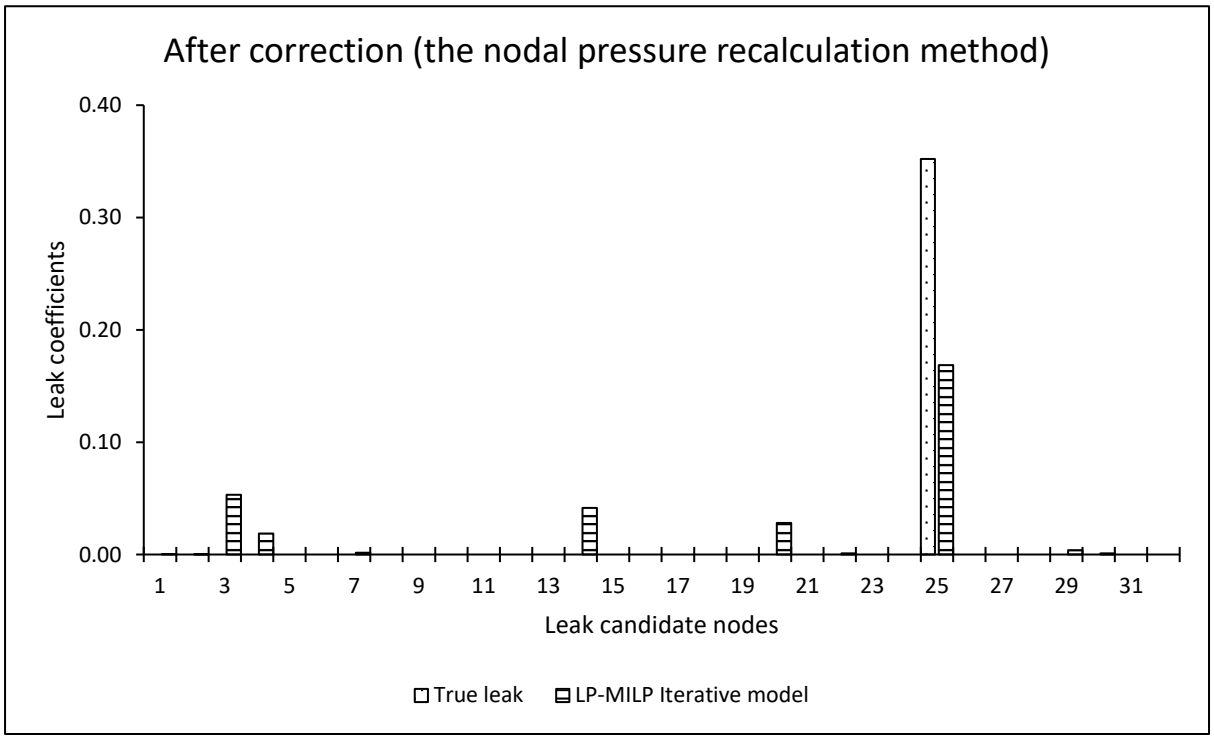

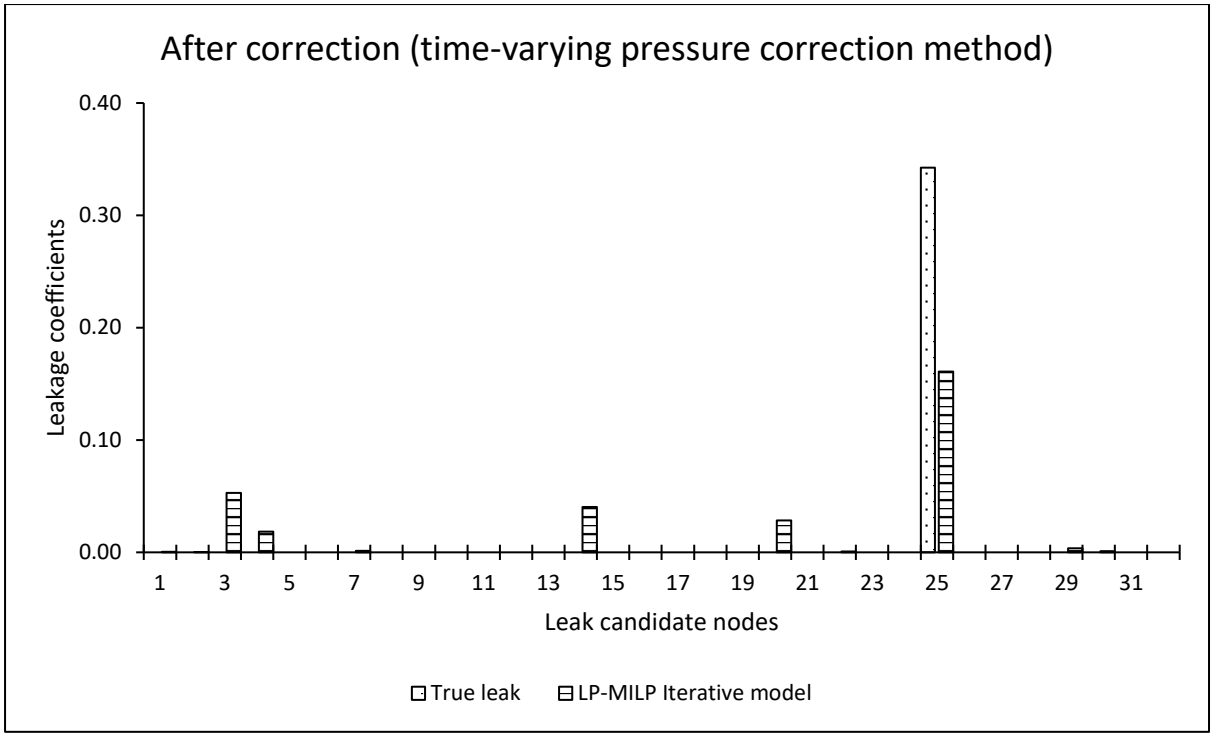

B. During peak demand conditions

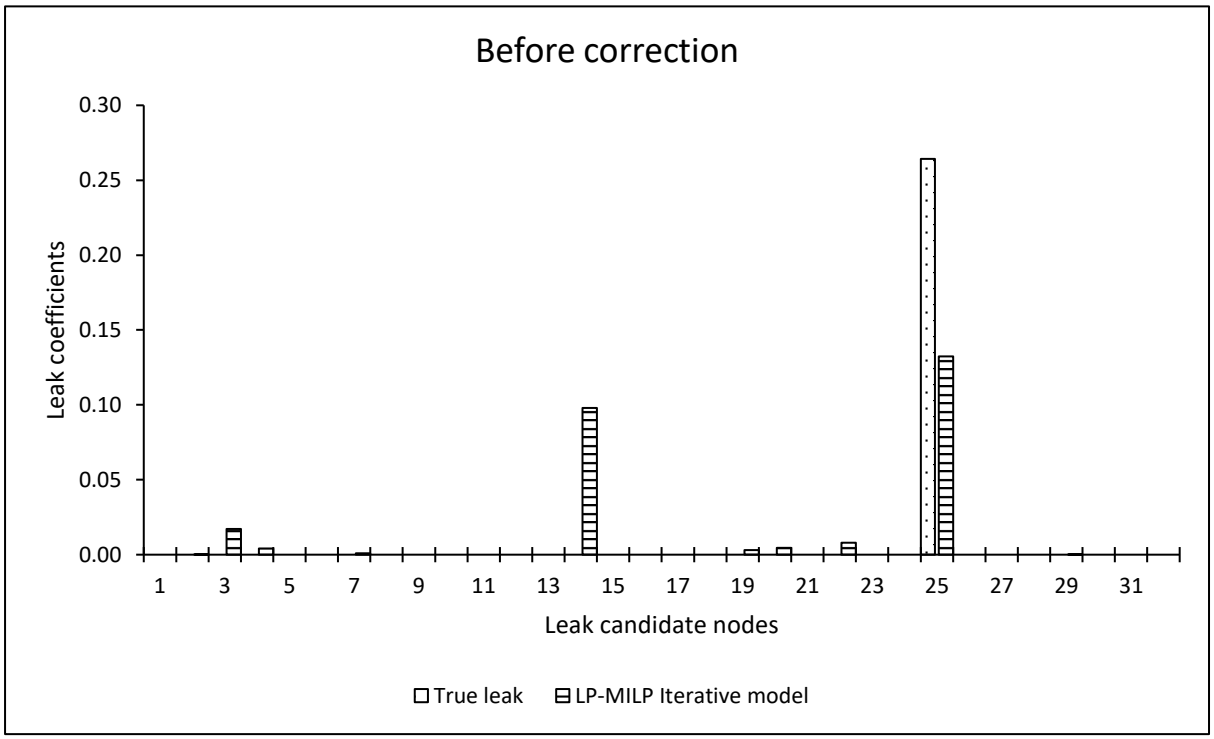

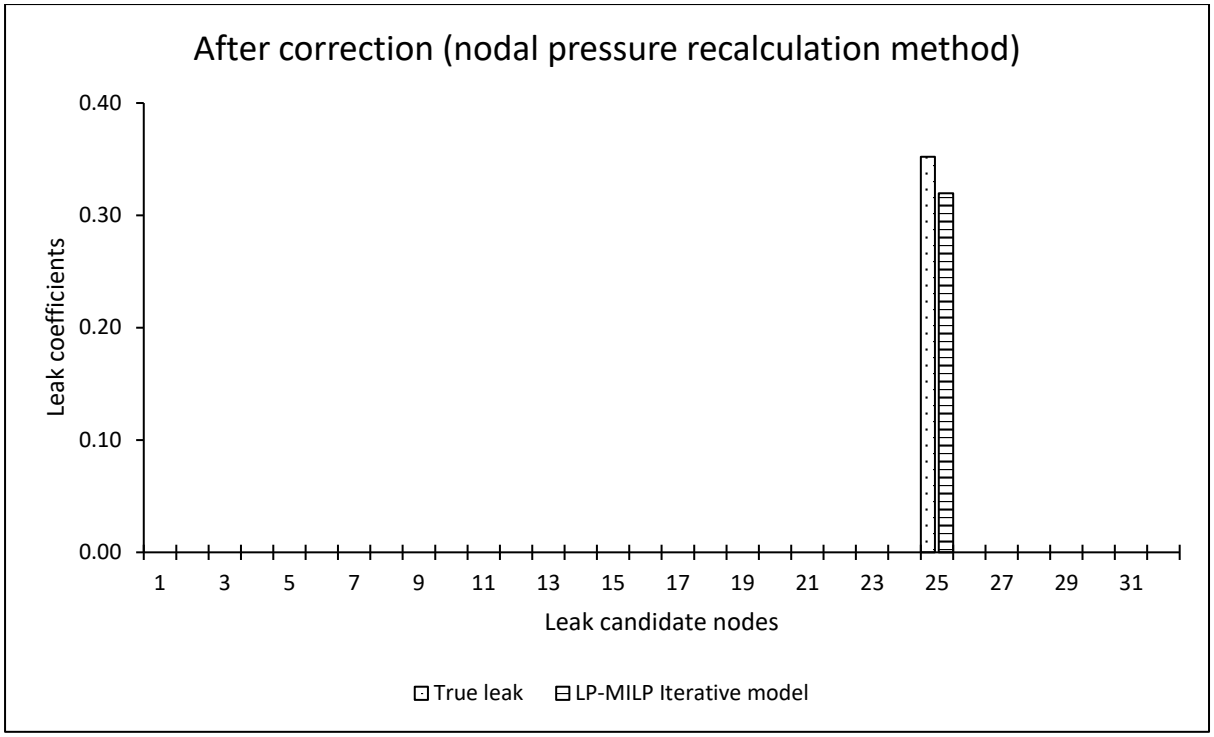
After correction (nodal pressure recalculation method)
Leak coefficients
0.40
0.30
0.20
0.10
0.00
1 3 5 7 9 11 13 15 17 19 21 23 25 27 29 31
Leak candidate nodes
True leak
LP-MILP Iterative model

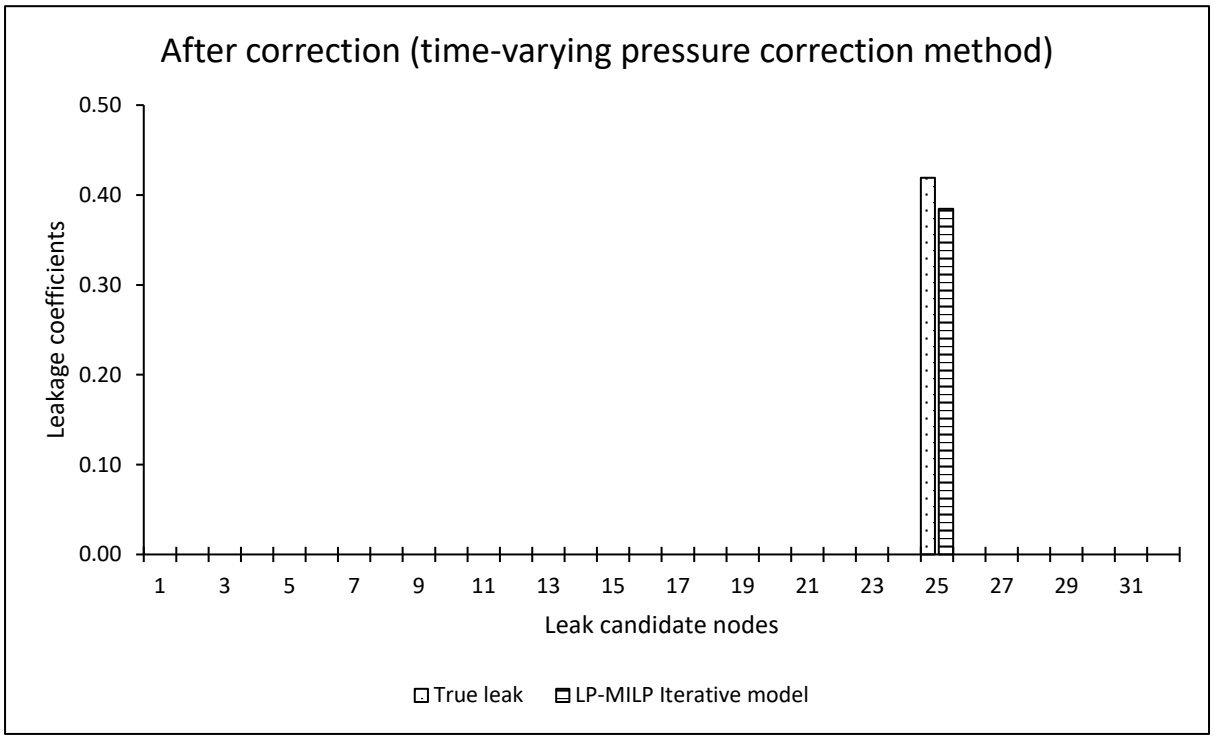
After correction (time-varying pressure correction method)
Leakage coefficients
0.50
0.40
0.30
0.20
0.10
0.00
1 3 5 7 9 11 13 15 17 19 21 23 25 27 29 31
Leak candidate nodes
True leak
LP-MILP Iterative model

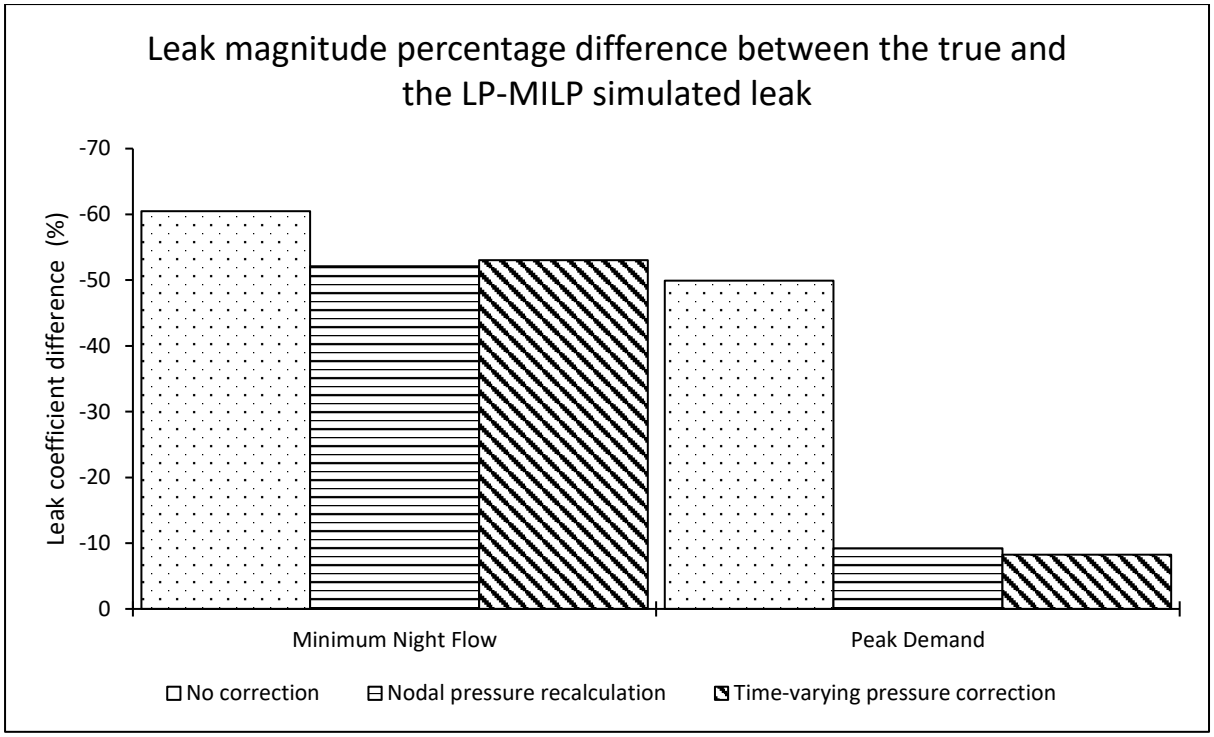
Leak magnitude percentage difference between the true and the LP-MILP simulated leak
Leak coefficient difference (%)
-70
-60
-50
-40
-30
-20
-10
0
Minimum Night Flow
Peak Demand
No correction
Nodal pressure recalculation
Time-varying pressure correction

Appendix E: Electronic documents

This appendix presents the following electronic documents on a compact disc (CD):

1. The source code and the dynamic link library (dll) of EPANET hydraulic modeling software, with the modified orifice formulation incorporated into it.
2. The stochastic model for the generation and distribution of leaks in standard water distribution pipe networks.
3. The input files of the three water distribution networks (i.e. small, medium and large) that were used in the evaluation of the modified orifice equation.